

# Organic Mass Spectrometry in Art and Archaeology

Editors **Maria Perla Colombini & Francesca Modugno**



 **WILEY**



# **Organic Mass Spectrometry in Art and Archaeology**





# Organic Mass Spectrometry in Art and Archaeology

Edited by

MARIA PERLA COLOMBINI AND FRANCESCA MODUGNO

*University of Pisa, Pisa, Italy*



A John Wiley and Sons, Ltd., Publication

This edition first published 2009  
© 2009 John Wiley & Sons, Ltd

*Registered office*

John Wiley & Sons Ltd, The Atrium, Southern Gate, Chichester, West Sussex, PO19 8SQ, United Kingdom

For details of our global editorial offices, for customer services and for information about how to apply for permission to reuse the copyright material in this book please see our website at [www.wiley.com](http://www.wiley.com).

The right of the author to be identified as the author of this work has been asserted in accordance with the Copyright, Designs and Patents Act 1988.

All rights reserved. No part of this publication may be reproduced, stored in a retrieval system, or transmitted, in any form or by any means, electronic, mechanical, photocopying, recording or otherwise, except as permitted by the UK Copyright, Designs and Patents Act 1988, without the prior permission of the publisher.

Wiley also publishes its books in a variety of electronic formats. Some content that appears in print may not be available in electronic books.

Designations used by companies to distinguish their products are often claimed as trademarks. All brand names and product names used in this book are trade names, service marks, trademarks or registered trademarks of their respective owners. The publisher is not associated with any product or vendor mentioned in this book. This publication is designed to provide accurate and authoritative information in regard to the subject matter covered. It is sold on the understanding that the publisher is not engaged in rendering professional services. If professional advice or other expert assistance is required, the services of a competent professional should be sought.

The publisher and the author make no representations or warranties with respect to the accuracy or completeness of the contents of this work and specifically disclaim all warranties, including without limitation any implied warranties of fitness for a particular purpose. This work is sold with the understanding that the publisher is not engaged in rendering professional services. The advice and strategies contained herein may not be suitable for every situation. In view of ongoing research, equipment modifications, changes in governmental regulations, and the constant flow of information relating to the use of experimental reagents, equipment, and devices, the reader is urged to review and evaluate the information provided in the package insert or instructions for each chemical, piece of equipment, reagent, or device for, among other things, any changes in the instructions or indication of usage and for added warnings and precautions. The fact that an organization or Website is referred to in this work as a citation and/or a potential source of further information does not mean that the author or the publisher endorses the information the organization or Website may provide or recommendations it may make. Further, readers should be aware that Internet Websites listed in this work may have changed or disappeared between when this work was written and when it is read. No warranty may be created or extended by any promotional statements for this work. Neither the publisher nor the author shall be liable for any damages arising herefrom.

***Library of Congress Cataloging-in-Publication Data***

Colombini, Maria Perla.

Organic mass spectrometry in art and archaeology / Maria Perla Colombini, Francesca Modugno.  
p. cm.

Includes bibliographical references and index.

ISBN 978-0-470-51703-1

1. Mass spectrometry. 2. Organic compounds—Analysis. I. Modugno, Francesca. II. Title.  
QD272.S6C63 2009  
702.8'8—dc22

2009009694

A catalogue record for this book is available from the British Library.

978-0-470-51703-1

Set in 10/12pt Times by Integra Software Services Pvt. Ltd, Pondicherry, India

Printed and bound in Italy by Printer Trento

**Cover Image**

On the cover: upper part of a clay lamp, from Antinoupolis, Egypt (inv. 718, unpublished, © Centro Studi Istituto Papirologico G. Vitelli, Università degli Studi di Firenze).

# Contents

<i>List of Contributors</i>	vii
<i>Acknowledgements</i>	ix
<i>Preface</i>	xi
<b>PART I INTRODUCTION</b>	<b>1</b>
<b>1 Organic Materials in Art and Archaeology</b>	<b>3</b>
<i>Maria Perla Colombini and Francesca Modugno</i>	
<b>2 Overview of Mass Spectrometric Based Techniques Applied in the Cultural Heritage Field</b>	<b>37</b>
<i>Gianluca Giorgi</i>	
<b>PART II DIRECT MASS SPECTROMETRIC ANALYSIS</b>	<b>75</b>
<b>3 Direct Mass Spectrometric Techniques: Versatile Tools to Characterise Resinous Materials</b>	<b>77</b>
<i>Erika Ribechini</i>	
<b>4 Direct Mass Spectrometry to Characterise Wax and Lipid Materials</b>	<b>97</b>
<i>Martine Regert</i>	
<b>5 GALDI-MS Applied to Characterise Natural Varnishes and Binders</b>	<b>131</b>
<i>Patrick Dietemann and Christoph Herm</i>	
<b>6 MALDI-MS Applied to the Analysis of Protein Paint Binders</b>	<b>165</b>
<i>Stepanka Kuckova, Radovan Hynek and Milan Kodicek</i>	

<b>PART III GAS CHROMATOGRAPHY/MASS SPECTROMETRY</b>	<b>189</b>
<b>7 GC/MS in the Characterization of Lipids</b>	<b>191</b>
<i>Maria Perla Colombini, Francesca Modugno and Erika Ribechini</i>	
<b>8 GC/MS in the Characterisation of Resinous Materials</b>	<b>215</b>
<i>Francesca Modugno and Erika Ribechini</i>	
<b>9 GC/MS in the Characterisation of Protein Paint Binders</b>	<b>237</b>
<i>Maria Perla Colombini and Gwénaëlle Gautier</i>	
<b>10 SPME/GC-MS in the Characterisation of Terpenic Resins</b>	<b>261</b>
<i>Jean Bleton and Alain Tchaplà</i>	
<b>11 Py-GC/MS of Organic Paint Binders</b>	<b>303</b>
<i>Ilaria Bonaduce and Alessia Andreotti</i>	
<b>12 Py-GC/MS of Natural and Synthetic Resins</b>	<b>327</b>
<i>Dominique Scalarone and Oscar Chiantore</i>	
<b>PART IV LIQUID CHROMATOGRAPHY/MASS SPECTROMETRY</b>	<b>363</b>
<b>13 Characterization of Organic Natural Dyes by Electrospray Mass Spectrometry Coupled with HPLC and/or Capillary Electrophoresis</b>	<b>365</b>
<i>Katarzyna Lech, Katarzyna Połec-Pawlak and Maciej Jarosz</i>	
<b>PART V OTHER MS-BASED TECHNIQUES</b>	<b>389</b>
<b>14 Compound-specific Stable Isotopes in Organic Residue Analysis in Archaeology</b>	<b>391</b>
<i>Richard P. Evershed</i>	
<b>15 ToF-SIMS Study of Organic Materials in Cultural Heritage: Identification and Chemical Imaging</b>	<b>433</b>
<i>Vincent Mazel and Pascale Richardin</i>	
<b>16 Accelerator Mass Spectrometry for <sup>14</sup>C Dating</b>	<b>459</b>
<i>Mariaelena Fedi</i>	
<b><i>Index</i></b>	<b>483</b>

# List of Contributors

**Alessia Andreotti**, Department of Chemistry and Industrial Chemistry, University of Pisa, Via Risorgimento 35, 56126 Pisa, Italy

**Jean Bleton**, Groupe de Chimie Analytique de Paris-Sud 11 (LETIAM) EA 4041, Institut Universitaire de Technologie d'Orsay, Plateau de Moulon, 91400 Orsay, France

**Ilaria Bonaduce**, Department of Chemistry and Industrial Chemistry, University of Pisa, Via Risorgimento 35, 56126 Pisa, Italy

**Oscar Chiantore**, Department of IPM Chemistry and Centre of Excellence NIS, University of Torino, Via Giuria 7, 10125 Torino, Italy

**Maria Perla Colombini**, Department of Chemistry and Industrial Chemistry, University of Pisa, Via Risorgimento 35, 56126 Pisa, Italy

**Patrick Dietemann**, Doerner Institut, Bayerische Staatsgemäldesammlungen, Barer Str. 29, D-80799 München, Germany

**Richard P. Evershed**, Organic Geochemistry Unit, Bristol Biogeochemistry Research Centre, School of Chemistry, University of Bristol, Cantock's Close, Bristol BS8 1TS, UK

**Mariaelena Fedi**, INFN Sezione di Firenze, Via Bruno Rossi 1, 50019 Sesto Fiorentino, Italy

**Gwénaëlle Gautier**, The Art Institute of Chicago, 111 South Michigan Avenue, Chicago, IL 60603-6404, USA

**Gianluca Giorgi**, Department of Chemistry, University of Siena, Via Aldo Moro, 53100 Siena, Italy

**Christoph Herm**, Studiengang Restaurierung, Hochschule für Bildende Künste Dresden, Güntzstr. 34, D-01307 Dresden, Germany

**Radovan Hyněk**, Institute of Chemical Technology, Department of Biochemistry and Microbiology, Technická 3, 166 28 Prague 6, Czech Republic

**Maciej Jarosz**, Faculty of Chemistry, Warsaw University of Technology, Noakowskiego 3, 00-664 Warsaw, Poland

**Milan Kodicek**, Institute of Chemical Technology, Department of Biochemistry and Microbiology, Technická 3, 166 28 Prague 6, Czech Republic

**Stepanka Kuckova**, Charles University, Department of Chemistry and Chemical Education, M.D. Rettigové 4, 116 39 Prague 1, Czech Republic and Institute of Chemical Technology, Department of Biochemistry and Microbiology, Technická 3, 166 28 Prague 6, Czech Republic

**Katarzyna Lech**, Faculty of Chemistry, Warsaw University of Technology, Noakowskiego 3, 00-664 Warsaw, Poland

**Vincent Mazel**, Laboratoire Matériaux et Santé, UFR de Pharmacie, Université Paris-sud XI, 92296 Chatenay Malabry Cedex, France

**Francesca Modugno**, Department of Chemistry and Industrial Chemistry, University of Pisa, Via Risorgimento 35, 56126 Pisa, Italy

**Katarzyna Połec-Pawlak**, Faculty of Chemistry, Warsaw University of Technology, Noakowskiego 3, 00-664 Warsaw, Poland

**Martine Regert**, CEPAM (Centre d'Etudes Préhistoire, Antiquité, Moyen Âge), UMR 6130, Université Nice Sophia Antipolis – CNRS, Bât. 1; 250, rue Albert Einstein, F-06560 Valbonne, France

**Erika Ribechini**, Department of Chemistry and Industrial Chemistry, University of Pisa, Via Risorgimento 35, 56126 Pisa, Italy

**Pascale Richardin**, C2RMF–CNRS UMR 171, Centre de Recherche et de Restauration des Musées de France, Palais du Louvre, Porte des Lions, 14, Quai François Mitterrand, 75001 Paris, France

**Dominique Scalarone**, Department of IPM Chemistry and Centre of Excellence NIS, University of Torino, Via Giuria 7, 10125 Torino, Italy

**Alain Tchapla**, Groupe de Chimie Analytique de Paris-Sud 11 (LETIAM) EA 4041, Institut Universitaire de Technologie d'Orsay, Plateau de Moulon, 91400 Orsay, France

# Acknowledgements

The editors would like to thank all the authors who contributed to this book and who believe in the importance of the dissemination of mass spectrometric techniques. They are grateful to Erika Ribechini, Ilaria Bonaduce, Ilaria Degano and all the research group of the Laboratory in Chemical Science for the Safeguard of Cultural Heritage at the Department of Chemistry and Industrial Chemistry of the University of Pisa, who helped considerably in the reviewing process. Thanks are also due to Adrian Wallwork and Anna Southern for proofreading sections of the book. Finally, we are grateful to Jenny Cossham, Richard Davies and the staff of John Wiley & Sons, Ltd for all their effort, patient assistance, and very useful suggestions.





# Preface

Early applications of chemical and physical analytical methods in studies on art materials and archaeological objects demonstrated that scientific investigation is an essential tool for acquiring information on the materials that make up an artwork and for assessing their decay, in order to plan restoration approaches. Chemical diagnosis, together with the investigation carried out by historians, archaeologists and art experts, is a valuable contribution to help identify the materials in paintings and ancient artefacts, as well as their state of conservation.

The development of scientific procedures that are able to use very minute samples (a few micrograms), together with the increased availability of advanced analytical instrumentation, have led to great interest in the chemical study of materials used in cultural heritage. This has given rise to a sharp increase in research studies at the interface between art, archaeology, chemistry and the material sciences. As a result, successful multidisciplinary collaborations have flourished among researchers in museums, conservation institutions, universities and scientific laboratories.

Thus, a new science, called Conservation Science, was born. This term came into use in the 1980s and is now widely adopted: the field includes both pure and applied research. Fundamental research is required specifically where knowledge gaps exist, for instance in the behaviour under natural ageing of new synthetic materials used both for restoration and for art purposes.

Organic substances can be identified both as the main constituents of an artwork or a cultural heritage object, and as secondary components, mixed with inorganic compounds. Organic materials can be found in the finish or decoration of the surfaces, or as residues of commodities, such as in ceramic or glass vessels. Moreover, the majority of restoration products applied as consolidants, adhesives, restoration paints and varnishes are of an organic nature.

Investigation into this wide range of substances is crucial for conservation since organic constituents are more prone to degradation due to the effects of light, temperature, moisture, biological agents and environmental oxidizing conditions. Their degradation pathways are thus often key in determining the overall decay of an object.

Over the past decade, particular attention has been focused on the characterization of organic materials occurring, for example, as the residues of food, medicines and balms in archaeology, as adhesives, and as binders in paints. The mixture of many materials in ancient recipes and technologies, and the chemical changes induced by ageing make it even more difficult to study these samples.

In this respect, research relies heavily on structural information at a molecular level, and thus the application of mass spectrometry plays a prominent role. This is mainly due to its

ability to obtain detailed compositional information of complex mixtures. In addition, the possibility of coupling mass spectrometry with chromatographic techniques, such as gas chromatography and high-performance liquid chromatography, make mass spectrometry the most powerful tool to investigate the complex and aged mixtures of organic molecules that are currently encountered as constituents of artistic, historic and archaeological objects.

In recent years, specialized journals and congresses have presented an increasing number of papers and case studies. However, with a few exceptions, due to its specialized and fragmentary nature such information is difficult to access.

This book offers an overview of the use of the techniques based on mass spectrometry for the analysis of organic substances in art and archaeological materials. The fundamental principles are illustrated along with procedures and mass spectrometric techniques. Case studies and examples show how these techniques can be used to reveal the history of the objects and how they were produced. A key issue is the search for fingerprints of the organic materials, which might reveal the techniques and the technologies used in the past. Another is the study of the decay processes of the constituent materials of heritage objects, which is crucial in terms of their conservation.

The examples given in the chapters start from sampling and sample pretreatments, and include data interpretation. Conclusions are then drawn which bring together chemical and archaeological data.

Since many difficult problems arise from the complex composition and alteration pathways of the materials considered, the book begins with a survey of organic materials used both in art and archaeology (Chapter 1) and a discussion of their behaviour under natural and artificial accelerated ageing and burial conditions. To help in understanding the various mass spectrometric methods and instruments, the main concepts in mass spectrometric instrumentation are discussed in Chapter 2. The wide variety of features offered by mass spectrometry makes the range of organic materials that can be studied very broad: it includes small volatile molecules such as monoterpenes in essential oils as well as macromolecules and proteins. Mass spectrometric based techniques are used for the accurate quantitative analysis of specific, well known species, and also for the identification of unknown, unexpected compounds such as degradation products on the basis of the mass spectra. The adoption of proteomic techniques in archaeometry has opened up new horizons in the study of biological residues.

Chapters 3–6 deal with direct mass spectrometric analysis highlighting the suitability of the various techniques in identifying organic materials using only a few micrograms of samples. Due to the intrinsic variability of artefacts produced in different places with more or less specific raw materials and technologies, complex spectra are acquired. Examples of chemometric methods such as principal components analysis (PCA) are thus discussed to extract spectral information for identifying materials.

Chapters 7–13 discuss several analytical approaches based on gas chromatography/mass spectrometry, pyrolysis-gas chromatography/mass spectrometry and liquid chromatography/mass spectrometry. Biomarkers for material identification are assessed and degradation mechanisms are examined, giving an in-depth insight of natural and synthetic resins, proteinaceous binders, plant gums, vegetable oils and waxes.

Finally, Chapters 14–16 deal with innovative applications in this field such as mass spectrometric compound-specific isotopic analysis, secondary ion mass spectrometry

(SIMS) to map specific compounds in cross-sections, and atomic isotopic analysis for dating using accelerator mass spectrometry (AMS).

This multi-authored book is aimed at:

- researchers who exploit analytical chemistry based on mass spectrometry to improve the knowledge and conservation of cultural heritage;
- students in instrumental analyses, chemical science and conservation science;
- archaeologists, art historians and museum conservators who cooperate with scientists in the study of materials.

We hope that this book will provide a useful source of information for people involved in conservation sciences and as a springboard for those who are just starting out in this fascinating field.

Maria Perla Colombini  
Francesca Modugno  
*University of Pisa, Italy*



# **Part I**

## **Introduction**



# 1

## Organic Materials in Art and Archaeology

*Maria Perla Colombini and Francesca Modugno*

### 1.1 Introduction

Men have always used the natural materials around us to produce functional objects and works of art. Paintings and other objects that are part of our cultural heritage, including textiles, books, sculptures, archaeological objects, furniture and the organic residues found in association with them (e.g. cosmetics, medicines, perfumes, food), contain a wide variety of organic materials from natural to synthetic.

Since ancient times, natural organic materials have been employed as paint binders, adhesives, waterproofing materials and so on, as reported in classical literature by Plinius the Elder and Vitruvius. Archaeological excavations often bring to light a wide variety of objects and materials that have been collected, processed and used by humans over time. Due to their long period underground, some of these materials and objects, especially those of an organic nature, have been partially or totally altered.

Being able to identify natural substances and their degradation products is a challenge. If we manage to do so, we then can shed light on the nature and the origin of the material employed, the artistic techniques used and the state of conservation. Organic materials are more subject to degradation than inorganic ones, so if we can understand their composition then we can ensure that ancient artefacts will remain part of our cultural heritage. This chapter outlines the main organic materials encountered in artistic and archaeological objects, along with their composition, basic behaviour and degradation pathways related to ageing. Table 1.1 summarizes the organic materials and how they were once used.

**Table 1.1** *Category, organic materials and uses*

Category	Organic materials	Uses
Proteins	Egg, milk and casein, animal glue, silk, wool, vegetable proteins (e.g. garlic, beans), human and animal tissues (e.g. mummies)	Paint binders, adhesives, textiles, commodities, parchment
Glycerolipids	Animal fats, vegetable oils (e.g. palm oil, olive oil) including drying oils (e.g. linseed, walnut, poppy seed)	Paint binders, varnishes, illuminants, commodities, ingredients of cosmetic and pharmaceutical preparations
Waxes	Beeswax, spermaceti, Chinese wax, lanolin (animal waxes); carnauba, candelilla, Japan wax, esparto (vegetable waxes); paraffin, ozokerite (fossil waxes)	Paint binders, coatings, sealants, writing tablets, ingredients of cosmetic and pharmaceutical preparations, sculptures
Natural resins	Pine resins, sandarac, copals, mastic, dammar, amber, frankincense, benzoe, styrax, myrrh, (plant resins); shellac (animal resin); tar and pitch (from thermal treatment of plant resins or wood)	Varnishes, coatings, waterproofing materials, paint binders, ingredients of cosmetic and pharmaceutical preparations
Polysaccharide materials	Starch, cellulose, plant gums (arabic gum, tragacanth, karaya, ghatti, guar, locust bean, fruit tree gum)	Paper, paint binders, adhesives
Bituminous materials	Bitumen, asphalt	Moulding materials, adhesive, pigment
Organic dyes	Cochineal, madder, kermes, saffron, purple, indigo, synthetic dyes	Colourants for dyeing textiles, paint materials
Synthetic polymers	Polyacrylates, cellulose nitrate, phenolic resins, polyethylene, poly(vinyl acetate), polystyrene	Paint binders, varnishes, coatings, consolidants, sculptures

## 1.2 Proteins

Proteins are macromolecules made up of one or more unbranched chains of amino acids which are joined together by peptide bonds between the carboxyl and amino groups of adjacent amino acid residues. Several amino acids are commonly found in animal and vegetable proteins: glycine (Gly), alanine (Ala), valine (Val), leucine (Leu), isoleucine (Ile), methionine (Met), proline (Pro), hydroxyproline, (Hyp), threonine (Thr), asparagine (Asn), glutamine (Gln), tyrosine (Tyr), cysteine (Cys), lysine (Lys), arginine (Arg), aspartic acid (Asp), phenylalanine (Phe), tryptophan (Trp), serine (Ser), glutamic acid (Glu), and histidine (His) [1].

The number and the type of amino acids and their sequence determine the surface charge of the protein, its molecular configuration and its unique chemical and physical properties. The function of a protein is dependent on its three-dimensional structure. A number of agents can disrupt this structure thus denaturing it, for example changes in pH, temperature, salt concentration, and the presence of reducing substances.



Both vegetable and animal proteins are encountered in art as textiles, leather and parchment, paint binders, and adhesives, and in archaeological objects as organic residues of commodities, or of human or animal tissues. Aged proteins are denaturized: as a result of the loss of water and of ageing, the tertiary and quaternary structures change, through the rearrangement of internal bonds between functional groups. Thus, their solubility and reactivity differ from the native ones, whereas in favourable cases the amino acid composition can remain mostly unchanged. Microbic degradation of protein is quite fast in the burial environment, whereas proteins are often present in quite a good state of conservation in the paint layers of paintings.

The determination of the amino acid profile of proteins after hydrolysis of peptide bonds can be used in specific cases for the differentiation and the identification of proteins in paint samples [2–7]. In paintings, animal proteins such as egg, casein and glue, were frequently used as binders for pigments in the tempera technique. Egg was mainly used as whole egg and egg yolk. A whole dry hen egg contains about 45% protein, 41% lipid and 2% cholesterol [2,8]. Milk is an aqueous emulsion of proteins and lipids: dry cow milk contains about 26% protein, 26% lipid, and sugars [2,8]. Casein is obtained by the acidic, enzymatic or thermal treatment of milk, and its main constituents are  $\alpha$ -casein,  $\beta$ -casein,  $\delta$ -casein, and  $\gamma$ -casein. Animal glue was obtained by boiling the skin, bones or cartilaginous parts of mammals and fish. It is made up of collagen, a protein characterised by the presence of a high content of glycine, proline and hydroxyproline [2]. One of the most important vegetable proteins is garlic (*Allium sativum*), a member of the Liliaceae family. Garlic contains 0.1–0.4% volatile oil, carbohydrates (making up 75% of the dry matter), and proteins (15–17% of the dry matter) [9] and was used as an adhesive in gildings [10]. Also plant gums such as arabic gum, which is mainly composed of polysaccharides, contain a minor proteinaceous fraction [11].

Table 1.2 gives the average amino acid composition of some animal and vegetable proteins found in art and archaeology.

During ageing, proteins react with other materials in the historical/archaeological object and, for instance, condensation and cross-linking reactions between proteins and glycerolipids may occur. Amino malonic aldehyde has been identified as a possible product of oxidative degradation of serine, phenylalanine and cysteine [13]. The further oxidation of this compound can lead to the formation of amino malonic acid. This compound has been detected in paint samples, and its presence increases in the course of ageing. Another important factor of protein degradation is pH changes which, in the presence of moisture, can cause the hydrolysis of peptide bonds. As a consequence, the molecular weight may change, and the serine and threonine may dehydrate. Alkaline treatments (commonly used in restoration) can partially hydrolyse proteins and produce cystine and dehydroalanine from cysteine [14]. The formation of oxalate salts on paint surfaces has also been observed, suggesting some kind of photo-oxidation [15]. The reduced solubility of proteins in ancient samples is related to denaturation and cross-linking processes during ageing: cations may act as catalysers for the protein oxidation, thus enhancing this phenomenon. Anaerobic degradation of proteins by micro-organisms may lead to the formation of molecules such as piperidone, benzoic acid and *p*-hydroxyphenylacetate [16].

Proteins are synthesized from L-amino acids. When the living organism has died, they start to spontaneously convert to the D-form through a process called racemization. The extent of racemization is measured by the ratio of D/L isomers and increases as a function of time and temperature, and can be used for geochronology or palaeothermometry. The longer racemization continues, the closer to 1 the ratio between the D- and L-forms

**Table 1.2** *Amino acid composition of proteinaceous materials (w/w %) [2,12]*

Amino acid	Egg white	Egg yolk	Casein	Animal glue (collagen)	Wool (keratin)	Silk (fibroin)	Garlic
Glycine	3.6	3.5	1.7	26.6	6.0	42.8	4.9
Alanine	6.3	5.6	2.7	10.3	3.9	33.5	6.2
Valine	8.3	6.4	7.2	2.5	5.5	3.3	5.8
Leucine	10.3	9.2	9.0	3.7	7.9	0.9	5.8
Isoleucine	6.2	5.1	6.0	1.9	3.8	1.1	3.0
Proline	4.5	4.5	13.2	14.4	6.7	0.5	3.1
Phenylalanine	5.2	3.9	5.1	2.3	3.7	1.3	4.9
Tyrosine	1.4	2.8	5.5	1.0	5.2	11.9	2.1
Serine	5.8	9.1	4.0	4.3	8.4	16.3	10.9
Threonine	3.7	5.6	2.7	2.3	6.6	1.4	—
Cystine	1.9	1.9	0.0	0.0	12.8	0.0	—
Methionine	1.2	2.3	2.3	0.9	0.6	0.0	0.8
Arginine	6.8	5.5	4.0	8.2	9.9	1.0	—
Histidine	2.4	2.4	3.6	0.7	3.0	0.4	—
Lysine	8.0	5.7	6.7	4.0	0.9	0.6	6.1
Aspartic acid	10.5	11.5	6.1	6.9	6.9	2.2	16.7
Glutamic acid	13.9	15.0	20.2	11.2	14.5	1.9	29.3
Hydroxyproline	0.0	0.0	0.0	12.8	0.0	0.0	0.3

becomes. Although it is not an absolute dating method, the extent of amino acid racemization has been used to date organic materials such as well-preserved fossils, teeth, bones, egg and mollusc shells, plants, calcium-rich soil sediments, as well as rock paintings and to evaluate the state of degradation of proteinaceous matter. The racemization of some amino acids can also be used to estimate the age of animals at the time of their death [17–20].

### 1.3 Glycerolipids

Oils and fats are mixtures of triglycerides, also known as triacylglycerols. They are basically esters of glycerol with fatty acids, and contain smaller amounts of other compounds, which include sterols and vitamins.

The physical and chemical properties of individual oils and fats are determined by the nature and proportions of fatty acids that enter into the triglycerides composition. Animal and dairy fat like plant oils are dominated by triacylglycerols, with steroids present as minor components, cholesterol and its esters being the most significant. The triacylglycerols of animal fats differ from plant oils since they contain more of the saturated fatty acids and consequently are solid at room temperature.

The fatty acid percentage composition of some fresh lipids which may be encountered in an archaeological context or in a painting is reported in Table 1.3.

Vegetable oils and dairy and animal fats were used extensively in ancient times in cookery, for lighting, and as ingredients of cosmetics, balms and medications [21–29]. Olive, almond, balanos, castor, coconut, linseed, moringa, palm, poppy, radish, safflower, and sesame oils were well known oleiferous species in the Mediterranean [21,30]. Data on

**Table 1.3** *Fatty acid percentage composition of some fresh vegetable oils and of animal lipids*

Oil	Palmitic acid (esadecanoic acid)	Stearic acid (octadecanoic acid)	Oleic acid (9-octadece- noic acid)	Linoleic acid (9,12-octa- decadienoic acid)	Linolenic acid (9,12,15- octadecatri- enoic acid)	Elaeostearic acid (9,11,13- octadecatri- enoic acid)	Ricinoleic acid (12- hydroxy-(Z)- 9-octadece- noic acid)	Gondoic acid (11- eicosenoic acid)	Erucic acid (13-docose- noic acid)
Linseed	6–8	3–6	14–24	14–19	48–60	—	—		
Walnut	3–7	0.5–3	9–30	57–76	2–16	—	—		
Poppyseed	8–12	2–3	12–17	55–65	3–8	—	—		
Olive	8–18	2–5	56–82	4–19	0.5–1	—	—		
Sunflower	5–6	4–6	17–51	38–74	—	—	—		
Castor	1–2	1–2	3–6	4–7	—	—	83–89		
Tung	3–5	2–4	8–11	12–15	0–3	75–85	—		
Palm	43–46	4–10	35–40	7–10	—	—	—	—	—
Rapeseed	2–6	1–3	20–30	17–22	6–10	—	—	13–16	20–40
Hen's egg	25–27	9–12	38–44	13–15	0–1	—	—	—	—
Lard	20–27	13–19	37–45	7–10	0–1	—	—	—	—

the use of oils are derived from papyri and from texts written by Theophrastus, Dioscorides and Pliny, which help to clarify the identification of plants cultivated for their oily seeds [30]. Lipids radically alter their original chemical composition as a consequence of degradation reactions [29,31,32]. The hydrolysis of triacylglycerols is a common process that leads to the formation of free fatty acids. Monoacylglycerols and diacylglycerols, which are produced by the partial hydrolysis of triacylglycerols, can survive in archaeological samples [32].

Unsaturated and especially polyunsaturated fatty acids in the triacylglycerol molecule are commonly subject to oxidation [33–37] via radical reactions with the inclusion of oxygen in the acyl chain, carbon-carbon bond cleavage, and the formation of lower molecular weight species. This phenomenon causes polymerization and cross-linking processes during the curing of drying oils (linseed oil, poppy seed oil, walnut oil, tung oil), highly polyunsaturated oils widely used as paint binders, varnishes and coatings. It leads to the formation of a polymeric network, generating a solid paint film.

The amount of free fatty acids increases with ageing and reflects the extent of hydrolysis of the triacylglycerols. The uptake of oxygen by double bonds leads to the formation of new oxygen containing functional groups and to the oxidative cleavage of fatty acid hydrocarbon chains. The products of the oxidation processes of lipids are generally  $\alpha,\omega$ -dicarboxylic fatty acids, hydroxycarboxylic acids and dihydroxycarboxylic acids [32,38,39]. Due to their relatively high solubility in water, which facilitates leaching once they have been buried, they are rarely detected in ancient artefacts [32].

Particular conservation conditions such as very arid environments, the absence of percolating water, and controlled storage conditions (e.g. paintings in museums) mean that relatively high amounts of hydroxyacids can be recovered along with dicarboxylic acids and dihydroxycarboxylic acids [29,39,40–42]. Aged drying oil paint films generally contain substantial amounts of dicarboxylic acids such as pimelic (1,7-heptanedioic, 7di), suberic (1,8-octanedioic, 8di), azelaic (1,9-nonanedioic, 9di) and sebacic (1,10-decane-dioic, 10di) acid, with azelaic acid being the most abundant.

The natural degradation processes of lipids can be accelerated or modified if the material is exposed to oxidizing conditions or to high temperatures, which occurs when cooking pottery, with oils used as illuminants, with drying oil prepolymerized by heating before use as paint binders, and with paint layers that are exposed to light and oxygen. Thus, the nature of degradation products depends on the composition of the original material, on the treatment of the material before or during its use, the presence of interacting species in the material, and on the environmental conditions.

It is thus quite difficult to distinguish between different degraded oils and fats on the basis of their fatty acid composition. The similarities in the composition of many vegetable oils used in ancient times and the way they might have been mixed together, means that degraded oils exhibit complex molecular patterns that usually prevent us from identifying the original botanical source.

Nevertheless, there are some vegetable oils that have a very specific composition. For example, castor oil consists of large amounts (83–89%) of 12-hydroxy-(Z)-9-octadecenoic acid (ricinoleic acid) which is not found in other natural lipids [21]. Ricinoleic acid produces a very characteristic oxidation product, 9,12-dihydroxyoctadecanoic acid [43], and both of these compounds can be considered as specific biomarkers for castor oil and have been used to assess its presence in ceramic lamps [43] and mummification balms [23].

Other oils show a very distinctive saturated fatty acid profile which in theory could be used for identification purposes in archaeological samples; for example moringa oil, which contains about 8% of long-chain saturated fatty acids (eicosanoic acid and docosanoic acid) which usually survive ageing [21,44], and coconut oil, which mainly consists of saturated triglycerides in which dodecanoic acid (lauric) and tetradecanoic acid (myristic) are the principal fatty acids [21]. All oils obtained from the seeds of Cruciferae such as rapeseed oil, turnip oil and radish oil, which were used in North Africa and in large areas of Europe and Asia [21,45], are characterised by a fatty acid profile showing some distinctive features: 5–15% (Z,Z)-9,12-octadecadienoic acid (linoleic acid), 10–30% (Z)-9-octadecenoic acid (oleic acid), 5–20% (Z)-11-eicosenoic acid (gondoic acid), 20–60% (Z)-13-docosenoic acid (erucic acid), 0.1–3% (Z)-15-tetracosenoic acid (nervonic acid), and about 4% long chain saturated fatty acids (eicosanoic acid, docosanoic acid, tetracosanoic acid) [21,46]. Mid to long chain  $\alpha,\omega$ -dicarboxylic fatty acids together with 11,12-dihydroxyeicosanoic acid and 13,14-dihydroxydocosanoic acid in ceramic vessels and oil lamps from Egypt have been reported [29,43,47]. These works demonstrated that the formation of these  $\alpha,\omega$ -dicarboxylic and dihydroxycarboxylic acids is related to the oxidation of erucic and gondoic acids, susceptible to degradation due to the presence of the double bond, so that a vegetable oil obtained from Brassicaceae seeds was identified.

A particular case is that of lipid materials as paint binders. Over the centuries, painting techniques have restricted the range of materials used to egg and drying oils [2]. The short list of possible candidates means that lipid materials in paint samples can generally be identified on the basis of their fatty acid profile. After ageing, drying oils are characterised by a higher amount of dicarboxylic acids than in egg lipids [40,41,48,49]. Moreover, steroids can survive in their original form or as degraded steroids such as cholesta-3,5-dien-7-one and 7-ketocholesterol [50–53]. Different drying oils can be distinguished on the basis of their palmitic over stearic acid (C16:0/C18:0) ratio [2,40]. This parameter is not significant in the case of mixtures of binders such as in the presence of *tempera grassa* (whole/yolk egg and drying oil) or in the presence of beeswax.

With regard to animal and dairy fats, the ratio of C16:0/C18:0 fatty acids has been used to identify animal fats and distinguish them from plant oils [21,43,54,55]. A content of C16:0 lower than that of C18:0 generally indicates an animal fat. The presence of odd numbered carbon straight chain fatty acids (C15, C17 and C19) and of significant amounts of branched chain fatty acids are considered characteristic of ruminant fats (sheep, cattle, goats, etc.) [56,57]. Ruminant fats also display a complex mixture of positional isomers of octadecenoic acid, resulting from the biohydrogenation of unsaturated dietary fatty acids in the rumen, characterised by double bonds located in various positions. This means a ruminant fat can be distinguished from non-ruminant fats (such as pig), which contain only the C18:1  $\Delta^9$  isomer [56,57].

Lipids from marine products have been studied less frequently. The detection of  $\omega$ -(*o*-alkylphenyl)alkanoic acids with 16, 18 and 20 carbon atoms together with isoprenoid fatty acids (4,8,12-trimethyltetradecanoic acid and phytanic acid) and substantial quantities of bones from fish and molluscs has provided evidence for the processing of marine animal products in vessels [58–60]. C16, C18, and C20  $\omega$ -(*o*-alkylphenyl)alkanoic acids are presumed to be formed during the heating of tri-unsaturated fatty acids (C16:3, C18:3 and C20:3), fatty acyl components of marine lipids, involving alkali isomerization, pericyclic (intermolecular Diels-Alder reaction) and aromatization reactions.

## 1.4 Natural Waxes

Natural waxes are highly heterogeneous lipid materials containing esters of long chain carboxylic acids, which are solid at room temperature and highly hydrophobic. Waxes of animal origin (beeswax, Chinese wax, lanolin, spermaceti wax), vegetable origin (carnauba, candelilla, esparto wax, Japan wax) and fossil waxes (paraffin wax, montan wax, ceresine) [2] have been used for many purposes such as sealants, surface coatings and polishes, casting and modelling materials, ingredients of balms and cosmetics, and lighting candles. Some chemical and physical features of natural waxes are reported in Table 1.4, and more details can be found in Chapter 4. In addition to natural waxes, a wide variety of synthetic waxes are used in restoration such as silicon waxes and polyethylene glycol.

### 1.4.1 Animal Waxes

Beeswax, obtained from the hives of bees, is the most commonly used natural wax for manufacturing works of art. Since prehistory, beeswax has been used as a waterproofing and sealing agent. The Egyptians used it in balms for mummies, in shipbuilding, to polish the surface of paintings, for lighting, and to make statues and writing tablets [2,61–66]. It was used by the Greeks and Romans to waterproof stone surfaces, as a protective agent and as a varnish [67]. Until the Middle Ages beeswax was used as a binder in a painting technique referred to as the encaustic technique [65,67]. Between the seventeenth and twentieth centuries the ceroplastic technique was developed for the realization of anatomical sculptures and botanical models [68].

**Table 1.4** *Chemical and physical features of natural waxes*

Wax	Melting range (°C)	Saponification number <sup>a</sup>	Iodine number <sup>b</sup>
<b>Animal</b>			
Beeswax	66–71	17–21	8–11
Chinese wax	80–83	11–15	1–2
Spermaceti	42–50	1–3	3–4
Lanolin	35–42		18–36
Ambergris	60–80	—	—
<b>Vegetable</b>			
Carnauba	82–86	4–8	12–15
Candelilla	67–79	16	14–37
Japan wax	50–60	206–237	4–13
<b>Mineral</b>			
Ceresin	54–77		7–9
Montan	76–92	23–27	10–16
Paraffin	46–68	—	—

<sup>a</sup>The saponification number is an indication of the number of acidic functionalities, and is the amount of KOH or NaOH (in mg) required to neutralize the acids in 1 g of lipid material.

<sup>b</sup>The iodine number is an indication of the degree of unsaturation of triglycerides, and is the amount of iodine (in mg) required to react with 1 g of lipid material.

The qualitative average composition of beeswax is quite constant and is made up of hydrocarbons (14%), monoesters (35%), diesters (14%), triesters (3%), hydroxymonoesters (4%), hydroxypolyesters (8%), monoacid esters (1%), acid polyesters (2%), free acids (12%) and free alcohols (1%) [2,69–73].

The aliphatic chains of beeswax compounds are mainly saturated and consequently extremely resistant to ageing. However, depending on the treatments undergone by the wax and the conservation conditions, some modifications to the original composition may occur. Since beeswax is solid at room temperature, thermal treatments were very commonly used to obtain a softened material to act as a binding medium or to be mixed with other materials. As a result, partial sublimation of the constituents can occur, leading to a change in the relative amounts of alkanes and esters [61,71,74–77]. Moreover, ambient humidity can cause a partial hydrolysis of beeswax esters, leading to the formation of free palmitic acid and long chain alcohols, which may also partially sublime, leading to changes in the acid and alcohol profiles.

Chinese wax is a white to yellowish-white, gelatinous, crystalline, water-insoluble substance obtained from the secretion of the scaled insect *Coccus ceriferus*, common in China and India. Chinese wax is used chiefly in the manufacture of polishes, sizes, and candles and is traditionally employed in Chinese medicine. It is basically made up of ceryl cerotate (esacosanoyl esacosanoate) and esacosanol [78,79].

Spermaceti wax (ambergris) is obtained from the precious oil in the head cavity of the sperm whale *Physeter macrocephalus*, and was used chiefly in balms, ointments, cosmetic creams, fine wax candles, pomades, textile finishing, and as a fuel for oil burning lamps. Nowadays, due to the current ban on whaling, authentic spermaceti wax is unavailable and the synthetic cetyl esters wax is used as a replacement for the naturally occurring material. The spermaceti wax composition includes cetyl palmitate (esadecanoyl esadecanoate), cetyl myristate, cetyl laurate, octyl stearate, octyl palmitate and cetyl alcohol [80,81]. Ambergris occurs as a biliary secretion of the intestines of the sperm whale and contains 46% cholestanol-type sterols [82].

Lanolin is a wax secreted by the sebaceous glands of sheep; it is obtained from wool and it has been used as a lubricant and as an ingredient in pharmaceutical preparations. It contains esters of long chain alkanolic acids, both linear and branched, and of hydroxyacids, cholesterol and lanosterol [2,83].

#### 1.4.2 Plant Waxes

These waxes are biosynthesized from plants and mainly contain esters made from long chain alcohols ( $C_{22}$ – $C_{34}$ ) and fatty acids with even carbon numbers.

Carnauba wax is obtained from the leaves of several species of palm trees in South America, such as *Copernicia cerifera* which grows in Brazil. It is made up of esters of long chain alcohols and acids with high carbon number, high molecular weight polyesters of hydroxyacids, and derivatives of *p*-hydroxy- and *p*-methoxycinnamic acid [84].

Ouricuri wax is an exudate on the underside of the leaves of the *Syagrus coronata* palm in northeastern Brazil and has similar properties and composition to Carnauba wax. Ouricuri wax is used in the manufacture of carbon paper, mould release agents and inks.

Candelilla wax is extracted from *Euphorbia cerifera* and *Euphorbia antisiphilitica*, which grow mainly in Mexico. The wax is collected from the root surface where the wax



acts as a protective coating. It is a dark yellow, hard and fragile solid, and it has been used to harden other waxes such as beeswax. Candelilla wax is used as a polishing material and in the manufacture of candles and sealing paper. Its main constituents are hydrocarbons (about 50%, between C<sub>29</sub> and C<sub>33</sub>), esters (28–29%), alcohols, free fatty acids (7–9%) and triterpenoid esters (12–14%). Entriacontane and miricylic alcohol [ $\text{CH}_3(\text{CH}_2)_{28}\text{CH}_2\text{OH}$ ] are the most abundant and characteristic compounds.

Many other plant waxes have also been exploited for various uses, including esparto wax, from esparto grass *Stipa tenacissima*, and Japan wax, from plants of the *Rhus* species.

### 1.4.3 Fossil Waxes

Ceresine is the white end-product of the purification of the fossil wax ozokerite, which is found in Miocene lignite deposits at considerable depths, by the separation of foreign and resinous matter and decolorisation by active agents. It is harder than paraffin wax, and has linear and cyclic hydrocarbons with high molecular weight [2]. It is used for waterproofing and oil absorption.

Paraffin waxes are also considered of mineral origin and are obtained from petroleum. The petroleum is distilled and the white colour of the wax is obtained by acid washing and purification. It has a typical melting point between about 47 °C and 64 °C. Its uses include candle making, casting and as a solidifier/stabilizer. The wax is composed of C<sub>20</sub>–C<sub>36</sub> n-alkanes (40–90%), isoalkanes and cycloalkanes.

Montan wax is obtained by solvent extraction of certain types of lignite or brown coal. It has a dark colour when not treated, but it is lighter when refined. Its chemical composition includes esters of C<sub>22</sub>–C<sub>32</sub> acids (53%), free acids (17%), free alcohols (1–2%), ketones (3–6%) and terpenoids (20–23%) [85].

Microcrystalline wax is found worldwide as a constituent of crude oil. It is removed by solvent extraction and distillation. The colour varies, depending on grade, from white to brown–black. It has many uses, including waterproofing paper and textiles, and as a sealant. This wax consists of a mixture of long chain (C<sub>41</sub>–C<sub>57</sub>) unsaturated hydrocarbons with an average molecular weight of 500–800.

## 1.5 Natural Resins

Plant resins are lipid-soluble mixtures of volatile and nonvolatile terpenoid and/or phenolic secondary compounds that are usually secreted in specialized structures located either internally or on the surface of the plant. Although terpenoid resins constitute the majority of the resins produced and used, some other important resins are phenolic. Phenolic resin components, which occur on the surfaces of plant organs, have been used particularly in medicines [86].

Natural terpenoid resins and resinous materials played a prominent role in ancient times – their intrinsic properties meant that they were used as adhesives, hydro-repellents, and coating and sealing agents [87–92]. They produced incense when burnt [92] and due to their antitoxic and antioxidant properties, they were also added to wine. In ancient Egypt, vegetable resins along with other natural organic compounds such as waxes, gums, oils and bitumen, were used to prepare mummification balms [23,88,93–97]. Resins and wood



from birch, pine and firs were used to produce tar and pitch in various regions of Europe and the Mediterranean.

Natural resins are substances with a high viscosity, semisolids or solid and insoluble in water. They are formed in the so-called 'resiniferous canals' of several trees. Many varieties of plants spontaneously exude resins as a product of their metabolism, to protect themselves against excessive loss of water and attack from micro-organisms.

From a chemical point of view, vegetable resins are a complex mixture of mono-, sesqui-, di- and triterpenes, which have, respectively, 10, 15, 20 and 30 carbon atoms per molecule. The mono- and sesquiterpenes are both present in most resins. The di- and triterpenes are rarely found together in the same resin, which means that terpenic resins can be divided into two main classes. Table 1.5 lists the botanical origin and the kind of terpenoid compounds of some natural resins.

Mono- and sesquiterpenoids are of limited use for the identification and classification of aged resins. Due to their volatility, they are rarely found in ancient samples except when they have been conserved in very particular conditions [88,98]. On the other hand, the di- and triterpenoids enable us to identify resins thereby identifying their botanical origin [2,99]. Figures 1.1 and 1.2 show the main diterpenoid and triterpenoid structures.

**Table 1.5** Botanical origin and chemical composition of terpenic resins

Class	Family	Genus (type of resin)	Composition
Coniferales	Pinaceae	<i>Pinus</i> (pine resin, colophony)	Abietadienic acids, pimaradienic acids
		<i>Abies</i> (Strasbourg turpentine)	Abietadienic acids, pimaradienic acids, <i>cis</i> -abienol
		<i>Larix</i> (Venice turpentine)	Abietadienic acids, pimaradienic acids, epimanol, larixol, larixyl acetate
	Cupressaceae	<i>Juniper</i> , <i>Cupressus</i> , <i>Tetraclinis articulata</i> (sandarac)	Pimaradienic acids (sandaracopimaric acid), communic acid, totarol
Guttiferales	Dipterocarpaceae	<i>Hopea</i> (dammar)	Dammaranes (hydroxydammaranone, dammaradienol), ursanes (ursonic acid, ursonaldehyde)
Terebinthales	Anacardiaceae	<i>Pistacia</i> (mastic)	Euphanes (masticadienonic acid, isomasticadienonic acid), oleanananes (oleanonic acid, moronic acid), dammaranes
	Burseraceae	<i>Commiphora</i> (myrrh)	$\alpha$ - and $\beta$ -amyrrin, euphanes, oleananes
		<i>Boswellia</i> (olibanum or frankincense) <i>Canarium</i> (elemi)	

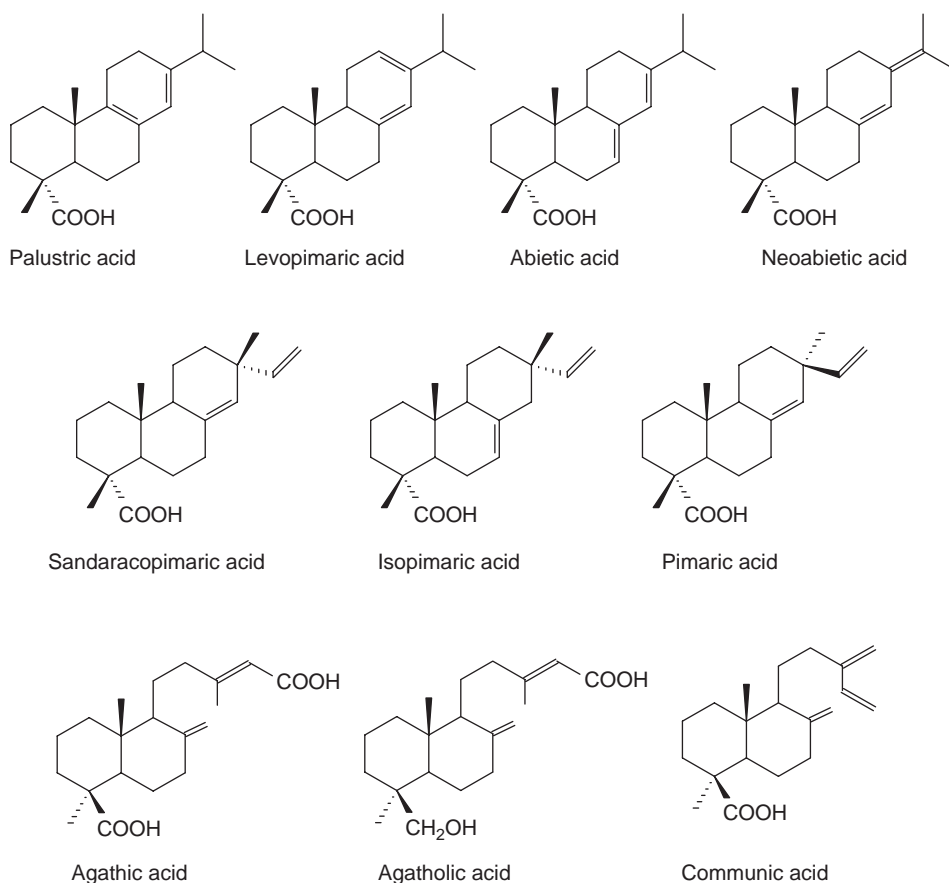


**Figure 1.1** Characteristic diterpenoid compounds of Pinaceae and Cupressaceae resins

Diterpenoid and triterpenoids in natural resins generally lead to one, two or three oxygen atoms in the form of acidic, carboxylic or alcoholic functionality and a variable degree of unsaturation.

### 1.5.1 Diterpenoid Resins

The plants that exude diterpenoid resins belong to the order of conifers. Pine resins (from the *Pinus* genus), Strasburg turpentine (from the *Abies* genus), Venice turpentine (from *Larix decidua*) were extracted from Pinaceae. Sandarac, juniper and cypress resins were extracted from trees of the Cupressaceae family: *Tetraclinis articulata*, *Juniperus* spp. and *Cupressus sempervirens*, respectively. Moreover, labdanum resin from the Cistaceae family (*Cistus* spp.) also belongs to the diterpenoid resins.

Pine resin, namely rosin or colophony, is one of the most widespread diterpenoid resins and has been used for waterproofing, for treating wood and paper, as varnish, as incense and as an ingredient in scented ointments. The main compounds present in fresh Pinaceae resins

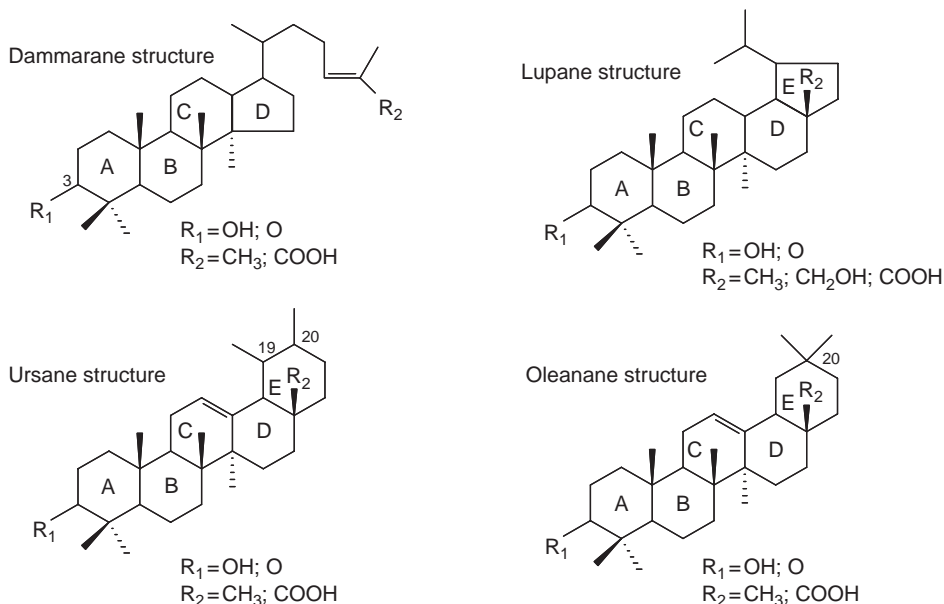


**Figure 1.2** General molecular formulae of triterpenes present in triterpenoid resins

are diterpenoid acids with either abietane or pimarane type skeletons (see Figure 1.1). Both kinds of acids are tricyclic: the abietadienic acids contain a conjugated double bond, whereas pimaradienic acids lack this conjugation, since a quaternary carbon separates the two double bonds. The absence of the conjugated double bond makes them more stable to oxidation processes than abietadienes [31]. Conifer resins, such as those of the pine family (Pinaceae), are characterised by a large volatile fraction (20–50%) with monoterpenes predominating over sesquiterpenes. Both classes most commonly occur as hydrocarbons with a few oxidized forms, often as trace components. Under natural conditions, monoterpenes volatilize with varying rapidity, providing, for example, the fragrant aromas in conifer forests during warm weather [86].

However, in many archaeological samples pimarane diterpenoids are often absent, and of the abietane compounds only dehydroabietic acid remains. In fact, dehydroabietic acid is present as a minor component in the fresh resins, but its abundance increases on ageing at the expense of the abietadienic acids since the latter undergo oxidative dehydrogenation to the more stable aromatic triene, dehydroabietic acid [2,18]. If oxygen is available, dehydroabietic acid can be oxidized to 7-oxodehydroabietic acid and 15-hydroxy-7-oxodehydroabietic acid. Since these diterpenoid compounds are often the dominant components in archaeological samples [95,97], they are considered characteristic for the presence of Pinaceae resins.

Of the Cupressaceae family, sandarac (from *Tetraclinis articulata*) has frequently been used as a paint varnish. It contains labdane compounds that account for the polymeric fraction of the resin (about 70%) [31]. The main monomeric diterpenoid present is sandaracopimaric acid, together with smaller amounts of 12-acetoxysandaracopimaric acid. Phenols, including totarol, are also present [31].

Labdanum resin (from the Cistaceae family) contains diterpenoid compounds with a labdane-type structure, namely laurifolic, cistenolic and labdanolic acids [100–103].

### 1.5.2 Triterpenoid Resins

Triterpenoid resins include gum resins from the Burseraceae family including myrrh and frankincense, and mastic resins (from *Pistacia* genus) [88]. Triterpenoid resins consist of mixtures of triterpenoid molecules with mainly pentacyclic and tetracyclic skeletons (see Figure 1.2). Tetracyclic triterpenes include dammarane and lanostane structures, characterised by the presence of a hydroxy or a keto group at position 3 and of a lateral chain bearing a double bond. Further possible functional groups are also usually present. Lanostane type molecules can be distinguished from dammarane molecules by the presence of a second double bond at position 7 or 8. Pentacyclic triterpenes can be divided into four main groups: ursane, oleanane, lupane and hopane. Ursane and oleanane triterpenes differ only in the position of one methyl group. The ursane type molecules bear one methyl group at position 20 and the other at position 19, while the oleanane ones bear the two methyl groups at position 20. The triterpenes with lupane and hopane skeletons have four six-membered rings and one five-membered ring (E) (Figure 1.2).

Frankincense, also known as olibanum, is obtained from trees belonging to the genus *Boswellia* (Burseraceae family). It is one of the best-known ancient plant resins. The ancient Egyptians were the first to use it as incense in embalming practices and in the preparation of medicines, cosmetics and perfumes, and today it is still used therapeutically. It contains pentacyclic triterpenoids belonging to oleanane, ursane or lupane type molecules and in particular of  $\alpha$ - and  $\beta$ -boswellic acids, and their *O*-acetates [104–111]. 11-Oxo- $\beta$ -boswellic acid and its acetyl derivative, identified in several *Boswellia* species, are also diagnostic for frankincense [112].

The survival of  $\alpha$ -boswellic acid,  $\beta$ -boswellic acid and their *O*-acetates, which have been isolated only from frankincense, has been demonstrated in archaeological samples [99,107,113]. These compounds are considered as very useful specific chemical markers for the identification of frankincense in resinous archaeological materials.

Mastic resin is derived from the genus *Pistacia* (Anacardiaceae family, four Mediterranean species: *P. atlantica*, *P. khinjuk*, *P. lentiscus* and *P. terebinthus*) and has been used as incense, as an adhesive and as varnish. Together with dammar resin and sandarac, it is one of the most commonly encountered resins in the formulation of varnishes for easel paintings. For this use, mastic was often applied in a mixture with linseed oil, giving an oleoresins varnish which suffered from yellowing and craquelures.

Mastic resins have many components in common with dammar and elemi. The main neutral triterpenoids are nor- $\alpha$ -amyrone, 28-norolean-17-en-3-one, hydroxydammarenone, oleanonic aldehyde together with triterpenoid acids (oleanonic, moronic, isomasticadienonic and masticadienonic) [92,114–122]. Unlike dammar resin, it does not contain ursanes, and contains a relatively higher amount of oleanic species.

Moronic, isomasticadienonic and masticadienonic acids are considered as characteristic and diagnostic molecules for assessing the presence of mastic resin in ancient samples [2,88,94,123,124].

It is also well known that during ageing, new compounds are formed by oxidation reactions. In fact, the presence of 20,24-epoxy-25-hydroxy-dammaren-3-one and 3-oxo-trisnor-

dammarano-20,24-lactone has been highlighted in several aged samples [125–127]. The first compound is produced via the cyclization of the lateral chain of the hydroxydammarenone, which then leads to the formation of a tetrahydrofuranic ring. The second is formed from 20,24-epoxy-25-hydroxy-dammarene-3-one by further oxidation reactions involving the formation of a lactone derivative.

In archaeological findings the occurrence of a high abundance of 28-norolean-17-en-3-one has been correlated to smouldering or burning processes undergone by *Pistacia* resins [94,123,124]. Mastic also contains a polymeric fraction (15–20%) identified as *cis*-1,4-poly- $\beta$ -myrcene [128].

Dammar resin was introduced into Europe in the nineteenth century, mainly as a paint varnish. It is still used today since it has good optical properties and low acidity. It is derived from various species (the genus *Hopea* and *Shorea* of the Dipterocarpaceae family). It is characterised by tetracyclic triterpenoids of the dammarane series and contains minor amounts of pentacyclic triterpenoids of the series of oleanane, ursane and hopane. It also contains a polymeric fraction named polycadinene or  $\beta$ -resene. Dammar resin triterpenoids undergo oxidation with ageing, as described for the components of mastic resin.

### 1.5.3 Phenolic Resins

Phenolic resins are mainly composed of aromatic esters: benzoe and storax were the most common in the Mediterranean [86].

Benzoe resin (also known as benzoin) comes from *Styrax* spp. (Styraceae family). In the *Styrax* genus the only species that occurs in the Mediterranean is *Styrax officinalis*, so this was probably the source of the resin in ancient times in that area. Benzoe mainly contains free cinnamic and benzoic acids, and their corresponding esters with cinnamyl, *p*-coumaryl and coniferyl alcohols. The amounts of these compounds are quite variable and depend on which species the resin was obtained from [129].

Storax resin is extracted from *Liquidambar orientalis* (Hamamelidiaceae) and *Altingia* and its major components are cinnamyl cinnamate and 3-phenylpropanyl cinnamate, with significant amounts of benzoic and cinnamic acids, and 3-phenylpropanol and cinnamyl alcohols [130,131]. The volatile content is very low and triterpenes (oleanonic and 3-epioleanolic acids and liquid ambronic acid) have also been observed [130,132].

### 1.5.4 Animal Resin

The resin of animal origin most used in the field of cultural heritage is shellac. It is a natural resin produced from the glandular secretion of an Indian scaled insect (*Laccifer lacca* Kerr, also known as *Kerria lacca*), which infests branches of numerous trees from the East Indies [133]. It began to be used in Europe towards the end of the sixteenth century [85] mainly as a varnish, known as 'French polish', for wooden objects, musical instruments, gildings, paintings, as an insulating material and as an adhesive in the restoration of pottery.

Shellac is a complex mixture made of mono- and polyesters of hydroxy-aliphatic and sesquiterpene acids, which can be separated into two fractions: the soft resin, soluble in ether, mainly consisting of monoesters [134], constituting about 30% of the total resin; and the hard resin, ether insoluble, which has quite a complex polyester composition, and

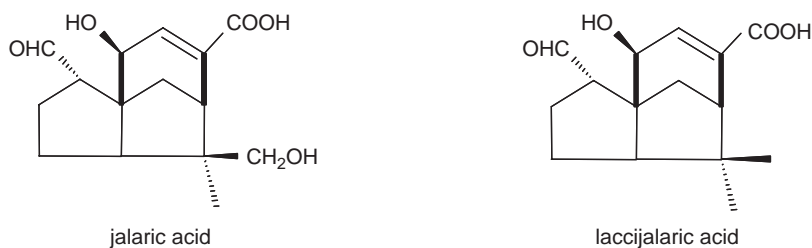


**Figure 1.3** Structures of the main sesquiterpenoid shellac compounds

accounts for the other 70% [135]. The main ester components of shellac are jalaric and laccijalaric acids (Figure 1.3), 9,10,16-trihydroxyhexadecanoic (aleuritic acid) and 6-hydroxytetradecanoic acids (butolic acid) [136–140].

### 1.5.5 Fossil Resins

Resins older than 40 000 years are considered to be fossil resins. The fossilization of resins begins with polymerisation and forms ambers and copals. Most of the ambers are derived from components of diterpenoid resins with a labdanoid structure; other ambers are based on polymers of sesquiterpene hydrocarbons such as cadinene, and may include triterpenoids; less common ambers from phenolic resins derive from polymers of styrene. Figure 1.4 shows the skeletal structures of the components which make up the polymers occurring in fossil resins [141].

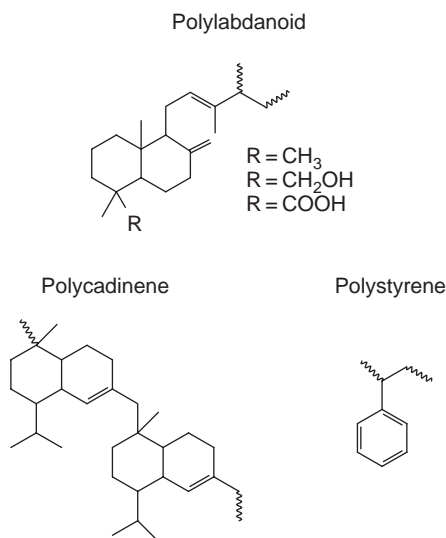


**Figure 1.4** Main structures of polymeric fossil resins

Amber deriving from the extinct species *Pinus succinifera* is known as Baltic amber or succinite and consists of dimers of abietic acids and copolymers of communol and communic acid. Amber is less soluble than the other resins, but partially soluble in hot oil, so it has been used as an ingredient in varnish.

Copals, sometimes referred to as immature amber, originate from Africa, Asia or central American countries and derive from the Araucariaceae and Leguminosae families. Polymerised communic acid and agathic acid are found as the main compounds in these fossil resins. The extreme hardness of copal results from polymers of resin acids such as ozoic acid, an enantiomer of communic acid that can polymerize and thus enable fossilization [86]. They are still commonly used today for varnishing and protecting wood.

### 1.5.6 Pitch and Tar

Natural resins and resinous wood were not only used in their natural form but were often subjected to hard-heating treatments and to distillation-type processes. This led to denser and stickier materials, referred to as tar or pitch [87,88].

Resins and wood from birch, pine and fir were used to produce tar and pitch in various regions of Europe and the Mediterranean [87–92,142–148], both for the production of adhesives and of hydro-repellents and coatings.

In Roman times tar and pitch from Pinaceae resinous wood were used to treat the inner surface of amphorae to store fluids such as wine [145,149] and to seal ship planks [89,144].

Heating treatments applied to natural resins and resinous wood profoundly modify the chemical composition of the original material. Diterpenoid compounds undergo aromatization, demethylation and decarboxylation reactions, with the formation of new compounds of a lower molecular weight that show a high degree of aromatisation [87,88]. In tar and pitch produced from Pinaceae resin and woods, retene is considered as a stable end product of these reaction pathways and nor-abietatrienes, simonellite and tetrahydrotene represent the intermediates of these reactions [87,89,150].

Birch bark was also used to produce pitch and tar. The pitch from Betulaceae bark has been found on arrowheads and flint tools from prehistoric ages and the pitch was probably a residue of the original adhesive [92,151,152]. Birch-bark pitch has also been identified in ceramic artefacts as an adhesive to coat, seal, or repair the inner surfaces of the vessels [90].

Betulin and lupeol, together with low amounts of lupenone, betulone and betulinic acid, are characteristic of birch bark [87,153–157]. All these compounds are pentacyclic triterpenoids with a lupane skeleton. In addition to triterpenoids, birch bark contains high amounts of a lipid material, called suberin [158].

## 1.6 Asphalt and Bitumen

Bitumen, asphalt, and other fossil organic materials such as coal, lignite and peat are found as natural deposits and have practically always been used in arts and handicrafts. Bitumen and asphalt were used in medicines and cosmetics, as pigments, as adhesives and in mummification balms in ancient Egypt [2,159,160].

These materials are chemically very complex and the composition of fossil organic matter depends on the kind of organism from which the deposit has formed [2].

Bitumen contains a solvent-soluble fraction referred to as maltenes, and an insoluble fraction called asphaltenes. The word bitumen is in some cases also used to indicate the residue of the distillation of petroleum.

Asphalt and bitumen contain isoprenoid compounds that derive from phytosterols, triterpenoids, and diterpenoids, which have defunctionalized and fragmented with a consequent loss of side chains. They mainly contain saturated compounds such as hopanes and steranes, but also small amounts of unsaturated and aromatized compounds. Bitumen generally contains a complete range of homologous series of n-alkanes, and the isoprenes pristane and phytane. The hopanes are biomarker compounds which can be related to their original biogenic precursors. Their ubiquity in sedimentary organic matter indicates that they are formed by the bacterial transformation of biological remains [2]. The identification, origin, uses and trade of bitumen has been widely described [161,162].

## 1.7 Polysaccharide Materials

Polysaccharides are polymers made up of many monosaccharides joined together by glycoside bonds, and include cellulose, starch, vegetable mucilage and plant gums.

Cellulose is a high molecular weight polymer of D-glucose with  $\beta(1-4)$ -glycosidic bonds, found in plant fibres; it is the major component of most plant tissues. Starch is another common polysaccharide, containing two polymers of glucose, amylose and amylopectin. It was used in some paint preparations and in the production of paper. Acid treatment of starch produces dextrans, which are used as adhesives and additives in water colour paintings.

Plant gums are naturally occurring polysaccharide exudates from several species of plants or extracted from the endosperm of some seeds. The polymers consist of aldopentoses, aldohexoses and uronic acids joined together by glycosidic bonds. Since ancient times, several plant gums have widely been used as paint media and sizing agents. The gums traditionally employed were Arabic gum (exuded by *Acacia senegal* and *Acacia seyal*), tragacanth gum (exuded by *Astragalus*) and fruit tree gum (obtained mainly from cherry, apricot, peach and plum trees). Locust bean, extracted from the kernels of the carob tree (*Ceratonia siliqua*), guar (from *Cyanopsis tetragonolobus*, Leguminosae), ghatti (from *Anogeissus latifolia*, Combretaceae) and karaya gum (from *Sterculia urens*, Sterculiaceae) were important materials mainly used in the Indian subcontinent. Natural gums present variable distributions in mean molecular mass of polymeric molecules, whereas the composition of the constituent sugar percentages remains reasonably constant and depends on the specie of the plant. The composition of monosaccharide differs from gum to gum and can thus be exploited for their identification [163,164]. Fucose, for example, is considered a marker for the recognition of tragacanth gum, since this sugar is absent in the other gums. Table 1.6 gives the saccharide composition of the most widespread gums.



**Table 1.6** *Percentage composition of plant gums and honey*

	Xylose	Arabinose	Ramnhose	Fucose	Galacturonic acid	Glucuronic acid	Glucose	Mannose	Galactose	Fructose
Arabic	—	37	11	—	—	7	—	—	45	—
Fruit tree	6	35	3	—	—	13	—	5	37	—
Locust bean	—	1	—	—	—	—	—	81	17	—
Karaya	—	—	25	—	7	4	—	—	64	—
Tragacanth	15	35	3	7	14	4	11	—	10	—
Guar	—	2	—	—	—	—	—	63	34	—
Ghatti	—	47	3	—	—	11	—	2	36	—
Honey	—	—	—	—	—	—	40	—	—	49

Gums are hydrophilic materials that easily undergo chemical hydrolysis with depolymerization, oxidation and microbiological attack. Leaching is a well-known phenomenon, and the inversion between arabinose and xylose content has been reported [164,165].

## 1.8 Organic Dyes

Natural organic colouring materials have been widely used to dye textiles and as pigments in paintings [165–168]. Investigation into natural colourants of historic importance mean that we gain a clearer idea of how the use and trade of pigments, dyestuff, dyed artefacts, and of dyeing technologies, differed from one geographical area to another. In the nineteenth century synthetic dyes began to replace natural ones, starting with the production of mauvein in 1856.

Organic dyes are fixed to the support by dispersion in a binder or by direct adsorption. Many organic dyes are used after precipitation with metal salts or metal hydroxides (mordants) as alum  $K_2(SO_4)_2$ ,  $Al_2(SO_4)_3 \cdot 24H_2O$  or potassium tartrate.

The chromophores contained in natural dyes are mainly flavonoids, anthrachinoids, indigoids and gallotannins. Other molecular types include carotenoids, benzochinons and anthocyanidins.

The most commonly used yellow dyes contain flavonoids (flavones and flavonols) and occur in plants as sugar derivatives. Weld (*Reseda luteola* L.), young fustic (*Cotinus coggyria* Scop.), dyer's broom (*Genista tinctoria* L.), sawwort (*Serratula tinctoria* L.), the berries of some species of rhamnus, old fustic (*Chlorophora tinctoria* L.), and quercitron bark (*Quercus velutina* L.) are the most common vegetable materials from which yellow dyes are extracted. After hydrolysis in the dye-bath to the parent aglycone, flavonoids bind to the fibre through a metal complex with the mordant via the carbonyl group and the adjacent phenolic group. Since many plants are rich in flavonoids, no individual source of yellow dye has become predominant – as did, for example, the red dyes madder and cochineal – and many different and local sources were in use at the same time.

All dyes are prone to fading caused mainly by chemical oxidation when exposed to light. The formation of low molecular mass products has been evidenced, such as 2,4-dihydroxybenzoic acid and 2,4,6-trihydroxybenzoic acid from morin degradation, in old fustic dyed samples [169] and from luteolin in weld and dyer's broom [170].

Debromination with ageing has been observed in the indigoid components of purple [171,172], and photochemical breakdown patterns of the three anthocyanidins contained in *Arrabidaea chica* red dye, produced by Andean Indian cultures in the tenth to fifteenth centuries, have been hypothesized [173]. Although identifying dye sources in ancient artefacts is quite difficult, it is helped considerably by understanding the fading and degradation mechanisms.

Table 1.7 lists the most widely used natural dyeing materials and their chemical composition.

**Table 1.7** Common natural dyeing materials and their chemical composition

Common name	Botanic name	Main chromophores					
<b>Anthraquinoid dyes</b>		Carminic acid	Kermesic acid	Flavokermesic acid	dc II	Laccaic acid A	Laccaic acid B
Cochineal	<i>Kermes vermilio</i>	—	+	+	—	—	—
	<i>Porphyrophora polonica</i>	+	+	+	+	—	—
	<i>Porphyrophora hameli</i>	+	+	+	+	—	—
	<i>Dactylopius coccus</i> Costa	+	+	+	—	—	—
	<i>Kerria lacca</i> Kerr	—	+	+	—	+	+
Madder	<i>Rubia tinctorum</i>	Alizarin	Purpurin	Xanthopurpurin	Munjistin	Pseudopurpurin	Other compounds
	<i>Rubia peregrina</i>	+	+	+	+	+	—
	<i>Rubia cordifolia</i>	—	+	—	—	+	—
	<i>Rubia akane</i> Nakai	+	+	+	+	+	Morin
	<i>Rubia akane</i> Nakai	—	+	—	—	+	—
Lady's bedstraw	<i>Galium verum</i> L.	+	+	+	—	+	—
	<i>Galium mollugo</i> L.	+	+	+	+	+	Rubiadin
Relbunium	<i>Relbunium</i>	—	+	+	+	+	—
	<i>hypocarpium</i> L.						
Morinda	<i>Morinda citrifolia</i> L.	—/+	—	—	—	—	Morin
<b>Indigoid dyes</b>							
		Indigotin	Indirubin	Monobromoindigotin	Dibromoindigotin	Dibromoindirubin	Other compounds
Woad	<i>Isatis tinctoria</i>	+	—	—	—	—	Quercetin, Kaempferol
Indigo	Various <i>Indigofera</i> species	+	+	—	—	—	Kaempferol

(continued overleaf)

**Table 1.7** (continued)

Common name	Botanic name	Main chromophores						
Indigo carmine	<i>Indigofera tinctoria</i>	—	—	—	—	—	—	Indigocarmine
Purple	<i>Muricidae</i> and <i>Rapaninae</i>	+	—	+	+	+	+	—
Orchil	<i>Rocella</i> and <i>Ochrolechia</i>	—	—	—	—	—	—	Orcein
<b>Flavonoid dyes</b>								
		Fisetin	Morin	Maclurin	Kaempferol	Quercetin		Other Compounds
Young fustic	<i>Cotinus coggyria</i> Scop.	+	—	—	—	—		Fustin, Sulfuretin
Old fustic	<i>Clorophora tinctoria</i> L.	—	+	+	+	—		—
Quercitron bark	<i>Quercus velutina</i> L.	—	—	—	—	+		Quercitrin
Persian berries	Rhamnus family	—	—	—	+	+		Rhamnetin
		Luteolin	Apigenin	Genistein	3-Methylquercetin			
Weld	<i>Reseda luteola</i> L.	+	+	—	—			
Dyer's broom	<i>Genista tinctoria</i> L.	+	—	+	—			
Rhamnus bark	<i>Rhamnus frangula</i> (cortex)	—	—	—	—			Glucofrangulin A and B, Franguline, Emodin
Sawwort	<i>Serratula tinctoria</i> L.	+	—	—	+			

Brazilwood	<i>Caesalpinia</i> species	Brazilin	Brazilein	Hematoxylin	Hematein
Logwood	<i>Hematoxylum campechianum</i>	+	+	+	+
		—	—	+	+

#### Tannin based dyes

Black alder	<i>Alnus glutinosa</i>	Gallic acid, quercetin, emodin
Sumac	<i>Rhus</i> genus	Gallic acid, ellagic acid, quercitrin, kaempferol
Black walnut	<i>Juglans nigra</i> , <i>Juglans regia</i> L., <i>Juglans cinerea</i> L.	Juglon
Walnut galls	Galls from <i>Cynips</i> species, <i>Quercus infectoria</i> Oliv.	Tannins
Silver birch	<i>Betula pendula</i> , <i>B. pubescens</i> , <i>B. nana</i> , <i>B. alleghaniensis</i> , <i>B. populifolia</i> , <i>B. papyrifera</i> , <i>B. lenta</i>	Tannins

#### Other dyes

Henna	<i>Lawsonia inermis</i>	Lawson
Sandalwood	<i>Pterocarpus santalinus</i>	Santalin A, Santalin B
Safflower	<i>Carthamus tinctorius</i> L.	Carthamina, Safflower Yellow A and B
Annatto	<i>Bixa orellana</i> L.	Bixin
Barberry	<i>Berberis vulgaris</i> L.	Berberin
Saffron	<i>Crocus sativus</i> L.	Crocin, crocetin
Turmeric	<i>Curcuma longa</i>	Curcumin, demethoxycurcumin, bisdemethoxycurcumin

---

## 1.9 Synthetic Polymers

Since the earliest production of synthetic materials in the mid nineteenth century, artists and restorers have explored their possibilities. After 1900 many artists became familiar with the new and modern materials such as cellulose nitrate and cellulose acetate. Thus modern artists replaced the traditional moulding in wax, casting in gypsum and expensive bronze with the newly available materials. The use of plastic in art objects occurred gradually: 1915 saw the first use of celluloid in sculptures, and after 1943 Plexiglas or Perspex [poly(methyl methacrylate), PMMA] was employed on account of its good resistance to ageing. In paintings, in addition to traditional materials such as drying oils and proteinaceous tempera, a range of synthetic polymers have been experimented with poly(vinyl acetate)s, alkyd resins and acrylic resins as the materials most used in the twentieth century [2,174,175].

Nearly all the polymers that industry has made available have been used in art or conservation [176]. Synthetic resins have been used as solidifiers, varnishes, coatings, paint binders, moulding and casting materials, clothing, jewellery, furniture and as materials for the display, support and storage of art objects.

The range of possible materials is very wide and depending on the function required they can be applied in many ways, for example:

- polymer solutions in a solvent, followed by evaporation of the solvent;
- emulsions or dispersions, usually in water;
- liquid pre-polymers which by chemical reaction form a polymer;
- liquid adhesives which remain as liquids;
- molten liquids which cool and form a solid.

As yet we are not fully aware of the chemical and physical behaviour of modern synthetic materials so this makes it difficult to characterise and conserve them. This is particularly true with regard to interactions with the components in art objects, interactions with additives (e.g. fillers, plasticizers, colourants), and changes in their properties during ageing. Since synthetic polymers are commercial products, the materials used in the past may significantly differ from modern materials of nominally the same composition, thus hampering characterisation and comparisons. Various types of degradation in plastics have been reported, the most commonly known being discoloration, deformation, embrittlement, cracking and crumbling, which are caused by moisture, heat and light.

Table 1.8 lists some synthetic materials and their use in art.

Synthetic coatings and varnishes, which are transparent and give colourless protective films, have for the most part replaced traditional natural paint varnishes (dammar resin, mastic resin, copals or colophony). The modern polymers used for this purpose include ketonic resins, acrylic and metacrylic resins, which have been employed due to their good refraction index, resistance to yellowing, and high transition temperature. Low glass transition temperatures lead, with time, to the inglobation of particulate in the coating layer, with a loss of transparency and gloss. One of the most widely used acrylic polymers is Paraloid B72, an ethyl-methyl methacrylate copolymer, which shows low tendency to reticulation with ageing and in fact remains quite soluble.

**Table 1.8** *Some synthetic materials and their use in art*

Material	Year of production	Main use	Added plasticizer	Notes
Cellulose nitrate (Celluloid)	1850	Moulding material, paints, glues, coatings, photographic films, varnishes	Camphor, phthalate esters	High flammability and degradability, with production of nitrogen dioxide
Cellulose acetate	1910	Moulding and extruding materials, fibres, photographic films		Degrades with hydrolysis of the acetate group and production of free acetic acid
Phenol-formaldehyde resin (Bakelite)	1906–1909	Enamels, moulding materials, jewellery, paints, consolidants	Wood flour	
Polyamides (nylons)	1934	Fibres, textiles, paint fixatives (Calaton)		No longer used as fixative due to the inclusion of dust
Vinyl polymers [polystyrene, PVC, polyethylene, polypropylene, poly(vinyl acetate), poly(vinyl alcohol), polyacrylonitrile]	~1920	Packaging, tubing, household goods, records, carpets, toys, water-based paint, adhesives, varnishes	Phthalate esters, poly(vinyl alcohol)	
Acrylic resins (Perspex, PMMA, Paraloid)	~1930	Varnishes, adhesives, glazing, sculptures, paint media		Sensitivity to sunlight. Methacrylates are subjected to bond cleavage. Acrylates undergo cross-linking reactions
Alkyd resins		Paints, varnishes	Drying oils	Very low solubility: the product becomes irremovable with ageing
Polyurethanes	1937	Foams, fibres, adhesives, coatings, sculptures, decorations		Tendency to yellowing, depolymerisation. Toxicity of isocyanates
Poly(ethylene glycol)s		Consolidants		Water soluble
Ketonic resins (Laropal K 80®, MS2A)	~1930	Varnishes	Seed oils	Quite stable with ageing with a low tendency to yellowing
Epoxy resins	1936	Adhesives, especially for glass repair		Resistant to acid, alkali and organic solvents. Tendency to yellowing with ageing

At the same time, natural adhesives such as casein glues, animal glue and polysaccharide gums have gradually been replaced by synthetic adhesives: vinyl thermoplastic adhesives [poly(vinyl acetate)], adhesives obtained by reticulation *in situ* of two components (as epoxy resins), represent very important materials in this field.

Thermoplastic synthetic resins as consolidants in restoration are now common. For example, poly(ethylene glycol)s with various molecular weights have been used to consolidate archaeological imbibed wood [177]. Normally materials that maintain a degree of solubility over time are preferred. In theory they can be removed, thus guaranteeing a certain reversibility of the intervention. These include vinyl resins and acrylic resins. Of the vinyl polymers, poly(vinyl acetate) shows good stability towards ageing and photooxidation. However with ageing it undergoes reticulation, and it consequently loses solubility and is difficult to remove. The commercial acrylic products that have found major application as consolidants are Paraloid B72 and Plexisol, which are characterised by less polarity and consequently by a better solubility in non-aggressive solvents.

## References

1. T.E. Creighton, *Proteins: Structures and Molecular Properties*, W.H. Freeman, New York, 1993.
2. J.S. Mills, R. White, *The Organic Chemistry of Museum Objects*, Butterworth Heinemann, Oxford, 1994.
3. M.P. Colombini, F. Modugno, Characterisation of proteinaceous binders in artistic paintings by chromatographic techniques, *Journal of Separation Science*, **27**, 147–160 (2004).
4. R. White, The characterisation of proteinaceous binders in art objects, *National Gallery Technical Bulletin*, **8**, 5–14 (1984).
5. S. Keck, T. Peters, Identification of protein-containing paint media by quantitative amino acid analysis, *Studies in Conservation*, **14**, 75–82 (1969).
6. M.R. Shilling, H.P. Khanjian, L.A.C. Souza, Gas chromatographic analysis of amino acids as ethyl chloroformate derivatives. Part 1: compositions of proteins associated with art objects and monuments, *Journal of American Institute for Conservation*, **35**, 45–59 (1996).
7. A. Andreotti, I. Bonaduce, M.P. Colombini, G. Gautier, F. Modugno, E. Ribechini, Combined GC/MS analytical procedure for the characterization of glycerolipid, waxy, resinous, and proteinaceous materials in a unique paint microsample, *Analytical Chemistry*, **78**, 4490–4500 (2006).
8. P. Cok, B. De Bernard, M.P. Radillo, F. Francescato, *Synoptic Food Composition Tables*, Edizioni Piccini, Padova, 1986.
9. US Department of Agriculture, Agricultural Research Service. 2007. USDA National Nutrient Database for Standard Reference, Release 20. Nutrient Data Laboratory Home Page, <http://www.ars.usda.gov/ba/bhnrc/ndl>.
10. I. Bonaduce, M.P. Colombini, S. Diring, Identification of garlic in old gildings by gas chromatography-mass spectrometry, *Journal of Chromatography A*, **1107**, 226–232 (2006).
11. D.M.W. Anderson, J.F. Howlett, C.G.A. McNab, The amino acid composition of the proteinaceous component of gum Arabic acacia Senegal (L.) Willd, *Food Additives and Contaminants*, **2**, 231–235 (1985).
12. B. Stuart, *Analytical Techniques in Materials Conservation*, John Wiley & Sons, Ltd, Chichester, 2007.
13. M.P. Colombini, F. Modugno, R. Fuoco, A. Tognazzi, A GC-MS study on the deterioration of lipidic paint binders, *Microchemical Journal*, **73**, 175–185 (2002).
14. A. Karpowicz, Ageing and deterioration of proteinaceous media, *Studies in Conservation*, **26**, 153–160 (1981).



15. L. Rampazzi, F. Cariati, G. Tanda, M.P. Colombini, Characterisation of wall paintings in the Sos Furrighesos necropolis (Anela, Italy), *Journal of Cultural Heritage*, **3**, 237–240 (2002).
16. C. Hecht, S. Bieler, C. Griehl, Liquid chromatographic-mass spectrometric analyses of anaerobic protein degradation products, *Journal of Chromatography A*, **1088**, 121–125 (2005).
17. B.J. Jonson, G.H. Miller, Archaeological applications of amino acid racemization, *Archaeometry*, **39**, 265–2872 (1997).
18. A.M. Pollard, C. Heron, *Archaeological Chemistry*, Royal Society of Chemistry, Cambridge, 1996, pp. 271–301.
19. E. Cappellini, B. Chiarelli, L. Sineo, A. Casoli, A. Di Gioia, C. Vernesi, M.C. Biella, D. Caramelli, Biomolecular study of the human remains from tomb 5859 in the Etruscan necropolis of Monterozzi, Tarquinia (Viterbo, Italy), *Journal of Archaeological Science*, **31**, 603–612 (2004).
20. F. Mori, R. Ponti, A. Messina, M. Flieger, V. Havlicek, M. Sinibaldi, Chemical characterization and AMS radiocarbon dating of the binder of a prehistoric rock pictograph at Tadrart Acacus, Southern West Libya, *Journal of Cultural Heritage*, **7**, 344–349 (2006).
21. M. Serpico, R. White, Oil, fat and wax, in *Ancient Egyptian Materials and Technology*, P. Nicholson and I. Shaw (Eds), Cambridge University Press, Cambridge, 2000, pp. 390–429.
22. K. Kimpe, P.A. Jacobs, M. Waelkens, Analysis of oil used in late Roman oil lamps with different mass spectrometric techniques revealed the presence of predominantly olive oil together with traces of animal fat, *Journal of Chromatography A*, **937**, 87–95 (2001).
23. A. Tchaplá, P. Mejanelle, J. Bleton, S. Goursaud, Characterisation of embalming materials of a mummy of the Ptolemaic era. Comparison with balms from mummies of different eras, *Journal of Separation Science*, **27**, 217–234 (2004).
24. P. Walter, P. Martinetto, G. Tsoucaris, R. Breniaux, M.A. Lefebvre, G. Richard, J. Talabot, E. Dooryhee, Making make-up in Ancient Egypt, *Nature*, 1999, **397**, 483–484.
25. R.P. Evershed, R. Berstan, F. Grew, M.S. Copley, A.J.H. Charmant, E. Barham, H.R. Mottram, G. Brown, Archaeology: formulation of a Roman cosmetic, *Nature*, **432**, 35–36 (2004).
26. E. Ribechini, F. Modugno, C. Baraldi, P. Baraldi, M.P. Colombini, An integrated analytical approach for characterizing an organic residue from an archaeological glass bottle recovered in Pompeii (Naples, Italy), *Talanta*, **74**, 555–561 (2008).
27. E. Ribechini, F. Modugno, R. Evershed, M.P. Colombini, Gas chromatographic and mass spectrometric investigations of organic residues from Roman glass unguentaria, *Journal of Chromatography A*, **1183**, 158–169 (2008).
28. S. Mirabaud, C. Rolando, M. Regert, Molecular criteria for discriminating adipose fat and milk from different species by nanoESI MS and MS/MS of their triacylglycerols: application to archaeological remains, *Analytical Chemistry*, **79**, 6182–6192 (2007).
29. M.P. Colombini, F. Modugno, E. Ribechini, Organic mass spectrometry in archaeology: evidence for Brassicaceae seed oil in Egyptian ceramic lamps, *Journal of Mass Spectrometry*, **40**, 890–898 (2005).
30. D.B. Sandy, The production and use of vegetable oils in Ptolemaic Egypt, *Bulletin of the American Society of Papyrologists*, Supplement 6 (1989).
31. R.P. Evershed, S.N. Dudd, M.S. Copley, R. Berstan, A.W. Stott, H. Mottram, S.A. Buckley, Z. Crossman, Chemistry of archaeological animal fats, *Accounts of Chemical Research*, **35**, 660–668 (2002).
32. M. Regert, H.A. Bland, S.N. Dudd, P.F. van Bergen, R.P. Evershed, Free and bound fatty acid oxidation products in archaeological ceramic vessels, *Proceedings of the Royal Society London B*, **265**, 2027–2032 (1998).
33. R.J. Hamilton, C. Kalu, E. Prisk, F.B. Padley, H. Pierce, Chemistry of free radicals in lipids, *Food Chemistry*, **60**, 193–199 (1997).
34. N.A. Porter, S.E. Caldwell, K.A. Mills, Mechanisms of free radical oxidation of unsaturated lipids, *Lipids*, **30**, 277–290 (1995).
35. L.A. O'Neill, The autoxidation of drying oils, *Chemistry & Industry*, 384–387 (1954).
36. W.E. Neff, W.C. Byrdwell, Characterization of model triacylglycerol (triolein, trilinolein and trilinolenin) autoxidation products via high-performance liquid chromatography coupled with atmospheric pressure chemical ionization mass spectrometry, *Journal of Chromatography A*, **818**, 169–186 (1998).

37. N.A. Porter, Chemistry of lipid peroxidation, *Methods in Enzymology*, **105**, 273–282 (1984).
38. W.J. Muizebelt, M.W.F. Nielen, Oxidative crosslinking of unsaturated fatty acids studied with mass spectrometry, *Journal of Mass Spectrometry*, **31**, 545–554 (1996).
39. F.O. Gülaçar, A. Buchs, A. Susini, Capillary gas chromatography-mass spectrometry and identification of substituted carboxylic acids in lipids extracted from a 4000-year-old Nubian burial, *Journal of Chromatography*, **479**, 61–72 (1989).
40. J.S. Mills, The gas chromatographic examination of paint media. Part I: Fatty acid composition and identification of dried oil films, *Studies in Conservation*, **11**, 92–107 (1966).
41. M.P. Colombini, F. Modugno, R. Fuoco, A. Tognazzi, A GC-MS study on the deterioration of lipidic paint binders, *Microchemical Journal*, **73**, 175–185 (2002).
42. M.P. Colombini, S. Francesconi, R. Fuoco, F. Modugno, Characterisation of proteinaceous binders and drying oils in wall painting samples by GC-MS, *Journal of Chromatography A*, **846**, 101 (1999).
43. M.S. Copley, H.A. Bland, P. Rose, M. Horton, R.P. Evershed, Gas chromatographic, mass spectrometric and stable carbon isotopic investigations of organic residues of plant oils and animal fats employed as illuminants in archaeological lamps from Egypt, *Analyst*, **130**, 860–871 (2005).
44. M.A. Somali M.A. Bajneid, S.S. Al-Fhaimani, Chemical composition and characteristics of *Moringa peregrina* seeds and seeds oil, *Journal of the American Oil Chemists Society*, **61**, 85–86 (1984).
45. P. Mayerson, Radish oil: a phenomenon in Roman Egypt, *Bulletin of the American Society of Papyrologists*, **38**, 109–117 (2001).
46. D. Grieco, G. Piepoli, Composizione degli acidi grassi contenuti nei lipidi estratti da semi e frutti oleosi, *Rivista Italiana delle Sostanze Grasse*, **XLI**, 283–287 (1964).
47. M.P. Colombini, G. Giachi, F. Modugno, E. Ribechini, Characterisation of organic residues in pottery vessels of the Roman age from Antinoe (Egypt). *Microchemical Journal*, **79**, 83–90 (2005).
48. A. Spyros, D. Anglos, Study of aging in oil paintings by 1D and 2D NMR spectroscopy, *Analytical Chemistry*, **76**, 4929–4936 (2004).
49. D.J. van den Berg, K.J. van den Berg, J.J. Boon, GC/MS analysis of fractions of cured and aged drying oil paints, *Advances in Mass Spectrometry*, **14**, D052100/1–D052100/8 (1998).
50. P. Agozzino, G. Avellone, I.D. Donato, F. Filizzola, Mass spectrometry for cultural heritage knowledge: gas chromatographic/mass spectrometric analysis of organic remains in Neolithic potsherds, *Journal of Mass Spectrometry*, **36**, 443–444 (2001).
51. S.A. Buckley, A.W. Stott, R.P. Evershed, Studies of organic residues from ancient Egyptian mummies using high temperature-gas chromatography-mass spectrometry and sequential thermal desorption-gas chromatography-mass spectrometry and pyrolysis-gas chromatography-mass spectrometry, *The Analyst*, **124**, 443–452 (1999).
52. M.P. Colombini, F. Modugno, E. Ribechini, The Egyptian mummies in the ‘Museo di Anatomia’ of the University of Pisa: a chemical approach for the characterization of balms, *Science and Technology for Cultural Heritage*, **13**, 83–87 (2004).
53. J.S. Mills, R. White, The identification of paint media from the analysis of their sterol composition, *Studies in Conservation*, **20**, 176–182 (1975).
54. S. Charters, R.P. Evershed, P.W. Blinkhorn, V. Denham, Evidence for the mixing of fats and waxes in archaeological ceramics, *Archaeometry*, **37**, 113–127 (1995).
55. S.A. Buckley, K.A. Clark, R.P. Evershed, Complex organic chemical balms of Pharaonic animal mummies, *Nature*, **431**, 294–299 (2004).
56. R.P. Evershed, S.N. Dudd, M.S. Copley, R. Berstan, A.W. Stott, H. Mottram, S.A. Buckley, Z. Crossman, Chemistry of archaeological animal fats, *Accounts of Chemical Research*, **35**, 660–668 (2002).
57. H.R. Mottram, S.N. Dudd, G.J. Lawrence, A.W. Stott, R.P. Evershed, New chromatographic, mass spectrometry and stable isotope approaches to the classification of degraded animal fats preserved in archaeological pottery, *Journal of Chromatography*, **833**, 209–221 (1999).
58. F.A. Hansel, M.S. Copley, L.A.S. Madureira, R.P. Evershed, Thermally produced  $\omega$ -(*o*-alkylphenyl)alkanoic acids provide evidence for the processing of marine products in archaeological pottery vessels, *Tetrahedron Letters*, **45**, 2999–3002 (2004).

59. O.E. Craig, M. Forster, S.H. Andersen, E. Koch, P. Crombé, N.J. Milner, B. Stern, G.N. Bailey, C. Heron, Molecular and isotopic demonstration of the processing of aquatic products in northern European prehistoric pottery, *Archaeometry*, **49**, 135–152 (2007).
60. E. Ribechini, M.P. Colombini, G. Giachi, F. Modugno, P. Pallecchi, A multi-analytical approach for the characterization of commodities in a ceramic jar from Antinoe (Egypt), *Archaeometry*, in press.
61. M. Regert, C. Rolando, Identification of archaeological adhesives using Direct Inlet Electron Ionization Mass Spectrometry, *Analytical Chemistry*, **74**, 965–975 (2002).
62. N. Garnier, C. Cren-Olivè, C. Rolando, M. Regert, Characterization of the archaeological beeswax by electron ionization and electrospray ionization mass spectrometry, *Analytical Chemistry*, **74**, 4868–4877 (2002).
63. C. Heron, N. Nemcek, K.M. Bonfield, The chemistry of Neolithic beeswax, *Naturwissenschaften*, **81**, 266–269 (1994).
64. R.P. Evershed, Biomolecular analysis by organic mass spectrometry, in *Modern Analytical Methods in Art and Archaeology*, E. Ciliberto and G. Spoto (Eds), Wiley Interscience, New York, 2000.
65. H.G. Bayer, The bust of Nefertiti, *Analytical Chemistry*, **54**, 619–628 (1982).
66. R.P. Evershed, S.J. Vaughan, S.N. Dudd, J.S. Soles, Fuel for thought? Beeswax in lamps and conical cups from late Minoan Crete, *Antiquity*, **71**, 979–985 (1997).
67. R. White, The application of gas-chromatography to the identification of waxes, *Studies in Conservation*, **23**, 57–58 (1978).
68. J.C.T. Chen, A.P. Amar, M.L. Levy, M.L.J. Apuzzo, The development of anatomical art and sciences: The ceruplastica anatomical models of la Specola, *Neurosurgery*, **45**, 883–891 (1999).
69. P. Tulloch, L.L. Hoffman, Canadian beeswax: analytical values and composition of hydrocarbons, free acids and long chain esters, *Journal of the American Oil Chemists Society*, **49**, 696–699 (1972).
70. P. Tulloch, Beeswax-composition and analysis, *Bee World*, **61**, 47–62 (1980).
71. A.P. Tulloch, Beeswax: structure of the esters and their component hydroxy acids and diols, *Chemistry and Physics of Lipids*, **6**, 235–265 (1971).
72. J.J. Jiménez, J.L. Bernal, S. Aumente, M.J. del Nozal, M.T. Martín, J. Bernal, Quality assurance of commercial beeswax: I. Gas chromatography–electron impact ionization mass spectrometry of hydrocarbons and monoesters, *Journal of Chromatography A*, **1024**, 147–154 (2004).
73. J.J. Jiménez, J.L. Bernal, S. Aumente, L. Toribio, J. Bernal, Quality assurance of commercial beeswax: II. Gas chromatography–electron impact ionization mass spectrometry of alcohols and acids, *Journal of Chromatography A*, **1007**, 101–116 (2003).
74. M. Regert, S. Colinart, L. Degrand, O. Decavallas, Chemical alteration and use of beeswax through time: accelerated ageing tests and analysis of archaeological samples from various environmental contexts, *Archaeometry*, **43**, 549–569 (2001).
75. R.P. Evershed, S.N. Dudd, V.A. Anderson-Stojanovic, E.R. Gebhard, New chemical evidence for the use of combed ware pottery vessel as beehives in ancient Greece, *Journal of Archaeological Science*, **30**, 1–12 (2003).
76. M.P. Colombini, G. Giachi, F. Modugno, P. Pallecchi, E. Ribechini, The characterization of paints and waterproofing materials from the shipwrecks found at the archaeological site of the Etruscan and Roman harbour of Pisa (Italy). *Archaeometry*, **45**, 659–674 (2003).
77. M. Regert, J. Langlois, S. Colinart, Characterisation of wax works of art by gas chromatographic procedures, *Journal of Chromatography A*, **1091**, 124–136 (2005).
78. A. Gascard, Ceryl alcohol and cerotic acid of Chinese wax, *Comptes Rendue*, **170**, 1326–1328 (1920).
79. A.P. Tulloch, Comparison of some commercial waxes by gas liquid chromatography, *Journal of the American Oil Chemists Society*, **50**, 367–371 (1973).
80. R. White, The application of gas chromatography to the identification of waxes, *Studies in Conservation*, **23**, 57–68 (1978).
81. T. Horiguchi, Y. Takase, Y. Arai, H. Ageta, Y. Showa, M. Tokyo, GC-MS study on ester components of spermaceti, *Natural Medicines*, **53**, 105–108 (1999).
82. C. Sell, The chemistry of ambergris, *Chemistry & Industry*, **20**, 516–520 (1990).

83. C. Chemtob, F. Fawaz, F. Puisieux, Analysis of ointments, oils, and waxes. XX. Chemical composition of waxy lanolin, *Annales Pharmaceutiques Francaises*, **33**, 243–251 (1975).
84. L.E. Vanderburg, E.A. Wilder, The structural constituents of carnauba wax, *Journal of the American Oil Chemists Society*, **47**, 514–518 (1970).
85. L. Masschelein-Kleiner, *Ancient Binding Media, Varnishes and Adhesives*, ICCROM Ed., Rome, 1995.
86. J.H. Langenheim, *Plant Resins, Chemistry, Evolution, Ecology, and Ethnobotany*, Timber Press, Portland, 2003.
87. A.M. Pollard, C. Heron, *Archaeological Chemistry*, Royal Society of Chemistry, Cambridge, 1996, pp. 239–270.
88. Serpico M., R. White, Resins, amber and bitumen, in *Ancient Egyptian Materials and Technology*, P. Nicholson and I. Shaw (Eds), Cambridge University Press, Cambridge, 2000, pp. 430–474.
89. N. Robinson, R.P. Evershed, W.J. Higgs, K. Jerman, Eglinton, G., Proof of a pine wood origin for pitch from Tudor (Mary Rose) and Etruscan shipwrecks: application of analytical organic chemistry in archaeology, *Analyst*, **112**, 637–643 (1987).
90. S. Charters, R.P. Evershed, L.J. Goad, C. Heron, P. Blinkhorn, Identification of an adhesive used to repair a roman jar, *Archaeometry*, **35**, 91–101 (1993).
91. M.P. Colombini, F. Modugno, E. Ribechini, Direct exposure electron ionization mass spectrometry and gas chromatography/mass spectrometry techniques to study organic coatings on archaeological amphorae, *Journal of Mass Spectrometry*, **40**, 675–687 (2005).
92. M.P. Colombini, F. Modugno, E. Ribechini, Chemical study of triterpenoid resinous materials in archaeological findings by means of direct exposure electron ionisation mass spectrometry and gas chromatography/mass spectrometry, *Rapid Communications in Mass Spectrometry*, **20**, 1787–1800 (2006).
93. S.A. Buckley, R.P. Evershed, Organic chemistry of embalming agents in Pharaonic and Graeco-Roman mummies, *Nature*, **413**, 837–841 (2001).
94. M.P. Colombini, F. Modugno, F. Silvano, M. Onor, Characterisation of the balm of an Egyptian mummy from the seventh century B.C., *Studies in Conservation*, **45**, 19–29 (2000).
95. U. Weser, Y. Kaup, H. Etspuler, J. Koller, U. Baumer, Embalming in the old kingdom of Pharaonic Egypt, *Analytical Chemistry*, **70**, 511A–516A (1998).
96. C. Vieillescazes, S. Coen, Caracterisation de quelques resines utilisees en Egypte ancienne, *Studies in Conservation*, **38**, 255–264 (1993).
97. M.L. Proefke, K.L. Rinehart, M. Raheel, S.H. Ambrose, S.U. Wisseman, Probing the mysteries of ancient Egypt. Chemical analysis of Roman period Egyptian mummy, *Analytical Chemistry*, **64**, 105A–111A (1992).
98. S. Hamm, J. Bleton, A. Tchaplá, Headspace solid phase microextraction for screening for the presence of resins in Egyptian archaeological samples, *Journal of Separation Science*, **27**, 235–243 (2004).
99. R.P. Evershed, P.F. van Bergen, T.M. Peakman, E.C. Leigh-Firbank, M.C. Horton, D. Edwards, M. Biddle, B. Kjølbye-Biddle, P.A. Rowley-Conwy, Archaeological frankincense, *Nature*, **390**, 667–668 (1997).
100. J. de Pascual Teresa, J.G. Urones, I.S. Marcos, P.B. Barcala, N.M. Garrido, Diterpenoid and other components of *Cistus laurifolius*, *Phytochemistry*, **25**, 1185–1187 (1986).
101. J. de Pascual Teresa, J.G. Urones, I.S. Marcos, F. Bermejo, P. Basabe, A rearranged labdane: salmantic acid from *Cistus laurifolius*, *Phytochemistry*, **22**, 2783–2785 (1983).
102. J. de Pascual Teresa, J.G. Urones, I.S. Marcos, L. Núñez, P. Basabe, Diterpenoids and flavonoids from *Cistus palinhæ*, *Phytochemistry*, **22**, 2805–2808 (1983).
103. M.T. Calabuig, M. Cortés, C.G. Francisco, R. Hernández, E. Suárez, Labdane diterpenes from *Cistus symphytifolius*, *Phytochemistry*, **20**, 2255–2258 (1981).
104. B. Mahajan, S.C. Taneja, V.K. Sethi, K.L. Dhar, Two triterpenoids from *Boswellia serrata* gum resin, *Phytochemistry*, **39**, 453–455 (1995).
105. E.M. Hairfield, H.H. Hairfield Jr, H.M. McNair, GC, GC/MS, and TLC of  $\beta$ -boswellic acid and O-acetyl- $\beta$ -boswellic acid from *B. serrata*, *B. carteri*, and *B. papyrifera*, *Journal of Chromatographic Science*, **27**, 127–133 (1989).

106. C. Mathe, G. Culioli, P. Archier, C. Vieillescazes, High-performance liquid chromatographic analysis of triterpenoids in commercial frankincense, *Chromatographia*, **60**, 493–499 (2004).
107. Mathe C., G. Culioli, P. Archier, C. Vieillescazes, Characterization of archaeological frankincense by gas chromatography-mass spectrometry, *Journal of Chromatography A*, **1023**, 277–285 (2004).
108. B. Buchele, T. Simmet, Analysis of 12 different pentacyclic triterpenic acids from frankincense in human plasma by high-performance liquid chromatography and photodiode array detection, *Journal of Chromatography B*, **795**, 355–362 (2003).
109. B. Buchele, W. Zugmaier, T. Simmet, Analysis of pentacyclic triterpenic acids from frankincense gum resins and related phytopharmaceuticals by high-performance liquid chromatography. Identification of lupeolic acid, a novel pentacyclic triterpene, *Journal of Chromatography B*, **791**, 21–30 (2003).
110. G. Culioli, C. Mathe, P. Archier, C. Vieillescazes, A lupane triterpene from frankincense (*Boswellia* sp., Burseraceae), *Phytochemistry*, **62**, 537–541 (2003).
111. P. Archier, C. Vieillescazes, Characterization of various geographical origin incense based on chemical criteria, *Analisis*, **28**, 233–237 (2000).
112. R.S. Pardhy, S.C. Bhattacharyya,  $\beta$ -Boswellic acid, acetyl- $\beta$ -boswellic acid, acetyl-11-keto- $\beta$ -boswellic acid and 11-keto- $\beta$ -boswellic acid, four pentacyclic triterpene acids from the resin of *Boswellia serrata* Roxb, *Indian Journal of Chemistry*, **16B**, 176–178 (1978).
113. P.F. van Bergen, T.M. Peakman, E.C. Leigh-Firbank, R.P. Evershed, Chemical evidence for archaeological frankincense: boswellic acids and their derivatives in solvent soluble and insoluble fractions of resin-like materials, *Tetrahedron Letters*, **38**, 8409–8412 (1997).
114. J. Koeller, U. Baumer, D. Grosser, E. Schmid, Arbeitshefte des bayerischen landesamtes fur denkmalpflege, *Arbeitsheft*, **81**, 347–358 (1997).
115. D.H.R. Barton, E. Seoane, Triterpenoids. Part XXII. The constitution and stereochemistry of masticdienonic acid, *Journal of the Chemical Society*, 4150–4157 (1956).
116. E. Seoane, Further crystalline constituents of gum mastic, *Journal of the Chemical Society*, 4158–4159 (1956).
117. R. Caputo, L. Mangoni, P. Monaco, G. Palumbo, Triterpenes of galls of *Pistacia terebinthus*: galls produced by *Pemphigus utricularius*, *Phytochemistry*, **14**, 809–811 (1975).
118. P. Monaco, R. Caputo, G. Palumbo, L. Mangoni, Triterpenes from the galls of *Pistacia lentiscus*, *Phytochemistry*, **12**, 1534–1537 (1973).
119. P. Monaco, R. Caputo, G. Palumbo, L. Mangoni, Neutral triterpenes from the galls of *Pistacia terebinthus*, *Phytochemistry*, **12**, 939–942 (1973).
120. R. Caputo, L. Mangoni, P. Monaco, G. Palumbo, Y. Aynehchi, M. Bagheri, Triterpenes from the bled resin of *Pistacia vera*, *Phytochemistry*, **17**, 815–817 (1978).
121. F.J. Marner, A. Freyer, J. Lex, Triterpenoids from gum mastic, the resin of *Pistacia lentiscus*, *Phytochemistry*, **30**, 3709–3712 (1991).
122. V.P. Papageorgiou, M.N. Bakola-Christianopolou, K.K. Apazidou, E.E. Psarros, Gas chromatographic-mass spectroscopic analysis of the acidic triterpenic fraction of mastic gum, *Journal of Chromatography A*, **769**, 263–273 (1997).
123. Y. Kaup, U. Baumer, J. Koller, R.E.M. Hedges, H. Werner, H. Hartmann, H. Etspueler, U. Weser, Zn2Mg alkaline phosphatase in an early Ptolemaic mummy, *Zeitschrift fuer Naturforschung C*, **49**, 489–500 (1994).
124. M. Serpico, R. White, The botanical identity and transport of incense during the Egyptian New Kingdom, *Antiquity*, **74**, 884–897 (2000).
125. G.A. van der Doelen, K.J. van den Berg, J.J. Boon, N. Shibayama, E.R. de la Rie, W.J.L. Genuit, Analysis of fresh triterpenoid resins and aged triterpenoid varnishes by high-performance liquid chromatography–atmospheric pressure chemical ionisation (tandem) mass spectrometry, *Journal of Chromatography A*, **809**, 21–37 (1998).
126. G.A. van der Doelen, J.J. Boon, Artificial ageing of varnish triterpenoids in solution, *Journal of Photochemistry and Photobiology A: Chemistry*, **134**, 45–57 (2000).
127. M.P. Colombini, F. Modugno, S. Giannarelli, R. Fuoco, M. Matteini, GC-MS characterization of paint varnishes, *Microchemical Journal*, **67**, 385–396 (2000).



128. K.J. van der Berg, J. van der Horst, J.J. Boon, O.O. Sudmeijer, Cis-1,4-poly- $\beta$ -myrcene; the structure of the polymeric fraction of mastic resin (*Pistacia lentiscus*) elucidated, *Tetrahedron Letters*, **39**, 2654–2648 (1998).
129. I. Pastorova, C.G. de Koster, J.J. Boon, Analytical study of free and ester bound benzoic and cinnamic acids of gum benzoin resins by GC-MS and HPLC-frit FAB-MS, *Phytochemical Analysis*, **8**, 63–73 (1997).
130. I. Pastorova, T. Weeding, J.J. Boon, 3-Phenylpropenylcinnamate, a copolymer unit in siegbur-gite fossil resin: a proposed marker for the Hamamelidaceae, *Organic Geochemistry*, **29**, 1381–1393 (1998).
131. F. Modugno, E. Ribechini, M.P. Colombini, Aromatic resin characterisation by gas chromatography-mass spectrometry: Raw and archaeological materials, *Journal of Chromatography A*, **85**, 164–173 (2006).
132. S. Huneck, Triterpenes. IV. Triterpene acids of *Liquidambar orientalis*, *Tetrahedron*, **19**, 479–482 (1963).
133. K.S. Brown, The chemistry of aphids and scale insects, *Chemical Society Reviews*, **4**, 263–288 (1975).
134. A.N. Singh, A. B. Upadhye, V.V. Mhaskar, Sukh Dev, Chemistry of lac resin-VI. Components of soft resin, *Tetrahedron*, **30**, 867–874 (1974).
135. R.G. Khurana, A.N. Singh, A.B. Upadhye, V.V. Mhaskar, Sukh Dev, Chemistry of lac resin-III. An integrated procedure for their isolation from hard resin; chromatography characteristics and quantitative determination, *Tetrahedron*, **26**, 4167–4175 (1970).
136. M.S. Wadia, R.G. Khurana, V.V. Mhaskar, Sukh Dev, Chemistry of lac resin-I. Butolic, jalaric and laksholic acids, *Tetrahedron*, **25**, 3841–3854 (1969).
137. A.N. Singh, A.B. Upadhye, M.S. Wadia, V.V. Mhaskar, Sukh Dev, Chemistry of lac resin-II. Laccijalaric acid, *Tetrahedron*, **25**, 3855–3867 (1969).
138. A.B. Upadhye, M.S. Wadia, V.V. Mhaskar, Sukh Dev, Chemistry of lac resin-IV. Pure lac resin-I: isolation and quantitative determination of constituent acids, *Tetrahedron*, **26**, 4177–4187 (1970).
139. A.B. Upadhye, M.S. Wadia, V.V. Mhaskar, Sukh Dev, Chemistry of lac resin-V. Pure lac resin-2: points of linkage of constituent acids, *Tetrahedron*, **26**, 4387–4396 (1970).
140. A.N. Singh, A.B. Upadhye, V.V. Mhaskar, DevSukh, A.V. Pol, V.G. Naik, Chemistry of lac resin-VII. Pure lac resin-3: structure, *Tetrahedron*, **30**, 3689–3693 (1974).
141. K.B. Anderson, J.C. Crelling (Eds), *Amber, Resinite, and Fossil Resins*, American Chemical Society, Washington, DC, 1995.
142. J. Koller, U. Baumer, D. Mania, High tech in the Middle Palaeolithic: Neanderthal-manufactured pitch identified, *European Journal of Archaeology*, **4**, 385–397 (2001).
143. M. Reunamen, R. Ekman, M. Heinonen, Analysis of Finnish pine tar and tar from the wreck of frigate St. Nikolai, *Holzforschung*, **43**, 33–39 (1989).
144. M.P. Colombini, C. Colombo, F. Modugno, F. Silvano, E. Ribechini, L. Toniolo, Chemical characterization of Egyptian amphorae from Fayum, *Geoarchaeological and Bioarchaeological Studies*, 157–160 (2005).
145. D. Urem-Kotsou, B. Stern, C. Heron, K. Kotsakis, Birch-bark tar at Neolithic Makriyalos, Greece, *Antiquity*, **76**, 962–967 (2002).
146. M. Regent, S. Vacher, C. Moulherat, O. Decavallas, Adhesive production and pottery function during the Iron Age at the site of Grand Aunay (Sarthe, France), *Archaeometry*, **45**, 101–120 (2003).
147. E. Ribechini, F. Modugno, M.P. Colombini, Direct exposure-(chemical ionization)-mass spectrometry for a rapid characterization of raw and archaeological diterpenoid resinous substances, *Microchimica Acta*, **162**, 405–413 (2008).
148. S.N. Dudd, R.P. Evershed, Unusual triterpenoid fatty acyl ester components of archaeological birch bark tars, *Tetrahedron Letters*, **40**, 359–362 (1999).
149. D.P.S. Peacock, D.F. Williams, *Amphorae and the Roman Economy: An Introductory Guide*, Longman, London, 1986, p. 49.
150. J. Connan, A. Nissenbaum, Conifer tar on the keel and hull planking of the Ma'agan Mikhael ship (Israel, 5th century BC): identification and comparison with natural products and artefacts employed in boat construction, *Journal of Archaeological Science*, **30**, 709–719 (2003).

151. M. Regert, S. Vacher, C. Moulherat, O. Decavallas, Adhesive production and pottery function during the Iron Age at the site of Grand Aunay (Sarthe, France), *Archaeometry*, **45**, 101–120 (2003).
152. P.P.A. Mazza, F. Martini, B. Sala, M. Magi, M.P. Colombini, G. Giachi, F. Landucci, C. Lemorini, F. Modugno, E. Ribechini, A new Palaeolithic discovery: tar-hafted stone tools in a European id-Pleistocene bone-bearing bed, *Journal of Archaeological Science*, **33**, 1310–1318 (2006).
153. R. Ekman, The suberin monomers and triterpenoids from the outer bark of *Betula verrucosa* Ehrh, *Holzforschung*, **37**, 205–211 (1983).
154. B.J.W. Cole, K.D. Murray, A.R. Alford, Y. Hua, M.D. Bentley, Triterpenes from the outer bark of *Betula nigra*, *Journal of Wood Chemistry and Technology*, **11**, 503–516 (1991).
155. B.J.W. Cole, M.D. Bentley, Y. Hua, Triterpenoid extractives in the outer bark of *Betula lenta* (black birch), *Holzforschung*, **45**, 265–268 (1991).
156. B.J.W. Cole, M.D. Bentley, Y. Hua, L. Bu, Triterpenoid constituents in the outer bark of *Betula alleghaniensis* (yellow birch), *Journal of Wood Chemistry and Technology*, **11**, 209–223 (1991).
157. M.M. O'Connell, M.D. Bentley, C.S. Campbell, B.J.W. Cole, Betulin and lupeol in bark from four white-barked birches, *Phytochemistry*, **27**, 2175–2176 (1988).
158. P.J. Holloway, Composition of suberin from the corks of *Quercus suber* and *Betula pendula*, *Chemistry and Physics of Lipids*, **9**, 158–170 (1972).
159. J. Connan, D. Dessort, Du bitume dans des baumes de momies égyptiennes (1295 av. J.C. - 300 ap. J.C.): détermination de son origine et évaluation de sa quantité, *Comptes Rendue Académie des Sciences de Paris Serie II*, **312**, 1445–1452 (1991).
160. A. Nissenbaum, Molecular archaeology: organic geochemistry of Egyptian mummies, *Journal of Archaeological Science*, **19**, 1–6 (1992).
161. J. Connan, R.P. Evershed, L. Biek, G. Eglinton, Use and trade of bitumen in antiquity and prehistory: molecular archaeology reveals secrets of past civilizations, *Philosophical Transactions: Biological Sciences*, **354**, 33–50 (1999).
162. J. Connan, O. Kavak, E. Akin, M.N. Yalc, K. Imbus, J. Zumberge, Identification and origin of bitumen in Neolithic artefacts from Demirkoy Hoyuk (8100 BC): Comparison with oil seeps and crude oils from southeastern Turkey, *Organic Geochemistry*, **37**, 1752–1767 (2006).
163. I. Bonaduce, H. Brecoulaki, M.P. Colombini, A. Lluveras, V. Restivo, E. Ribechini, GC-MS characterization of plant gums in samples from painted works of art, *Journal of Chromatography A*, **1175**, 275–282 (2007).
164. V. Pitthard, P. Finch, GC-MS analysis of monosaccharide mixtures as their diethyldithioacetal derivatives: Application to plant gums used in art works, *Chromatographia*, **53**, S317–S321 (2001).
165. J.H. Hofenk de Graaff, *The Colorful Past. Origin, Chemistry and Identification of Natural Dyestuffs*, Abegg-Stiftung, Riggisberg, 2004.
166. H. Zollinger, *Color Chemistry. Syntheses, Properties and Applications of Organic Dyes and Pigments*, Wiley-VCH, Weinheim, 2003.
167. E.W. Fitzhugh (Ed.), *Artists' Pigments. A Handbook of Their History and Characteristics*, Vol. **3**, Oxford University Press, New York, 1997.
168. J. Cannon, M. Cannon, *Dye Plants and Dyeing*, The Herbert Press, London, 1994.
169. E.S.B. Ferreira, A. Quye, H. McNab, A.N. Hulme, Photo-oxidation products of quercetin and morin as markers for the characterisation of natural flavonoid yellow dyes in ancient textiles, *Dyes in History and Archaeology*, **18**, 63–72 (2002).
170. M.P. Colombini, A. Andreotti, C. Baraldi, I. Degano, J.J. Łucejko, Colour fading in textiles: A model study on the decomposition of natural dyes, *Microchemical Journal*, **85**, 174–182 (2007).
171. Z.C. Koren, Photochemical vat dyeings of the biblical purple tekhet and argaman dyes, Paper presented at the 13th meeting of Dyes in History and Archaeology, Royal Museum of Scotland, Edinburgh, 1994.
172. C.J. Cooksey, R.S. Sinclair, Colour variations in Tyrian purple dyeing, *Dyes in History and Archaeology*, **20**, 127–135 (2005).

173. J. Wouters, I. Van den Berghe, B. Devia, Understanding historic dyeing technology: a multi-faced approach, in *Scientific Analysis of Ancient and Historic Textiles*, R. Janaway and P. Wyeth (Eds), Archetype Publications, London, 2005, pp. 187–193.
174. T. van Oosten, Y. Shashoua, F. Waentig, *Plastics in Art. History, Technology, Preservation*, Siegl, Munich, 2002.
175. F. Cappitelli, Y. Shashoua, E. Vassallo (Eds), *Macromolecules in Cultural Heritage*, Wiley-VCH, Weinheim, 2006.
176. C.V Horie, *Materials for Conservation, Organic Consolidants, Adhesives and Coatings*, Butterworth Heinemann, Oxford, 1987.
177. P. Hoffmann, On the stabilisation of waterlogged oak-wood with PEG. Designing a two-step treatment for multi quality timber, *Studies in Conservation*, **31**, 103–113 (1986).



# 2

## Overview of Mass Spectrometric Based Techniques Applied in the Cultural Heritage Field

*Gianluca Giorgi*

### 2.1 Introduction

Most materials from cultural heritage are composed of complex mixtures of different molecules having a wide range of chemico-physical properties. Most of them are at a trace level, whilst others are in high amounts.

The study and characterization of these molecules can yield information on the use and function of the material, as well as on the customs of the people who used it, their way of life and other useful information invaluable to reconstruct the historical, cultural and social background of a given period in a given geographical area.

To obtain reliable information it is necessary to identify and characterize *each component* in the material. To fulfil this aim, methodologies characterized by high selectivity, specificity and sensitivity are required. Mass spectrometry (MS) is one of the most powerful methodologies for identifying, structurally characterizing, and quantitating wide classes of molecules, ranging from small to very big species.

MS is based on the production of gas phase ions and on their separation according to their mass-to-charge ( $m/z$ ) ratios. It was introduced at the end of the nineteenth century and for a long time it was confined to the physical sciences, being used to study elementary particles of matter. Pioneering works by J. J. Thomson, F. W. Aston and A. J. Dempster provided the basis for the determination of the isotopes of elements. In the 1940s, MS

found applications in chemistry in the characterization of hydrocarbon mixtures that were of great interest to oil companies. However, due to the lack of separation methods, the results were difficult to interpret.

During the following decades, in order to characterize different classes of molecules, many efforts were made to find a relationship between the mass spectrum and the molecular structure. Owing to technological innovation and advances in instrumentation, mass spectrometers became more and more sophisticated and versatile tools for different applications in chemistry. At the end of the 1970s, wide classes of volatile organic molecules with low to medium molecular weight could be characterized by this methodology.

The introduction of *soft* ionization techniques, such as *plasma desorption* (PD),[1] *field desorption* (FD)[2] and *fast atom bombardment* (FAB),[3] marked the beginning of a new era for MS. In fact, they allowed MS to extend its applications to wide classes of nonvolatile, polar, thermally unstable and high molecular weight analytes. This opened up new horizons for MS in many unexpected fields, such as biology, biomedicine and biotechnology, in which this methodology had not previously found any possible application.

The growing interest for the identification and characterization of polar and large compounds caused the development and the introduction of new ionization techniques, such as *electrospray ionization* (ESI)[4], and *matrix assisted laser desorption ionization* (MALDI),[5] and their more recent improvements, thus establishing new MS based approaches for studying large molecules, polymers and biopolymers, such as proteins, carbohydrates, nucleic acids.

Parallel to the development of mass spectrometric instrumentation and methodologies, the improvements of separation techniques, such as gas chromatography (GC), high performance liquid chromatography (HPLC) and capillary electrophoresis (CE), and of their coupling with MS allowed the study of complex mixtures, that are generally encountered in most studies.

Nowadays, MS plays an important role in many fields of scientific and technological research for identification, structural characterization and quantitative determination of wide classes of compounds. Its unique capabilities, such as high sensitivity, high selectivity, accuracy in molecular weight determination, and ability to analyze complex mixtures, give this methodology great importance in the solution of problems not easily handled by other techniques.

An overview of the principles and instrumentation of MS, its powerful ability and utility in the identification, structural characterization and quantitation of analytes, together with applications in cultural heritage, are presented in this chapter.

## 2.2 Features of Mass Spectrometry

MS has characteristic features, in particular:

1. *Sensitivity.* MS is an extremely sensitive method. Nowadays, substances over a wide range of molecular weight can be measured [at the attomol ( $10^{-18}$  mol) or subattomol level].

2. *Specificity and selectivity.* In most of cases, a mass spectrum is produced by just one molecule and a given molecule produces only one mass spectrum. It follows that a mass spectrum is unequivocally related to the *chemical structure* of the compound that produced it.
3. *Speed.* The time needed to obtain a mass spectrum is in the range of  $10^{-3}$ –1 s.
4. Another feature, unfortunately not as positive as the previous ones, is the cost of the instrumentation. Several decades ago, when MS applications were limited to a few fields, the cost was high. Nowadays, owing to the great development in instrumentation and technology, together with greater commercialization, the cost of instrumentation is assuming less and less importance. Costs vary from a few tens of thousands to a million Euros, depending on the type and performance of the instrumentation.

### 2.2.1 Mass Spectrometry Studies of Ions in the Gas Phase

All approaches that use MS are based on the study of *ions in the gas phase*. Briefly, we will try to clarify what this means.

In the gas phase species are isolated, far from each other. It follows that their behaviour is not influenced by solvation, as occurs in solution, or by reticular forces, as in the crystalline state. Thus, the gas phase allows the study of the *intrinsic properties* of a given species, that are only dependent on its chemico-physical properties, i.e. its molecular weight, type of atoms (C, N, O, ...) involved, connections between them, etc.

According to the IUPAC definition, an ion is an ‘atomic or molecular particle having a net electric charge’.[6] In contrast to molecules, that are neutral entities and consequently have no charge, ions have a net electric charge. Owing to this, and in contrast to molecules, ions can be accelerated, decelerated, moved and driven in any direction. As for all charged species, ion movements are influenced by different forces, and in particular by an electric field, a magnetic field and a radiofrequency. One, two or all three of these forces are used in mass spectrometers to study ions. In every mass spectrometer, independently from its features and performance, ions are generated, accelerated, driven, analyzed and detected.

Generally we are used to dealing with molecules. However, MS studies *ions*. Consequently, the first event that *must* occur inside the mass spectrometer is the transformation of molecules into ions. This process is called *ionization* and it occurs in the first part of a mass spectrometer: the *ion source*.

Molecules can be small, like  $\text{CH}_4$ , large, or very large, like some biopolymers with molecular weights of millions of daltons. They can be organic, inorganic, polar, apolar, etc. Mass spectrometry can study all of them. However, one ionization technique cannot ionize all kinds of molecules but different ionization techniques are now available. Their choice is based on the chemico-physical properties of the molecule, such as molecular weight, polarity, thermal stability, etc.

Whilst for a molecule it is enough to specify its molecular weight (MW), this is not true for ions. In fact, an ion is defined by its mass ( $m$ ) and by its charge ( $z$ ). Both even-electron ions, like  $\text{H}_3\text{O}^+$ , and radical ions, i.e. radicals that carry an electric charge, like  $\text{CH}_4^{+\bullet}$ , can be formed in a mass spectrometer. With MS it is possible to study positive or negative ions: molecules with basic properties are easily protonated, while those having acidic character are more easily deprotonated.

## 2.3 Information that can be Obtained by Mass Spectrometry

A lot of information regarding identification, structural characterization, quantitation, gas phase ion chemistry and thermodynamics can be obtained by MS.

### 2.3.1 Identification and Structural Characterization of Unknowns

Just for a moment, imagine that your eyes are covered. You are dealing with an unknown object that has been placed into your hands. The first information you receive is the object's weight. According to this, you can discard wide classes of objects whose weight is totally different from that, and you can focus your attention on those whose weight is roughly similar to that of the object you are holding.

It is likely that when you have unknown compounds, such as those that can be extracted from an archaeological material, knowledge of their weight is important for their identification. MS can measure it. Hence, when you introduce a given compound into a mass spectrometer you can determine its molecular weight. Accordingly, you can restrict the number of possible compounds.

However, knowledge of only the molecular weight of a given molecule is not selective and specific information. Indeed, different objects with totally different shape, function, colour, etc., may have the same weight; a lot of molecules may even have the same molecular weight. For example, if the molecular weight is 100 Da, a lot of atomic compositions (i.e.  $C_6H_{12}O$ ,  $C_5H_8O_2$ ,  $C_5H_8S$ , ...) as well as several chemical structures are possible. It follows that molecular weight determination is *necessary* but not *sufficient* information for the identification of a given molecule.

Referring back to the last example, consider that the object falls from your hands and breaks. However, your eyes have now been uncovered. Now you can see not the object but its fragments. Note that each fragment is lighter than the entire object. By reassembling the fragments, finally you can see the object and its shape. Only at this stage can you *unambiguously* identify the object.

A MS experiment is similar to this example: owing to the determination of *both* the molecular weight *and* nature and weights of *fragment ions* it is possible to unambiguously identify a given molecule.

### 2.3.2 Quantitation

Once the analyte has been identified and characterized, it is possible to determine its quantity. This is important information in a lot of fields and in cultural heritage in particular. There are specific experimental set-ups for quantitative analysis, such as selected ion monitoring (SIM) and multiple reaction monitoring (MRM). By considering that MS is highly sensitive, it is possible to carry out quantitative determinations of compounds at trace level.[7,8]

### 2.3.3 Chemical Reactions and Thermochemistry

A mass spectrometer can be also used as a gas phase laboratory and a lot of reactions can be done inside it. Furthermore chemico-physical properties, such as proton affinity, the energetics of gas phase processes and many other thermochemical parameters can be

**Table 2.1** Information obtainable by mass spectrometry

Experiment	→	Information
Mass spectrum	→	Molecular weight, structural information
High resolution + accurate mass	→	Stoichiometry ( $C_nH_mO_w, \dots$ )
SIM, SRM, MRM	→	Quantitation
Tandem MS	→	Structural information, quantitation
Ion mobility	→	Analyte cross section, conformation
MS imaging	→	Analytes' mapping

SIM, selected ion monitoring; SRM, selected reaction monitoring; MRM, multiple reaction monitoring.

obtained by MS experiments. Although these are both very important and useful, these aspects are beyond the scope of the present chapter.

### 2.3.4 Summary of Information Obtainable by Mass Spectrometry

In addition to the information described above, a lot of other information can be obtained by MS. An overview is reported in Table 2.1. It is noteworthy that ion mobility and MS imaging are emerging fields of modern MS: the former allows the characterization of the *shape* (conformation) and *cross-section* of gas phase ions, while the latter provides *molecular mapping* of different analytes present in an object, such as organs, tissues and organisms. Applications to cultural heritage materials, such as ceramics, paintings, marble, statues, etc., might follow soon.

Some of the experimental approaches reported in Table 2.1 are described in this chapter.

## 2.4 The Mass Spectrometer

Before describing the single parts, let us examine the general features of a mass spectrometer (Figure 2.1). In every MS experiment the first step is the introduction of the sample into the mass spectrometer. It follows that the first part of every instrument is the *inlet system* that allows the introduction of the sample, generally molecules, into the mass spectrometer. There are different ways to introduce the sample, depending on its purity and properties.

You already know that MS studies ions. So, once molecules have been introduced inside the mass spectrometer, they must be ionized, i.e. transformed into *ions*. The ionization process occurs in the *ion source* by using an ionization technique. There are different ionization techniques depending on the physico-chemical properties of the molecules.

The ions thus produced are accelerated and driven from the source to the *analyzer* that separates them according to their  $m/z$  ratios. Finally, the *detector* reveals ions.

All mass spectrometers have different stages of pumping in order to maintain the analyzer and detector regions under high vacuum, i.e.  $10^{-7}$ – $10^{-8}$  torr or higher. Depending upon the ionization technique, the inlet system and the ion source must be/

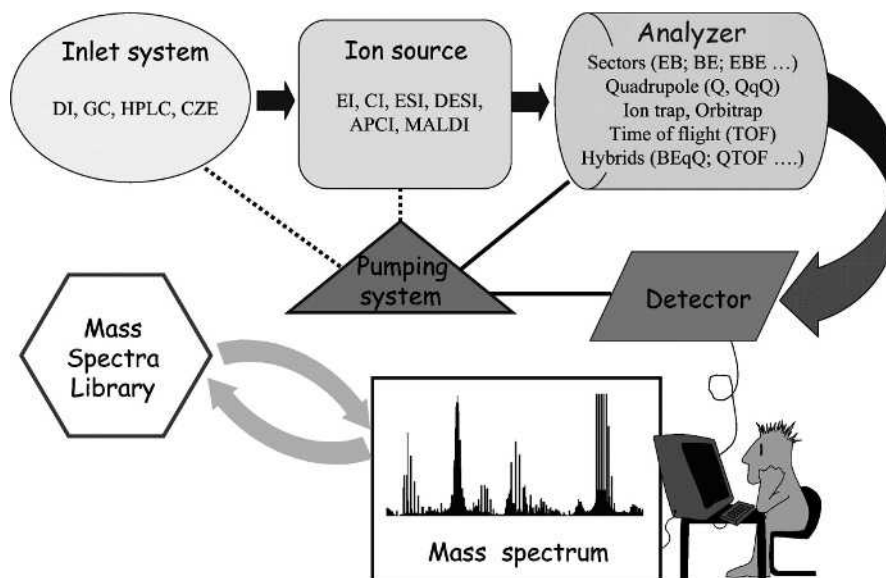


**Figure 2.1** Mass spectrometric approach. DI, direct inlet; GC, gas chromatography; HPLC, high performance liquid chromatography; CZE, capillary zone electrophoresis; EI, electron ionization; CI, chemical ionization; ESI, electrospray ionization; DESI, desorption electrospray ionization; APCI, atmospheric pressure chemical ionization; MALDI, matrix-assisted laser desorption ionization; B, magnetic analyzer; E, electrostatic analyzer

must not be/may be under vacuum. A schematic diagram of a mass spectrometer is shown in Figure 2.1.

The *mass spectrum* is the result of a MS experiment. It is a plot of relative abundances of the ions produced inside the mass spectrometer against their  $m/z$  ratios.

Once a mass spectrum has been obtained, it is possible to perform a library search, in different databases installed in the local computer or in remote servers through the Internet that can help in identification of unknowns.

## 2.5 Inlet System and Sample Introduction in a Mass Spectrometer

Generally it is not possible to introduce a material, e.g. a piece of ceramic, as it is, into a mass spectrometer: an appropriate sample preparation procedure, basically consisting of analytes extraction from the substrates and in their preliminary purification, precedes the mass spectrometric analysis.

There are several devices for introducing a sample into a mass spectrometer. Their choice is based on the purity and chemico-physical properties of the sample.

The simplest way is the introduction of a sample directly in the ion source through a direct inlet whose design depends upon the ionization technique used. As an example,

if electrospray is used, the direct introduction of the sample in the ion source is achieved through flow injection of a solution. In other cases, such as for electron or chemical ionization, the simplest direct inlet device consists of a capillary in which one drop of the solution of the analyte is deposited in it. This capillary is supported on a probe that it is introduced directly into the ion source. More complex direct inlets are constituted by filaments of different metals on which a drop of the solution is deposited. The filament, supported on a probe, is introduced into the ion source and a current is applied to it. It causes a rapid heating of the sample thus allowing its evaporation to the gas phase. These devices are known by different acronyms, such as direct temperature mass spectrometry (DTMS)[9], direct inlet mass spectrometry (DI-MS)[10] and direct exposure-mass spectrometry (DE-MS)[11]. These techniques are useful and rapid for obtaining a fingerprint of solid samples, such as archaeological materials.

If different analytes are introduced directly into the mass spectrometer at the same time the result will be a mass spectrum formed by the superimposition of each mass spectrum of each component of the mixture. This will be not easily interpretable and will be meaningless.

However, one generally has to identify, characterize and quantify analytes that are present in complex mixtures. This is the case in the analysis of extracts obtained from cultural heritage materials, such as ceramics, paintings, monuments, etc. In these cases separation methods are required prior the mass analysis so that several components arrive in the ion source one at a time. It follows that MS must be coupled to a separation technique for analysis of mixtures. This *coupling* is generally *on-line* and it allows the combination of complementary features: high sensitivity, selectivity and specificity offered by MS with high performance in separation, typical of a separation technique that often cannot unambiguously identify an unknown analyte.

A summary of the available couplings of MS with separation techniques is given in Table 2.2.

**Table 2.2** *Couplings of mass spectrometry with separation techniques for analysis of mixtures*

Separation technique	MS ionization method <sup>a</sup>	Comment
Gas chromatography (GC)	El	• Separation of mixtures of volatile and gas phase stable compounds
	CI	• Derivatization is often required
High performance liquid chromatography (HPLC)	ESI, APCI, APPI	• Separation of polar, ionic, nonvolatile, high molecular weight and thermally labile analytes
		• Buffer restriction and appropriate flow rates
Capillary zone electrophoresis (CZE)	ESI	<ul style="list-style-type: none"> <li>• Separation of a wide variety of polar and charged species at high sensitivity</li> <li>• Relatively high chemical background</li> <li>• Proper safety interlocks</li> </ul>

<sup>a</sup> APPI, atmospheric pressure photoionization.

## 2.6 The Ion Source and Ionization Techniques

Through a direct inlet or a separation technique the sample is introduced into the ion source (the region in which the ionization occurs, i.e. the mass spectrometer region where a neutral molecule is transformed into an *ion*). The design of the ion source is dependent on the ionization technique.

A wide variety of ionization techniques is nowadays available and one can choose the most suitable on the basis of different factors, such as the chemico-physical properties of the analyte under investigation, its molecular weight, polarity, etc.

There are different ways to ionize a molecule ( $M$ , Scheme 2.1): extraction of an electron from gas phase molecules ( $M_g$ ), yielding radical cations [Equation (2.1)], as occurs in electron ionization, or addition of one [Equation (2.2); CI, MALDI, etc.)] or more protons [Equation (2.3); ESI]. Similarly, molecules can be ionized by the formation of negative ions due to single [Equation (2.4)] or multiple proton abstraction [Equation (2.5)].

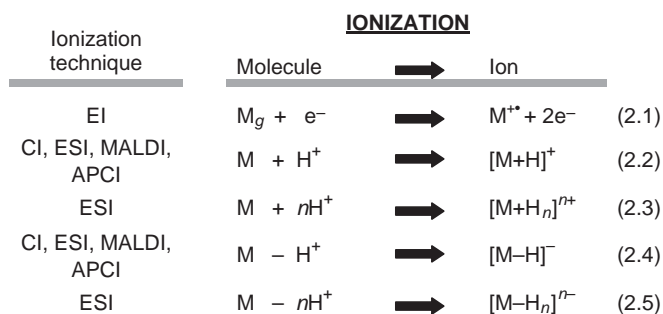
EI and CI are the most commonly used ionization techniques for the analysis of volatile, nonpolar, low molecular weight (up to 700–900 Da) and thermally stable compounds. These techniques can be also useful for studying non highly volatile molecules, but in these cases, preliminary chemical reactions, such as derivatization, have to be performed in order to obtain derivatives with increased volatility.

The introduction and development of more recent ionization techniques, such as ESI, APCI and MALDI, have allowed the study of nonvolatile and thermally unstable compounds.

A classification of the main ionization techniques used in the study of samples from cultural heritage is reported in Table 2.3. Each ionization method will be illustrated in detail in the following sections of this chapter.

### 2.6.1 Gas Phase Ionization Techniques

Gas phase ionization techniques ionize the molecules that are in the gas phase. It is possible to bring molecules to the gas phase only of compounds that are volatile. To fulfil this requirement, a molecule must be nonpolar, not too big (molecular weight <1000 Da) and thermally stable, i.e. it must not decompose when heated. Although these are harsh



**Scheme 2.1** Main ionization reactions occurring in mass spectrometry



**Table 2.3** Classification of the main ionization techniques used in the study of samples from cultural heritage

Ionization technique	Analyte properties	Working phase	Ionizing agent	General features
Electron ionization (EI)	Volatile, nonpolar, low MW, thermostable molecules	Gas	Electrons (eV)	Hard technique, odd-electron ions, fragments
Chemical ionization (CI)			Reagent gas	Soft technique, protonated/deprotonated molecules, even-electron ions, no fragments, adducts
Atmospheric pressure chemical ionization (APCI)	Low to medium high MW, medium polar to polar compounds	Liquid	Corona discharge	Spray technique, even-electron ions, scarce fragmentation
Electrospray ionization (ESI)	Polar, low to very high MW molecules	Liquid	Electric field (kV)	Spray soft technique, even-electron ions, multicharged ions, no fragments, adducts
Desorption electrospray ionization (DESI)	Polar, low to medium high MW molecules	Solid	Primary ions	Desorption soft technique, protonated/deprotonated molecules, even-electron ions, no fragments. Suitable for imaging mass spectrometry
Matrix assisted laser desorption ionization (MALDI)	Polar, low to very high MW molecules	Solid	Photons (laser beam)	Desorption soft technique, protonated/deprotonated molecules, even-electron ions, no fragments, adducts. Suitable for imaging mass spectrometry

restrictions, the range of volatile molecules is very wide, encompassing large amounts of analytes, most being of interest from the cultural heritage perspective.

The most important gas phase ionization techniques are electron ionization and chemical ionization. The latter will be described in Section 2.6.2.

### 2.6.1.1 Electron Ionization

EI is probably the most used ionization technique in the study of cultural heritage. In EI the ionization of a molecule is produced by electrons. Often this technique and its acronym EI are referred as ‘electron impact’, but this terminology is inappropriate. The term ‘impact’ implies a crash, a collision between two or more objects. In the case of EI no such impact or crash occurs.

The EI process might be simplified as follows. Imagine that a girl with long hair is waiting for a train on a station platform. In the meantime another train passes close to her at speed without stopping. While the train is passing the girl's long hair is disturbed in the air: in fact, the energy of the train is partially transferred to the air and, in turn, the air transfers part of this energy to the hair so that the hair moves.

An analogous process occurs in EI: an electron beam with an appropriate energy passes *in proximity* to the gas phase molecules and transfers part of its energy to them. If the transferred energy is enough high, an electron is extruded from the molecule.

The EI source is formed by a tungsten or rhenium filament, an anode, an ion repeller, a magnet, and a series of lenses for extracting, focusing and accelerating the ions formed (Figure 2.2).

The electron beam, formed by heating the filament, crosses the source attracted by the anode located in front of the filament. Gas phase sample molecules, introduced in the source (generally heated at 200°C or more), interact with the electron beam. As the filament–anode distance is short (1–3 cm), the electron–molecule interaction time should be extremely short. To increase it, one pole of a magnet is put just behind the filament and the other behind the anode. The presence of the magnet causes the trajectory of the electrons to become helicoidal so that the distance that each electron covers increases greatly. As a consequence, the electron–molecule interaction time becomes longer thus causing a high ionization yield. Once the ions are formed, they are pushed out of the source towards the analyzer by the action of the extracting, focusing and accelerating lenses.

It has been estimated that the electron–molecule interaction occurs in a very short time ( $\sim 10^{-16}$  s) and its product is the ejection of one electron from the molecule according to Equation. (2.1). The ions so formed constitute the *molecular ion* ( $M^{+\bullet}$ ). It is produced directly from the molecule but it is a positive ion. In fact, an electron has a negative charge and its removal from a neutral species causes the formation of a positively charged ion. In addition, molecules are neutral species with an even number of electrons that are paired two by two in the orbitals. When one of these is removed, there is a remaining odd number,

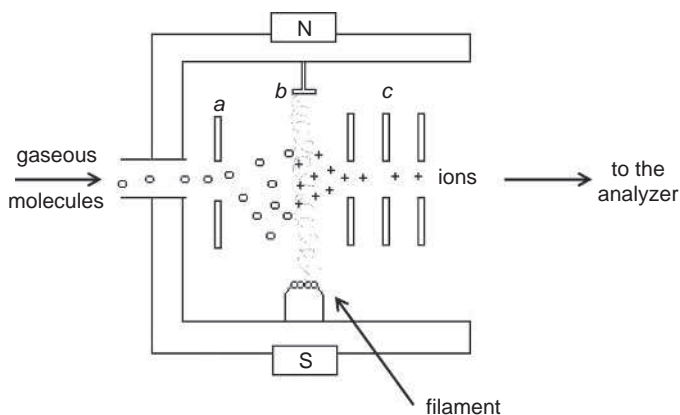


**Figure 2.2** Schematic view of the electron ionization source. *a*, Ion repeller; *b*, anode; *c*, acceleration and focalization plates; *N*, *S*, magnet poles

and one electron is unpaired. Species with an unpaired electron are called radicals. It follows that the molecular ion is both a positively charged ion (or cation) and a radical, i.e. it is a 'radical cation'. These two features appear in the notation  $M^{+\bullet}$ , where the plus sign indicates the positive charge and the dot the unpaired electron.

The electron removal from a molecule is not a spontaneous process but it requires an amount of energy corresponding to the first ionization potential (IP). For most organic molecules the value is roughly around 10 eV. It has become convention to use a standard potential of 70 eV applied to the filament emitting electrons. This value is much higher than the IP values, but there are a lot of steps preceding the energy transfer to the gaseous molecules, and in each step part of the energy is lost.

In any case, an excess of energy, small or large depending on the IP of the molecule, is deposited on the molecular ion. It follows that  $M^{+\bullet}$  is in an excited state and, like everything in nature, it tends to return to its ground state by dissipating its excess energy. This occurs through *fragmentation* that consists of the breaking of covalent bonds from which *fragment ions* originate. It follows that a mass spectrum obtained by EI is characterized by the presence of fragment ions, that give important information for the structural characterization of the analyte (see above).

The EI technique is well established, sensitive and suitable for qualitative and quantitative applications.

## 2.6.2 'Soft' Ionization Techniques

The term *soft* is opposite to *hard* and both these terms are used to refer to the amount of energy deposited onto the molecule during the ionization process. In the case of EI (see above) a large amount of energy is deposited onto the molecular ion. It causes abundant fragmentation and structural information can be obtained. However, if the amount of excess energy is too large, the molecular ion might be undetectable thus not allowing molecular weight determination of the analyte.

In *soft* ionization methods the excess energy deposited onto the ionized molecule is very small and stable even-electron ions are formed. This leads to easy determination of the molecular weight of the analyte, but as fragmentation is absent or it occurs to a very low extent, structural information is missing in the mass spectrum. However, one can obtain structural information by causing ion fragmentation out of the source by means of tandem mass spectrometry experiments (see below).

Owing to *soft* conditions, the mass spectra obtained by this kind of ionization techniques are also characterized by the presence of *adduct* ions, i.e. ionic species formed by weak interactions between the ions and other chemical species (see below).

*Soft* ionization methods can be classified into different groups: (a) those occurring in the gas phase; (b) spray ionization techniques; (c) desorption ionization techniques.

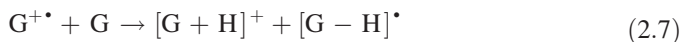
### 2.6.2.1 Gas Phase Soft Ionization: Chemical Ionization (CI)

CI was described for the first time by Munson and Field in 1966.[12] It soon became a widely used technique mainly due to its ability to provide molecular weight information in those cases where it was not possible using EI.

The CI technique requires an excess of reagent gas to be present in the ion source that is maintained at a pressure ranging from 1 torr, for conventional CI sources, to a few

microtorr, for internal ion trap sources. The most commonly used reagents are isobutane, methane and ammonia but liquids, such as acetonitrile, methanol, acetone, amines and ethers, can also be used.

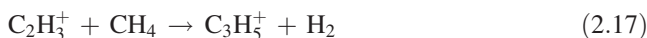
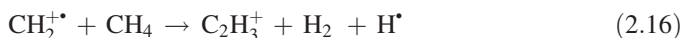
The processes occurring in CI are shown in Equations (2.6)–(2.8):



where G is the reagent gas, M is the analyte molecules and PA is the gas phase proton affinity.

The EI of the reagent gas (G) produces molecular ions  $G^{+\bullet}$  [Equation (2.6)] that can react with a reagent gas molecule yielding even-electron  $[G + H]^+$  reagent ions [Equation (2.7)]. The latter cause the ionization of the analyte molecules (M): if the gas phase proton affinity of M is greater than that of G, a proton transfer from  $[G+H]^+$  to M occurs. In this way, *protonated molecules* (sometimes referred to as *pseudomolecular* or *quasimolecular ions*) of the analyte, i.e.  $[M + H]^+$ , are formed [Equation (2.8)]. It follows that the protonated molecules have a mass shift +1 with respect to the molecular weight of the molecule.

It has to be considered that, in addition to its molecular ion, the EI of the reagent gas G produces further species due to ion-molecule reactions occurring inside the ion source. The main ionic species produced when methane is used as reagent gas are summarized in Equations (2.9)–(2.18).



For example, the species  $CH_3^+$  can react with neutral methane thus yielding the cation  $C_2H_5^+$  [Equation (2.12)]. In turn, the latter can react with the analyte yielding an addition product  $[M + (C_2H_5)]^+$  whose  $m/z$  value is 29 u higher than the molecular weight of the

analyte [Equation (2.13)]. Similarly, the species  $\text{C}_3\text{H}_7^+$  and  $\text{C}_3\text{H}_5^+$  can add to the analyte yielding ions  $[\text{M} + 43]^+$  [Equation (2.15)] and  $[\text{M} + 41]^+$  [Equation (2.18)], respectively.

Other gas phase reactions can occur under CI conditions. They are anion abstraction, charge exchange and electrophilic addition. Furthermore, CI can be used to produce negative ions, such as  $[\text{M}-\text{H}]^-$  or radical anions  $\text{M}^{\cdot-}$ . These reactions are beyond the scope of this chapter and more specialized literature is recommended.[13]

### 2.6.2.2 Spray Ionization Techniques

The ionization techniques described above occur in ion sources that are maintained under high vacuum. In contrast, spray ionization techniques operate at atmospheric pressure: a solution spraying from a capillary is ionized at atmospheric pressure and the ions produced are driven into the high vacuum of the mass analyzer where they are separated. The use of spray and desorption ionizations does not require volatilization of the sample before ionization. This means that all these techniques can ionize nonvolatile, polar and large to very large compounds.

The most important techniques belonging to this class are electrospray ionization (ESI), atmospheric pressure chemical ionization (APCI) and, more recently, atmospheric pressure photoionization (APPI). At present the latter does not have applications in cultural heritage, so it will be not described here.

*Electrospray ionization.* Although the electrospray phenomenon was known since the beginning of the twentieth century, and the first description of its principle was published in 1968,[14] the breakthrough for ESI came in the mid 1980s from work by John Fenn[4] and a Russian research group.[15] (Fenn was jointly awarded the Nobel Prize for Chemistry in 2002.)

The term *electrospray* reveals important features of the process: first of all, and differently from the ionization methods described so far, the ionization occurs on a *spray*. This is produced by forcing a liquid to pass through a capillary, as occurs with perfume dispensers. This causes the formation of millions and millions of small droplets. The first part of the ionization's term contains further important information: an electric field (3–5 kV) is applied to the capillary and it causes ionization (Figure 2.3). The overall effect is the formation of small liquid-charged droplets from which gas phase ions are formed. ESI is governed by a large number of chemical and physical parameters that

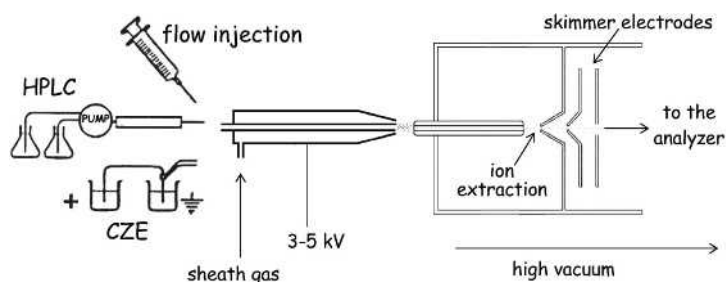


Figure 2.3 Electrospray ion source

together determine the quality of the process. At the exit of the capillary, the liquid assumes a characteristic shape, called a Taylor cone, from which the jet of charged particles emanates. There are two main theories to explain the electrospray process: the charge residue model (CRM)[14] and the ion evaporation model (IEM).[16]

According to the former, during their travel from the exit capillary to the entrance of the high vacuum region, that are 1–3 cm apart, the charged droplets, each containing ions and solvent molecules, undergo evaporation of the solvent with a consequent reduction of their size and increase of the field at their surface. This causes a ‘Coulomb explosion’, due to high charge density, and ion escape occurs. The ions so generated are transferred to the high vacuum region of the mass spectrometer and are driven to the mass analyzer.

ESI can be used to produce protonation or deprotonation of the analyte. A requisite of a molecule to be ionized by ESI is its polarity: nonpolar compounds cannot be ionized by this technique.

ESI mass spectra are characterized by protonated/deprotonated molecules and adduct ions, i.e.  $[M + H]^+$ ,  $[M + Na]^+$ ,  $[M + HCOO]^-$ . A key feature of the electrospray process is the formation of *multiply charged ions*. An empirical rule states that a molecule generally takes a charge every thousand units of molecular weight. This allows the measurement of very high molecular weight molecules at low  $m/z$  values. For example, if the analyte has a molecular weight of 20 000 Da, and if it has twenty protonable sites,  $[M + 20H]^{20+}$  ions at  $m/z (20\,000 + 20)/20 = 1001$ , which fall in the  $m/z$  range available on all analyzers, will be formed (see below).

**Atmospheric Pressure Chemical Ionization.** As its name reveals, APCI[16] is a CI carried out at atmospheric pressure instead of under vacuum, as occurs for classical CI. As for ESI, the sample must be in a solution that is continuously flowing into the APCI source (flow rate between 0.2 and 2 ml min<sup>-1</sup>). The solution passes through a pneumatic nebulizer and is desolvated in a heated quartz tube or heating block, thus producing vaporization of solvent and analyte molecules (Figure 2.4).

Since APCI is a chemical ionization, it needs a gas. Indeed, a nebulising gas (generally nitrogen) is introduced into the source. The gas molecules are ionized by a corona discharge (analogous to the filament used in CI) thus forming the primary ions, mainly composed of  $N_2^{+\bullet}$  and  $N_4^{+\bullet}$ . In turn, the latter ionize the vaporized solvent molecules by

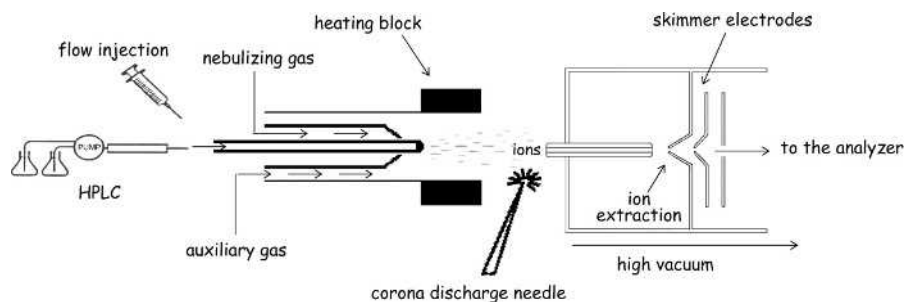


**Figure 2.4** The APCI source

proton transfer, so forming  $\text{H}_3\text{O}^+$ ,  $\text{NH}_4^+$  and  $(\text{H}_2\text{O})_n\text{H}^+$ . The latter are reactant ions that ionize the sample molecules.

APCI can be used for polar and relatively polar compounds with molecular weights up to about 100–1500 Da and produces singly charged ions with fragmentation to some extent.

### 2.6.2.3 Desorption Ionization Techniques

The term ‘desorption ionization’ indicates those ionization techniques in which the production of ions is based on a desorption process. This consists of the rapid addition of energy to a sample in a condensed phase (i.e. liquid or solid) with subsequent production and emission of stable ions in the gas phase. These are generally even electron species that fragment only to a limited extent. The development of desorption methods has amplified the impact and utility of MS in a lot of fields, such as biology, biochemistry and proteomics.

Over the years, a lot of desorption ionization techniques have been introduced to MS, such as plasma desorption, field desorption, laser desorption, secondary ion mass spectrometry, fast atom bombardment, matrix assisted laser desorption and desorption electrospray ionization. Most of them are actually no longer used. In the following paragraphs, both matrix assisted laser desorption (MALDI) and desorption electrospray ionization (DESI) will be discussed.

*Matrix Assisted Laser Desorption Ionization.* During the development of MS, a lot of studies have been devoted to the use of laser light as an energy source for ionizing molecules. As a result, in the mid 1980s MALDI[5] was introduced and soon applied to the study of large molecules.[18] Koichi Tanaka was jointly awarded the Nobel Prize for Chemistry in 2002 for the study of large biomolecules by MALDI.

In contrast to the other ion sources, the MALDI source may operate under high vacuum or under atmospheric pressure. In the latter case the acronym AP-MALDI (atmospheric pressure matrix assisted laser desorption ionization) is used.

A lot of features of MALDI are conveyed by its name: it is a desorption ionization, produced by a laser beam, and assisted by a matrix (Figure 2.5). The analyte (1 pmol or less) is mixed with a suitable matrix in a 1:1000 or higher molar ratio. The matrix is composed of a compound with a strong absorption at the wavelength of the laser used. These two factors, matrix excess and its strong absorption, ensure that the energy from the laser pulse is absorbed by the matrix and not by the analyte, thus avoiding its decomposition. Nicotinic acid, sinapinic acid (SA), 2,5-dihydroxy benzoic acid (2,5-DHB) and 2-(4-hydroxyphenylazo)benzoic acid (HABA) are some of the most commonly used matrices for MALDI.

Solutions of the analyte and the matrix (from nanolitre to microlitre amounts) are deposited or spotted on a flat metal target plate. Owing to evaporation of the solvent, matrix and analyte co-crystallize. Short laser pulses (1–20 ns) bombard the solid and cause the sample and matrix to be volatilized. The formation of ions occurs by acid–base reaction between the ionized matrix molecules and the analyte molecules (Figure 2.5).

The product of the desorption process is the formation of singly charged (protonated or deprotonated) molecules of the analyte, with dimensions ranging from a few hundred daltons to several hundred thousand daltons. It follows that, contrary to ESI, in the study of

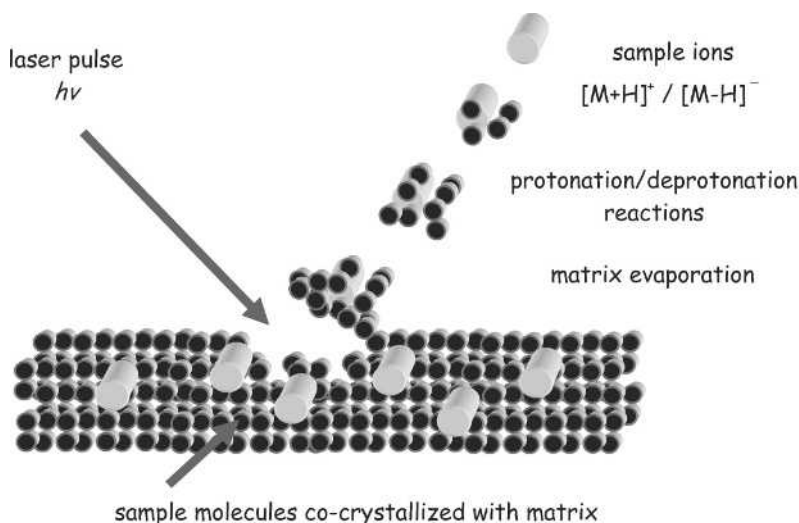


**Figure 2.5** Schematic view of MALDI

‘elephant’ molecules by MALDI, analyzers with very high  $m/z$  ranges are needed. The only analyzer having this feature is the time of flight (TOF) analyzer (see below). For this reason, the coupling MALDI-TOF is widely used.

**Desorption Electrospray Ionization (DESI).** DESI is a novel *gentle* ionization method for surface analysis (Figure 2.6).[19,20] Like classical ESI, it operates at atmospheric pressure. No sample preparation is required. A solvent passes through the capillary of the electrospray source; charged droplets are produced (primary ions) and they are directed to a solid sample. Their impact with the surface causes sample molecules to be ionized and

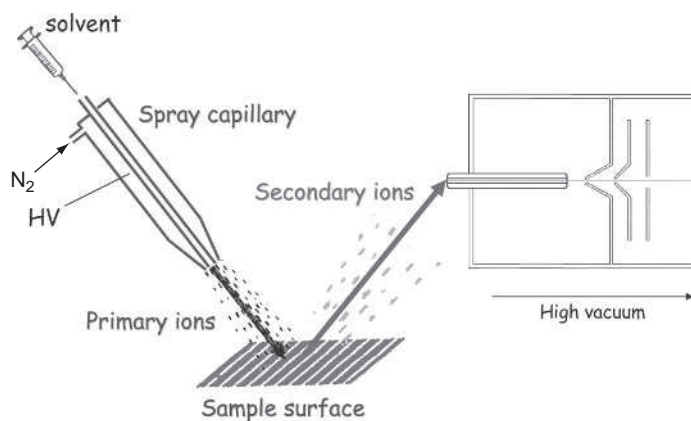


**Figure 2.6** Schematic diagram of a DESI source



the formation of gas phase ions (secondary ions) that enter the high vacuum region of the analyzer. DESI mass spectra are similar to those obtained by classical ESI. A lot of experimental variables, such as nature of primary ions, gas flow rate, incident spray angle on the surface, and nature of the surface, have to be evaluated and optimized for high quality results.

Using DESI, high quality mass spectra have already been obtained for a wide range of molecules by directly interrogating a diverse range of surfaces. It might be also applied to characterize cultural heritage material.

### 2.6.3 Ionization Techniques for Inorganic Materials

There is a branch of MS specially designed for dealing with the analysis of inorganic materials.[21,22] Different specific ionization techniques, such as inductively coupled plasma mass spectrometry (ICP-MS),[23] glow discharge mass spectrometry (GD-MS)[24] and secondary ion mass spectrometry (SIMS),[25] are available and they are widely used in cultural heritage applications. Their description is beyond the scope of this chapter.

## 2.7 The Analyzer

Once the ions are formed in the ion source, they are accelerated towards the mass analyzer where separation according to their  $m/z$  ratio occurs. Before describing the main analyzers, it is better to consider one feature common to all of them: the resolution.

### 2.7.1 Resolution

Resolution or resolving power is the ability of a mass spectrometer, and in particular of its analyzer system, to separate ions with different  $m/z$  ratios. An example of mass spectra obtained at different resolutions is reported in Figure 2.7: by increasing the resolution the peak shape becomes more and more narrow thus allowing the separation of ions with their  $m/z$  values differing in decimals ( $10^{-1}$ – $10^{-3}$ ).

When resolution refers to two peaks it can be defined by Equation (2.19) (Figure 2.8):

$$R = \frac{m}{\Delta m} \quad (2.19)$$

where  $m$  is the nominal  $m/z$  value of the ions to be separated and  $\Delta m$  is their  $m/z$  difference calculated by considering the exact monoisotopic masses. Two peaks are considered to be resolved also in the presence of a valley, of a specified fraction of either peak height, between them (Figure 2.8a). Resolution can be also determined by considering a single peak by using its width  $\Delta m$  at a given height. If the peak width is taken at 50% of its height, the resolution is defined as the full width at half maximum (FWHM, Figure 2.8b).

The possibility to have well resolved peaks allows the measurement of the accurate mass of an ion, i.e.  $m/z$  values significant to four decimals, and to calculate its elemental composition.

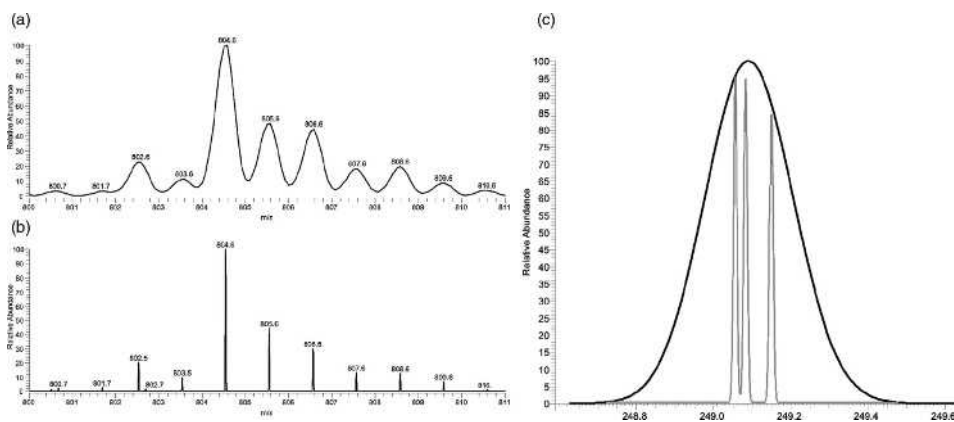


**Figure 2.7** Mass spectra recorded at different resolutions. Mass spectrum obtained by a two-dimensional ion trap at low resolution (a) and by an Orbitrap at resolving power 50 000 (b). Mass spectrum of a mixture of three isobaric species  $[C_{19}H_7N]^+$ ,  $[C_{20}H_9]^+$ ,  $[C_{13}H_{19}N_3O_2]^+$  obtained at low resolution (black line) and at resolving power 50 000 (grey line) (c). It is noteworthy that at low resolution the three peaks are completely unresolved

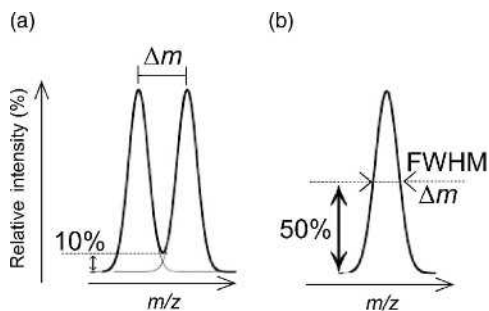


**Figure 2.8** Resolution at 10% valley (a) and at full width at half maximum (FWHM, b)

### 2.7.2 Analysis of Ions in Time and in Space

Based on the main methods of ion separation, analyzers can be classified into two main groups: those based on the separation of ions in space or the separation of ions in time. The former separate ions while they are travelling over a distance (some metres in the case of sector instruments, centimetres in the quadrupole) (Table 2.4). In contrast, when separation occurs in time, ions are confined in a small region of space and their separation occurs by varying some parameters (Table 2.4).

Magnetic and electrostatic sectors, quadrupole, and time of flight analyzers belong to the first group, while ion trap, Orbitrap and Fourier transform ion cyclotron resonance analyzers separate ions in time.

**Table 2.4** Mass spectrometry analyzers and their features

Ion separation in space					
Analyzer	Force	Separation based on	$m/z$ range	Resolution	Mass accuracy
Double focusing (EB, BE)	Magnetic field + electrostatic field	Ion momentum + kinetic energy	10 000	10 000	<10 ppm
Quadrupole (Q)	Electric field + radiofrequency	Ion stability/instability	2000-4000	Unit (0.2 u FWHM)	No (>20 ppm)
Time of flight (TOF)		Velocity	>100 000	>10 000	2–5 ppm
Ion separation in time					
Analyzer	Force	Separation based on	$m/z$ range	Resolution	Mass accuracy
Ion trap	Electric field + radiofrequency	Frequency of ion orbits	10 000	<500	No
Fourier transform ion cyclotron resonance (FT-ICR)	Magnetic field + electric field + radiofrequency	Frequency of ion orbits	>10 000	>100 000	<1 ppm
Orbitrap	Electric field	Frequency of harmonic oscillation	<6000	<150 000	1–5 ppm

The choice of an analyzer depends on the kind of studies and applications that will be carried out:  $m/z$  range, resolution, mass accuracy, scan speed, number of mass separations, are some of the parameters that have to be considered.

### 2.7.3 Ion Separation in Space

#### 2.7.3.1 Magnetic and Electrostatic Fields: Double Focusing Mass Spectrometers

The magnet (B) was the first analyzer introduced to MS and it separates ions according to their momentum. It is generally coupled to an electrostatic sector (E) that separates ions according to their kinetic energy. The presence of both of these analyzers allows a double focalization of an ion beam to be obtained: one according to momentum, and consequently to  $m/z$  values, the other according to kinetic energy. The uses of double focusing mass spectrometers range from the acquisition of a simple mass spectrum to the possibility of two steps of mass separation, high resolution and accurate mass measurements. Different factors, mainly their complex needs, high maintenance and high cost, have restricted double focusing mass spectrometers to very specific applications, such as in the environmental field.

### 2.7.3.2 The Quadrupole Mass Filter

The quadrupole mass filter (Q, Figure 2.9) is composed of four parallel cylindrical, or ideally hyperbolic, rods to which a direct current (DC) and a radiofrequency (RF) are applied. The separation of ions according to their  $m/z$  ratio occurs by scanning simultaneously DC and RF, but maintaining their ratio to be constant. For a given value of DC and RF only ions with a given  $m/z$  value will be able to pass through the entire quadrupole and they will be transmitted to the detector. By changing DC and RF another family of resonant ions will be transmitted and so on. A complete scan allows all the  $m/z$  values in a given range to be analysed.

Quadrupole mass spectrometers are generally bench-top instruments, of relatively low cost, easy to manage and widely used for routine analysis.

### 2.7.3.3 Time of Flight Analyzer

The TOF analyzer separates ions according to the time they spend travelling inside a tube, i.e. the flight tube (Figure 2.10).

The ion beam formed in the source is accelerated towards the flight tube. Since the kinetic energy ( $E_k$ ) is related to the mass ( $m$ ) by Equation (2.20), a charged species with high molecular weight will take more time than a low molecular weight compound to reach the detector.

$$E_k = 1/2 mv^2 \quad (2.20)$$

where  $v$  is velocity.

From the flight time it is possible to determine the  $m/z$  ratios of the ions.

Although the first generation of TOF analyzers were formed by just a drift tube and had low resolution (Figure 2.10a), many improvements have been made over the years. In particular, the introduction of a 'reflectron', located at the end of the flight tube, improved the TOF performances a lot. In fact, once accelerated in the source, ions with the same  $m/z$  value do not have exactly the same kinetic energy. Thus they arrive at the detector at

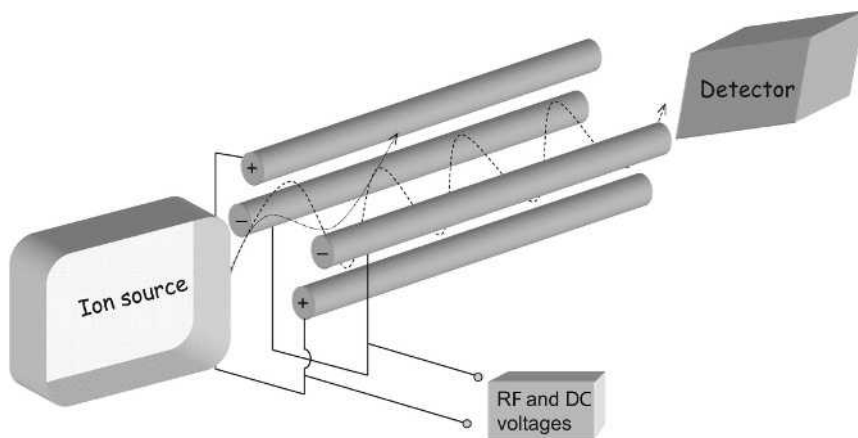


**Figure 2.9** The quadrupole analyzer

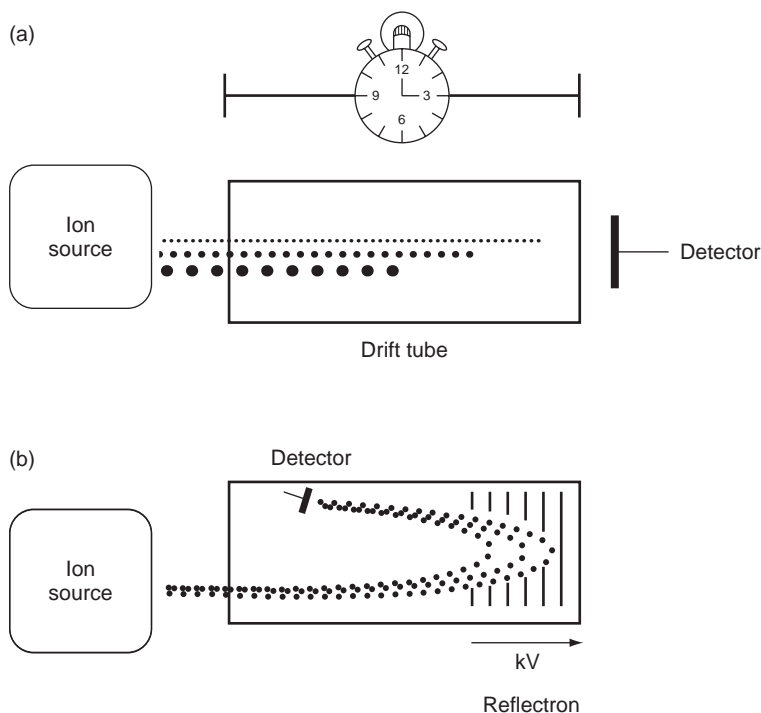


**Figure 2.10** Time of flight analyzer: drift tube (a) and reflectron (b)

different times, causing peak broadening and a consequent low resolution. The reflectron consists of a series of electrostatic lenses with increasing potential and provides compensation for the energy spread of the ion beam (Figure 2.10b). In fact, ions with high kinetic energy are able to penetrate deep into the electric field generated by the lenses and consequently they cover a longer distance. In contrast, ions with the same  $m/z$  values, but with lower kinetic energy, penetrate to a less extent in the reflectron and they cover a shorter distance. As a consequence, all ions having the same  $m/z$  value will arrive at the same time at the detector yielding a narrow peak and increasing resolution.

The great advantage of the TOF analyzer is that it has no restriction on the  $m/z$  range, being able to analyze ions with  $m/z$  values ranging from a few hundred to 500000 and higher. This is an important feature for its coupling with MALDI in the study of large molecules. In fact, as ions produced by MALDI are generally singly charged species, their  $m/z$  values can be extremely high and an analyzer able to explore such high  $m/z$  ranges, i.e. TOF, is needed. Owing to its scan speed, high resolution and mass accuracy capabilities, TOF is currently coupled with all ionization techniques.

## 2.7.4 Ion Separation in Time

### 2.7.4.1 Three- and Two-Dimensional Ion Traps

The ion trap is one of the most recently introduced analyzers. It is strictly related to the quadrupole mass filter and it uses the same forces of the quadrupole analyzer, i.e. electric

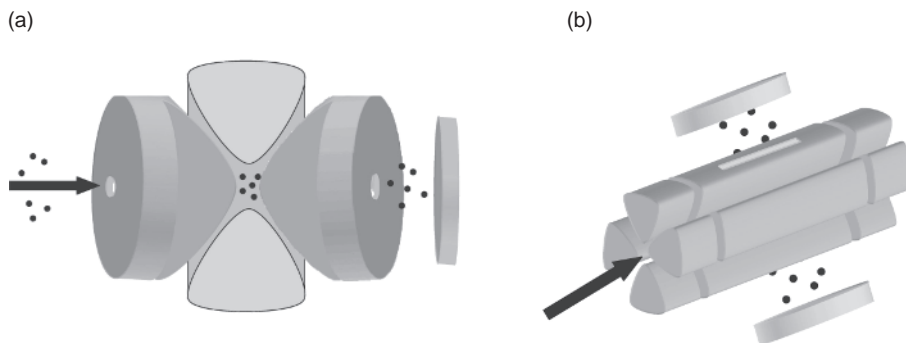


**Figure 2.11** Three-dimensional (a) and linear (b) ion trap mass analyzers. Arrows indicate the entrance of ions from the source. Detectors are depicted as plates

field and radiofrequency. According to the movement of ions inside them, ion traps can be divided into two groups: three- and two-dimensional (linear) ion traps. In the former, ions, that are confined and maintained near the centre of the ion trap, have complex movements in three dimensions, like bees in the sky. However, in linear ion traps, ion movements are almost in a two-dimensional plane, like a snake on land.

A three-dimensional ion trap is formed by three electrodes, two end caps and a ring electrode; in the linear ion trap different electrodes form each of the four edges (Figure 2.11).

The ions introduced into the trap are maintained on stable orbits applying DC and RF potential to the electrodes. To separate ions, according to their  $m/z$ , a RF scan is made. While the RF amplitude increases, ions with higher  $m/z$  values are destabilized and they leave the ion trap moving towards the detector.

Ion trap mass spectrometers are widely used and can be easily interfaced with all the ionization techniques.

One of the most interesting aspects of ion trap mass spectrometers is represented by the possibility of carrying out multi mass separation steps with only one analyzer (see Section 2.9).

#### 2.7.4.2 *Analyzers with Fourier Transform Treatment of the Signal*

FT-ICR and the Orbitrap belong to this group. In these analyzers the  $m/z$  values of the ions are not directly measured, but they are obtained by Fourier transform treatment of the signal (Figure 2.12).

*The Orbitrap.* The Orbitrap analyzer,[26] invented by Alexander Makarov, has been defined by the company that commercially produces it as ‘the first totally new mass analyzer to be introduced to the market in more than 20 years’. Its name recalls the concept of trapping ions. Indeed, ions are trapped in an electrostatic field produced by two electrodes: a central spindle-shaped and an outer barrel-like electrode. Ions are moving in harmonic, complex spiral-like movements around the central electrode while shuttling back and forth over its long axis in harmonic motion with frequencies

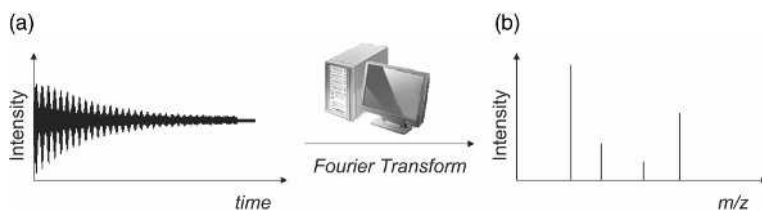


**Figure 2.12** Time-domain free-ion decay signal (a). Fourier-transformed mass spectrum (b)

dependent only on their  $m/z$  values (Figure 2.13). The latter can be determined by Fourier transform treatment of the signal. Note that, in contrast to other trapping analyzers, neither RF nor a magnet field are used. This means that the Orbitrap is simple to use and easily maintained.

The Orbitrap allows very high resolution to be achieved (the resolving power in commercial instruments is 100 000, rivalling that of FT-ICR instruments) and routine mass measurement accuracies less than 2 ppm. It finds applications in many fields, such as biology, proteomics, food chemistry and cultural heritage.

*Fourier Transform Ion Cyclotron Resonance.* The FT-ICR analyzer is based on the interaction of a charged species with an external magnetic field produced by superconducting magnets. A charged species subject to a magnetic field covers a circular trajectory. The rotational frequency of a certain ion on this orbit is called the ‘natural cyclotronic frequency’ and it is dependent on the magnetic field and on the  $m/z$  ratio of the ion. An additional RF is applied and the net result is a spiral motion. To obtain the mass spectrum the RF is scanned while the magnetic field is maintained constant.

In FT-ICR mass spectrometers, ion isolation and detection occur in the same region. In fact all ions coming from the source are simultaneously excited applying a RF pulse of a

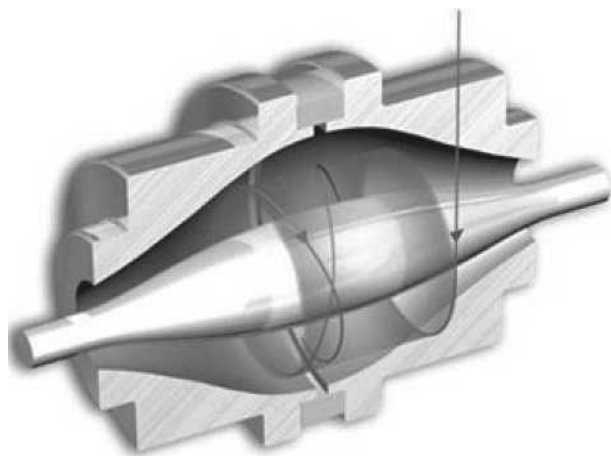


**Figure 2.13** The Orbitrap analyzer. From the Thermo web site (<http://www.thermo.com>)

large wide band. The resulting signal is then converted by Fourier transform to obtain the mass spectrum.

The main feature of this analyzer is its extremely high resolution. However, owing to the difficulty of operation and its very high cost, the FT-ICR analyzer cannot be used for routine purposes.

## 2.8 Detector

Once ions have been produced and analysed they must be detected. Indeed, the detector is the final part of a mass spectrometer. At the start of MS, detectors were composed of a fluorescent screen or a photographic plate; the modern instruments are equipped with detectors able to transform the signal produced by the ion beam into an electric current that is transmitted to the data system.

Actually there is a variety of different types of detectors whose choice is determined by the instrument design and applications. A review of MS detectors has been published recently.[27]

## 2.9 Tandem Mass Spectrometry and MS<sup>n</sup>

The concept of tandem generally recalls to mind tandem bicycles in which at least two cyclists ride the same bicycle. If the cyclists want to avoid falling, they must synchronize their movements and the trajectory of the tandem! Similarly, tandem MS[28] involves two or more partners, in the specific case the analyzers, which are synchronized. This is particularly important for obtaining structural information and for quantitative analysis.

In other words, in tandem MS experiments two (MS/MS or MS<sup>2</sup>) or more (MS<sup>n</sup>) sequential stages of mass analysis (which can be separated spatially or temporally) are used in order to examine selectively the decomposition of given ions, occurring out of the ion source, in a mixture of ions. Type and performances of the analyzers determine the kind of MS<sup>n</sup> experiments that can be carried out. There are two main kinds of reactions that cause decomposition of ions occurring out of the source:

- (a) those spontaneously produced by *metastable ions*. As they involve just ions, these are unimolecular reactions.
- (b) those induced by collision of ions with a gas, generally nitrogen, helium or argon. These unspontaneous decompositions are referred to as collision-induced dissociation (CID) or collision-activated decomposition (CAD) reactions and, as they involve two reagents, they are bimolecular reactions.

While metastable decompositions have been extensively studied for many decades, nowadays the use of tandem MS is almost exclusively limited to the study of decompositions caused by collision. Different kinds of experiments can be carried out by tandem MS: the most common is the *product ion scan*. This is carried out by selecting ions with a given *m/z* value among all those formed in the source and detecting selectively their *product ions* formed due to CIDs. It follows that at least two analyzers (the tandem) are required. In



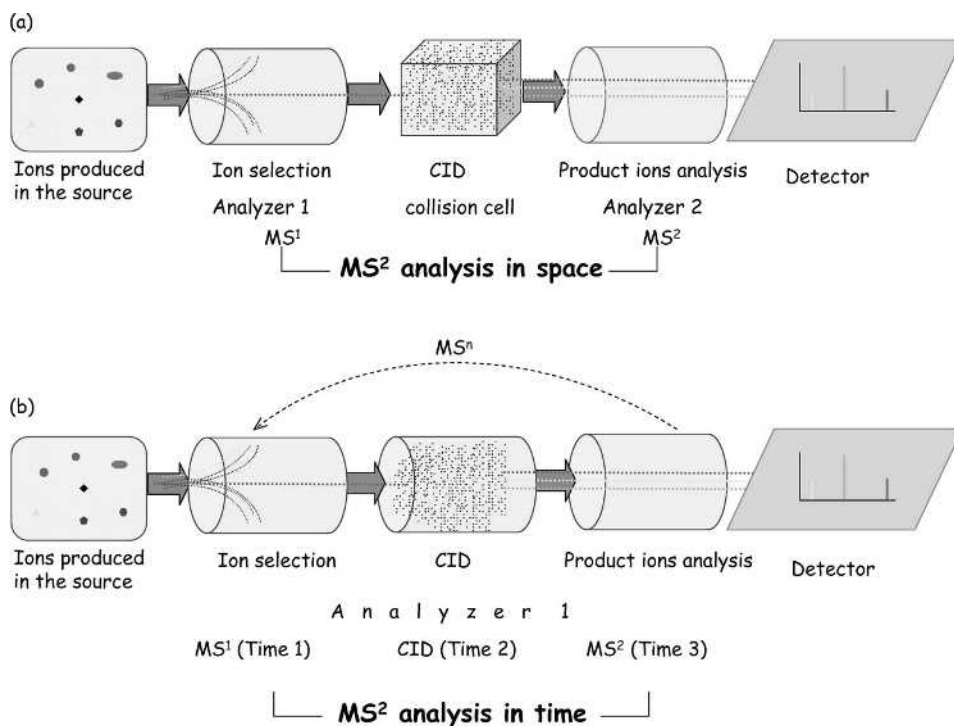


**Figure 2.14** Tandem mass spectrometry product ion scan experiments: in space (a) and in time (b)

particular, the first analyzer is fixed in such a way that only ions with a specific  $m/z$  value can pass through it, while all the others are eliminated (Figure 2.14a). The second analyzer scans over a  $m/z$  range in order to detect all the product ions formed owing to CIDs in a collision cell located in between the two analyzers. To increase the efficiency of collisions, a voltage (collision energy) is applied to the collision cell. The two, or more, analyzers constituting the tandem may be the same, for example quadrupoles, but their coupling can be also hybrid, as occurs in BE, Q-IT and Q-TOF.

One of the most common couplings of analyzers for tandem MS is the triple quadrupole. Its notation is QqQ, where the capital Q indicates a quadrupole analyzer and the lowercase q is for a RF-only quadrupole that constitutes the collision cell.

The processes just described are valid for analyzers separating ions in space: while ions are travelling, there is separation of the ions of interest, their decomposition is due to CID and there is analysis of product ions. Two analyzers are required for MS/MS experiments, three for MS[3], and so on.

The situation is different for analysis in time (Figure 2.14b). In this case, the three main processes, i.e. ion separation, CID and analysis of product ions, occur inside the same analyzer just changing the forces acting on the ions over time. Hence, in an ion trap, it is possible to isolate the ions of interest, by application of a suitable RF and voltages to its electrodes, to apply a supplementary voltage for CID with the helium present inside it, and to

carry out analysis of the product ions. All this occurs in just one analyzer. Furthermore it is possible to perform isolation-CID-isolation-CID-analysis of product ions in order to obtain MS<sup>3</sup> spectra, but it is also possible to repeat the cycle several times to obtain MS<sup>n</sup> spectra.

An example showing the usefulness of CID-MS/MS experiments is shown in Figure 2.15. The lipid extract obtained from a ceramic vessel recovered from the thirteenth century church of Sant' Antimo in Piombino (Central Italy) has been analysed by APCI in positive mode. The resulting mass spectrum shows several peaks (Figure 2.15a). As APCI has been used no or limited fragmentation is expected; thus each peak is due to a protonated molecule. This large number of peaks indicates a mixture of compounds, and it represents a fingerprint of the material under investigation.

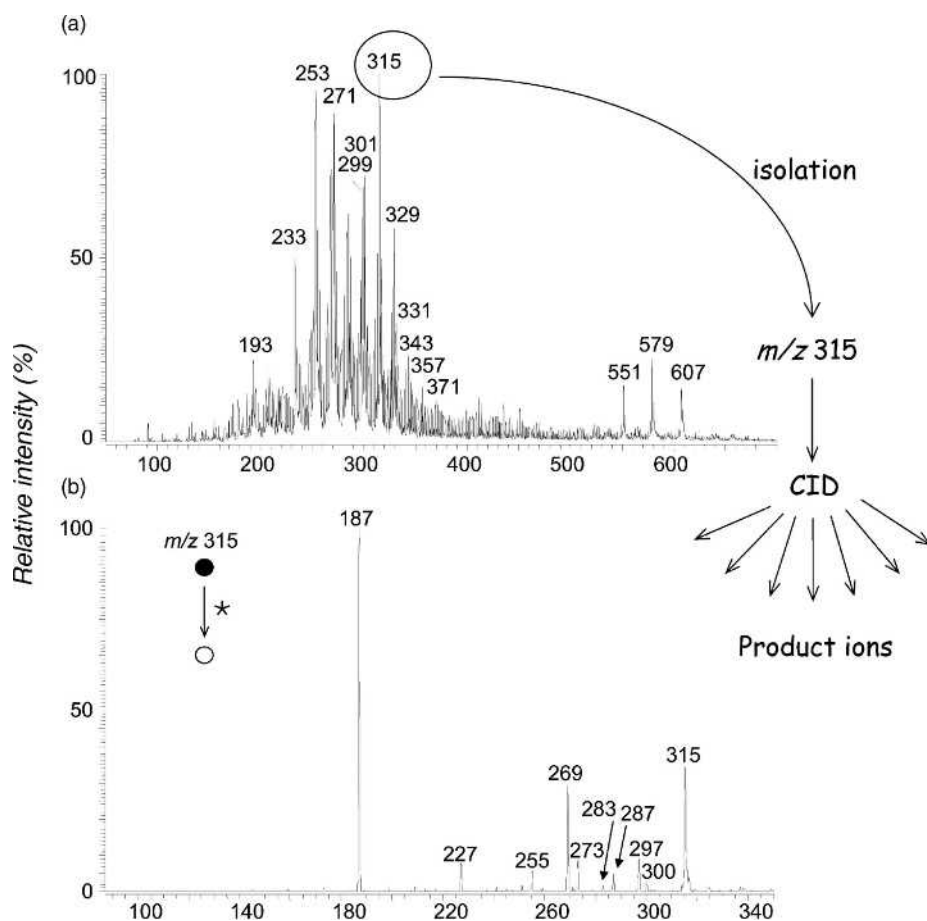


**Figure 2.15** APCI (+) mass spectrum of the lipid extract obtained from a ceramic vessel recovered from the thirteenth century church of Sant'Antimo in Piombino (Central Italy) (a). The APCI-MS/MS spectrum obtained by selecting ions at  $m/z$  315 (b). The latter made it possible to determine that ions at  $m/z$  315 are due to protonated 7-oxodehydroabiatic acid. (Adapted from ref. [29])

When ions at  $m/z$  315 are isolated and submitted to CID, the product ion spectrum shown in Figure 2.15(b) is obtained. Product ions at  $m/z$  300, 297, 273 and 269 can be attributed to losses of a methyl radical, water, cyclopropane and formic acid, respectively. These decompositions, together with other information and a more detailed study of the MS[2] spectrum, enable the identification of the compound with  $[M+H]^+$  at  $m/z$  315 as protonated 7-oxodehydroabietic acid.

## 2.10 The Mass Spectrum

As already stated, the mass spectrum is a two-dimensional graph that reports the  $m/z$  ratio of ions (abscissa) and their relative intensity (ordinate). The most abundant ions are assigned as 100%. A mass spectrum can be displayed as peak profiles or as bar graphs corresponding to the peak centroids, i.e. the weighted centre of mass of the peak, or as a table (Figure 2.16). The most abundant ions in a mass spectrum constitute the *base peak* whose intensity is assumed equal to 100%.

The appearance of the mass spectrum is greatly determined by the amount of energy deposited on the molecule during the ionization: if it is high, as occurs in EI, the mass spectrum is characterized by the molecular and fragment ions. In this case, the mass spectrum can be defined as the fingerprint of the chemical species which produced it. In fact it contains a lot of structural information: the molecular mass, those of fragment ions as well as useful information on functional groups and elements present/absent in the analyte. However, if the amount of energy deposited on the molecule during the ionization is small, as occurs in soft ionizations, the mass spectrum shows only the presence of the protonated/deprotonated molecule, and eventually a few adduct ions but not fragment ions.

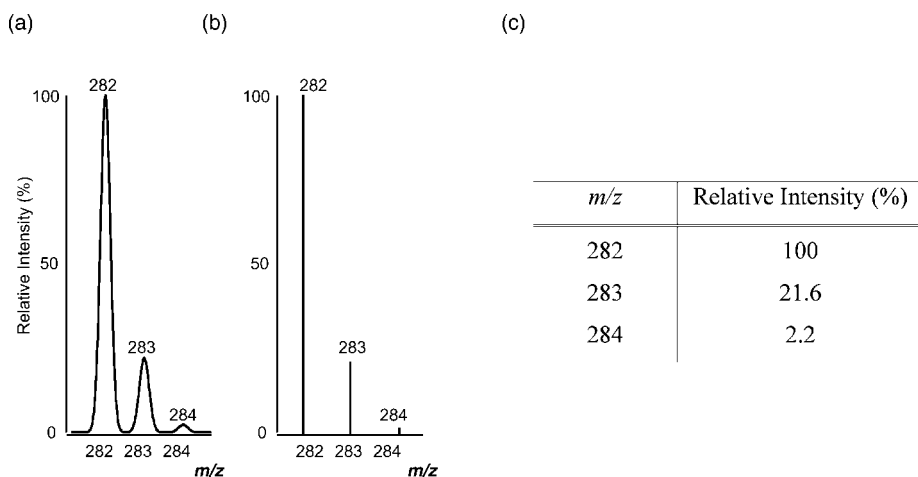


**Figure 2.16** Different ways to represent a mass spectrum: peak profile (a), bar graph (b) and table (c)

There are some features common to all mass spectra like the presence of isotopes. Their knowledge and the use of the nitrogen rule can help in their interpretation.

### 2.10.1 The Isotopes

When we look at a mass spectrum we can observe that a single peak is never isolated but there is one or more small peaks accompanying it to its right (Figure 2.16). These peaks are due to the isotopes of the elements. Isotopes are atoms of the same element that have the same number of protons and electrons but a different number of neutrons. The total number of protons and neutrons constitutes the *mass number* and it is indicated as a superscript preceding the atomic symbol, i.e.  $^1\text{H}$ ,  $^{12}\text{C}$ ,  $^{23}\text{Na}$ .

On account of having the same number of electrons and protons, isotopes of a given element have identical chemical properties and reactivity. However, since they differ in the number of neutrons, they have different atomic masses. As MS measures and discriminates mass, isotopes are detected and they are present in every mass spectrum, independent of the ionization technique used, instrumentation, etc.

Isotopic displays contain a wealth of important and useful information: they can reveal what types of elements are contained in a molecule; their study is valuable in high resolution and in accurate mass determination; and they can also reveal the charge state of an ion, which is particularly useful when ESI is used.

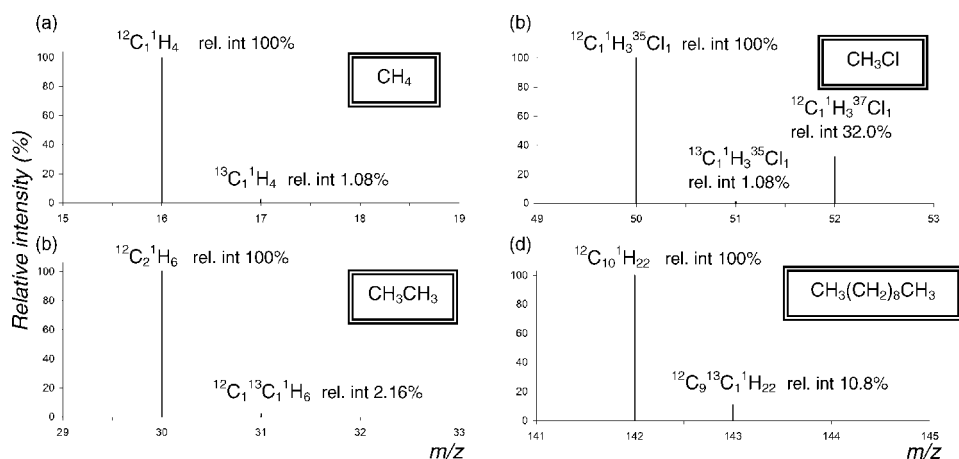
Isotopes can be naturally occurring or of synthetic origin, and they can be divided into two main groups: stable and unstable. The former are atoms without any spontaneous degradation, such as  $^{13}\text{C}$ ,  $^1\text{H}$  and  $^{35}\text{Cl}$ , while the latter have a decay in time, such as  $^{14}\text{C}$  and  $^3\text{H}$ . MS studies stable isotopes. A branch of MS, i.e. isotope ratio mass spectrometry (IRMS), devoted to the study of isotope abundances, is receiving more and more interest.[30] Its principles and applications in cultural heritage are presented in the following chapters.

Natural isotopic abundances of common elements present in organic molecules are reported in Table 2.5. According to the nomenclature introduced by McLafferty,[31] an element can be classified as A, A + 1, A + 2, etc., where A refers to the most abundant isotope of the element, A + 1 to its isotope 1 u heavier, and so on. By examining Table 2.5 it can be seen that carbon and nitrogen can be categorized as A + 1 type elements because their second most abundant isotope, i.e.  $^{13}\text{C}$  and  $^{15}\text{N}$ , respectively, are 1 u heavier than that of the most abundant. A closer study of Table 2.5 shows that, with the exception of silicon, not always present in organic molecules, the highest A + 1 contribution is given by  $^{13}\text{C}$  with a percentage of 1.08% with respect to that of  $^{12}\text{C}$ . Similarly, from Table 2.5 it appears that chlorine and bromine are A + 2 elements with very abundant isotopes differing 2 u from the most abundant. All the isotopic peaks of an ion constitute the *isotopic cluster* of that ion.

The isotopic cluster of the molecular ion of methane (Figure 2.17a) is formed by two ions at  $m/z$  16 and 17, the latter due to the isotopic contribution of  $^{13}\text{C}$ . If that at  $m/z$  16 has relative abundance of 100%, that for the ion at  $m/z$  17 is:  $1.08$  (relative abundance of  $^{13}\text{C}$ )  $\times$  1 (number of carbon atoms) = 1.08%. The case is similar for ethane (Figure 2.17b). Also, the isotopic cluster of the molecular ion of decane ( $\text{C}_{10}\text{H}_{22}$ ) is formed by two main ions (Figure 2.17d). The relative abundance of that at  $m/z$  143 is:  $1.08 \times 10 = 10.8\%$ .

**Table 2.5** Natural isotopic abundances and monoisotopic masses of common elements

Element	Isotope	A		Isotope	A + 1		Isotope	A + 2	
		Mass (u) [32]	%		Mass (u) [32]	% [33]		Mass (u) [32]	% [33]
H	<sup>1</sup> H	1.007825	100	<sup>2</sup> H	2.014102	0.01			
C	<sup>12</sup> C	12.000000	100	<sup>13</sup> C	13.003355	1.08			
N	<sup>14</sup> N	14.003074	100	<sup>15</sup> N	15.000109	0.37			
O	<sup>16</sup> O	15.994915	100	<sup>17</sup> O	16.999132	0.04	<sup>18</sup> O	17.999160	0.20
F	<sup>19</sup> F	18.998403	100						
Si	<sup>28</sup> Si	27.976927	100	<sup>29</sup> Si	28.976495	5.08	<sup>30</sup> Si	29.973770	3.35
P	<sup>31</sup> P	30.973762	100						
S	<sup>32</sup> S	31.972071	100	<sup>33</sup> S	32.971458	0.80	<sup>34</sup> S	33.967867	4.52
Cl	<sup>35</sup> Cl	34.968853	100				<sup>37</sup> Cl	36.965903	31.96
Br	<sup>79</sup> Br	78.918338	100				<sup>81</sup> Br	80.916291	97.28
I	<sup>127</sup> I	126.904468	100						

**Figure 2.17** Comparison of the isotopic clusters of the molecular ion for (a) methane, (b) ethane, (c) chloromethane and (d) decane

As the  $A + 2$  contribution of  $^{37}\text{Cl}$  and  $^{81}\text{Br}$  is high, their presence is easy to be determined. In fact, the occurrence of an isotopic cluster in which two ions are separated by 2 u and the heaviest has the same intensity of the lightest suggests that the ion contains a bromine atom. The isotopic cluster of chloromethane ( $\text{CH}_3\text{Cl}$ , Figure 2.17c) is formed by three ions:  $^{12}\text{C}_1^1\text{H}_3^{35}\text{Cl}_1$  ( $m/z$  50),  $^{13}\text{C}_1^1\text{H}_3^{35}\text{Cl}_1$  ( $m/z$  51),  $^{12}\text{C}_1^1\text{H}_3^{37}\text{Cl}_1$  ( $m/z$  52), due to the most abundant isotopes, to the isotopic contribution of  $^{13}\text{C}$  and to that of  $^{37}\text{Cl}$ , respectively. If the relative intensity of the former is 100%, those of the others will be:

ions at  $m/z$  51: main contribution due to  $^{13}\text{C}$ : relative intensity =  $1.08 \times 1 = 1.08\%$ ;

ions at  $m/z$  52: main contribution due to  $^{37}\text{Cl}$ : relative intensity =  $31.96 \times 1 = 31.96\%$ .

### 2.10.2 The Nitrogen Rule

In addition to the study of the isotopic cluster, useful information on analyte identity can be obtained by the nitrogen rule. It states that *if a molecule contains an odd number of nitrogen atoms, its molecular weight must be an odd number. However, if an even number of nitrogen atoms or no nitrogen is present, its molecular weight must be an even number.*

Hence, the presence in an EI spectrum of the molecular ion at  $m/z$  109 suggests that the molecule must contain an odd number of nitrogen atoms, while if it is at  $m/z$  232 the molecule may contain no nitrogen atoms or an even number of them.

Similarly, if in a CI(+) mass spectrum we observe the species  $[M + H]^+$  at  $m/z$  164, it follows that the molecular weight is 163, and consequently the molecule must contain an odd number of nitrogen atoms.

### 2.10.3 Mass Spectra Obtained by Electron Ionization

A hypothetical example of reactions occurring when EI is used, and the resulting mass spectrum are reported in Figure 2.18. You already know that the molecular ion  $[M]^{\bullet+}$  has the same weight as the neutral parent compound. It is on the right in the  $m/z$  axis of the mass spectrum, being the heaviest ion from which all the fragmentation pathways originate and, as a consequence, the  $m/z$  ratios of fragment ions are less than that of the molecular ion. The  $[M]^{\bullet+}$  relative intensity is closely related to its structure and it can greatly vary from one class of compounds to another. For example, aromatic compounds produce stable molecular ions, with high relative intensities and very limited fragmentation, while for other classes of compounds the molecular ion may have different abundances or be absent altogether.

If during fragmentation a neutral molecule is eliminated, the charge and the unpaired electron remain on the same species and the fragment ions are odd-electron species, like the molecular ion. However, if the fragmentation implies charge and radical separation, the fragment ions will be even-electron species. Of course, only charged species will be present in the mass spectrum, while molecules and radicals cannot be detected.

Fragment ions can be produced by simple cleavages of covalent bonds: for example, a simple cleavage occurring in  $[\text{molecule}]^{\bullet+}$  can yield  $[\text{mo}]^+$  and  $[\text{lecule}]^{\bullet}$  and only the charged species  $[\text{mo}]^+$  will be present in the mass spectrum (Figure 2.18). However, fragmentation may also involve rearrangement reactions in which moieties that are far from each other in the ion became close and can be eliminated. For example, the species  $[\text{molle}]^{\bullet+}$  can be produced from  $[\text{molecule}]^{\bullet+}$  only through a so-called rearrangement reaction (Figure 2.18).

As an example, the EI mass spectrum of nonacosan-15-one, a marker commonly related to leafy waxes of *Brassicaceae*, such as cabbage and analogous vegetable species,[34] is reported in Figure 2.19. Its molecular ion ( $m/z$  422) has a relative intensity of 8%, while the base peak is at  $m/z$  225 due to cleavage at the carbonyl group (Figure 2.19). Several ions differing for  $-\text{CH}_2-$  units (▼) are produced by fragmentations of different bonds in the hydrocarbon chain.

Mass spectra obtained by EI are highly reproducible on different instrumentation and over the time. This allows mass spectra libraries to be built in which an unknown mass spectrum can be searched by using an algorithm. Indeed, a lot of EI mass spectra libraries containing hundreds of thousands of mass spectra, such as the NIST/EPA/NIH

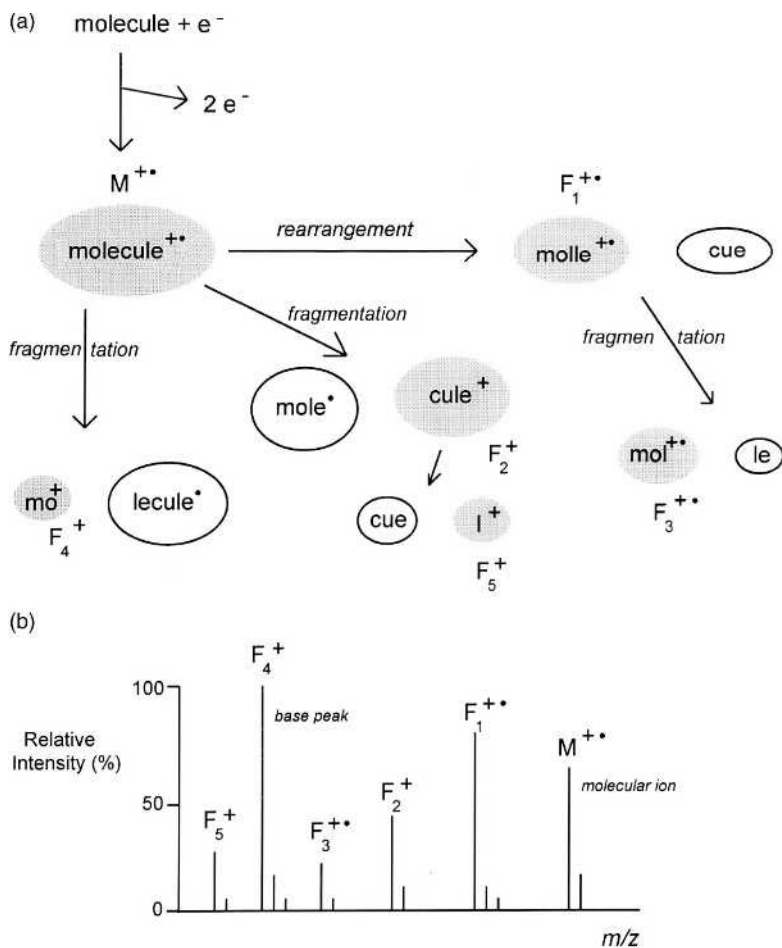


**Figure 2.18** Schematic diagram showing the hypothetical behaviour of a molecule ionized by electron ionization (a) and its mass spectrum (b)

Mass Spectral Library[35] and the Wiley Registry of Mass Spectral Data[36] are now available to help mass spectrometrists in the identification of unknowns.

#### 2.10.4 Mass Spectra Obtained by Soft Ionization Techniques

If during the ionization the amount of energy deposited on the molecule is low, as occurs in *soft* techniques, i.e. CI, ESI, DESI and MALDI, the mass spectrum is very simple. It is characterized by protonated/deprotonated molecules, and eventually few adduct ions but very few or no fragment ions. This implies that it is easy to obtain the molecular weight of the analyte under investigation, but structural information is missing. As an example, the ESI mass spectrum of a small molecule is reported in Figure 2.20. There are two main ions: one at  $m/z$  556 and another at  $m/z$  578. As the mass spectrum has been obtained in positive

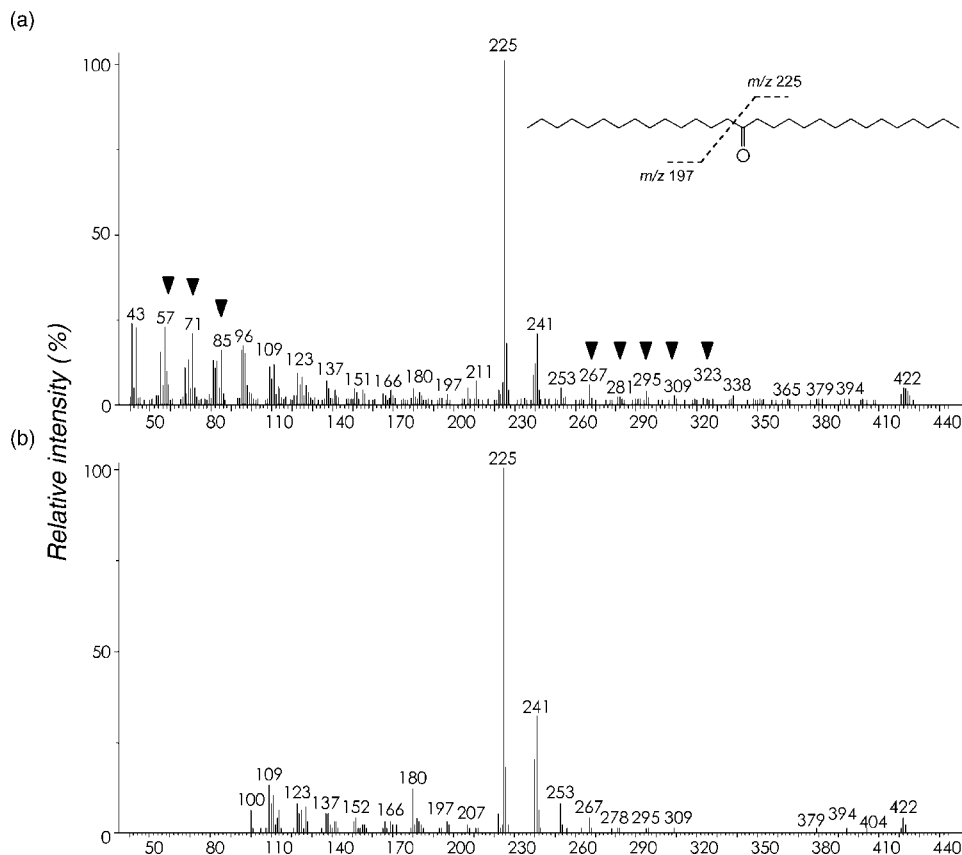


**Figure 2.19** Comparison between the electron ionization mass spectrum obtained in my laboratory (a) and that reported in the NIST library[35] (b) of nonacosan-15-one

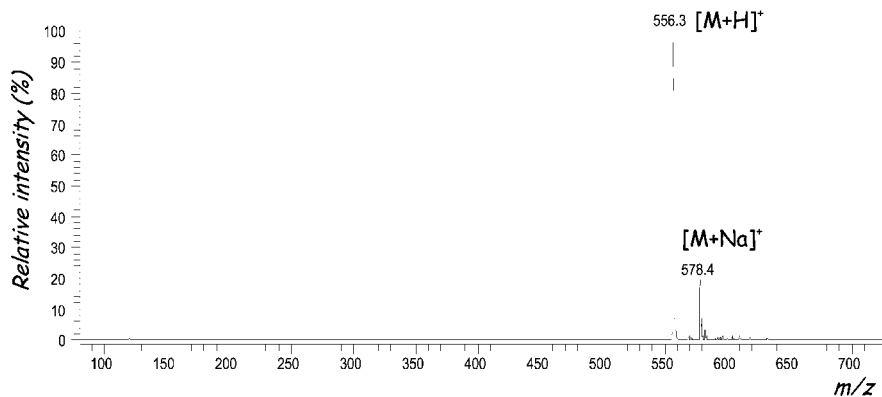


**Figure 2.20** Electrospray positive ion mass spectrum of a small molecule



mode, it is likely that the former ion corresponds to the protonated molecule and, as a consequence, its molecular weight is 555 Da. It follows that it must contain an odd number of nitrogen atoms. In addition, as the intensity of the isotopic ion at  $m/z$  558 is quite low, it means that the molecule does not contain either chlorine or bromine atoms.

The other intense ion is at  $m/z$  578 and it differs 22 u from the ion at  $m/z$  556, or 23 u from the molecular weight. It is attributable to an adduct of the molecule with sodium, whose presence is almost ubiquitous.

No structural information is obtainable from this mass spectrum and tandem MS is needed for structural characterization of the analyte.

ESI is also able to ionize not only small but also ‘elephant’ molecules. In this case multicharged ions are produced (see Section 2.6.2.2). A typical ESI spectrum of a large molecule is shown in Figure 2.21.

Protonation, and analogously deprotonation, is not an ‘all or nothing’ phenomenon: in fact a given large molecule can be charged to different extents thus producing ions with different  $m/z$  values (Figure 2.21). It follows that the ions present in an ESI mass spectrum represent the same molecule but with different charge states. As it appears from Figure 2.21, two main features can be found in an ESI spectrum of a large molecule:

- There is a rough Gaussian distribution of the peak intensities. In fact the majority of molecules will take a given number of protons, producing the ion with the highest intensity (i.e.  $m/z$  942 in Figure 2.21). There will be other molecules that took a higher number of protons, yielding ions on the left of the highest peak (i.e.  $m/z$  817 in Figure 2.21), but also others that are protonated to a lesser extent, yielding ions on the right of the highest peak (i.e.  $m/z$  1748 in Figure 2.21). This explains why a statistical distribution of charge states is present in the mass spectrum.
- The distance between two consecutive peaks increases on moving from left to right. In fact, by decreasing the number of protons that are added or lost, there is a slight reduction in mass but a big reduction in the  $m/z$  value.

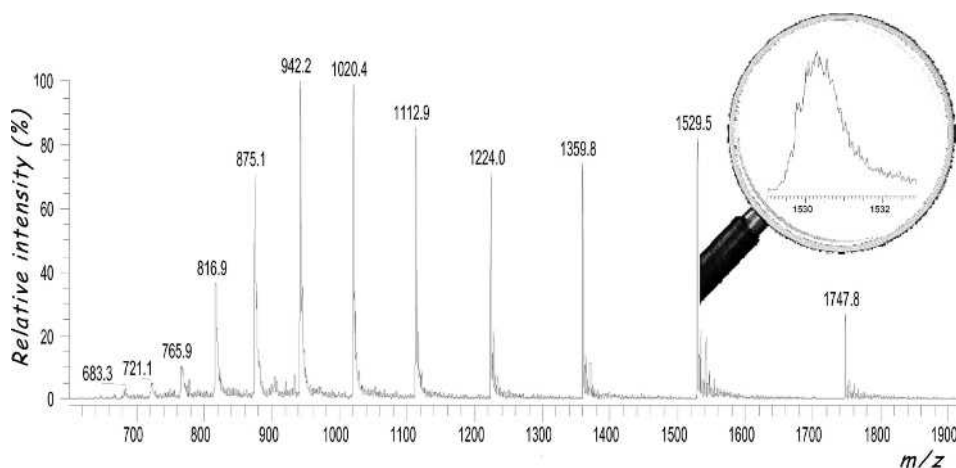


**Figure 2.21** Electrospray positive ion mass spectrum of cytochrome *c*, a large molecule

As shown in Figure 2.21, information for the determination of the molecular weight is not *directly* displayed in the mass spectrum. However, it is possible to obtain it from the spectrum.

Let us consider the mass spectrum in Figure 2.21 and some ions, for example those at  $m/z$  1020. As this mass spectrum has been obtained in positive mode, these ions are produced by addition of  $n$  protons to the molecule ( $M$ ) yielding the species  $\{[M+nH]^{n+}\}/n$ . The ion to the left of this species, i.e.  $m/z$  942, is produced by the molecule which added one proton more, and as a consequence, it has taken an additional charge, yielding the species  $\{[M+(n+1)H]^{(n+1)}\}/(n+1)$ . It is possible to make a system with two equations and two unknowns, i.e.  $M$  and  $n$ , and obtain the number of charges of the ions:

$$\begin{cases} 1020 = \frac{[M + nH]^{n+}}{n} \\ 942 = \frac{[M + (n+1)H]^{(n+1)}}{n+1} \end{cases} \quad \Rightarrow \quad n = 12$$

By replacing the value of  $n$  in the two equations we obtain  $M = 12\,228$  and  $M = 12\,233$  with the average value,  $M_{av} = 12\,230.5$ . By reiterating the process for all peaks and for different combinations of peaks we can obtain the molecular weight with good accuracy. The computer can do it quite easily: the entire process is called *deconvolution* and many sophisticated algorithms have been developed for this. The deconvolution of the spectrum reported in Figure 2.21 is depicted in Figure 2.22. Figure 2.22a shows the charge attribution of each peak, whilst Figure 2.22b shows the deconvoluted spectrum, with the

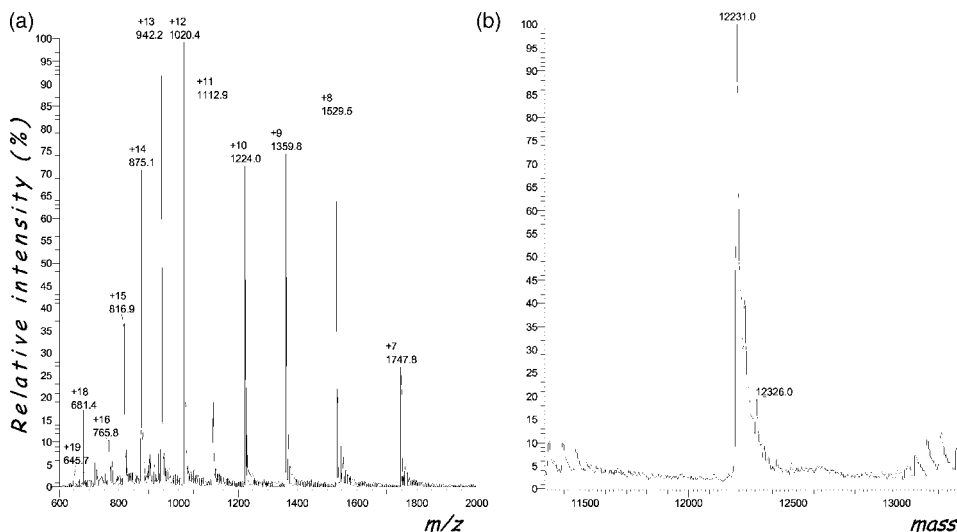


**Figure 2.22** Charge attribution (a) and deconvolution (b) of the electrospray positive ion mass spectrum of cytochrome c (see Figure 2.21)

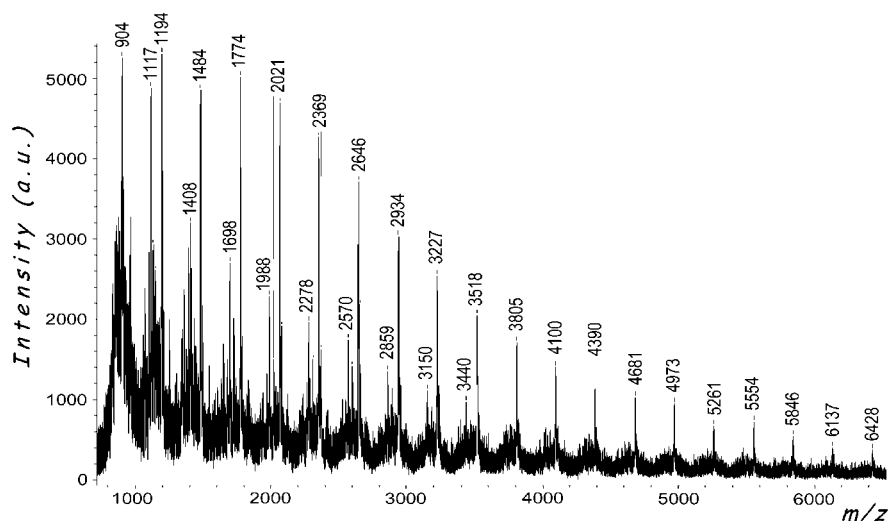


**Figure 2.23** MALDI (+) mass spectrum of a synthetic polymer

molecular weights indicated. It is worth noting that on the abscissa of the deconvoluted spectrum, produced *in silico* by the computer, the mass instead of the  $m/z$  value is used.

It is important to remember the two features of an ESI spectrum of multicharged ions. In fact, a quick glance at the mass spectrum shown in Figure 2.23 might lead to error. In fact, the peaks show a statistical distribution with high relative intensities on the left that decrease on moving to the right. However, different from every ESI spectrum, the distance between two consecutive peaks is the same over all of the  $m/z$  region. It excludes the presence of multicharged ions while promotes the possibility that the sample is composed of molecules whose molecular weights differ by a constant value. Indeed, Figure 2.23 is a MALDI mass spectrum of a polymer whose components differ by 290 u.

## 2.11 New Developments in Mass Spectrometry

### 2.11.1 Mass Spectrometry Imaging

MS imaging is an emerging, new technique for molecular mapping and imaging of molecule analytes present in an object. The concept involves mounting the object on a sample holder that can be accurately moved in the  $x$ - $y$  plane. A primary beam hits the sample: analyte ions are desorbed and a mass spectrum is obtained. It is recorded together with the position of the sample. The sample is moved a few micrometres and another spectrum is collected. The process is repeated thousands of times; from the analysis of the spectra and the position of the sample it is possible to reconstruct the spatial distribution, or mapping, of a given analyte in a sample. MALDI-TOF has been the first approach used for MS imaging with pioneering work done by R. Caprioli.[37,38] A crucial step is matrix deposition and different techniques have been developed for this purpose. More recently

DESI has also been introduced into MS imaging.[39] SIMS is also used for surface imaging and depth profiling.[40]

MS imaging is extensively used for biological applications, in analysis of tissues and small organisms, but its applications are in principle unlimited. Hence, it should be possible for applications in cultural heritage to become available soon.

## References

1. D. F. Torgerson, R. P. Skowronski and R. D. Macfarlane, New approach to the mass spectroscopy of non-volatile compounds, *Biochem. Biophys. Res. Commun.*, **60**, 616–621 (1974).
2. H. D. Beckey, Field ionization mass spectrometry, *Res. Dev.*, **20**, 26–31 (1969).
3. M. Barber, R. S. Bordoli, R. D. Sedgwick and A. N. Tyler, Fast atom bombardment of solids (F.A.B.): a new ion source for mass spectrometry, *J. Chem. Soc. Chem. Commun.*, 325–327 (1981).
4. M. Yamashita and J. B. Fenn, Electrospray ion source. Another variation on the free-jet theme, *J. Phys. Chem.*, **88**, 4451–4459 (1984).
5. M. Karas and F. Hillenkamp, Laser desorption ionization of proteins with molecular masses exceeding 10,000 daltons, *Anal. Chem.*, **60**, 2299–2301 (1988).
6. A. D. McNaught and A. Wilkinson, *Compendium of Chemical Terminology*, International Union of Pure and Applied Chemistry, 2nd Edition, Blackwell Science, 1997.
7. I. Lavagnini, F. Magno, R. Seraglia and P. Traldi, *Quantitative Applications of Mass Spectrometry*, Chichester, J. Wiley & Sons, 2006.
8. R. Boyd, R. Bethem, C. Basic and D. Matthews, *Trace Quantitative Analysis by Mass Spectrometry*, J. Wiley & Sons, New York, 2008.
9. K. J. Van den Berg, J. J. Boon, I. Pastorova and L. F. M. Spetter, Mass spectrometric methodology for the analysis of highly oxidized diterpenoid acids in Old Master paintings, *J. Mass Spectrom.*, **35**, 512–533 (2000).
10. M. Regert and C. Rolando, Identification of archaeological adhesives using Direct Inlet Electron Ionization Mass Spectrometry, *Anal. Chem.*, **74**, 965–975 (2002).
11. E. Ribechini, F. Modugno and M. P. Colombini, Direct exposure-(chemical ionization)-mass spectrometry for a rapid characterization of raw and archaeological diterpenoid resinous substances, *Microchimica Acta*, **162**, 405–413 (2008).
12. M. S. B. Munson and F. H. Field, Chemical Ionization Mass Spectrometry. I. General Introduction, *J. Am. Chem. Soc.*, **88**, 2621–2630 (1966).
13. A. G. Harrison, *Chemical Ionization Mass Spectrometry*, CRC Press, Boca Racon (FL), 1983.
14. M. Dole, L. L. Mack, R. L. Hines, R. C. Mobley, L. D. Ferguson and M. B. Alice, Molecular beams of macroions, *J. Chem. Phys.*, **49**, 2240–2249 (1968).
15. M. L. Aleksandrov, L. N. Gall, V. N. Krasnov, V. I. Nikolaev, V. A. Pavlenko and V. A. Shkurov, Ion extraction from solutions at atmospheric pressure – a method for mass-spectrometric analysis of bioorganic substances, *Dokl Akad Nauk SSSR*, **277**, 379–383 (1984) (in Russian).
16. J. V. Iribarne and B. A. Thomson, On the evaporation of small ions from charged droplets, *J. Chem. Phys.*, **64**, 2287–2289 (1976).
17. D. I. Carroll, I. Dzidic, R. N. Stillwell, K. D. Haegele and E. C. Horning, Atmospheric pressure ionization mass spectrometry. Corona discharge ion source for use in a liquid chromatograph-mass spectrometer-computer analytical system, *Anal. Chem.*, **47**, 2369–2373 (1975).
18. K. Tanaka, H. Waki, Y. Ido, S. Akita, Y. Yoshida, T. Yoshida and T. Matsuo, Protein and polymer analyses up to  $m/z$  100 000 by laser ionization time-of-flight mass spectrometry, *Rapid Commun. Mass Spectrom.*, **2**, 151–153 (1988).
19. Z. Takáts, J. M. Wiseman and R. G. Cooks, Ambient mass spectrometry using desorption electrospray ionization (DESI): instrumentation, mechanisms and applications in forensics, chemistry, and biology, *J. Mass Spectrom.*, **40**, 1261–1275 (2005).

20. R. G. Cooks, Z. Ouyang, Z. Takáts and J. M. Wiseman, Ambient Mass Spectrometry, *Science*, **311**, 1566–1570 (2006).
21. W. Henderson and J. S. McIndoe, *Mass Spectrometry of Inorganic and Organometallic Compounds: Tools–Techniques–Tips*, John Wiley & Sons, Ltd, Chichester, 2005.
22. J. R. de Laeter, *Applications of Inorganic Mass Spectrometry*, John Wiley & Sons, Ltd, New York, 2001.
23. S. Nelms (Ed.), *Inductively Coupled Plasma Mass Spectrometry*, Blackwell Publishing, Oxford, 2005.
24. A. Bogaerts and R. Gijbels, Fundamental aspects and applications of glow discharge spectrometric techniques, *Spectrochim. Acta, Part B*, **53**, 1–42 (1998).
25. A. Benninghoven, F. G. Rüdenauer and H. W. Werner, *Secondary Ion Mass Spectrometry: Basic Concepts, Instrumental Aspects, Applications, and Trends*, John Wiley & Sons, Ltd, New York, 1987.
26. Q. Hu, R. J. Noll, H. Li, A. Makarov, M. Hardman and R. G. Cooks, The Orbitrap: a new mass spectrometer, *J. Mass Spectrom.*, **40**, 430–443 (2005).
27. D. W. Koppenaal, C. J. Barinaga, M. B. Denton, R. P. Sperline, G. M. Hieftje, G. D. Schilling, F. J. Andrade and J. H. Barnes IV, MS detectors, *Anal. Chem.*, **77**, 418A–427A (2005).
28. K. L. Bush, G. L. Glish and S. A. McLuckey, *Mass Spectrometry/Mass Spectrometry*, VCH, New York, 1988.
29. L. Salvini, A. Pecci and G. Giorgi, Cooking activities during the Middle Age: organic residues in ceramic vessels from the Sant’Antimo Church (Piombino, Central Italy), *J. Mass Spectrom.*, **43**, 108–115 (2008).
30. I. T. Platzner, *Modern isotope ratio mass spectrometry*, John Wiley & Sons, Ltd, Chichester, 1997.
31. F. W. McLafferty and F. Tureček, *Interpretation of Mass Spectra*, 4th Edition, University Science Books, Mill Valley, 1993.
32. (a) G. Audi and A. H. Wapstra, The 1993 atomic mass evaluation: (I) Atomic mass table, *Nucl. Phys. A*, **565**, 1–65 (1993); (b) G. Audi and A. H. Wapstra, The 1995 update to the atomic mass evaluation, *Nucl. Phys. A*, **595**, 409–480 (1995).
33. K. J. R. Rosman and P. D. P. Taylor, Table of isotopic masses and natural abundances, *Pure Appl. Chem.*, **71**, 1593–1607 (1999).
34. S. Charters, R. P. Evershed, A. Quye, P. W. Blinkhorn and V. Reeves, Simulation experiments for determining the use of ancient pottery vessels: the behaviour of epicuticular leaf wax during boiling of a leafy vegetable, *J. Archaeol. Sci.*, **27**, 1–27 (1997).
35. Standard Reference Data Program, NIST/EPA/NIH Mass Spectral Library, Version 2.0f, National Institute of Standards and Technology, Gaithersburg, MD.
36. Wiley Registry of Mass Spectral Data, 8th Edition, John Wiley & Sons, Ltd, New York, 2008.
37. R. M. Caprioli, T.B. Farmer and J. Gile, Molecular imaging of biological samples: localization of peptides and proteins using MALDI-TOF MS, *Anal. Chem.*, **69**, 4751–4760 (1997).
38. M. Stoeckli, P. Chaurand, D. E. Hallahan and R. M. Caprioli, Imaging mass spectrometry: A new technology for the analysis of protein expression in mammalian tissues, *Nature Med.*, **7**, 493–496 (2001).
39. J. M. Wiseman, D. R. Ifa, Q. Song and R. G. Cooks, Tissue imaging at atmospheric pressure using Desorption Electrospray Ionization (DESI) mass spectrometry, *Angew. Chem. Int. Edn*, **45**, 7188–7192 (2006).
40. A. J. Paul, Organic and molecular imaging by ToF-SIMS – at the cutting edge, *Spectrosc. Eur.*, **17**, 25–27 (2005).

## General Bibliography

- B. Ardrey, *Liquid Chromatography–Mass Spectrometry: An Introduction*, AnTS Analytical Techniques in the Sciences, John Wiley & Sons, Ltd, Chichester, 2003.
- J. R. Chapman, *Practical Organic Mass Spectrometry: A Guide for Chemical and Biochemical Analysis*, 2nd Edition, John Wiley & Sons, Ltd, Chichester, 1995.
- C. Dass, *Fundamentals of Contemporary Mass Spectrometry*, Wiley-Interscience, New York, 2007.

- E. De Hoffmann and V. Stroobant, *Mass Spectrometry: Principles and Applications*, 3rd Edition, John Wiley & Sons, Ltd, Chichester, 2007.
- R. L. Grob and E. F. Barry (Eds), *Modern Practice of Gas Chromatography*, 4th Edition, John Wiley & Sons, Ltd, New York, 2004.
- J. H. Gross, *Mass Spectrometry. A Textbook*, Springer Verlag, Berlin–Heidelberg, 2004.
- M. L. Gross and R. M. Caprioli (Eds), *Encyclopedia of Mass Spectrometry*, Elsevier Science, Oxford, 2003.
- R. A. W. Johnstone and M. E. Rose, *Mass Spectrometry for Chemists and Biochemists*, 2nd Edition, Cambridge University Press, Cambridge, 1996.
- W. M. A. Niessen, *Liquid Chromatography–Mass Spectrometry*, 3rd Edition, Chromatographic Science Series Vol. **97**, CRC Press LLC, New York, 2006.
- J. T. Watson and O. D. Sparkman, *Introduction to Mass Spectrometry: Instrumentation, Applications, and Strategies for Data Interpretation*, 4th Edition, Chichester, Wiley, 2007.

# **Part II**

## **Direct Mass Spectrometric Analysis**





# 3

## Direct Mass Spectrometric Techniques: Versatile Tools to Characterise Resinous Materials

*Erika Ribechini*

### 3.1 Introduction

A wide range of natural substances may be found in association with archaeological findings, artefacts and works of art. Of these, natural plant resins and resinous materials are known to have been extensively used by ancient populations and by artists in every historical period. The chemical and physical properties of resinous materials made them popular for use as glues, hydro-repellents, coatings and sealing materials for handicrafts [1–12], as well as varnishes and binders in works of art [13]. These substances were also used as fundamental ingredients in make up, remedial preparations and ritual balms. Due to their antitoxic and antioxidant properties, they were also added to wines [6]. For their various applications, plant resins were either used in their natural form or were subjected to pyrolysis and to distillation-type processes, in order to obtain denser and stickier materials, such as tar and pitch [1,5,6].

Resinous substances do not have any characteristic morphology. As a result, studying their chemical composition is the only way to establish their origin. The identification of such substances is a real challenge from an analytical standpoint due not only to the complexity of the chemical composition of these natural substances and their mixtures, but also to changes in the chemical composition caused by human activities such as heating, or mixing materials in order to modify their properties depending on their specific use.

Moreover, degradation due to ageing under the influence of different burial circumstances or museum environment can induce further changes in the composition of the original materials. For instance, in archaeological contexts, the presence of water or humidity could favour the solubilisation of organic materials and the subsequent loss of several classes of compounds. However, entrapment in certain archaeological environments could lead to an enhancement in the preservation of organic materials. For example, decomposition is slowed down by very dry conditions such as arid or cold climates. Moreover, exposure to light radiation, in particular UV, and/or to heating treatments as well as the preservation in warm/hot environments can favour thermo-oxidative phenomena leading to the formation of oxidised compounds. These phenomena, for example, are responsible for the yellowing of terpenoid paint varnishes.

Scientific research has clearly shown that analytical methodologies based on mass spectrometry are unrivalled tools for deriving detailed compositional information (chemical structures and compound distribution) and for reliably identifying resinous substances in cultural heritage objects. In particular, gas chromatography coupled with mass spectrometry (GC/MS) has proven to be an extremely useful analytical technique for characterising archaeological resinous substances on the basis of the identification of specific molecular markers (see Chapter 8) [1,2,4–10,13–15]. However, this technique often requires time-consuming sample pretreatment, which normally entails extraction, purification, hydrolysis and derivatisation reactions, and long times for the data acquisition and evaluation. Thus, other techniques based on direct mass spectrometry that can reduce sample manipulation and analysis time are now being focused on. Direct Inlet-Mass Spectrometry (DI-MS), Direct Exposure-Mass Spectrometry (DE-MS) and Direct Temperature Resolved Mass Spectrometry (DTMS) have demonstrated their potential for characterising resinous substances in archaeological findings and works of art [16–24]. Moreover, mass spectrometric techniques based on the direct introduction of a micro-sample into the ionization source are able, in a fast single run, to detect the presence of mixtures of resinous materials with other organic substances. For instance, on the basis of DE mass spectra the presence of beeswax has been determined as a major component, along with lower proportions of other lipids and coniferous resin, in several organic residues recovered from Roman glass unguentaria [23]. Another study using DI-MS pointed out the intentional mixing of birch bark tar and beeswax used as an adhesive in repairing a ceramic vessel from the Iron Age [19].

Although these direct in-source mass spectrometric techniques present different instrumental features, they are all types of desorption/pyrolysis mass spectrometry. These techniques require very small amounts of untreated sample (a few nanograms), and they can be performed rapidly, just a few minutes for heating and data acquisition. They are particularly sensitive and can identify the nature of the main molecular constituents present in samples and provide a fingerprint together with general information on the nature of organic materials. They may be useful for providing initial hypotheses regarding the substances present in a sample and their state of degradation.

In the following sections, the instrumental features of direct mass spectrometry based techniques (DI-MS, DE-MS and DTMS) are presented, followed by a discussion of some mass spectra of standard compounds and reference materials. Finally, a series of case studies related to the presence of resinous materials in archaeological findings and works of art are reported and discussed.

### 3.2 Features of Direct Mass Spectrometry Based Techniques

The most attractive features are:

- sensitivity, as just a few nanograms of sample is sufficient to acquire good spectra;
- speed, as they require just a few minutes for each analysis;
- minimal sample manipulation and preparation, as the samples can be analysed in a solid state or just dissolved in a proper solvent.

These techniques represent a form of desorption/pyrolysis mass spectrometry, where the sample undergoes a controlled heating within the ion source of the spectrometer. The sample components are desorbed or pyrolysed over the heating range, and are ionised [by electron ionisation (EI) or chemical ionisation (CI)] and analysed as a function of time. Thus, it is possible to obtain a graph representing the total ion current (TIC) as a function of the time (that is of temperature) and a set of mass spectral data, averaging the mass spectra in the desired time range. The employment of fast ramp rates ensures that the volatilisation of the sample occurs rapidly and that thermal degradation is minimised. The controlled heating of the probe also means that slower ramp rates can be used for separating the sample constituents according to their molecular weight and eventually, to their polarity and thermal stability. Consequently through volatilisation, low molecular weight and volatile components are released first, and then the high molecular weight/polymeric fraction is removed. The polymeric fraction is released under thermolytic regime (pyrolysis regime) at higher temperatures.

In DI-MS, solid or liquid samples are introduced into a small glass cup and then the cup is inserted into a spring-loaded holder (probe tip). This is heated by a coiled heater up to a maximum of 450 °C thus allowing the sample to be volatilised. The probe can be heated in two different ways: ballistic mode or temperature-programme mode. In ballistic mode the probe heats at the maximum rate (150 °C min<sup>-1</sup>) up to the final temperature desired. In the temperature-programme mode the probe heats at a specified rate (from 10 to 100 °C min<sup>-1</sup>) up to the final set up temperature.

In DE-MS, once the sample has been dissolved in a suitable solvent or at solid state, it is placed onto the small loop at the end of a rhenium filament. Once inside the ion source, a current passes through the filament to heat it and the sample rapidly desorbs. The low thermal inertia of the rhenium filament produces rapid heating rates and high surface temperatures. The loop carries out an important function for the analysis of liquid samples as it favours the evaporation of the solvent due to the phenomenon of superficial tension. The probe is heated in current-programme mode, with a maximum current of 1000 mA corresponding to approximately 1000 °C. Typical ramp rates are 20–500 mA s<sup>-1</sup> even though the maximum ramp rate allowed is 1000 mA s<sup>-1</sup>. This means that volatilisation from the filament occurs more rapidly than when using the glass cup in DI-MS. As a result, less thermal degradation of the sample occurs.

In DTMS the sample suspended in a suitable solvent is applied to a platinum/rhodium filament (Pt/Rh 9:1) of the direct insertion probe. The probe is inductively heated at a rate of 0.5–1 A min<sup>-1</sup> to a maximum temperature of 800 °C. This means that the temperature is linearly increased from ambient to 800 °C in 1–2 min.

### 3.3 Mass Spectra of Reference Molecules and Materials

On account of the chemical complexity of resinous materials and the complexity of the mass spectra arising from the analysis by direct mass spectrometry based techniques, to determine the specific ions and ion fragments it is of primary importance to analyse standard compounds and reference materials, such as raw natural substances and/or natural materials artificially aged in the laboratory. Establishing characteristic ions and ion fragments is fundamental in order to identify resinous materials in archaeological findings and works of art. With this in mind, a series of mass spectra of standard compounds and reference materials obtained by DE-MS, DTMS and DI-MS are now presented and discussed along with some results.

Figure 3.1 shows the DE-MS spectra of  $\alpha$ -amyrine and of oleanolic acid as examples of the fragmentation of triterpenoid molecules [16]. They are obtained using electron ionisation at 70 eV. In both mass spectra, the intense peaks at  $m/z$  189, 203 and 218 can be related to the typical fragmentation pathway of oleanane and ursane type molecules bringing a double bond at position 12 [16,25], as shown in Figure 3.2, where the scheme of fragmentation for the urs-12-ene type molecules is reported. The fragmentation pathway is the same for olean-12-ene type molecules since these two series of compounds have the same carbon skeleton and differ only in the position of one methyl group. The peak at  $m/z$  218 occurs due to a classical retro Diels-Alder fission of ring C [16,25–27], and peaks at  $m/z$  189 and 203 arise from fragmentation rearrangements of the radical ion at  $m/z$  218.

In the mass spectra of  $\alpha$ -amyrine, a peak was observed at  $m/z$  426, relating to the molecular ion, along with peaks at  $m/z$  411 and 408, arising from the fragmentation of the molecular ion by the loss of a methyl radical and of a water molecule, respectively. The peak at  $m/z$  393 is due to the loss of a methyl radical and a water molecule.

The mass spectrum of oleanolic acid, a triterpenoid acid with double bond in position 12 and a carboxylic moiety in position 17 of the ring E, is also characterised by the presence of a peak at  $m/z$  248. The formation of this radical ion is due to a retro Diels-Alder fragmentation of the ring C, as shown in Figure 3.3 [16,25], analogous to the one reported for the formation of an ion at  $m/z$  218. The molecular ion of oleanolic acid occurs at  $m/z$  456. Moreover, in the mass spectrum peaks at  $m/z$  438, 411 and 410 are also evident and are caused by the loss of water,  $\text{CO}_2\text{H}^\cdot$  radical and  $\text{HCO}_2\text{H}$  from ring E, respectively. The loss of a methyl radical and of water leads to the formation of the peak at  $m/z$  423.

Figures 3.4–3.6 report the average mass spectra obtained, respectively, for frankincense resin, mastic resin and birch bark tar [16]. Moreover, in each spectrum the main ion and ion radical fragments are assigned, and for each material the main molecular markers are shown.

It is interesting to note that in DE mass spectra of lupane type molecules bringing an hydroxyl group at position 3 (typical of birch bark tar), the ion fragment at  $m/z$  189 arises from the fragmentation of the C ring system by cleavage of the 9–11 and 8–14 bonds followed by the loss of a water molecule [16,25,28] as shown in Figure 3.7.

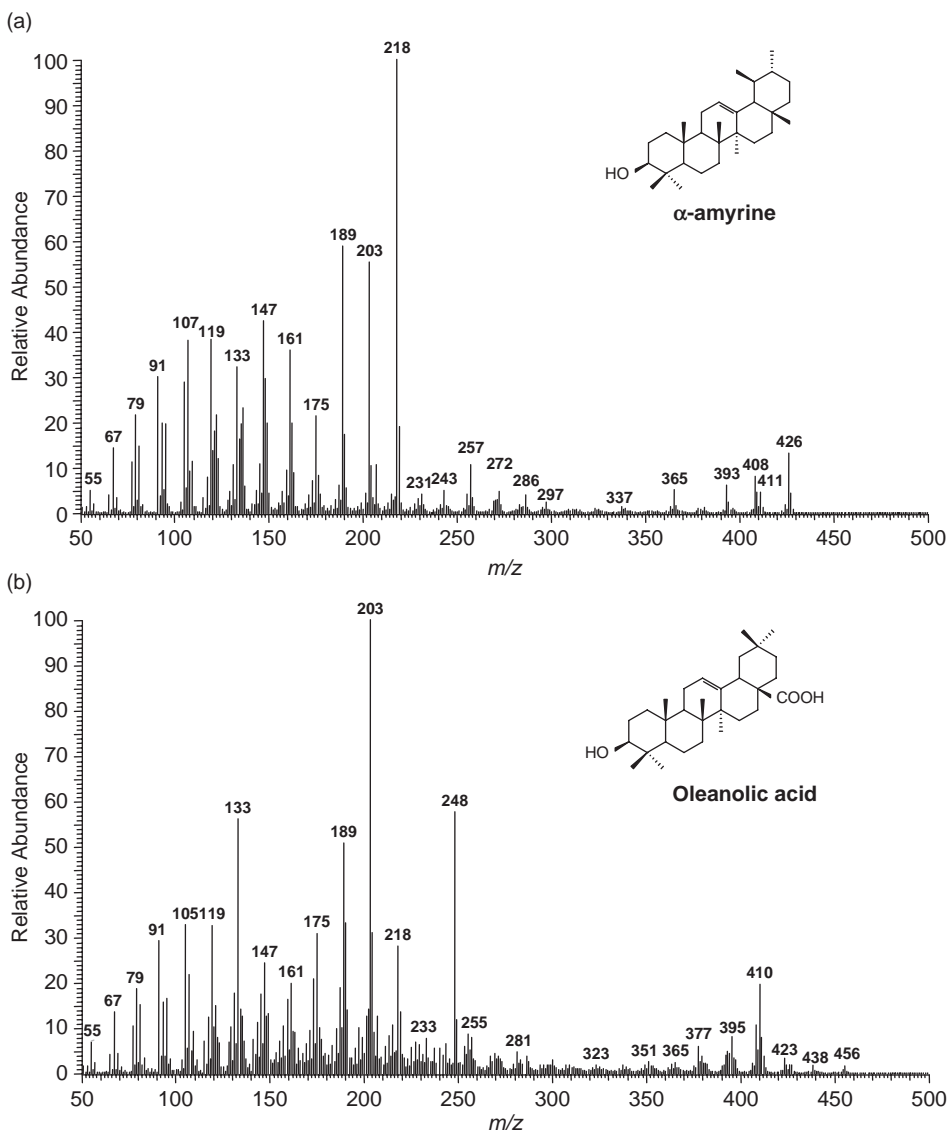


**Figure 3.1** Mass spectra of (a)  $\alpha$ -amyryne and (b) oleanolic acid obtained by DE-MS

The techniques based on the direct introduction of the sample in the mass spectrometer can also be used with CI. This allows just a small amount of fragmentation. Due to the fact that less energy is used than in the EI mode, CI produces relatively stable molecular ions and ion fragments, and does not give as extensive fragmentation as readily as EI does. Figure 3.8 compares the mass spectra of 7-oxo-dehydroabietic acid obtained by DE-MS using EI at 70 eV and CI with isobutane. In both these

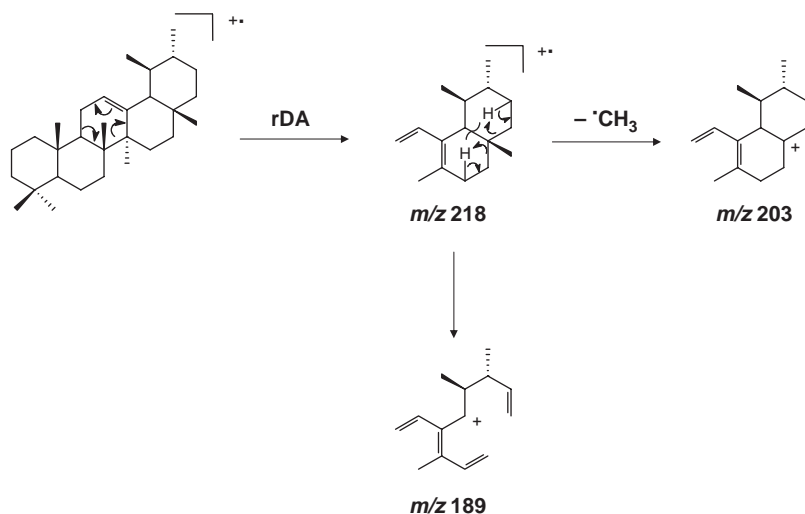


**Figure 3.2** Scheme of fragmentation for the urs-12-ene type molecules that leads to the formation of radical ions and ions at  $m/z$  218, 203 and 189

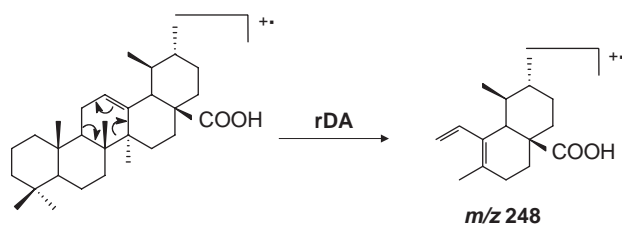


**Figure 3.3** Scheme of fragmentation for the urs-12-ene-17-oic type molecules that leads to the formation of radical ion at  $m/z$  248

conditions this acid shows a similar fragmentation pathway [18]. Figure 3.9 shows the scheme of the fragmentation pathway of 7-oxo-dehydroabietic acid under EI at 70 eV [29,30–32].

In the EI mass spectrum the occurrence of the molecular ion peak at  $m/z$  314 is evident along with a peak relative to the loss, from the molecular ion, of the methyl group at position 20 (as a methyl radical) at  $m/z$  299. The loss of the neutral fragment  $\text{HCOOH}$  then leads to the formation of peak at  $m/z$  253. Finally, the subsequent elimination of the isopropyl group along with the back transfer of one of its hydrogen atoms ( $\text{C}_3\text{H}_6$ ) gives rise to the peak at  $m/z$  211. The fragmentation pathway of 7-oxo-dehydroabietic acid under CI by isobutane is quite similar to the one obtained in the EI mode. In any case, with CI mass spectra can be acquired with more intense molecular or protonated molecular ion peaks. In the case of 7-oxo-dehydroabietic acid, the protonated molecular ion peak ( $m/z$  315)

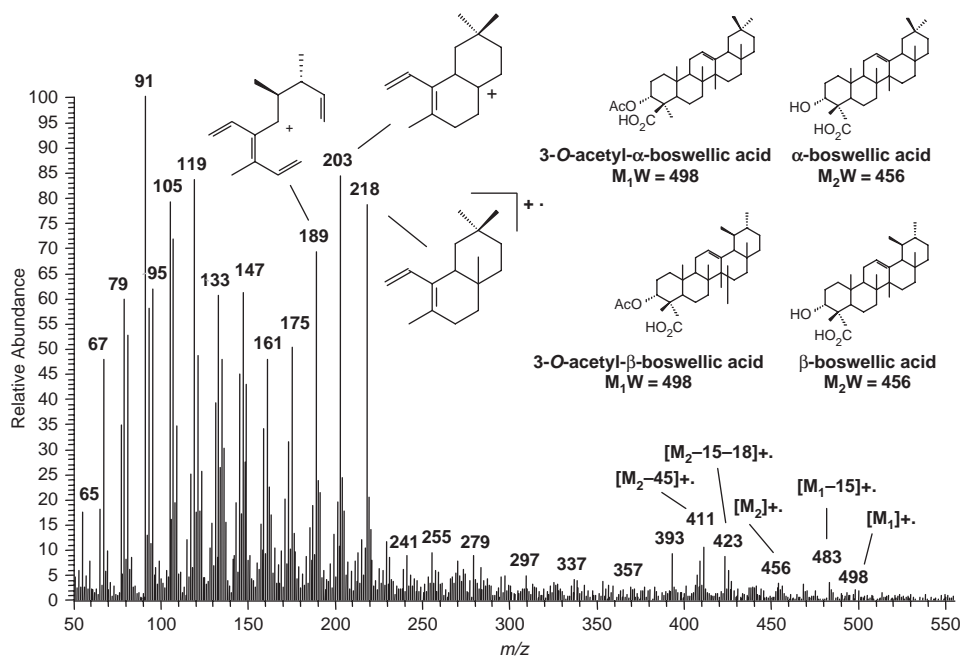


Figure 3.4 Mass spectrum of frankincense resin obtained by DE-MS

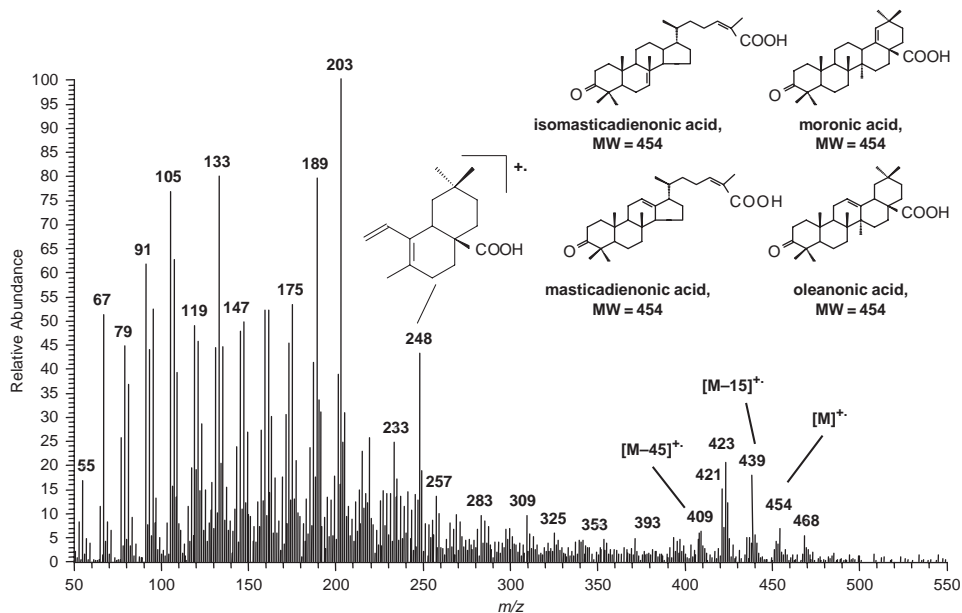
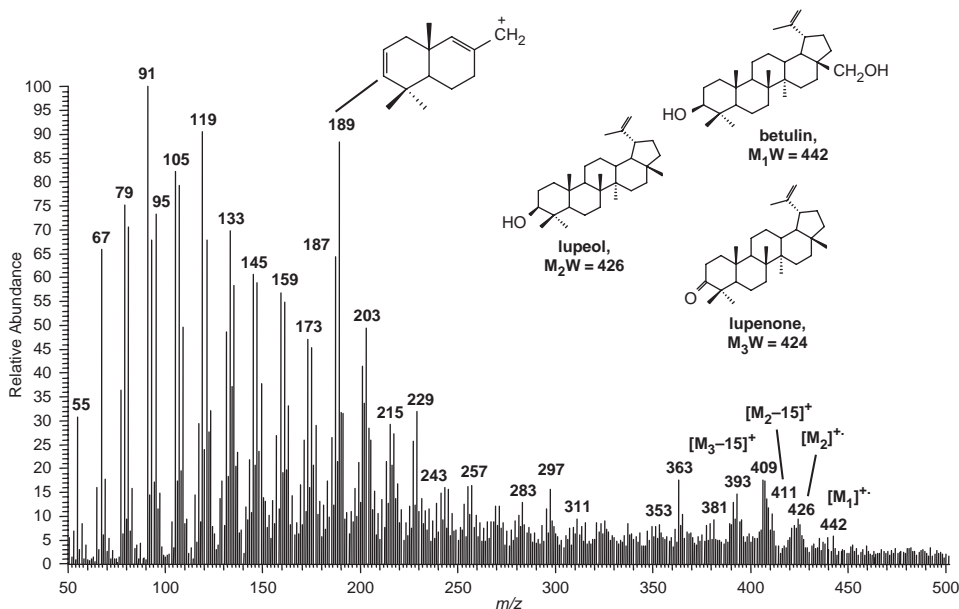
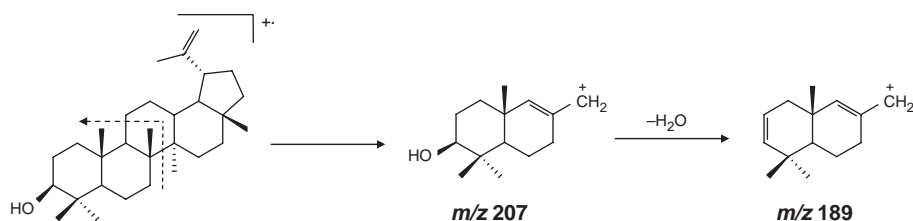


Figure 3.5 Mass spectrum of mastic resin obtained by DE-MS



**Figure 3.6** Mass spectrum of birch bark tar obtained by DE-MS

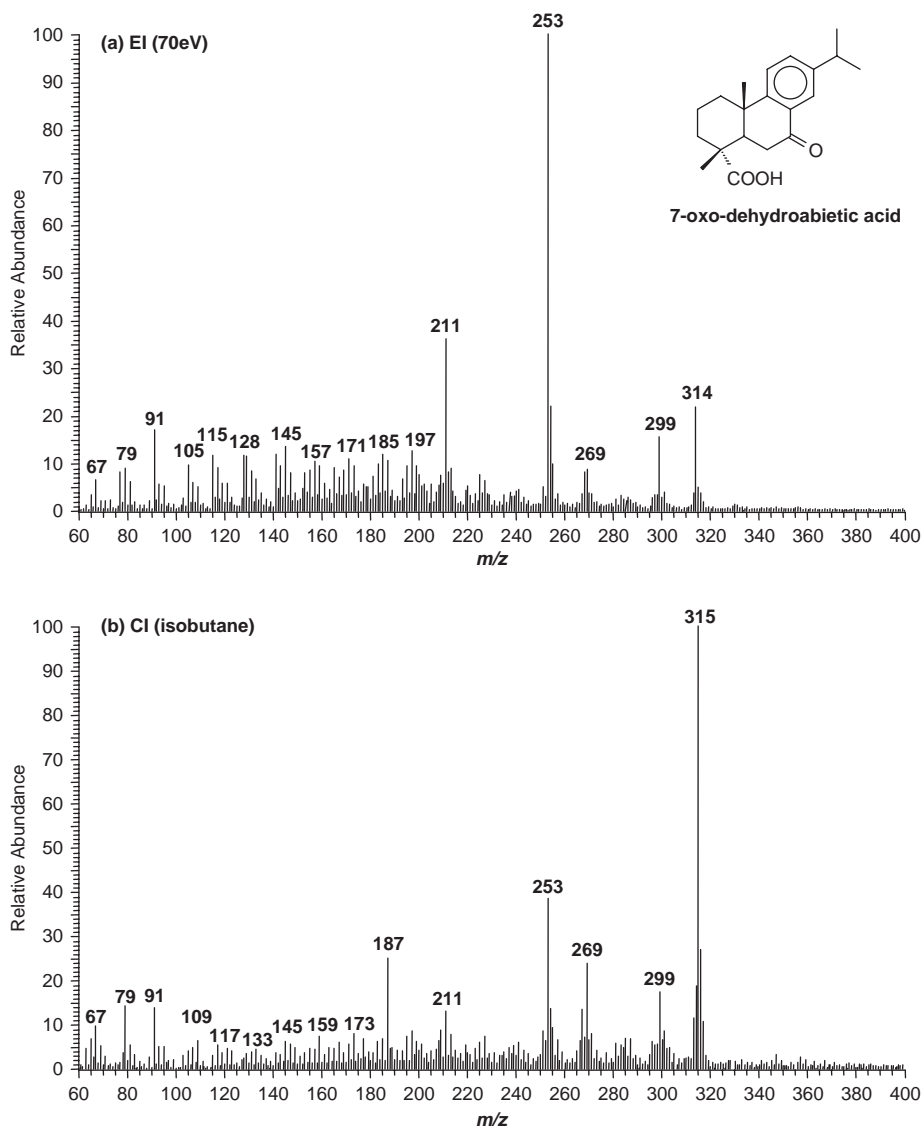


**Figure 3.7** Scheme of fragmentation for lupane type molecules that leads to the formation of the characteristic ion fragment at  $m/z\ 189$

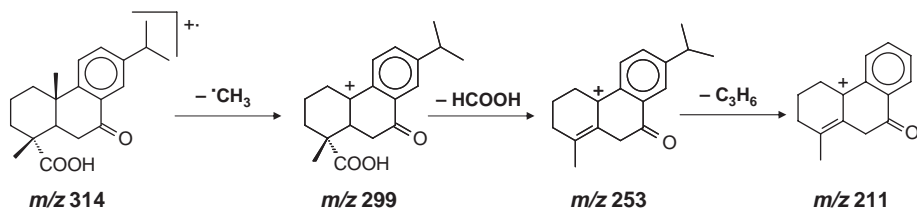
represents the base peak. The presence of the keto group, which increases the proton affinity of the molecule, gives it great stability. The mass spectra have a lower amount of noise because of the reduced fragmentation.

Figure 3.10 shows the mass spectra obtained by using DE-MS to analyse a sample of aged colophony from a varnish layer (colophony layered on a glass tile and naturally aged since 1976). The mass spectra are obtained using EI and CI. The mass spectrum of aged colophony obtained using EI at 70 eV presents the base peak at  $m/z\ 253$  formed by the fragmentation of 7-oxo-dehydroabietic acid; other intense peaks are at  $m/z\ 211$ , 299 and 314 which also arise from the fragmentation of 7-oxo-dehydroabietic acid, and at  $m/z\ 239$  and 285 which are related to the fragmentation of dehydroabietic acid. In addition, the ion fragments at  $m/z\ 315$  and 330 reveal the presence of highly oxidised tricyclic diterpenic molecules which arise from the oxidation of dehydroabietic acid





**Figure 3.8** Mass spectra of 7-oxo-dehydroabietic acid obtained by DE-MS using (a) electron ionisation at 70 eV and (b) chemical ionisation with isobutane



**Figure 3.9** Fragmentation pathway of 7-oxo-dehydroabietic acid

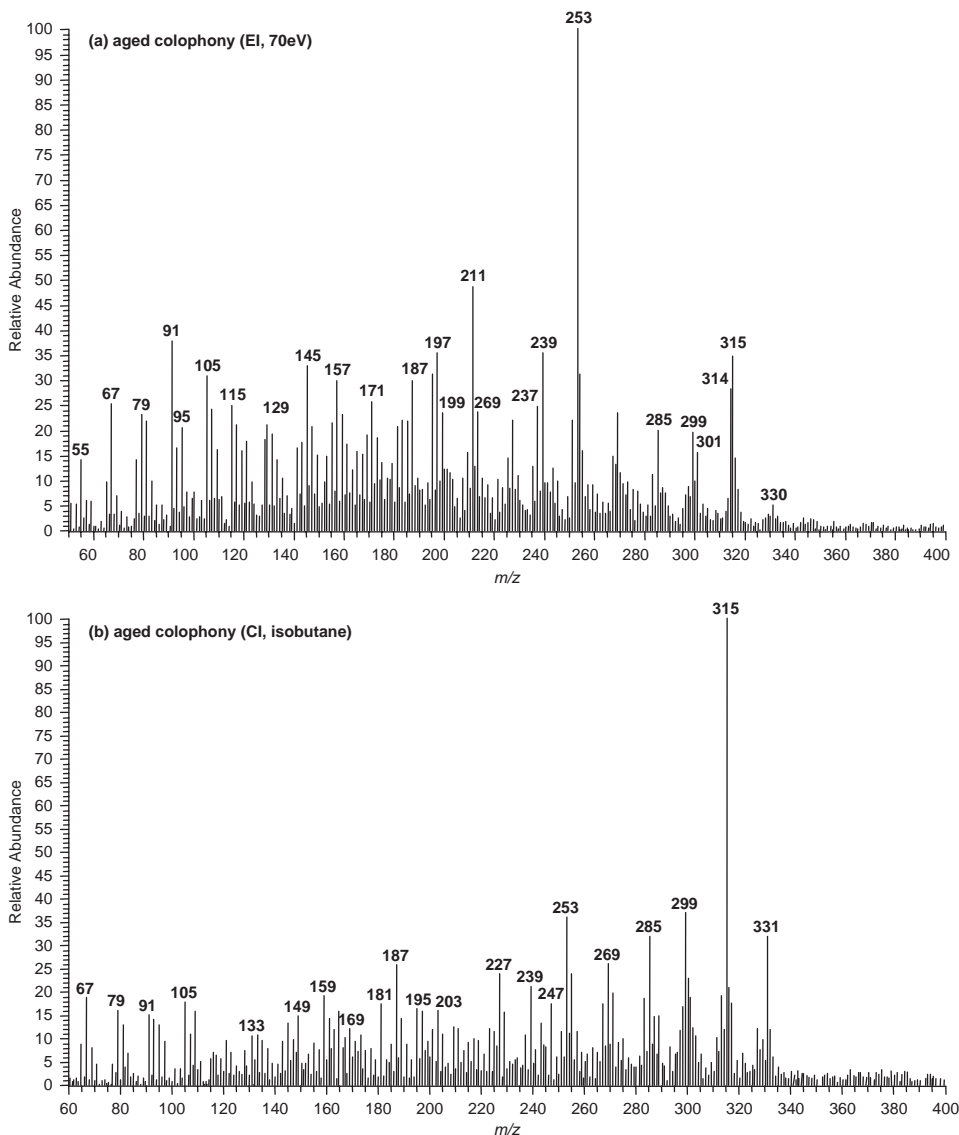


**Figure 3.10** Mass spectra of aged colophony obtained by DE-MS using (a) electron ionisation at 70 eV and (b) chemical ionisation with isobutane

and 7-oxo-dehydroabiatic acid with the inclusion of other oxygen atoms (formation of keto or hydroxyl groups) [17]. The mass spectrum of aged colophony obtained by CI with isobutane presents the base peak at  $m/z$  315, the protonated molecular ion of 7-oxo-dehydroabiatic acid. Other intense peaks are at  $m/z$  299 and 253, which also arise from 7-oxo-dehydroabiatic acid fragmentation and at  $m/z$  285 and 239, which are formed by the fragmentation of dehydroabiatic acid as seen previously. In this spectrum

too, the fragment at  $m/z$  331 reveals highly oxidised tricyclic diterpenoid molecules such as 7-oxo-15-hydroxy-dehydroabietic acid [18].

In both the mass spectra, the simultaneous presence of ion fragments related to 7-oxo-dehydroabietic acid and highly oxidised tricyclic diterpenes demonstrates the higher degree of oxidation of the aged colophony with respect to the fresh pine resin [17–19]. In the mass spectra, the peaks attributed to abietadienic and pimaradienic acids are not evident, indicating their depletion in the course of the resin ageing.

DTMS was used to study the ageing pathway of natural resins employed as varnishes in paintings [33]. This study was carried out by the complementary use of ammonia chemical ionisation ( $\text{NH}_3/\text{CI}$ ) and EI at 16 eV. EI promotes fragmentation of a molecule yielding structural information, while  $\text{NH}_3/\text{CI}$  mainly produces  $[\text{M}+\text{H}]^+$  or  $[\text{M}+\text{NH}_4]^+$  ions yielding molecular weight information. In particular, the analysis of raw and artificially aged dammar, mastic, colophony, copal and sandarac resin highlighted that, with ageing, cross-linking processes affect these organic substances with the formation of compounds at higher molecular weights [20,21,33]. Figure 3.11

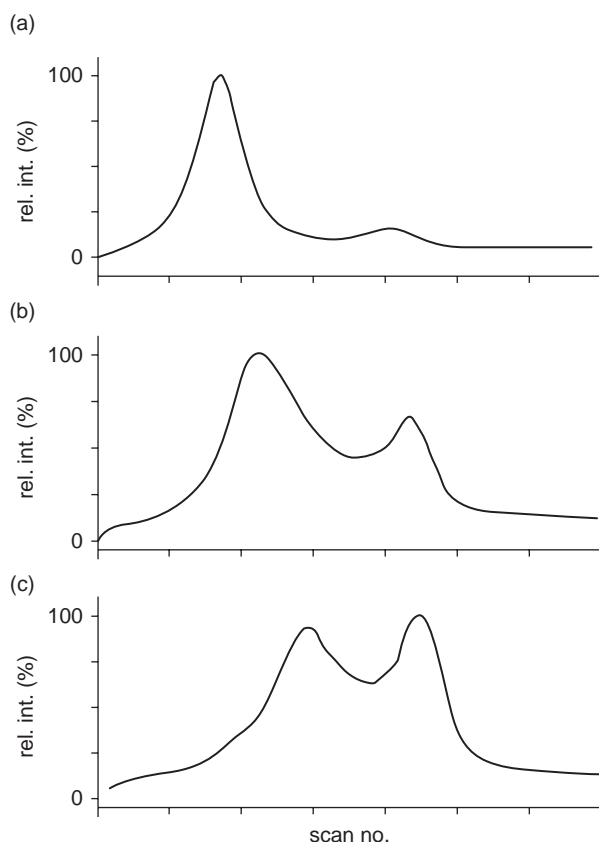


**Figure 3.11** DTMS total ion currents of (a) fresh dammar resin and dammar after (b) 1 week or (c) 2 weeks of artificial ageing. Reproduced from *J. Photochem. Photobiol., A*, **134**, 13, Copyright 2000, with permission from Elsevier

shows the DTMS TICs of raw and artificially aged dammar resin. By comparing the abundances of the volatilisation region (first peak, corresponding to volatile compounds) and the pyrolysis region (second peak, corresponding to cross-linked/polymerised material) of the TIC curves, it is evident that the polymerised fraction increases during the ageing of the resins.

### 3.4 Case Studies: Direct inlet mass-spectrometry (DI-MS)

DI-MS using EI was applied to the characterisation of natural substances in ancient adhesives to obtain molecular information on these substances in order to identify them [19]. DI-MS has considerable potential for extending the knowledge of the various natural resources used by prehistoric people for making adhesives.

#### 3.4.1 Analysis of a Brownish-orange Deposit from a Ceramic Sherd Recovered at La Fangade (France)

DI-MS was used to analyse a brownish-orange deposit observed on a ceramic sherd dated back to the 12th–11th century BC (Bronze Age) and found at the archaeological site of La Fangade (France). The analysis showed that pine resin was the main organic constituent in the sample. The mass spectrum was characterised by a base peak at  $m/z$  239 and a main fragment at  $m/z$  285 (Figure 3.12).

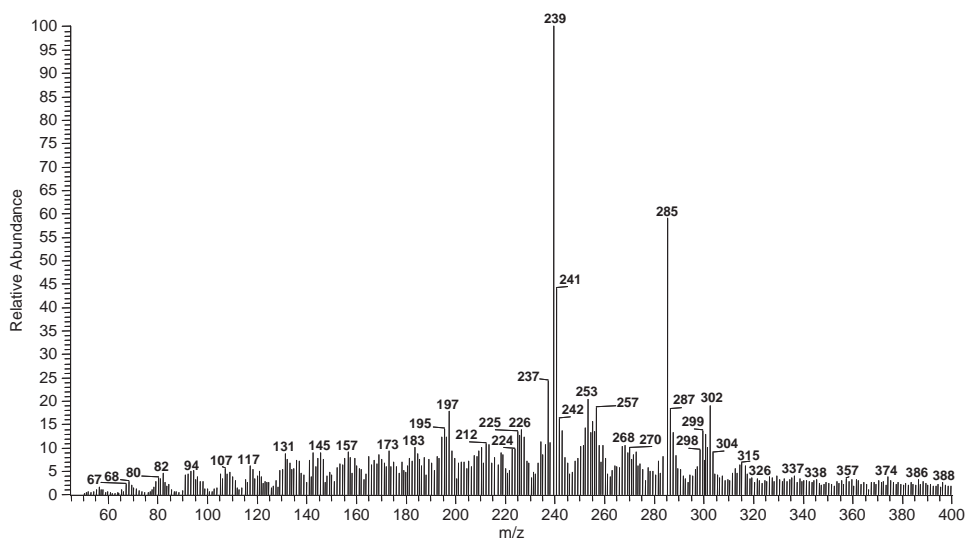


**Figure 3.12** Mass spectrum of the organic material sampled from a ceramic sherd from the Bronze Age site of La Fangade (France). The spectrum was obtained by means of DI-MS. Reproduced from *Anal. Chem.*, Regert and Rolando, **74**, 5, 965–975, Copyright 2002, with permission from American Chemical Society

Both ion fragments are known to be the main peaks of the mass spectrum of a pine resin. In particular, the base peak at  $m/z$  239 is characteristic of the fragmentation of dehydroabietic acid. This acid is the main degradation marker formed by aromatisation of abietadienic acids, which are the major constituents of raw pine resins. DI-MS gave data not only on the class of materials present but also on the degree of oxidation. In fact, the low intensity of fragments at  $m/z$  253 and 314 produced by the fragmentation of 7-oxodehydroabietic acid under EI at 70 eV indicates that the pine resin has not undergone any significant oxidation process, probably because of the anaerobic burial environment of the archaeological site where the sample had been preserved.

### 3.4.2 Analysis of a Blackish Residue Present on the Chape of a Sword Discovered at Argancy (Moselle, France)

A second application of DI-MS was in the analysis of archaeological adhesive of a blackish amorphous residue present on the chape of a bronze sword, discovered in a tomb from the Iron Age (ca. 800–700 BC) at the archaeological site of Argancy (Moselle, France). In the mass spectrum (Figure 3.13) the ion fragment at  $m/z$  189, which is characteristic of triterpenoid compounds, is evident and represents the base peak.

The general pattern of the mass spectrum and the presence of peaks at  $m/z$  424, 426 and 442, attributed, respectively, to the molecular ions of lupeol, lupenone and betulin, suggest the presence of birch bark tar. This study provided the first evidence that birch bark tar was used for assembling bronze tools during the Iron Age in Europe.

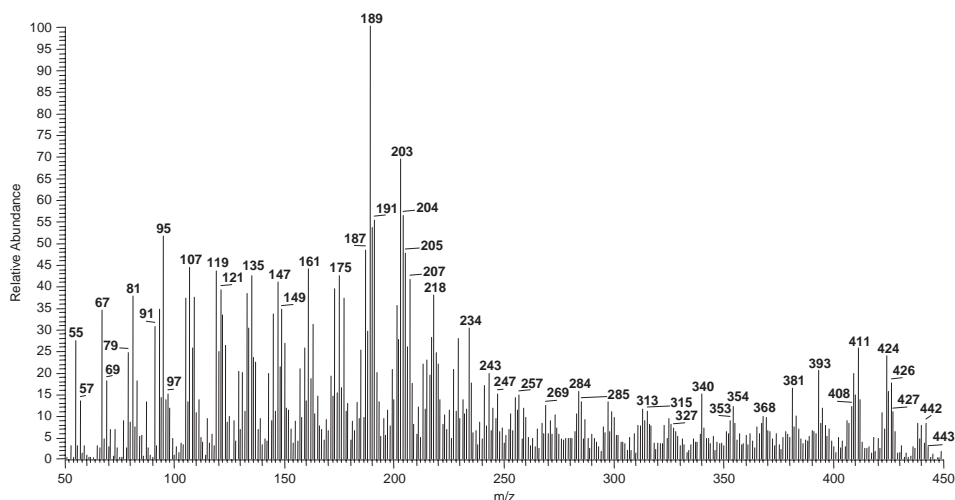


**Figure 3.13** Mass spectrum of the black material collected from a bronze chape of a sword from the Iron Age period. The spectrum was obtained by means of DI-MS. Reproduced from *Anal. Chem.*, Regert and Rolando, **74**, 5, 965–975, Copyright 2002, with permission from American Chemical Society

### 3.5 Case Studies: Direct Exposure-Mass Spectrometry (DE-MS)

DE-MS was employed in the characterisation of resinous materials from Roman ceramic vessels, Palaeolithic stone tools, Roman glass unguentaria and amphorae [14,16,18,23].

#### 3.5.1 Analysis of the Organic Residue from a Ceramic Censer Recovered in Antinoe (Egypt) [16]

The first example regards the use of DE-MS in the study of an amorphous material sampled from a censer recovered Antinoe archaeological site and dated back to the V-VII cent. AC. The mass spectrum (Figure 3.14) proved that ion fragments at  $m/z$  189 and 203 were the most abundant, highlighting the occurrence of triterpenoid compounds. The general pattern of the mass spectrum appears to be very similar to that of mastic resin, especially in the range  $m/z$  400–500. In addition, the occurrence of an ion at  $m/z$  248, consistent with the fragmentation of oleanonic acid by a retro Diels-Alder fragmentation of the ring C, seems to indicate that mastic is the main component of the sample.

The results show that DE-MS alone provides evidence of the presence of the most abundant components in samples. On account of the relatively greater difficulty in the interpretation of DE-MS mass spectra, the use of multivariate analysis by principal component analysis (PCA) of DE-MS mass spectral data was used to rapidly differentiate triterpene resinous materials and to compare reference samples with archaeological ones. This method classifies the spectra and indicates the level of similarity of the samples. The output is a two- or three-dimensional scatter plot in which the geometric distances among the various points, representing the samples, reflect the differences in the distribution of ion peaks in the mass spectra, which in turn point to differences in chemical composition of

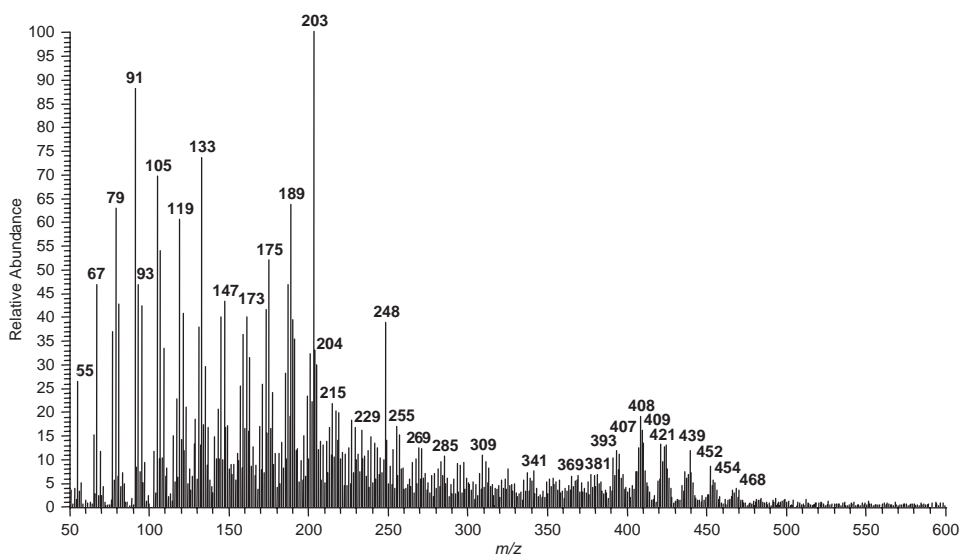


**Figure 3.14** Mass spectrum of the sample from the censer found in the archaeological site at Antinoe (Egypt) obtained by DE-MS [16]

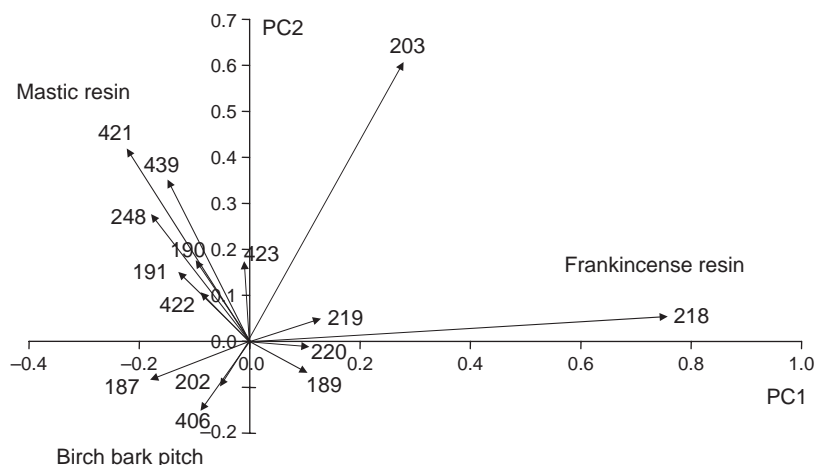


**Figure 3.15** Significant mass fragments in PCA analysis of DE-MS data of the examined triterpenoid substances and the value of their loadings in calculating PC1 and PC2

the samples. Mass spectral data (relative abundance of selected  $m/z$  value ranges) corresponding to six replicates of reference samples of frankincense, mastic and birch bark pitch were submitted to PCA based on the covariance matrix after row normalisation of the data. The samples of the three resins are located in three distinct areas of the scatter plot of the first two principal components (PCs), which accounts for 89% of the variance of the data. The 15 variables (mass fragments) with the highest weights (loadings) were  $m/z$  187, 189, 190, 191, 202, 203, 218, 219, 220, 248, 406, 421, 422, 423 and 439. The loading values (Figure 3.15) show that a high intensity of  $m/z$  218 determined the position of frankincense on the right of the scatter plot, at positive values of PC1. However, the value of PC2 is crucial for differentiating between mastic and birch bark pitch. A high intensity of  $m/z$  203, 421, 439 and 248 accompanied by a relatively low intensity of  $m/z$  202, 187 and 406 resulted in a placing at positive values of PC2. This is characteristic of mastic resin rather than birch bark pitch. The mass spectral data obtained from samples collected from the censer were treated in the same manner together with the reference data, and the relative scatter plot is shown in Figure 3.16.

The first two PCs account for 85% of the total variance of the data set. The PCA highlights that the sample is placed in the area of the mastic resin cluster. This confirmed the hypothesis made on the basis of a qualitative examination of the mass spectra, even though the sample is clearly shifted at lower values of PC2 with respect to the centroid of the mastic cluster. This was attributed to the presence of other substances mixed with the resin, and/or to a different quantitative distribution of the triterpenoids present in the censer with respect to the reference raw mastic resin.

### 3.5.2 Analysis of the Organic Residue from a Roman Amphora Recovered in Liguria (Italy) [18]

Another interesting application of DE-MS was in the examination of a resinous archaeological substance sampled from the material contained in a Roman amphora (2nd–4th

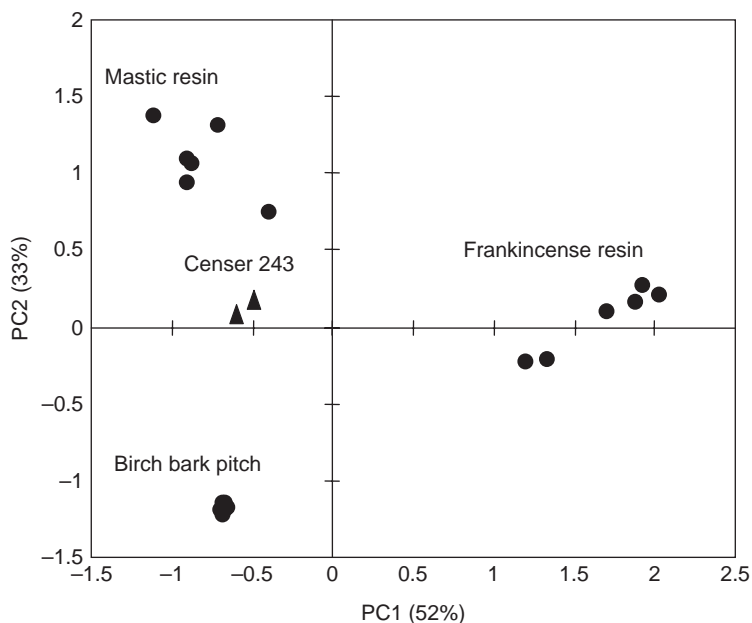


**Figure 3.16** PCA scatter plot of mass spectral data recorded by DE-MS for mastic resin, frankincense resin, birch bark pitch and organic residue recovered from the ceramic censer from Antinoe (Egypt)

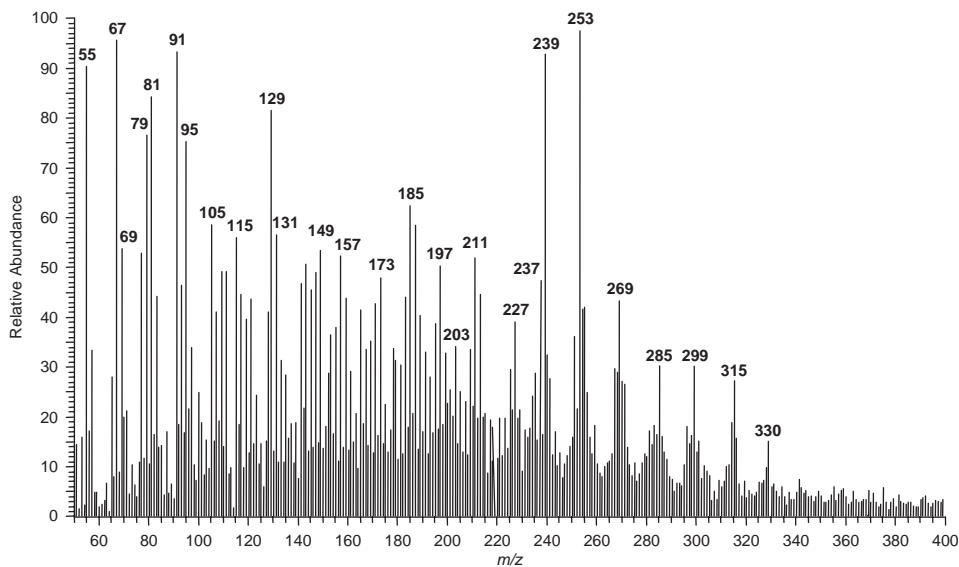


**Figure 3.17** DE mass spectrum of the resinous material collected from the Roman amphora recovered from a waterlogged archaeological site in Liguria (Italy) [18]



centuries AD) recovered from a waterlogged archaeological site in Liguria (Italy) [18]. In this case DE-MS was employed in CI mode using isobutane as reagent gas. On account of the small amount of energy involved in the fragmentation pathway, DE-CI(isobutane)MS managed to make a rapid distinction between pine resin and pine pitch, which would not have been feasible with EI at 70 eV. In fact, the DE-CI mass spectra contained a limited number of peaks and exhibited major molecular adducts which thus provided the molecular weights of the main constituents.

Figure 3.17 shows the mass profile of the resinous material collected from the Roman amphora. It shows the presence of abietane skeleton diterpenoids due to the occurrence of the peaks at  $m/z$  315, 299, 285, 253 and 239. Furthermore, a high degree of oxidation of the resin was ascertained by the abundance of peaks at  $m/z$  315 and 253, deriving from 7-oxo-dehydroabietic acid, and those at  $m/z$  331 and 329, from highly oxidised tricyclic diterpenoid molecules. Finally, the presence of retene was evidenced by the peaks at  $m/z$  234 and 219. The results showed that a pitch from *Pinaceae* had been in the amphora.

### 3.6 Case Studies: Direct Temperature Resolved Mass Spectrometry (DTMS)

#### 3.6.1 Analysis of Varnishes Collected from Paintings

DTMS was applied to determine the nature of several varnish samples collected from various paintings preserved in Dutch museums [20]. DTMS allowed the low molecular weight part (volatiles) to be separated from the polymeric part of the sample. Two different types of varnish (triterpenoid and diterpenoid) were thus identified and the degree of oxidation was ascertained. It was found that triterpenoid varnishes were characterised by molecular ions in the region  $m/z$  410–460 and high peaks at  $m/z$  143. The latter peak corresponds to the ion fragment obtained by the cleavage of the side chain of ocotillone-type molecules, which are typical of aged triterpenoid materials containing molecules with a dammarane skeleton such as dammar resin [20]. Diterpenoid varnish mass spectra present molecular ions in the region  $m/z$  300–330. Peaks at  $m/z$  253, 299 and 315 indicate the presence of 7-oxo-dehydroabietic acid and other highly oxidised diterpenoids.

### 3.7 Conclusions

Direct mass spectrometry based techniques such as DI-MS, DE-MS and DTMS are unique in their ability to yield complete chemical structure assignments and to identify a great variety of resinous amorphous materials.

Despite the complexity of the chemical composition of the resinous materials, in a few minutes such techniques provide a mass spectral fingerprint, which highlights the compounds that are the main components in the sample. They avoid any sampling treatment before analysis. They have thus enabled diterpenoid resinous materials from *Coniferae*, and several triterpenoid materials to be clearly identified. In particular, the DE-MS technique is able to distinguish between different triterpenoid materials such as mastic resin, frankincense resin and birch bark tar. In fact, using PCA on DE-MS mass

spectral data at selected  $m/z$  ranges, corresponding to the fragmentation of triterpenoid molecules, means that the three resinous substances can be separated graphically into three separate clusters in the PCA scatter plot. Thus, the chemical differences and similarities between the samples can be understood more easily. The three resinous materials are collocated in three well defined areas of the scatter plot which accounts for 89% of the total variance.

The degree of oxidation of *Pinaceae* resins can also be ascertained using such techniques but in EI mode at 70 eV they failed to distinguish between pine resin and pine pitch. In fact, retene and related compounds, and methyl dehydroabietate do not form any characteristic fragment ion in sufficient abundance to be used as a marker. The ability to identify the presence of pine resin or pine pitch is useful in order to reconstruct the technological methods that were once used to produce an artefact. DE-CI(isobutane)MS has proved to be a fast tool for distinguishing between pine resin and pine pitch. In fact, due to the small amount of energy involved in the fragmentation pathway, the DE-CI mass spectra contained a limited number of peaks and exhibited major molecular adducts directly providing the molecular weights of the main constituents.

## References

1. K. Evans and C. Heron, Glue, disinfectant and chewing gum: natural products chemistry in archaeology, *Chem. Ind.*, **12**, 446–449 (1993).
2. E. W. H. Hayek, P. Krenmayr, H. Lohninger, U. Jordis, W. Moche and F. Sauter, Identification of archaeological and recent wood tar pitches using gas chromatography/mass spectrometry and pattern recognition, *Anal. Chem.*, **62**, 2038–2043 (1990).
3. J. S. Mills and R. White, The identity of the resins from the late Bronze Age shipwreck at Ulu Burun (Kas), *Archaeometry*, **31**, 37–44 (1989).
4. A. M. Pollard and C. Heron, The chemistry and use of resinous substances, in *Archaeological Chemistry*, RSC Paperbacks, Cambridge, 1996.
5. M. Serpico and R. White, Resins, amber and bitumen, in *Ancient Egyptian Materials and Technology*, P. Nicholson and I. Shaw (Eds), Cambridge University Press, Cambridge, 2000.
6. N. Robinson, R. P. Evershed, W. J. Higgs, K. Jerman and G. Eglinton, Proof of a pine wood origin for pitch from Tudor (Mary Rose) and Etruscan shipwrecks: application of analytical organic chemistry in archaeology, *Analyst*, **112**, 637–643 (1987).
7. S. Charters, R. P. Evershed, L. J. Goad, C. Heron and P. Blinkhorn, Identification of an adhesive used to repair a roman jar, *Archaeometry*, **35**, 91–101 (1993).
8. S. A. Buckley and R. P. Evershed, Organic chemistry of embalming agents in Pharaonic and Graeco-Roman mummies, *Nature*, **413**, 837–841 (2001).
9. M. P. Colombini, F. Modugno, F. Silvano and M. Onor, Characterisation of the balm of an Egyptian mummy from the seventh century B.C., *Stud. Conserv.*, **45**, 19–29 (2000).
10. U. Weser, Y. Kaup, H. Etspuler, J. Koller and U. Baumer, Embalming in the old kingdom of pharaonic Egypt, *Anal. Chem.*, **70**, 511A–516A (1998).
11. C. Vieillescazes and S. Coen, Carcterisation de quelques resines utilisees en Egypte ancienne, *Stud. Conserv.*, **38**, 255–264 (1993).
12. M. L. Proefke, K. L. Rinehart, M. Raheel, S. H. Ambrose and S. U. Wisseman, Probing the mysteries of ancient Egypt. Chemical analysis of Roman period Egyptian mummy, *Anal. Chem.*, **64**, 105A–111A (1992).
13. J. S. Mills and R. White, *Organic Chemistry of Museum Objects*, Butterworth-Heinemann, London, 1999.
14. M. P. Colombini, G. Giachi, F. Modugno, P. Pallecchi and E. Ribechini, Characterisation of paints and waterproofing materials of the shipwrecks found in the archaeological site of the Etruscan and Roman harbour of Pisa (Italy), *Archaeometry*, **45**, 649–664 (2003).

15. B. Stern, C. Heron, L. Corr, M. Serpico and J. Bourriau, Compositional variations in aged and heated pistacia resin found in late Bronze Age Canaanite amphorae and bowls from Amarna, Egypt, *Archaeometry*, **45**, 457–469 (2003).
16. F. Modugno, E. Ribechini and M. P. Colombini, Chemical study of triterpenoid resinous materials in archaeological findings by means of direct exposure electron ionisation mass spectrometry and gas chromatography/mass spectrometry, *Rapid Commun. Mass Spectrom.*, **20**, 1787–1800 (2006).
17. M. P. Colombini, F. Modugno and E. Ribechini, Direct exposure electron ionization mass spectrometry and gas chromatography/mass spectrometry techniques to study organic coatings on archaeological amphorae, *J. Mass Spectrom.*, **40**, 675–687 (2005).
18. E. Ribechini, F. Modugno and M. P. Colombini, Direct Exposure-(chemical ionisation) Mass Spectrometry for a rapid characterization of raw and archaeological diterpenoid resinous materials, *Microchim. Acta*, **162**, 405–413 (2008).
19. M. Regert and C. Rolando, Identification of archaeological adhesives using Direct Inlet Electron Ionization Mass Spectrometry, *Anal. Chem.*, **74**, 965–975 (2002).
20. G. A. Van Der Doelen, K. J. Van Den Berg and J. J. Boon, Comparative chromatographic and mass-spectrometric studies of triterpenoid varnishes: fresh material and aged samples from paintings, *Stud. Conserv.*, **43**, 249–264 (1998).
21. D. Scalarone, J. van der Horst, J. J. Boon and O. Chiantore, Direct-temperature mass spectrometric detection of volatile terpenoids and natural terpenoid polymers in fresh and artificially aged resins, *J. Mass Spectrom.*, **38**, 607–617 (2003).
22. M. Regert, J. Langlois, E. Laval, A.-S. Le Hô and S. Pagès-Camagna, Elucidation of molecular and elementary composition of organic and inorganic substances involved in 19th century wax sculptures using an integrated analytical approach, *Anal. Chim. Acta*, **577**, 140–152 (2006).
23. E. Ribechini, F. Modugno, M. P. Colombini and R. P. Evershed, Gas chromatographic and mass spectrometric investigations of organic residues from roman glass unguentaria, *J. Chromatogr. A*, **1183**, 158–169 (2008).
24. M. Regert, T. Deviese, A. S. Le Ho and A. Rougeulle, Reconstructing ancient Yemeni commercial routes during the Middle Ages using structural characterization of terpenoid resins, *Archaeometry*, **50**, 668–695 (2008).
25. H. Budzikiewicz, J. M. Wilson and C. Djerassi, Mass spectrometry in structural and stereochemical problems. XXXII. Pentacyclic triterpenes, *J. Am. Chem. Soc.*, **85**, 3688–3699 (1963).
26. J. Karliner and C. Djerassi, Terpenoids. LVII. Mass spectral and nuclear magnetic resonance studies of pentacyclic triterpene hydrocarbons, *J. Org. Chem.*, **31**, 1945–1956 (1966).
27. L. Ogunkoya, Application of mass spectrometry in structural problems in triterpenes, *Phytochem.*, **20**, 121–126 (1981).
28. J. Schmidt and S. Huneck, Mass spectroscopy of natural products. V. Mass spectroscopic studies of ring A substituted allobetulane derivatives, *Org. Mass Spectrom.*, **14**, 646–655 (1979).
29. T. L. Chang, T. E. Mead and D. F. Zinkel, Mass spectra of diterpene resin acid methyl esters, *J. Am. Oil Chem. Soc.*, **48**, 455–461 (1971).
30. H. E. Audier, S. Bory, G. Defaye, M. Fetizon and G. Moreau, Spectre de masse des terpenes – II. Influence du noyau aromatique sur la fragmentation des diterpenes tricycliques, *Bull. Soc. Chim. Fr.*, **10**, 3181–3186 (1966).
31. H. E. Audier, S. Bory, M. Fetizon and N. T. Anh, Spectre de masse des terpenes – III. Influence des liaisons ethyleniques sur la fragmentation des diterpenes, *Bull. Soc. Chim. Fr.*, **12**, 4002–4010 (1966).
32. C. R. Enzell, Mass spectrometric studies of diterpenes – IV. Aromatic diterpenes, *Tetrahedron Lett.*, **19**, 2135–2143 (1966).
33. G.A. van der Doelen and J. J. Boon, Artificial ageing of varnish triterpenoids in solution, *J. Photochem. Photobiol., A*, **134**, 45–57 (2000).



# 4

## Direct Mass Spectrometry to Characterise Wax and Lipid Materials

*Martine Regert*

### 4.1 Introduction

Animal fats, beeswax and vegetable oils have been exploited for a long time; the first examples date from the Palaeolithic period (Niven, 2007). The exploitation of beeswax is attested in various Neolithic European sites (Heron *et al.*, 1994; Regert *et al.*, 2001a). The start of the extraction of oil from plants is more difficult to assess. The use of vegetable oils may date back to the Neolithic period (Regert *et al.*, 2003a) but it is undeniably chemically demonstrated for more recent times (Copley *et al.*, 2001; Colombini *et al.*, 2005a).

Although several archaeological clues including bone remains, pollen assemblages or iconography, may provide information related to the utilization of these products during prehistory, more direct evidence comes from the chemical analysis of amorphous organic residues that are preserved in ancient ceramic vessels (Evershed *et al.*, 1997a, b, 2002; Copley *et al.*, 2003; Regert, 2007). Beeswax was also encountered in various other objects of our cultural heritage such as writing tablets, seals on ancient documents, sculptures and paintings (Regert, 2008). Other waxes, from animal, plant or fossil origin are also of importance, particularly in wax sculptures (Regert *et al.*, 2005).

These natural substances covered a wide range of uses. They could be used as pure materials or as part of complex mixtures containing resins, starch, pigments or dyes, depending on the purpose for which they were employed.

From a chemical standpoint, ancient lipids and waxes are made of complex molecular mixtures containing fatty acids, *n*-alcohols, *n*-alkanes, and also long chain compounds such as triacylglycerols (TAGs), monoesters, hydroxy esters or diesters. Chromatographic techniques, usually linked with mass spectrometry, are methods of choice for their characterisation. However, these analyses are necessarily preceded by time-consuming pretreatment steps that depend upon the biomolecular constituents present in the matter. Before performing any separation analysis, it may be useful to proceed to direct inlet, or direct exposure, electron ionisation mass spectrometry (DI EI-MS or DE EI-MS) on tiny samples. These methods are of great interest for several reasons. First of all, they are adapted to the analysis of a minimal amount of sample (<100 µg). They represent an interesting mode of sample introduction that reduces or eliminates sample manipulation. Lastly, they are fast methods that allow a mass spectrum of a complex sample to be obtained in a few minutes. Hence, they allow the rapid treatment of a large number of samples that may be easily classified in several categories depending on their mass spectral pattern.

Such methods were recently shown to be efficient fingerprinting tools to assess the different kinds of lipid and wax substances present in a sample, as well as some additives, particularly plant resins (see Chapter 3).

In specific cases, when long chain compounds such as esters and TAGs have survived and have not yet been hydrolysed or oxidised, it may be useful to carry out soft ionisation techniques in order to fully characterise the structure of these biomarkers by direct infusion into an electrospray source after adapted purification treatments.

In the present chapter, we first provide some general information concerning the chemistry of waxes and lipids currently encountered in various items from our cultural heritage and we detail the main protocols based on direct mass spectrometry that have been developed so far. We then discuss the mass spectra obtained by EI-MS on a range of reference substances and materials sampled from museum and archaeological artefacts. We then focus on the recent possibilities supplied by electrospray ionisation for the elucidation of the structure of biomarkers of beeswax and animal fats.

## **4.2 Description, Origin and Chemistry of Lipids from our Cultural Heritage**

The interpretation of the analytical data obtained from ancient materials relies on a good knowledge of the various natural or synthetic substances that may be involved in the samples investigated. Accordingly, we describe here the main characteristics of waxes, animal fats and vegetable oils, not only from a chemical point of view, but also considering their properties, origin and uses.

### **4.2.1 Waxes**

Waxes do not form a homogeneous group from both chemical and biological points of view. They are made of a great variety of molecular compounds and they originate from

both animals and plants. Some of them are also from geological origin (fossil matter). Nevertheless, they present a set of common chemical and biological properties that means they are considered as a specific and particular class of substances. Whatever their origin, all waxes are hydrophobic substances. Some of them are protective coatings, particularly when they originate from the plant kingdom. They are solid at room temperature: depending on their chemical composition, their melting point varies between 40°C and 100°C. They are all made of complex molecular mixtures containing various homologous compounds such as fatty acids, *n*-alkanes, *n*-alcohols and esters.

Their hydrophobicity and their plasticity were appreciated and used for a long time in a wide range of activities. To our knowledge, the first wax to have been exploited is beeswax. Beeswax is produced by various species of bees in the world, and it has a melting point between 62°C and 64°C. It mainly contains homologous series of even-numbered fatty acids (C<sub>22</sub>–C<sub>34</sub>, C<sub>24</sub> being the predominant compound), odd-numbered *n*-alkanes (C<sub>21</sub>–C<sub>33</sub>, C<sub>27</sub> being the major compound) and even-numbered palmitic esters from C<sub>40</sub> to C<sub>52</sub> (Tulloch and Hoffman, 1972; Kolattukudy, 1976). Hydroxy esters, diesters and hydroxy diesters also form part of beeswax to a lesser extent.

Another animal wax mentioned in the field of cultural heritage, although not often attested by chemical analysis, is spermaceti (Mills and White, 1994). Used for several purposes including medicines, cosmetics and lighting (candles), this substance may be obtained from whale oil extracted from the head cavities of sperm whale (*Physeter macrocephalus*). It has a melting point of 44°C (Mills and White, 1994) and it is made of even-numbered esters in the range C<sub>26</sub>–C<sub>36</sub>. Recent work showed that contrary to beeswax in which all the esters are derived from a single fatty acid (palmitic acid), the esters present in spermaceti contain several different even-numbered fatty acid moieties from C<sub>10</sub> to C<sub>18</sub> (Regert *et al.*, 2005).

The main vegetable substances, candelilla and carnauba, referred to as waxes in the field of cultural heritage are issued from plants growing in the American continent. The first, candelilla wax, is produced by the leaves of various species of *Euphorbia* and contains a mixture of odd-numbered *n*-alkanes with 29–31 carbon atoms, *n*-C<sub>31</sub> predominating; the second, carnauba wax, originates from several palm trees, such as *Copernicifera cerifera* and is made of homologous series with even-numbered constituents including *n*-alcohols (C<sub>28</sub>–C<sub>34</sub>, C<sub>32</sub> predominating) and long chain esters in the range C<sub>48</sub>–C<sub>62</sub>, C<sub>56</sub> being the main compound. A third substance, known as Japan wax, is also usually considered as a vegetable wax although it mainly contains fatty biomarkers, namely TAGs, tripalmitin being the major constituent.

Fossil waxes, also incorrectly known as mineral waxes, are mainly made of odd- and even-numbered *n*-alkanes presenting various distributions. Paraffin has a simple pattern from C<sub>21</sub> to C<sub>35</sub>, maximising at C<sub>27</sub>, whereas ozokerite presents a bimodal distribution around C<sub>27</sub> and C<sub>42</sub>.

Table 4.1 summarises the main characteristics of the waxes discussed in this chapter.

#### 4.2.2 Animal Fats and Vegetable Oils

Animal fats and vegetable oils form a more coherent group than waxes from a chemical point of view. When they are fresh, i.e. when they have not yet been submitted to any degradation process, they indeed contain more than 90% TAGs. Depending on the nature

**Table 4.1** *Origin and main biomarkers of waxes discussed*

Name of wax	Origin	Main biomarkers
Beeswax	Produced by bees	Even-numbered fatty acids (C <sub>22</sub> –C <sub>34</sub> ) Odd-numbered <i>n</i> -alkanes (C <sub>21</sub> –C <sub>33</sub> ) Even-numbered palmitic esters (C <sub>40</sub> –C <sub>52</sub> ) Even-numbered esters (C <sub>26</sub> –C <sub>36</sub> )
Spermaceti	Extracted from head cavities of sperm whales	Odd-numbered <i>n</i> -alkanes (C <sub>29</sub> –C <sub>31</sub> )
Candelilla wax	Protective coating of leaves from <i>Euphorbia</i> , particularly growing in Mexico and southern USA	Even-numbered <i>n</i> -alcohols (C <sub>28</sub> –C <sub>34</sub> ) Even-numbered esters (C <sub>48</sub> –C <sub>62</sub> )
Carnauba wax	Protective coating of leaves from several American palm trees	Triacylglycerols, palmitin as major compound
Japan wax	Protective coating of kernels from small shrubs (sumac plants, <i>Rhus</i> genus) growing in China or Japan	Series of odd and even-numbered <i>n</i> -alkanes with a simple distribution
Paraffin	Fossil matter obtained by distillation of petroleum	Series of odd and even-numbered <i>n</i> -alkanes with a bimodal distribution
Ozokerite	Fossil matter obtained by distillation of petroleum	

of the fatty acids involved in the structure of these biomarkers, and particularly on their degree of unsaturation, the fatty matter is at solid or liquid state at room temperature. Vegetable oils are known to contain a greater amount of unsaturated fatty acids than animal fats and are thus more easily oxidised and polymerised.

Although some fatty substances may be well preserved over time in particular conditions (Evershed *et al.*, 1997b, 2002; Dudd and Evershed, 1998; Dudd *et al.*, 1999; Mirabaud *et al.*, 2007; Regert, 2007; Regert *et al.*, 2001b), their TAG content is usually greatly modified by a series of alteration processes including hydrolysis and oxidation (Evershed *et al.*, 1992; Dudd *et al.*, 1998; Regert *et al.*, 1998) that have to be taken into account for the detection of animal fats and vegetable oils. Due to their high molecular weight, their low volatility and their labile character, one must note that their analysis by direct mass spectrometry is more efficient using a soft ionisation mode such as electrospray ionisation (ESI) than electron ionisation (EI) (Mirabaud *et al.*, 2007).

### 4.3 Analytical Methodology

Investigations based on direct mass spectrometry analysis aiming at identifying waxes and other lipids in museum or archaeological items were first carried out at the end of



the 1990s on beeswax and some vegetable oils in the EI mode (Regert, 1996). They were then extended to other ionisation modes, particularly ESI, and applied to a wider range of reference and ancient materials (Garnier *et al.*, 2002; Regert and Rolando, 2002; Mirabaud, 2007; Mirabaud *et al.*, 2007; Ribechini *et al.*, 2008a, b). These two main modes of ionisation were used in response to different and complementary purposes: the EI mode appeared to be a straightforward, rapid and screening tool that provided general fingerprints on complex samples with a minimum of sample treatment whereas ESI aimed at providing precise compositional information on specific high molecular weight compounds previously purified and possibly lithiated. The specificities of these two approaches are described below; sample preparation, analytical conditions, advantages and limits of each method are reported and briefly discussed.

### 4.3.1 Direct Mass Spectrometry in the Electron Ionisation Mode

Direct introduction of a sample, either in solid or liquid state, in the ion source of a mass spectrometer may be achieved through two procedures: the first one is based on the use of a direct insertion probe (DIP); the second one necessitates a direct exposure probe (DEP). Direct introduction followed by heating of the sample in the ion source of the mass spectrometer is also known as direct temperature resolved mass spectrometry (DTMS).

The DIP consists of a probe at the end of which a small glass vial may receive a sample. This latter may be a solid fragment, a liquid substance or a solution. After introduction into the ion source, the vial is heated through a heating element present in the probe at a temperature that routinely does not go over 450°C with a maximum ramp of temperature that varies depending on the mass spectrometer used. During the heating operation of the probe, the sample is slowly volatilised and then ionised into the source of the mass spectrometer. This method is an interesting way to analyse solid samples without any previous sample manipulation. A tiny grain of matter of ~100 µm length may indeed be selected under a binocular lens, placed into the sample holder and directly introduced into the ion source. A drop of liquid matter or of a sample diluted in an adequate solvent may also be analysed in this way.

The DEP ends with a filament wire onto which a drop of sample is deposited. After evaporation to dryness, the probe is introduced into the source of the mass spectrometer and is rapidly heated to a temperature that can reach 1000°C. This probe is ideal for the study of high molecular weight or polymeric components. It is mostly dedicated to the analysis of samples in the liquid state. Although a small solid fragment of matter may be placed on the filament, this critical operation may lead to the loss of the sample, especially if it is particularly small. To avoid such a difficult handling, the sample may be ground and homogenised in a mini-mortar and then made into suspension with a few drops of appropriate solvent (Scalarone *et al.*, 2003).

When the samples are previously dissolved in a solvent, solutions at 1 mg ml<sup>-1</sup> are usually used (Regert and Rolando, 2002; Colombini *et al.*, 2005b; Ribechini *et al.*, 2008a, b).

During the analysis, the ion source is generally maintained at a temperature around 200°C, between 180°C and 230°C, depending on the investigators (Regert and Rolando, 2002; Scalabrone *et al.*, 2003; Regert *et al.*, 2006, 2008; Ribechini *et al.*, 2008).

Because wax and lipid substances may contain high molecular constituents, a first run is usually performed with a scan range from  $m/z$  50 to 900 or 1000. In a second step, if the mass spectrum excludes the presence of high molecular weight compounds, and if enough matter is available for analysis, another run is performed over a narrower scan range, often between  $m/z$  50 and 500 (Colombini *et al.*, 2005b).

One must note that the analyser device of the mass spectrometer has a particular importance with respect to the spectra obtained. In particular, the 'ion trap analyser is noted for its discrimination against ions with  $m/z$  values below 100' (Regert and Rolando, 2002) and tends to produce spectra on which the molecular ions are particularly intense even when using the EI mode. Therefore, the pattern of the mass spectra for a same product may differ between analysers and several differences, including the position of the base peak, the ratio between some peaks and the presence of peaks resulting from specific molecular rearrangements in an ion trap analyser have already been reported (Regert *et al.*, 2001a; Regert and Rolando, 2002).

Whatever the analyser and the analytical conditions chosen, the spectrum obtained corresponds to the sum of the spectra of all the individual compounds present in the sample investigated. Spectra have thus to be cautiously interpreted using a set of reference data from single commercial or synthesised compounds, reference raw and aged natural substances and mass spectral libraries.

### 4.3.2 ESI MS and ESI MS/MS Analysis

The first developments of soft ionisation methods such as ESI or atmospheric pressure chemical ionisation in the field of cultural heritage were published at the beginning of the century (Kimpfe *et al.*, 2001, 2002, 2004; Garnier *et al.*, 2002; Guash-Jané *et al.*, 2004, 2006a, b; Mirabaud *et al.*, 2007). These methods mostly dealt with issues concerning fats and waxes, but also with those of ancient wine, and they were usually preceded by a liquid chromatography step that allowed the separation of the compounds of interest before their characterisation by mass spectrometry (Kimpfe *et al.*, 2001, 2002; Guash-Jané *et al.*, 2004, 2006a, b). In some cases however, it was possible to gain compositional information from direct infusion ESI MS and ESI MS/MS analysis, particularly for the study of diesters and hydroxy esters of beeswax and of TAGs isolated from reference and archaeological animal fats (Garnier *et al.*, 2002; Mirabaud *et al.*, 2007).

In contrast to direct mass spectrometry used in the EI mode, ESI often requires specific pretreatments of the samples to purify the components of interest, to increase their yield of ionisation and consequently to improve selectivity and sensitivity. It is thus not a preliminary step of analysis but a method that forms part of an analytical strategy that allows the presence of well preserved high molecular long chain compounds to be shown before their fine characterisation by ESI techniques (Regert *et al.*, 2003a; Mirabaud, 2007; Mirabaud *et al.*, 2007).

To summarise, a fractionation step allows the isolation of the compounds of interest from the other molecular constituents, particularly from the fatty acids that are well-ionised. To compensate for the low ionisation yield of some compounds, such as TAGs, the solutions may be doped with a cation. Samples are then directly infused into the ion electrospray source of the mass spectrometer. A first spectrum provides an overview of the main molecular compounds present in the solution based on the peaks related to molecular cations. The MS/MS experiment is then performed to elucidate the structure of each high molecular compound. Table 4.2 shows the different methods of sample preparation and analysis of nonvolatile compounds as esters and TAGs from reference beeswax, animal fats and archaeological samples.

Figure 4.1 summarises analytical methodologies in which direct mass spectrometry was used, either in the EI mode or by ESI.

**Table 4.2** Summary of the different methods of sample preparation and analysis by direct ESI MS and ESI MS/MS

Sample	Sample preparation	ESI analysis
Contemporary beeswax	Isolation of the diesters and hydroxyesters/alcohols fraction by anion-exchange chromatography with an aminopropyl cartridge from a solution of $1 \text{ mg ml}^{-1}$ of raw beeswax in $\text{CHCl}_3/\text{MeOH}$ (2:1, v/v) Preparation of 0.1% trifluoroacetic acid (TFA) solution from fractionated beeswax	Micromass Quattro II triple-stage quadrupole fitted with an electrospray ion source for ESI MS and ESI MS/MS (MRM mode) analysis
Archaeological sample containing beeswax	Solvent extraction of beeswax from ceramic sherds and preparation of 0.1% TFA solution	
Contemporary animal fats	Solvent extraction and addition of a doping reagent (2% lithium chloride in methanol)	Applied Biosystems Q-q-TOF analyser equipped with a nanoelectrospray ion source for nano ESI MS and nano ESI MS/MS analysis
Archaeological sample containing well preserved TAGs from animal fats	Solvent extraction of the total lipid extracts from ceramic sherds and charred surface residues Isolation of DAGs and TAGs on silica solid-phase cartridges Formation of lithiated adducts from the TAG fraction by addition of 2% lithium chloride in methanol	

From Garnier *et al.*, 2002 and Mirabaud *et al.*, 2007.

DAG, diacylglycerol; TAG, triacylglycerol.

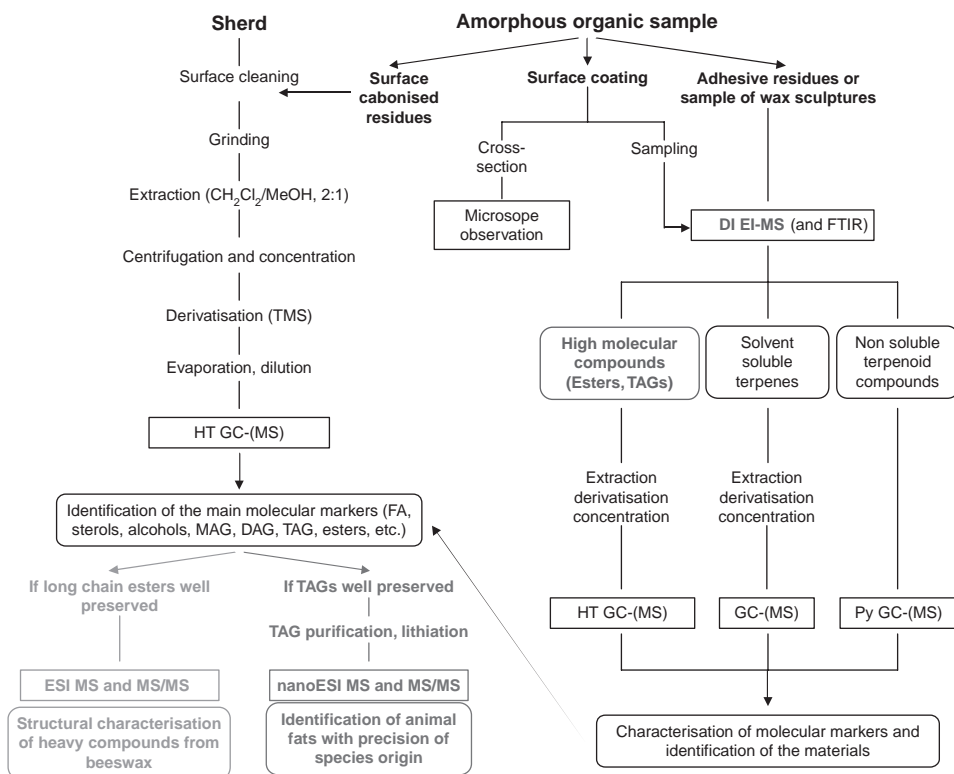


**Figure 4.1** Analytical strategy in which direct mass spectrometry analyses using either electron ionisation or electrospray are used for detecting and identifying lipid substances in archaeological and museum samples

#### 4.4 DI and DE EI-MS of Reference Substances

As direct mass spectrometry does not allow any separation at the molecular level, the main difficulty associated with this technique is the interpretation of the mass spectral fingerprints obtained by volatilisation and thermal degradation of complex multicomponent mixtures (Scalarone *et al.*, 2003). Mass spectral fingerprints are indeed obtained by averaging the mass spectra in the desired time range and correspond to the summation of mass spectra of several constituents and products (Colombini *et al.*, 2005b). Their interpretation is based on a good knowledge of spectra of pure single compounds and of raw, synthetic and aged natural substances (Regert and Rolando, 2002).

This section details the mass spectra of reference molecular constituents and of various substances including waxes and vegetable oils that were recently investigated in order to establish comprehensive correlation between the mass spectra obtained on archaeological and museum samples and the main organic materials involved in their composition.

#### 4.4.1 Individual Molecular Constituents

Mass spectra of numerous single compounds are available in reference libraries. However these spectra have not always been obtained in the same conditions as those used in DE or DI EI-MS modes and the spectra of molecules of specific interest in the field of cultural heritage have not been systematically registered. It is thus of importance to achieve mass spectra on a set of standard molecular constituents in order to study their mass spectral fingerprint in detail before investigating the more complex mass spectra of multicomponent materials.

In most cases, mass spectra on single compounds were obtained with reference materials provided by commercial suppliers. This is the case for fatty acids, diacids and TAGs (Ribechini *et al.*, 2008a). Nevertheless when the molecules of interest are not commercially available it may be useful to synthesise and purify them in the laboratory as shown for the esters of beeswax (Garnier *et al.*, 2002).

The mass spectrum of palmitic acid obtained by DE-MS with a Polaris Q ion trap external ionisation mass spectrometer is presented in Figure 4.2 (Ribechini *et al.*, 2008a). Dominated by a base peak at  $m/z$  87, it presents a visible molecular peak at  $m/z$  256, accompanied by a fragment at  $m/z$  257, possibly formed by rearrangement in the ion trap. The loss of the

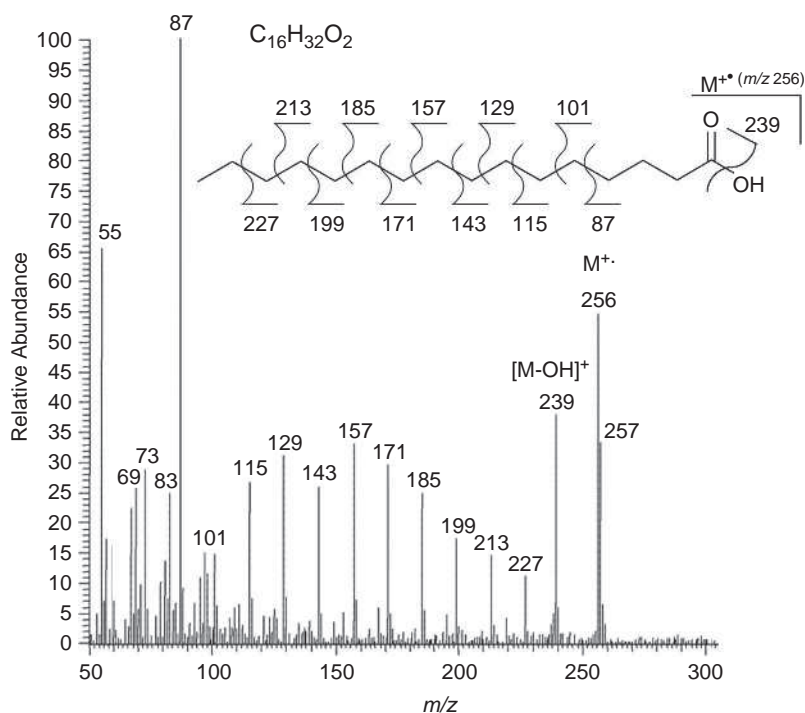


**Figure 4.2** Mass spectrum of palmitic acid and main fragmentation mechanisms. This spectrum was obtained by DE-MS with a Polaris Q ion trap external ionisation mass spectrometer. Reproduced from Talanta, 74, Ribechini *et al.*, 2008a, Copyright 2008 with permission from Elsevier

hydroxy group from the carboxy function is responsible for the formation of the  $m/z$  239 peak. Other noticeable peaks regularly spaced every  $m/z$  14 units from 87 to 227 arise from the cleavage of the hydrocarbon chain of the fatty acid (Ribechini *et al.*, 2008a).

Unsaturated monocarboxylic acids provide spectra with very low intense molecular peaks at  $m/z$  282 for oleic acid ( $C_{18:1}$ ) and  $m/z$  338 for erucic acid ( $C_{18:1}$ ) according to the results published by Ribechini and co-workers (Ribechini *et al.*, 2008a). Intense peaks were also observed at  $m/z$  264 for oleic acid and  $m/z$  320 for erucic acid, corresponding to the loss of a molecule of water. Other fragments at  $m/z$  265 and 321 arise from the loss of an hydroxy radical for, respectively, oleic and erucic acids. Other fragmentations resulting from the cleavage of the carbon backbone are also described (Ribechini *et al.*, 2008a).

Spectra of dicarboxylic acids, namely azelaic ( $C_9$ ) and sebacic ( $C_{10}$ ) acids are characterised by the absence of their molecular peak at, respectively,  $m/z$  188 and 202 (Ribechini *et al.*, 2008a). They both present a base peak at  $m/z$  83 and significant fragments corresponding to  $\{[M+H]^+\}$ ,  $\{[M+H]^+-H_2O\}$  and  $\{[M-2(H_2O)]^+\bullet\}$  species, as shown in Figure 4.3 (Ribechini *et al.*, 2008a).

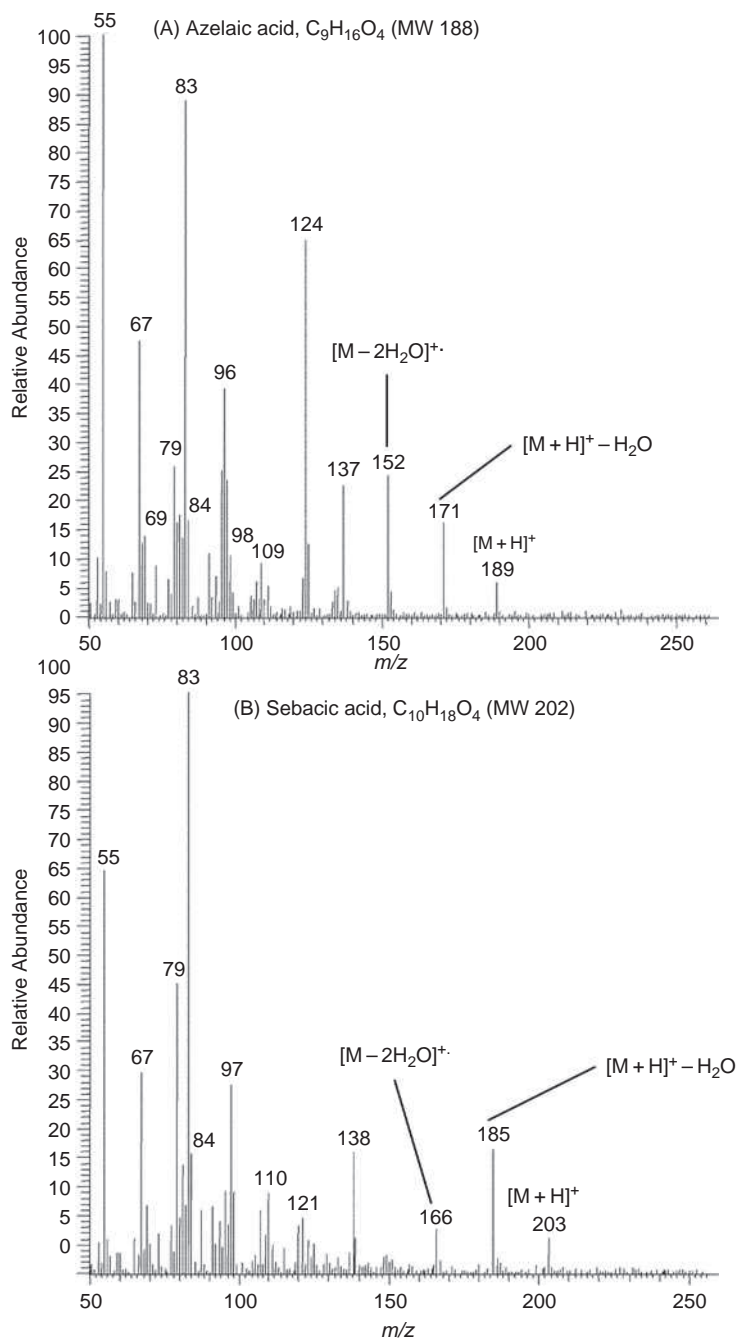
Mass spectra of TAGs are dominated by a base peak corresponding to the loss of an acylium group  $[M-RCO_2]^+$  at  $m/z$  495, 551 and 607 for, respectively, trimyristin, tripalmitin and tristearin (see Figure 4.4 for mass spectrum of tristearin; Ribechini *et al.*, 2008a). As for diacids, the molecular ion is not detected probably because of extensive fragmentation occurring with anionisation energy of 70 eV. The other fragments of importance are given in Figure 4.4.

Figure 4.5 shows the mass spectrum of a palmitic ester chemically synthesised (for details of the synthesis, see Garnier *et al.*, 2002). This spectrum was obtained by DI EI-MS with a ThermoFinnigan GCQ ion trap external ionisation mass spectrometer (Regert and Rolando, 2002). Depending on the analyser used, the base peak may be observed either at  $m/z$  256 or 257, respectively, corresponding to  $[C_{15}H_{31}CO_2H]^+\bullet$  and  $[C_{15}H_{31}CO_2H + H^+]$  fragments. Other peaks at  $m/z$  239, 336, 381 and 592 may be interpreted as resulting from the following fragments  $[C_{15}H_{31}CO]^+$ ,  $[C_{24}H_{48}]^+$ ,  $[CO_2C_{24}H_{49}]^+$ , and  $M^+\bullet$  (Regert and Rolando, 2002).

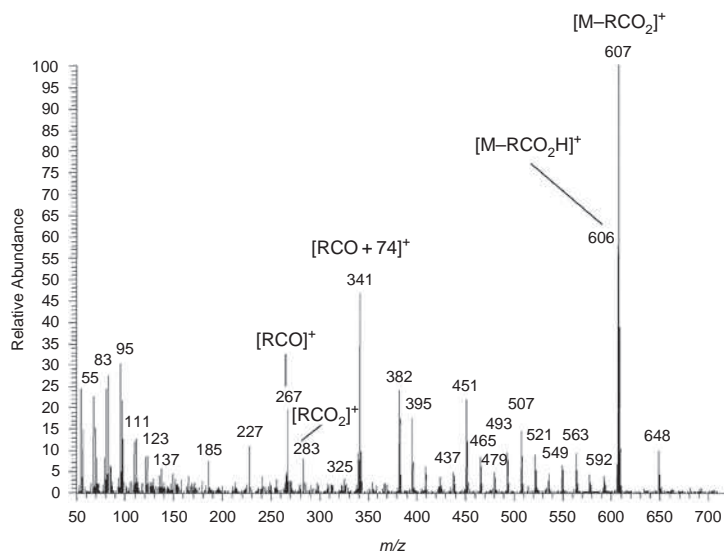
All these results obtained on commercial pure molecular constituents may now be exploited for interpreting more complex mass spectral fingerprints achieved on natural substances.

#### 4.4.2 Authentic Natural Substances

The most common wax exploited by human beings through time is beeswax as already mentioned. This animal substance presents a very characteristic mass spectrum dominated by a base peak at either  $m/z$  256 or 257 depending on the analyser used. The relative simplicity of the mass spectrum obtained may be explained by the fact that the main monoesters present are made of a single fatty acid moiety, namely palmitic acid. The fragmentation of these compounds arises through the formation of  $[C_{15}H_{31}CO_2H]^+\bullet$  and  $[C_{15}H_{31}CO_2H + H^+]$  ions as previously discussed (Figure 4.6a). Spectra obtained with an ion trap analyser show a series of peaks regularly spaced by 28 mass units from  $m/z$  592 to  $m/z$  732 corresponding to the molecular ions of even-numbered palmitic esters from  $C_{40}$  to  $C_{52}$ . In the low  $m/z$  range, a pattern with peaks regularly spaced by 14 mass units may be related to cleavage of the hydrocarbon chains present in *n*-alkanes, fatty acids and wax



**Figure 4.3** Mass spectra of (a) azelaic acid and (b) sebacic acid obtained by DE-MS with a Polaris Q ion trap external ionisation mass spectrometer. Reproduced from Talanta, 74, Ribechini et al., 2008a, Copyright 2008 with permission from Elsevier



	[RCO] <sup>+</sup>		[M-RCO <sub>2</sub> H] <sup>+</sup>			
Trimyristin (MW 722, C <sub>45</sub> H <sub>86</sub> O <sub>6</sub> )	211	285	494	<b>495</b>	536	564
Tripalmitin (MW 806, C <sub>51</sub> H <sub>98</sub> O <sub>6</sub> )	239	313	550	<b>551</b>	592	620
Tristearin (MW 890, C <sub>57</sub> H <sub>110</sub> O <sub>6</sub> )	267	341	606	<b>607</b>	648	676
	[RCO + 74] <sup>+</sup>		[M-RCO <sub>2</sub> ] <sup>+</sup>			

**Figure 4.4** Mass spectrum of tristearin and main characteristics of DE-MS spectra of triacylglycerols obtained on a Polaris Q ion trap external ionisation mass spectrometer. Reproduced from Talanta, **74**, Ribechini et al., 2008a, Copyright 2008 with permission from Elsevier

esters of beeswax (Regert and Rolando, 2002). Other peaks at  $m/z$  239, 336 and 381 that were already discussed for the mass spectrum of C<sub>40</sub> ester, were also observed.

From the animal waxes, the mass spectrum of spermaceti was registered by DI EI-MS with a Shimadzu QP 2010 mass spectrometer equipped with a quadrupole analyser (Figure 4.6b). As for beeswax, spermaceti contains wax esters but with different molecular weights, distribution and structures (Table 4.1). Its mass spectrum presents some common characteristics with that of beeswax, considering the formation of the main peaks observed. Indeed, in the mass range 400–525, peaks regularly spaced every  $m/z$  28 units from 424 to 508, maximising at  $m/z$  452, correspond to the molecular peaks of the even-numbered esters from C<sub>28</sub> to C<sub>34</sub>, the main one containing 30 carbon atoms (Figure 4.6b). In the region of the spectrum between  $m/z$  200 and 300, a series of peaks at  $m/z$  201, 229, 257 and 285 arises from the fission of the



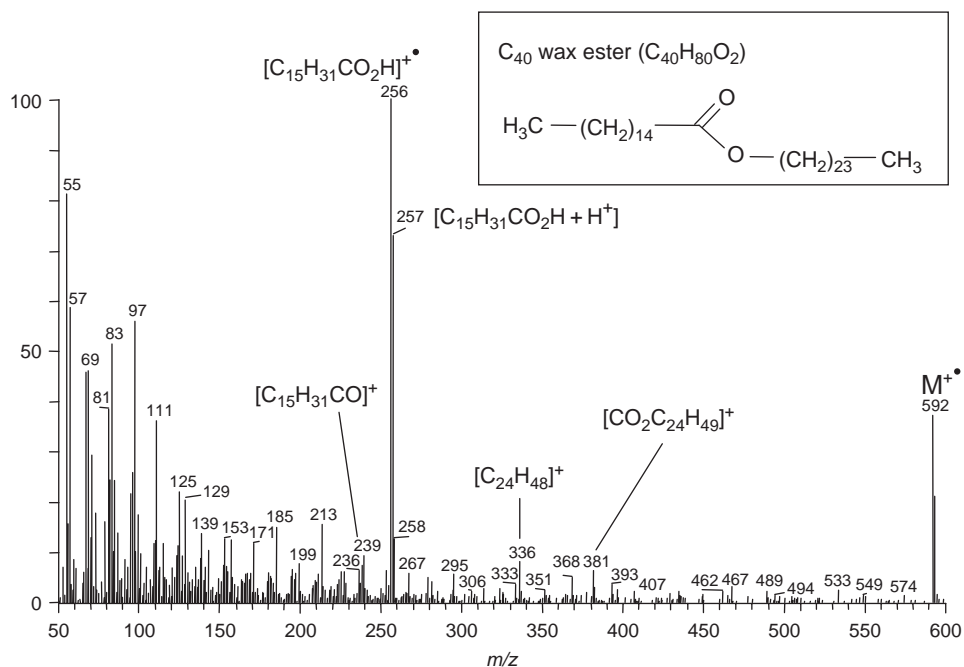


**Figure 4.5** Mass spectrum of synthesised tetracosanyl palmitate obtained by DI EI-MS on a GCQ Finnigan device equipped with an ion trap analyser. Adapted from Regert and Rolando, 2002

alkyl-oxygen bond of the esters and corresponds to  $[C_nH_{2n+1}CO_2H + H]^+$  ions, with  $n = 11, 13, 15$  and  $17$ . The presence of these fragments indicates that several fatty acid moieties are involved in the esters of spermaceti (Regert *et al.*, 2005). Low intensity peaks at  $m/z$  200, 228, 256 and 284 corresponding to  $[C_nH_{2n+1}CO_2H]^{\bullet+}$  radical ions are also observed. Their low intensity compared with that of  $[C_nH_{2n+1}CO_2H + H]^+$  ions may be attributed to the use of a quadrupole analyser for acquiring this spectrum whereas  $[C_nH_{2n+1}CO_2H]^{\bullet+}$  radical ions versus  $[C_nH_{2n+1}CO_2H + H]^+$  ions are predominant when using ion trap analysers (Regert and Rolando, 2002). Lastly, the base peak of the mass spectrum is at  $m/z$  57. This peak is followed by a series of peaks regularly spaced every 28 mass units indicative of the cleavage of the carbon skeleton of long chain compounds. Once again, this spectrum illustrates the differences observed between ion trap and other analysers. Although fragments below  $m/z$  100 are discriminated in ion trap analysers, they are more intense in other analysers. In mass spectra of wax esters acquired with ion trap analysers, the base peak corresponds to  $[C_nH_{2n+1}CO_2H]^{\bullet+}$  radical ions whereas it corresponds to the cleavage of the carbon backbone of long chain compounds when the analysis is performed with a quadrupole.

Mass spectra of reference vegetable and fossil waxes were also acquired by DI EI-MS with a Shimadzu QP 2010 mass spectrometer equipped with a quadrupole analyser (Figures 4.7–4.9). The mass spectrum of carnauba is dominated by a base peak at  $m/z$  57. At low mass range the pattern observed is that already discussed for other waxes with peaks spaced every 28 mass units corresponding to the fragmentation of long linear carbon chains. Two other areas of interest may be mentioned: one between  $m/z$  250 and 450

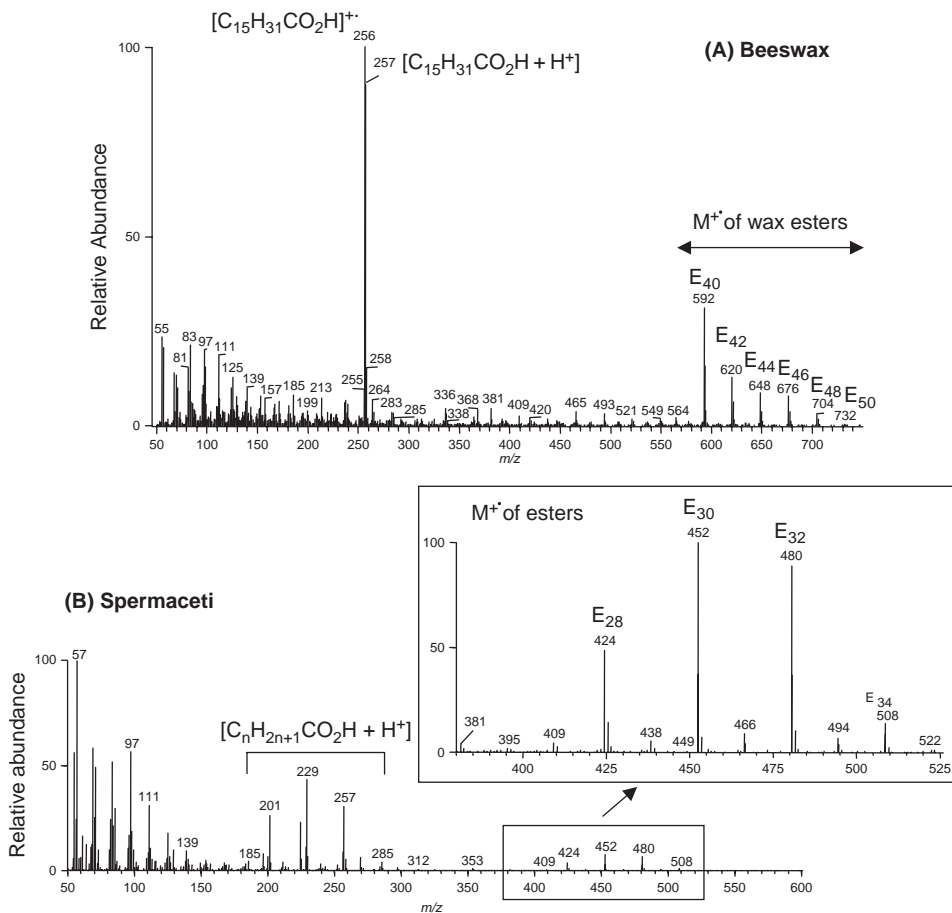


**Figure 4.6** (a) Mass spectrum of beeswax obtained by DI EI-MS on a GCQ Finnigan device equipped with an ion trap analyser. Adapted from Regert and Rolando, 2002. (b) Mass spectrum of spermaceti obtained by DI EI-MS on a Shimadzu QP 2010 mass spectrometer equipped with a quadrupole

corresponding to  $[C_nH_{2n+1}CO_2H+H^+]$  ions issued from fragmentation of wax esters, with  $n = 15, 17, 19, 21, 23, 25$  and  $27$ ; the other one between  $m/z$  700 and 900 with a series of peaks at  $m/z$  733, 761, 789, 817 (main peak), 845 and 873 relative to  $[M+H^+]$  ions of wax esters. As in the case of spermaceti, these results confirm that the esters constituting carnauba are more complex than those of beeswax and contain several different fatty acid moieties (Regert *et al.*, 2005).

Japan wax does not contain any wax ester but only TAGs dominated by tripalmitin ( $T_{48}$ ).<sup>1</sup> Its mass spectrum is thus very similar to that of this last compound with noticeable

<sup>1</sup> TAGs are abbreviated as  $T_x$  where  $x$  is relative to the Equivalent Carbon Number (ECN) that corresponds to the number of carbon atoms of all the acyl moieties of the TAG.

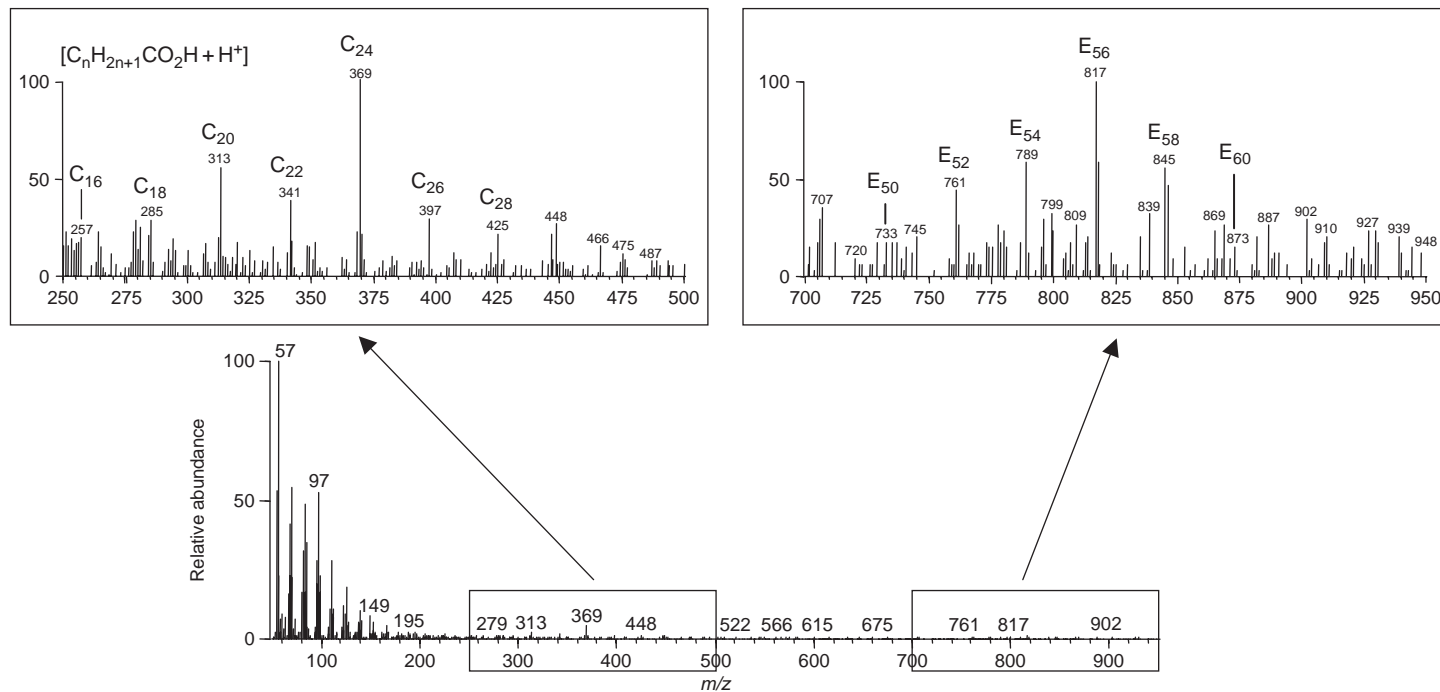


**Figure 4.7** Mass spectrum of carnauba wax obtained by DI EI-MS on a Shimadzu QP 2010 mass spectrometer equipped with a quadrupole

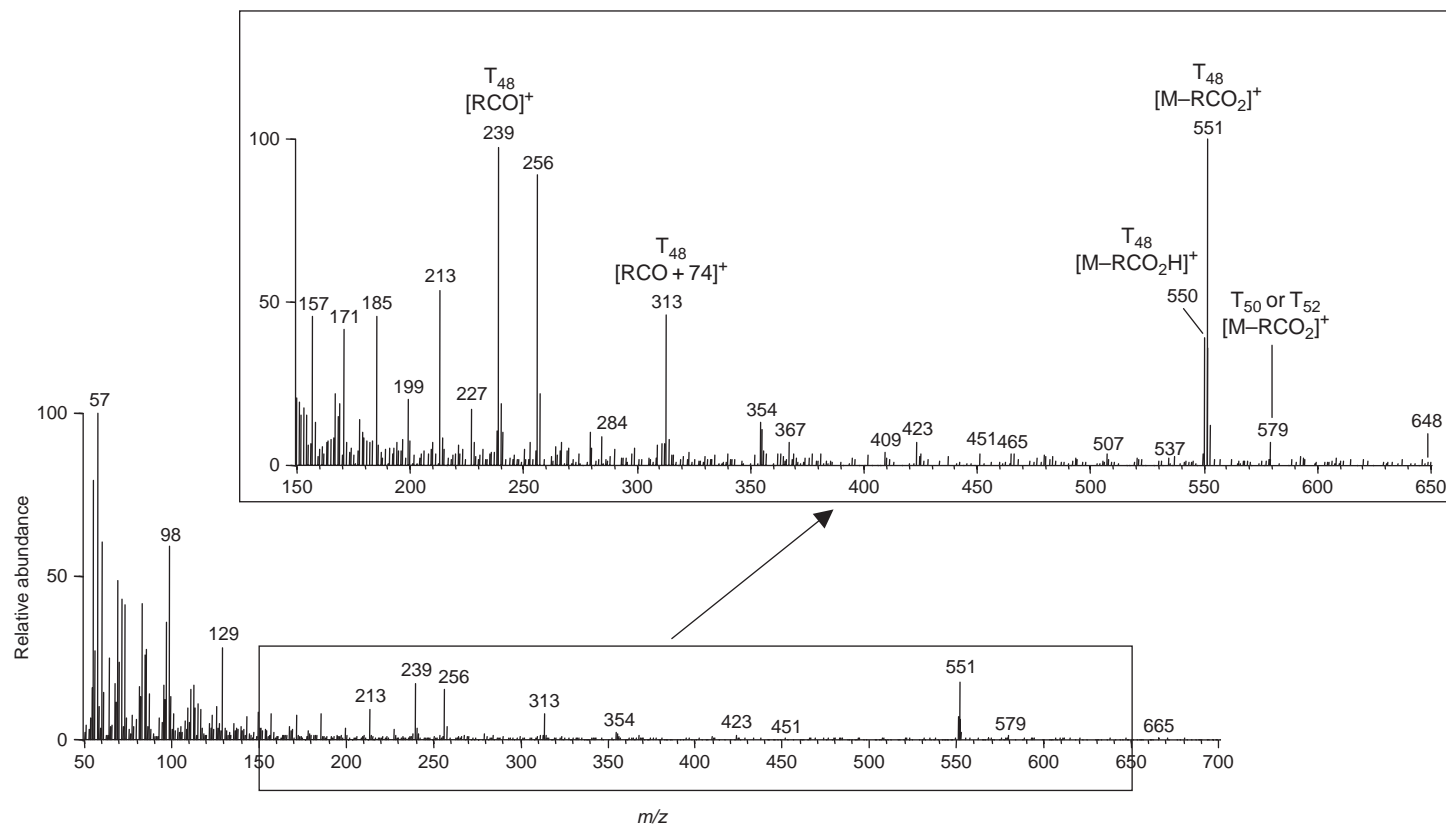


**Figure 4.8** Mass spectrum of Japan wax obtained by DI EI-MS on a Shimadzu QP 2010 mass spectrometer equipped with a quadrupole

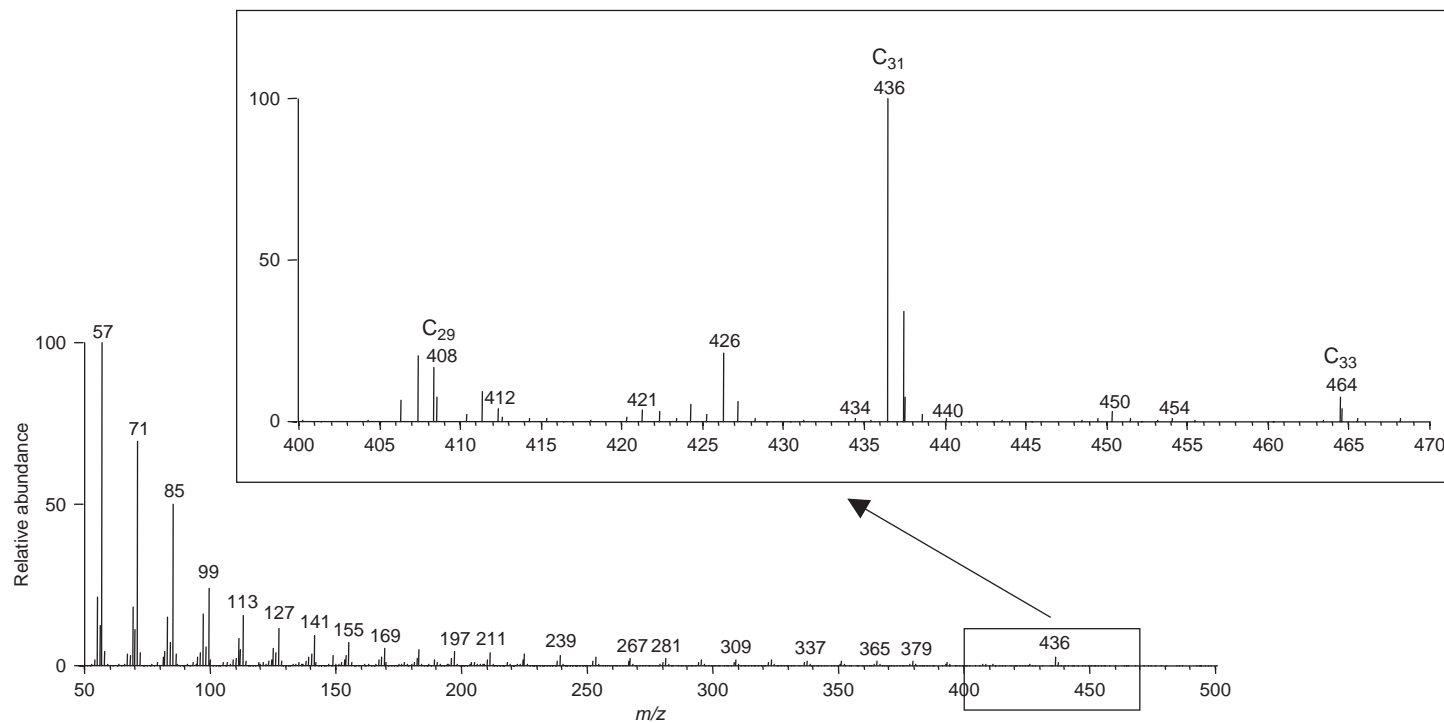


**Figure 4.9** Mass spectrum of candelilla wax obtained by DI EI-MS on a Shimadzu QP 2010 mass spectrometer equipped with a quadrupole

peaks at  $m/z$  551, 550, 313 and 239, respectively, corresponding to  $[M-RCO_2]^+$  formed by the loss of an acylium group,  $[M-RCO_2H]^+$  arising from the loss of an acylium group and the addition of an hydrogen,  $[RCO+74]^+$  relative to the glycerol backbone linked with a palmitic acid and an hydroxy group, and the acylium group  $[RCO]^+$ , all issued from the fragmentation of tripalmitin (Figure 4.8). A peak at  $m/z$  579 indicates the presence of other TAGs. This fragment may indeed be formed by the loss of an acylium group  $[RCO]^+$ , containing 16 or 18 carbon atoms from, respectively,  $T_{50}$  or  $T_{52}$  TAG.

Candelilla, paraffin and ozokerite are all formed by a series of *n*-alkanes. Their mass spectrum, obtained by DI EI-MS with a Shimadzu QP 2010 mass spectrometer equipped with a quadrupole analyser, is characterised by a base peak at  $m/z$  57 corresponding to the radical ion  $[CH_3(CH_2)_3]^+$  formed by the cleavage of the carbon backbone, followed by peaks regularly spaced 14 mass units apart (Figure 4.9). In the case of candelilla, the molecular ions of the three main *n*-alkanes ( $C_{29}$ ,  $C_{31}$  and  $C_{33}$ ), respectively, at  $m/z$  408, 436 and 464, maximising at  $m/z$  436, are observed. In the case of paraffin and ozokerite that contain longer chain compounds, molecular peaks until  $m/z$  464 ( $C_{33}$ ) and 534 ( $C_{38}$ ) could be seen (data not shown).

The last substances for which DI EI-MS spectra were acquired with the aim to identify them in ancient items are vegetable oils (Regert and Rolando, 2002). Three kinds of oils, namely olive oil, linseed oil and poppy seed oil, were investigated by DI EI-MS with a GCQ ThermoFinnigan mass spectrometer equipped with an ion trap analyser (Figure 4.10). These three oils present common patterns in the mass range  $m/z$  800–900, 550–650 and 300–350, respectively, corresponding to fragments of TAGs, diacylglycerols and monoacylglycerols. These common features make them very difficult to distinguish only using direct mass spectrometry analysis but provide interesting fingerprints to detect their presence in complex mixtures if they are well preserved.

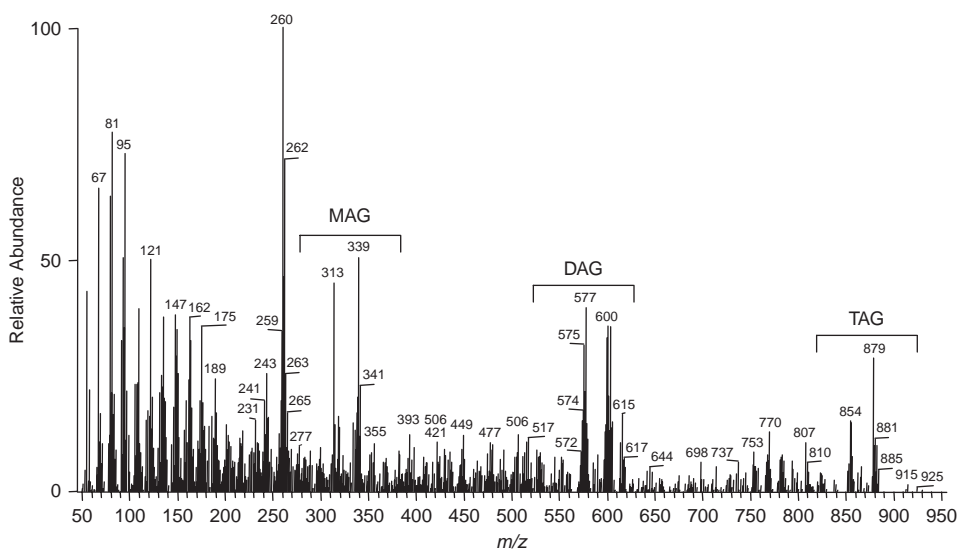


**Figure 4.10** Mass spectrum of poppy seed oil obtained by DI EI-MS on a GCQ Finnigan device equipped with an ion trap analyser. Adapted from Regert and Rolando, 2002

All these data are not of the same significance for detecting and identifying natural substances in complex and degraded mixtures usually present in samples from archaeological or museum items.

On one hand, some materials are characterised by a few noticeable but very informative peaks that are not common to many substances. This is the case for waxes, including beeswax, spermaceti and carnauba, which contain long chain esters. Their mass spectrum exhibits two main types of fragments: those formed by the fission of the alkyl-oxygen bond of the esters corresponding to  $[C_nH_{2n+1}CO_2H]^{\bullet+}$  radical ions and  $[C_nH_{2n+1}CO_2H+H^+]$  ions; the others related to the molecular weight ( $M^{\bullet+}$  or  $M+1$ ) of monoesters. Materials mainly made of TAGs such as Japan wax or vegetable oils also present clear mass spectra with specific features. Most of these substances may be easily distinguished from each other by their mass spectrum, even in the case of mixtures since they present characteristic peaks in different mass ranges. This is the case for beeswax, spermaceti, carnauba and Japan wax. However, for other materials, it is only possible to be precise about their nature (vegetable oils for example) without any more information on the species from which they are issued.

On the other hand, materials for which mass spectra present features that are common to many products will be difficult to detect by the only direct mass spectrometry approach when mixed with other substances. In particular, the fingerprint of *n*-alkanes from candelilla, paraffin or ozokerite may be easily recognised in the case of a pure material, even though discriminating between these three products is probably a difficult task. However, when they are mixed with other substances, their signal is likely to be hidden by peaks arising from other products, particularly those of waxes that contain a lot of long chain constituents that give rise to the formation of a pattern very close to that of mixtures of *n*-alkanes at low mass range.

## 4.5 Results obtained by Direct Mass Spectrometry using the Electron Ionisation Mode on Archaeological Samples and Wax Sculptures

To our knowledge, two main types of object have been investigated using direct mass spectrometry in the EI mode with the aim of detecting and identifying the main wax and lipid substances they were made of: organic residues sampled from glass bottles and ceramic vessels; and wax sculptures exhibited in museums. In this section, we describe and discuss the mass spectra obtained for these items and we examine their contribution to the field of cultural heritage.

### 4.5.1 Archaeological Samples

The most ancient sample in which the presence of beeswax was determined by DI EI-MS is dated to the second Iron Age period. It is an organic visible residue sampled from a sherd discovered at the site of Grand Aunay located at Yvré-l'Évêque, about 5 km from Le Mans, in the administrative division of Sarthe, France (Regert and Vacher, 2001; Regert *et al.*, 2003b). This site was occupied from the third to the first centuries BC. During the excavation carried out at the end of the 1990s, a set of amorphous organic remains, either as free lumps in the sediment or as charred surface residues in ceramic vessels, was

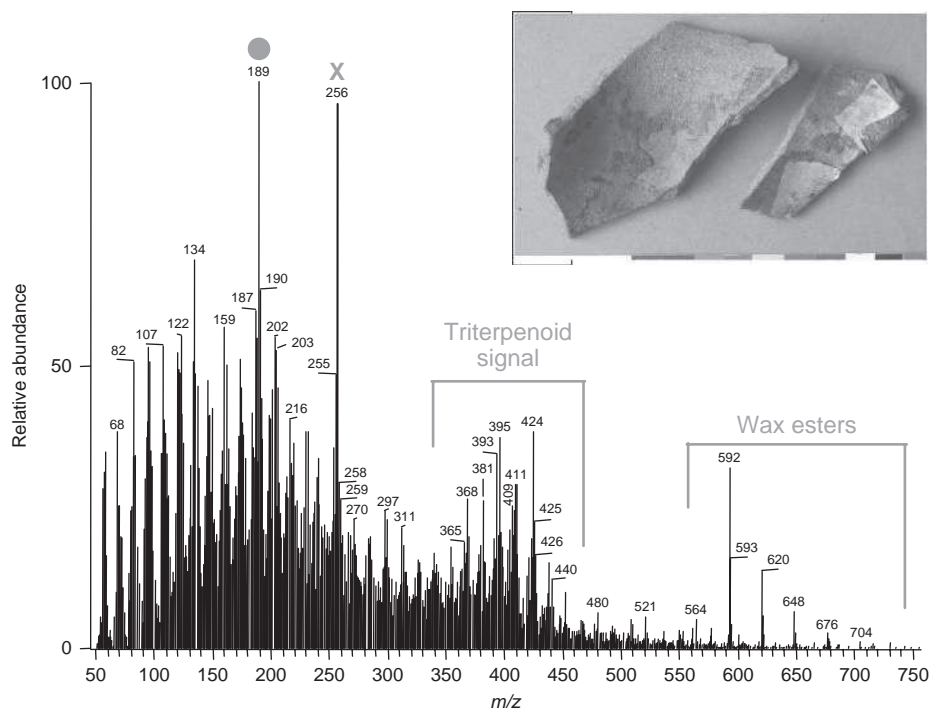


**Figure 4.11** Mass spectrum of an archaeological sample made of a mixture of beeswax and birch bark tar from a residue sampled on a ceramic sherd from the Iron Age site of Grand Aunay (Sarthe, France). The spectrum was obtained by DI EI-MS on a GCQ Finnigan device equipped with an ion trap analyser. Adapted from Regert and Rolando, 2002 (see colour Plate 1)

recovered. Among them, one provided a complex mass spectrum of particular interest, which is reported in Figure 4.11. Regularly spaced peaks at  $m/z$  592, 620, 648 and 704, as well the high intense peak (relative abundance of 95%) at  $m/z$  256, undoubtedly indicate the presence of beeswax. However, several other peaks, including the base peak at  $m/z$  189, that do not belong to the mass spectrum of beeswax or to any other wax or lipid substance, were also observed. The base peak and the peaks detected in the range  $m/z$  350–450 may be assumed to come from the mass spectrum of a single material. Indeed, the fragment at  $m/z$  189 arises from the fragmentation of the ring system of triterpenoids with a lupane skeleton, followed by the loss of a water molecule (Regert and Rolando, 2002; Modugno *et al.*, 2006). By comparison with spectra already published on standards and on triterpenoid resins and tars, the fragments at  $m/z$  381, 393, 409, 411, 424 and 426 can be directly related to the occurrence of lupeol, lupenone and betulin (Modugno *et al.*, 2006): peaks at  $m/z$  424 and 426 correspond, respectively, to the molecular ions of lupenone and lupeol; ions at  $m/z$  409 and 411 are formed by the loss of a methyl group from these two molecules and the fragment at  $m/z$  393 arises from the loss of  $\cdot\text{CH}_2\text{OH}$  and  $\text{H}_2\text{O}$  from betulin (Regert and Rolando, 2002). All these data, as well as the general fingerprint of the spectrum between  $m/z$  50 and 450, strongly suggest the presence of birch bark tar, an adhesive produced by a controlled heating



of white birch bark since the middle Palaeolithic in Europe (Grünberg *et al.*, 1999; Koller *et al.*, 2001; Grünberg, 2002). Further analysis of this sample by high temperature gas chromatography-mass spectrometry (HT GC-MS) confirmed this hypothesis (Regert *et al.*, 2003b). In that case, direct mass spectrometry was particularly efficient for identifying a mixture of materials with very different mass spectral fingerprints. This result is of prime importance in the field of archaeology. Indeed, archaeologists had hypothesised for a long time that tar or resin had to be mixed with a clay or ochre temper and a plastifier such as beeswax to obtain good quality adhesives. This assumption was based on archaeological experiments and ethnological data but no evidence for such mixtures was found until recently, although many samples of ancient adhesives were analysed. Therefore, the incorporation of beeswax to birch bark tar, demonstrated by DI EI-MS analysis, may be considered as an improvement in making adhesive that occurred during the second Iron Age. This innovation gives evidence for the diversification of adhesive making at a period when processes based on temperature control, particularly in the field of metallurgy, had been developed and had reached a high level of know-how (Regert and Rolando, 2002).

More recently, DE EI-MS investigations were performed on the organic content of a Roman glass bottle discovered at the site of Pompeii in Italy (Ribechni *et al.*, 2008a). The spectrum obtained was dominated by a base peak at  $m/z$  87 typical of a fatty acid fragment  $[(CH_2)_3COOH]^+$ . Other noticeable peaks at  $m/z$  115, 129, 143, 157, 171, 185, 199, 213 and 227 are also characteristic of the presence of fatty acids and correspond to the cleavage of their carbon skeleton. The high abundance of the peak at  $m/z$  256, which corresponds to the molecular ion of palmitic acid, suggests that this molecular constituent is the main compound present in the sample. The fragment at  $m/z$  284 indicates the presence of stearic acid in low amount (Ribechni *et al.*, 2008a). Although these data do not allow the proposal of any hypothesis about the substance present in the sample, it shows that the glass bottle contained a fatty matter still rich in palmitic and stearic acids. Further investigations by GC-MS completed these data and led to the identification of a set of oxidised compounds (hydroxy saturated and unsaturated monocarboxylic acids and diacids) giving evidence for the presence of an oxidised fatty matter of vegetable origin (Ribechni *et al.*, 2008a).

These results show that, depending on the lipid substances present in a sample, direct mass spectrometry may allow the identification of all the lipid substances present in a material, in particular when their mass spectral fingerprints do not overlap, or to determine the main molecular constituents still preserved in the sample.



#### 4.5.2 Wax Sculptures

From a methodological viewpoint, the case of wax sculptures is quite different from that of amorphous organic materials discovered during the course of archaeological excavations. First of all, at variance with archaeological organic residues, for which nothing is known about the substances they contain, the presence of wax, whatever its nature or origin, is a constant in wax sculpture. Furthermore, only minute samples are available due to the unique character of works of art. Samples have thus to be carefully recovered with a sterile scalpel blade or the extremity of a needle. The operation is usually performed under binocular lenses to minimise the size of the sample. The location of the sample is cautiously chosen to avoid affecting the integrity of the sculpture, ideally on the back side in small interstices that often exist in wax items.




We report here the results recently obtained in the framework of a research programme that aims at determining the different materials involved in wax sculptures of the 19th and the beginning of the 20th century (Regert *et al.*, 2005, 2006; Lattuati-Derieux *et al.*, 2008). Most of the sculptures investigated are exhibited at the well known Orsay museum in Paris (Table 4.3). One is from the Musée de la Révolution Française in Vizille (France).

All the spectra presented in this section were recorded by DI EI-MS using a ThermoFinnigan GCQ ion trap external ionisation mass spectrometer. In most cases, mass spectra qualitatively comparable with that described above for beeswax and with those already reported in the literature (Regert and Rolando, 2002) were obtained

**Table 4.3** Summary of the results obtained by DI EI-MS on a series of sculptures from French museums and details of complementary information obtained by HT GC-MS

Characteristics of the sculpture	Photograph	DI EI-MS results	Complementary HT GC-MS data
1. Chest of <i>Aline</i> , (300 × 208 × 168 cm), ~1882, by Paul Gauguin, Orsay museum (no. inv. RF4697), Paris, France (Photograph D. Bagault, C2RMF)		Pine resin and beeswax	Pine resin and beeswax
2. Wax sketch <i>La Semeuse</i> (50 × 50 cm), 1887, by Louis-Oscar Roty, Orsay museum (no. inv. RF4374), Paris, France (Photograph D. Bagault, C2RMF)		Pine resin and beeswax	Pine resin and beeswax, possibly mixed with a fatty substance

**Table 4.3** (continued)

Characteristics of the sculpture	Photograph	DI EI-MS results	Complementary HT GC-MS data
3. Wax sculpture <i>La Critique Artistique</i> (21 cm tall), 1896, by François Rupert Carabin, Orsay museum (no. inv. RF4643), Paris, France (Photograph D. Bagault, C2RMF)		Pine resin and beeswax	Pine resin, beeswax and a fatty substance, probably of plant origin
4. Preparatory wax sculpture by Aimé-Jules Dalou (1928–1902), Musée de la Révolution Française (no. inv. 1889MRF2003-9), Vizille, France (Photograph L. Chicoineau)		Pine resin, material with a high amount of tripalmitin and a low amount of beeswax	Pine resin (main material), Japan wax, low amount of beeswax and paraffin
5. Head of <i>Degas</i> , 6 × 6 × 9 cm, 1910, by Paul Valéry, Orsay museum (no. inv. RF4461), Paris, France (Photograph D. Baugault, C2RMF)		Beeswax	Beeswax and paraffin

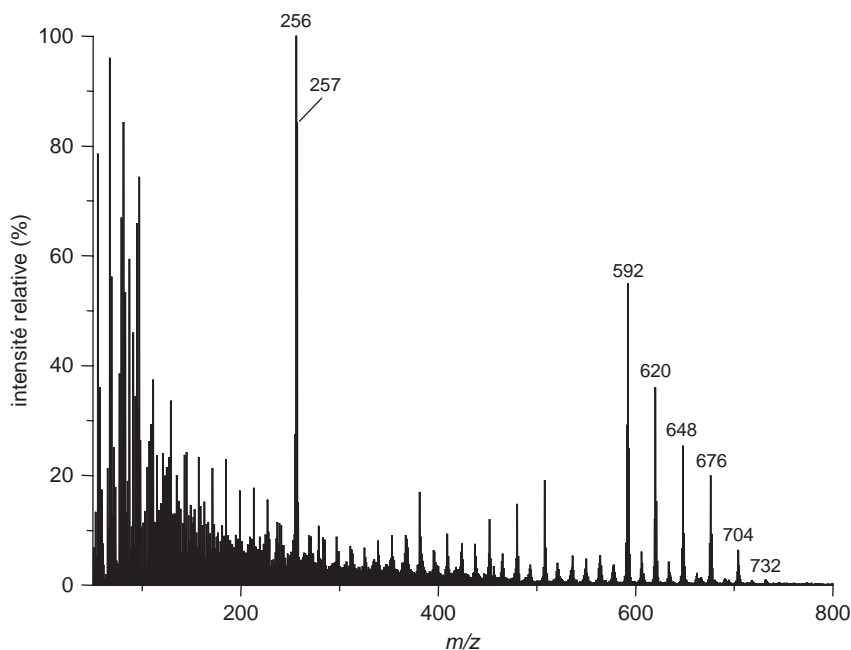


**Figure 4.12** Mass spectrum typical of beeswax (wax sculpture of the head of Degas by Paul Valéry). Spectrum obtained by DI EI-MS on a GCQ Finnigan device equipped with an ion trap analyser

(Figure 4.12). Three different cases were encountered: (i) whatever the time range considered on the total ion current (TIC) trace of the desorption curve, the mass spectrum obtained is the same and corresponds to that of beeswax (Figure 4.12); (ii) depending on the time range on which mass spectra were averaged, different spectra are obtained corresponding to beeswax and other materials, mainly pine resin; (iii) beeswax is detected in very low amount and the spectra are dominated by peaks corresponding to other fatty substances and to resins (Figure 4.13).

The only work of art in which beeswax was the single material detected by DI EI-MS is the head of Degas manufactured by Paul Valéry in 1910 (Figure 4.12). Further HT GC-MS analyses confirmed that beeswax was the main substance used by Valéry but they also showed that paraffin was added (data not shown). These results illustrate the fact that the presence of paraffin is very difficult to detect in samples from wax sculptures by direct mass spectrometry methods, because its mass spectrum is largely overlapped by that of beeswax when these two materials are mixed together. Starch, detected by a specific micro-chemical test, and different inorganic tempers and pigments containing iron, zinc or barium were also added to the wax paste. This recipe thus appears quite simple compared with the diversity of materials that were used in manufacturing wax sculptures in this period (Regert *et al.*, 2005, 2006). This may be explained by the fact that Valéry was a poet and writer and only occasionally spent his time sculpting.

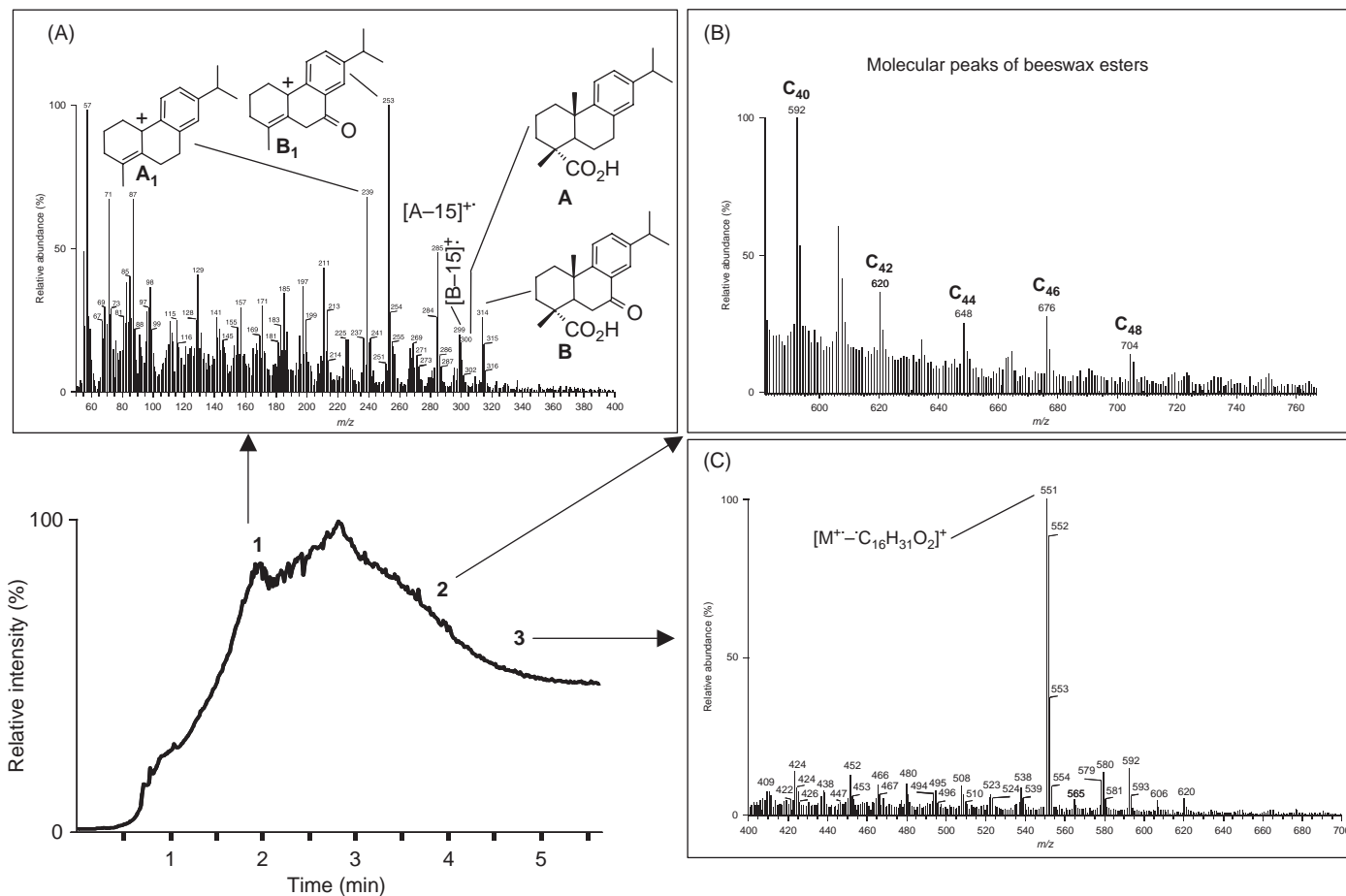


**Figure 4.13** Total ion current trace and mass spectra obtained by DIEL-MS on a GCQ Finnigan device equipped with an ion trap analyser on a sample from a sculpture by A.-J. Dalou showing a mixture of pine resin (a), beeswax (b) and a fatty substance containing tripalmitin (c). Adapted from Regert et al., 2006

Most other sculptures were shown to contain mainly pine resin mixed with beeswax (Table 4.3). In the first part of the TIC trace, the spectrum obtained was dominated by a base peak at  $m/z$  239 or 253 and other characteristic fragments were observed at  $m/z$  285, 300 and 314. Such a fingerprint is in agreement with spectra of oxidised pine resins already published (Regert and Rolando, 2002; Colombini *et al.*, 2005b). Indeed, fragments at  $m/z$  300, 285 and 239 may correspond to, respectively, (i) the molecular ion of dehydroabietic acid (DA), an aromatisation product of abietadienic acids, (ii) a fragment formed from DA by loss of a methyl group and (iii) another fragment arising from the loss of a methyl group followed by that of a the neutral fragment  $[\text{HCO}_2\text{H}]$  (Regert and Rolando, 2002; Colombini *et al.*, 2005b). The fragments at  $m/z$  314 and 253 suggest the presence of a compound formed by oxidation of pine resin biomarkers, namely 7-oxo-dehydroabietic acid. The peak at  $m/z$  314 is related to the molecular ion of this degradation marker and the fragment at  $m/z$  253 results from the loss of a methyl group followed by that of neutral formic acid. The spectrum obtained by averaging the data at the end of the TIC trace presents a fingerprint similar to that of beeswax. Once again, substances with mass spectra overlapped by those of beeswax or pine resin could not be detected by DI EI-MS but they were confirmed by complementary investigations carried out by HT GC and HT GC-MS. This is the case for the paraffin and fatty substances given in Table 4.3.

The case of the sculpture manufactured by Aimé-Jules Dalou was more complex than all the others. Indeed, mass spectra were averaged on three main zones of the TIC trace as shown in Figure 4.13. At the beginning of the desorption curve, the average spectrum indicates the presence of an oxidised pine resin. A very noisy spectrum in which the molecular ion of beeswax esters could be detected was then obtained. The mass spectrum of the last material desorbed was very simple and dominated by a base peak at  $m/z$  551. At this stage of the analytical strategy, it is difficult to assign this spectrum to a specific material. However, since Japan wax is the only wax in which palmitin is the main compound, the presence of this substance was suspected (Regert *et al.*, 2005, 2006). The HT GC and HT GC-MS investigations confirmed this hypothesis and showed in addition the presence of paraffin in the recipe used by Dalou. This organic mixture made of pine resin, Japan wax, paraffin and a low amount of beeswax is the most complex that we have encountered up to now. It shows how innovative the sculptors of the 19th century could be in the choice of their wax pastes for sculpting.

#### **4.6 Recent Advances in ESI MS and ESI MS/MS for the Analysis of Ancient Waxes and Animal Fats**

Although EI MS is an efficient way to provide structural information on several molecular constituents of various lipid substances it only provides partial information and it is particularly not suitable for the study of the low volatile components. High molecular weight and nonvolatile compounds are particularly difficult to analyse in this way and it may therefore be interesting to explore the possibilities of other ionisation modes such as electrospray for an accurate structural study of high molecular constituents such as monoester and diester species of beeswax (Garnier *et al.*, 2002) and TAGs of animal fats

(Mirabaud *et al.*, 2007). Analytical methodologies were first developed and adapted on model samples of beeswax, animal fats and dairy products of different origins (cow, sheep and goat) and then transferred to archaeological materials sampled in the sedimentary matrix or on various ceramic vessels.

#### 4.6.1 Long Chain Compounds of Beeswax

The first step of analysis led to obtaining an ESI MS spectral pattern of authentic beeswax that could be divided into three main areas (Garnier *et al.*, 2002). At low mass range, below  $m/z$  500, the mass spectrum was characterised by a complex fingerprint that was not studied in detail. Fragments at  $m/z$  255 and 257 were nevertheless noted and interpreted as ions corresponding to protonated palmitoleic and palmitic acids. At mass range  $m/z$  500–900, the protonated fragments of three main different homologous series of biomarkers were observed. The most intense peaks were assigned to monounsaturated monoesters. Regularly spaced every  $m/z$  28 mass units, from 591 to 703, these peaks give evidence for the easy ionisation of such species. Saturated palmitic monoesters gave rise to the ions at  $m/z$  593, 621, 649, 677 and 705 and even-numbered saturated hydroxy monoesters from  $C_{40}$  to  $C_{46}$  were detected as protonated species at  $m/z$  609, 637, 665 and 693. At high mass range, for  $m/z$  840–1010, the mass spectrum shows typically protonated molecular ions  $[M+H]^+$  of saturated diesters and saturated hydroxy diesters (Figure 4.14, Garnier *et al.*, 2002).

To gain insight into the structure of these biomarkers, ESI MS/MS analyses were carried out by selecting the protonated molecular ions of the compounds of interest in the first quadrupole of the mass spectrometer. This cation was then collided with argon at a chosen energy in the second quadrupole and analysed in the third quadrupole (Garnier

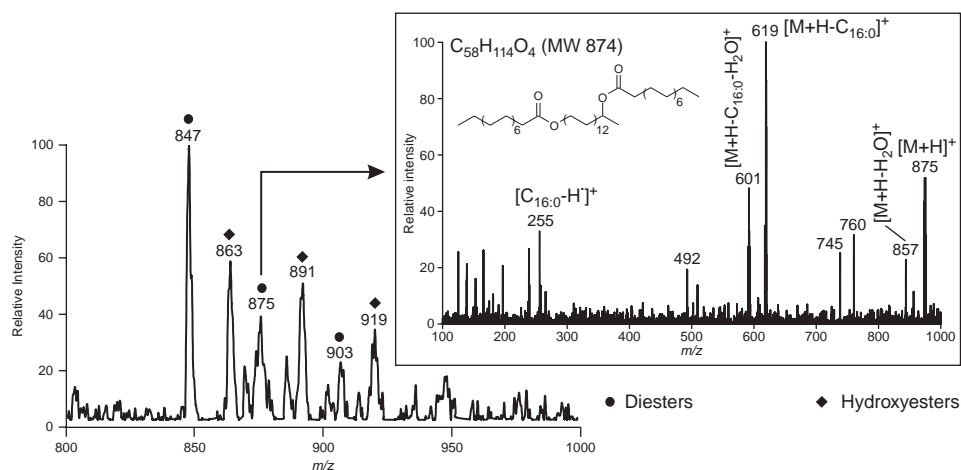


**Figure 4.14** Mass spectrum obtained by ESI MS of beeswax in the mass range  $m/z$  800–1000 and mass spectrum obtained by ESI MS/MS of hexacosanedioyl-1,15-dipalmitoyl. Adapted from Garnier *et al.*, 2002

*et al.*, 2002). For each compound, it was possible to obtain a mass spectrum that could highlight its structure. For example, Figure 4.14 shows the mass spectrum that allowed the identification of one of the diesters present in beeswax, namely hexacosanediol-1,15-dipalmitoyl.

Using this methodology, a series of archaeological samples was investigated. From thirty Etruscan ceramic vessels from archaeological levels of the site of La Castellina corresponding to human occupation during the late eighth and the seventh centuries BC (Garnier *et al.*, 2002), one yielded a spectral signal that could be related to the presence of beeswax. This beehive product was also identified in other samples discovered as free lumps in the sediment. In particular, ESI MS and ESI MS/MS operations were efficient for detecting and characterising monoesters, hydroxy monoesters and diesters in these archaeological materials (Garnier *et al.*, 2002).

#### 4.6.2 Triacylglycerols of Animal Fats

All the mass spectra obtained by nanoESI MS analysis of lithiated model animal fats present common features. They are dominated by peaks related to the molecular cation of lithiated adducts of TAGs and diacylglycerols (Figure 4.15). In dairy products, it was possible to detect TAGs from T<sub>24</sub>, giving evidence for the high sensitivity of this method since, to our knowledge, such small TAGs with 24 and 26 ECN were never detected by any analytical method used until now (Mirabaud *et al.*, 2007). This spectrum is an interesting way to assess the TAG and diacylglycerol distribution in animal fats whether they are saturated or unsaturated. Furthermore, it allows the use of a very tiny amount of matter down to 1 nmol  $\mu\text{l}^{-1}$  with an injection flow of about 200 nl min<sup>-1</sup> (Mirabaud *et al.*, 2007).

To further elucidate the structure of the TAG biomarkers, their mass spectrum was acquired using nanoESI MS/MS. In the mass spectra obtained, a series of peaks at high mass range corresponds to the loss of fatty acid fragments  $[\text{M}+\text{Li}-\text{RCOOH}]^+$  and lithiated fatty acid moieties  $[\text{M}+\text{Li}-\text{RCOOLi}]^+$  from the lithiated adduct cation; at low mass range, the corresponding acylium ions  $\text{RCO}^+$  are formed from the precursor TAG (Figure 4.15, Mirabaud *et al.*, 2007). Because nanoESI MS and nanoESI MS/MS analyses were performed without any pre-separation, the spectra are quite complex and correspond to the loss of all the fatty acids involved in TAG isomers with the same ECN and the same number of unsaturations. These results were used to draw graphs where the relative intensity of the peak corresponding to the loss of a specific fatty acid was plotted against the number of carbon atom of the fatty acid considered (Mirabaud *et al.*, 2007). The graphs obtained in this way for various reference fats were compared and it was possible to propose new criteria to distinguish model samples based on their nature (subcutaneous animal fats or dairy products) and their species (cow, sheep and goat). Such a methodology was then applied to selected archaeological samples in which the presence of well preserved animal fats was previously shown by HT GC and HT GC-MS analysis. Vessels containing cow milk, goat milk and sheep adipose fat from the Neolithic site of Clairvaux XIV could thus be discriminated in this way (Mirabaud, 2007; Mirabaud *et al.*, 2007).



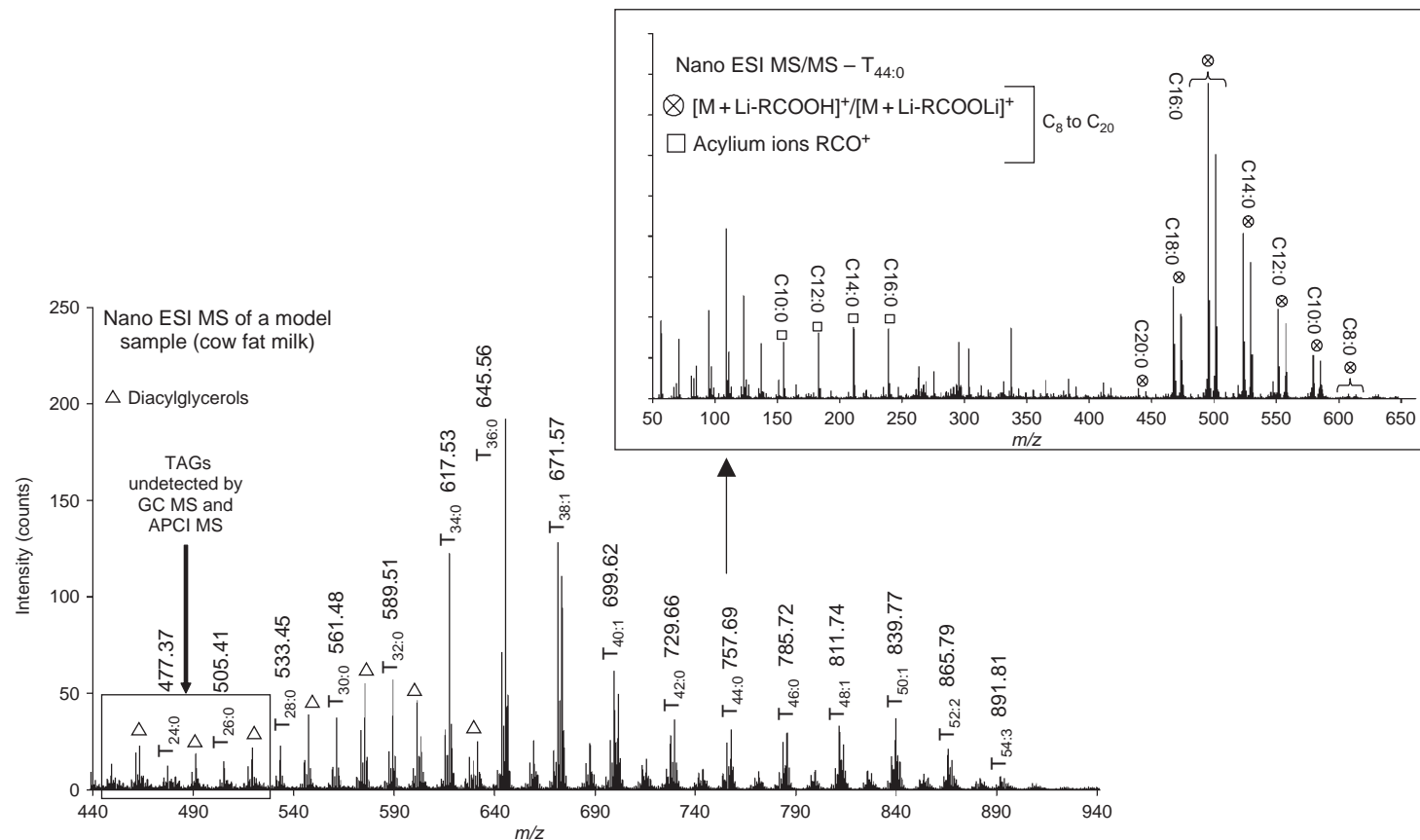


**Figure 4.15** Mass spectrum obtained by nanoESI MS of a model sample of cow fat milk and mass spectrum obtained by nanoESI MS/MS of the triacylglycerol  $T_{44:0}$ . Adapted from Mirabaud et al., 2007

## 4.7 Conclusions

Although most of the analytical studies focused on lipid substances encountered in archaeological objects and museum works of art are carried out using separation techniques, direct mass spectrometry represents an alternative or a complementary analytical way for identifying such complex materials.

EI following introduction into the mass spectrometer using a direct inlet or an exposure probe appears to be a suitable method that minimises sample manipulation, rapidly acquires a high number of spectra, analyses minute samples and distinguishes several materials based upon their mass spectral fingerprint. It may thus be considered as a valuable preliminary step, relying on a fast fingerprinting procedure, in the general strategy leading to the elucidation of the fine structure of the molecular markers still preserved in ancient materials (Figure 4.1). In the case of pure materials, the mass spectrum obtained is very characteristic. However, when several substances are mixed, spectra of different products may overlap, preventing the detection of the presence of some compounds. For example, materials only made of *n*-alkanes, such as candelilla wax, paraffin or ozokerite, are particularly difficult to detect when associated with other waxes. Mixtures of various waxes and resins or tars may nevertheless be detected in wax sculptures or in archaeological samples. The degree of alteration of the materials detected in a sample may also be assessed by this method. In addition to the determination of the main products present in a sample, the detection of long chain compounds such as esters or TAGs is helpful for establishing appropriate sample treatments and analytical conditions for chromatographic analysis that may follow the direct mass spectrometry step.

In contrast to DI or DE EI-MS analysis, investigations relying on ESI MS and ESI MS/MS usually have to be performed as the last stage of analytical strategies (Figure 4.1). When some substances are detected by EI-MS or GC analyses, ESI methods allow the structure of biomarkers of interest in selected samples to be ascertained more soundly. In the case of beeswax, it was shown to be a powerful tool for increasing the number of biomarkers determined in both authentic and archaeological samples, giving rise to the structural elucidation of hydroxy esters, diesters and hydroxy diesters. For animal fats, the use of ESI, in combination with HT GC and HT GC-MS screening analysis, allows the determination of the nature of the fats, especially when the profile of TAGs is particularly altered (distinction between subcutaneous animal fats and fatty materials from dairy products) and to distinguish the species from which the animal substances are issued (cow, goat or sheep).

Hence, direct mass spectrometry techniques, either using EI or ESI, appear to be powerful and innovative analytical tools for elucidating the structure of the main biomarkers present in a wide range of waxes and lipids that may be preserved in archaeological objects and in museum works of art. In most cases, they have nevertheless to be cautiously exploited in combination with other complementary analytical techniques.

## Acknowledgements

We are very grateful to the Ministère de la Culture et de la Communication for financial support provided by the research programme PNRC 2006–2008. We wish to thank Juliette Langlois for the acquisition of some of the spectra presented here. Lastly, we express our

gratitude to the curators, particularly Anne Pinget and Alain Chevalier, and to the archaeologist Stéphane Vacher, for providing access to museum and archaeological items.

## References

- M. P. Colombini, F. Modugno and E. Ribechini, Organic mass spectrometry in archaeology: evidence for Brassicaceae seed oil in Egyptian ceramic lamps, *Journal of Mass Spectrometry*, **40**, 890–898 (2005a).
- M. P. Colombini, F. Modugno and E. Ribechini, Direct exposure electron ionization mass spectrometry and gas chromatography/mass spectrometry techniques to study organic coatings on archaeological amphorae, *Journal of Mass Spectrometry*, **40**, 675–687 (2005b).
- M. S. Copley, J. R. Rose, A. Clapham, D. N. Edwards, M. C. Horton and R. P. Evershed, Processing palm fruits in the Nile Valley – biomolecular evidence from Qasr Ibrim, *Antiquity*, **75**, 538–542 (2001).
- M. S. Copley, R. Berstan, S. N. Dudd, G. Docherty, A. Mukherjee, V. Straker, S. Payne and R. P. Evershed, Direct chemical evidence for widespread dairying in prehistoric Britain, *Proceedings of the National Academy of Sciences of the United States of America*, **100**, 1524–1529 (2003).
- S. N. Dudd and R. P. Evershed, Direct demonstration of milk as an element of archaeological economies, *Science*, **282**, 1478–1481 (1998).
- S. N. Dudd, M. Regert and R. P. Evershed, Assessing microbial contributions to absorbed acyl lipids during laboratory degradations of fats and oils and pure triacylglycerols absorbed in ceramic potsherds, *Organic Geochemistry*, **29**, 1345–1354 (1998).
- S. N. Dudd, R. P. Evershed and A. M. Gibson, Evidence for varying patterns of exploitation of animal products in different prehistoric pottery traditions based on lipids preserved in surface and absorbed residues, *Journal of Archaeological Science*, **26**, 1473–1482 (1999).
- R. P. Evershed, H. R. Mottram, S. N. Dudd, S. Charters, A. W. Stott, G. J. Lawrence, A. M. Gibson, A. Conner, P. W. Blinkhorn and V. Reeves, New criteria for the identification of animal fats preserved in archaeological pottery, *Naturwissenschaften*, **84**, 402–406 (1997a).
- R. P. Evershed, S. J. Vaughan, S. N. Dudd and J. S. Soles, Fuel for thought? Beeswax in lamps and conical cups from Late Minoan Crete, *Antiquity*, **71**, 979–985 (1997b).
- R. P. Evershed, S. N. Dudd, M. S. Copley, R. Berstan, A. W. Stott, H. Mottram, S. A. Buckley and Z. Grossman, Chemistry of archaeological animal fats, *Accounts of Chemical Research*, **35**, 660–668 (2002).
- R. P. Evershed, C. Heron, S. Charters and L. J. Goad, The survival of food residues: new methods of analysis, interpretation and application. In: A. M. Pollard (ed.), *New Developments in Archaeological Science*. Proceedings of the British Academy, 77, Oxford University Press, Oxford, 1992, 293 p.
- N. Garnier, C. Cren-Olivé, C. Rolando and M. Regert, Characterization of archaeological beeswax by electron ionization and electrospray ionization mass spectrometry, *Analytical Chemistry*, **74**, 4868–4877 (2002).
- J. M. Grünberg, Middle Palaeolithic birch-bark pitch, *Antiquity*, **76**, 15–16 (2002).
- J. M. Grünberg, H. Graetsch, U. Baumer, and J. Koller, Untersuchung der mittelpaläolithischen ‘Hartzreste’ von Königsau. Ldkr. Aschersleben-Stassfurt, *Jahresschrift für mitteldeutsche Vorgeschichte*, **81**, 7–38 (1999).
- M. R. Guasch-Jané, M. Ibern-Gómez, C. Andrés-Lacueva, O. Jáuregui and R. M. Lamuela-Raventós, Liquid chromatography with mass spectrometry in tandem mode applied for the identification of wine markers in residues from ancient Egyptian vessels, *Analytical Chemistry*, **76**, 1672–1677 (2004).
- M. R. Guasch-Jané, C. Andrés-Lacueva, O. Jáuregui and R. M. Lamuela-Raventós, The origin of the ancient Egyptian drink Shedeh revealed using LC/MS/MS, *Journal of Archaeological Science*, **33**, 98–101 (2006a).
- M. R. Guasch-Jané, C. Andrés-Lacueva, O. Jáuregui and R. M. Lamuela-Raventós, First evidence of white wine in ancient Egypt from Tutankhamun’s tomb, *Journal of Archaeological Science*, **33**, 1075–1080 (2006b).

- C. Heron, N. Nemcek, K. M. Bonfield, D. Dixon and B. S. Ottaway, The chemistry of Neolithic beeswax, *Naturwissenschaften*, **81**, 266–269 (1994).
- K. Kimpe, P. A. Jacobs and M. Waelkens, Analysis of oil used in late Roman oil lamps with different mass spectrometric techniques revealed the presence of predominantly olive oil together with traces of animal fats, *Journal of Chromatography A*, **937**, 87–95 (2001).
- K. Kimpe, P. A. Jacobs and M. Waelkens, Mass spectrometric methods prove the use of beeswax and ruminant fat in late Roman cooking pots, *Journal of Chromatography A*, **968**, 151–160 (2002).
- K. Kimpe, C. Drybrooms, E. Schrevens, P. A. Jacobs, R. Degeest and M. Waelkens, Assessing the relationship between form and use of different kinds of pottery from the archaeological site Sagalassos (southwest Turkey) with lipid analysis, *Journal of Archaeological Science*, **31**, 1503–1510 (2004).
- P. E. Kolattukudy (ed.), *Chemistry and Biochemistry of Natural Waxes*, Elsevier, New York, 1976.
- J. Koller, U. Baumer, and D. Mania, High-tech in the Middle Palaeolithic: Neandertal-manufactured pitch identified, *European Journal of Archaeology*, **4**, 385–397 (2001).
- A. Lattuati-Derieux, S. Thao, J. Langlois, M. Regert, First results on headspace-solid phase microextraction-gas chromatography/mass spectrometry of volatile organic compounds emitted by wax objects in museums, *Journal of Chromatography A*, **1187**, 239–249 (2008).
- J. S. Mills and R. White, *The Organic Chemistry of Museum Objects*, Butterworth-Heinemann, Oxford, 1994.
- S. Mirabaud, *Développements méthodologiques en spectrométrie de masse pour l'analyse des composés organiques archéologiques. Etude du site néolithique de Clairvaux XIV*. Unpublished PhD thesis, Université des Sciences et Technologiques de Lille, 2007.
- S. Mirabaud, C. Rolando and M. Regert, Molecular criteria for discriminating adipose fat and milk from different species by nanoESI MS and MS/MS of their triacylglycerols: application to archaeological remains, *Analytical Chemistry*, **79**, 6182–6192 (2007).
- F. Modugno, E. Ribechini and M.-P. Colombini, Chemical study of triterpenoid resinous materials in archaeological findings by means of direct exposure electron ionisation mass spectrometry and gas chromatography/mass spectrometry, *Rapid Communications in Mass Spectrometry*, **20**, 1787–1800 (2006).
- L. Niven, From carcass to cave: Large mammal exploitation during the Aurignacian at Vogelherd, Germany, *Journal of Human Evolution*, **53**, 362–382 (2007).
- M. Regert, *Les composés organiques en préhistoire : nouvelles approches analytiques*. Unpublished PhD thesis, Université de Paris X, 351 p. (1996).
- M. Regert, Investigating the history of prehistoric glues through gas chromatography – mass spectrometry, *Journal of Separation Science*, **27**, 244–254 (2004).
- M. Regert, Elucidating pottery function using a multi-step analytical methodology combining infrared spectroscopy, mass spectrometry and chromatographic procedures, *British Archaeological Reports*, **S1650**, 61–76 (2007).
- M. Regert, Des chasseurs de miel néolithiques aux sculpteurs du 19<sup>ème</sup> siècle : une histoire des produits de la ruche et des cires revisitée par la chimie analytique, *Actualité Chimique*, **318**, 52–57 (2008).
- M. Regert and C. Rolando, Identification of archaeological adhesives using direct inlet electron ionization mass spectrometry, *Analytical Chemistry*, **74**, 965–975 (2002).
- M. Regert and S. Vacher, Des adhésifs organiques sur un site de La Tène au Grand Aunay, *Archéopages*, **4**, 20–29 (2001).
- M. Regert, H. A. Bland, S. N. Dudd, P. F. van Bergen and R. P. Evershed, Free and bound fatty acid oxidation products in archaeological ceramic vessels. *Proceedings of the Royal Society of London*, **B265**, 2027–2032 (1998).
- M. Regert, S. Colinart, L. Degrand and O. Decavallas, Chemical alteration and use of beeswax through time: accelerated ageing tests and analysis of archaeological samples from various environmental contexts, *Archaeometry*, **43**, 549–569 (2001a).
- M. Regert, S. N. Dudd, P. F. van Bergen, P. Pétrequin and R. P. Evershed, Investigations of both extractable and insoluble polymeric components: organic residues in Neolithic ceramic vessels from Chalain (Jura, France), *British Archaeological Reports*, **S939**, 78–90 (2001b).

- M. Regert, N. Garnier, O. Decavallas, C. Cren-Olivé and C. Rolando, Structural characterization of lipid constituents from natural substances preserved in archaeological environments, *Measurement Science and Technology*, **14**, 1620–1630 (2003a).
- M. Regert, S. Vacher, C. Moulherat, O. Decavallas, Study of adhesive production and pottery function during Iron Age at the site of Grand Aunay (Sarthe, France), *Archaeometry*, **45**, 101–120 (2003b).
- M. Regert, J. Langlois and S. Colinart, Characterisation of wax works of art by gas chromatographic procedures, *Journal of Chromatography A*, **1091**, 124–136 (2005).
- M. Regert, J. Langlois, E. Laval, A.-S. Le Hô and S. Pagès-Camagna, Elucidation of the molecular and elementary composition of organic and inorganic substances involved in 19th century wax sculptures using an integrated analytical approach, *Analytica Chimica Acta*, **577**, 140–152 (2006).
- M. Regert, T. Devière, A.-S. Le Hô and A. Rougelle, Reconstructing ancient Yemeni commercial routes during the Middle-Ages using structural characterisation of terpenoid resins, *Archaeometry*, **50**, 668–695 (2008).
- E. Ribechini, F. Modugno, C. Baraldi, P. Baraldi and M. P. Colombini, An integrated analytical approach for characterizing an organic residue from an archaeological glass bottle recovered in Pompeii (Naples, Italy), *Talanta*, **74**, 555–561 (2008a).
- E. Ribechini, F. Modugno, M. P. Colombini and R. P. Evershed, Gas chromatographic and mass spectrometric investigations of organic residues from Roman glass unguentaria, *Journal of Chromatography A*, **1183**, 158–169 (2008b).
- D. Scalarone, J. van der Horst, J. J. Boon and O. Chiantore, Direct-temperature mass spectrometric detection of volatile terpenoids and natural terpenoid polymers in fresh and artificially aged resins, *Journal of Mass Spectrometry*, **38**, 607–617 (2003).
- A. P. Tulloch and L. L. Hoffman, Canadian beeswax: analytical values and composition of hydrocarbons, free acids and long chain esters, *Journal of the American Oil Chemists' Society*, **49**, 696–699 (1972).



# 5

## GALDI-MS Applied to Characterise Natural Varnishes and Binders

*Patrick Dietemann and Christoph Herm*

### 5.1 Introduction

Mass spectrometry is used to identify unknown compounds by means of their fragmentation pattern after electron impact. This pattern provides structural information. Mixtures of compounds must be separated by chromatography beforehand, e.g. gas chromatography/mass spectrometry (GC-MS) because fragments of different compounds may be superposed, thus making spectral interpretation complicated or impossible. To obtain complementary information about complex mixtures as a whole, it may be advantageous to have only one peak for each compound that corresponds to its molecular mass ( $[M]^+$ ). Even for thermally labile, nonvolatile compounds, this can be achieved by so-called ‘soft’ desorption/ionisation techniques that evaporate and ionise the analytes without fragmentation, e.g. matrix-assisted laser desorption/ionisation mass spectrometry (MALDI-MS).

Two slightly different laser desorption/ionisation methods were developed simultaneously by Karas and Hillenkamp [1] and Tanaka *et al.* [2]. Whereas Karas and Hillenkamp used small organic matrix molecules to assist and facilitate the desorption and ionisation of analytes (MALDI), Tanaka *et al.* used ultra-fine metal powders and glycerol. Zumbühl *et al.* first analysed natural triterpenoid resins, dammar and mastic, both

by particle suspensions and MALDI-MS with small organic acids [3, 4]. Graphite-assisted laser desorption/ionisation mass spectrometry (GALDI-MS) using graphite particles without any liquid matrix was found to be superior to crystalline organic matrices for these materials. Signal levels were generally higher, and the spectra were not complicated by matrix adducts that greatly complicated spectral interpretation.

Thus, although Karas and Hillenkamp's MALDI method is much more widely used today (see Chapter 6), this chapter deals with the GALDI method, which is a variation of Tanaka's *et al.* particle method. In particular, the use of GALDI-MS to study degradation processes in natural resins by following changes of mass distributions during ageing is demonstrated in Section 5.2, whereas Section 5.3 describes the use of GALDI-MS as an easy and straightforward method of identifying diverse organic materials used in works of art, since no sample preparation is necessary.

The MALDI technique involves mixing the sample with a matrix and desorbing it with a laser, usually a nitrogen UV laser. The matrix absorbs the laser energy and desorbs, while the analytes co-desorb. In the gas phase, the matrix assists the ionisation of the analytes, in most cases by protonation or deprotonation. The resulting ions can then be separated by a mass analyser, usually a time-of-flight mass spectrometer. The properties required for a matrix are also fulfilled in Tanaka *et al.*'s method, but with a two-phase matrix: small particles and a liquid with a low vapour pressure. The small particles absorb the laser energy and heat the liquid matrix containing the analyte. Heating is very fast owing to the large surface of the ultra-fine particles [5], and desorption is achieved without excessive heating of the liquid. Therefore, thermally labile compounds may also be desorbed and ionised without extensive fragmentation. Materials for the particles range from cobalt [2], silicon [6], and titanium nitride [5] to graphite [7–9]. Particle diameters are in the low nanometre to the low micrometre range.

The addition of a liquid matrix, usually glycerol, improves the reproducibility of the mass spectra because inhomogeneities caused by analyte and matrix co-crystallisation are avoided. In some cases, it also enhances signal intensity and resolution. However, analytes can also be desorbed from dry surfaces [7–9].

For molecules larger than 10–30 kDa [5, 8], particle suspension methods are generally considered to be less sensitive, less soft and accompanied by a higher degree of analyte fragmentation compared with MALDI-MS [10], although Tanaka *et al.* were able to detect proteins with masses >100 kDa [2]. However, these conclusions were drawn from peptide and protein analyses and might be different for other types of analytes. For small- and medium-sized molecules, as found in most natural resins, lipids and waxes used in art and archaeology, analysis with particle suspensions is unproblematic [8].

GALDI-MS is an easy and straightforward method to analyse organic binding media because no sample preparation is necessary: a slurry of 2- $\mu\text{m}$  graphite particles in methanol, doped with a small amount of sodium chloride, is pipetted onto a sample tip and allowed to dry. A solution of the sample in any suitable solvent is pipetted on the sample tip and also allowed to dry. The sample quantity has to be varied empirically to optimise the signal and the resolution [3]. If too much sample is applied, poor spectra are obtained and the graphite particles are covered with material that prevents direct desorption from particle surfaces. In this case, the initially grey graphite can sometimes appear black and glossy.

The slurry of graphite in methanol is doped with sodium chloride to enhance signal intensity [3]. Excess sodium ions suppress protonated species as well as adducts with the



ubiquitous potassium ions [11] and therefore avoids signal confusion resulting from the simultaneous occurrence of these species. Sodium iodide can be used as an alternative to sodium chloride [12].

Although Zumbühl *et al.* reported that GALDI-MS is superior for the analysis of natural triterpenoid resins compared with MALDI-MS [3, 4], Scalarone *et al.* demonstrated that MALDI-MS nevertheless works if sample and matrix are applied to cellulosic surfaces of thin-layer chromatography plates [12]. Possibly, the cellulose surface structure allows a better analyte/matrix interaction and a better energy transfer from the matrix to the analyte molecules. However, spectral interpretation is complicated because analytes can be protonated  $[M+H]^+$ , dehydrated  $[M-H_2O+H]^+$  or sodium adducts  $[M+Na]^+$ . The identities of signals are thus ambiguous. In GALDI-MS, analytes are detected as sodium adducts, and protonation as well as dehydration after protonation do not normally occur (see Section 5.2.1) because no proton-providing matrix is present.

The drawback of GALDI is the possible contamination of the ion source with graphite powder that can cause short circuits. The authors have found that the application of thin graphite films and low laser powers minimise the amount of sputtering in the ion source. However, modern commercial spectrometers have compact ion sources that can be easily contaminated, and care should be taken in the use of this methodology. The same is true for turbomolecular pumps if they are located directly below the ion source.

## 5.2 Studying the Ageing of Natural Triterpenoid Resin Varnishes

Dammar and mastic, natural triterpenoid resins, have long been used as varnishes for paintings and are still widely used today [4, 13]. Varnishes fulfil aesthetic functions, they saturate the colours and give gloss to the paintings, but they also protect them from environmental influences. Their main drawback is that they deteriorate rather quickly, although they still fulfil the optical functions for quite a long time despite the chemical degradation. However, the pronounced yellowing of thick layers of varnish can significantly change the appearance of a painting. Brittle cracking degrades both the optical properties of the varnish and its protective function over time. Old varnishes are then often removed with rather polar solvents, which can damage the painting by swelling and leaching of paint components [14–16]. It is therefore desirable to deepen our understanding of the ageing behaviour of these resins for a better protection of valuable works of art.

Various authors have studied the ageing of triterpenoid resins to understand and possibly slow their deterioration [3, 4, 12, 13, 17–36]. The main degradation pathway is autoxidation, an oxidative radical chain reaction [37, 38]: after formation of radicals, oxygen from the air is inserted, leading to peroxides. The peroxides can be homolytically cleaved, resulting in new radicals that continue the chain reaction. The cleavage of peroxide bonds can be induced thermally or photochemically.

### 5.2.1 Characterisation of Pure Single Triterpenes

A study of the photoageing of single triterpenes was undertaken to establish the suitability of the GALDI-MS method [39]. The triterpenes served as a simplified reference system for the more complex natural triterpenoid resins, dammar and mastic. Seven triterpenes were

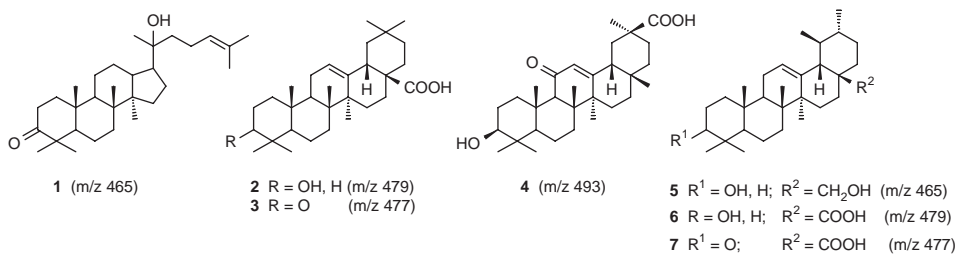


**Figure 5.1** Structures of the pure triterpenes studied by GALDI-MS: hydroxydammar-20-one (20-hydroxydammar-24-en-3-one) **1**, oleanolic acid (3-hydroxyolean-12-en-28-oic acid) **2**, oleanonic acid (3-oxoolean-12-en-28-oic acid) **3**, 18 $\beta$ -glycyrrhetic acid ((3 $\beta$ ,18 $\beta$ ,20 $\beta$ )-3-hydroxy-11-oxoolean-12-en-29-oic acid) **4**, uvaol (urs-12-en-3,28-diol) **5**, ursolic acid (3-hydroxyurs-12-en-28-oic acid) **6**, and ursonic acid (3-oxours-12-en-28-oic acid) **7**

chosen to evaluate the influence of different functional groups or carbon skeletons on the ageing behaviour of pure triterpenes (Figure 5.1). Compounds **1–3** are known components of both dammar and mastic resins, **6** and **7** are components of dammar. The ageing of hydroxydammar-20-one (**1**) and oleanolic acid (**2**) was also investigated by van der Doelen [21].

The results demonstrate that GALDI-MS leads to intact desorption of the triterpenoids. Fragmentation in the spectrometer was found to be insignificant for all triterpene reference substances. Thus each signal in the mass spectrum of natural or aged samples is believed to correspond to one (or several) intact component(s) (see Figures 5.2 and 5.4a) [39]. Carboxylic acid protons can sometimes be exchanged for sodium, leading to additional signals at  $[M+2Na-H]^+$  for acids. Results obtained by GALDI-MS were always highly reproducible in terms of relative signal intensities. In Figures 5.2–5.4, signals marked with crosses (mainly at  $m/z$  413, 469, 483, and 507) are attributed to contamination of the spectrometer with diffusion pump oil, which interfered with the signals of the triterpenes.

Because signal intensities depend on sodium affinity, compounds containing more oxygen atoms show higher signal intensities and are detected more sensitively, as can be seen in the mass spectrum of an equimolar mixture of five triterpenes (Figure 5.2b). The triterpenes show different signal intensities, even though they were all present in the same concentrations. The combined signal of **1** and **5** has the same intensity as that of **3**, although it is caused by two substances. The signals of **2** and **3** are similar, thus there are no big differences between an OH and a C=O group with respect to mass-spectral sensitivity. Compound **4** reveals the highest sodium affinity. It is not clear whether this is only due to the increased polarity or whether it is specific to the unsaturated keto group in this molecule. Steric factors probably also play a role, e.g. the different location of the acid group in the structure may play a role.

Artificial photoageing of the single triterpenes with fluorescence tubes for 300 h [39] results in a remarkably wide variety of products, indicating multiple radical-attack points and the progressive reaction of initial products (Figures 5.2–5.4). Hydrogen abstraction by attacking peroxy radicals will preferentially produce the most stable radicals in tertiary, allylic, or oxygenated positions, first leading to a relatively small number of abundant products. As oxidation progresses, a triterpenoid will be oxidised at many different

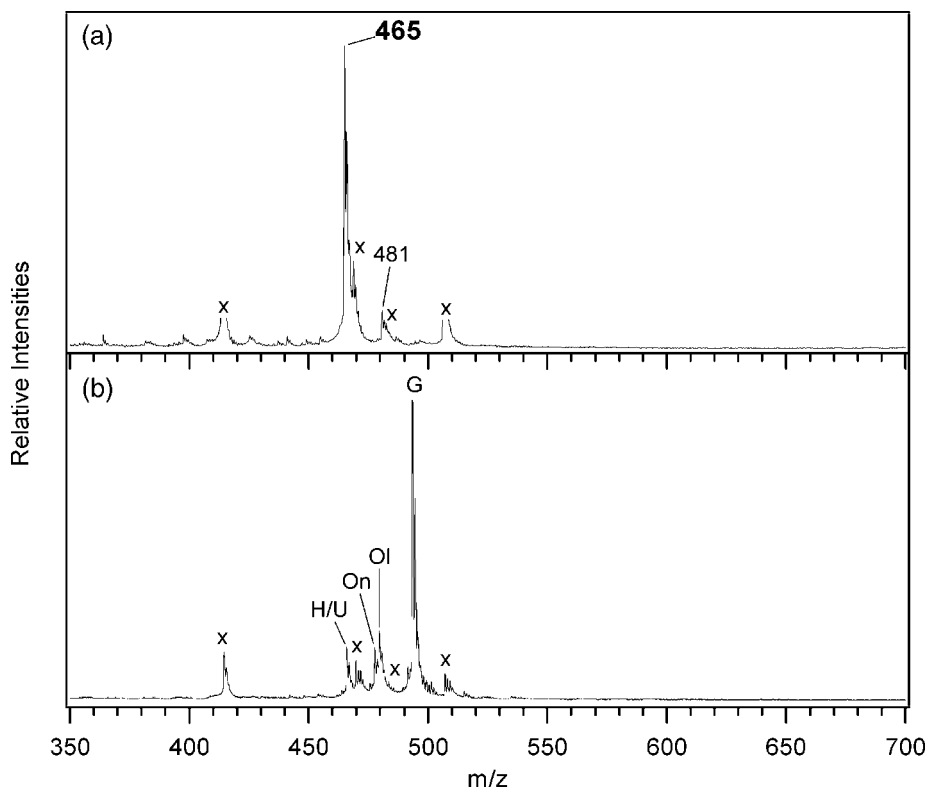


**Figure 5.2** GALDI mass spectra of (a) fresh hydroxydammarone (**1**, sodium adduct  $[M+Na]^+$  at  $m/z$  465) and (b) an equimolar mixture of hydroxydammarone (**1**: H,  $m/z$  465), uvaol (**5**: U,  $m/z$  465), oleanonic acid (**3**: On,  $m/z$  477), oleanolic acid (**2**: Ol,  $m/z$  479), and glycyrrhetinic acid (**4**: G,  $m/z$  493) [39]. In (a), a small amount of  $(M+16)$  is visible at  $m/z$  481 in the unaged sample. Signals marked with crosses at  $m/z$  413, 469, 483, and 507 are contaminants in the spectrometer

locations because abstraction is not completely specific. A large number of oxygen atoms can therefore be incorporated, and a large variety of ageing products is expected. Such a complex MS pattern was found for all artificially aged triterpenes measured by GALDI-MS, differing mainly in the extent of oxidation. As the signal intensity of the initial triterpene decreases, groups of signals with mass increments of 16 or 14 Da develop (Figure 5.3). Different numbers of oxygen atoms are incorporated, leading to signals with a mass difference of 16 Da. Simultaneous loss of hydrogen (e.g. by allylic oxidation or oxidation from alcohols to acids) leads to mass increases of 14 Da. Different combinations of 14 and 16 Da increments lead to signal groups becoming broader and less distinct with increasing mass. At least seven oxygen atoms can be incorporated into a single triterpene. Degradation products arising from cleavage reactions appear at lower masses than the initial triterpenes (Figures 5.2–5.4). Very small amounts of cross-linking products were observed in aged single triterpenes, but they were not studied in detail.

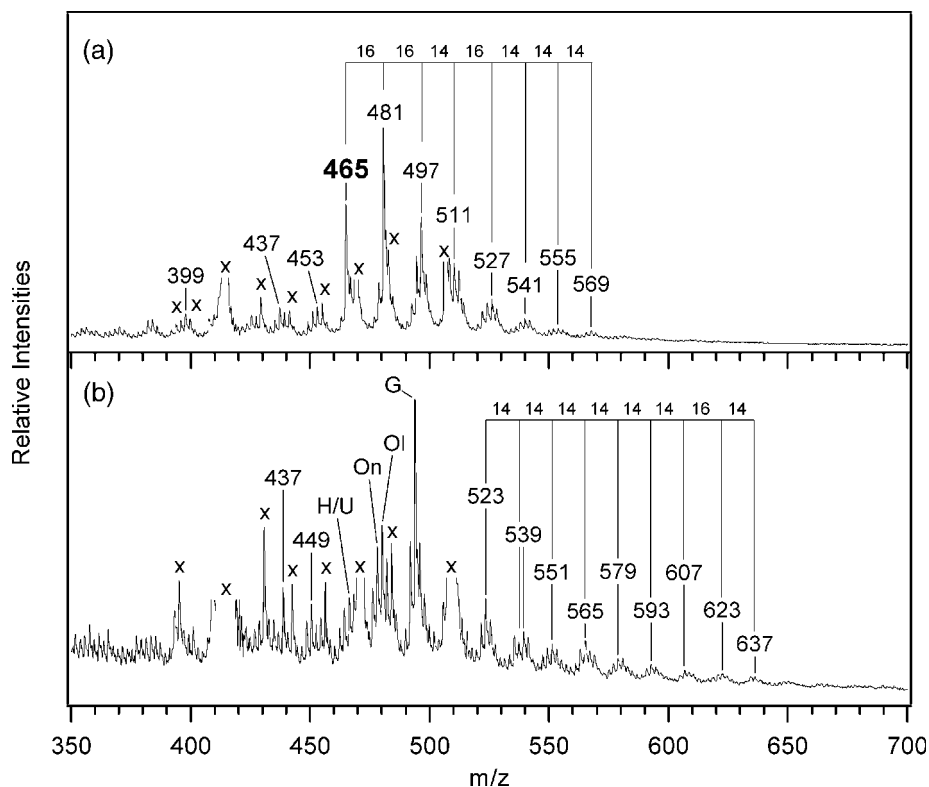


**Figure 5.3** GALDI mass spectra of the samples depicted in Figure 5.2 photoaged for 300 h: hydroxydammarone (a) and the equimolar mixture (b) [39]. Photoageing results in strong oxidation and degradation of the initial triterpenes. Progressive oxidation can be followed by mass increments of 16 and 14 Da. Signals marked with crosses at  $m/z$  413, 469, 483, and 507 are contaminants in the spectrometer. Signals with crosses at  $m/z$  < 460 may have small contributions from contaminants

To simulate a simplified 'resin', equimolar amounts of five triterpenes were mixed and artificially aged. Artificial ageing of the mixture of the triterpenes led to very strong oxidation (Figure 5.3b). The initial triterpenes were almost totally degraded and a large variety of compounds was formed. The signal groups with 14/16 Da mass increments observed in aged pure triterpenes were nevertheless preserved in the mixture. Substances with masses of up to 700 Da and over were formed. It is evident that the mixture is more reactive than the single components alone. This is presumably because the mixture contains a greater variety of functional groups and more combinations of groups in proximity that can react with each other.

Although single compounds cannot be fully identified by GALDI-MS, considerable chemical information regarding ageing is directly available from the mass increments observed. Ageing with too much UV light results in complete cleavage of ketones such as hydroxydammarone (1) or oleanonic and ursonic acid (3, 7) by the Norrish reaction

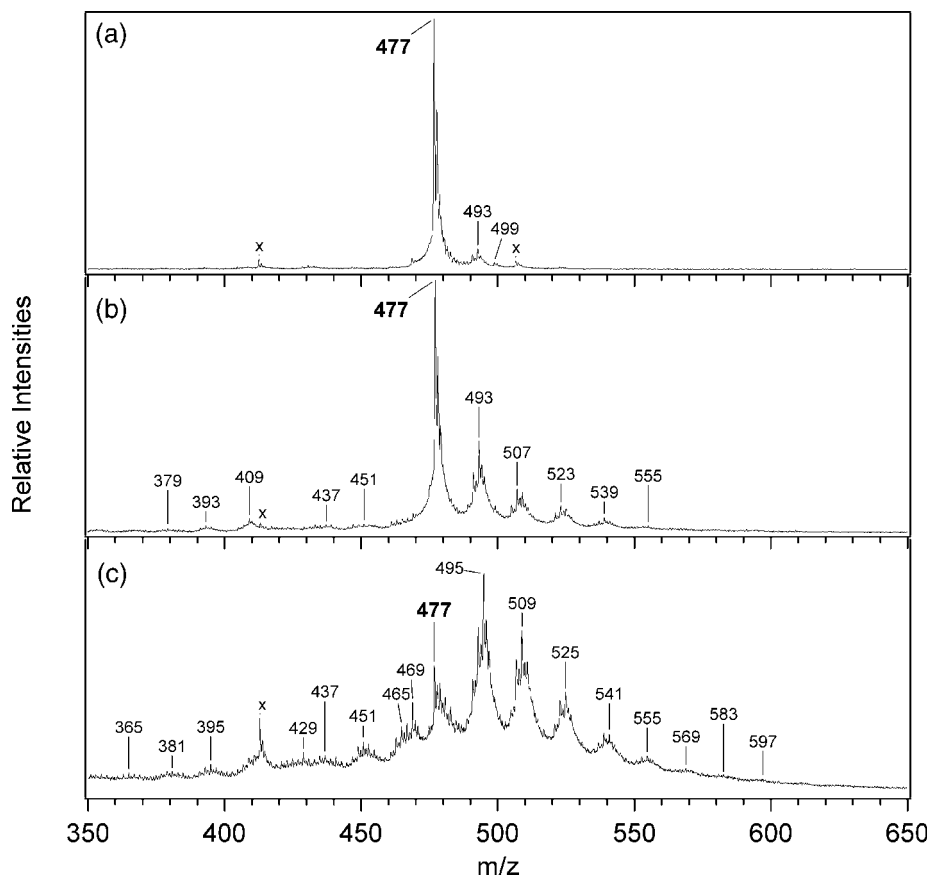


**Figure 5.4** GALDI mass spectra of ursonic acid (**7**,  $m/z$  477): fresh (a), photoaged with (b) and without (c) glass filter. Spectrum (b) depicts the normal ageing pattern (cf. Figure 5.3), but ageing without glass filter – and therefore with much more UV light – results in a mass shift of ( $M+2$ ) in spectrum (c) relative to (b), which is explained by Norrish reactions

(Figure 5.5), as demonstrated by nuclear magnetic resonance (NMR) [3] and GC-MS [24]. The corresponding acid ageing products appear at masses (for **1**:  $m/z$  483; for **3**, **7**:  $m/z$  495) differing by two units from the main natural ageing products (**1**:  $m/z$  481; **3**, **7**:  $m/z$  491/493). Only very small signal intensities were found at the masses of Norrish cleavage products under all ageing conditions, and the same is true for naturally aged resins. However, in samples that were artificially aged without a glass filter, i.e. with large amounts of light in the UV range, the expected shift in the pattern was indeed found (Figure 5.4c). GC-MS analysis confirmed that the dominant ageing product in that sample was indeed the expected Norrish product (3,4-seco-urs-12-en-3,28-dioic acid  $m/z$  495). Thus, GALDI-MS is able to distinguish between this artificial and the natural ageing pathways.

In this study, only compounds with saturated ketone groups were found to be strongly oxidised after artificial ageing with simulated window-filtered daylight [39]. Compounds

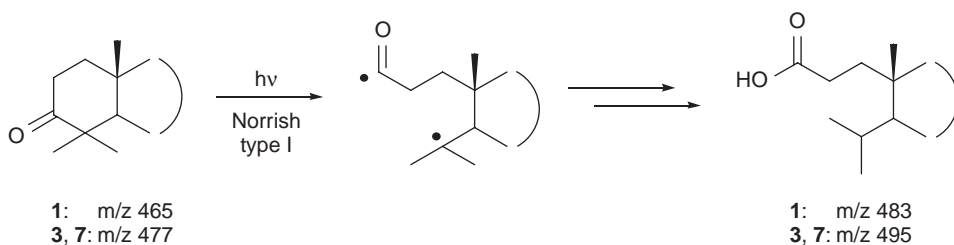


**Figure 5.5** Norrish reaction of a triterpenoid (e.g. dammarane, oleanane or ursane type) leading to ring opening and subsequent oxidation of the ketone to the corresponding acid

without such a group revealed only weak oxidation. Thus it was concluded that ketones are the main initiators of autoxidation under these conditions. Surprisingly, the one unsaturated ketone studied (**4**) did not react in the same way and was only weakly oxidised.

Although no considerable amounts of Norrish products were observed, this reaction could still be responsible for initiating autoxidation and the strong degradation of the saturated ketones. Owing to the fact that peroxides induced by even small rates of the Norrish reaction can be efficiently cleaved by saturated ketones via sensitising mechanisms [38, 40], this might in the end still lead to a high degree of oxidation because this oxidation is autocatalytic. However, the single triterpenes studied were not purified prior to ageing, and minor amounts of impurities or by-products from synthesis may also play an important role in initiating autoxidation [39].

### 5.2.2 Characterisation of Triterpenoid Resins and Varnishes

Triterpenoid resins used as varnishes on paintings were first studied with GALDI-MS by Zumbühl *et al.* [3, 4]. He realised that freshly bought commercial resin, usually considered 'fresh', is actually in an advanced stage of oxidation. Additional experiments were performed later on with improved mass resolution that allowed more detailed conclusions [34–36].

The GALDI mass spectra of fresh dammar and mastic resins (Figures 5.6a and 5.7b) can be readily explained by the well-known components identified by GC-MS [22, 23, 33, 36] (Tables 5.1 and 5.2). In the case of mastic, it is obvious that commercially available resins are considerably oxidised compared with the really fresh resin only a few days after harvesting (Figure 5.7a and b). This is not surprising because there is usually a gap of 1–2 years between harvesting and selling [35]. Furthermore, the resins are then often stored in cupboards for several years before application as varnishes on paintings. The effect is not as pronounced with dammar. This can be explained by the fact that dammar usually occurs in larger beads, and the autoxidation of resins is mainly a surface phenomenon [18, 31, 35]. Samples taken from the surface and the interior of the same dammar bead do indeed display a large difference in the degree of oxidation, as expected (data not shown). However, it is clear that autoxidation of dammar and mastic starts after exudation on the tree and not just after application as a varnish.

As soon as the resin is applied as a varnish, oxidation is dramatically accelerated due to the increased surface-to-volume ratio. Accordingly, a large dependency of the degree of oxidation on the layer thickness is observed [36]. The same oxidation pattern and mass

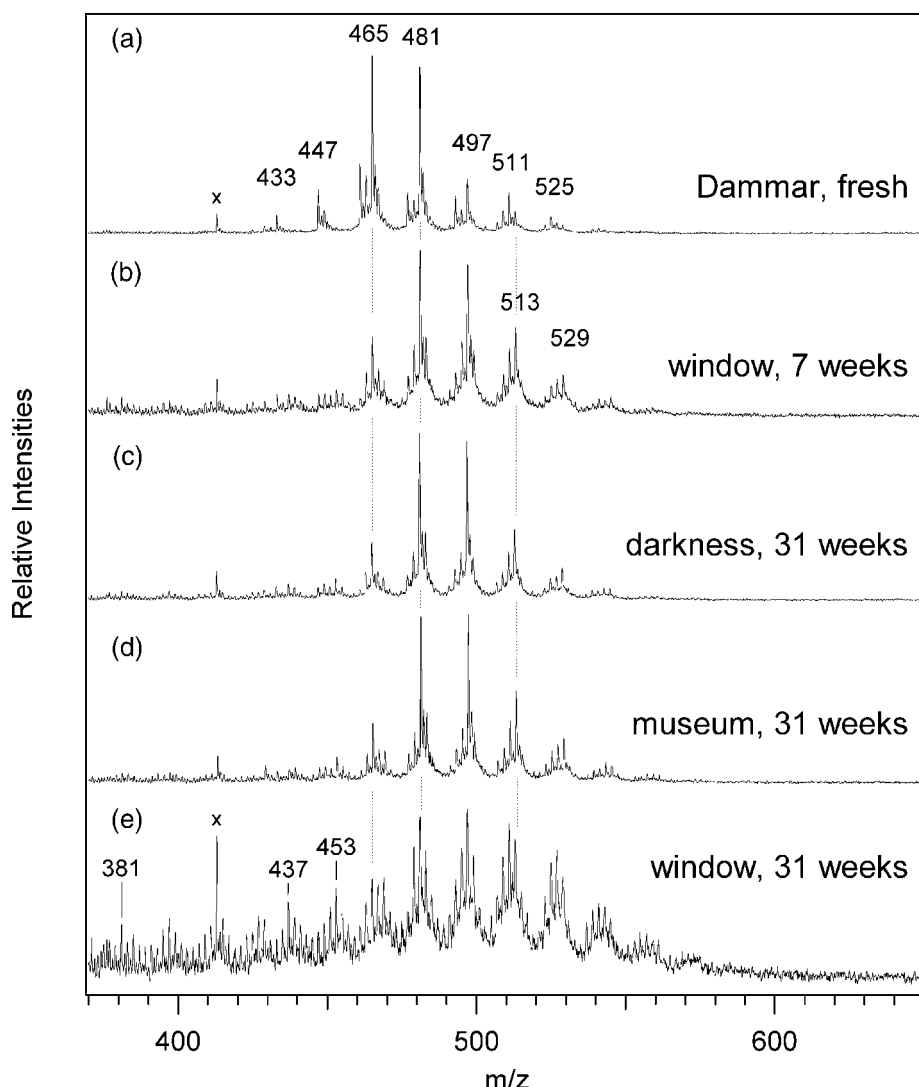


**Figure 5.6** GALDI mass spectra of dammar, fresh (a) and naturally aged under different conditions: in a window after 7 weeks (b), as well as in the dark (c), under museum conditions (d) and in a window after 31 weeks (e) [36]. Strong oxidation and degradation can be seen after a few weeks under all ageing conditions, and the ageing patterns are very similar. Oxidation under museum conditions is not much more pronounced than in darkness

increments of 14 and 16 Da are observed as those found for the single triterpenes discussed above (Figures 5.6 and 5.7). In dammar, the mass spectra are dominated by the compounds with  $m/z$  465 and 481, and oxidation can easily be followed by their progressive ageing products at  $m/z$  497, 513, 529, etc. In mastic, the pattern is more complicated because the ageing products of components at  $m/z$  461–467 and 477 are superimposed. Initial oxidation

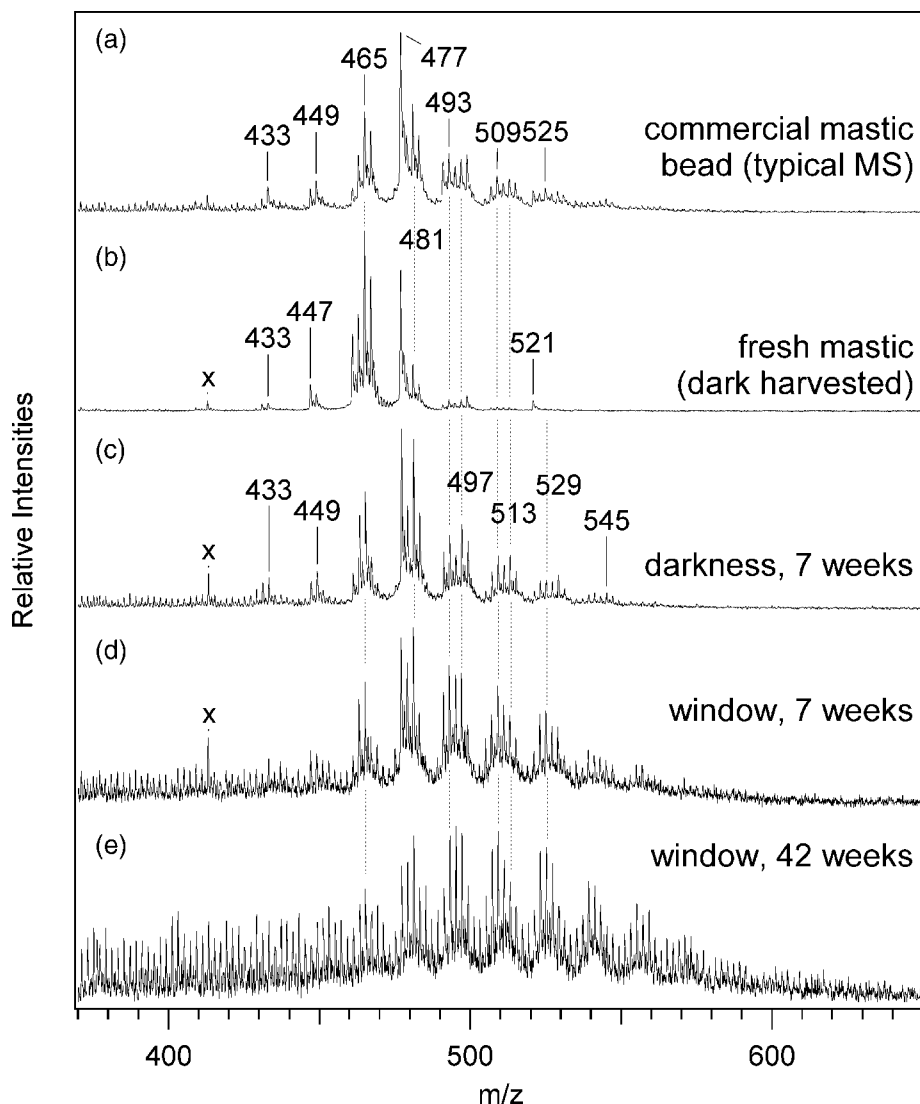


**Figure 5.7** GALDI mass spectra of mastic. Commercially available mastic (a) in an advanced state of oxidation as can be seen by comparison with really fresh mastic a few days after harvesting (b). As with dammar, oxidation and degradation progress quickly in both light and darkness. The same mastic as in (b) is depicted after natural ageing in the dark after 7 weeks (c), and in a window after 7 weeks (d) and 42 weeks (e)

is obvious (Figure 5.7b and c), but further degradation mainly broadens the signal groups and the space between groups is filled (cf. Figure 5.7c and d). Intermediate degradation states are therefore difficult to distinguish (cf. full set of GALDI mass spectra in Appendix of Ref. [33]). With extensive degradation, however, the original signal groups become rather indistinct (Figure 5.7e).



**Table 5.1** Components of fresh dammar resin, as reported in the literature [34], with corresponding  $m/z$  values of the sodium adducts (see Figure 5.6a)

$m/z$ [M+Na] <sup>+</sup>	Compound	Molecular formula
433	Nor-amyrone	C <sub>29</sub> H <sub>46</sub> O
447	Dammaradienone	C <sub>30</sub> H <sub>48</sub> O
449	Dammaradienol	C <sub>30</sub> H <sub>50</sub> O
461	Oleanonic aldehyde, ursonic aldehyde	C <sub>30</sub> H <sub>46</sub> O <sub>2</sub>
463	Oleanolic aldehyde, ursolic aldehyde	C <sub>30</sub> H <sub>48</sub> O <sub>2</sub>
465	Hydroxydammaranone, hydroxyhopanone	C <sub>30</sub> H <sub>50</sub> O <sub>2</sub>
467	Dammarenediol	C <sub>30</sub> H <sub>52</sub> O <sub>2</sub>
477	Oleanonic acid, ursonic acid	C <sub>30</sub> H <sub>46</sub> O <sub>3</sub>
479	Oleanolic acid, ursolic acid	C <sub>30</sub> H <sub>48</sub> O <sub>3</sub>
481	Dammarenolic acid, 20,24-epoxy-25-hydroxy-dammaran-3-one	C <sub>30</sub> H <sub>50</sub> O <sub>3</sub>
493	Hydroxyoleanonic lactone	C <sub>30</sub> H <sub>46</sub> O <sub>4</sub>
497	Shoreic acid, eichlerianic acid	C <sub>30</sub> H <sub>50</sub> O <sub>4</sub>
509	3-Acetoxy-22-hydroxy-hopanone	C <sub>32</sub> H <sub>54</sub> O <sub>3</sub>
511	Asiatic acid	C <sub>30</sub> H <sub>48</sub> O <sub>5</sub>
523	23-Hydroxy-2,3-secours-12-ene-2,3,28-trioic acid (2→23)-lactone	C <sub>30</sub> H <sub>44</sub> O <sub>6</sub>

**Table 5.2** Components of fresh mastic resin, as reported in the literature [34], with corresponding  $m/z$  values of the sodium adducts (see Figure 5.7b)

$m/z$ [M+Na] <sup>+</sup>	Compound	Molecular formula
433	Nor-β-amyrone, nor-lupeone	C <sub>29</sub> H <sub>46</sub> O
435	Nor-β-amyrin	C <sub>29</sub> H <sub>48</sub> O
447	Dammaradienone, β-amyrone, 3-oxo-malabarica-14(26),17E,21-triene	C <sub>30</sub> H <sub>48</sub> O
449	Tirucallol, β-amyrin, germanicol, lupeol, 3-hydroxy-malabarica-14(26),17E,21-triene	C <sub>30</sub> H <sub>50</sub> O
461	Oleanonic aldehyde	C <sub>30</sub> H <sub>46</sub> O <sub>2</sub>
463	28-Hydroxy-β-amyrone	C <sub>30</sub> H <sub>48</sub> O <sub>2</sub>
465	Hydroxydammaranone, (8R)-3-oxo-8-hydroxypolypoda-13E,17E,21-triene	C <sub>30</sub> H <sub>50</sub> O <sub>2</sub>
467	(3L,8R)-3,8-Dihydroxypolypoda-13E,17E,21-triene	C <sub>30</sub> H <sub>52</sub> O <sub>2</sub>
477	Oleanonic acid, moronic acid, masticadienonic acid, isomasticadienonic acid, 18αH-oleanonic acid	C <sub>30</sub> H <sub>46</sub> O <sub>3</sub>
479	Oleanolic acid, 3-epi-masticadienolic acid, 3-epi-isomasticadienolic acid	C <sub>30</sub> H <sub>48</sub> O <sub>3</sub>
509	3-Acetoxy-hydroxydammaranone	C <sub>32</sub> H <sub>54</sub> O <sub>3</sub>
521	3-O-acetyl-2-epi-masticadienolic acid, 3-O-acetyl-2-epi-isomasticadienolic acid	C <sub>32</sub> H <sub>50</sub> O <sub>4</sub>

In addition to the oxidation products, there are also degradation products with lower masses than the initial triterpenoids as well as cross-linking products. Degradation products can be seen in all aged samples, in pure triterpenes (Figures 5.3 and 5.4) and in the resins (Figures 5.6 and 5.7). They are already present very early in the ageing process (Figure 5.6b

and 5.7c), thus extensive oxidation is not needed for their formation. Some degradation products with low molecular weight have been identified by GC-MS, but again the GALDI mass spectra show that a much broader variety of many more compounds has developed. Cross-linking of triterpenoids occurs during ageing; however, this has not been studied extensively with GALDI-MS. Formation of dimers and trimers has been observed in both artificially and naturally aged dammar and mastic films [3, 34]. It is remarkable that not only oligomers are formed, but also many compounds with molecular weights between those of triterpenoid oligomers. This has been explained by the cross-linking of triterpenoids with degradation products from the ageing process [3, 34] and degraded parts of the resin polymers [12] that consist of a polycadinene in dammar [41] or polymyrcene in mastic [42].

A natural ageing study was undertaken to investigate the influence of light and resin composition on the ageing process [33, 36]. Dammar and different mastic resins were naturally aged in darkness, under museum conditions (max. 300 lux, no UV light) and behind a window (high light levels with UV). Oxidation proceeded very rapidly, within a few weeks (cf. Figures 5.6b–e, 5.7c and d), regardless of the ageing conditions. A comparison of varnishes aged in the dark and in the light reveals that the ageing processes are very similar under both conditions [36] because the mass spectrometric patterns are almost identical. These conclusions were further supported by data from electron paramagnetic resonance studies on the radical processes involved in autoxidation [34, 36]. Thus, autoxidation does not stop in the dark, despite the lower rate of radical formation. Presumably even the fresh resins are in such an advanced state of oxidation that enough peroxides are formed to maintain the autoxidation pathway by thermally induced homolytic cleavage of peroxide bonds.

Oxidation under moderate, controlled light conditions, as in a museum, was actually not much more pronounced than without any light (cf. Figure 5.6c and d), although high amounts of light with UV led to extensive degradation. Therefore, we can confirm that the effort of museums to protect their objects from light as far as possible is a highly effective measure. These findings are also supported by infrared spectroscopic data [36].

The resin composition was indeed found to influence the ageing processes: in mastic, the polymer fraction was shown to reduce the oxidation of triterpenoids (Figure 5.8). This was found for both natural ageing [33, 36] and artificial ageing. Because the polymer, a polymyrcene, contains many double bonds that can easily be oxidised [42], it might act as a radical stabiliser. The mastic samples shown in Figure 5.8 were obtained from three aliquots of the same mastic solution, the polymer part of the first aliquot was removed and added to the third.

### 5.2.3 Conclusions

Application of GALDI-MS to the ageing of natural resins provided insights into the ageing pathways and their dynamics. The influence of ageing conditions, mainly the amount of light, as well as the resin composition was studied, thus increasing our understanding of the processes involved. GALDI-MS is an ideal tool to monitor and study the ageing and especially oxidation of organic materials such as resins because analytes are detected as sodium adducts. Therefore, more strongly oxidised compounds are detected more sensitively due to their higher sodium affinities. This is in contrast to GC-MS, which has lower response factors to highly oxidised, thermally labile polar compounds. GC-MS is an extremely

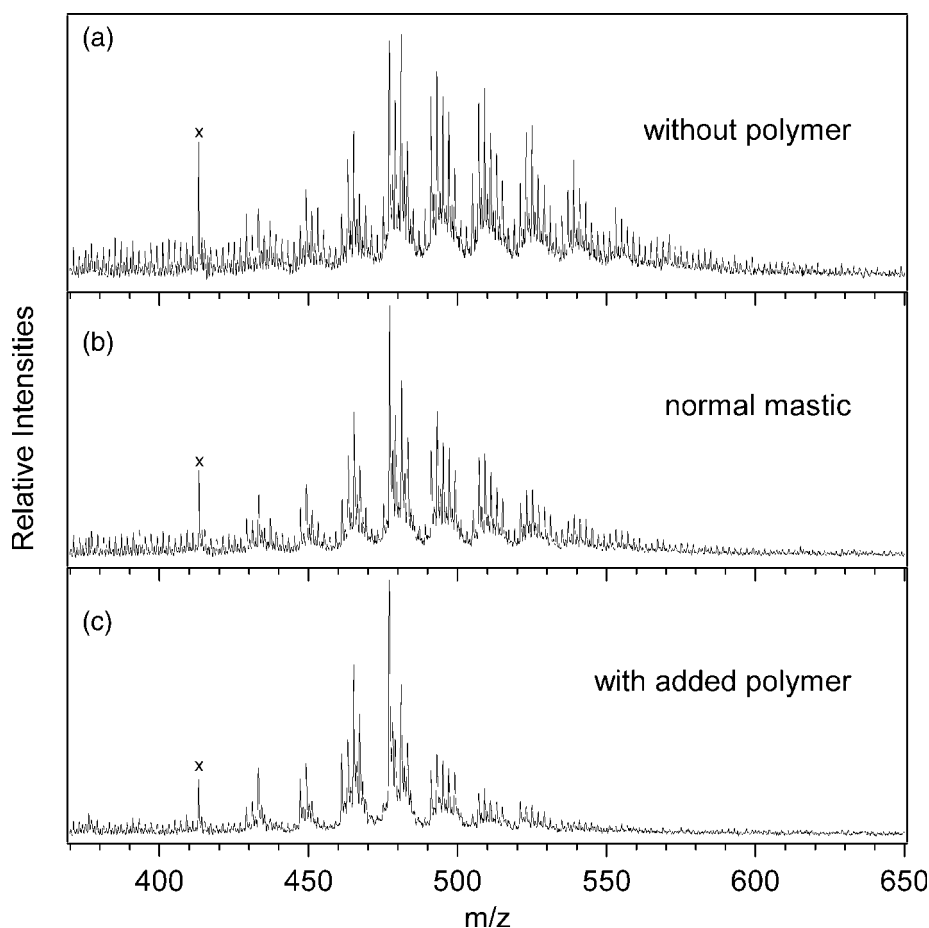


**Figure 5.8** GALDI mass spectra of mastic with variable amounts of polymer, artificially aged for 880 h [36]: (a) without polymer; (b) normal mastic; and (c) with added polymer. Oxidation and decomposition is enhanced with lower amounts of polymer, thus the mastic polymer retards oxidation of the triterpenoids

powerful and valuable tool to identify single compounds to deduce ageing pathways [43, 44], but GALDI-MS is better suited to providing a broader overview of the changes. Therefore, the two methods are complementary, and the results of both methods should be considered.

Ageing of a single triterpene leads to a surprisingly broad range of ageing products. Up to seven oxygen atoms or more can be incorporated into each triterpene. As a consequence, the complex composition of aged varnishes is not due to the formation of a few ageing products from a large number of initial compounds (as could be expected by the results of van der Doelen and Boon [21, 43]), but rather the complexity of the ageing products of each single component.

Ageing of natural resins mainly proceeds by autoxidation and strong oxidation occurs within a very short time – within weeks and months rather than years and decades. Oxidation is more pronounced in light, but it also proceeds in darkness. Reduced intensities of

UV-filtered light, as in a museum, effectively reduces the amount of oxidation to almost the same level that occurs in darkness. The polymer fraction of mastic was found to reduce the degree of oxidation in the material, possibly by acting as a radical scavenger.

### 5.3 Application to Organic Materials of Artworks

#### 5.3.1 Methodological Aspects

Besides the well-established chromatographic/mass spectrometric or spectroscopic methods there is always a need for complementary methods for the study of organic materials from art objects. The application of laser desorption/ionisation mass spectrometry (LDI-MS) methods to such materials has been reported only sporadically [12, 45–48]; however, it is apparently increasing in importance. After GALDI-MS had been applied to triterpenoid resins, as described in Section 5.2, this relatively simple method was evaluated for a wider range of binders and other organic substances used for the production or conservation of artwork. Reference substances as well as original samples from works of art were analysed.

Sample preparation was carried out with various solvents, depending on the solubility of the sample; sometimes gentle warming was necessary. Whereas mostly tetrahydrofuran (THF) in addition to methanol, ethanol and water were used for polar substances, cyclohexane and toluene proved suitable for nonpolar waxes and free fatty acids.

The majority of the GALDI-MS experiments followed the method for triterpenoid resins described in Section 5.1. Fine-grain silicon powder ( $\varnothing < 78 \mu\text{m}$ ) was tried as an alternative matrix, but it did not show any advantages over graphite. In some cases in which the sodium chloride doped graphite matrix did not give satisfactory spectra, silver trifluoroacetate was added in order to produce silver adducts. However, this variation increased the signal intensities only for natural rubber (see Figure 5.9).

The detection limit of the method was determined using a dilution series of three different substances. Without delayed extraction [49], the detection limit lay between  $1 \mu\text{g}$  and  $0.1 \mu\text{g}$ ; i.e.  $< 3.5 \text{ nmol}$  for stearic acid (MW 284),  $< 2.1 \text{ nmol}$  for 18 $\beta$ -glycyrrhetic acid (MW 470), and  $< 1.1 \text{ nmol}$  for trielaeostearin from tung oil (MW 873). Delayed extraction decreased the detection limit for glycyrrhetic acid by the order of one magnitude. Generally, GALDI mass spectra of polymeric materials with a broad molecular weight distribution showed that the sensitivity of the instrument decreased with increasing  $m/z$  values.

The time-of-flight mass spectrometer was usually operated in the positive mode in order to detect the cationic sodium adducts of the analyte molecules. The anions of H-acidic substances were detected in the negative mode. This mode significantly enhanced the signals of acidic compounds, e.g. free fatty acids compared with ester signals in the mass spectra of beeswax and tung oil.

Generally, it is not possible to determine a chemical substance from a single  $m/z$  value because several isomers can contribute to the peak. This is especially true of aged natural binders. Consequently, interpretation of GALDI-MS results can be ambiguous and initial assignments should only be made with the aid of analytical data from independent experiments (e.g. infrared spectroscopy) and from the literature. However, after peak patterns have been established and marker substances determined from reference measurements, complex organic materials can nevertheless be identified in samples from art objects. An error of  $\pm 2 \text{ Da}$  due to calibration errors has to be considered in the figures shown.

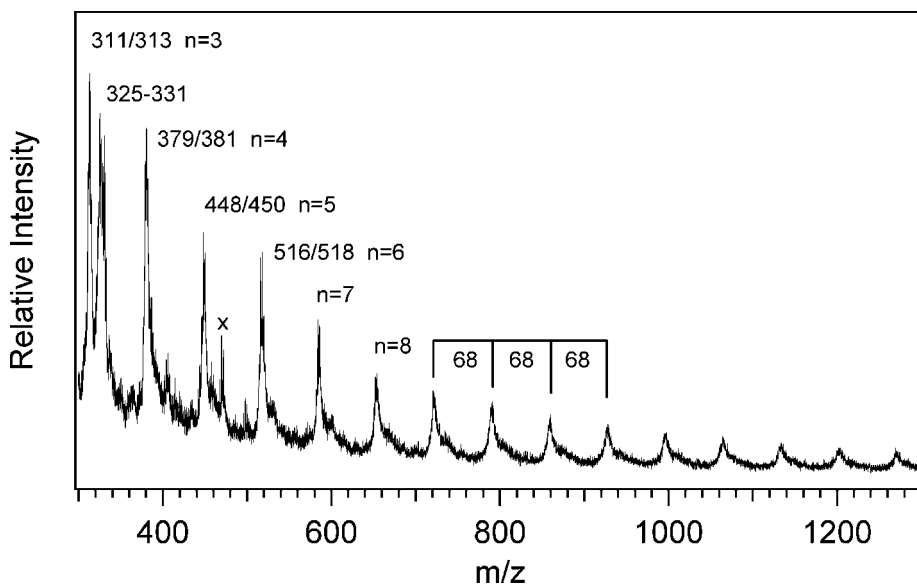


**Figure 5.9** GALDI mass spectrum of natural rubber (from toluene/THF solution) on silver-doped graphite matrix. The signal spacing of 68 Da corresponds to the isoprene monomer

It should be mentioned that the GALDI-MS method described here readily revealed mass spectra of chemically different organic dyes and pigments (diazo dyes, phthalocyanines, anthraquinones, triarylmethines, indigoids). The majority of these dyes showed the molecular masses expected from theory. Furthermore, some organic dyes (Brilliant Green CI 42040, Phthalocyanine Green CI 74260/PG7) applied directly to the blank target of the mass spectrometer produced intensive mass spectra as well. This variant without a matrix is similar to LDI-MS, which has already been reported as a successful method for the analysis of synthetic dyes [50].

### 5.3.2 Natural Resins

A number of different diterpenoid resins (burgundy resin, Canada balsam, colophony, Congo copal, Zanzibar copal, sandarac, spruce resin, Venetian turpentine from larch) generally showed similar patterns with a main signal at  $m/z$  325. This corresponds to the sodium adducts of several isomeric diterpenoid acids ( $C_{20}H_{30}O_2$ , e.g. pimaric acid, palustric acid and abietic acid). For example, Figure 5.10 shows a typical GALDI mass spectrum of rosin. Rosin, or colophony, is the distillation residue from different pine resins. In addition to the predominant signal at  $m/z$  325, it shows a series of higher masses ( $m/z$  337, 339, 355, 373, etc.). Mass increments of 14 or 16 Da indicate repeated incorporation of oxygen and loss of hydrogen, based on similar ageing pathways as discussed for triterpenoid resins in Section 5.2.2. The most intense signals exactly match the molecular masses of oxidised abietic acids, which were identified as main components of resin samples from old paintings [44] (see Table 5.3). Highly oxidised species with even more

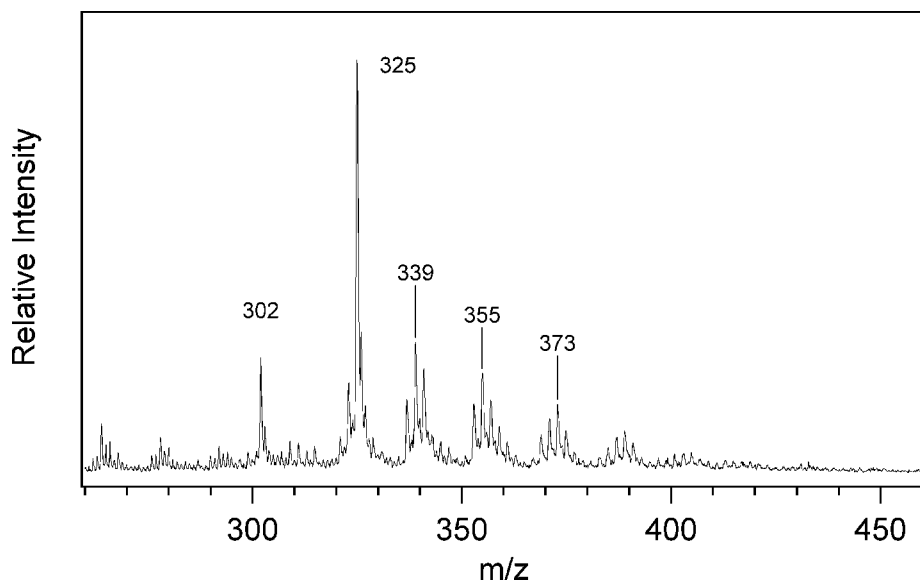


**Figure 5.10** GALDI mass spectrum of rosin (colophony; from THF solution). The typical signal pattern of diterpenoids is visible;  $m/z$  325 corresponds to isomeric diterpenoid acids, e.g. abietic acid (see Table 5.3)

**Table 5.3** Prominent peaks in the mass spectrum of rosin (see Figure 5.10). Compounds marked with an asterisk are mentioned as constituents of diterpenoid varnishes from old pictures in the literature

$m/z$ $[M+Na]^+$	Compound	Molecular formula
325	Abietic acid and isomers (MW = 302)	$C_{20}H_{30}O_2$
337	7-Oxodehydroabietic acid*	$C_{20}H_{26}O_3$
339	Hydroxydehydroabietic acids*	$C_{20}H_{28}O_3$
355	Dihydroxydehydroabietic acids*	$C_{20}H_{28}O_4$
373	Trihydroxyabietic acid or isomer	$C_{20}H_{30}O_5$

oxygen (3–5 atoms) can be recognised. The additional signal at  $m/z$  302 cannot be directly correlated to the sodium adducts of diterpenoids. However, it equals the molecular weight of the positive molecule ion of the abietic acid isomers. At even higher masses ( $m/z$  600–750), a group of weak signals with maxima in the range of  $m/z$  655–675 indicate cross-linking of the diterpenoids.

Although the mass spectra of aged diterpenoid resins are generally not characteristic enough for a clear identification, some natural products show characteristic peaks above  $m/z$  325. These signals can be explained by particular constituents of the respective resins, so-called biomarkers. For example, copaiba balsam shows an intense peak at  $m/z$  385, which can be attributed to 3-acetoxy-copaiferic acid [51] (see Figure 5.11). Another

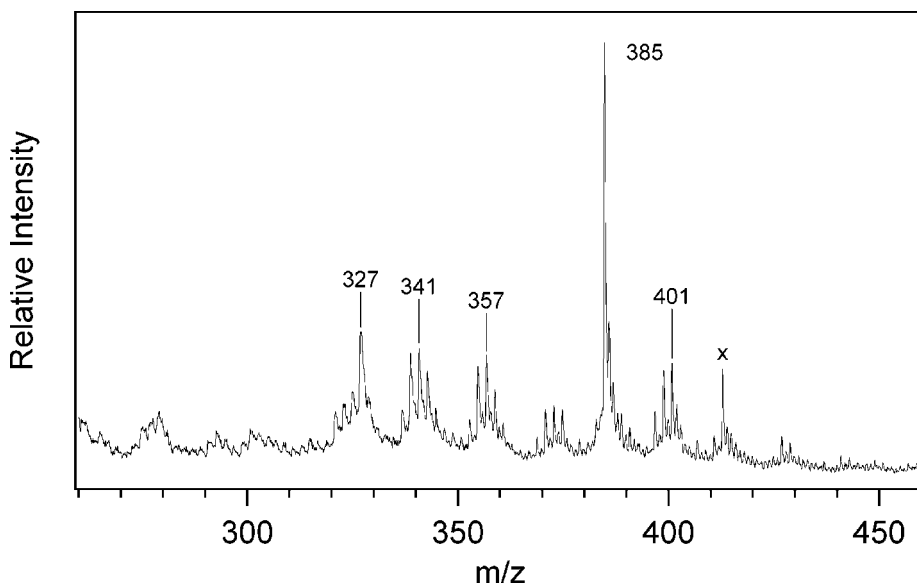


**Figure 5.11** GALDI mass spectrum of copaiba balsam. The most intense peak ( $m/z$  385) can be attributed to 3-acetoxy-copaiferic acid

example is larch resin, in which an enhanced peak at  $m/z$  371 corresponds to larixyl acetate ( $C_{22}H_{36}O_3$ ) [52, 53].

GALDI-MS was used to analyse elemi, a triterpenoid resin, as well as mastic and dammar, which are discussed in detail in Section 5.2. As for most diterpenoid resins, the mass spectra were not characteristic enough for a clear identification of the particular resin. Generally, the mass spectra are dominated by ageing products with  $[M+Na]^+ = m/z$  477–481 ( $C_{30}H_{46}O_3$ – $C_{30}H_{50}O_3$ ). Although neither diterpenoid nor triterpenoid resins can be distinguished reliably, their presence in binding media may be reliably established by GALDI-MS on the basis of their characteristic peak patterns in the range of  $m/z$  320–380 or  $m/z$  450–600, respectively.

Other resins may be identified more easily. For example, the GALDI mass spectrum of a methanolic extract of shellac is shown in Figure 5.12. Shellac is described in the literature as a cross-linked oligomer of two aliphatic hydroxy acids (butolic acid and aleuritic acid, see Table 5.4) with several related sesquiterpenoid carboxylic acids (jalaric and laccijalaric acids, and their reduction and oxidation products) [52, 54]. The mass spectrum of shellac is dominated by a characteristic peak at  $m/z$  570, which can most probably be attributed to the ester of laccijalaric acid with aleuritic acid within a deviation of  $\pm 4$  Da. Smaller peaks in this region indicate further monoesters among the above-mentioned hydroxy acids. A complex pattern of signals at  $m/z$  267–327 may be caused by the free acids. However, there is interference by peaks from the graphite matrix. Additionally, the mass spectrum shows weak signals of diesters at  $m/z \approx 800$  and of triesters at  $m/z \approx 1120$ .

Aloe is an example of a yellow-coloured natural plant juice that was used as yellow pigment or glaze. The GALDI mass spectrum of *Aloe hepatica*, a historic sample from the

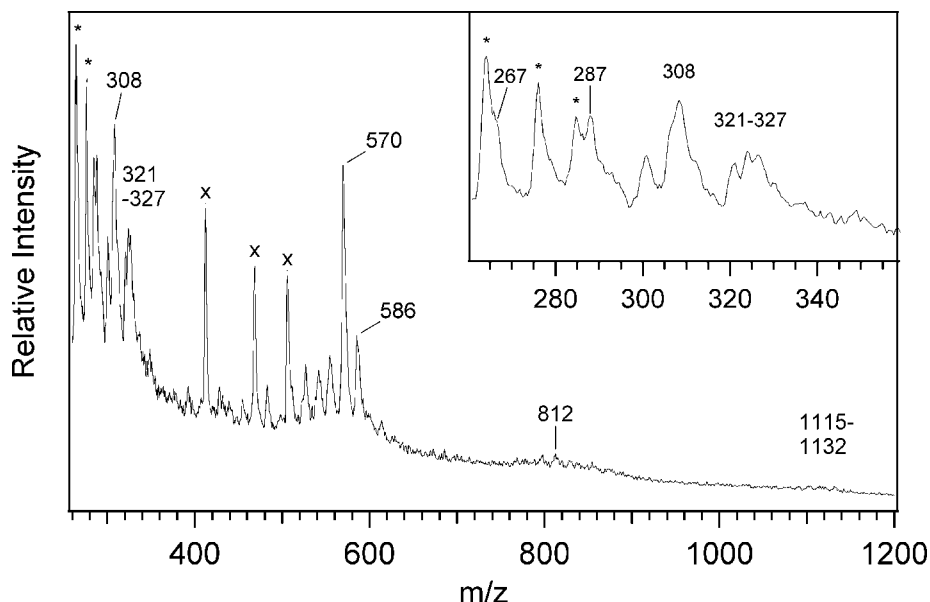


**Figure 5.12** GALDI mass spectrum of shellac (from methanol solution). Peaks at  $m/z \approx 570$  are related to esters of aliphatic hydroxy acids with sesquiterpenoid carboxylic acids (see text and Table 5.4). Signals marked with crosses are contaminants in the spectrometer that accumulated over time ( $m/z$  413, 469, and 507); peaks marked (\*) are contaminating graphite clusters from the matrix ( $m/z$  264, 276, 288).

**Table 5.4** Prominent peaks in the mass spectrum of shellac (see Figure 5.12), interpretation following the literature

$m/z$ $[M+Na]^+$	Compound	Molecular formula
267	Butolic acid (6-hydroxytetradecanoic acid)	$C_{14}H_{28}O_3$
287	Laccijalaric acid	$C_{15}H_{20}O_4$
303	Jalaric acid	$C_{15}H_{20}O_5$
305	Laksholic acid	$C_{15}H_{22}O_5$
319	Shellolic acid	$C_{15}H_{20}O_6$
327	Aleuritic acid (9,10,16-trihydroxyhexadecanoic acid)	$C_{16}H_{32}O_5$
573	Ester of aleuritic acid and laccijalaric acid	$C_{31}H_{50}O_8$
589	Ester of aleuritic acid and jalaric acid	$C_{31}H_{50}O_9$
818	Diester of butolic/aleuritic/laksholic acid	$C_{45}H_{78}O_{11}$

nineteenth century, is dominated by two characteristic peak doublets at  $m/z$  431/447 and 577/593. Literature mentions the anthraquinone aloe-emodine in the form of its 8- $\beta$ D-glucoside as the main colouring component of aloe resin ([55], p. 228). The main peak at  $m/z$  432 in the mass spectrum (Figure 5.13 and Table 5.5) matches the molecular mass of the glucoside, i.e. this dye is desorbed as a molecular radical cation in this experiment. The very high intensity of this molecular peak compared with other peaks in the mass spectrum



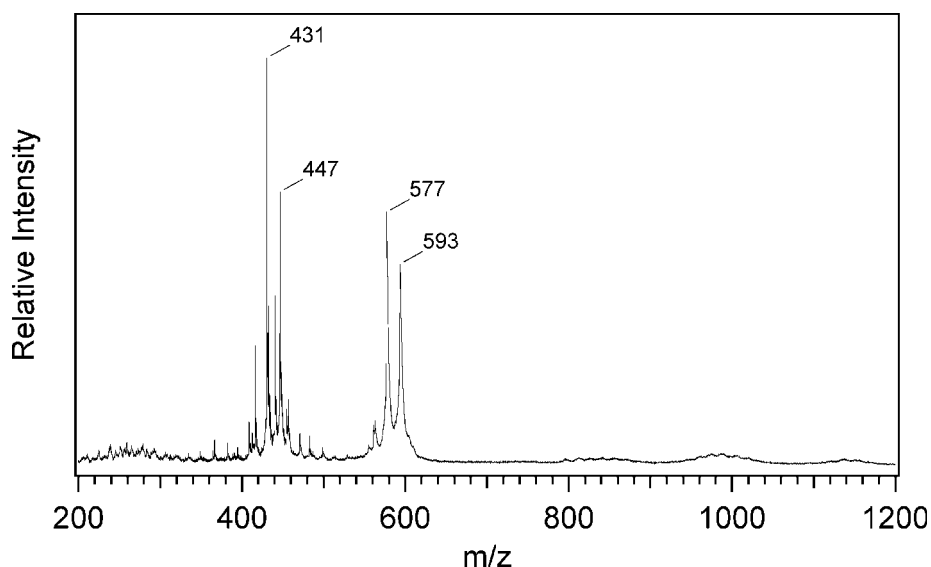


**Figure 5.13** GALDI mass spectrum of aloe resin (from THF solution). The two doublets correspond to mono- and diglucosides of aloe-emodin and their oxidation and reduction products, respectively (see Table 5.5)

**Table 5.5** Prominent peaks in the mass spectrum of aloe resin (see Figure 5.13), interpretation following the literature. The dyes are not detected as sodium adducts but as radical cations formed by direct absorption and ionisation of the laser energy

MW	Compound	Molecular formula
432	Aloe-emodin-glucoside <b>8</b>	$C_{21}H_{20}O_{10}$
448	Oxidation product of <b>8</b>	$C_{21}H_{20}O_{11}$
578	Reduction product of <b>9</b>	$C_{27}H_{30}O_{14}$
594	Aloe-emodin-diglucoside <b>9</b>	$C_{27}H_{30}O_{15}$

is another example of the high effectiveness of the desorption of dyes as molecular ions compared with the sodium adduct. The spacing of 162 Da (matching glucosidyl,  $C_6H_{10}O_5$ ) leads to another intense peak with  $m/z$  594, which can consequently be identified as a diglucoside of aloe-emodin. Finally, a molecule with one less oxygen is identified in the mass spectrum at  $m/z$  577 as well.

The GALDI mass spectrum of natural rubber (poly-2-methyl-1,3-butadiene) on a silver-doped graphite matrix (Figure 5.9) shows an equidistant sequence of signal groups beginning at  $m/z \approx 311/313$  and detectable up to  $\approx 2000$ . The spacing of 68 Da between the groups matches the molecular weight of isoprene ( $C_5H_8$ ). The intensity of the groups decreases with increasing  $m/z$  value. Considering the atomic mass of the silver isotopes (107/109 Da), the multiplets can be attributed to oligomers of isoprene with  $n \geq 3$ . The double peaks spaced by 2 Da also hint at silver adducts. Additionally, a group of peaks at

$m/z$  325–331 might indicate oxidised trimers. Although not representing the true molecular weight distribution, GALDI-MS shows a characteristic spectrum of polyisoprene.

### 5.3.3 Waxes

The GALDI-MS measurements covered a selection of natural ester waxes, both from animal (beeswax, shellac wax, spermaceti) and vegetable sources (candelilla, cane, carnauba, cotton fibre, esparto, ouricouri). Generally, the waxes were readily distinguishable by their characteristic distribution of molecular masses. In some cases, markers could be identified on the basis of literature data.

Beeswax is the most important wax in the technology of objects of art and antiquity. According to the literature [52, 56], beeswax consists of hydrocarbons, free fatty acids and different esters (monoesters, diesters, triesters, hydroxy monoesters and hydroxy polyesters) (Table 5.6). The oligomeric esters are composed of diols and hydroxy acids. The

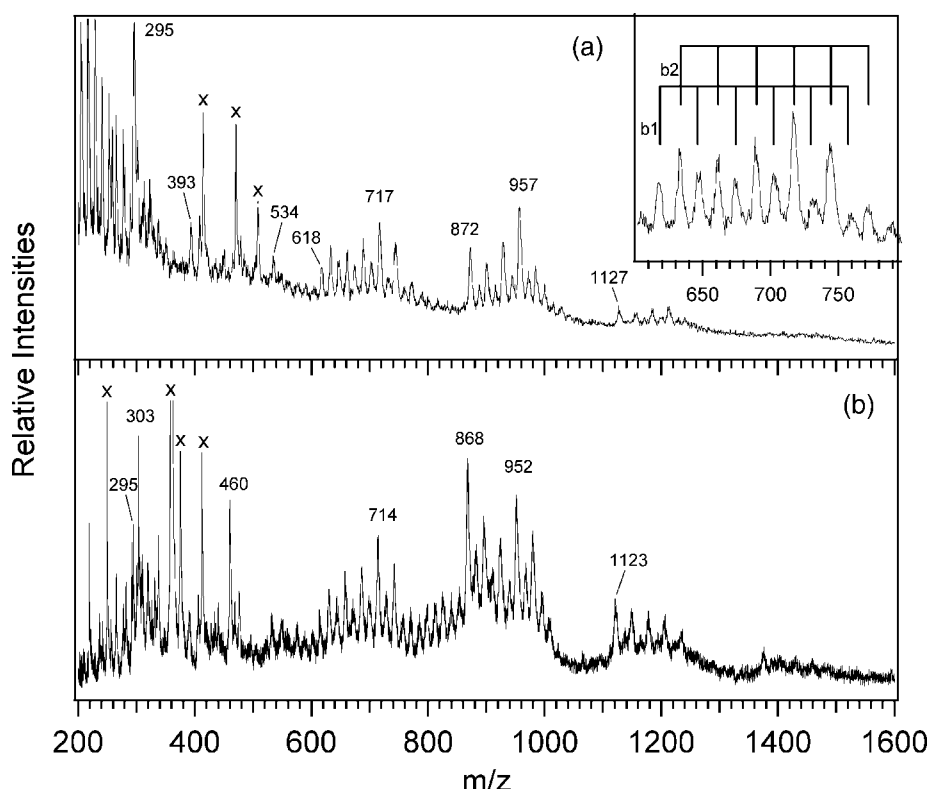


**Figure 5.14** GALDI mass spectra of (a) beeswax (from THF solution) and (b) medieval white wax seal (from toluene-THF solution). See Table 5.6 for an interpretation. In (a), pattern b1 indicates monoesters and b2 indicates hydroxy monoesters; the mass increments of 28 Da correspond to  $(CH_2)_2$  groups. Signals around  $m/z$  850–1000 indicate diesters, those at  $m/z$  1100–1300 indicate triesters

**Table 5.6** Prominent peaks in the mass spectrum of beeswax (see Figure 5.14), interpretation following the literature [57, 61]

$m/z$ $[M+Na]^+$	Compound	Molecular formula
279	(a) free fatty acids: $n = 16$ (palmitic acid)	$C_nH_{2n}O_2$
391	$n = 24$ (lignoceric acid)	
531	$n = 34$ (psyllastearic acid)	
295	(a) hydroxy fatty acids, $n = 16$	$C_nH_{2n}O_3$
616	(b) monoesters, $n = 40$	$C_nH_{2n}O_2$
716	(b) hydroxy monoesters, $n = 46$	$C_nH_{2n}O_3$
870	(c) diesters, $n = 56$	$C_nH_{(2n-2)}O_4$
954	$n = 62$	
1124	(d) triesters, $n = 72$	$C_nH_{(2n-4)}O_6$

mass spectrum of beeswax obtained by GALDI-MS cannot be interpreted in great detail here. In general, it is characterised by four groups of signals (Figure 5.14a):

- (a)  $m/z$  280–600: free fatty acids ( $n = 16$ –34) and hydroxy acids ( $n = 16$ –24);
- (b)  $m/z$  600–750: (1) monoesters  $C_nH_{2n}O_2$  ( $n = 40$ –48) and (2) hydroxy monoesters  $C_nH_{2n}O_3$  ( $n = 40$ –48); the hydroxy monoesters are more prominent than the monoesters;
- (c)  $m/z$  870–1000: diesters  $C_nH_{2n-2}O_4$  ( $n = 56$ –64) and hydroxy diesters  $C_nH_{2n-2}O_5$  ( $n = 60$ –64); the diesters are more prominent than the hydroxy diesters;
- (d)  $m/z$  1100–1250: triesters  $C_nH_{2n-4}O_6$  ( $n = 72$ –80).

Particularly the ester signal groups (b–d) are typical for beeswax and were detected in various mixtures containing beeswax. Several beeswax samples from different regions showed a very similar composition. The spacing between the peaks of each series is 28 Da because only homologous alkyl chains with even carbon numbers exist, both in the acid and the alcohol moieties. The existence of hydroxyl derivatives is evident through an interlaced series of peaks that differ by the atomic mass of oxygen (16 Da) from the acids in group (a) and esters in groups (b) and (c), respectively. The paraffin fraction of beeswax did not appear in the GALDI mass spectra. Similarly, ozokerite (a natural paraffin wax) did not produce peaks in the GALDI-MS spectrum.

Several historic wax samples were analysed successfully with GALDI-MS. It was found that a group of eighteen white seals from medieval documents (thirteenth to fourteenth century) from the archive of the Canton of Lucerne (Switzerland) all mainly consisted of beeswax. For example, the mass spectrum of a white seal from 1377 (inventory no. URK636/12663) is shown in Figure 5.14b. The typical pattern of beeswax, as described for the reference sample, can be clearly recognised. An additional peak at  $m/z$  303 may be caused by abietic acid in the form of the molecule cation ( $C_{20}H_{30}O_2$ , MW 302), as found for rosin (see Section 5.3.2). This hints at the use of a diterpenoid resin, which was a common hardener for beeswax. A more detailed discussion of the composition of medieval white wax seals has been published elsewhere [57].

Another group of investigated samples came from the wax filler material of fourteen silver plates from a medieval reliquary shrine (Chasse des enfants de Saint Sigismond from St Maurice, Switzerland, twelfth to thirteenth century) [58]. Again, GALDI-MS generally

proved beeswax to be the main component. Three of the fillers additionally showed signals typical of diterpenoid resins.

In addition to the natural waxes, a number of synthetic waxes were analysed with GALDI-MS: carboxylic acids (Hoechst wax-L, -S), esters (Hoechst wax-FL, -H, -O), and glycol esters (Hoechst wax-KP, -KPS). In most cases, significant mass spectra were obtained. The mass spectrum of polyethylene glycol (Carbowax 6000) showed a series of signals; the spacing of  $m/z$  44 between the signals corresponds to one oxyethylene unit.

#### 5.3.4 Oils and Fats

Fatty acids, which are important constituents of many natural products, e.g. palmitic and stearic acids, readily produce signals in GALDI-MS. They were detected in most of the spectra of oils and fats as well as ester waxes. Frequently, high concentrations of carboxylic acids (e.g. in beeswax or blooming on paintings) produced additional signals at  $m/z = [MW+45]^+$  caused by their  $[M+2Na-H]^+$  ions. Protonated fatty acids were additionally detected in the cases of shellac and beeswax. In contrast to the free fatty acids, their poorly soluble salts with divalent cations ( $Mg^{2+}$ ,  $Ca^{2+}$ ,  $Co^{2+}$ ,  $Zn^{2+}$ ,  $Pb^{2+}$ ), so-called metal soaps, did not produce signals with GALDI-MS.

Generally, the GALDI mass spectra of common drying oils (e.g. linseed, poppyseed, walnut, tung) as well as the non-drying castor oil are composed of three groups of signals that are assigned to (a) free fatty acids, their oxidation products and monoglycerides, (b) diglycerides and (c) triglycerides. The abundance of certain fatty acids that are characteristic for each oil ('fatty acid profile') influences the relative intensity of the different di- and triglycerides. For example, the quick-drying tung oil is characterised by a high proportion of a triglyceride of C-18 acids with nine double bonds ( $C_{57}H_{92}O_6$ ,  $m/z$  896  $[M+Na]^+$ ), which can be related to the high content of 18:3-*elaeostearic* acid in this oil. The most abundant triglyceride in a non-dried linseed oil, which had been stored airtight for 35 years, shows a broader peak at  $m/z \approx 902$ , which corresponds to a triglyceride of three C-18 acids with six double bonds ( $C_{57}H_{98}O_6$ ) (see Figure 5.15a).

To study the drying process, glass slides were coated with different drying oils (linseed oil, boiled linseed oil, and linseed standoil) that had been stored airtight for 35 years in the SIAR collection. The test plates cured naturally in the laboratory under sunlight through window glass. After 2 weeks of natural ageing, this oil showed an increased variety of di- and triglycerides in the THF extract (Figure 5.15b and Table 5.7). Signals with  $m/z = 500$ – $650$  indicate diglycerides, including those with azelaic acid. Triglycerides are found in the region of  $m/z = 800$ – $1000$ . There were also peaks at higher masses (up to  $m/z = 1111$ ). The spacing of approximately the molecular weight of glycerol (MW 92) to the triglycerides suggests dimeric glycerides with three or four fatty acid moieties. After 4 months of natural curing, the oil film was insoluble in THF and GALDI-MS gave no result.

These results from aged drying oils suggest that GALDI-MS is not the analytical method of choice for dry oil paint. However, additional data on the composition of paint was obtained in particular cases, as illustrated by the following case studies. They show that soluble, low molecular weight compounds from oil paints, such as fatty acids, di- and triacyl glycerols as well as diterpenoids, can be detected by GALDI-MS.

The Swiss painter Cuno Amiet (1868–1961) carried out experiments with binding media from at least 1902 onwards. Today, many of his paintings show several ageing phenomena that probably are due to the nature of the applied painting technique. On the

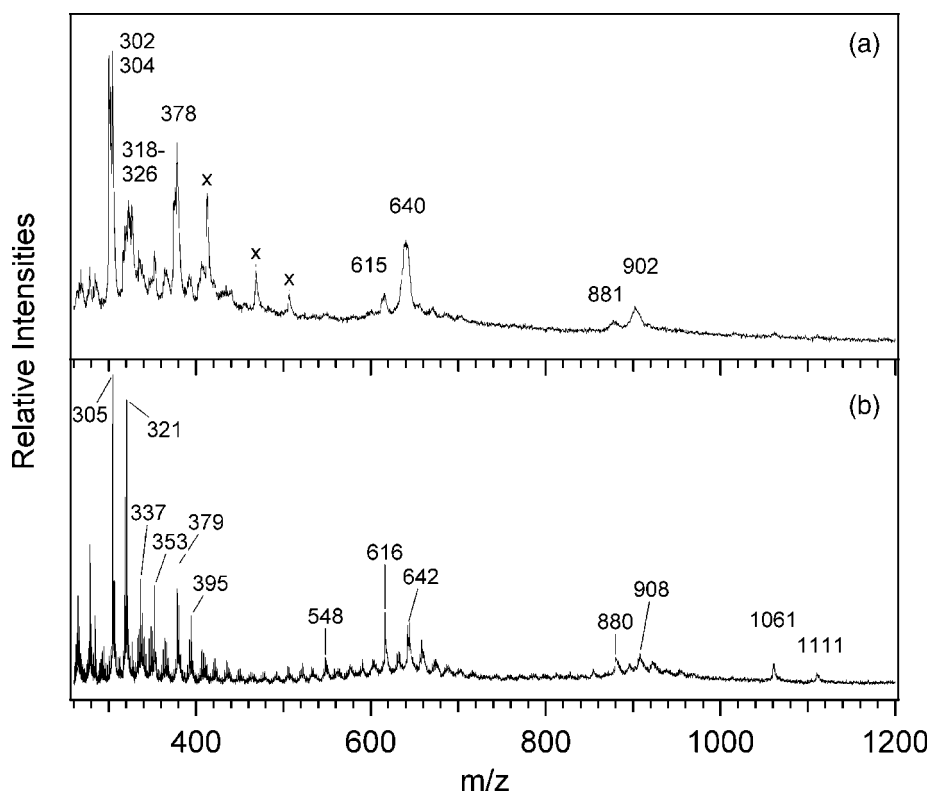


**Figure 5.15** GALDI mass spectra of (a) linseed oil (35 years airtight storage; from THF solution) and (b) linseed oil as in (a) after 2 weeks of natural ageing (from THF solution). Signal groups of free fatty acids, their oxidation products, and monoglycerides ( $m/z < 500$ ) can be distinguished from diglycerides ( $m/z 500\text{--}800$ ), and triglycerides ( $m/z 800\text{--}1000$ ) (see Table 5.7)

**Table 5.7** Prominent peaks in the mass spectra of linseed oil (see Figure 5.15) and oil paint (see Figure 5.16a and b), and tentative attribution to compounds

$m/z$ $[M+Na]^+$	Compound	Molecular formula
301, 303, 305, 307	18:3 / 18:2 / 18:1 / 18:0 fatty acids	$C_{18}H_{30}O_2\text{--}C_{18}H_{36}O_2$
317, 319, 321	Monoxides of 18:3 / 18:2 / 18:1 fatty acids	$C_{18}H_{30}O_3\text{--}C_{18}H_{34}O_3$
335	Dioxide of 18:2 fatty acid	$C_{18}H_{32}O_4$
353	16:0-Monoglyceride (monostearin)	$C_{19}H_{38}O_4$
377	18:2-Monoglyceride (monolinolin)	$C_{21}H_{38}O_4$
395	18:1-Monoglyceride-(monoolein-) oxide	$C_{21}H_{40}O_5$
547	(18:2)-Azelate-diglyceride	$C_{30}H_{52}O_7$
616	16:0-(18:2)-Diglyceride and isomers	$C_{37}H_{68}O_5$
618	16:0-(18:1)-Diglyceride and isomers	$C_{37}H_{70}O_5$
640	(18:2)-Diglyceride and isomers	$C_{39}H_{68}O_5$
644	Di-(18:1)-glyceride and isomers	$C_{39}H_{72}O_5$
880	16:0-(18:1)-(18:2)-Triglyceride and isomers	$C_{55}H_{100}O_6$
902	Tri-(18:2)-glyceride and isomers	$C_{57}H_{98}O_6$
908	Tri-(18:1)-glyceride and isomers	$C_{57}H_{104}O_6$
1060–1110	Dimeric glycerides	$C_{60}H_mO_n$

painting 'The Post House at Oschwand' (1915, private collection), thick oil paint lies over the preparation layer. Premature cracks in the overlaying second paint layer suggest that the first layer dried slowly. The mass spectrum of a THF extract of this paint shows diglycerides that are composed of the non-drying oleic (18:1) acid, as indicated by the peaks at  $m/z$  645 and 618 in the mass spectrum (Figure 5.16). An intense peak at  $m/z$  309 is assigned to stearic acid ( $C_{18}H_{36}O_2$ ). The peak at  $m/z$  336 could be caused by a dioxide of linolic acid, although other oxides of fatty acids do not appear with the same intensity in the mass spectrum. In another area on the same painting, a soft, colourless material was found on the surface. The GALDI mass spectrum clearly shows the typical pattern of an oxidised diterpenoid resin with main peaks at  $m/z$  338 and 354. A small amount of diglycerides appears at  $m/z$  645. The resinous material seems to have separated from the overlaying paint (probably a distemper made from resin) and has accumulated on the surface – a microscopic investigation did not give any indication that the painting had ever been varnished.

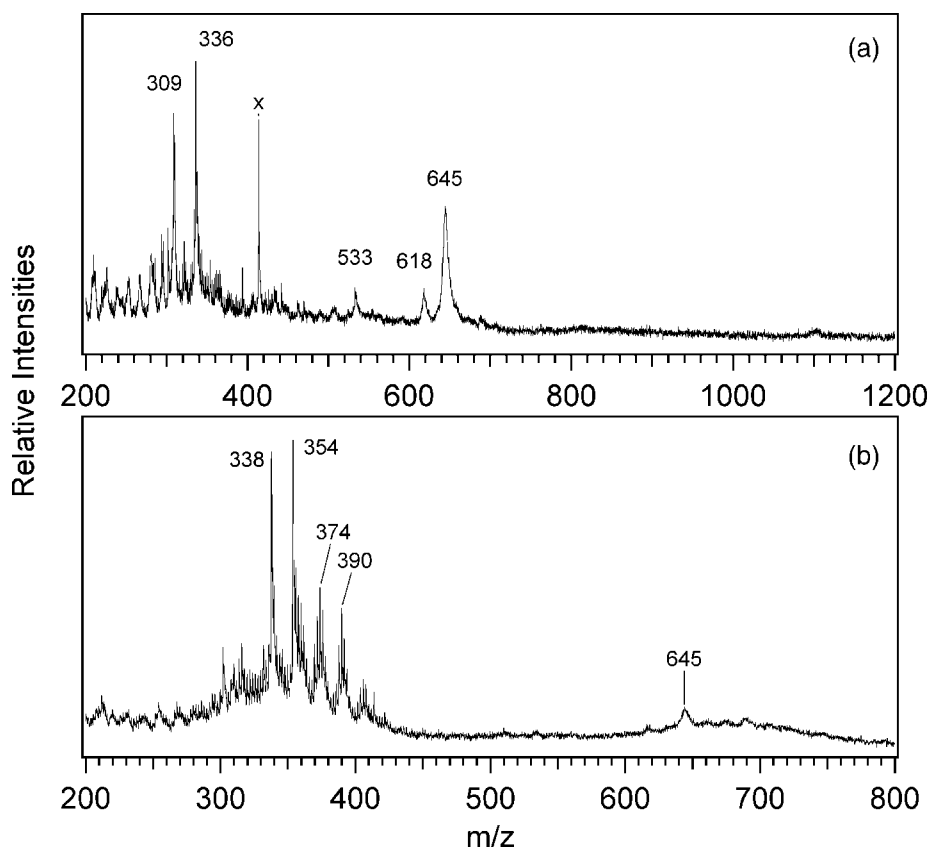


**Figure 5.16** GALDI mass spectra of binding material from the painting 'The Post House at Oschwand' by Cuno Amiet (1915): (a) slow drying oil paint (diglycerides at  $m/z \approx 645$ ); (b) resinous material on the surface (diterpenoids  $m/z$  300–400)

Another painting by Cuno Amiet ('Standard Rose', 1913, private collection) showed a whitish bloom. GALDI-MS readily revealed palmitic acid ( $m/z$  279  $[M+Na]^+$ ) as the main component, while efflorescence on several other paintings of the twentieth century (e.g. by Alfred J. Jensen, 1903–1981) showed signals of a mixture of palmitic and stearic acid.

Fats are defined as triglycerides that are solid at ambient temperature. Similar to the oils, a number of natural fats (beef tallow, cow butter, coconut) gave characteristic mass spectra. So-called Japan wax was used as raw material for a specific painting colour of the times around 1900, the 'Raffaelli solid oil colours', which were patented in 1903. The GALDI mass spectrum of Japan wax (cyclohexane extract) is dominated by a typical pattern of tripalmitin and three higher homologues in accordance with the literature ([52], p. 52). Minor signals of products of hydrolysis (diglycerides) and oxidation can be seen as well (Figure 5.17a and Table 5.8).

Various original 'Raffaelli solid oil colours' were analysed with GALDI-MS along with original samples, supposedly the same paint material, from a painting by the inventor of this paint, Jean-Francois Raffaelli ('Le défilé devant la maison de Victor Hugo pour ses 80

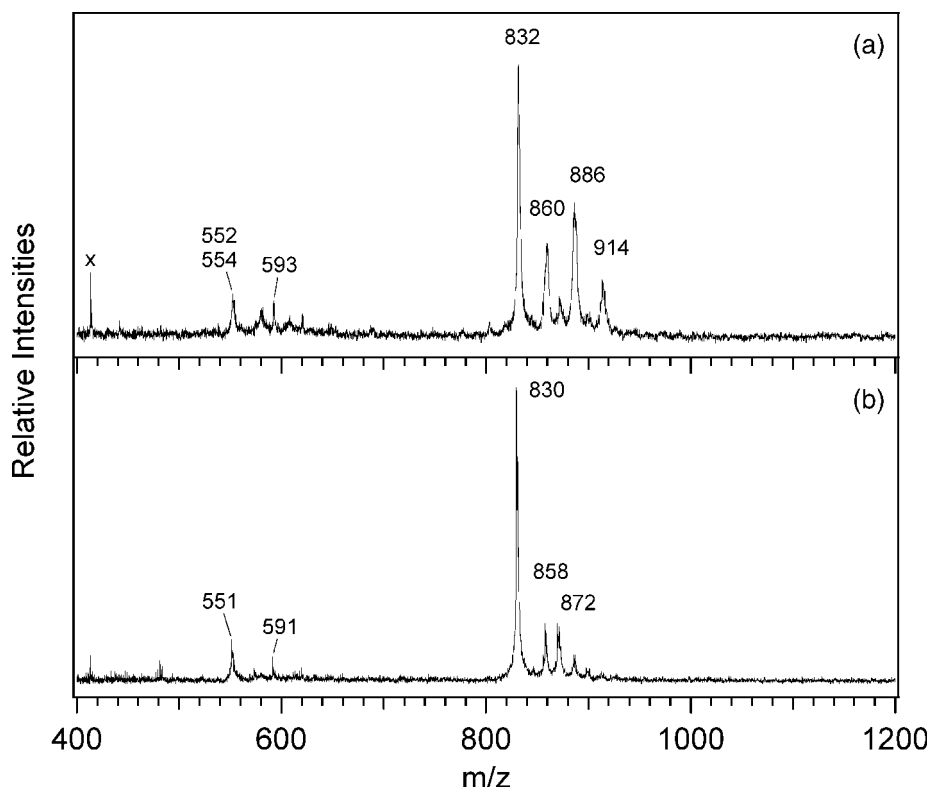


**Figure 5.17** GALDI mass spectra of (a) Japan wax and (b) a dark blue paint sample from Jean-Francois Raffaelli 'Le défilé devant la maison de Victor Hugo pour ses 80 ans' (1902, Musée Victor Hugo, Paris) [59]. Both spectra are dominated by tripalmitin ( $m/z$  830) and higher homologues (see Table 5.8)

**Table 5.8** Prominent peaks in the mass spectra of Japan wax and 'Raffelli solid oil colour' (see Figure 5.17), and tentative attribution to compounds

$m/z$ [M+Na] <sup>+</sup>	Compound	Molecular formula
549	Oleic-azelaic-diglyceride	C <sub>30</sub> H <sub>54</sub> O <sub>7</sub>
551	Stearic-azelaic diglyceride	C <sub>30</sub> H <sub>56</sub> O <sub>7</sub>
591	Dipalmitine	C <sub>35</sub> H <sub>68</sub> O <sub>5</sub>
830	Tripalmitine	C <sub>51</sub> H <sub>98</sub> O <sub>6</sub>
858	Stearo-dipalmitine	C <sub>53</sub> H <sub>102</sub> O <sub>6</sub>
872	Oxidised oleo-dipalmitine	C <sub>53</sub> H <sub>100</sub> O <sub>7</sub>
886	Distearo-palmitine	C <sub>55</sub> H <sub>106</sub> O <sub>6</sub>
914	Tristearine	C <sub>57</sub> H <sub>110</sub> O <sub>6</sub>

ans', 1902, Paris, Musée Victor Hugo) and from a work by the Swiss painter Ferdinand Hodler ('Landscape at Chateau d'Oex', c. 1905, private collection) [59]. In each case, GALDI-MS revealed patterns similar to Japan wax, e.g. in a sample from the painting by Raffaelli (see Figure 5.17b). In addition to the main component tripalmitin, smaller peaks again indicate the presence of higher homologues, diglycerides (stearic/azelaic acid-diglycerides) and oxidation products. This GALDI-MS investigation proved that the 'Raffaelli solid oil colours' consist of Japan wax on the one hand and that the investigated paintings were made of this specific paint on the other.

In New Guinea, an oil known as tigas oil or *nguat*, is obtained from the tree *Camposperma brevipetiolata* (Volkart). This oil is applied to the human body and is also used in the production of a coating material for ethnographic objects. The main components of tigas oil are campospermonol [1-hydroxy-3-(nonadec-10'-en-2'-onyl)benzene, C<sub>25</sub>H<sub>40</sub>O<sub>2</sub>] and 5-hydroxy-5-(nonadec-10'-en-2'-onyl)cyclohex-2-enone (C<sub>25</sub>H<sub>42</sub>O<sub>3</sub>) [60]. The GALDI mass spectrum of such an oil shows signals at  $m/z$  396 and 414, which can be directly attributed to these substances (Figure 5.18a). Small signals at  $m/z \approx 785$  indicate an oxidised dimer of campospermonol. Other low-intensity signal groups at  $m/z$  662 and 678 can be explained by the loss of one phenolic group from the dimers.

We also investigated the polychromy of a *mai* mask from Papua New Guinea (Inv. No. 27496, Museum der Kulturen, Basel) [61]. A sample of the coating was extracted with propanone and analysed by GALDI-MS. The mass spectrum shows the triplet at the same position as in tigas oil; however, the oxidation product at  $m/z$  414, which is a minor component in fresh tigas oil, is the predominant component in this case (Figure 5.18b). Almost no campospermonol ( $m/z$  395) remained. The mass spectrum of the extract from the coating also shows another triplet with values 90–94 Da below those observed with tigas oil ( $m/z$  320–338). This difference could be explained by the loss of the phenolic group ( $m/z$  94) from the aforementioned compounds, if tigas oil was used. An interpretation of the results is presented in Table 5.9.

### 5.3.5 Synthetic Binders

Low molecular weight cyclohexanone resins have been used as picture varnishes since the 1950s. Their synthesis from cyclohexanone and methyl cyclohexanone in the presence of



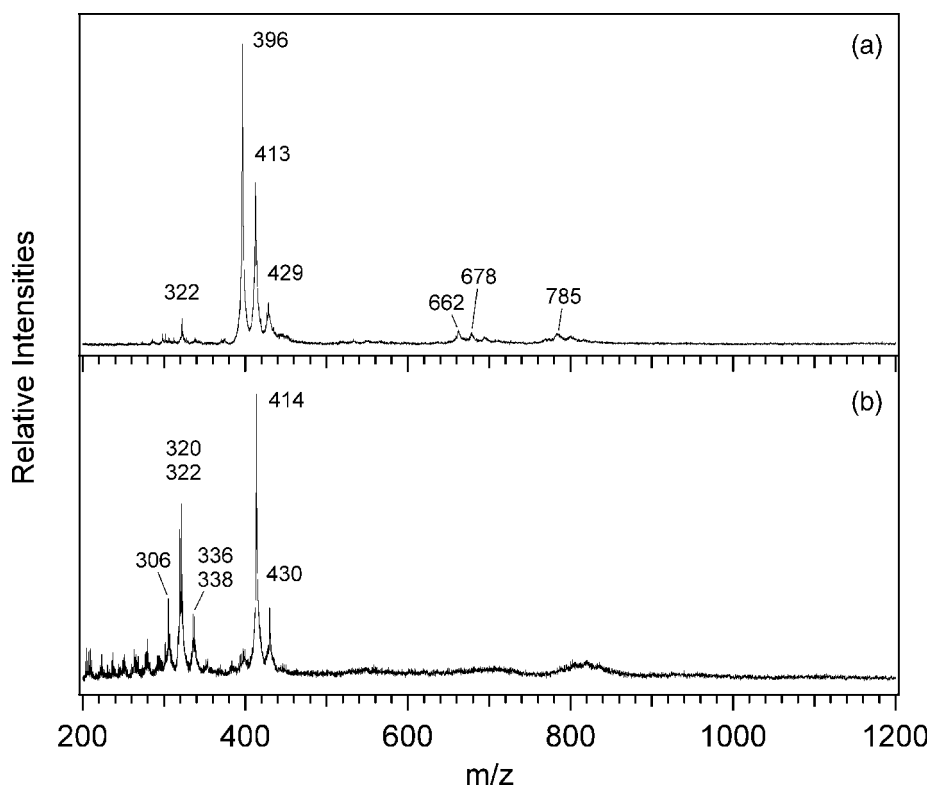


**Figure 5.18** GALDI mass spectra of (a) tigaso oil (from THF solution) and (b) coating of a mai mask (from acetone solution) [61]. The spectra are dominated by camgnospermonol ( $m/z$  395) and one of its oxidation products ( $m/z$  413) (see Table 5.9)

**Table 5.9** Prominent peaks in the mass spectra of tigaso oil and an extract from the coating of a mai mask, and a tentative assignment to the compounds (see Figure 5.18a and b). Compounds marked with an asterisk are mentioned as constituents of tigaso oil in the literature

$m/z$ $[M+Na]^+$	Compound	Molecular formula
303	Nonadecenone*	$C_{19}H_{36}O$
319	Nonadecenone, oxidised <b>10</b>	$C_{19}H_{36}O_2$
321	Hydroxy-nonadecanone	$C_{19}H_{38}O_2$
336	Oxidation product of <b>10</b>	$C_{19}H_{36}O_3$
337	Dihydroxy-nonadecan-2-one	$C_{19}H_{38}O_3$
395	1-Hydroxy-3-(nonadec-10'-en-2'-onyl)-benzene* = camgnospermonol <b>11</b>	$C_{25}H_{40}O_2$
413	5-Hydroxy-5-(nonadec-10'-en-2'-onyl)cyclohex-2-enone* <b>12</b>	$C_{25}H_{42}O_3$
429	Oxidation product of <b>12</b>	$C_{25}H_{42}O_4$
661		$C_{44}H_{68}O_2$
677		$C_{44}H_{68}O_3$
785	Dimer of camgnospermonol <b>11</b> , oxidised	$C_{50}H_{82}O_5$

alkaline methanol, sometimes followed by hydration, leads to oligomers with a complicated molecular structure [62]. For example, the GALDI mass spectrum of Ketone Resin N shows an equidistant sequence of signal groups beginning at  $m/z \approx 310$  up to  $m/z$  1420 (Figure 5.19a). The intensity of the groups decreases with increasing  $m/z$  value. These multiplets can be attributed to oligomers of cyclohexanone with three and more monomer units. The signal at  $m/z$  325 indicates a trimer containing one additional methylene group ( $C_{19}H_{28}O_3$ ,  $m/z$  327  $[M+Na]^+$ ), whereas there is no straightforward explanation for the signals at  $m/z$  347. The spacing between the groups is approximately 109 Da, which is closer to methylcyclohexanone (MW 112) than cyclohexanone (MW 98). Although Ketone Resin N is produced from pure cyclohexanone, statistically almost one methyl group seems to be introduced with each polymerisation step. This supports a condensation mechanism that includes formaldehyde, as proposed by de la Rie and Shedrinsky [62] rather than an aldol condensation followed by a Hofmann elimination [63]. The spacings of 14–16 Da within the multiplets in the mass spectra of cyclohexanone resin can be explained by differing contents of methylene or oxygen groups, respectively.

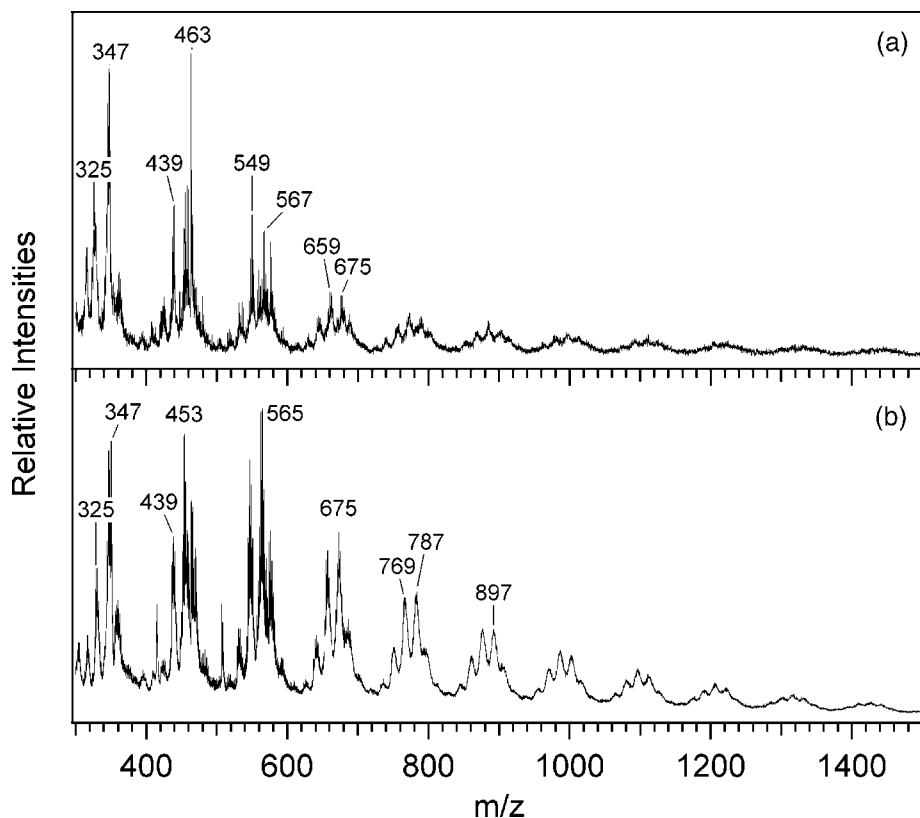


**Figure 5.19** GALDI mass spectra of (a) Ketone Resin N (from THF solution) and (b) ketone resin varnish from a painting (from THF solution). The signal groups generally correspond to cyclohexanone units

Another product, AW2 resin, has been produced by BASF from a mixture of cyclohexanone and methylcyclohexanone. A sample from 1972 shows a very similar GALDI mass spectrum to that of Ketone Resin N. The prominent signal at  $m/z$  376 indicates a trimer containing two  $\text{CH}_2\text{O}$  groups ( $\text{C}_{20}\text{H}_{30}\text{O}_5$ ,  $m/z$  373  $[\text{M}+\text{Na}]^+$ ). However, the spacing of the multiplets is slightly higher (approximately 117 Da) than that of Ketone Resin N. This shows the introduction of statistically more than one methyl group per condensation and is due to the co-condensation of methylcyclohexanone.

The varnish on a modern painting ('Mont Salève' by Alexandre Perrier, 1916, private collection) showed a mass spectrum (Figure 5.19b) almost identical to that of Ketone Resin N. The use of a cyclohexanone resin as a picture varnish seems uncommon because copolymers such as AW2 were preferred by conservators [62]. An investigation into cyclohexanone resins by direct temperature-resolved MS (DTMS) is reported in the literature [22, 64]. Similar mass spectrometric patterns were achieved with masses accurately reflecting the values expected for the oligomers.

Whereas GALDI-MS detects low molecular weight synthetic resins, common synthetic polymers, such as various acrylic polymers, polystyrene, and cellulose nitrate, did not produce any mass spectra using this method.

### 5.3.6 Aqueous Binding Media

Several water-soluble binders, both natural and synthetic, were investigated by GALDI-MS: animal glue (glutin) and synthetic cellulose ethers [hydroxyethyl methyl cellulose (Tylose<sup>®</sup> MH300) and carboxymethyl cellulose (Tylose<sup>®</sup> C300 and C600)]. No mass spectrum was achieved in any case. Obviously, the GALDI-MS procedure described here is not suitable for polymeric, aqueous binding media.

### 5.3.7 Conclusions

GALDI-MS was shown to be an advantageous method for the analysis of oxygen-containing, low molecular weight organic substances such as resins, ester waxes, fatty acids, fats and oils, ketone resins and dyestuffs. In contrast, neither nonpolar substances (hydrocarbons) nor aqueous high molecular weight binders (proteins, carbohydrates) gave positive results.

Once natural marker substances for natural materials have been defined by analysing reference materials, binding media from works of art can be identified. On account of the straightforward sample preparation and the relatively low complexity, GALDI-MS is a valuable enrichment of the repertoire of analytical methods for the identification of binding media and other organic substances used in the production of artistic objects. Furthermore, as shown for tigas oil, this method has potential for the analysis of natural products in general.

Owing to the fact that organic substances have to be separated from a complex sample, transferred to the mass spectrometer target and desorbed, it seems impossible so far to analyse cross-linked binding media from artwork (e.g. dried oil, aged proteins, cross-linked synthetic polymers). Application of classical methods of sample treatment for

chromatography, either chemical (hydrolysis) or thermal (pyrolysis), occasionally followed by chemical derivatisation, may widen the application field for GALDI-MS to insoluble or nondesorbable samples.

## Acknowledgements

We would like to thank Richard Knochenmuss and Renato Zenobi for continuous support and advice. We are grateful to Ursula Baumer for measuring GC-MS of artificially aged ursonic acid, and Corina Hunger-Pfeiffer for measuring the GALDI-MS of the cyclohexanone varnish. Original 'Raffaelli solid oil colours' were provided by one of the three contemporary suppliers, Winsor & Newton (Harrow, UK). Tigaso oil was imported from Papua New Guinea and kindly provided by Marianne Klaus. Financial support from the Swiss National Science Foundation (SNF) (project nos 20-52422.98 and 12-61848.00) is gratefully acknowledged.

## References

1. M. Karas, and F. Hillenkamp, Laser Desorption Ionization of Proteins with Molecular Masses Exceeding 10 000 Daltons, *Anal. Chem.*, **60**, 2299–2301 (1988).
2. K. Tanaka, H. Waki, Y. Ido, S. Akita, Y. Yoshida, and T. Yoshida, Protein and Polymer Analyses up to  $m/z$  100 000 by Laser Ionization Time-of-flight Mass Spectrometry, *Rapid Commun. Mass Spectrom.*, **2**, 151 (1988).
3. S. Zumbühl, R. Knochenmuss, S. Wülfert, F. Dubois, M.J. Dale, and R. Zenobi, A Graphite-Assisted Laser Desorption/Ionisation Study of Light-induced Aging in Triterpene Dammar and Mastic Varnishes, *Anal. Chem.*, **70**, 707–715 (1998).
4. S. Zumbühl, R.D. Knochenmuss, and S. Wülfert, Rissig und blind werden in relativ kurzer Zeit alle Harzessenzfirnisse, *Z. Kunsttechnol. Konserv.*, **12**, 205–219 (1998).
5. M. Schürenberg, K. Dreisewerd, and F. Hillenkamp, Laser Desorption/Ionization Mass Spectrometry of Peptides and Proteins with Particle Suspension Matrices, *Anal. Chem.*, **71**, 221–229 (1999).
6. M.J. Dale, R. Knochenmuss, and R. Zenobi, Two-phase Matrix-assisted Laser Desorption/Ionisation: Matrix Selection and Sample Pretreatment for Complex Anionic Analytes, *Rapid Commun. Mass Spectrom.*, **11**, 136–142 (1997).
7. J. Sunner, E. Dratz, and Y.C. Chen, Graphite Surface-assisted Laser Desorption/Ionization Time-of-flight Mass Spectrometry of Peptides and Proteins from Liquid Solutions, *Anal. Chem.*, **67**, 4335–4342 (1995).
8. M.J. Dale, R. Knochenmuss, and R. Zenobi, Graphite/Liquid Mixed Matrices for Laser Desorption/Ionization Mass Spectrometry, *Anal. Chem.*, **68**, 3321–3329 (1996).
9. H.J. Kim, J.K. Lee, S.J. Park, H.W. Ro, D.Y. Yoo, and D.Y. Yoon, Observation of Low Molecular Weight Poly(methylsilsesquioxane)s by Graphite Plate Laser Desorption/Ionization Time-of-flight Mass Spectrometry, *Anal. Chem.*, **72**, 5673–5678 (2000).
10. K. Dreisewerd, The Desorption Process in MALDI, *Chem. Rev.*, **103**, 395–425 (2003).
11. R. Knochenmuss, A. Stortelder, K. Breuker, and R. Zenobi, Secondary ion-molecule Reactions in Matrix-assisted Laser Desorption/Ionization, *J. Mass Spectrom.*, **35**, 1237–1245 (2000).
12. D. Scalarone, M.C. Duursma, J.J. Boon, and O. Chiantore, MALDI-TOF Mass Spectrometry on Cellulosic surfaces of Fresh and Photo-aged Di- and Triterpenoid Varnish Resins, *J. Mass Spectrom.*, **40**, 1527–1535 (2005).
13. E.R. de la Rie, Old Master Paintings: A Study of the Varnish Problem, *Anal. Chem.*, **61**, 1228A–1240A (1989).

14. N. Stolow, Solvent Action, in *On Picture Varnishes and their Solvents*, R.L. Feller, N. Stolow and E.H. Jones (Eds), National Gallery of Art, Washington, DC, 1985, pp. 47–116.
15. D. Erhardt, and J.-S. Tsang, The Extractable Components of Oil Paint Films, in *Cleaning, Retouching and Coatings. Technology and Practice for Easel Paintings and Polychrome sculpture*, J.S. Mills and P. Smith (Eds), Contributions to the IIC Brussels Congress, International Institute for Conservation, London, 1990, pp. 93–97.
16. K. Sutherland, The Extraction of Soluble Components from an Oil Paint Film by a Varnish Solution, *Stud. Conserv.*, **45**, 54–62 (2000).
17. E.R. de la Rie, Stable Varnishes for Old Master Paintings, PhD thesis, University of Amsterdam, 1988.
18. E.R. de la Rie, Photochemical and Thermal Degradation of Films of Dammar Resin, *Stud. Conserv.*, **33**, 53–70 (1988).
19. E.R. de la Rie, and C.W. McGlinchey, Stabilized Dammar Picture Varnish, *Stud. Conserv.*, **34**, 137–146 (1989).
20. E.R. de la Rie, and C.W. McGlinchey, The Effect of a Hindered Amine Light Stabilizer on the Aging of Dammar and Mastic Varnish in an Environment Free of Ultraviolet Light, in *Cleaning, Retouching and Coatings. Technology and practice for Easel Paintings and Polychrome Sculpture*, J.S. Mills and P. Smith (Eds), Contributions to the IIC Brussels Congress, International Institute for Conservation, London, 1990, pp. 160–164.
21. G.A. Van der Doelen, Molecular Studies of Fresh and Aged Triterpenoid Varnishes, PhD thesis, University of Amsterdam, 1999.
22. G.A. Van der Doelen, K.J. Van den Berg, and J.J. Boon, Comparative Chromatographic and Mass-spectrometric Studies of Triterpenoid Varnishes: Fresh Material and Aged Samples from Paintings, *Stud. Conserv.*, **43**, 249–264 (1998).
23. G.A. Van der Doelen, K.J. Van den Berg, J.J. Boon, N. Shibayama, E.R. de la Rie, and W.J.L. Genuit, Analysis of Fresh Triterpenoid Resins and Aged Triterpenoid Varnishes by High-performance Liquid Chromatography-Atmospheric Pressure Chemical Ionisation (Tandem) Mass Spectrometry, *J. Chromatogr. A*, **809**, 21–37 (1998).
24. G.A. Van der Doelen, K.J. Van den Berg, and J.J. Boon, A Comparison of Weatherometer Aged Dammar Varnishes and Aged Varnishes from Paintings, in *Proceedings of the Conference 'Art et Chimie' – La couleur*, J. Goupy and J.P. Mohen (Eds), Paris, France, 1998, CNRS Editions, Paris, 2000, pp. 146–149.
25. S. Zumbühl, Einfluss der Oxidationsprodukte auf das mechanische Filmverhalten von Naturharzfirnissen, Diploma thesis, Schule für Gestaltung, Bern, 1996.
26. L. Carlyle, N.E. Binnie, G. Van der Doelen, J. Boon, B. McLean, and A. Ruggles, Traditional Painting Varnishes Project: Preliminary Report on Natural and Artificial Aging and a Note on the Preparation of Cross-sections, in *Postprints of Firnis, Material Aesthetik Geschichte, International Kolloquium*, AdR, Braunschweig, 1998, pp. 110–127.
27. M.P. Colombini, F. Modugno, S. Giannarelli, R. Fuoco, and M. Matteini, GC-MS characterization of paint varnishes, *Microchem. J.*, **67**, 385–396 (2000).
28. E. Wenders, Dammar als Gemäldefirnis, *Z. Kunsttechnol. Konserv.*, **15**, 133–162 (2001).
29. D. Scalapone, J. Van der Horst, J.J. Boon, and O. Chiantore, Direct-temperature Mass Spectrometric Detection of Volatile Terpenoids and Natural Terpenoid Polymers in Fresh and Artificially Aged Resins, *J. Mass Spectrom.*, **38**, 607–617 (2003).
30. U. Weilhammer, Der Einfluss von Kunstharzübersätzen auf das Alterungsverhalten von Naturharzfirnissen, *Z. Kunsttechnol. Konserv.*, **17**, 397–406 (2003).
31. C. Theodorakopoulos, and V. Zafiropoulos, Uncovering of Scalar Oxidation within Naturally Aged Varnish Layers, *J. Cult. Heritage*, **4**, 216s–222s (2003).
32. C. Theodorakopoulos, *The Eximer Laser Ablation of Picture Varnishes*, PhD thesis, Royal College of Art, London, 2005.
33. P. Dietemann, Towards More Stable Natural Resin Varnishes for Paintings, PhD thesis, Swiss Federal Institute of Technology, Zurich, 2003.
34. P. Dietemann, M. Kälin, S. Zumbühl, R. Knochenmuss, S. Wülfert, and R. Zenobi, A Mass Spectrometry and Electron Paramagnetic Resonance Study of Photochemical and Thermal Aging of Triterpenoid Varnishes, *Anal. Chem.*, **73**, 2087–2096 (2001).

35. P. Dietemann, M. Kälin, R. White, C. Sudano, R. Knochenmuss, and R. Zenobi, Chios Gum Mastic – Freshly Harvested vs. Commercial Resin and its Implications to Aging of Varnishes, *Z. Kunsttechnol. Konserv.*, **19**, 119–130 (2005).
36. P. Dietemann, C. Higgitt, M. Kälin, M.J. Edelmann, R. Knochenmuss, and R. Zenobi, Aging and Yellowing of Triterpenoid Resin Varnishes – Influence of Aging Conditions and Resin Composition, *J. Cult. Heritage*, **10**, 30–40 (2009).
37. G. Scott, *Atmospheric Oxidation and Antioxidants Vol. I*, Elsevier Science, Amsterdam, 1993.
38. R.L. Feller, *Accelerated Aging, Photochemical and Thermal Aspects*, The Getty Conservation Institute, Los Angeles, 1994.
39. P. Dietemann, M.J. Edelmann, C. Meisterhans, C. Pfeiffer, S. Zumbühl, R. Knochenmuss, and R. Zenobi, Artificial Photoaging of Triterpenes Studied by Graphite-assisted Laser Desorption/Ionization Mass Spectrometry, *Helv. Chim. Acta*, **83**, 1766–1777 (2000).
40. G. Geuskens, D. Baeyens-Volant, G. Delaunois, Q. Lu Vinh, W. Piret, and C. David, Photo-oxidation of Polymers – II. The Sensitized Decomposition of Hydroperoxides as the Main Path for Initiation of the Photo-oxidation of Polystyrene Irradiated at 253.7 nm, *Eur. Polym. J.*, **14**, 299–303 (1978).
41. B.G.K. Van Aarssen, H.C. Cox, P. Hoogendoorn, and J.W. De Leeuw, A Cadinene Biopolymer Present in Fossil and Extant Dammar Resins as a Source for Cadinanes and Bicadinanes in Crude Oils from South East Asia, *Geochim. Cosmochim. Acta*, **54**, 3021–3031 (1990).
42. K.J. Van den Berg, J. Van der Horst, J.J. Boon, and O.O. Sudmeijer, Cis-1,4-poly- $\beta$ -myrcene; the Structure of the Polymeric Fraction of Mastic Resin (*Pistacia lentiscus* L.) Elucidated, *Tetrahedron Lett.*, **39**, 2645–2648 (1998).
43. J. Boon, and G. Van der Doelen, Advances in the Current Understanding of Aged Dammar and Mastic Triterpenoid Varnishes on the Molecular Level, in *Postprints of Firmis, Material Aesthetik Geschichte, International Kolloquium*, AdR, Braunschweig, 1998, pp. 92–104.
44. K.J. Van den Berg, J.J. Boon, I. Pastorova, and L.F.M. Spetter, Mass Spectrometric Methodology for the Analysis of Highly Oxidized Diterpenoid Acids in Old Master Paintings, *J. Mass Spectrom.*, **35**, 512–533 (2000).
45. O.F. van den Brink, J.J. Boon, P.B. O'Connor, M.C. Duursma, and R.M.A. Heeren, Matrix-assisted laser desorption/ionization Fourier transform mass spectrometric analysis of oxygenated triglycerides and phosphatidylcholines in egg tempera paint dosimeters used for environmental monitoring of museum display conditions, *J. Mass Spectrom.*, **36**, 479–492 (2001).
46. I. Rogner, 'Characterisation of East Asian Lacquers by Laser Desorption Mass Spectroscopy (LD-MS)' in *Ostasiatische und europäische Lacktechniken*, in *Arbeitshefte des Bayerischen Landesamtes für Denkmalpflege*, Vol. 112, M. Kühnleth (Ed.), Karl M. Lipp Verlag, Munich, 2000, pp. 121–124.
47. J.D.J. Van den Berg, N.D. Vermist, L. Carlyle, M. Holcapek, and J.J. Boon, Effects of Traditional Processing Methods of Linseed Oil on the Composition of its Triacylglycerols, *J. Sep. Sci.*, **27**, 181–199 (2004).
48. R. D'Agata, G. Grasso, S. Parlato, S. Simone, and G. Spoto, The Use of Atmospheric Pressure Laser Desorption Mass Spectrometry for the Study of Iron-gall Ink, *Appl. Phys. A*, **89**, 91–95 (2007).
49. M.L. Vestal, P. Juhasz, and S.A. Martin, Delayed Extraction Matrix-assisted Laser Desorption Time-of-flight Mass Spectrometry, *Rapid Commun. Mass Spectrom.*, **9**, 1044–1050 (1995).
50. J.J. Boon, and T. Learner, Analytical Mass Spectrometry of Artists' Acrylic Emulsion Paints by Direct Temperature Resolved Mass Spectrometry and Laser Desorption Ionisation Mass Spectrometry, *J. Anal. Appl. Pyrol.*, **64**, 327–344 (2002).
51. I.D. Van der Werf, K.J. van den Berg, S. Schmidt, and J.J. Boon, Molecular Characterization of Copaiba Balsam as Used in Painting Techniques and Restoration Procedures, *Stud. Conserv.*, **45**, 1–18 (2000).
52. J.S. Mills, and R. White, *The Organic Chemistry of Museum Objects*, 2nd edn, Butterworth-Heinemann, Oxford, 1994.
53. J. Koller, U. Baumer, D. Grosser, and K. Walch, 'Larch turpentine and Venetian Turpentine' in *Baroque and Rococo Lacquers*, in *Arbeitshefte des Bayerischen Landesamtes für Denkmalpflege*, Vol. 81, K. Walch and J. Koller (Eds), Karl M. Lipp Verlag, Munich, 1997, pp. 359–378.

54. M.P. Colombini, I. Bonaduce, and G. Gautier, Molecular Pattern Recognition of Fresh and Aged Shellac, *Chromatographia*, **58**, 58–61 (2003).
55. H. Schweppe, *Handbuch der Naturfarbstoffe*, ecomed, Landsberg, 1993.
56. M. Regert, J. Langlois, and S. Colinart, Characterisation of Wax Works of Art by Gas Chromatographic Procedures, *J. Chromatogr. A*, **1091**, 124–136 (2005).
57. R. Cozzi, I Sigilli Medioevali: composizione e fenomeni di degrado dei 'sigilli bianchi', Diploma thesis, Berner Fachhochschule, 2001.
58. C. Herm, La Chasse des enfants de Saint Sigismond de l'Abbaye de Saint-Maurice: Analysis of the Filler Material using Graphite-assisted Laser Desorption / Ionisation Mass Spectrometry, in *Medieval Reliquary Shrines and Precious Metal Objects*, K. Anheuser and C. Werner (Eds), Archetype, London, 2006, pp. 17–24.
59. D. Gros, and C. Herm, Die Ölfarbenstifte des J.-F. Raffaelli, *Z. Kunsttechnol. Konserv.*, **18**, 1–28 (2004).
60. L.K. Dalton, and J.A. Lambertson, Studies of the Optically Active Compounds of Anacardiaceae Exudates I. The Long-chain Alicyclic Keto Alcohol of Tigaso Oil, *Aust. J. Chem.*, **11**, 46–63 (1958).
61. M. Klaus, Die Übermodellierungsmasse auf mai-Masken vom Mittleren Sepik in Papua Neuguinea: Problemstellungen der Konservierung-Restaurierung, Diploma thesis, Haute École d'Arts appliqués du Canton de Neuchâtel, La-Chaux-des-Fonds, 2002.
62. E.R. de la Rie, and A.M. Shedrinsky, The Chemistry of Ketone Resins and the Synthesis of a Derivative with Increased Stability and Flexibility, *Stud. Conserv.*, **34**, 9–19 (1989).
63. J. Koller, and U. Baumer, Kunstharzfirnisse, Teil III: Die niedermolekularen (nichtpolymeren) Kunstharzfirnisse, *Restauro*, 26–38 (2001).
64. J.J. Boon, and J. van Och, A Mass Spectrometric Study of the Effect of Varnish Removal from a 19th Century Solvent-sensitive Wax Oil Painting, in *Preprints ICOM Committee for Conservation, 11th Triennial Meeting*, J. Bridgland (Ed.), James & James, London, 1996, pp. 197–205.





# 6

## MALDI-MS Applied to the Analysis of Protein Paint Binders

*Stepanka Kuckova, Radovan Hynek and Milan Kodicek*

### 6.1 Introduction

Proteins are the most complicated molecular structures present in the biosphere. From an analytical point of view, their identification represents one of the most challenging tasks for a chemist. Their backbone is formed by a linear polypeptide chain created from 20 proteinogenic amino acids; its length varies from 100 to 2000 amino acid residues, connected by amid (peptide) bonds. No rules, limiting the number of combinations or excluding any sequence of amino acids in the chain, are known up to now. Thus,  $20^{100}$  small proteins containing hundreds of amino acid residues may exist theoretically. The order of amino acid residues, which is encoded by order of deoxyribonucleotides in the corresponding DNA segment (gene), is decisive for the identity of the protein; this is called the primary structure of the protein.

Biosynthesis of the polypeptide chain is realised by a complicated process called translation. The basic polypeptide chain is subsequently chemically modified by the so-called posttranslational modifications. During this sequence of events the peptide chain can be cleaved by directed proteolysis, some of the amino acids can be covalently modified (hydroxylated, dehydrogenated, amidated, etc.) or different so-called prosthetic groups such as haem (haemoproteins), phosphate residues (phosphoproteins), metal ions (metalloproteins) or (oligo)saccharide chains (glycoproteins) can be attached to the molecule by covalent bonds. Naturally, one protein molecule can be modified by more means.

Thus, proteins and particularly their naturally occurring mixtures may possess a wide range of different physical and chemical properties as a consequence of the variability of their chemical structure described above. Generally, proteins decrease the surface tension of water; consequently, the particles that are dispersed into the water can interact better. Furthermore, some proteins are prone to aggregate into complex supra-molecular structures (collagens and materials derived from them like glue, gelatine, etc.) and connect particles of inorganic mixture components. This is why, since ancient times, various easily available proteins have been employed as additives to powdery materials in order to bind them together and improve their final properties. The longest known application of protein binders is their utilisation in colour layers of artworks as well as in coats and mortars that were often required to endure exposure to extreme conditions.

Nowadays, there exist several reasons why protein binders in historical materials attract general attention. Correct determination of the involved protein binder is essential for assessment of the painting technique used (e.g. illumination, casein, egg, and egg yolk tempera), which helps to improve restoration methods; for restoration purposes it is pivotal to know the composition of colour layers for selecting the appropriate technique for removal of overpaintings and following consolidation of the original layers. As remarked above, the determination of the protein binder type is crucial for the assessment of painting techniques from an art history point of view, widening our technological and artistic knowledge and improving the understanding of developments in painting techniques from medieval times to the present day. Determination of protein binders can also be useful for recognising the individual painting schools, which kept almost the same techniques for many decades or even centuries. That is why the knowledge of protein composition of binders can help in verification of artwork studied. Finally, outstanding properties of certain historical building materials, in which protein binders were used, can inspire contemporary architects and house-builders.

For a proper understanding of the protein binder's function in artworks and historical building materials, it is essential to identify the individual proteinaceous additives and to distinguish them even in materials where they are present in very small amounts, in insoluble forms and often in matrices unsuitable from an analytical point of view. For many materials the appropriate analytical methodology has not been found up to now and, in general, this type of analyses has not become a routine technique. Thanks to the recent development of proteomics (Section 6.2) most of the afore-mentioned problems have been resolved; mass spectrometry forms a fundamental platform for this new methodology.

### **6.1.1 Main Proteinaceous Binders Used in Art and in Historical Building Materials**

Of course, only easily available proteinaceous materials could be used in historical materials, particularly egg (whole or either yolk or white), glue (from bovine or porcine bones or skin, but also from rabbit or fish), gelatine, milk, curd, whey, and blood. In the following paragraphs the basic characteristics of the main groups of these proteins are discussed.

Egg yolk and white were used in paintings either separated or, more often, together. Egg or egg yolk temperas served as the most common protein binders in colour layers of artworks. Egg white alone was used in book illustrations, but it was usually not involved in other artworks because colour layers containing it were too fragile. Egg yolk in temperas has always been popular because of the higher content of lipids, which make the layers elastic and increases their adhesion to the surface.

Egg white contains, apart from water (88%), mainly proteins (~11%), saccharides, mineral compounds and traces of lipids. The most abundant proteins (mostly glycoproteins) are ovalbumin (54%), ovotransferin (13%), ovomocoid (11%), lysozyme (3.5%), other globulins (4%) and ovomucin (1.5–2%); some other proteins, e.g. ovomucoprotein, ovomicroglobulin and avidin [1], are present in traces (<1%).

Egg yolk contains mainly lipids (32–34%), proteins (16%), saccharides, mineral compounds, vitamins, dyes and water (48%). It is formed by two distinguishable fractions: plasma and granules. The plasma contains mostly lipids (90% of total solids) and proteins. Granules contain mainly acidic phosphoproteins (fosvitin, lipovitellins and low-density lipoproteins), which are soluble only in higher ionic strength water solutions.

*Milk* is a complex emulsion containing many proteins as well as low-molecular-weight compounds. Bovine milk contains six predominant proteins ( $\kappa$ -,  $\alpha_{S1}$ -,  $\alpha_{S2}$ - and  $\beta$ -caseins,  $\alpha$ -lactalbumin and  $\beta$ -lactalbumin) and other proteins like globular glycoproteins, macroglobulin and serum albumin. The technology that allows separating milk into two components – curd and whey – has been known for ages. All types of casein are acidic phosphoproteins existing in milk in the form of calcium salts; they form the major protein component of milk and curd, while whey contains mainly  $\alpha$ - and  $\beta$ -lactalbumin,  $\alpha$ - and  $\beta$ -lactoglobulin, globular glycoproteins, macroglobulin and serum albumin [2]. Since ancient times milk, curd and whey have been used in building materials, mainly in murals, plaster and mortars, but not very frequently in paintings because of their inappropriate properties.

Animal *glues and gelatine* have been used as adhesives with a wide spectrum of application for a long time; in Egypt animal glues were added into mortars 4000 years ago. Industrial production of glues started in the Netherlands in 1690, slightly later in England (1700) and a century later in the USA (1808). Glues can be extracted by boiling materials like bones, skin or various connective tissues. Their major component is the denatured and hydrolysed collagen, an extracellular glycoprotein containing large amounts of glycine, proline and its posttranslationally hydroxylated derivative hydroxyproline. The chemical composition of animal glues and gelatine is very similar; they mainly contain fragments of collagen. Gelatine is prepared by a longer boiling process than glues and thus it contains smaller collagen fragments. Glues are more polydisperse, containing a mixture of similar peptides with different molecular weights. Molecular weights of animal glues vary in the range of 20 000–250 000 Da and gelatine in the range of 20 000–100 000 Da. Glues and gelatine swell in warm water, forming a colloid solution, but after becoming dry they become rather insoluble as their functional groups in the side chains mutually interact forming a polymer net.

Animal glues from various biological raw materials differ in molecular weight and in the portion of low-molecular-weight compounds and impurities. Hide and bone glue (usually bovine or porcine) are the most produced collagenous materials. Bone glue contains fats and peptides formed by keratin decomposition; it has relatively low adhesiveness and is acidic with pH ranging from 5.8 to 6.3. Neutral hide glue exhibits better characteristics. Even

higher quality is possessed by rabbit glue, used also as a background for gold coating, and isinglass (fish glue), which is clear, perfectly adhesive and in contrast to other glues it does not darken. Distinction of individual glues and gelatine represents an extremely complicated analytical problem because of small differences in chemical structure, similar amino acid composition and even in the similar primary structure of their proteins and peptides.

Animal *blood* is a mixture of liquid plasma and so-called blood bodies of which more than 99% form erythrocytes (red cells). In blood plasma, more than 150 proteins can be identified; its most abundant proteins are serum albumin (>60%) and glycoprotein fibrinogen (~10%) and other coagulation factors, haptoglobin, ceruloplasmin, transferrin, ferritin, haemosiderin, etc. Erythrocytes contain a high concentration of haemoglobin, the conjugated protein formed by the polypeptide globin and the prosthetic group haem containing an iron atom [3–5]. The blood addition to mortars adjusts their consistency and modifies the workability time (Section 6.1.3).

### **6.1.2 Proteins in Colour Layers of Easel Paintings, Murals, Polychrome Statues, etc.**

Colour layers of artworks are a combination of powder dyes or pigments with binders. Although the binders form the minority of the colour layer, the name of the painting techniques are derived from them; at present the most common techniques are oil and tempera.

According to the predominant component, the binders are usually divided into protein, oil, polysaccharide, and resin binders. In this section we shall focus on protein binders but it is worth mentioning that in the majority of natural ‘non-protein’ binders a minority protein component is usually present as well. Thus many of the analytical techniques described here can be (with certain limitations) applied to them as well. Although in colour layers of artworks and particularly in paintings protein binders are relatively abundant (up to 10%), their identification is often limited by a small amount of sample that is usually available for analysis (tens or hundreds of micrograms at most [6]).

Nowadays, reliable identification of proteins in binders is considered to be problematic. Attempts have been made to identify them using classical or pyrolysis gas chromatography, and high performance liquid chromatography [7–15] or capillary zone electrophoresis [16, 17]. Interference with  $\text{Ca}^{2+}$ ,  $\text{Cu}^{2+}$  and  $\text{Fe}^{3+}$  ions, which originate from common inorganic components of the colour layer, occurs when identification of amino acids is carried out by high-performance liquid chromatography (HPLC) with UV or fluorescent detectors or by gas chromatography with a flame ionisation detector (GC-FID) or mass spectrometer (GC-MS). Influence of ions on analysis by GC-FID can be eliminated by addition of  $\text{Na}_2\text{EDTA}$  [18] or by using ion exchange chromatography (cation exchange resin) [19]; alternatively, protein material can be extracted from the sample before the hydrolysis [19]. The situation is complicated by the fact that some polysaccharide binders themselves contain proteins; e.g. Arabic gum, which was often used in combination with protein binders, contains approximately 3% of proteins. The identification based on ratios of individual amino acids is not reliable in such complex binders. Different gas chromatography or HPLC techniques are able to identify only animal glue, casein and egg. Bone glue, rabbit glue, hide glue and isinglass (fish glue) are indistinguishable by the above methods because of similar distribution of individual amino acids.

In the last decade, modern biochemical methods have been used for analysis of protein binders [20,21]; in one case a group led by A. Heginbotham identified egg proteins in a seventeenth century painting using immunofluorescent microscopy and enzyme-linked immunosorbent assay (ELISA) [20].

### 6.1.3 Proteins in Historical Building Materials

Early on in ancient Egypt and Rome, builders added various inorganic and organic additives to the mortar. The inorganic materials they used, amongst other things, were pulverised bricks, potsherds, broken glass, pottery, ash or clay as filling agents to replace locally scarce and expensive lime and sand [22,23].

The organic additives used can be divided into two groups. The first group contains the compounds used as the filling or reinforcing materials like straw, sawdust, other plant filamentous materials, and animal dung (mainly from horse and goat). The second group contains the so-called modifiers that, even in small amounts, can adjust certain mortar properties; they may change the water distribution in fresh mortar and the speed of its desiccation during which they initiate crystallisation and thus change the properties of hardened mortar (Table 6.1) [22, 24].

With the introduction of new building technologies, namely application of synthetic polymeric additives, the natural organic additives gradually disappeared [24]. At present, builders are returning to them; in particular, biomolecules (saccharides and their derivatives, oils, waxes, etc.) produced by biotechnological procedures have been reintroduced [25].

**Table 6.1** Organic additives in mortars and their classification by their effects on fresh and hardened mortars. Some of the protein additives are matched into more, sometimes even contradicting, categories, due to their different influence on fresh and moderately hardened mortars [22,24]

Meaning	Effect	Material
Accelerator	Accelerating firmness and increasing early firming	Egg white, blood, sugar, grease, curd, starch
Setting retarder	Extending workability time	Sugar, treacle, fruit syrup, blood, egg white, gluten
Plasticiser	Improving workability, consolidation of fresh mortar	Milk, egg white, fats, oils, sugar, colophony
Aerator	Improving permanency and frost proof	Malt, beer, urine
Sealing and hydrophobic additive	Providing waterproof character	Fats, oils, wax, asphalt, sugar
Adhesive	Improving cohesion	Colophony, gelatine, animal glue, casein
Firmer	Increasing firmness	Treacle, fruit syrup, fats, oils
Stiffening agent	Adjusting mortar consistence	Sour milk, casein, cheese, rye dough, gluten, plant gums, blood, collagen, gelatine

A great part of the organic additives contains various amounts of proteinaceous materials. The identification of proteinaceous binder could help to explain the unusual properties of the mortars, such as high firmness, hydrophobicity of surfaces, and, for frescoes, high stability [24].

Current research related to biological additives is focused particularly on their influence on the properties of mortars, namely on porosity, tensile strength, compressive strength, drying shrinkage, etc. [23, 24, 26]. The identification of proteinaceous additives used in historical buildings has been marginal for many years and no reliable methods are properly described in the literature.

## 6.2 Proteomics of Protein Binders: Peptide Mass Mapping Using Mass Spectrometry

As shown in the previous sections, identifying a small amount of a protein (in the order of tens of picomoles) represents a difficult problem for traditional methods of chemical analysis. The situation is even more complicated when a protein mixture of variable composition should be identified in a complex matrix containing dyes, oils, inorganic pigments, lime, etc.; moreover, the analysed materials come often from the Middle Ages or even ancient times and the proteins in them could have undergone various modifications (e.g. oxidation, photodecomposition and microbial digestion) over the centuries.

During the last two decades, the methodology for mastering this challenging task has been developed by biochemists. The branch of biochemistry that seeks to identify all or at least the great majority of proteins occurring in cells, tissues or even entire organisms under the given physiological or pathological conditions is called proteomics. Its experimental procedure (Figure 6.1) is usually based on three steps, which are described in detail in Sections 6.2.1–6.2.3:

- Protein (as pure as possible) is specifically cleaved with a protease under defined conditions. Thus the mixture of peptides, specific for the given protein, is produced. In classical proteomic approach this step is generally preceded by separation of individual proteins, usually by two-dimensional electrophoresis.
- Then the mass spectrum of the mentioned peptide mixture is measured. The set of molecular mass values (peak list) corresponding to individual peptides is characteristic for the protein and can be considered as its fingerprint.
- The obtained peak list together with other data (biological species, possible posttranslational modifications of amino acids, etc.) is then submitted to a software tool (usually publicly available) and searched against a certain protein database, which leads to protein identification. The majority of available software tools also offer information on the statistical probability of protein identification.

This procedure is called Peptide Mass Mapping (PMM), which is defined as a means of protein identification by comparing observed masses ( $m/z$  values) with predicted masses of digested proteins contained in a database.

Recently, the above technique has been used for the identification of proteinaceous binders [27]. It was correctly anticipated that for each relatively well-defined protein

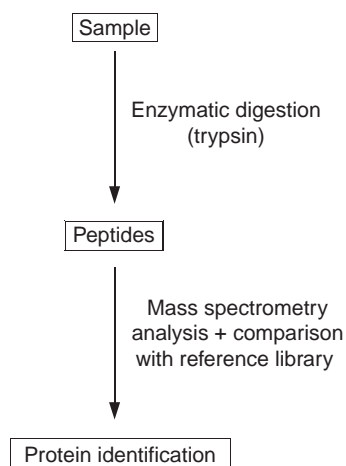


**Figure 6.1** A scheme of peptide mass mapping

mixture (animal glue, egg, milk, etc.) the characteristic ‘peptide mass fingerprint’ could be obtained. By this method it is possible to identify not only a single proteinaceous binder, but even combinations of them (e.g. milk proteins and whole egg), which is generally quite difficult with other analytical methods. Experience from biochemical experiments demonstrates that the method is very sensitive; the detection limit for e.g.  $\beta$ -casein (the characteristic milk protein) is about 18 fmol [28], which means that a sufficient amount of sample can be less than 0.5  $\mu\text{g}$  in the case of the colour layer of paintings. Such a low detection limit is essential for successful analysis of historical mortars, in which the protein concentration can be very low and the amount of sample must be proportionally larger.

### 6.2.1 Proteolytic Cleavage

Proteases (endopeptidases or proteinases) commonly used for specific cleavage of proteins are summarised in Table 6.2. Trypsin is almost always used as an enzyme of first choice; it is highly specific and stable, has an appropriate pH-optimum and is commercially available in high purity and quality. When the results obtained are ambiguous, or the trypsin cannot be used for any other reason, a different protease can be easily chosen. In all experiments, described here, the trypsin cleavage was applied.

**Table 6.2** The most often used endopeptidases in peptide mass mapping

Enzyme	pH optimum	Specific cleavage <sup>a</sup>
Chymotrypsin	7–8	-Phe † X- , -Tyr † X- , -Trp † X- , -Leu † X-
Endoproteinase V8 <sup>b</sup>	4–7.8	-Glu† X- , Asp† X-
Pepsin	1.5–2.5	-X † Phe † X- , -X † Tyr † X- , -Leu † Glu-
Trypsin	7–9	-Arg † X- , -Lys † X-

<sup>a</sup>X indicates arbitrary amino acid and † the protein cleavage sites.

<sup>b</sup>From *Staphylococcus aureus*.

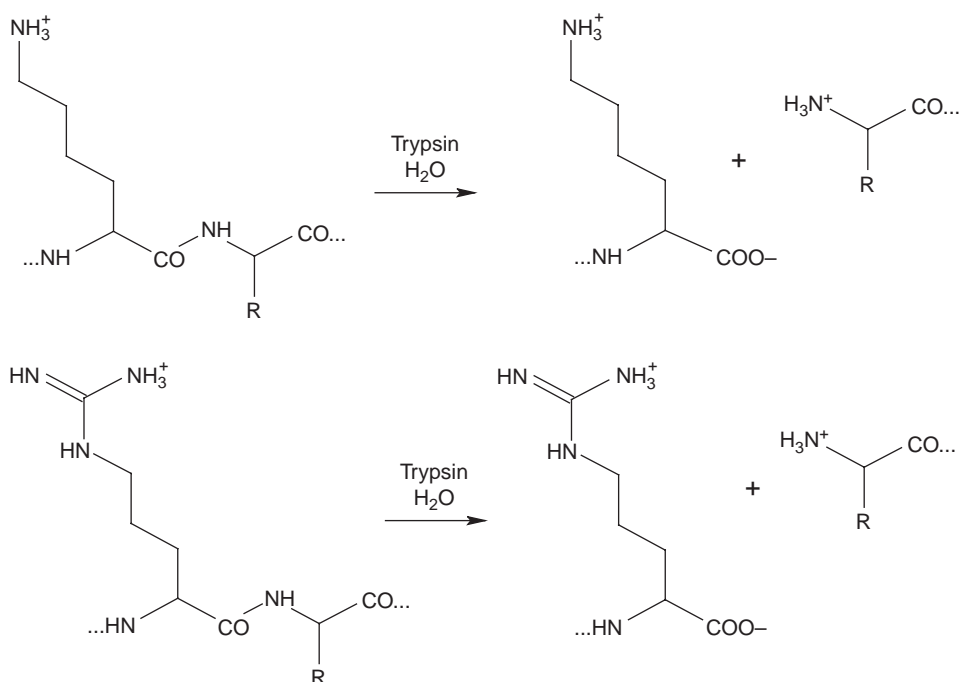


**Figure 6.2** The tryptic digestion of peptide bonds

Trypsin (EC 3.4.21.4) is a serine endopeptidase with high specificity for peptide bonds behind positively charged amino acid residues of lysine and arginine (Figure 6.2) (if the subsequent amino acid is not proline). It is produced in the pancreas of vertebrates and excreted in the form of inactive zymogen trypsinogen to duodenum; there it is activated by enzymatic cleavage of N-terminal hexapeptide. It is a relatively small protein; e.g. bovine trypsinogen has a molecular weight of 24 kDa. As a result of trypsin autocatalysis, its peaks with  $m/z$  equal to 842 and 2211 are often found in mass spectra and can be used for calibration as internal standards. Commercially available trypsin contains traces of chymotrypsin; consequently, it is supplied with an inhibitor of chymotrypsin, namely L-1-tosylamido-2-phenylethylchloromethylketone (TPCK). Trypsin cleaves optimally in the pH range of 7–9 (isoelectric point 9.4) and is inactivated at pH higher than 11. It is reversibly inactivated also in acidic media; that is why its stock solutions are held at a pH of approximately 3. Trypsin loses its activity under the denaturing conditions of 1 M guanidine hydrochloride or 30% ethanol.

### 6.2.2 Mass Spectrometry in Peptide Mass Mapping

From a historical point of view, it is fascinating to observe how technical and theoretical development of mass spectrometry has caused the rise of proteomics. Although different ways of specific protein cleavage were well understood by the 1960s, the dramatic development of mass spectrometry at the turn of the millennium fulfilled the dream of



biochemists – to identify minute amounts of proteins in biological materials, and thus to study the expression of individual genes, which is one of the most important biological processes.

Different types of mass spectrometers may be used for determination of molecular weights of peptides resulting from specific enzyme cleavage. Nowadays, matrix-assisted laser desorption/ionisation time-of-flight (MALDI-TOF) mass spectrometry is probably the most popular method because it does not require preliminary chromatographic separation of peptides and thus is relatively fast with high throughput potential [29]. This type of mass spectrometry has been used to obtain the data presented in the examples reported in the following sections. The potential of other mass spectrometric methods in the analysis of proteinaceous binders is briefly discussed in Section 6.5.

### 6.2.3 Database of Protein Binders

Identification of proteins by the peptide mass mapping method is based on the comparison of molecular weights of peptides ( $m/z$  values), obtained by enzyme cleavage of unknown protein, with those of peptide fragments in a database (usually publicly available [30]). The number of hits (in the range of selected tolerance e.g.  $\pm 0.2$  Da), which means the number of experimentally obtained peptide masses matching theoretical masses in the database, is reflected by the so-called score; a higher score means a higher reliability of protein identification. The score (%) represents the ratio of the number of peaks, corresponding to a certain binder, to the number of all peaks found in the interval from 900 to 2000 Da. In other words, the mass fingerprint of the studied protein is compared with that of known protein in the database.

A database of protein binders, which includes molecular weights of peptides produced by tryptic cleavage of the commonly used protein binders (yolk, egg white, casein, milk, whey, curd, gelatine as well as rabbit, bone, hide, and fish glue), has been recently developed [29]. This database can be used for protein mixture identification; its principle is the same as the PMM method described in Section 6.2.2, working with individual proteins – it compares the mass fingerprints of analogous protein mixtures. Now, when the database is more or less complete, it is possible to load a peak list, obtained after tryptic cleavage of unknown binder samples, and to get the score value characterising the reliability of identification not of an individual protein but of a binder mixture instead. The final decision about the type of binder depends on the score value which represents the ratio of the number of hits to the number of all peaks in the spectrum; in some cases (which is not unusual in proteomics) personal experience and responsibility of the researcher also plays a significant role in mass spectrum interpretation.

For the user's peace of mind, it would be desirable to understand the  $m/z$  values saved in the database. The individual  $m/z$  values should be assigned to definite peptide sequences of proteins contained in a certain protein binder. This assignment of the peptide sequences is not easy for many reasons: the individual binders are rich mixtures of proteins, which are usually posttranslationally modified to a large extent. Nevertheless, some individual proteins originating from reference binders were found in the Internet database *ExPASy* [30], their specific enzyme cleavage was simulated using the program *Mass-2.0-alpha4* and their  $m/z$  values were finally discovered in the measured mass spectra [31].

### 6.3 Experiments: Sample Preparation, Mass Spectra Measurement and Analysis

In this section the technique of PMM, using MALDI-TOF mass spectrometry, is described in detail. This method has been used both for model samples as well as for mortars and painting fragments (Section 6.4). It should be emphasised that the samples could be treated analogically if a different mass spectrometric technique was used.

#### 6.3.1 Digestion of Proteins by Trypsin

The solution of trypsin [ $2\text{ }\mu\text{g}$  in  $100\text{ }\mu\text{l}$  of  $50\text{ mmol l}^{-1}\text{ NH}_4\text{HCO}_3/(\text{NH}_4)_2\text{CO}_3$  buffer pH 7.5] is used for specific enzyme digestion.

When a colour layer of an artwork is analysed, a drop ( $5\text{--}10\text{ }\mu\text{l}$ ) of this solution is localised on the sample surface. This method of enzymatic digestion can be, in principle, applied to all types of samples that occur in restoration practice – fragments, cross-sections, microtome slices, etc. The samples are digested in closed microtubes to prevent evaporation of the solution. In the case of the cross-sections and microtome slices, it is essential to ensure the wetness of sample surface for the whole time of digestion.

The powdery sample (e.g. a mortar) is mixed with  $60\text{--}100\text{ }\mu\text{l}$  of trypsin solution (see above). Usually  $5\text{--}10\text{ mg}$  of model fresh mortar, containing about  $100\text{ }\mu\text{g}$  of proteins, is sufficient for a reliable identification. In the case of older samples (model samples aged for 9 months were tested) about  $100\text{ mg}$  of the material was necessary. Similar amounts of samples from buildings of different age (Section 6.4.4) were needed.

#### 6.3.2 Searching for the Appropriate Cleavage Time of the Reference Samples

The choice of the appropriate time for the enzymatic cleavage is a critical point of sample preparation. All types of the reference proteinaceous binders (Section 6.2.3) were cleaved from 1 to 24 h at laboratory temperature  $20\text{--}25\text{ }^\circ\text{C}$ . The peptide peaks in the interval  $900\text{--}2000\text{ Da}$  were registered; below  $900\text{ Da}$  the peaks of the matrix interfere and above  $2000\text{ Da}$  the incompletely cleaved oligopeptides are present which makes interpretation difficult. The best result, i.e. the highest number of peaks, was obtained after digestion for 2 h at laboratory temperature [32].

For determining the appropriate cleavage time of building materials, the seven model mortar samples containing different proteinaceous additives were digested by trypsin for 1–24 h (Figure 6.3). The highest number of peaks was found after 2- and 4-h digestion; in order to speed up the analysis, the 2-h period was preferred in all experiments described in the following sections.

#### 6.3.3 The Concentration and Purification of Peptides on the Reverse Phase

Before measuring the mass spectra, it is appropriate to concentrate and refine the peptides that are released into the solution by trypsin-catalysed hydrolysis of proteins. The reverse phase  $\text{C}_{18}$  in the  $10\text{ }\mu\text{l}$  tip of the automatic pipette (commercially available ZIP-TIP, Millipore Corporation, Bedford, MA, USA) was used. The peptides that are rather

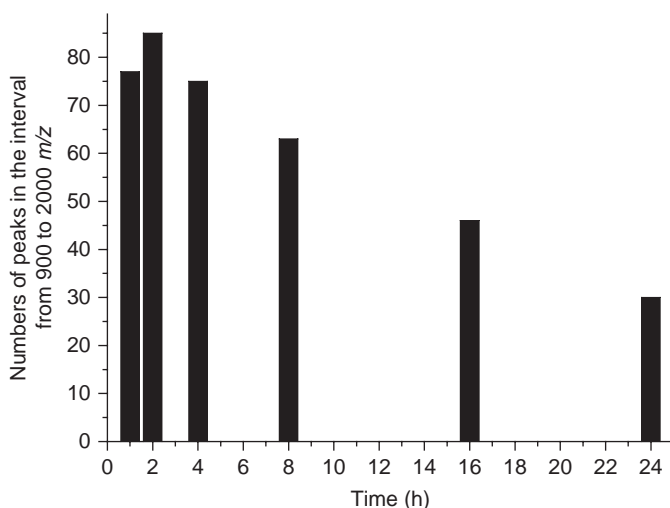


**Figure 6.3** The time dependence of the number of peaks found after tryptic cleavage of egg white model mortar

hydrophobic are retained on the reverse phase, while the ballast components, e.g. inorganic salts, stay in solution and can be easily washed out from the microcolumn. Finally, the column is washed by a small volume of elution solution [acetonitrile/0.1% trifluoroacetic acid, 1/1 (v/v)] and the peptides are released [33].

### 6.3.4 Sample Measurement by MALDI-TOF Mass Spectrometry

The 2  $\mu$ l of the concentrated peptide solution was mixed with 4  $\mu$ l of 2,5-dihydroxybenzoic acid [ $\sim 7$  mg in 500  $\mu$ l of the mixture of acetonitrile/0.1% trifluoroacetic acid, 1/2 (v/v)]. The resulting mixture was applied to the MALDI steel plate and left to crystallise. Afterwards, the MALDI-TOF mass spectra were measured by a BIFLEX IV instrument (Bruker, Germany) under appropriate conditions (potential 19 kV on the plate and 15.05 kV on the deflector, positive reflector mode – potential 20 kV, laser intensity 50 or 60%). The range of detected masses was from 600 to 3000 Da. For the external calibration the standard mixture of peptides M-Pep was used.

### 6.3.5 Data Analysis: Application of ‘Protein Binders Library’

Recently, a library of proteinaceous binders most frequently used in artworks and building materials (egg white, egg yolk, whole egg, casein, bovine milk, whey, curd, fish glue, bone glue, hide glue, rabbit glue, gelatine, and blood) has been built [29]. This library contains the  $m/z$  values of the most often occurring peptides that were obtained after 2-h trypsin digestion of reference binders at laboratory temperature and the database is described in Section 6.2.3. Thus, comparison of the measured peak list of the sample with that of the library allows a reliable assignment of the protein to be achieved.

## 6.4 Examples of Peptide Mass Mapping

In this section the experiments for the identification of proteinaceous binders contained in the model and artwork samples are summarised.

### 6.4.1 Model Samples of Colour Layers

The model samples were prepared at the Academy of Fine Arts in Prague (Czech Republic) in the summer of 2005. The samples, simulating the most typical ground layers used in the nineteenth century [34], were supplied for analysis as ‘samples of unknown composition’ under the codes S1–S10 (Table 6.3).

The results are summarised in Table 6.4, where the  $m/z$  peak values that were assigned to the peptides of the reference binder are shown; the meaning of ‘score’ is explained in Section 6.2.3.

**Table 6.3** *Composition of the model samples of the typical ground layers (recipes from the nineteenth century [33])*

Component	Sample									
	S1	S2	S3	S4	S5	S6	S7	S8	S9	S10
Rotter bolus (g)	6.7	6.8	6.9	7.3	7.2	7.6	6.9	6.7	7.9	6.8
Linseed oil (ml)	2.0	–	–	3.0	–	1.5	1.5	–	–	2.0
Whole egg (ml)	7.0	–	9.0	–	9.0	2.5	–	–	–	–
Egg yolk (ml)	–	9.0	–	–	–	–	2.5	4.0	4.0	7.0
Egg white (ml)	–	–	–	6.0	–	–	–	–	–	–
Hide glue (ml)	–	–	–	–	–	5.0	5.0	5.0	5.0	–
Water (ml)	–	–	–	–	–	–	–	–	–	2.0

**Table 6.4** *Composition of the proteinaceous binders in the model ground layers identified by peptide mass mapping*

Sample	Proteinaceous binders		Measured peak $m/z$ values
	Expected	Found (score%)	
S1	Whole egg	Whole egg (55%)	1020, 1048, 1050, 1064, 1085, 1106, 1114, 1150, 1164, 1226, 1345, 1401, 1406, 1428, 1436, 1445, 1560, 1562, 1859
S2	Egg yolk	Whole egg (42%)	900, 910, 915, 931, 935, 973, 989, 999, 1048, 1085, 1099, 1106, 1114, 1134, 1150, 1164, 1168, 1324, 1342, 1375, 1401, 1406, 1435, 1436, 1567, 1608
S3	Whole egg	Whole egg (yolk) <sup>a</sup> (30%)	915, 1099, 1234, 1255, 1268, 1445
S4	Egg white	Whole egg (white) <sup>a</sup> (38%)	1234, 1345, 1687, 1859
S5	Whole egg	Whole egg (29%)	903, 989, 1020, 1153, 1234

**Table 6.4** (continued)

Sample	Proteinaceous binders		Measured peak $m/z$ values
	Expected	Found (score%)	
S6	Whole egg	Whole egg (52%)	1020, 1048, 1085, 1088, 1105, 1177, 1201, 1240, 1267, 1303, 1401, 1406, 1445, 1563, 1566, 1587, 1656
	Hide glue	Animal glue (rabbit) <sup>a</sup> (30%)	942, 1088, 1095, 1105, 1201, 1221, 1265, 1267, 1303, 1453, 1465, 1469, 1501, 1566, 1568
S7	Egg yolk	Whole egg (yolk) <sup>a</sup> (40%)	1020, 1105, 1177, 1240, 1267, 1303, 1401, 1406, 1453, 1560, 1563, 1566, 1656, 1859
	Hide glue	Animal glue (hide) <sup>a</sup> (40%)	1267, 1303, 1453, 1465, 1469, 1501, 1560, 1566
S8	Egg yolk	Whole egg (22%)	1020, 1105, 1177, 1240, 1255, 1267, 1303, 1454, 1533, 1562, 1563, 1567, 1586, 1656, 1795
	Hide glue	Animal glue (hide, rabbit) <sup>a</sup> (15%, 25 %)	1095, 1099, 1105, 1105, 1205, 1221, 1267, 1303, 1453, 1465, 1501, 1550, 1562, 1586, 1637, 1795, 1947
S9	Egg yolk	Whole egg (39%)	956, 979, 1013, 1020, 1105, 1153, 1240, 1267, 1303, 1305, 1440
	Hide glue	Animal glue (hide, rabbit) <sup>a</sup> (29%, 26%)	942, 967, 1105, 1162, 1221, 1267, 1303, 1455, 1469, 1501, 1562, 1568
S10	Egg yolk	Whole egg (33%)	999, 1046, 1048, 1085, 1106, 1114, 1150, 1164, 1195, 1201, 1324, 1374, 1401, 1406, 1418, 1437, 1445, 1560, 1562, 1607, 1859
	–	Animal glue or gelatine (9%, 10%)	1099, 1104, 1106, 1114, 1195, 1201, 1406, 1560, 1562, 1816, 1947, 1980

<sup>a</sup> In the brackets the type of proteinaceous binder is specified according to experimental results.

The type of proteinaceous binder was correctly identified in all model samples. In only one case (S10), the animal glue was additionally identified, although the restorer who prepared these model samples declared that the sample contained only egg binder. It is possible that this sample was contaminated during its preparation or during laboratory treatment. The results indicate that this method does not allow reliable identification of the presence of individual egg yolk and egg white; most probably it is caused by the presence of a trace of egg white that is always present in the egg yolk preparations (and vice versa) and can be detected by the highly sensitive PMM method. The identification of individual types of animal glues will never be reliable by MALDI-TOF mass spectrometry because of their similar composition; the application of ESI (electrospray ionisation)-MS/MS (Section 6.5) could possibly overcome this problem. Only the fish glue, whose peptide

structure differs significantly from the other animal glues, can be reliably identified by the method described here.

### 6.4.2 Model Samples of Mortars

The seven model mortar samples with proteinaceous binders and a blank were prepared in the authors' laboratory and are described in Table 6.5. The binders were added to the basic mixture containing sand, lime and water (4:1:1 w/w/w). The samples were shaped into plates of dimensions 20x10x2.5 cm and left to dry under outdoor conditions.

The samples, containing about 0.1% proteins, were analysed by the PMM method. The  $m/z$  values of the peaks were compared with those of the given proteinaceous additive in the database (Table 6.6) [29]. It can be seen that the scores range from 20 to nearly 100%. Analogously to the case of colour layers, it was not often possible to reliably distinguish between individual components of the material (egg yolk vs whole egg, whey and curd vs milk, etc.), because of the imperfect separation of the proteins; nevertheless the main raw materials (milk, egg and collagenous materials like animal glue or gelatine) can be reliably distinguished.

The decrease of peak numbers was observed, when the spectra of the same amounts of fresh (1–2 weeks old) and aged (9 months old) mortars were compared. This decrease might be caused by activity of ubiquitous microorganisms that live on the mortar surfaces in biofilms. Especially in mild climate conditions, algae and cyanobacteria [35] can appear here; moulds (*Aspergillus*, *Penicillium*, *Fusarium*, *Mucor*) [36] and bacteria (*Arthrobacter*, *Bacillus*, *Micrococcus*, *Staphylococcus*) [37,38] have been discovered as well. The microorganisms secrete various hydrolytic enzymes that can decompose the organic additives, namely proteins, and make their sample identification less sensitive.

The proteins in the mortars can be modified by gradual oxidation or other chemical processes. In mass spectra the peaks that can be interpreted as oxygen incorporation (the mass shift of +16 Da) or ammonia release (–15 Da) can be sometimes indicated. This observation is not surprising as several amino acids (Met, Trp, Tyr, etc.) can be oxidised under these conditions; similarly, Gln and Asn can gradually release their ammonia by long-term hydrolysis in a wet inorganic matrix.

**Table 6.5** *Composition of the model mortar samples*

Proteinaceous binder	Binder weight (g)	Dry mortar mixture (kg)
Whey <sup>a</sup>	50	1.6
Bone glue <sup>b</sup>	50	1.6
Curd	40	1.6
Milk	75	1.6
Egg white	40	1
Egg yolk	25	1
Whole egg	60 (1 piece)	1
Blank	–	1.6

<sup>a</sup> The whey solution was prepared by stirring of 40 g of whey powder in 500 ml of water.

<sup>b</sup> The bone glue solution was prepared by stirring of 4 g of pulverised bone glue in 500 ml of water.

**Table 6.6** Identification of the proteinaceous binders in the model mortar samples by peptide mass mapping [32]

Binder	Results and scores (%)		Values of $m/z$ found in the database [29] for aged samples
	Fresh	Aged	
Whey	Milk (33%) Whey (21%)	Milk (28%)	971, 979, 997, 1106, 1367, 1441, 1590, 1669, 1762
Bone glue	Bone glue (40%)	Bone glue (15%) Rabbit glue (18%)	963, 991, 1019, 1048, 1150, 1162, 1179, 1193
Curd	Curd (64%) Milk (61%)	Curd (32%) Milk (46%)	955, 933, 977, 993, 1090, 1092, 1094, 1150, 1155, 1219, 1251, 1625, 1653, 1701, 1718, 1881
Milk	Milk (97%)	Milk (44%)	933, 968, 997, 1022, 1074, 1092, 1094, 1097, 1106, 1108, 1122, 1124, 1150, 1155, 1166, 1209, 1301, 1324, 1341, 1424, 1567, 1590, 1625, 1653, 1701, 1703, 1729, 1762, 1807, 1881 1779
Egg white	Egg white (63%)	Egg white (25%)	928, 988, 995, 1024, 1047, 1135, 1144, 1234, 1279, 1301, 1346, 1535, 1556, 1582, 1631, 1670, 1688
Egg yolk	Egg yolk (31%) Whole egg (71%)	Egg yolk (20%)	1025, 1048, 1077, 1085, 1134, 1252, 1268
Whole egg	Whole egg (61%)	Whole egg (57%)	928, 946, 973, 1025, 1042, 1047, 1077, 1083, 1085, 1134, 1144, 1147, 1164, 1179, 1268, 1280, 1301, 1346, 1367, 1390, 1419, 1446, 1506, 1535, 1556, 1582, 1631, 1845, 1960

### 6.4.3 Artwork Case Studies

Applications of PMM for the analyses of proteinaceous binders in artworks are summarised in Table 6.7 [21,39–43]. The analyses of the most interesting paintings by E. Munch, are described in detail here.

The samples, taken from the Edward Munch paintings (Table 6.8) [39], were provided by Munch-Museet in Oslo as small fragments weighing several microgrammes (samples P1, P2a, P2b, P3). The detailed description of the painting technique, stratigraphy of the colour layers, and inorganic pigments are published elsewhere [40,41].

Based on contemporary art techniques, it was presumed that the sample P2a contained whole egg. This presumption was confirmed by PMM analysis of this extremely small

**Table 6.7** *Identification of proteinaceous binders in art objects*

Artwork description	Historical allocation	Proteinaceous binder	References
Melancholy (E. Munch) Munch-Museet in Oslo	1891–1892	Egg white/ Whole egg	[40,41]
Young Woman Embracing Death (E. Munch) Munch-Museet in Oslo	1893	Whole egg + Rabbit glue	[40,41]
Sitting Nude and Grotesque Masque (E. Munch) Munch-Museet in Oslo	1893	Whole egg + Rabbit glue	[39]
Separation (E. Munch) Munch-Museet in Oslo	1893	Whole egg + Rabbit glue	[39]
Portrait of Friedrich Nietzsche (E. Munch) Munch-Museet in Oslo	1905	Whole egg + Rabbit glue	[39]
St John the Evangelist (right altar wing, M. Coxie)	Sixteenth century	Whole egg + Rabbit glue	[21]
Crucifixion (unknown author) Church of St John the Baptist in Hlučín	1540–1560	Rabbit glue	[42]
Francis I (J. Zitterer) Moravian gallery	1792	Egg yolk / whole egg	[43]
Curtain from the Karlín theatre, Prague	Nineteenth century	Whole egg + Rabbit glue	Not published

**Table 6.8** *Description of four samples from the paintings by E. Munch*

Painting (year)	Sample code	Layer description	Proteinaceous binder
Sitting nude and grotesque masque (1893)	P1	Brown layer + white ground layer	Whole egg + Rabbit glue
Separation (1893)	P2a P2b	Pink layer Red and blue layer + ground layer	Whole egg Whole egg + Rabbit glue
Portrait of Friedrich Nietzsche (1905)	P3	Red and blue layer + ground layer	Whole egg + Rabbit glue



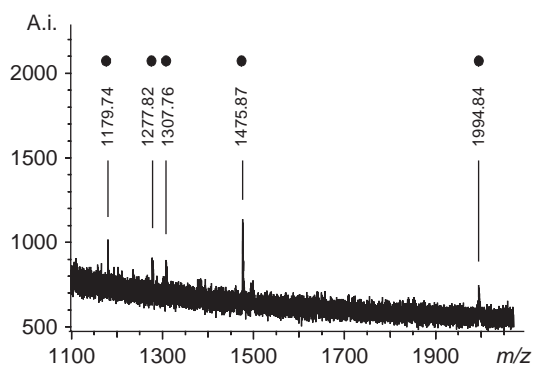


**Figure 6.4** Mass spectrum of sample P2a from 'Separation 2'. The peaks of egg white are labelled

sample (Figure 6.4). In the samples P1, P2b, and P3 that contained both colour and ground layers, whole egg and animal glue (most probably rabbit) were found (Figure 6.5). From these results it can be concluded that the colour layers contain egg tempera and the ground layers contain rabbit glue.

According to previous analyses of these paintings, the colour layers contain a high concentration of phosphorus (in the order of units of per cent) [40]; this led restorers to the assumption that they contain casein which was ruled out by our detailed analysis. Thus, a high concentration of phosphorus coming from the proteinaceous binder is excluded because of the low concentration of phosphorus in the most phosphorylated binder (casein, max. 5% phosphorus) and the amount in the colour layer (up to 10%). The source of phosphorus was discovered by powder X-ray microdiffraction; it comes from aluminium phosphate that was probably used as a substrate for the precipitation of red organic lake [40].

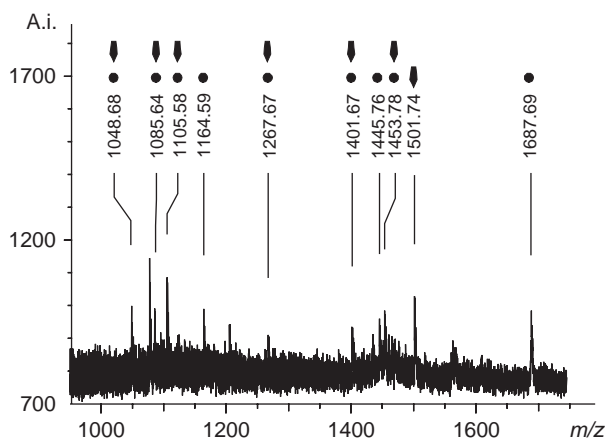


**Figure 6.5** Mass spectrum of sample P3 from 'Portrait of Friedrich Nietzsche'. The mass peaks of animal glue are labelled by the arrows and the mass peaks of whole egg by the dots

#### 6.4.4 Mortars from Historical Buildings

Several samples of materials from historical buildings have been analysed by the PMM method and the results are summarised in Table 6.9. In nearly all of them proteinaceous binders were reliably identified [32, 44, 45].

The most interesting results [44] of the samples from the Romanesque rotunda of Saint Catherine in Znojmo (Czech Republic) are reported in Table 6.10 (Figure 6.6).

**Table 6.9** *Description of mortar samples taken from secular and sacral architecture*

Sample origin <sup>a</sup>	Period	Analysed material	Proteinaceous additives
Castle Bauska (Latvia)	Fifteenth century	Inner mortar	Collagens
Castle Švihov	Middle age	Artificial stone	Collagens
Castle Pernštejn	Middle age	Mortar of the oriel roof	Whole egg
Castle Štamberk	Fourteenth century	Mortar	Milk proteins
Castle Lemberk	Middle age	Stucco decoration	Collagens
Chateau in Náměšť nad Oslavou	Middle age	Artificial marble	Collagens
Castle in Český Krumlov	Gothic	Plaster	Collagens
Rotunda of Saint Catherine in Znojmo	Romanesque	Mortar	Milk proteins and collagens
Bridge in Roudnice nad Labem	1333–1340	Mortar	Milk proteins
Church Svojšín	Twelfth century	Mortar	Whole egg
Lobkowicz Palace at Prague Castle	Baroque	Artificial stone	Collagens

<sup>a</sup> All samples except Castle Bauska come from the Czech Republic.

**Table 6.10** *Results obtained in the analysis of mortar samples*

Sample	Place of sampling	Description	Proteinaceous additives
1	Outer part of vertex	Lean mortar taken from the vertex centre	Bone glue or gelatine
1A	Outer part of vertex	Rich mortar taken from the vertex centre	–
2	Outer part of vertex	Mortar from the expungement of the 'rim' at ashlars masonry	Bone glue or gelatine
3	Inner part of vertex	Mortar from the expungement between the centre and the rest of the aisle construction	Curd or whey
4	Inner part of vertex	Lean mortar from the construction of the vertex centre	Curd or whey
8	Inner part of vertex	Mortar from the expungement between the vault-stone of the apse and rotunda aisle masonry	Curd or whey
10	Rotunda aisle	Mortar from the rotunda aisle	–

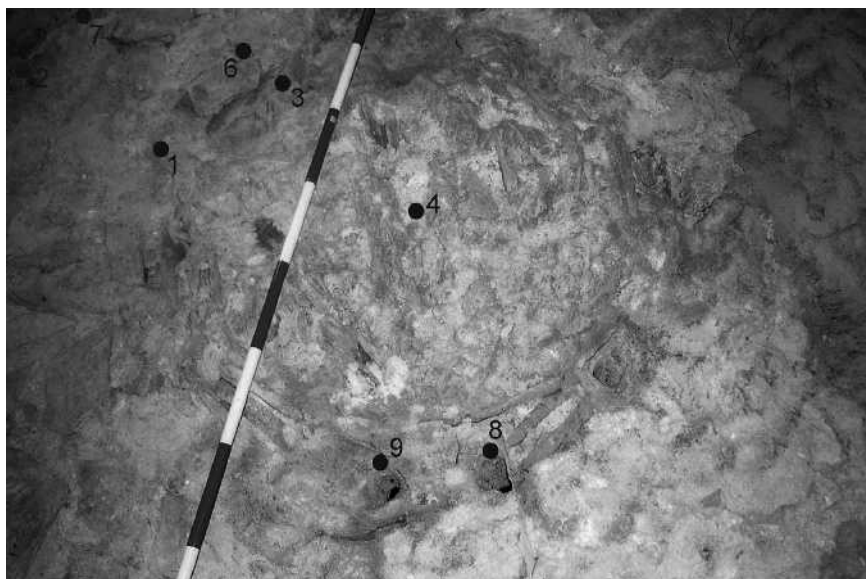


**Figure 6.6** Photograph from the vertex of the rotunda of Saint Catherine in Znojmo (Czech Republic). The places of sampling are labelled. Samples with numbers 6, 7 and 9 were not analysed because they were parts of bricks and stone. (Courtesy of Dr Jaromír Kovárník)

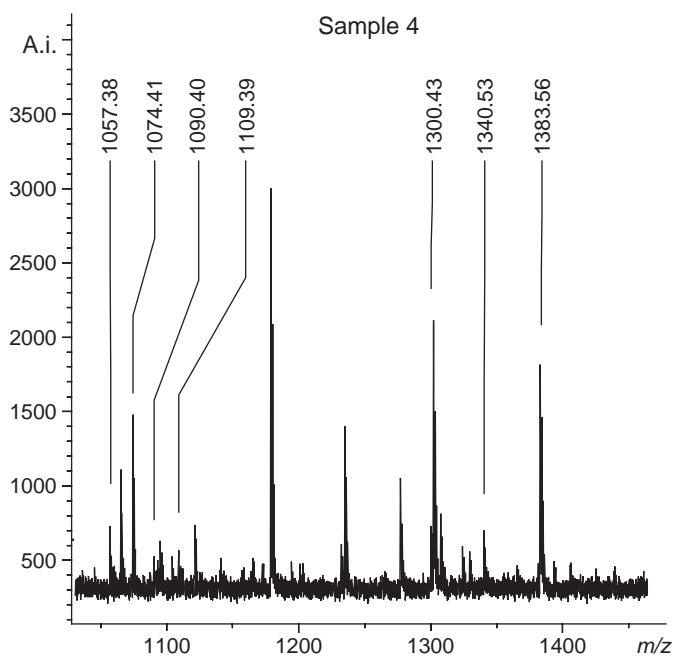


**Figure 6.7** Mass spectrum obtained from sample 4. The peaks corresponding to milk proteins are labelled

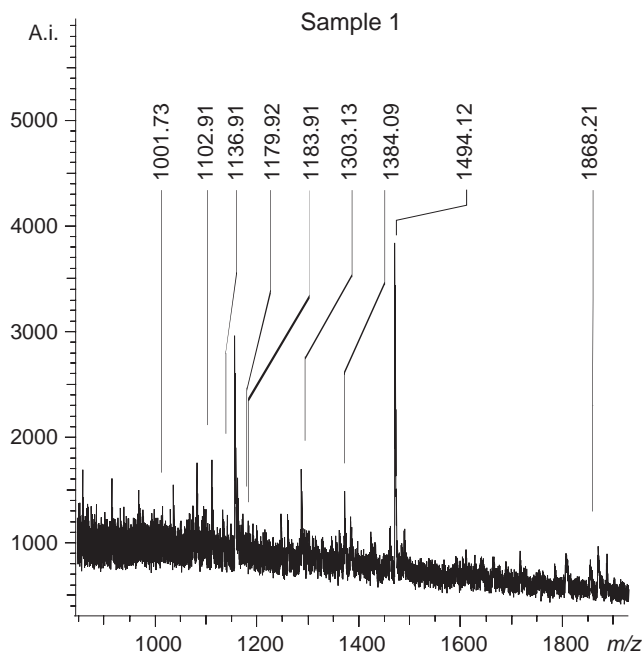


**Figure 6.8** Mass spectrum obtained from sample 1. The peaks corresponding to collagen are displayed

The samples can be divided into three groups: (1) samples 3, 4 (Figure 6.7) and 8 contain mainly milk proteins; (2) samples 1 (Figure 6.8) and 2 contain mainly collagens; and (3) samples 1A and 10 do not contain any proteinaceous additive. These three groups match the three different places of sampling. The first group was taken from the inner part of the vertex, while the second one from the outer part (Figure 6.6). In the third group, sample 1A was the second layer of sample 1 (it was so-called rich mortar because of its protective properties caused by the addition of some oleic hydrophobic material); sample 10 was taken from the rotunda aisle. It may be supposed that the higher amount of milk proteins in the inner part of the vertex was added to increase the mortar firmness while the collagens were added to create a better workability and increase the adhesivity of the mortar.

All these results have confirmed that the described methodology can be used for the identification of proteinaceous binders in solid samples taken from historical objects. The method facilitates the distinction of the basic types of proteinaceous additives (milk proteins from collagenous, etc.) that are contained in low concentrations in medieval or even older samples.

## 6.5 Conclusions

The application of PMM enables the identification of proteinaceous binders in a more reliable and sensitive way than the more commonly used ‘classical’ analytical methods.

The fascinating experience with 1000-year-old mortar, in which the protein concentration was extremely low, has shown that by using this method it is possible to work in fields where other methods fail. In the case of easel paintings, small samples are usually available; the advantage of the method described here also lies in the true microdestructive character. Moreover, as most samples, mainly in the case of paintings, often contain more than one proteinaceous binder (see e.g. E. Munch 'Portrait of Friedrich Nietzsche', Section 6.4.3), it is very encouraging that the PMM allows the simultaneous determination of at least two of them.

MALDI-TOF mass spectrometry is a very direct and favourable method for PPM because of the simple sample preparation and mainly because of the rapid spectra recording (without the chromatographic separation). It can be supposed that in the future more sophisticated mass spectrometry methods will be used in this analytical field; they are slower, but they can offer more information about the binder present. The lower number of peaks will then be sufficient for identification because the peptides will be sequenced and compared with a single protein database. For instance, nano liquid chromatography/nano ESI/Q-q-TOF MS/MS has recently been applied to model samples that contained ovalbumin and whole egg. This method successfully identified whole egg in samples taken from Benedetto Bonfigli's triptych ('The Virgin and Child', St John the Baptist, St Sebastian) and 'Virgin and Child' by Niccola di Pietro Gerini [46].

## References

1. <http://www.aces.edu/dept/family/foodsafety/Eggs-2003-ppt/Eggs-2003.ppt>. Cited 14 September 2005.
2. J. Velíšek, *Chemie potravin 1*, OSSIS, Tabor, pp. 43–48, 2002.
3. <http://www.biomedici.ic.cz/download/materials/Fyziologie/Krev.pdf>. Cited 18 August 2007.
4. <http://www.nem.pce.cz/ocni/Bakalarky%20web/HEMATOLOGIE.htm>. Cited 18 August 2007.
5. <http://www.lf3.cuni.cz/physio/Physiology/education/materialy/krev/krev1.ppt>. Cited 18 August 2007.
6. R. Mateo-Castro, J.V. Gimeno-Adelantado, F. Bosch-Reig, A. Doménech-Carbó, M.J. Casas-Catalán, L. Osete-Cortina, J. De la Cruz-Cañizares, M.T. Doménech-Carbó: Identification by GC-FID and GC-MS of amino acids, fatty and bile acids in binding media used in works of art, *Fresenius J. Anal. Chem.*, **369**, 642–646 (2001).
7. M.P. Colombini, F. Modugno, Characterisation of proteinaceous binders in artistic paintings by chromatographic techniques, *J. Sep. Sci.*, **27**, 147–160 (2004).
8. F. Caruso, S. Orecchio, M.G. Cicero, C. Di Stefano, Gas chromatography–mass spectrometry characterization of the varnish and glue of an ancient 18th century double bass, *J. Chromatogr., A*, **1147**, 206–212 (2007).
9. A. Andreotti, I. Bonaduce, M.P. Colombini, G. Gautier, F. Modugno, E. Ribechini, Combined GC/MS analytical procedure for the characterization of glycerolipid, waxy, resinous, and proteinaceous materials in a unique paint microsample, *Anal. Chem.*, **78**, 4490–4500 (2006).
10. F. Capitelli, F. Koussiaki, THM-GCMS and FTIR for the investigation of paints in Picasso's *Still Life*, *Weeping Woman* and *Nude Woman in a Red Armchair* from the Tate Collection, London, *J. Anal. Appl. Pyrol.*, **75**, 200–204 (2006).
11. M. Carbin, R. Stevanato, M. Rovea, P. Traldi, D. Favretto, Curie-point pyrolysis gas chromatography mass spectrometry in the art field. The characterization of proteinaceous binders, *Rapid Commun. Mass Spectrom.*, **10**, 1240–1242 (1996).

12. I. Bonaduce, M.P. Colombini, Gas chromatography/mass spectrometry for the characterisation of organic materials in frescoes of the Monumental Cemetery of Pisa (Italy), *Rapid Commun. Mass Spectrom.*, **17**, 2523–2527 (2003).
13. J.V. Gimeno-Adelantado, R. Mateo-Castro, M.T. Domenech-Carbo, F. Bosch-Reig, A. Domenech-Carbo, J. De la Cruz-Canizares, M.J. Casas-Catalan, Analytical study of proteinaceous binding media in works of art by gas chromatography using alkyl chloroformates as derivatising agents, *Talanta*, **56**, 71–77 (2002).
14. G. Chiavari, N. Gandini, P. Russo, D. Fabbri, Characterisation of standard tempera painting layers containing proteinaceous binders by pyrolysis gas chromatography mass spectrometry, *Chromatographia*, **47**, 420–426 (1998).
15. G. Chiavari, G. Lanterna, C. Luca, M. Matteini, S. Prati, I.C.A. Sandu, Analysis of proteinaceous binders by in-situ pyrolysis and silylation, *Chromatographia*, **57**, 645–648 (2003).
16. I. Gluch, A. Urbanska, I. Zadrozna, K. Pawlak, M. Jarosz, Identification of proteinaceous binding media used for paintings by capillary electrophoresis with electrospray MS detection, *Chem. Analit.*, **51**, 195–210 (2006).
17. S.M. Harrison, I. Kaml, V. Prokoratova, M. Mazanek, E. Kenndler, Characterisation and identification of proteinaceous binding media (animal glues) from their amino acid profile by capillary zone electrophoresis, *Anal. Bioanal. Chem.*, **382**, 1520–1526 (2005).
18. J. De la Cruz-Cañizares, M.T. Doménech-Carbó, J.V. Gimeno-Adelantado, R. Mateo-Castro, F. Bosch-Reig, Suppression of pigment interference in the gas chromatographic analysis of proteinaceous binding media in paintings with EDTA, *J. Chromatogr., A*, **1025**, 277–285 (2004).
19. M.P. Colombini, F. Modugno, A. Giacomelli, Two procedures for suppressing interference from inorganic pigments in the analysis by gas chromatography-mass spectrometry of proteinaceous binders in paintings, *J. Chromatogr., A*, **846**, 101–111 (1999).
20. A. Heginbotham, V. Millay, M. Quick, The use of immunofluorescence microscopy (IFM) and enzyme-linked immunosorbent assay (ELISA) as complementary techniques for protein identification in artists' materials, *J. Am. Inst. Cons.*, **45**, 89–105 (2006).
21. R. Hynek, S. Kuckova, J. Hradilova, M. Kodicek, Matrix-assisted laser desorption/ionization time-of-flight mass spectrometry as a tool for fast identification of protein binders in color layers of paintings, *Rapid. Commun. Mass Spectrom.*, **18**, 1–5 (2004).
22. L.B. Sickels, Organic additives in mortars, *Edinburgh Uni. Res. J. Architect.*, 8–19 (1980).
23. S. Chandra and J. Aavik, Influence of proteins on some properties of portland cement mortar, *Int. J. Cement Compos. Lightweight Concrete*, **9**, 91–94 (1987).
24. P. Rovnaníková, *Omítky. Chemické a technologické vlastnosti*, STOP, Prague, 2002.
25. J. Plank, Applications of biopolymers and other biotechnological products in building materials, *Appl. Microbiol. Biotechnik.*, **66**, 1–9 (2004).
26. J. Jasiczak and K. Zielinski, Effect of protein additive on properties of mortar, *Int. J. Cement Compos. Lightweight Concrete*, **28**, 451–457 (2006).
27. Š. Kučková, Identifikace proteinových pojiv v barevné vrstvě uměleckých děl metodou hmotnostní spektrometrie, Diploma thesis, VŠCHT Praha, 2006.
28. Y. Ma, Y. Lu, H. Zeng, D. Ron, W. Mo, T.A. Neubert, Characterization of phosphopeptides from protein digests using matrix-assisted laser desorption/ionization time-of-flight mass spectrometry and nanoelectrospray quadrupole time-of-flight mass spectrometry, *Rapid Commun. Mass Spectrom.*, **15**, 1693–1700 (2001).
29. S. Kuckova, R. Hynek, M. Kodicek, Identification of proteinaceous binders used in art-works by MALDI-TOF mass spectrometry. *Anal. Bioanal. Chem.*, **388**, 201–206 (2007).
30. <http://www.expasy.ch>. Cited 21 September 2006.
31. <http://mmass.biographics.cz/>. Cited 24 April 2006.
32. S. Kuckova, M. Crhová, R. Hynek, M. Kodicek, Proteomická analýza proteinových aditiv v historických maltách. *Ve službách archeologie*, **1**, 43–47 (2008).
33. <http://www.millipore.com/userguides.nsf/docs/p36110>. Cited 18 March 2007.
34. R. Massey, *Formulas for Painters*, Watson-Guption Publications, New York, 1967.
35. Ch.C. Gaylarde, P.M. Gaylarde, A comparative study of the major microbial biomass of biofilms on exteriors of buildings in Europe and Latin America, *Int. Biodeter. Biodegr.*, **55**, 131–139 (2005).

36. L. Laiz, G. Piñar, W. Lubitz, C. Saiz-Jimenez, Monitoring the colonization of monuments by bacteria: cultivation versus molecular methods, *Environ. Microbiol.*, **5**, 72–74 (2003).
37. M. Gódyová, B. Uher, A. Šimonovičová, J. Švec, Mikrobiálna biodeteriorácia kameňa, *Bull. československej spoločnosti mikrobiol.*, **2**, 37–48 (2003).
38. M. Gódyová, A. Šimonovičová, E. Franková, Biodeteriorácia kamenných substrátov pôdnymi mikromycétami, *Mykologické listy*, **74**, 17–22 (2000).
39. S. Kuckova, J. Hradilova, M. Kodicek, I. Nemec, T. Grygar, P. Bezdictka, D. Hradil, *New Approach to the Organic Analysis of Paintings: Example of Edvard Munch's Canvases*, Non-Destructive Testing and Microanalysis for the Diagnostics and Conservation of the Cultural and Environmental Heritage, Lecce, 2005.
40. D. Konvalinkova, J. Hradilova, D. Hradil, P. Sacha, B. Casadiego, M. Novotna, M. Denderova, I. Vernerova, M. Vojtiskova, T. Joudova, B. Hrebickova, H. Millionova, D. Frank, M. Rumlova, T. Popova, L. Helfertova, J. Michalkova, *Restoration of Modern and Contemporary Art (in Czech)*, National Gallery in Prague, Ministry of Culture of the Czech Republic, internal report, Prague, p. 495, 2002.
41. J. Hradilova, D. Hradil, S. Bakardjieva, M. Vojtiskova, A. Langrova, Z. Korbelova, M. Novotna, *Laboratory Research of Selected Paintings of Frantisek Kupka and Edvard Munch (in Czech)*, Academy of Fine Arts in Prague, internal report, Prague, p. 138, 2002.
42. J. Hradilová, D. Hradil, *Zpráva o laboratorním průzkumu– Ukřižování. –(olej na plátně)*, Academy of Fine Arts in Prague, unpublished material, Prague.2002.
43. <http://www.alma-lab.cz/pdf/zpravaj0504.pdf>. Cited 10 January 2008.
44. S. Kuckova, R. Hynek, M. Kodicek, Identification of proteinaceous binders in the mortars from rotunda of Saint Catherine in Znojmo (Czech Republic), *J. Cult. Heritage* (in press).
45. M. Drdáký, Z. Slížková, Mechanical characteristics of historic mortars from tests on small-sample non-standard specimens. In *Proceedings of 3rd Baltic Conference of Silicate Materials, Latvia*, pp. 9–11, 2007.
46. C. Tokarski, E. Martin, Ch. Rolando, C. Cren-Olivé, Identification of proteins in Renaissance paintings by proteomics, *Anal. Chem.*, **78**, 1494–1502 (2006).





# **Part III**

## **Gas Chromatography/Mass Spectrometry**



# 7

## GC/MS in the Characterization of Lipids

*Maria Perla Colombini, Francesca Modugno and Erika Ribechini*

### 7.1 Introduction

Lipids represent a remarkable class among the organic substances found in archaeological remains and works of art. They can derive from many sources, including vegetable oils, animal lipids, and waxes, and they have been used in many different ways in art and everyday activities. Lipid materials have been used extensively by ancient and modern populations as food, illuminants, waterproofing materials, binders, ingredients in medicines, cosmetics and balms.

Fats and oils, constituted by acylglycerolipids, represent a major subgroup of lipids. They are the most common class of medium-size molecules produced by living organisms. They are the main constituents of the storage fat cells in plants and animals. They have quite a similar chemical composition, as they are mainly composed of triglycerides, triesters of glycerol with fatty acids (FAs).

The saturated hydrocarbon moieties give lipids an aliphatic character, and thus hydrophobic properties, which limit their loss from artefacts by water leaching. However, they are subject to chemical and microbiological alterations; since they have a limited number of reactive sites, they are relatively less susceptible to structural modification and degradation than polysaccharides, proteins and nucleotides.

Entrapment in certain archaeological environments can enhance lipid preservation. For example, decomposition is slowed down by dry conditions such as arid or cold climates. In charred residues, the activity of micro-organisms present in organic tissues stops and the outer surfaces are fused, providing a barrier against microbial attack. This means that lipids are often encountered in many different environments associated with artworks and archaeological objects. They appear as constituents, decoration materials or residues of the materials originally contained in a vessel.

Some oils of plant origin with siccative properties have been used as paint binders, in order to disperse and apply pigments and varnishes. These oils are characterized by 'semidrying' properties (such as cottonseed, sesame oil) or by 'drying' properties (linseed, poppy seed, walnut, safflower, tung oil) – this means they form solid films when exposed to air. Drying oils contain high levels of polyunsaturated FAs in the triglycerides, and the siccative property is linked to the number of conjugated double bonds in the acyclic chains. Basically, an oil may be defined as 'drying' when the percentage of double bonds in the FAs is higher than 65% of the total FA composition. The identification and the study of the ageing of drying oils used as paint binders has become a fundamental issue for the conservation of paintings.

Although analytical procedures based on GC/MS analysis usually involve a relatively long analysis time, requiring a wet chemical pretreatment of the samples, they are unsurpassed in their capacity to unravel the molecular composition of the lipids used in works of art and in archaeological findings at a molecular level. In addition to obtaining a qualitative molecular profile, GC permits quantitative or semi-quantitative measurements on specific molecules.

There are a huge number of applications of GC/MS to lipid analysis in cultural heritage reported in the literature. Lipid characterization, together with the study of lipid degradation processes, is an important research area in conservation science [1–31].

This chapter gives an overview of GC/MS analytical procedures used for lipid determination, and a summary of the complex issue of lipid chromatographic data interpretation in paintings and archaeological objects. Some examples and case studies are also included.

## 7.2 Analytical Procedures

Many analytical procedures based on GC/MS have been described for the analysis of a wide range of lipid materials in samples from art and historical objects [2,3,7,11,17,21,26]. Wet chemical pretreatments are generally needed before GC/MS analysis, in order to:

- extract or solubilize compounds of interest;
- decompose high molecular weight lipid compounds (triglycerides, cerides, polyesters) into smaller molecules (FAs and alcohols), by cleavage of ester bonds;
- clean-up the sample to eliminate interferents;
- transform FAs and other polar compounds into volatile molecules, by performing suitable derivatizing reactions.

Extraction is usually performed in a solvent such as dichloromethane (DCM), chloroform, methanol, or a mixture of them, to obtain the so-called total lipid extracts (TLEs).

Samples may vary from a few mg to 10–50 mg, and the amount of solvent is between 1 ml and 5 ml. Ultrasounds are normally applied during extraction with a laboratory sonicator. When archaeological organic residues in unglazed ceramic vessels are being investigated, grinding potsherds into fine powder, and then adding the solvent, maximizes the contact between the residue and the solvent, and then provides data on lipid materials entrapped in the ceramic pores [32]. Lipids entrapped in the pores of archaeological ceramic vessels appear to be relatively well preserved and protected from oxidation and environmental action, thus representing a source of information on food residues and consequently on the diets of ancient times. As absorption of lipids by the ceramic matrix is generally not homogeneous throughout the wall of the vessel, taking samples from different portions of the vessel is recommended when possible.

A critical aspect is the different solubility of specific lipid molecules in the solvents, which may result in a different distribution of lipids in the solution with respect to the residue. The analytical procedures thus need to be validated with suitable reference materials.

Contamination must be carefully avoided in the manipulation of samples: wearing gloves and running frequent blanks is strictly necessary in the analysis of lipids. Squalene and cholesterol are among the lipid components of human skin, so their occurrence in a lipid extract may suggest contamination [4]. In laboratory blanks palmitic and stearic acids are commonly encountered, and they should be carefully quantified, in order to assess their limit of detection (LOD) and level of quantification (LOQ)<sup>1</sup>. This entails carefully determining their blank signal together with the standard deviation. Moreover, when analysing organic materials in buried archaeological objects, the contribution of soil lipid should be always checked, by analysing the extract of samples of sediment collected at the same time as the objects themselves.

The lipid extracts obtained can then be separated into different fractions and analysed in order to simplify data interpretation and optimize the chromatographic conditions for each class of compounds. Aliquots of the TLEs can be separated into polar and nonpolar fractions using bonded aminopropyl solid-phase extraction cartridges. According to this procedure [19] the nonpolar fraction is collected by elution with 2:1 v/v DCM/isopropanol. Flushing the cartridge with acetic acid in diethylether results in the elution of the polar fraction. The nonpolar fraction can be further separated on an activated silica gel column, using solvents of increasing polarity, i.e. hexane, hexane/DCM (9:1), DCM, DCM/methanol (1:1 w/w) and methanol, which give the hydrocarbon fraction, aromatic fraction, wax ester fraction, esters/alcohol fraction and polar fraction, respectively.

In the analysis of paint samples, a stepwise extraction of the various lipid and resinous components has been proposed [33] which uses isooctane, methanol, chloroform/methanol (7:3) and methanol/oxalic acid (10%). The last extraction releases FAs from the metal soaps.

A specific sample pretreatment can be used to analyse lipids and proteins in a single paint microsample. This entails extracting proteinaceous matter with ammonia solution to

---

<sup>1</sup> LOD is defined as the amount of analyte corresponding to a signal equal to the average blank signal plus three times its standard deviation; LOQ is commonly defined as the amount of analyte corresponding to a signal equal to the average blank signal plus 10 times its standard deviation.

separate it from lipids, followed by re-extracting the free FAs from the acidic hydrolysate of proteins with diethylether [30].

Chemolysis of ester bonds is performed by hydrolysis or methanolysis. Acidic methanolysis, for 24 h at 80 °C, cleaves ester bonds by transesterification, obtaining the fatty acid methyl esters (FAMES), and has been used to simultaneously study oils, waxes, tannins, resins and polysaccharides in samples collected from embalming materials from Egyptian mummies [17]. Transesterification with trimethyl sulfonium hydroxide in methanol is also used [33,34].

Generally, alkaline saponification in hydroalcoholic KOH is the most widespread approach [11–13]. This allows us to cleave ester bonds and, if necessary, to separate the saponifiable fraction (acids) and unsaponifiable fraction (alcohols, sterols, and hydrocarbons). Generally, 3 h of saponification in 10% KOH in water/methanol (3:1) at 60 °C achieves a quantitative yield for triglycerides. Wax esters are less prone to hydrolysis and generally need stronger conditions. Quantitative hydrolysis of beeswax long chain esters has been obtained using 10% KOH in ethanol assisted by microwaves, for 60 min at 80 °C and at 200 W [21].

In the case of paint samples where lipids are often admixed with proteinaceous binders, in some cases acidic hydrolysis is proposed to simultaneously hydrolyse proteins and triglycerides in the same step [35,36], although in acidic conditions the hydrolysis of triglycerides is not quantitative.

In all cases, in order to make polar molecules volatile so that they can be separated by GC, derivatizing reactions on polar functional groups are usually performed. Carboxylic functional groups can be transformed into the corresponding 2-propyl esters [35], methyl esters [18], ethylchloroformate derivatives [36], *t*-butyldimethylsilyl esters [9] and trimethylsilyl ester derivatives [3,12,30].

The many derivatizing reagents commercially available include methanolic HCl and diazomethane for methylation, and *N,O*-bis(trimethylsilyl)trifluoroacetamide (BSTFA), with or without 1% trimethylchlorosilane (TMCS), for silylation. Using BSTFA, hydroxyl moieties also can be silylated, giving the corresponding trimethylsilyl ethers.

Instead of the wet chemical hydrolysis and derivatization before GC/MS analysis, methods based on pyrolysis-GC/MS with *in situ* thermally assisted hydrolysis and methylation or silylation can be used, as described in detail in Chapters 11 and 12.

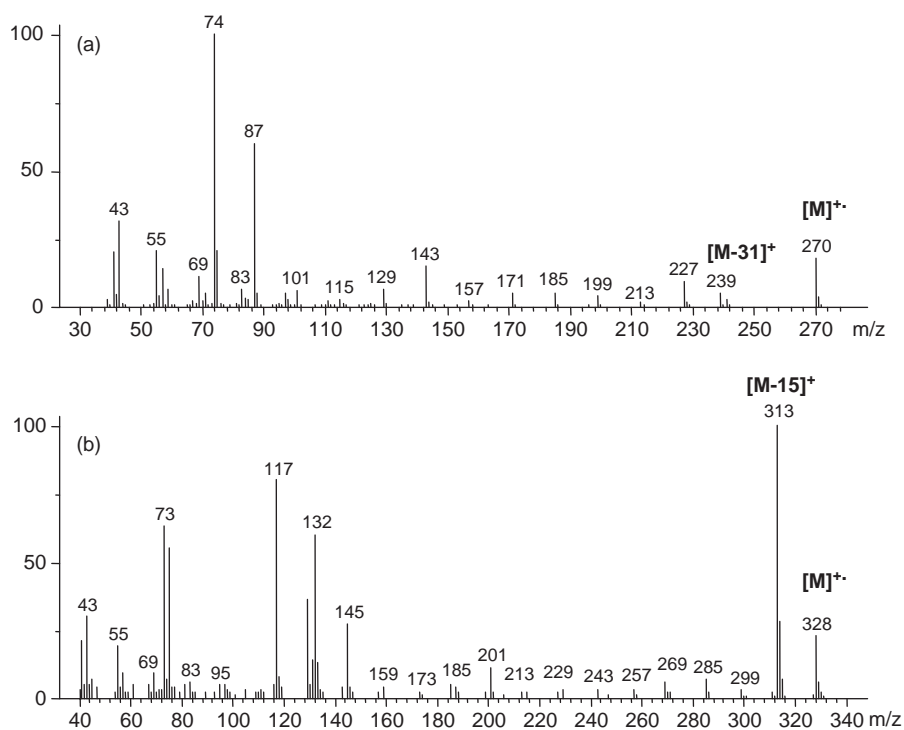
GC/MS separation of mixtures of the compounds are usually performed on capillary columns with low and mid polarity and a length in the range of 30–50 m, with a total separation time of 20–40 min, and temperature ramping from 40 to 300 °C. Total ion current (TIC) profiles are often obtained using ion trap or quadrupole analysers. Quantification is performed by selected-ion monitoring (SIM) detection using calibration curves.

Table 7.1 reports the ions commonly used in SIM acquisition for the quantification of trimethylsilyl (TMS) and *t*-butyldimethylsilyl (TBDMS) derivatives.

As an example, Figure 7.1 shows the mass spectra of palmitic acid, after methylation and trimethylsilylation, respectively. In the mass spectra of FAMES, the molecular ion (in Figure 7.1a it is at  $m/z$  270) is clearly seen, and the ion  $[M-31]^+$ , representing the loss of a methoxyl group as radical, (in Figure 7.1a it is at  $m/z$  239) is abundant. The mass spectra of TMS ethers and esters are characterized by weak or absent molecular ions; the  $[M-15]^+$  (in Figure 7.1b it is at  $m/z$  313) ion formed by loss of a methyl radical is generally abundant and in the case of alcoholic functions, the loss of a trimethylsilanol molecule  $[M-90]^+$  is

**Table 7.1** Ions for trimethylsilyl (TMS) and *t*-butyldimethylsilyl (TBDMS) derivatives of lipid compounds useful for quantitation in selected-ion monitoring

Analyte	TMS derivative ion, $m/z$ (MW-15)	TBDMS derivative ion, $m/z$ (MW-57)
Decanoic acid	229	229
Lauric acid	257	257
Myristic acid	285	285
Pentadecanoic acid	299	299
Palmitic acid	313	313
Heptadecanoic acid	327	327
Oleic acid	339	339
Stearic acid	341	341
Nonadecanoic acid	355	355
Eicosanoic acid	369	369
Oxalic acid	219	261
Malonic acid	233	275
Succinic acid	247	289
Glutaric acid	261	303
Adipic acid	275	317
Pimelic acid	289	331
Suberic acid	303	345
Azelaic acid	317	359
Sebacic acid	331	373
Cholesterol	368 (MW-90)	443

**Figure 7.1** Mass spectra of palmitic acid after (a) methylation and (b) trimethylsilylation

also diagnostic. These two peaks are often used for quantification in SIM. Moreover, the peak at  $m/z$  73, corresponding to the TMS group, is important in nearly all the spectra of TMS derivatives.

Since the analysis of terpenic compounds is often performed together with lipids, silylation has the advantage of being able to differentiate between carboxylic acids and naturally occurring methyl esters, which can be found for example in some terpenic resins and extracted together with lipids.

All the approaches based on a chemolysis step and GC analysis give detailed information on the FA and alcohol profiles, but do not reveal anything about the extent of the hydrolysis of any triglycerides and wax esters in the sample.

Determining the degree of hydrolysis of lipids is particularly interesting when degradation is being studied, since the hydrolysis of the ester bond is one of the main decay paths for triglycerides and wax esters.

To measure the degree of hydrolysis and the distribution of tri-, di- and monoglycerides, the extracts need to be analysed directly by high temperature gas chromatography/mass spectrometry (HTGC/MS). With HTGC/MS molecular mixtures of compounds over a large range of molecular weight can be studied, by adopting short nonpolar capillary columns (10–15 m) with a thin stationary phase and a temperature of up to 350 °C. Acylglycerides and wax esters can be analysed directly using HTGC, which then gives a chromatographic fingerprint of the material without any structural modification. This approach can provide a great deal of valuable information regarding the nature of aged organic residues.

However, direct analysis of extractable compounds only gives information on free, nonpolymeric compounds. Thus, chemolysis is needed even when HTGC is used, to characterize particularly heavy molecules, such as the very long chain esters of carnauba wax [37], or to release molecules involved in polymerized substances, such as the suberin in birch bark tar or reticulated glycerides in oil paintings. In paint samples and in the presence of metal salts, the degradation of triglycerides leads to the formation of metal soaps, which are only solubilized in strong alkaline or acidic conditions. The formation of metal carboxylates known as ‘metal soaps’ has been recently recognized as an important aspect of the appearance and alteration of paint layers, and it is connected to the reactivity of FAs with pigments [38,39].

### 7.3 GC/MS Lipid Data Interpretation

Identifying a specific natural source of lipids after GC/MS analysis is not always straightforward. The occurrence of mixtures, the unspecific FA composition of many lipid materials, the fact that materials may be physically handled during pretreatment before use and the deep changes induced by ageing, mean that extreme caution is required when interpreting FA profiles.

Although predicting the fate of the components in these complex organic materials may be difficult, it is particularly useful to consider the chemical transformations they are likely to have been undergone during preparation, cooking and ageing. Many specific studies in the last 20 years have been carried out by means of artificial ageing and experimental



archaeology, to reconstruct the decay patterns of lipid materials in artworks and in archaeological materials [1,3,6,9,12,13,27,29,30,32,40].

Several processes often occur in lipids, including oxidation, hydration, dehydration, decarboxylation, esterification, aromatization, hydrolysis, hydrogenation and polymerization. In fact, the chemistry of these materials can be affected, for example, by heat (anthropogenic transformations), humidity, pH, and microbial attacks.

All this highlights that it would be quite difficult to distinguish between different oils and fats on the basis of their FA composition after degradation. In particular, if we consider the similarities in the composition of many materials used in ancient times, and how they might have been mixed together, it is clear that the complex molecular patterns exhibited by degraded lipids mean that the specific source cannot be identified, except on favourable occasions.

Sometimes it is possible only to assess the presence or absence of glycerolipids.

Animal and dairy fats can be differentiated from plant lipids on the basis of the FA distribution: animal fats generally contain less palmitic acid than stearic acid, while palmitic acid predominates over stearic acid in plant oils.

Plant lipids generally have an even number of carbon FAs, while animal lipids include odd-numbered carbon chain FAs, and, in some cases, branched chain FAs formed by bacterial activity in the digestive tract of ruminant mammals [5,41]. Branched FAs can also be formed in low amounts from other kind of lipids as a result of microbial activity after burial.

Sterols are seldom detected in archaeological residues due to their low concentration and the tendency to undergo chemical degradation. In any case, the presence of sterols or of their oxidation products in a sample can help distinguish between animal and plant lipid materials: cholesterol is the most abundant animal sterol, while campesterol and sitosterol are the two major plant ones.

Only a few specific kinds of lipids can be identified on the basis of the characteristic features of the FA profile and the presence of specific biomarkers. For example, oils obtained from the seeds of *Brassicaceae*, such as rapeseed oil, are characterized by abundant amounts of uncommon FA such as gondoic (Z-11-eicosenoic) acid and erucic (Z-13-docosenoic) acid and, after ageing their oxidation products. Other examples are reported in Table 7.2 and in Chapter 1.

Interpreting FA profiles in archaeological food residues is particularly difficult due to the general predominance of palmitic acid and stearic acid, to the depletion of unsaturated acyl chains after heating, and to the mixing of the original materials which normally makes the FA profile quite unspecific. Although there has always been an interest in studying the residues found in association with archaeological objects, the full potential of lipid molecular fingerprints in biomolecular archaeology and biomolecular palaeontology has not yet been reached. Gas chromatography/combustion-isotope ratio mass spectrometry (GC/C/IRMS) FA analysis is proving to be a complementary tool for investigating the source of lipids in food residues and sediments, for example for distinguishing between ruminant and monogastric animal lipids, as described in Chapter 14.

The analysis of paint samples represents a peculiar case, in which the identification of lipids is made virtually possible by the fact that the range of used materials is limited to drying oils (linseed, poppy seed, walnut, tung), egg yolk, and beeswax. Safflower oil (from

**Table 7.2** Some examples of lipid chemical features and molecular biomarkers that have been used to highlight lipid sources in archaeological organic residues

Molecular profile	Lipid source	Reference
Odd-numbered carbon branched and straight-chain fatty acids (C <sub>15</sub> , C <sub>17</sub> and C <sub>19</sub> ), positional isomers of octadecenoic acid	Fat from ruminant animals	[5]
Isoprenoid fatty acids (4,8,12-trimethyl-tetradecanoic acid and phytanic acid), $\omega$ -( <i>o</i> -alkylphenyl)alkanoic acids with 16, 18 and 20 carbon atoms	Heated marine lipids	[42,43]
Hydroxyoctadecanoic (ricinoleic) acid, 9,12-dihydroxyoctadecanoic acid	Castor oil	[17,44]
Z-11-eicosenoic (gondoic) acid, Z-13-docosenoic (erucic) acid, 11,12-dihydroxyeicosanoic acid, 13,14-dihydroxydocosanoic acid	Oils from <i>Brassicaeae</i> seeds	[12,44,45]
Odd-numbered carbon alkanes, abundant palmitic acid, tetracosenoic (lignoceric) acid, palmitate esters, long-chain alcohols	Beeswax	[11,23,27]
<i>n</i> -Nonacosane, nonacosane-15-one, nonacosan-15-ol	<i>Brassica</i> leaf wax	[32,46]
Coprostanol (5 $\beta$ -coprostanol), lithocholic acid, cholest-5-en-7-one-3 $\beta$ -ol	Manure, faecal deposition	[4,47,48,49]

the seeds of *Carthamus tinctorius*) and sunflower oil have also been used, alone or mixed with other drying oils to enhance the siccative properties.

The product of cross-linking and oxidation processes in drying oils is described as a porous polymeric fraction with a wide range of molecular weight. The chemical structure that can be influenced by age, thickness and the presence of pigments, while nonbonded species are present in the interstices: free mono- and dicarboxylic acids, mono-, di- and triglycerides, aldehydes, ketones, etc.

Lipids are generally identified in paint samples by evaluating characteristic ratio values of FA amounts and comparing them with naturally or artificially aged reference paint layers. Molar or weight contents are obtained after quantification based on calibration curves.

High amounts of  $\alpha,\omega$ -dicarboxylic acids (mainly suberic, azelaic and sebacic) in a paint sample are indicative of the presence of an aged drying oil. This is because dicarboxylic acids, of which azelaic is the most abundant, are produced during the auto-oxidation of the polyunsaturated acyclic chain present in drying oils.

The ratio between the amounts of azelaic and palmitic acids (A/P) is a parameter for differentiating drying oils from egg lipids in paint samples because the amount of dicarboxylic acid formed in the ageing of egg lipids is considerably less than it is in drying oils. Values of A/P >1 indicate a drying oil, values of A/P <0.3 are typical of egg lipids,

while intermediate values of the A/P ratio are observed for 'tempera grassa', where egg and a drying oil are mixed together. The sum of the amounts of dicarboxylic acids ( $\Sigma D$ ) can also be used as an index to identify the type of lipid binder: generally,  $\Sigma D$  is much more than 30% of the total FA content if drying oil is the only lipid binder, and  $\Sigma D$  is less than 10% if there are no drying oils. Clearly, A/P and  $\Sigma D$  are strictly dependent on the level of oxidation, degradation and polymerization, so the values observed are influenced by many factors such as the pre-heating of the oil media before use, the age of the paint, the conservation environment, and the interaction with pigments.

When heating treatments are applied to obtain stand oils, the following chemical modifications are likely to occur: cross-linking of triacylglycerols, isomerization of double bonds, and formation of dimers through Diels-Alder cyclization [50,51]. As a result of double bond isomerization, the amounts of suberic and sebacic acids increase with respect to azelaic acid. Consequently, the ratio of suberic acid to azelaic acid may help to indicate a pre-polymerized oil [52,53].

The quantification of glycerol, in addition to FAs and dicarboxylic acids, has also been found to be useful in identifying drying oils in paint samples. The ratios of palmitic acid to glycerol (P/G), and of azelaic acid to glycerol (A/G), help us to understand the chemical transformations occurring during curing and ageing [8].

The ratio of palmitic acid to stearic acid (P/S) can be used to differentiate between drying oils, since these two saturated monocarboxylic acids are less subject to chemical reactions during treatment and ageing. Also, they have a similar chemical reactivity, so their ratio can be hypothesized to be relatively unaltered during ageing. The P/S ratio approach was pioneered by Mills [10], and has been subsequently adopted in a number of studies [7–9]. Typical values of the P/S ratio are 1–2 for linseed oil, 2–3 for walnut oil, 3–8 for poppy seed oil and 2.5–3.5 for egg.

Evaluating the P/S ratio requires particular care: first, because of the presence of mixtures of more than one binder, such as egg and oil in 'tempera grassa'; secondly, due to the presence of waxes, and in particular beeswax, which has been widely used as a coating and restoration material; and thirdly, due to the contribution of FAs from other sources such as fouling or micro-organisms, which can considerably alter the P/S values from those expected for reference materials. For instance, because the ratio for walnut oil falls between the value of linseed oil, poppy oil and egg lipids, using the P/S ratio it is not possible to differentiate between pure walnut oil, and mixtures of linseed and poppy oil or egg.

A recent study on artificially aged paint layers highlighted the possible decrease of P/S ratio with ageing, due to the preferential loss of palmitic acid with respect to stearic acid, under the influence of the concentration of pigments [38].

Calculating the P/S ratio from the corresponding peak area ratios or by using one point calibration method leads to erroneous interpretations [54] because the P/S ratio depends on sample dilution. An accurate quantitation of FA is thus needed to evaluate this important parameter correctly.

The ratio of oleic acid to stearic acid (O/S) is another parameter used for assessing the degree of ageing of a lipid paint binder. This ratio is considered as an index of oxidation because the oleic acid double bond is particularly reactive towards oxidation, so normally the content of oleic acid in aged paintings is very low, with an O/S value around 0.1–0.2 [55].

The differentiation of lipid media in samples from artworks on the basis of their sterol content has been attempted, but the tendency of sterols to oxidize means that they can rarely be detected in thin paint layers [56].

Natural waxes are another class of lipids of extreme interest in cultural heritage. Analytical methods based both on HTGC/MS [3,13,23,24,26,27,31,57] and GC/MS [11,13,21,30] are regularly used to identify these materials in archaeological finds and works of art. Waxes tend to be very stable over time, and have a very specific composition. The methods that use HTGC/MS base the identification of waxes on the presence and the distribution of long chain hydrocarbons, long chain FAs, long chain esters and long chain hydroxy esters. Beeswax is characterized by odd-numbered linear hydrocarbons (C21–C33), even-numbered long chain FAs (C22–C34 peaking at C24), long chain palmitate esters (C40–C52 peaking at C46), and long chain hydroxypalmitate esters (C40–C52) when the solvent-soluble fraction is analysed directly. Due to the low volatility of the main constituents of beeswax, analytical methods based on conventional GC/MS need a preliminary hydrolysis step to break down the esters and identify them in terms of the occurrence of odd-numbered linear hydrocarbons (C21–C33), even-numbered long chain FAs (C22–C34 peaking at C24) and long chain alcohols (C24–C34 peaking at C30) produced in the cleavage of ester bonds, and the presence of very high proportions of palmitic acid.

Although beeswax is a very stable and chemically inert material, studies have verified that the composition of beeswax found in archaeological environments may show some significant alterations compared with that of fresh material. The main changes observed are due to:

- the partial hydrolysis of the esters, leading to the formation of free palmitic acid and long chain alcohols;
- partial alteration of the distribution (depletion or disappearance) of the odd-numbered hydrocarbons [11,13, 23,24].

This phenomenon has been investigated [27] by artificially ageing beeswax. It was hypothesized that the loss of alkanes was due either to the fact that the wax was heated during use or to its sublimation over the centuries under particular environmental conditions. Figure 7.2 summarizes the chemical mechanisms involved in beeswax degradation [27].

Other waxes have not been studied to the same extent as beeswax. They derive from a variety of plant, animal and also mineral sources, as described in Chapter 1, where more detailed information on their chemical composition is reported. HTGC/MS analysis after solvent extraction has been successfully used to identify spermaceti, candellila and Japan waxes which have been used in the manufacture of works of art [37]. In particular, in the case of spermaceti wax it has been possible to understand the structure of the various isomers of even-numbered esters ranging from C<sub>26</sub> to C<sub>34</sub>, as well as odd-numbered esters detected in low amounts. The mass spectra obtained demonstrated for the first time that spermaceti esters are mainly composed of hexadecanol and octadecanol moieties associated with a range of FAs containing 10–20 carbon atoms.

The following subsections describe some case studies dealing with GC/MS procedures used to investigate lipid materials in archaeological objects and paintings.

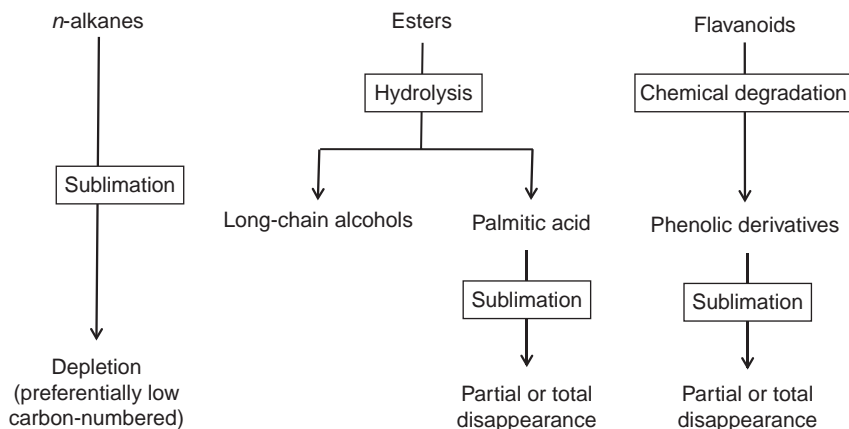


**Figure 7.2** Summary of the main chemical transformations undergone by beeswax during accelerated ageing tests. Reprinted from *Archaeometry*, 2001, **43**, 549–569, Regert, Colinart, Degrand and Decavallas, with permission from Wiley-Blackwell

### 7.3.1 Case Study 1: Analysis of Residues of Illuminants in Roman Lamps from Antinoe (Egypt)

The Necropolis of Antinoe is located about 9.5 km south of Beni Hasan, in a village called Sheikh Abada, on the east bank of the Nile, in Egypt, about 300 km south of Cairo. Findings include various types of ceramic vessels (bowls, plates, balms, censers) dated between the sixth and seventh centuries AD. The collection of ceramics, which is now kept at the Istituto Papirologico Vitelli in Florence (Italy) [58], has meant that the residues of the products that people cooked, stored or otherwise used in Roman Egypt can be chemically studied. The results described below relate to the analysis of residues of the dark material in two clay lamps (nos 718 and 809) of the collection.

After alkaline hydrolysis and extraction of acidic and neutral compounds, the samples were submitted to GC/MS analyses. They gave similar chromatographic patterns, as shown in Figure 7.3.

The acidic extracts consisted of a series of linear monocarboxylic saturated FAs ranging from 9 to 24 carbon atoms with hexadecanoic acid (palmitic) and octadecanoic acid (stearic) as the most prominent; along with a high abundance of long chain acids ( $C_{20}$ – $C_{24}$ ), a series of  $\alpha,\omega$ -dicarboxylic acids, ranging from 4 up to 14 carbon atoms, with nonanedioic acid (azelaic) as the main constituent of this group; a series of  $\omega$ -hydroxycarboxylic acids ranging from 8 up to 14 carbon atoms; and three long chain dihydroxycarboxylic acids with 18, 20 and 22 carbon atoms, namely, 9,10-dihydroxyoctadecanoic acid, 11,12-dihydroxyeicosanoic acid and 13,14-dihydroxydocosanoic acid. Each of the dihydroxycarboxylic acids is present as a pair of *threo-erythro* isomers. The predominance of C9 dicarboxylic acid (azelaic acid) together with the presence of 9,10-dihydroxylated acids indicates that oxidation in position 9 of the acyclic chain has occurred. In particular, 9,10-dihydroxyoctadecanoic acid is known to be formed from oleic acid.

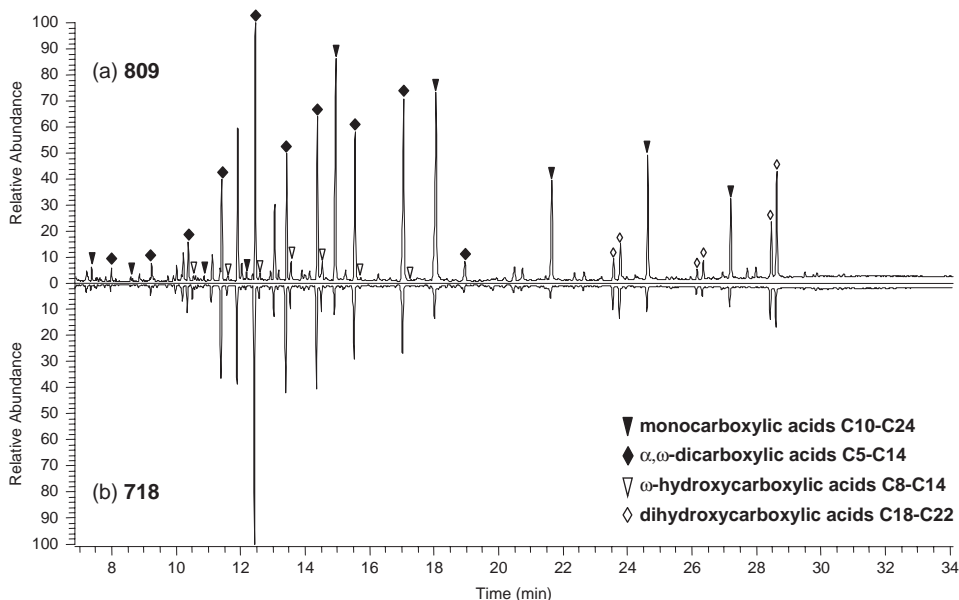


**Figure 7.3** GC/MS chromatogram of the acidic fraction of (a) sample 809 and (b) sample 718 [12]

With the same mechanism, 11,12-dihydroxyeicosanoic acid and 13,14-dihydroxydocosanoic acid, which are a very distinctive feature of these samples, can be directly ascribed to the oxidation processes of gondoic and erucic acids. Since the only seed oils that contain high amounts of gondoic and erucic acids are those derived from *Brassicaceae* [12,59,60], the results obtained can be interpreted as chemical evidence of a seed oil derived from the *Brassicaceae* species used for lighting purposes. Of the various oil sources, *Brassicaceae* (known also as *Cruciferae*) seeds are mentioned as having being used in ancient times in North Africa and in many parts of Europe and Asia. *Brassica* spp. (turnip and rape), *Raphanus sativus* (radish) and *Sinapis* spp. (mustard) are among the possible sources. *Brassicaceae* seeds have been found in several archaeological sites [1,60]. The most ancient seeds described in the literature as *Brassica* spp. and *Sinapis* spp. were found in Mesopotamia (3000 BC) as charred residues [1].

Radish oil is supposed to be one of the most common oil crop products in Roman Egypt [61], as mentioned also by Pliny in *Naturalis Historia* (XV:7; XIX:26), though the source of this oil may not only be *Raphanus sativus* but other *Cruciferae* species as well.

It is impossible to reveal the botanical species from which the seed oil used in the examined lamps was actually produced, e.g. to say whether the oil came from radish as reported by Pliny or from another *Brassicaceae* plant such as rapeseed. However, the detection of the characteristic markers in lamps from Antinoe, one of the main urban centres of Roman Egypt, represents a chemical confirmation of the widespread use of cruciferous oil at that time, and is consistent with ancient documents [61,62]. This identification is

supported by the results obtained in the ageing tests and analysis performed on *Brassica juncea* oil and on the pure gondoic and erucic acids. It has been possible to demonstrate that 11,12-dihydroxyeicosanoic acid and 13,14-dihydroxydocosanoic acid are markers for cruciferous seed oil in archaeological residues [12,44].

### 7.3.2 Case study 2: Analysis of Residues in Glass Unguentaria from Oplontis (Naples, Italy)

Gas chromatographic and mass spectrometric techniques, including HTGC/MS and GC/MS of neutral and acid fractions, were employed to study the composition and to identify the origins of the organic materials used to manufacture balm residues surviving in a series of glass unguentaria recovered from the excavations of a Roman villa in the ancient town of Oplontis (Naples, Italy) [13]. The results highlight the complexity involved in the interpretation of molecular fingerprints of mixtures of lipids of unknown origin.

HTGC/MS and GC/MS analyses provided detailed molecular compositions, and showed the presence of a wide range of compound classes including mid and long chain FAs, long chain hydroxy acids, *n*-alkanols, alkandiol, *n*-alkanes, long chain monoesters, phytosterols and diterpenoid acids. Figure 7.4 shows the TIC profile of the trimethylsilylated TLEs of the contents of a glass unguentarium 73291 obtained by HTGC/MS.

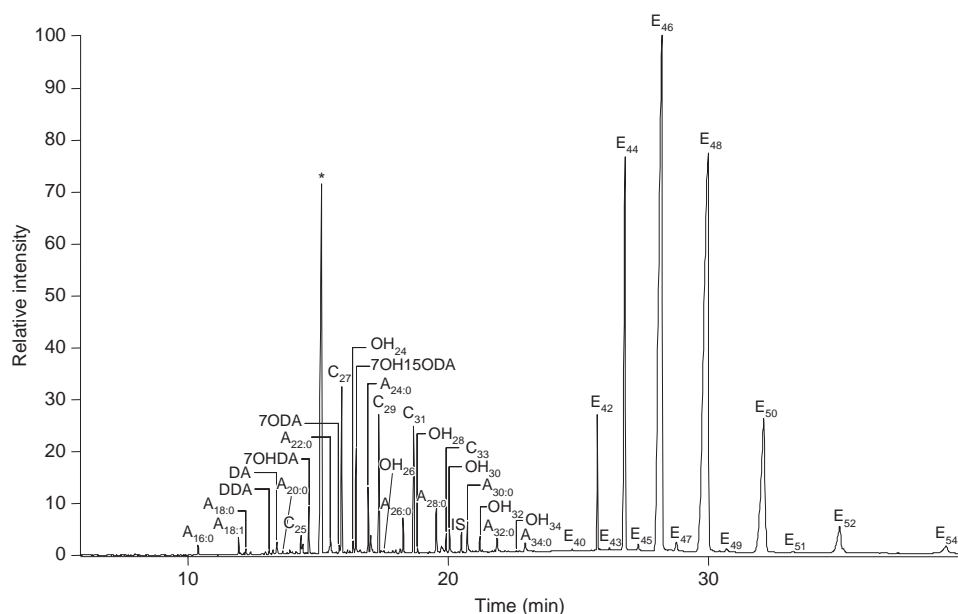


**Figure 7.4** Total ion current profile of the trimethylsilylated total lipid extracts of the contents of a glass unguentarium 73291 obtained by HTGC/MS.  $A_{x,y}$ , FAs of chain length  $x$  and degree of unsaturation  $y$ ;  $C_x$ , *n*-alkanes of chain length  $x$ ;  $OH_x$ , *n*-alkanols of chain length  $x$ ;  $E_x$ , long chain monoesters of chain length  $x$ ; DDA, didehydroabiatic acid; DA, dehydroabiatic acid; 7OHDA, 7-hydroxy-dehydroabiatic acid; 7ODA, 7-oxo-didehydroabiatic acid; 7OH15ODA, 7-hydroxy-15-oxo-dehydroabiatic acid; IS, *n*-tetratriacontane internal standard [13]



Characteristic biomarkers and their distributions indicate the presence of beeswax, *Pinaceae* resin and another wax, as the main organic constituents of all of the preparations examined. The occurrence of phytosterols and of long chain monoesters (odd and even long chain esters in the C40–C54 range), in which the acyl moiety was not exclusively palmitic acid, suggested the presence of a second waxy-lipid constituent of plant origin. The mass spectrum observed for the chromatographic peak attributed to a long chain ester containing 50 carbons is reported in Figure 7.5. The fragments clearly indicate that several esters co-elute. In fact, long chain esters are known to provide one main fragment characteristic of the acid moiety of the ester, namely  $[C_nH_{2n}CO_2H+H]^+$  [3], while the mass spectra recorded for the contents from the unguentaria present several peaks and seem to indicate that every chromatographic peak could be associated with several (from two to six) aliphatic long chain monoesters with the same molecular weight. In the mass spectrum of E<sub>50</sub> carbon atoms (Figure 7.5), the peaks at  $m/z$  257, 285, 313, 341, 369 and 397 indicate the co-elution of triacontanyl-hexadecanoate, octacosanyl-octadecanoate, hexacosanyl-eicosanoate, tetracosanyl-docosanoate, docosanyl-tetracosanoate and eicosanyl-hexacosanoate, respectively. The mass spectrum of each chromatographic peak provides the qualitative composition of the isomeric mixture and allows us to quantitatively evaluate the various isomers present. Interestingly, the composition of the various isomeric mixtures of each chromatographic peak is almost constant in the seven samples investigated, suggesting a common origin.

The results are consistent with the beeswax that was used in the preparation of the cosmetics preserved in the unguentaria, while the other lipids are most likely the residue of

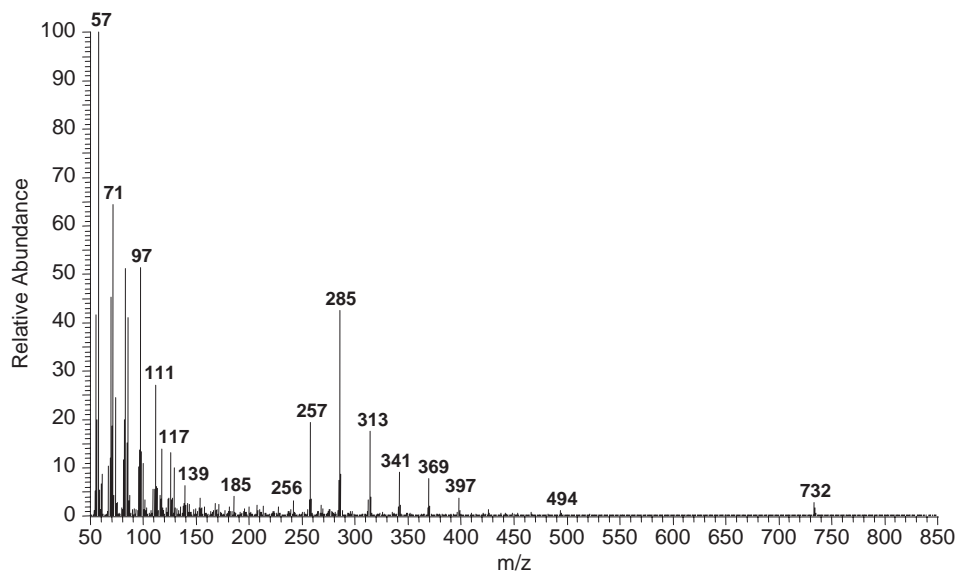


**Figure 7.5** Mass spectrum of the chromatographic peak labelled E<sub>50</sub> in Figure 7.4, corresponding to a long chain monoester containing 50 carbon atoms, observed in the HTGC/MS analysis of the content of a glass unguentarium 73291 [13]



some as yet unidentified plant extract(s), possibly deriving from the cuticular waxes of flowers and/or leaves.

### 7.3.3 Case Study 3: Characterization of Lipid Paint Binders in Paintings

A painting is a complex heterogeneous matrix, whose chemical composition continuously changes over the course of time depending on several factors: specific interactions between pigment and binder, conservation conditions such as changes in temperature and humidity, exposure to air pollutants, and prolonged exposure to natural or artificial light.

In the last few years the characterization of the organic constituents of paint media by GC analysis has received increasing attention, due to the fact that organic materials used as binders or varnish are likely to be involved in the degradation process.

Among the various organic substances used by artists in the past, traditional paint binders of a lipid nature are represented by egg yolk in the tempera technique and drying or siccative oils in the oil technique. Drying oils have been used both in easel paintings and in wall paintings. In addition to being widely adopted as paint media, drying oils were used as ingredients of gilding mordents and paint varnishes in Europe and in the Mediterranean area, often mixed with natural terpenic resins. Drying oils in Europe were not only used in easel paintings, but also on wall paintings, for example 'The Legend of the True Cross' by Piero della Francesca, in the church of St Francesco in Arezzo (Italy), which dates back to 1452 [63].

Many studies have characterized lipids in paintings and, as seen in the previous sections, the determination of the FA profile by GC/MS is the most common approach for the identification of lipid paint materials [6,8,10,55]. For restoration and preservation purposes, it is important not only to identify the original substances used in the painting, but also to characterize their degradation products. For this reason, and due to the necessity to minimize sampling from painted artworks, research in this field has often involved the preparation of collections of reference paint layers, using traditional materials and techniques reconstructed on the basis of old treatises. These are then used to validate analytical procedures, highlight interactions between inorganic and organic paint materials, and investigate ageing patterns. [9,38,64]. Natural and artificial ageing by means of light, heat and exposure to environmental pollutants have played a prominent role in the advancement of the knowledge in paint media analysis and conservation.

The chromatogram in Figure 7.6 shows a typical profile of an aged drying oil. It was obtained in the analysis of a reference layer of linseed oil on glass pertaining to the reference paint material collection of Opificio delle Pietre Dure (Florence, Italy), artificially aged by irradiation with a mercury lamp at 365 nm for 21 days, at a temperature of 20 °C and 80% relative humidity [9].

The profile is characterized by substantial amounts of dicarboxylic acids, mainly formed in the oxidation of polyunsaturated C18 acids (linoleic acid, C18:2 and linolenic acid, C18:3), which are no longer detected after ageing. The presence of short chain dicarboxylic acid, and in particular of oxalic acid, is also characteristic of aged lipid layers. Moreover, in the 30–35 min interval, several peaks are detected and attributed to oxidized species of unsaturated C18 acids. Figure 7.7 reports the mass spectrum of the peak at 31.84, attributed to 13-OH-9-octadecenoic acid or 14-OH-9-octadecenoic acid. Its

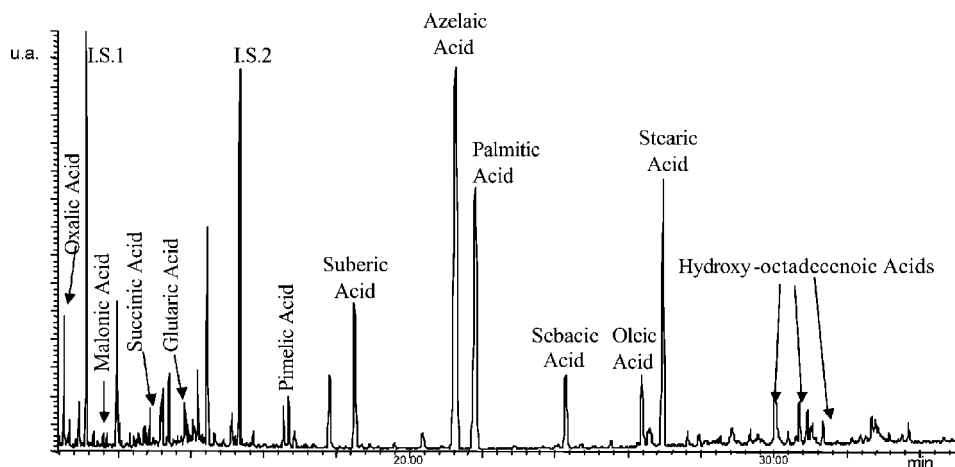


**Figure 7.6** Total ion current profile of the acidic fraction of a sample from a linseed oil reference paint layer (Opificio delle Pietre Dure, Florence, Italy), after saponification and silylation of carboxylic and hydroxylic groups [9]

*N*-methyl-*N*-trimethylsilyl (MTBS) derivative is characterized by fragments at  $m/z$  469 ( $M-57^+$ , loss of a *t*-butyl group), 413 ( $469-57 + H^+$ , corresponding to the loss of another *t*-butyl group and the addition of one proton). The fragments at  $m/z$  73, 75, 117, 129, 147 are due to rearrangement of the silyl moiety. The fragment at  $m/z$  337 corresponds to  $[C_{17}H_{31}COOSi(CH_3)_2]^+$ . Further fragmentation depends on the position of the OH group in the chain.

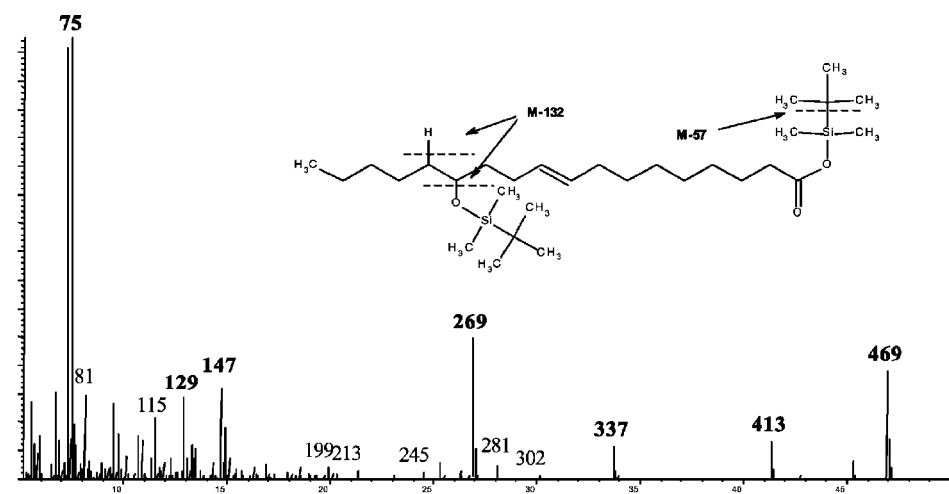


**Figure 7.7** Mass spectrum of the oxidation product corresponding to the peak at 31.84 min in Figure 7.6, identified as 13(14)-OH-9-octadecenoic acid [9]

Other octadecenoic acids carrying hydroxyl groups in the chain are present in the considered time range: their formation derives from the oxidation of the unsaturated C18 FAs linoleic acid, linolenic acid and oleic acid.

To show some examples of the many cases of lipid paint materials reported in the literature, Table 7.3 reports the results of characteristic parameters obtained in the quantitative analysis of FAs in a series of samples (<1 mg) from paintings on various supports.

*'Madonna con Bambino in Trono e due Angeli' by Cimabue.* The TIC profile obtained by GC/MS for the acidic fraction of the sample is shown in Figure 7.8. The low value of the A/P ratio and the low content of dicarboxylic acid ( $\Sigma D$ ) meant that the presence of a drying oil could be ruled out, and the lipid material in the sample was attributed to the use of egg yolk as binder. This was further confirmed by quantitative amino acid analysis [66]. Though the presence of egg was fully evident, the P/S value has a lower value than expected for egg: the constancy of this ratio is still a matter of debate, and has been discussed in the literature [38]. An explanation for this phenomenon is that the deposition on the paint layer of fouling containing stearic acid can also contribute to lowering the value of the P/S ratio. Oxalic acid was detected in considerable amounts, giving indication of oxidation of organic matter. In the chromatogram, peaks identified as derivatives of abietadiene acid, dehydroabietic acid and 7-oxo-dehydroabietic acid highlight the use of colophony, which was probably used as a coating. In the unsaponifiable fraction, neither cholesterol nor its oxidation products were detected, confirming the hypothesis that sterols tend to be completely degraded and no longer detectable in aged paintings.

**Table 7.3** Characteristic parameters for lipid identification in samples from some works of art

	P/S	A/P	O/S	$\Sigma D$	Ref.
Panel painting 'Madonna con Bambino in Trono e due Angeli' attributed to Cimabue (1240–1302) and conserved in the National Gallery (London). The sample contained white lead and ultramarine blue pigments	0.8	0.1	0.6	2.8	[9]
Sample collected from a painting on copper leaf by F. Boucher, dated 1750, containing white lead, Prussian blue and carbon black pigments	1.8	1.0	0.3	31.0	[9]
Sample from the easel painting 'Dama con Liocorno' by Raffaello (1505–1506, Galleria Borghese, Rome). The sample contained white lead and azurite pigments	2.5	1.8	0.2	62.4	[9]
Sample from the wall painting in the Messer Filippo cell, in the medieval Tower of Spilamberto (Modena, Italy). The sample contained red earth rich in Fe(III) oxides (haematite and goethite)	1.9	0.3	0.0	27.2	[65]

P/S, palmitic acid vs stearic acid; A/P, azelaic acid vs palmitic acid; O/S, oleic acid vs stearic acid;  $\Sigma D$ , sum of dicarboxylic acids (suberic, azelaic and sebacic).

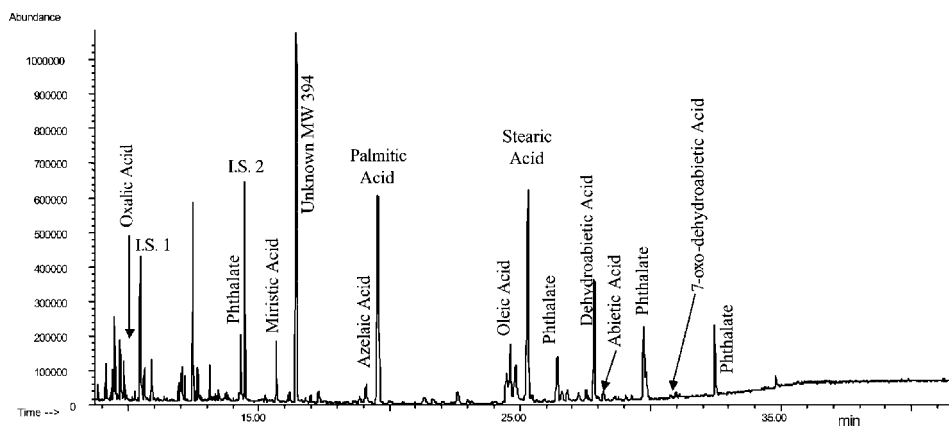


**Figure 7.8** Total ion current profile of the MTBS derivatives in the acidic fraction of a sample from 'Madonna con Bambino in Trono con Angeli' (Cimabue) [9]

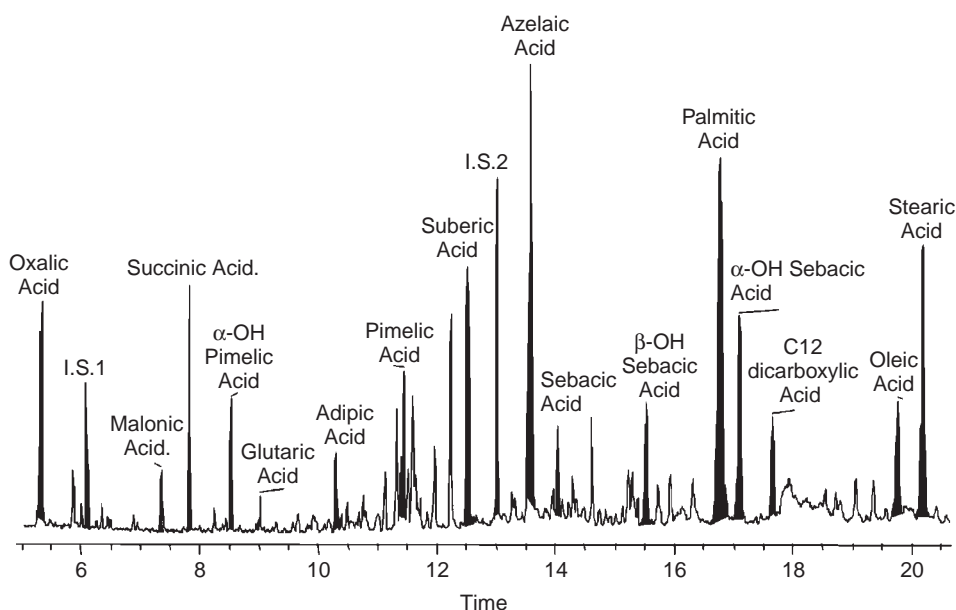


**Figure 7.9** Total ion current profile of the TMS derivatives in the acidic fraction of a sample from a painted copper leaf (Boucher) [9]

*Painting on copper leaf by Boucher.* Figure 7.9 shows the TIC profile relative to the TMS derivatives of FAs from the sample [9]. The values of the parameters reported in Table 7.3 indicate that the binder was linseed oil. The FA composition shows a high content of dicarboxylic acid together with oxidation products. In this case, due to the

presence of metallic copper as a support, it may be hypothesized that the metal increases the speed of the oxidation processes, thus facilitating the formation of different degradation compounds: short chain dicarboxylic acids are produced in significant amounts.

'*Dama con Liocorno*' by Raffaello. The analysed sample contained a substantial amount of dicarboxylic acid, which highlights the presence of a drying oil, as suggested by the values reported in Table 7.3. The high P/S value highlights that lipids from egg yolk were also present, and again the presence of egg was confirmed by protein analysis [9]. As in the above case, no cholesterol or cholestenes were detected. The O/S ratio showed an almost complete degradation of the unsaturated oleic acid, while a high amount of oxalic acid was found. An extensive oxidation of the paint layer occurred and, as suggested when white lead is present, the formation of short dicarboxylic acids was favoured with respect to hydroxy-C18 acids.

*Wall painting in the Messer Filippo cell, Tower of Spilamberto (Modena, Italy).* The painted surface is in an advanced state of deterioration: the detachment of the pictorial matter from the plaster is evident, efflorescence is present, and the pictorial coating is almost completely covered by a grey-whitish film formed by microcrystalline gypsum, as proved by micro-Raman investigations. The FA profile, characterized by an A/P ratio of 0.3, suggests that the lipid does not derive from a drying oil, and is compatible with egg lipids. Protein analysis highlighted an amino acid pattern compatible with that of egg, so a tempera technique may have been used [65]. In the chromatograms, phosphates, sulfates and oxalates were also detected. Phosphates are related to the presence of the egg protein, oxalates are the degradation products of organic compounds due both to bio-organism metabolism and chemical oxidation of the egg substrate, and sulfates are related to the formation of gypsum.

The analytical techniques proposed in the literature generally give reliable information on lipids present in the paint layer. However, the presence of lipid mixtures and of particular environmental conservation conditions may affect the lipid pattern to such an extent that their identification may be very difficult and sometimes erroneous. Thus, a multianalytical approach is recommended which integrates chromatographic data with techniques such as mapping based on Fourier transform infrared spectroscopy or SIM on cross-sections, in order to better understand the distribution of lipids in the various paint layers.

## References

1. Serpico M., White R. *Ancient Egyptian Materials and Technology*, eds P. Nicholson and I. Shaw, Cambridge University Press, Cambridge, 2000: 390–429.
2. Evershed R.P., Organic residues analysis in archaeology: the archaeological biomarker revolution, *Archaeometry*, 2008, **50**, 895–924.
3. Evershed R.P., Biomolecular analysis by organic mass spectrometry, in *Modern Analytical Methods in Art and Archaeology*, eds E. Ciliberto and G. Spoto, Wiley Interscience, New York, 2000: 177–239.
4. Evershed R.P., Biomolecular archaeology and lipids, *World Archaeology*, 1993, **25**, 74–93.
5. Evershed R.P., Dudd S.N., Copley M.S., Berstan R., Stott A.W., Mottram H., Buckley S.A., Crossman Z., Chemistry of archaeological animal fats, *Accounts of Chemical Research*, 2002, **35**, 660–668.

6. Mills J.S., White R., *The Organic Chemistry of Museum Objects*, Butterworth-Heinemann, Oxford, 1994: 31–44.
7. Casadio F., Giangualano I., Piqué F., Organic materials in wall paintings: the historical and analytical literature, *Reviews in Conservation*, 2004, **5**, 63–80.
8. Shilling M.R., Khanjian H.P., Gas chromatographic determination of the fatty acid and glycerol content of lipids. I: The effects of pigments and ageing on composition of oil paints, *ICOM Committee for Conservation Preprints 11th Triennial Meeting*, James and James, London, 1996: 220–227.
9. Colombini M.P., Modugno F., Fuoco R., Tognazzi A., A GC/MS study on the deterioration of lipidic paint binders, *Microchemical Journal*, 2002, **73**, 175–185.
10. Mills J.S., The gas chromatographic examination of paint media. Part I: Fatty acid composition and identification of dried oil films, *Studies in Conservation*, 1966, **11**, 92–107.
11. Colombini M.P., Giachi G., Modugno F., Pallecchi P., Ribechini E., Characterisation of paints and waterproofing materials of the shipwrecks found in the archaeological site of the Etruscan and Roman harbour of Pisa (Italy), *Archaeometry*, 2003, **45**, 649–664.
12. Colombini M.P., Modugno F., Ribechini E., Organic mass spectrometry in archaeology: evidence for Brassicaceae seed oil in Egyptian ceramic lamps, *Journal of Mass Spectrometry*, 2005, **40**, 890–898.
13. Ribechini E., Modugno F., Colombini M.P., Evershed R.P., Gas chromatographic and mass spectrometric investigations of organic residues from Roman glass unguentaria, *Journal of Chromatography A*, 2008, **1183**, 158–169.
14. Colombini M.P., Giachi G., Modugno F., Ribechini E. Characterisation of organic residues in pottery vessels of the Roman age from Antinoe (Egypt). *Microchemical Journal* 2005, **79**, 83–90.
15. Ribechini E., Modugno F., Baraldi C., Baraldi P., Colombini M.P., An integrated analytical approach for characterizing an organic residues from an archaeological glass bottle recovered in Pompeii (Naples, Italy), *Talanta*, 2008, **74**, 555–561.
16. Gülaçar F.O., Buchs A., Susini A. Capillary gas chromatography-mass spectrometry and identification of substituted carboxylic acids in lipids extracted from a 4000-year-old Nubian burial. *Journal of Chromatography* 1989, **479**, 61–72.
17. Tchaplá A., Mejanelle P., Bleton J., Goursaud S. Characterisation of embalming materials of a mummy of the Ptolemaic era. Comparison with balms from mummies of different eras. *Journal of Separation Science*, 2004, **27**, 217–234.
18. Mottram H.R., Dudd S.N., Lawrence G.J., Stott A.W., Evershed R.P., New chromatographic, mass spectrometry and stable isotope approaches to the classification of degraded animal fats preserved in archaeological pottery, *Journal of Chromatography*, 1999, **833**, 209–221.
19. Evershed R.P., Dudd S.N., Charters S., Mottram H., Stott A.W., Raven A., Van Bergen P.F., Bland H.A., Lipids as carriers of anthropogenic signals from prehistory, *Philosophical Transactions of the Royal Society of London, Series B: Biological Sciences*, 1999, **354**, 19–31.
20. Kimpe K., Jacobs P.A., Waelkens M. Analysis of oil used in late Roman oil lamps with different mass spectrometric techniques revealed the presence of predominantly olive oil together with traces of animal fat. *Journal of Chromatography A*, 2001, **937**, 87–95.
21. Bonaduce I., Colombini M.P., Characterisation of beeswax in works of art by gas chromatography-mass spectrometry and pyrolysis-gas chromatography-mass spectrometry procedures, *Journal of Chromatography A*, 2004, **1028**, 297–306.
22. Buckley S.A., Stott A.W., Evershed R.P., Studies of organic residues from ancient Egyptian mummies using high temperature-gas chromatography-mass spectrometry and sequential thermal desorption-gas chromatography-mass spectrometry and pyrolysis-gas chromatography-mass spectrometry, *The Analyst*, 1999, **124**, 443–452.
23. Evershed, R.P., Vaughan, S.J., Dudd, S.N., Soles, J.S., Fuel for thought? Beeswax in lamps and conical cups from late Minoan Crete, *Antiquity*, 1997, **71**, 979–985.
24. Heron, C., Nemeck, N., Bonfield, K.M., Dixon, D. Ottaway, B.S., The chemistry of Neolithic beeswax, *Naturwissenschaften*, 1994, **81**, 266–269.

25. Evershed R. P., Heron C., Goad J., Analysis of organic residues of archaeological origin by high-temperature gas chromatography and gas chromatography-mass spectrometry, *Analyst*, 1990, **115**, 1339–1342.
26. Regert M., Investigating the history of prehistoric glues by gas chromatography-mass spectrometry, *Journal of Separation Science*, 2004, **27**, 244–254.
27. Regert M., Colinart S., Degrand L., Decavallas O., Chemical alteration and use of beeswax through time: accelerated ageing tests and analysis of archaeological samples from various environmental contexts, *Archaeometry*, 2001, **43**, 549–569.
28. Regert M., Bland H. A., Dudd S. N., van Bergen P. F., Evershed R. P., Free and bound fatty acid oxidation products in archaeological ceramic vessels, *Proceedings of the Royal Society London B*, 1998, **265**, 2027–2032.
29. Dudd S. N., Regert M., Evershed R. P., Assessing microbial lipid contributions during laboratory degradations of fats and oils and pure triacylglycerols absorbed in ceramic potsherds, *Organic Geochemistry*, 1998, **29**, 1345–1354.
30. Andreotti A., Bonaduce I., Colombini M.P., Gautier G., Modugno F., Ribechini E., Combined GC/MS analytical procedure for the characterization of glycerolipid, waxy, resinous, and proteinaceous materials in a unique paint microsample, *Analytical Chemistry*, 2006, **78**, 4490–4500.
31. Regert M., Langlois J., Laval E., Le Hô A.-S., Pagès-Camagna S., Elucidation of molecular and elementary composition of organic and inorganic substances involved in 19th century wax sculptures using an integrated analytical approach, *Analytica Chimica Acta*, 2006, **577**, 140–152.
32. Evershed R.P., Experimental approaches to the interpretation of absorbed organic residues in archaeological ceramics, *World Archaeology*, 2008, **40**, 26–47.
33. Koller J., Baumer U., An investigation of the 'Lacquers of the West'. A methodical survey, in *Japanese and European Lacquerware*, ed. M. Kühlenthal, Karl M. Lipp Verlag, Munich, 2000: 339–348.
34. Baumer U., Binding media analysis at the Doerner Institut, in *Proceedings of MASC (User's Group for Mass Spectrometry and Chromatography) 2007 GCMS Workshop*, Philadelphia Museum of Art, 2007, <http://www.mascgroup.org>.
35. Casoli A., Musini P.C., Palla G., Gas chromatographic-mass spectrometric approach to the problem of characterizing binding media in paintings, *Journal of Chromatography A*, 1996, **731**, 237–246.
36. Mateo Castro R., Domenech Carbo M.T., Peris Martinez V., Gimeno Adelantado J.V., Bosch Reig F., Study of binding media in works of art by gas chromatographic analysis of amino acids and fatty acids derivatized with ethyl chloroformate, *Journal of Chromatography A*, 1997, **778**, 373–381.
37. Regert M., Langlois J., Colinart S., Characterisation of wax works of art by gas chromatographic procedures, *Journal of Chromatography A*, 2005, **1091**, 124–136.
38. Keune K., Hoogland F., Boon J.J., Peggie D., Higgitt C., Comparative study of the effect of traditional pigments on artificially aged oil paint systems using complementary analytical techniques, *Preprints of 15th Triennial Meeting of ICOM Committee for Conservation* Vol. II, New Delhi, 2008: 833–842.
39. Keune K., *Binding medium, pigments and metal soaps characterized and localized in paint cross sections*, PhD Dissertation, University of Amsterdam, 2005.
40. Barnard H., Ambrose S.H., Beehr D.E., Forster M.D., Lanehart R.E., Malainey M.E., Parr R.E., Rider M., Solazzo C., Yohe II R.M., Mixed results of seven methods for organic residue analysis applied to one vessel with the residue of a known foodstuff, *Journal of Archaeological Science*, 2007, **34**, 28–37.
41. Dudd S. N., Regert M., Evershed R.P., Assessing microbial lipid contributions during laboratory degradations of fats and oils and pure triacylglycerols absorbed in ceramic potsherds, *Organic Geochemistry*, 1998, **29**, 1345–1354.
42. Craig O.E., Forster M., Andersen S.H., Koch E., Crombé P., Milner N.J., Stern B., Bailey G.N., Heron II C.P., Molecular and isotopic demonstration of the processing of aquatic products in Northern European prehistoric pottery, *Archaeometry*, 2007, **49**, 135–152.



43. Hansel F.A., Copley M.S., Madureira L.A., Evershed R.P., Thermally produced  $\omega$ -(*o*-alkylphenyl)alkanoic acids provide evidence for the processing of marine products in archaeological pottery vessels, *Tetrahedron Letters*, 2004, **45**, 2999–3002.
44. Copley M.S., Bland H.A., Rose P., Horton M., Evershed R.P., Gas chromatographic, mass spectrometric and stable carbon isotopic investigations of organic residues of plant oils and animal fats employed as illuminants in archaeological lamps from Egypt, *Analyst*, 2005, **130**, 860–871.
45. Romanus K., Van Neer W., Marinova E., Verbeke K., Luypaerts A., Accardo S., Hermans I., Jacobs P., De Vos D., Waelkens M., Brassicaceae seed oil identified as illuminant in Nilotic shells from a first millennium AD Coptic church in Bawit, Egypt, *Analalytical Bioanalytical Chemistry*, 2008, **390**, 783–793.
46. Evershed R.P., Heron C., Goad L.J., Epicuticular wax components preserved in potsherds as chemical indicators of leafy vegetables in ancient diets, *Antiquity*, 1991, **65**, 540–544.
47. Knights B.A., Dickson C.A., Dickson J.H., Breeze D.J., Evidence concerning the Roman military diet at Bearsden, Scotland in the 2nd century, *Journal of Archaeological Science*, 1983, **10**, 139–152.
48. Lin D.S., Conner W.E., Napton L.K., Heizer R.F., The steroids of 2000-year old human coprolites, *Journal of Lipid Research* 1978, **19**, 215–221.
49. Simpson I.A., van Bergen P.F., Perret V., Elhmmali M.M., Roberts D.J., Evershed R.P., Lipid biomarkers of manuring practice in relict anthropogenic soils, *The Holocene*, 1999, **9**, 223–229.
50. van den Berg J.D.J., Vermist N.D., Carlyle L., Holcapek M., Boon J.J., Effects of traditional processing methods of linseed oil on the composition of its triacylglycerols, *Journal of Separation Science*, 2004, **27**, 181–199.
51. van den Berg J.D.J., Vermist N.D., Boon J.J., MALDI-TOF-MS and ESI-FTMS of oxidized triacyl glycerols and oligomers in traditionally prepared linseed oils used in oil paintings, *Advances in Mass Spectrometry*, 2001, **15**, 823–824.
52. Mills J.S., White R., Organic mass spectrometry of art materials: work in progress, *National Gallery Technical Bulletin*, 1982, **6**, 3–18.
53. Katsibiri O., Boon J.J., Investigation of the gilding technique in two post-Byzantine wall paintings using micro-analytical techniques, *Spectrochimica Acta, Part B: Atomic Spectroscopy*, 2004, **59B**, 1593–1599.
54. Tsakalof A.K., Bairachtari K.A., Chryssoulakis I.D., Pitfalls in drying oils identification in art objects by gas chromatography, *Journal of Separation Science*, 2006, **29**, 1642–1646.
55. Colombini M.P., Fuoco R., Modugno F., Menicagli E., Giacomelli A., GC-MS characterisation of proteinaceous and lipid binders in UV aged polychrome artefacts, *Microchemical Journal*, 2000, **67**, 291–300.
56. Mills J.S., White R., The identification of paint media from the analysis of their sterol composition, *Studies in Conservation*, 1975, **20**, 176–182.
57. Evershed R.P., Dudd S.N., Anderson-Stojanovic V.A., Gebhard E.R., New chemical evidence for the use of combed ware pottery vessel as beehives in ancient Greece, *Journal of Archaeological Science*, 2003, **30**, 1–12.
58. Guidotti, M.C., Pesì, L., *La ceramica da Antinoe nell'Istituto papirologico G. Vitelli*, Studi e Testi di Papirologia, N.S. 6, *Istituto papirologico G. Vitelli, Firenze*, 2004.
59. Grieco D., Piepoli G. Composizione degli acidi grassi contenuti nei lipidi estratti da semi e frutti oleosi. *Rivista Italiana delle Sostanze Grasse*, 1964, **XLI**, 283–287.
60. O'Donoghue K., Clapham A., Evershed R.P., Brown T.A. Remarkable preservation of biomolecules in ancient radish seeds, *Proceedings of the Royal Society London B*, 1996, **263**, 541–547.
61. Mayerson P. Radish oil: a phenomenon in Roman Egypt, *Bulletin of the American Society of Papyrologists*, 2001, **38**, 109–117.
62. Sandy D.B. The production and use of vegetable oils in Ptolemaic Egypt, *Bulletin of the American Society of Papyrologists*, 1989, Supplement 6.
63. Colombini M.P., Francesconi S., Fuoco R., Modugno F., Characterisation of proteinaceous binders and drying oils in wall painting samples by GC-MS, *Journal of Chromatography A*, 1999, **846**, 101–111.



64. Schilling M.R., Khanjian H.P., Carson D.M., Fatty acid and glycerol content of lipids. Part II. Effects of ageing and solvent extraction on the composition of oil paints, *Techne*, 1997, **5**, 71–78.
65. Ospitali F., Rattazzi A., Colombini M.P., Andreotti A., di Leonardo G., XVI century wall paintings in the 'Messer Filippo' cell of the tower of Spilamberto: Microanalyses and monitoring, *Journal of Cultural Heritage*, 2007, **8**, 323–327.
66. Colombini M.P., Modugno F., Menicagli E., Fuoco R., Giacomelli A., GC-MS characterization of proteinaceous and lipid binders in UV aged polychrome artefacts, *Microchemical Journal*, 2000, **67**, 291–300.



# 8

## GC/MS in the Characterisation of Resinous Materials

*Francesca Modugno and Erika Ribechini*

### 8.1 Introduction

In the cultural heritage field, the chemical characterisation of resinous materials is a complex task due to the high number of possible materials and the fact that they are complex mixtures of many similar chemical species from the terpene class. Consequently, characterising these kinds of materials and recognizing them in aged samples, such as those from paintings or archaeological objects, entails characterising the components at a molecular level.

The most widely adopted analytical approach to the study of natural resinous materials is gas chromatography/mass spectrometry (GC/MS) [1–29]. This hyphenated technique reveals the presence of specific compounds that act as biomolecular markers. The use of biomolecular markers for resinous material identification is based on the so-called biomarker concept which originated in the field of ‘chemical fossils’. It is based on the idea that when certain naturally occurring compounds are deposited in a sedimentary environment, they undergo changes as a result of diagenesis and maturation. They lose their functional groups but their basic carbon skeleton remains intact. Thus, it is possible to establish a precursor–product relationship between naturally occurring compounds and their analogues present in the sediments [30]. In archaeological and cultural heritage chemistry, biomarkers are considered as diagnostically stable molecules present in the original material and preserved intact in archaeological environments or formed over the centuries due to ageing. Identifying the molecular composition and, thus the presence of biomolecular markers, is essential in order to gain information about the type of organic

substances that were originally present in an object and to understand the alteration processes that have modified their original composition. More exactly, molecular biomarkers can be related to:

- the botanical origin: the plant source from which the resin or the pitch was obtained;
- the anthropogenic modifications: the alterations and changes in the chemical composition intentionally induced by man before the use of a substance in order to modify its properties in view of a specific use;
- the natural decay: the transformations due to environmental causes and/or ageing.

High performance separation techniques, such as GC coupled with MS, can be used to separate mixtures of terpenes, and then identify them and their relative amounts [1–4]. Unfortunately, in some cases the chromatographic profiles obtained using GC are too complex for a full interpretation. Also, only a few natural terpenoid compounds are commercially available as standards, thus in several cases identification must be based on mass spectra interpretation. For this reason, the analysis of reference raw materials of known botanical origin is an important step in the set up of analytical procedures and for supporting data interpretation. Artificial ageing can also be of great help in providing useful reference materials and for studying decay processes.

The analysis of organic materials by GC/MS requires a pretreatment of the sample, one important step being the extraction of the compounds of interest from the matrix. This is crucial with resinous materials from historical objects due to the uniqueness of such samples and to the small amount of the organic fraction usually contained in them. This means the extraction methods must be highly efficient. The methods generally adopted can be divided into three main groups:

- Extraction with organic solvents. The most common method used usually involves chloroform, dichloromethane and methanol, alone or in a mixture. In some cases during the extraction an ultrasonic bath is used in order to improve the recovery of the analytes.
- Alkaline hydrolysis, in some cases carried out with the help of a microwave system, followed by extraction with organic solvents (normally *n*-hexane and diethyl ether), allows neutral and acidic compounds to be separated into two fractions, and the chromatographic data to be more easily interpreted.
- Headspace solid phase microextraction (HS-SPME). With this extraction technique, it is possible to concentrate volatile compounds thus allowing their detection even at trace levels, as in the case of volatile and semi-volatile terpenes in archaeological findings [7,31]. Chapter 10 outlines how resinous materials are investigated using HS-SPME-GC/MS.

In resinous materials, the presence of molecules bringing hydroxy and carboxylic moieties usually requires a derivatization step before chromatographic analysis. Derivatization reactions are required to render polar, nonvolatile and thermolabile compounds suitable for gas chromatographic analysis [32]. The reduction of polarity by derivatization leads to better peak shapes due to the minimization of detrimental and non-specific column adsorptions. Furthermore, the derivatization reactions can also be a particularly useful tool in those cases in which underivatized molecules give rise to mass spectra of poor diagnostic value. In fact, the fragmentation of derivative compounds often results in the formation of diagnostic fragment ions [32,33]. Methylation and silylation, in particular trimethylsilylation, are the most common derivatization reactions for the

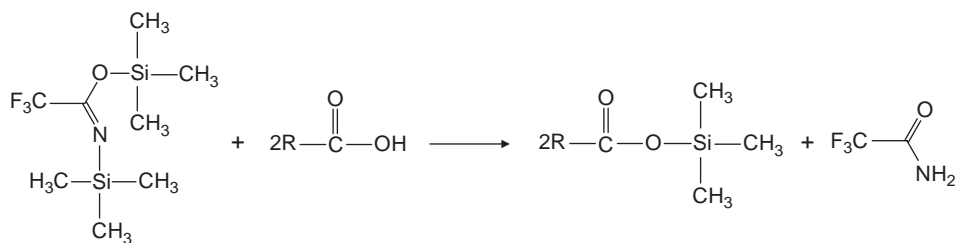


**Figure 8.1** Reaction scheme for the formation of a trimethylsilyl ester between BSTFA and an organic carboxylic acid

GC/MS analyses of resinous materials. Trimethylsilylating (TMS) reagents [such as *N,O*-bis(trimethylsilyl)trifluoroacetamide, BSTFA] are able to derivatize groups with an active/polar proton (OH, NH and SH), converting them into TMS ethers and/or esters. Figure 8.1 shows the reaction scheme for the formation of a TMS ester between BSTFA and an organic carboxylic acid. Methylation reagents such as diazomethane or TMS-diazomethane are able to convert organic acids into methyl esters.

The electron ionization (EI) mass spectra of TMS ethers and esters are generally characterised by weak or absent molecular ions. The  $[M-15]^+$  ion formed by loss of a methyl radical is generally abundant and in the case of alcoholic functions, the loss of a trimethylsilanol molecule  $[M-90]^+$  is also diagnostic. The peak at  $m/z$  73, corresponding to the TMS group, is important in nearly all the TMS-derivative mass spectra. Figure 8.2 shows the fragmentation of TMS esters and ethers in mass spectrometric analyses.

In addition to GC/MS, high performance liquid chromatography (HPLC/MS) has been used to analyse natural resins in ancient samples, particularly for paint varnishes containing mastic and dammar resins [34]. A partial limitation of chromatographic techniques is that they do not permit the analysis of the polymeric fraction or insoluble fraction that may be present in the native resins or formed in the course of ageing. Techniques based on the direct introduction of the sample in the mass spectrometer such as direct temperature resolved mass spectrometry (DTMS), direct exposure mass spectrometry (DE-MS) and direct inlet mass spectrometry (DI-MS), and on analytical pyrolysis (Py-GC/MS), have been employed as complementary techniques to obtain preliminary information on the

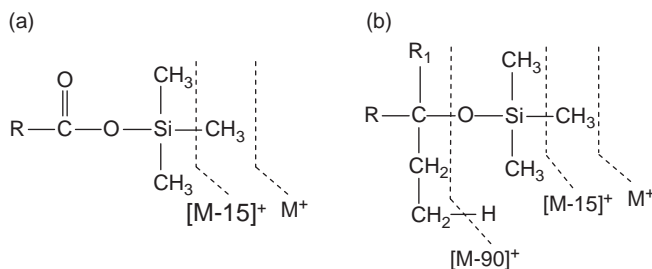


**Figure 8.2** Fragmentation of trimethylsilyl esters (a) and ethers (b) in mass spectrometric analyses

sample and to investigate the insoluble or polymeric fraction as well. These techniques do not generally require sample pretreatment, which is necessary for GC analysis, however the interpretation of the results obtained is generally less straightforward than for GC/MS. Chapters 3, 4, 11 and 12 deal with pyrolysis-based techniques and how they are used when studying resinous and lipid materials.

Other MS based analytical approaches have occasionally been applied to ancient resin samples, in particular for paint varnishes. Such techniques include FABS (fast atom bombardment mass spectrometry) [35], MALDI (matrix assisted laser desorption-ionization mass spectrometry) and GALDI (graphite assisted laser desorption-ionization mass spectrometry) [36–38].

Fourier transform infrared (FTIR) spectroscopy,  $^{13}\text{C}$  nuclear magnetic resonance (NMR) spectroscopy, ultraviolet-visible (UV-VIS) and fluorescence spectroscopy can be integrated with chromatographic techniques especially in the study of ageing and degradation of terpenic materials. They can be used to study the transformation, depletion or formation of specific functional groups in the course of ageing.

The following paragraphs describe some case studies related to procedures based on GC/MS techniques to archaeological and art objects.

## 8.2 Case Studies

### 8.2.1 Archaeological Frankincense

Frankincense, also known as *olibanum*, has been obtained since ancient times from trees belonging to the genus *Boswellia* (family *Burseraceae*). It is one of the best-known ancient plant resins. Evershed *et al.* provided the first chemical evidence of frankincense resin from an archaeological site [5,6], in a sample collected in the cellar of a house at the site of Qasr Ibrîm (AD 400–500, Egyptian Nubia). The study was carried out by means of an analytical procedure based on GC/MS which entails organic solvent extraction (2:1 v/v, dichloromethane/propan-2-ol) and a derivatization reaction with BSTFA. The survival of  $\alpha$ -boswellic acid,  $\beta$ -boswellic acid and their *O*-acetates, pentacyclic triterpenes specific chemical markers which have been isolated only from frankincense, was demonstrated by their mass spectra and by a comparison with the results obtained by analysing raw frankincense. Mass spectra of  $\alpha$ -boswellic acid,  $\beta$ -boswellic acid and their *O*-acetates in the form of TMS derivatives are reported in Figure 8.3. The mass spectra were obtained using EI at 70 eV and an ion trap as analyser.

### 8.2.2 Archaeological Pine Pitch

An analytical procedure based on alkaline hydrolysis and silylation (BSTFA) followed by GC/MS analysis was used to examine 53 samples of tarry-like materials derived from two archaeological sites: Medinet Madi in Fayum (Egypt) and Pisa San Rossore in Tuscany (Italy) [8]. In both sites a high number of amphorae and vessels were recovered, many of which presented residues of a dark and sometimes shiny resinous coating on their internal surfaces. GC/MS highlighted dehydroabietic acid, 7-oxo-dehydroabietic acid, 15-hydroxy-7-oxo-dehydroabietic acid and 15-hydroxy-dehydroabietic acid in the acidic fraction, and retene, tetrahydrotetene, norabietatriene, norabietatetraene, and methyl

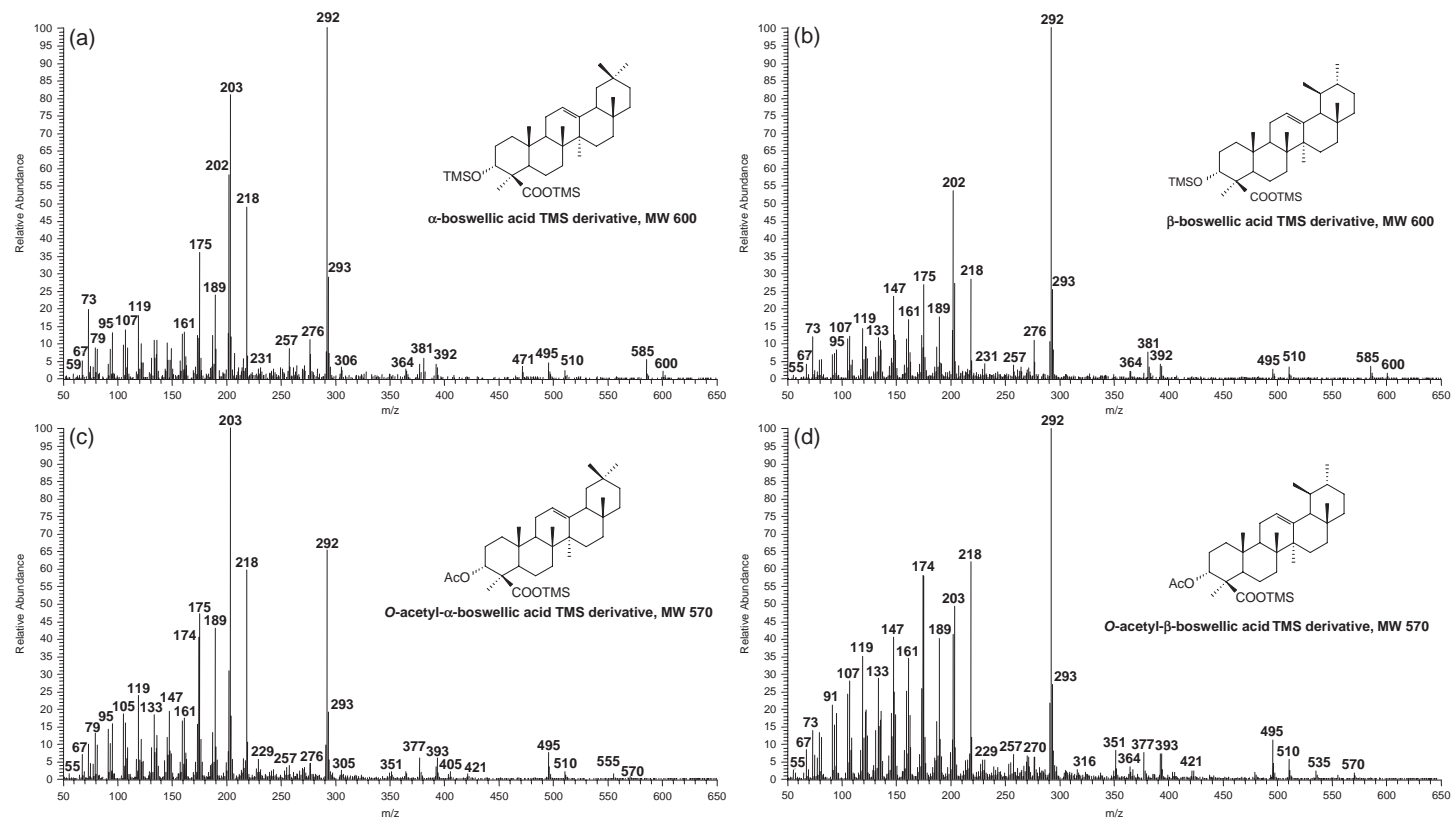


**Figure 8.3** Mass spectra of (a)  $\alpha$ -boswellic acid, (b)  $\beta$ -boswellic acid and (c,d) their O-acetates in the form of TMS derivatives

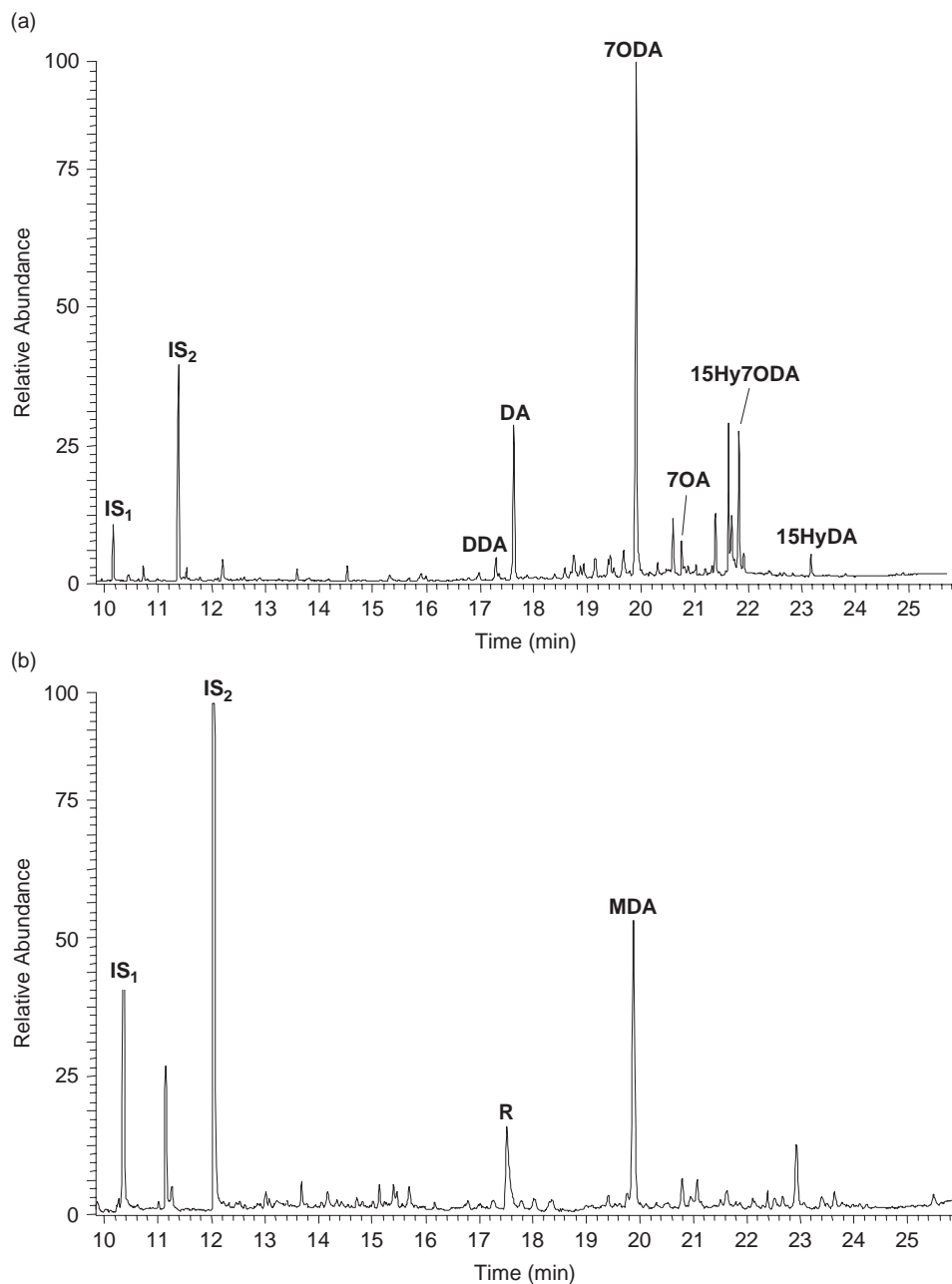


**Figure 8.4** Total ion current chromatograms of the (a) acidic and (b) neutral fractions of a sample collected from an amphora recovered in Fayum. DDA, didehydroabiatic acid; DA, dehydroabiatic acid; 7ODA, 7-oxo-dehydroabiatic acid; 7OA, 7-oxo-abietic acid; 15Hy7ODA, 15-hydroxy-7-oxo-dehydroabiatic acid; 15HyDA, 15-hydroxy-dehydroabiatic acid; R, retene; MDA, methyl dehydroabietate.  $IS_1$ , internal standard, hexadecane;  $IS_2$ , internal standard, tridecanoic acid



dehydroabietate in the neutral fraction. Figure 8.4 shows the total ion current (TIC) chromatograms of the acidic and neutral fractions of a sample collected from an amphora from Fayum.

These oxidized and aromatized abietanes proved that the amphorae had been water-proofed with a pitch produced from resinous wood of plants from the *Pinaceae* family. In fact, in tar and pitch produced from *Pinaceae* resin and woods, retene is considered as a stable end-product of these reaction pathways and norabietatrienes, simonellite and tetrahydroretene represent the intermediates of these reactions [2,8]. Furthermore, the occurrence of methylated diterpenoid acids indicates that the pitch was obtained by a pyrolytic treatment of resinous pine wood. The methanol released in the hard heating of wood reacts easily with diterpenic acids to produce, above all, methyl dehydroabietate [2,8], which is absent in pitch produced by heating resin alone. Figure 8.5 shows the thermal degradation pathway leading to the formation of the characteristic compounds present in pine pitch.

To highlight and explain the quantitative chemical differences between the pitches found in the two archaeological sites, a chemometric evaluation of the GC/MS data (normalized peak areas) by means of principal component analysis (PCA) was performed. The PCA scatter plot of the first two principal components (Figure 8.6) highlights that the samples from Pisa and Fayum are almost completely separated into two clusters and that samples from Fayum form a relatively compact cluster, while the Pisa samples are

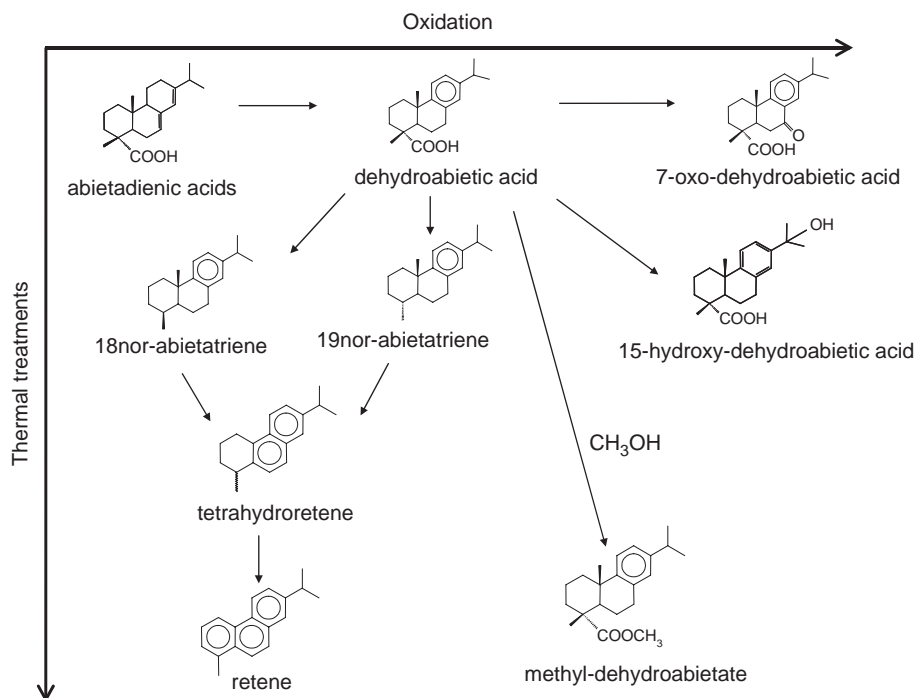


**Figure 8.5** Oxidation and thermal degradation pathway leading to the formation of the characteristic compounds present in pine pitch

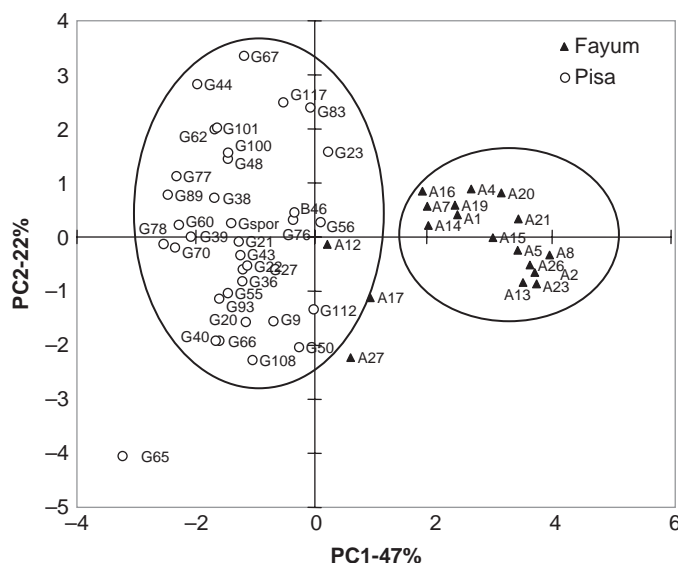


**Figure 8.6** PCA scatter plot of GC/MS data for the 53 samples of waterproofing material collected from amphorae

scattered over a wider area of the PCA plot. The amphorae from the Pisa archaeological site belonged to loads from different ships that had been wrecked in the same harbour. Thus, the variance in the chemical composition of Pisa samples takes into account the differences that arise when the pitch was produced with similar technologies but in different Mediterranean sites and probably also manufactured at different times.

The loading plot of the first two principal components (Figure 8.7) indicates that the two clusters are mainly differentiated, in their position on the PC1, by the relative amounts of oxidized abietanes, with the Fayum samples presenting greater oxidation. In particular, 7-oxo-dehydroabietic acid has a significant positive loading on PC1. This can be related to the environmental conditions in Fayum (hot and dry) and Pisa (waterlogged). If the difference in environmental conditions explains the various amounts of oxidized diterpenic acids, the presence of a relatively higher amount of retene in the Egyptian amphorae would seem to indicate that pitch production in this case was conducted at higher temperatures and for a longer duration.

### 8.2.3 Archaeological Bark Tar

Regert *et al.* studied [9] a series of 30 Neolithic hafting adhesives from lake dwellings at Chalain (France) using an analytical procedure based on GC/MS analysis involving solvent extraction (dichloromethane) and trimethylsilylation. In the majority of the samples a series of triterpenoid compounds with a lupane structure was clearly identified on the basis of their TMS mass spectra. In particular, the presence of betulin, betulone, lupenone, lupeol and lupa-2,20(29)-dien-28-ol allowed birch bark tar to be identified. In other samples the co-occurrence of other plant biomarkers such as  $\alpha$ -amyrin,  $\beta$ -amyrin

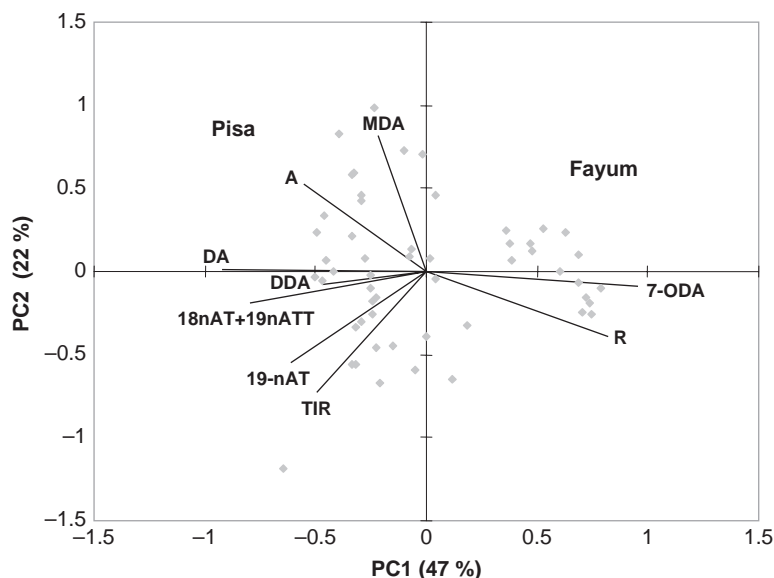


**Figure 8.7** PCA loading plot of GC/MS data for the 53 samples of waterproofing material collected from amphorae

and  $\beta$ -sitosterol suggested that these adhesives might have been derived from other vegetable barks such as oak, beech and alder barks.

Given that betulin and lupeol together with low amounts of lupenone, betulone and betulinic acid are known to be characteristic of birch bark [39–43], the other compounds were considered as characteristic of the degradation reactions undergone by bark during the heating processes necessary to produce the pitch. In particular, betulin is partly transformed into lupa-2,20(29)-dien-28-ol by dehydration, whereas lupeol leads to the formation of a triterpenoid hydrocarbon identified as lupa-2,20(29)-diene. Lupa-2,20(29)-dien-28-ol and lupa-2,20(29)-diene are thus indicative of a thermal treatment and, depending on the duration and the intensity of the hard-heating treatment, their proportion changes. Furthermore, the amounts of lupenone and betulone, naturally present in fresh birch bark only in small amounts, may increase during tar production by the oxidation of lupeol and betulin, respectively [10].

Mass spectra of betulin, betulone, lupenone, lupeol, lupa-2,20(29)-dien-28-ol and lupa-2,20(29)-diene are reported in Figure 8.8. The mass spectra are obtained using EI at 70 eV and an ion trap as analyser.

GC/MS has also been used to investigate acidic and neutral fractions (after alkaline hydrolysis, separation and trimethylsilylation) of a resinous sample collected from a flint flake dated back to the lower Palaeolithic (roughly 200 000 BC) and recovered near Arezzo in Italy [11]. The results show that the organic material recovered on the flint flake was a pitch obtained from birch bark by a pyrolysis type process. In fact, the main components of the acidic fraction are a series of linear  $\alpha,\omega$ -dicarboxylic acids ranging from 16 to 22 carbon atoms and a series of  $\omega$ -hydroxycarboxylic acids ranging from 16 to 22 carbon

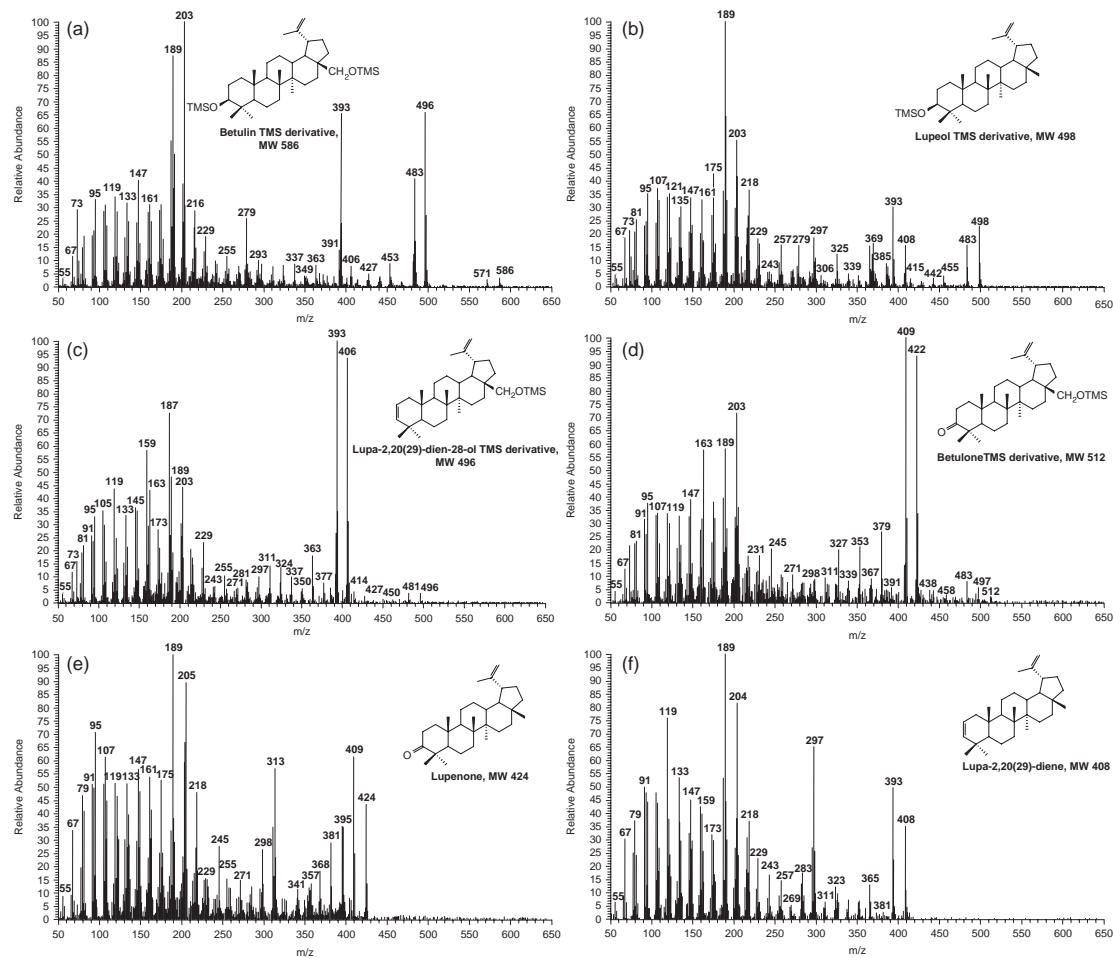


**Figure 8.8** Mass spectra of (a) betulin (TMS derivative), (b) lupeol (TMS derivative), (c) lupa-2,20(29)-dien-28-ol (TMS derivative), (d) betulone (TMS derivative), (e) lupenone and (f) lupa-2,20(29)-diene

atoms. The neutral fraction was principally made up of triterpenoids with a lupane skeleton: betulin followed by lupeol, lupadienol, betulone and lupadiene. Figure 8.9 shows the gas chromatograms of the acidic and neutral fractions of the sample collected from the flint flake.

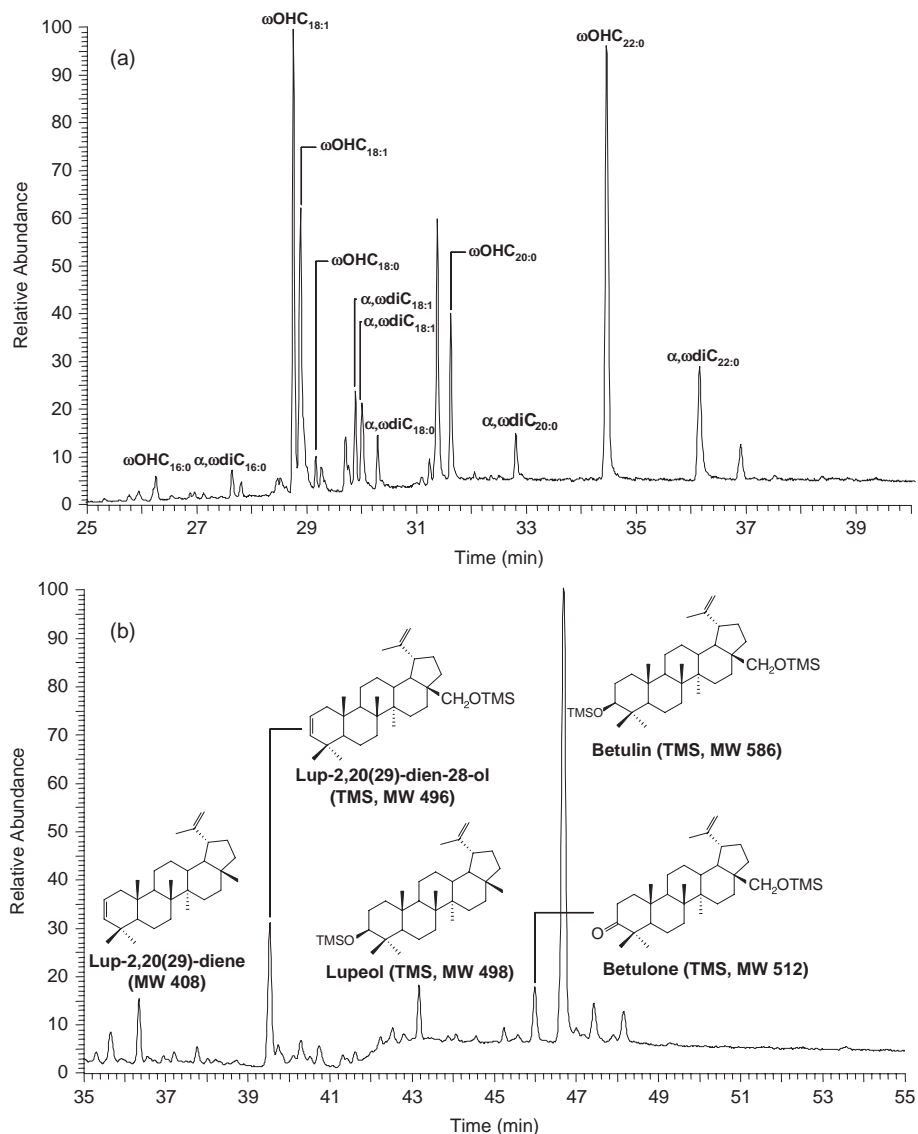


**Figure 8.9** Total ion current chromatograms of (a) acidic and (b) neutral fractions of the sample collected from the Palaeolithic flint flake.  $\omega\text{OHC}_{x:y}$  are hydroxy fatty acids of chain length  $x$  with the hydroxy group at position  $\omega$  and with  $y$  double bonds;  $\alpha,\omega\text{diC}_{x:y}$  are  $\alpha,\omega$ -dicarboxylic fatty acids of chain length  $x$  and with  $y$  double bonds

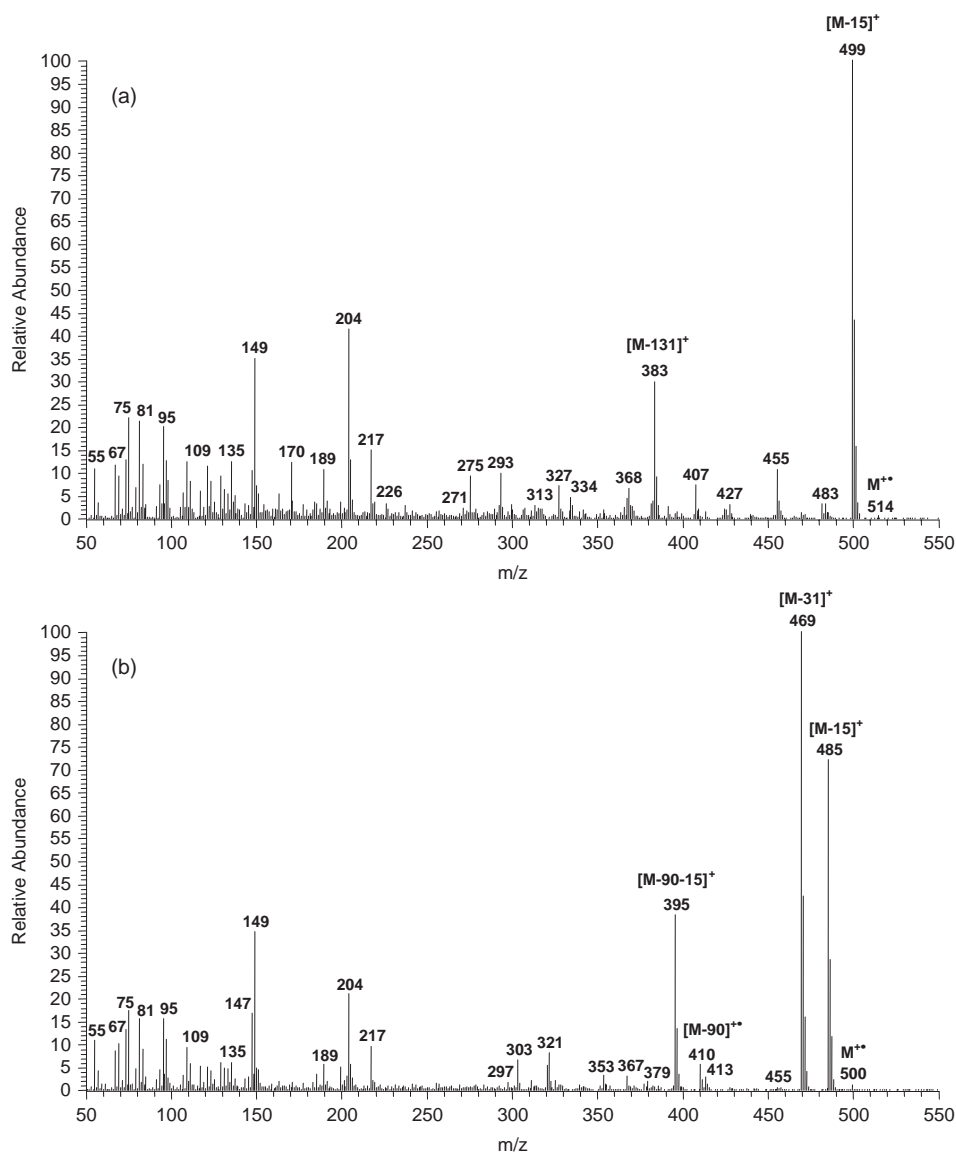


**Figure 8.10** Mass spectra of (a)  $\alpha, \omega$ -docosandioic acid and (b)  $\omega$ -hydroxydocosanoic acid after derivatization with BSTFA

As an example, Figure 8.10 shows the mass spectra of  $\alpha, \omega$ -docosandioic acid and  $\omega$ -hydroxydocosanoic acid.

The EI mass spectra of  $\alpha, \omega$ -dicarboxylic acids and  $\omega$ -hydroxycarboxylic acids are characterised by ions arising from the fragmentation of the TMS ester and ether moieties and from fragmentation due to interactions between the two TMS

functionalities, involving TMS transfer from the ester or ether group to the other ester group [44]. Therefore, ions and radical ions at  $m/z$  204, 217, as well as  $[M-15]^+$  and  $[M-131]^+$ , are characteristic of  $\alpha,\omega$ -dicarboxylic acids, and ions at  $m/z$  204, 217, as well as  $[M-15]^+$ ,  $[M-31]^+$ ,  $[M-90]^+$ , and  $[M-90-15]^+$ , are characteristic of  $\omega$ -hydroxycarboxylic acids. The peaks at  $[M-90]^+$  can be attributed to the loss of a molecule of trimethylsilanol from the molecular ion by a rearrangement process, while the peak at  $[M-90-15]^+$  is related to the consecutive loss of trimethylsilanol and a methyl radical. The peak corresponding to  $[M-15]^+$  can be related to the loss of a methyl radical from the TMS group.

Lupane type molecules, and long chain  $\alpha,\omega$ -dicarboxylic acids and  $\omega$ -hydroxycarboxylic acids are characteristic of the suberin of birch bark [45,46]. Chemically the suberin of birch bark is considered a biopolyester mainly composed of hydroxy, epoxy and dicarboxylic acids. In particular,  $\alpha,\omega$ -dicarboxylic acids and  $\omega$ -hydroxycarboxylic acids are formed by the breakdown of the ester bonds present in the suberin during the alkaline hydrolysis used in the sample pretreatment as revealed by the analysis of reference birch bark pitch. Nevertheless, suberin hydrolysis may also have been induced by ageing during the burial period, and not only by the sample pretreatments. Thus, to test if part of the suberin structure survived the hard-heating treatment and the long period of burial, the authors decided to also analyse the sample directly after solvent extraction with dichloromethane, avoiding any alkaline treatments. It was observed that the recovery of the suberin monomers (as free acids) was about 20% less than it had been after the alkaline hydrolysis treatment. Thus, it was possible to conclude that part of the original structure of suberin was still preserved in the archaeological material.

#### 8.2.4 Archaeological Mastic Resin

Mastic is a triterpenic resin from several species of the genus *Pistacia* and has been widely used since ancient times in the Mediterranean area. By means of GC/MS analyses, moronic, isomasticdienonic and masticdienonic acids have been found in a number of aged and archaeological samples and are considered as characteristic and diagnostic molecules for assessing the presence of mastic resin in ancient samples [11–17]. Moreover, several authors [15–17] have suggested that the occurrence of a high abundance of 28-norolean-17-en-3-one can be correlated to a smouldering or burning process undergone by *Pistacia* resins. The molecular structures of some triterpenoids typical of mastic resin are reported in Figure 8.11.

The compositional variations of mastic resin found in late Bronze Age Canaanite amphorae and bowls (most likely censers) from Amarna (18th Dynasty of the New Kingdom, 1300 BC) have been investigated by an analytical procedure based on GC/MS analysis following dichloromethane extraction and methylation of carboxylic functionalities with diazomethane. This study highlighted that the abundance of 28-norolean-17-en-3-one [MW 410; mass spectrum (abundance in brackets): 410 (20), 395 (8), 191 (65), 175 (22), 163 (100), 55 (35)] in ancient samples is not matched by the archaeological evidence for heating and that it is therefore not possible to use this compound as a biomarker for the identification of mastic resin submitted to thermal treatments [13]. Moreover, in addition to methyl moronate, methyl oleanonate, methyl

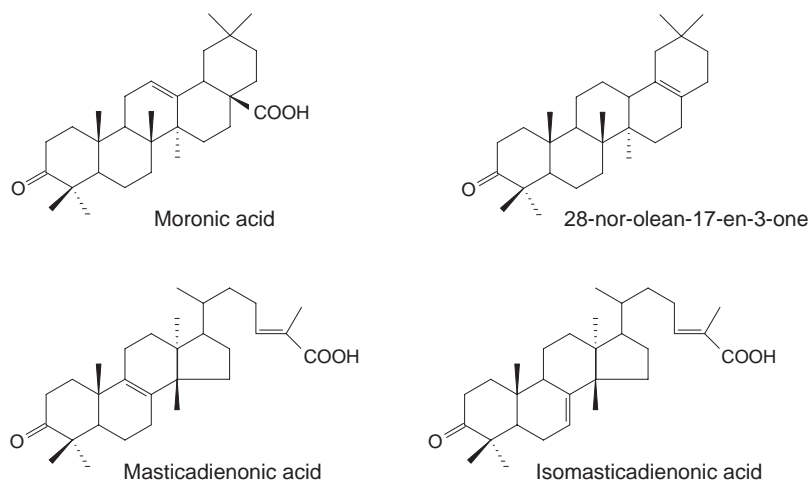


**Figure 8.11** Triterpenoids typical of mastic resin

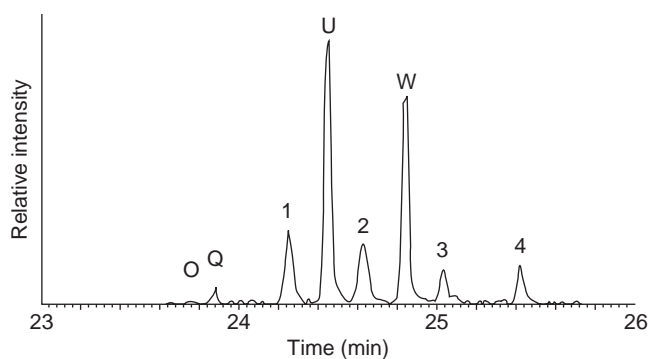


**Figure 8.12** Mass chromatogram of  $m/z$  453 of the organic residues extracted from a bowl recovered from Amarna. O, methyl moronate; Q, methyl oleanonate; U, methyl masticadienonate; W, methyl isomasticadienonate; 1–4, unidentified compounds with a base peak at  $m/z$  453. Reproduced from B. Stern, C. Heron, L. Corr, M. Serpico, J. Bourriau, *Archaeometry*, **45**, 457–469. Copyright 2003, with permission from Blackwell

masticadienonate and methyl isomasticadienonate, whose mass spectra are characterised by the presence of a peak at  $m/z$  453, a number of yet unidentified compounds with a base peak at  $m/z$  453 was present in seven (out of ten) bowls but not in the Canaanite amphorae (Figure 8.12). This suggested that the presence of these compounds is an indication of a heated mastic resin.

### 8.2.5 Archaeological Aromatic Resin

GC/MS has provided the first chemical evidence of the presence of benzoe resin in an archaeological material from the Mediterranean area [18]. The procedure was



based on alkaline hydrolysis, solvent extraction and trimethylsilylation followed by GC/MS analysis. It was first used to study the chemical composition of raw benzoe and storax resins, water-insoluble exudates of trees of the *Styrax* and *Liquidambar* genus. This analytical procedure allowed the authors to characterise the main components of the two resins and, even though both resins simultaneously contain cinnamic acid, benzoic acid and cinnamyl alcohol as major compounds, important differences in the chemical composition of the two resins permit to distinguish between them. In fact, benzoe resin is characterised by the presence of 4-hydroxybenzaldehyde, vanillin, 3-hydroxybenzoic acid, 4-hydroxybenzoic acid and vanillic acid. However, 4-hydroxy-benzenepropanol, *p*-hydroxycinnamic acid, 3-phenyl-2-propanol and triterpenoid acids (oleanonic and oleanolic) are distinctive of storax resin. These data were used to unambiguously identify the aromatic compounds observed in an organic residue from an Egyptian ceramic censer (fifth to seventh centuries AD) as being derived from benzoe resin. Figure 8.13 shows the chromatogram of the acidic fraction of the sample collected from the censer.

### 8.2.6 Terpenoid Paint Varnishes

One of the many uses of terpenic resins is as the main ingredient in paint varnishes. Such varnishes are applied on the surface of paintings to protect the paint layer and to confer gloss and saturation to colours. It is important to know the characteristics

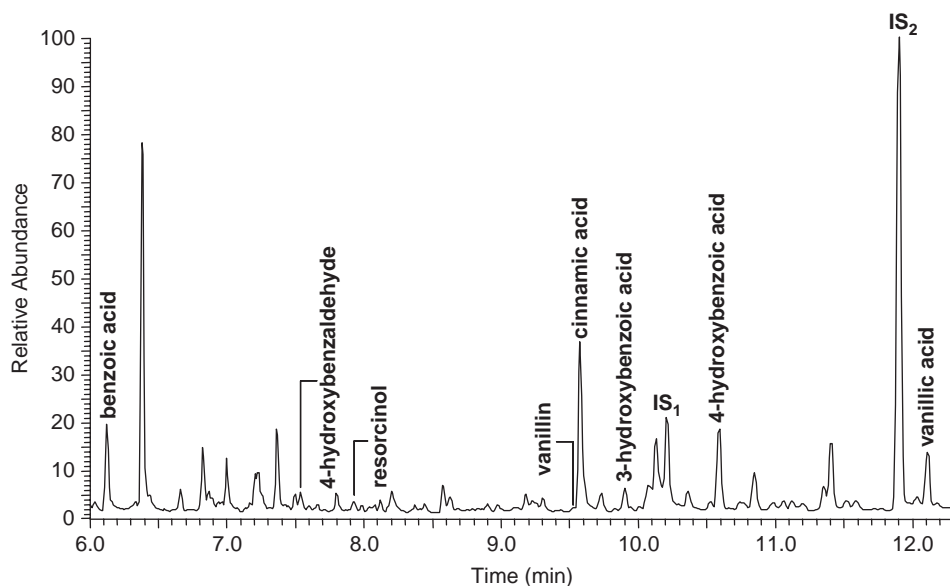


**Figure 8.13** Total ion current chromatogram of the acidic fraction of the sample collected from the Roman-Egyptian censer showing the presence of benzoe resin. *IS*<sub>1</sub>, internal standard, hexadecane; *IS*<sub>2</sub>, internal standard, tridecanoic acid

of the varnish in order to select the cleaning treatments for restoring the paintings. Terpenoid varnishes have been analysed by GC/MS throughout the identification of diterpenoid and triterpenoid compounds. Due to the polarity of acidic and alcoholic moieties of the terpenoid compounds, usually a derivatization step prior to GC/MS analysis is performed. Silylation with BSTFA or with *N*-*tert*-butyldimethylsilyl-*N*-methyl-trifluoroacetamide, and methylation with TMS-diazomethane or with diazomethane are the most common methods [19–23]. Van den Berg *et al.* [21] proposed an interesting double derivatization procedure for the study of diterpenoid varnishes. It entails the use of TMS-diazomethane followed by trimethylsilylation with BSTFA. This procedure produced the methylation of the acidic moieties and the trimethylsilylation of the alcoholic moieties. Figure 8.14 shows the mass spectra of 15-hydroxy-7-oxo-dehydroabietic acid obtained using methylation, methylation followed by trimethylsilylation, and trimethylsilylation. Even though a different derivatization step, these kinds of esters give a characteristic and similar fragmentation pattern which involves loss of an ester group, loss of a C<sub>20</sub> methyl group as a radical, and loss of water or trimethylsilanol from hydroxyl moieties.

GC/MS is particularly suitable for studying the complex organic mixtures commonly found in paint samples. A GC/MS analytical procedure [23] for the identification of lipids, waxes, proteins, and resinous materials in the same microsample from works of art has been used to study an Italian easel painting on canvas from the seventeenth to eighteenth centuries. As far as the painting varnish is concerned, a mixture of pine and dammar resins was identified on the basis of the presence of didehydroabietic acid, dehydroabietic acid and 7-oxo-dehydroabietic acid for the pine resin, and of shoreic acid, oleanonic acid, ursonic acid, nor- $\alpha$ -amyrone, nor- $\beta$ -amyrone, 20,24-epoxy-25-hydroxydammar-3-one, hydroxydammar-3-one, 20,24-epoxy-25-hydroxydammar-3-ol, oleanonic aldehyde and ursonic aldehyde for dammar resin. Shoreic acid, 20,24-epoxy-25-hydroxydammar-3-one and 20,24-epoxy-25-hydroxydammar-3-ol, which are not present in fresh raw dammar resin, are the products of the oxidation of dammar-3-ol, hydroxydammar-3-one and hydroxydammar-3-ol. This is related to the oxidation of the side chain of dammar-3-ol skeleton-type molecules leading to the formation of a side chain of the ocotillone type [20,47]. The mass spectra of ocotillone type products are dominated by a peak at  $m/z$  143, as shown in the mass spectrum of 20,24-epoxy-25-hydroxydammar-3-one in Figure 8.15.

The same procedure [23] was employed to study the painting from an Etruscan marble sarcophagus from the fourth century BC. This study ascertained the presence of animal glue and egg as the organic materials originally employed in the decoration. The use of shellac resin as a restoration material was highlighted on the basis of a distinctive gas chromatographic profile characterised by the presence of typical sesquiterpenoid acids, namely epilaccishellic, laccishellic, epishellic, shellic acids, and aleuritic acid. The mass spectra of epilaccishellic acid and epishellic acid are shown in Figure 8.16. The mass spectra of laccishellic acid and shellic acid, being epimers of epilaccishellic acid and epishellic acid, feature to a very similar fragmentation pattern.

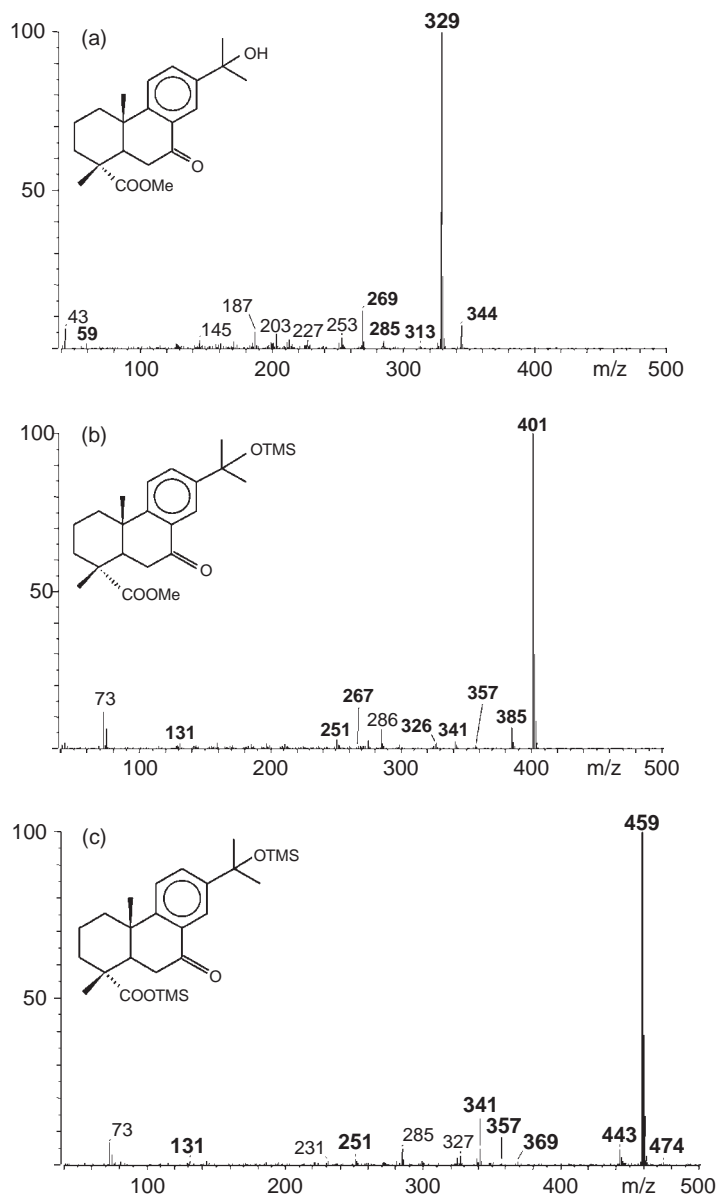


**Figure 8.14** Mass spectra of 15-hydroxy-7-oxo-dehydroabietic acid after (a) methylation, (b) methylation followed by trimethylsilylation and (c) trimethylsilylation. Reproduced from K. J. van den Berg, J. J. Boon, I. Pastorova, L. F. M. Spetter, *J. Mass Spectrom.*, **35**, 512–533. Copyright 2000, with permission from John Wiley & Sons, Ltd

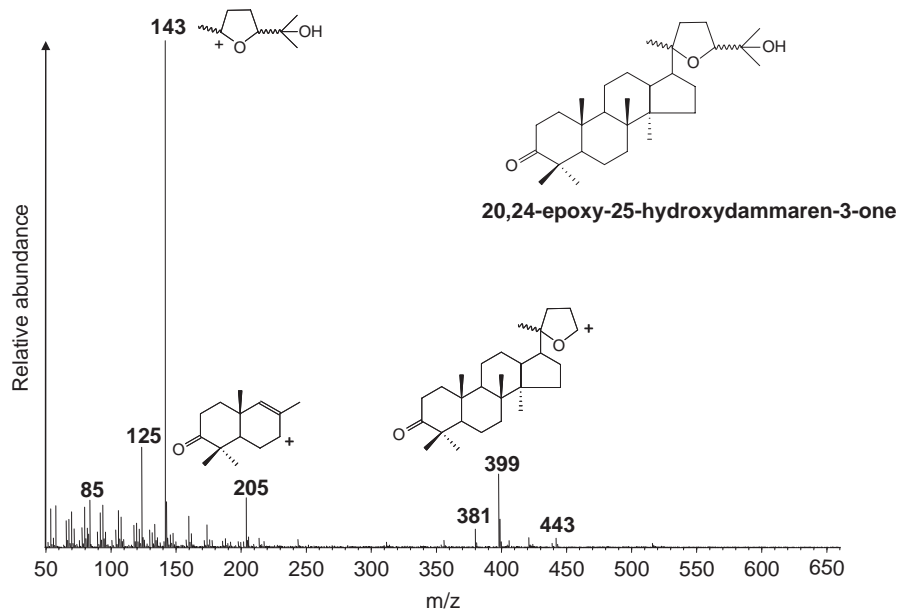


**Figure 8.15** Mass spectrum of 20,24-epoxy-25-hydroxydammar-3-one

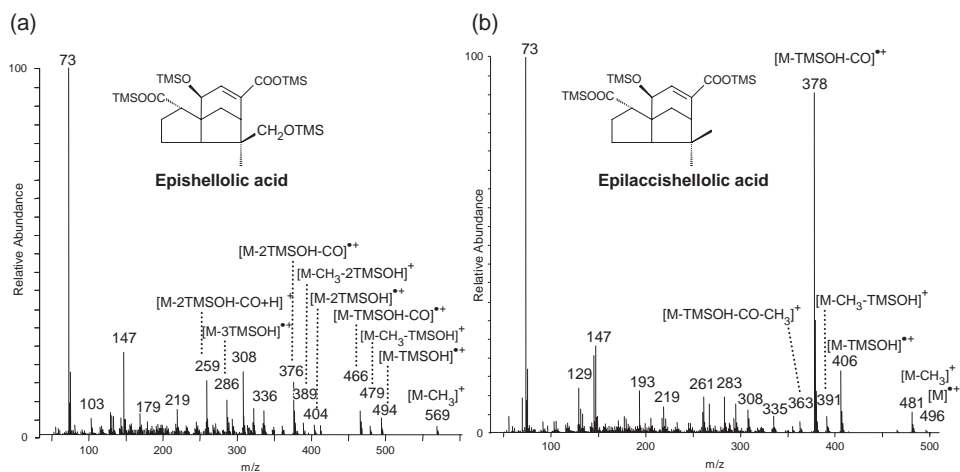


**Figure 8.16** Mass spectra of (a) epishellolic acid and (b) epilaccishellolic acid after derivatization with BSTFA

### 8.3 Conclusions

Although analytical procedures based on GC/MS analysis entail relatively long analysis times and a wet chemical pretreatment of the samples, they are unsurpassed in their

capacity to unravel the molecular composition of resinous materials both in archaeological findings and in works of art. Sample pretreatments generally include extraction of the analytes and derivatization to make them volatile. For this reason, it is good practice to perform a preliminary screening of the samples by FTIR or by a direct mass spectrometric technique. Such techniques can be used to ascertain the presence of organic materials and to learn about the type of possible materials so that the best pretreatment condition before GC analysis can be chosen.

The derivatization step, usually with BSTFA, is essential especially in cases where underivatized molecules give rise to mass spectra that are of poor diagnostic value. The fragmentation of TMS derivative compounds results in the formation of diagnostic fragment ions. Thus, on the basis of mass spectra of TMS derivatives, it is possible to identify the composition of the organic residues, any new compounds, and the presence of specific compounds acting as biomolecular markers. All this is essential to establish the origin of natural substances present in the samples. The analysis of raw and naturally and accelerated aged reference resinous materials is of paramount importance for identifying residues from archaeological findings and works of art and for understanding how these natural organic substances degrade.

Some high molecular weight substances, such as highly polymerized terpenic resins or fossil resins, cannot be directly analysed by GC/MS. In these cases online analytical pyrolysis combined with GC/MS can be used. Pyrolysis-GC/MS applications are described in Chapters 11 and 12.

## References

1. M. Serpico, R. White, Resins, Amber and Bitumen, in *Ancient Egyptian Materials and Technology*, P. Nicholson and I. Shaw (Eds), Cambridge University Press, Cambridge, 2000, pp. 430–474.
2. A. M. Pollard, C. Heron, *Archaeological Chemistry*; RSC Paperbacks, Cambridge, 1996.
3. R. P. Evershed, Biomolecular Analysis by Organic Mass Spectrometry, in *Modern Analytical Methods in Art and Archaeology*, E. Ciliberto and G. Spoto (Eds), Wiley Interscience, New York, 2000, pp. 177–230.
4. J. S. Mills, R. White, *The Organic Chemistry of Museum Objects*, 2nd Edition, Butterworth Heinemann Ltd, Oxford, 1994.
5. P. F. van Bergen, T. M. Peakman, E. C. Leigh-Firbank, R. P. Evershed., Chemical evidence for archaeological frankincense: boswellic acids and their derivatives in solvent soluble and insoluble fractions of resin-like materials, *Tetrahedron Lett.*, **38**, 8409–8412 (1997).
6. R. P. Evershed, P. F. van Bergen, T. M. Peakman, E. C. Leigh-Firbank, M. C. Horton, D. Edwards, M. Biddle, B. Kjølbye-Biddle, P. A. Rowley-Conwy, Archaeological frankincense, *Nature*, **390**, 667–668 (1997).
7. S. Hamm, J. Bleton, J. Connan, A. Tchaplal, A chemical investigation by headspace SPME and GC–MS of volatile and semi-volatile terpenes in various olibanum samples, *Phytochemistry*, **66**, 1499–1514 (2005).
8. M. P. Colombini, F. Modugno, E. Ribechini, Direct exposure electron ionization mass spectrometry and gas chromatography/mass spectrometry techniques to study organic coatings on archaeological amphorae, *J. Mass Spectrom.*, **40**, 675–687 (2005).
9. M. Regert, J. Delacotte, M. Menu, P. Petrequin, C. Rolando, Identification of Neolithic hafting adhesives from two lake dwellings at Chalain (Jura, France), *Ancient Biomol.*, **2**, 81–96 (1998).
10. M. Regert, Investigating the history of prehistoric glues by gas chromatography-mass spectrometry, *J. Sep. Sci.*, **27**, 244–254 (2004).

11. F. Modugno, E. Ribechini, M. P. Colombini, Chemical study of triterpenoid resinous materials in archaeological findings by means of direct exposure electron ionisation mass spectrometry and gas chromatography/mass spectrometry, *Rapid Commun. Mass Spectrom.*, **20**, 1787–1800 (2006).
12. S. A. Buckley, R. P. Evershed, Organic chemistry of embalming agents in Pharaonic and Greco-Roman mummies, *Nature*, **413**, 837–841 (2001).
13. B. Stern, C. Heron, L. Corr, M. Serpico, J. Bourriau, Compositional variations in aged and heated Pistacia resin found in late bronze age Canaanite amphorae and bowls from Amarna, Egypt, *Archaeometry*, **45**, 457–469 (2003).
14. J. S. Mills, R. White, The identity of the resins from the late Bronze Age shipwreck at Ulu Burun (Kas), *Archaeometry*, **31**, 37–44 (1989).
15. Y. Kaup, U. Baumer, J. Koller, R. E. M. Hedges, H. Werner, H. Hartmann, H. Etspueler, U. Weser, Zn<sub>2</sub>Mg alkaline phosphatase in an early Ptolemaic mummy, *Z. Naturforsch. C*, **49**, 489–500 (1994).
16. M. Serpico, R. White, The botanical identity and transport of incense during the Egyptian New Kingdom, *Antiquity*, **74**, 884–897 (2000).
17. M. P. Colombini, F. Modugno, F. Silvano, M. Onor, Characterization of the balm of an Egyptian mummy from the seventh century B.C., *Stud. Conserv.*, **45**, 19–29 (2000).
18. F. Modugno, E. Ribechini, M. P. Colombini, Aromatic resin characterisation by gas chromatography–mass spectrometry: raw and archaeological materials, *J. Chromatogr., A*, **1134**, 298–304 (2006).
19. J. S. Mills, R. White, Natural resins of art and archaeology: their sources, chemistry and identification, *Stud. Conserv.*, **22**, 12–31 (1977).
20. G. A. van der Doelen, J. J. Boon, Artificial ageing of varnish triterpenoids in solution, *J. Photochem. Photobiol., A*, **134**, 45–57 (2000).
21. K. J. van den Berg, J. J. Boon, I. Pastorova, L. F. M. Spetter, Mass spectrometric methodology for the analysis of highly oxidized diterpenoid acids in Old Master paintings, *J. Mass Spectrom.*, **35**, 512–533 (2000).
22. M. P. Colombini, F. Modugno, S. Giannarelli, R. Fuoco, M. Matteini, GC/MS characterization of paint varnishes, *Microchem. J.*, **67**, 385–396 (2000).
23. A. Andreotti, I. Bonaduce, M. P. Colombini, G. Gautier, F. Modugno, E. Ribechini, Analytical procedure for the characterization of glycerolipid, waxy, resinous, and proteinaceous materials in a unique paint microsample, *Anal. Chem.*, **78**, 4490–4500 (2006).
24. J. Koller, U. Baumer, D. Mania, High tech in the Middle Palaeolithic: Neanderthal-manufactured pitch identified, *Eur. J. Archaeol.*, **4**, 385–397 (2001).
25. M. Reunamen, R. Ekman, M. Heinonen, Analysis of Finnish pine tar and tar from the wreck of frigate St. Nikolai, *Holzforschung*, **43**, 33–39 (1989).
26. M. P. Colombini, C. Colombo, F. Modugno, F. Silvano, E. Ribechini, L. Toniolo, Chemical characterization of Egyptian amphorae from Fayum, *Geoarchaeol. Bioarchaeol. Stud.*, 157–160 (2005).
27. D. Urem-Kotsou, B. Stern, C. Heron, K. Kotsakis, Birch-bark tar at Neolithic Makriyalos, Greece, *Antiquity*, **76**, 962–967 (2002).
28. M. Regent, S. Vacher, C. Moulherat, O. Decavallas, Adhesive production and pottery function during the Iron Age at the site of Grand Aunay (Sarthe, France), *Archaeometry*, **45**, 101–120 (2003).
29. S. N. Dudd, R. P. Evershed, Unusual triterpenoid fatty acyl ester components of archaeological birch bark tars, *Tetrahedron Lett.*, **40**, 359–362 (1999).
30. R. P. Philp, J. N. Oung, Biomarkers: occurrence, utility and detection, *Anal. Chem.*, **60**, 887A–896A (1988).
31. M. Regert, V. Alexandre, N. Thomas, A. Lattuati-Derieux, Molecular characterisation of birch bark tar by headspace solid-phase microextraction gas chromatography–mass spectrometry: a new way for identifying archaeological glues, *J. Chromatogr., A*, **1101**, 245–253 (2006).
32. R. P. Evershed, Advances in silylation, in *Handbook of Derivatives for Chromatography*, 2nd Edition, K. Blau and J. Halket (Eds), John Wiley & Sons, Ltd, Chichester, 1993, pp. 52–92.

33. J. Segura, R. Ventura, C. Jurado, Derivatization procedures for gas chromatographic–mass spectrometric determination of xenobiotics in biological samples, with special attention to drugs of abuse and doping agents, *J. Chromatogr., B*, **713**, 61–90 (1998).
34. G. A. Van der Dolen, K. J. van der Berg, J. J. Boon, Comparative chromatographic and mass-spectrometric studies of triterpenoid varnishes: fresh material and aged samples from paintings, *Stud. Conserv.*, **43**, 249–264 (1998).
35. M. L. Proefke, L. R. Kenneth, M. Raheel, S. H. Ambrose, S. U. Wissenman, Chemical analysis of a Roman period Egyptian mummy, *Anal. Chem.*, **64**, 105–111 (1992).
36. S. Zumbuhl, R. Knochenmuss, S. Wulfert, F. Dubois, J. M. Dale, R. Zenobi, A graphite-assisted laser desorption/ionization study of light induced aging in triterpene dammar and mastic varnishes, *Anal. Chem.*, **70**, 707–711 (1998).
37. P. Dietemann, M. J. Edelmann, C. Meisterhans, C. Pfeiffer, S. Zumbuhl, R. Knochenmuss, R. Zenobi, Artificial photoaging of triterpenes studied by graphite-assisted laser desorption/ionization mass spectrometry, *Helv. Chim. Acta*, **3**, 1766–1777.
38. P. Dietemann, S. Zumbuhl, R. Knochenmuss, R. Zenobi, Aging of triterpenoid resin varnishes on paintings studied by graphite-assisted laser desorption/ionization mass spectrometry, *Adv. Mass Spectrom.*, **15**, 909–910 (2001).
39. R. Ekman, The suberin monomers and triterpenoids from the outer bark of *Betula verrucosa* Ehrh, *Holzforschung*, **37**, 205–211 (1983).
40. B. J. W. Cole, K. D. Murray, A. R. Alford, Y. Hua, M. D. Bentley, Triterpenes from the outer bark of *Betula nigra*, *J. Wood Chem. Technol.*, **11**, 503–516 (1991).
41. B. J. W. Cole, M. D. Bentley, Y. Hua, Triterpenoid extractives in the outer bark of *Betula lenta* (black birch), *Holzforschung*, **45**, 265–268 (1991).
42. B. J. W. Cole, M. D. Bentley, Y. Hua, L. Bu, Triterpenoid constituents in the outer bark of *Betula alleghaniensis* (yellow birch), *J. Wood Chem. Technol.*, **11**, 209–223 (1991).
43. M. M. O’Connell, M. D. Bentley, C. S. Campbell, B. J. W. Cole, Betulin and lupeol in bark from four white-barked birches, *Phytochemistry*, **27**, 2175–2176 (1988).
44. J. Rontani, C. Aubert, Trimethylsilyl transfer during electron ionization mass spectral fragmentation of some  $\omega$ -hydroxycarboxylic and  $\omega$ -dicarboxylic acid trimethylsilyl derivatives and the effect of chain length, *Rapid Commun. Mass Spectrom.*, **18**, 1889–1895 (2004).
45. R. Ekman, The suberin monomers and triterpenoids from the outer bark of *Betula verrucosa* Ehrh, *Holzforschung*, **37**, 205–211 (1983).
46. E. W. H. Hayek, P. Krenmayr, H. Lohninger, U. Jordis, W. Moche, F. Sauter, Identification of archaeological and recent wood tar pitches using gas chromatography/mass spectrometry and pattern recognition, *Anal. Chem.*, **62**, 2038–2043 (1990).
47. G. A. van der Doelen, K. J. van den Berg, J. J. Boon, N. Shibayama, E. R. de la Rie, W. J. L. Genuit, Analysis of fresh triterpenoid resins and aged triterpenoid varnishes by high-performance liquid chromatography-atmospheric pressure chemical ionization (tandem) mass spectrometry, *J. Chromatogr., A*, **809**, 21–37 (1998).





# 9

## GC/MS in the Characterisation of Protein Paint Binders

*Maria Perla Colombini and Gwénaëlle Gautier*

### 9.1 Introduction

Science provides tools that allow an objective analysis of the information pertaining to the chemical composition and the physical and structural properties of the materials that compose a work of art. The identification of binding media in paintings is fundamental in any conservation plan as it gives insight into deterioration processes, but it also leads to greater understanding and interpretation of painting techniques. The information gained is valuable both to conservators and art historians, and therefore it is essential to construct compatible conservation interventions in order to guarantee appropriate conditions for long-term preservation [1].

In general, paintings have a complicated layered structure. The physical support is typically a rigid plaster or wood, stretched canvas, or mounted paper or parchment. The next layer is the ground layer or priming (e.g. gypsum and animal glue) used to prepare the support for the following paint layers. In order to obtain the coloured film-forming paint capable of adhering to the ground layer, pigments are dispersed into an organic binder to form one or more paint layers. Often an outer layer of varnish may have been applied by artists or previous restoration programmes to protect the work.

In centuries prior to the industrial revolution, before the development of manufactured paints, a painter was not only an artist, but also a 'formulator of paints', thus experimenting with a multitude of materials as paint. Organic paint binders typically were adhesive to the ground layer and also provided a matrix capable of suspending the coloured pigments. Specific binders were needed to form stable films with aesthetic visual properties. In European artwork,

these are found to be essentially proteinaceous binders, polysaccharide gums, and siccative oils. Additional natural organic materials widely found in paintings consist of plant resins, waxes, and organic dyestuffs. Resins and waxes served mainly as protective coatings and alternative binding media, while dyestuffs were used as colouring agents [2]. The characterisation of all these materials is beyond the scope of this chapter and is discussed in detail in other sections of the book. Here the focus is on a description of the current practices used in the characterisation of proteinaceous components of paint media.

The proteinaceous binders are one of the main constituents of the wide range of organic materials and are a central component of the artist's palette. In the technique referred to as *tempera*, artists commonly used proteinaceous binders derived from egg, milk or casein, and collagen glues derived from animal skins or bones. These can be used independently, mixed together, or in a more complex mixture with siccative oils (as in the *tempera grassa* technique) or plant gums.

Egg has been widely used as a binder since ancient times either in its entirety, as just the white, or just the yolk. The egg white, also referred to as egg albumen or glair, has also found additional uses as glue for gilding, varnish, priming to coat plaster, and for retouching purposes [3,4]. It forms particularly resistant and elastic films. Its permeability and solubility decreases with ageing due to the denaturation of the hydrophilic proteins. Although the protein-rich parts of an egg are typically separated into two groups, the egg albumen and the egg yolk, they do not significantly differ in their amino acid contents. Over 50% of hen egg albumen is a glycoprotein called ovalbumin, another 15% is conalbumin (also a glycoprotein), and about 3% is lysozyme. The remaining part of the albumen contains salts, lecithin, and carbohydrates. The yolk contains phosvitin (phosphoprotein),  $\alpha$ - and  $\beta$ -lipovitellins (lipoproteins containing phospholipids) and  $\alpha$ -,  $\beta$ - and  $\gamma$ -livetins. All the proteins of egg contain moderate amounts of asparagine, glutamine, and leucine.

Milk has been often used instead of egg and has been frequently employed with blue pigments [4]. The concentration of protein in milk is relatively low, and typically varies from 3.0 to 4.0%. The protein falls into two major groups: caseins (80%) and whey proteins (20%). Casein, which is a phosphoprotein complex, can easily be filtered after precipitation by acidifying and heating skimmed milk. The white powder can be applied as a binding medium after being dissolved in an aqueous solution of  $\text{Ca}(\text{OH})_2$ ,  $\text{Na}_3\text{PO}_4$  or  $\text{Na}_2\text{B}_4\text{O}_7 \cdot 10\text{H}_2\text{O}$ . Casein tempera, made from skimmed milk and lime, has been used since very early times. It possesses a notable adhesive power and has long served as a binder for wall paintings [2]. In addition to the casein, whey proteins, which include  $\beta$ -lactoglobulin and  $\alpha$ -lactalbumin, also form a significant part of the other proteinaceous component of milk.

Diluted animal glue was widely used as binding medium to prepare the ground layer (with gypsum) [3] and as a pigment binder. It has also been used to retouch gilding and as a mordant [4]. Animal glue is relatively soluble in water in comparison with other proteinaceous binders, composed of egg or casein, even after ageing. Preparation is relatively simple, involving the treatment with hot water (80–90°C) of specific collagen-containing animal/fish tissues (including the various parts such as skin, muscle tissue, bone, and hide). This glue is a nearly colourless (though it shows a slightly yellowish discoloration in the dry state), transparent and amorphous substance. Collagen is a typical example of the fibrous proteins formed from very long, thin fibres of amino acids covalently bonded in a specific sequence. There are a number of different types of collagen, but they all consist of molecules which contain three polypeptidic  $\alpha$ -chains in the particular conformation of

a triple helix. The  $\alpha$ -chains are rigidly held together by a strong hydrogen-binding interaction between the hydroxyl group of the hydroxyproline and the amino hydrogens of adjacent glycine units. Without the hydrogen bonds the structure is unstable. Each  $\alpha$ -chain has an amino acid sequence which is mainly a repeating structure, with glycine as every third residue and either proline or hydroxyproline often preceding the glycine residues. Glycine therefore accounts for roughly 26% of the total amino acidic content.

In their native states, proteins are folded into complex three-dimensional structures. A delicate balance of hydrophobic and electrostatic interactions, and hydrogen bonds between the side chains of the amino acids contribute to the formation of these unique structures. In the case of proteins, the unique structure is highly correlated with a particular function. The structure, and therefore function of the protein, is extremely susceptible to variations in the drying processes, pH, temperature, or environmental parameters. Denaturation of the protein corresponds to a randomization of the native three-dimensional structure where the secondary and tertiary structures are destroyed. In addition to these physical changes, chemical processes are also a serious concern. Proteins, for example, have a strong tendency to complex with metallic cations and can be very photosensitive. The reactions typically associated with degradation due to ageing can be influenced by the presence of sulfur and sugars and strongly depend on conditions of pH, temperature and relative humidity. Biological attacks from micro-organisms also have significant effects which will be discussed. Finally, other environmental factors such as pollutants can accelerate degradation processes and reactions. These include the formation of free radicals, the formation of chemical by-products from condensation, oxidation, and cross-linking reactions [5]. It is necessary to have a general overview of the processes which occur naturally and those which can be introduced and accelerated during the steps of sample preparation because they interfere with protein identification.

### 9.1.1 Metallic Cation Interference

Proteins have a great capacity to bind with metal ions. Currently, information pertaining to the interactions between the amino acids and metallic cations inside the pictorial film is limited. However, metallic pigments are highly reactive elements in paint media, mainly by forming strong complexes. In addition, other cations that may come from support and dryers act in the same way as those which are contained in pigments. Complexes formed with the transition metals such as copper, zinc, mercury and silver, tend to be very strong and can occur in conjunction with several amino acid functional groups.

Over time, loss of binding power by light induced and metal catalysed oxidation of the polymer system occurs. Some amino acidic residues are more sensitive to this degradation/interaction and thus the proteins subjected to ageing will respond in different ways according to the different pigments present. The catalytic oxidation takes into consideration most of all the amino acids with functional groups containing O, N, and S, such as histidine, proline, arginine, lysine, methionine, cysteine, and serine, that can coordinate to the metallic cations. In the literature, it is reported that, following the reactions with metals, carbonyl groups may be formed on the lateral chain of such amino acids [6]. The interactions with these cations also give rise to interferences during the analytical treatment that are evidenced by changes on the profile of the relative amino acid percentages obtained [7–9], and this may obstruct a correct identification of the proteinaceous binder.

Schilling and Khanjian *et al.* [7] demonstrated that pigments reduced the concentration of amino acids that possess certain functional groups: acidic (aspartic acid, glutamic acid); hydroxyl (threonine, serine); basic (lysine); sulfur-containing (methionine); and aromatic (phenylalanine). The authors referred to them as 'reactive'. They highlighted that aspartic acid, glutamic acid, serine, and threonine are particularly sensitive to hematite, ochre, umber, azurite, and malachite. In addition, they showed that some pigments interfered with the recovery of the internal standard (norleucine). The same effect was recently confirmed in a study of the effect of increasing concentration of azurite in tempera replicas [10].

A decrease of the total recovery of proteins from tempera layers has been correlated with the presence of inorganic cations [11–16] that may reduce the solubility of the organic materials due to cross-linking reactions where cations may be active as catalysers.

### 9.1.2 Biological Degradation and Interferences

Growth of micro-organisms on paintings may cause aesthetic and structural damage as well as alter chemical composition of painted artwork, directly affecting the original protein content. The main consequence of micro-organisms due to their metabolic activity (such as the excretion of enzymes, inorganic and organic acids and of complex forming substances) is the dissolution of minerals of the substrate [17]. After an initiation period of growth, the microflora may turn into a biofilm, which continues to live at extremely low levels of metabolic activity. Chemical, physical and biological activities may be screened or shielded for a very long period of time. Furthermore when an organic substance is exposed to micro-organisms (such as yeast, bacteria, and mould), fermentation takes place. Unlike the denaturation process, fermentation alters the properties of an organic material and causes irreversible changes within the material. The action of enzymes, either present in the organic substrate itself or secreted by the active micro-organisms is also often considered part of the fermentation process. During the fermentation process, peptide bonds can be broken, sugars can be digested and altered, and amino acids can be broken down. Yeast for example, which is commonly known for its effect on sugars, can derive some of its nutritional requirement from the amino acid lysine.

The formation of pigmented biofilms, biomineralisation, the dissolution of metals by acids and chelating agents, the degradation of organic binders and consolidants, and the degradation and discoloration of pigments are some of the damaging occurrences triggered by microbial growth [18–20]. The degree of damage is strictly correlated with the type and dimension of the involved organisms, the kind of material and the state of its conservation, the environmental conditions, the micro-climatic exposure, and the level and the types of air pollutants [21]. It is now well recognised that micro-organisms can cause damage on paintings. However, most of the published reports are essentially lists of the micro-organisms isolated from painted surfaces [22–24], while information on the actual chemical damage to the organic materials is very limited [22,25–27].

### 9.1.3 Action Induced by Environmental Conditions

Environmental factors such as temperature (increases), humidity (violent change), pH and exposure to UV radiation can also influence the stability of the proteins, causing changes in their structure and lowering the resistance to biodeterioration. This decay is also influenced by the presence of other components such as lipids, carbohydrates, mineral

constituents and impurities [21]. In fact, photodecomposition includes the breakdown of hydrogen bonds and the destruction of disulfide bonds (creating two reactive -SH groups). The aromatic amino acids (phenylalanine, tryptophan and tyrosine) absorb UV light and are thereby oxidised. Furthermore, it is known that amino acids can become separated from the protein chain by the action of light, which implies that the peptide bond itself is responsible for UV light absorption [28]. The pH change is another important factor that, in the presence of moisture, can induce hydrolysis of peptidic bonds. Consequently decomposition occurs, molecular weight changes, dehydration in serine and threonine may result [6], and cysteine in alkaline pH degrades to cystine and dehydroalanine [29].

For the above reasons, the identification of proteinaceous paint media, and in general organic paint constituents in works of art, is still considered a difficult challenge for the chemist. Summarising, one has to consider the following:

- a paint sample by its structure is heterogeneous, proteinaceous paint media may be present along with several other natural and synthetic organic substances;
- in the tiny paint sample (<1 mg), the protein content typically is low and at most 10% w/w;
- aged proteins are denaturised and as a result they are barely soluble in water and organic solvents;
- proteins may interact with the other inorganic and organic materials present in the painting;
- proteins are also sensitive to environmental and storage conditions (bacterial and fungal attacks, light and moisture degradation);
- degradation compounds may be present as a result of ageing, restoration treatment, and pollution.

To address these concerns, chromatographic techniques have been the most widely adopted approach for specific identification of the proteinaceous materials in paint media and of their by-products resulting from the degradation processes [11,30,31]. The range of chromatographic techniques applied to the characterisation of the proteinaceous constituents in paint includes paper chromatography [32,33], thin-layer chromatography (TLC) [34–36], ionic exchange chromatography [37,38], reversed phase high-performance liquid chromatography with pre-column derivatisation [14,39–45], gas chromatography [7,15,16,30,46–57], and pyrolysis combined with gas chromatography-mass spectrometry (Py-GC/MS) [58–66]. Gas chromatography (GC) and gas chromatography-mass spectrometry (GC/MS) are among the most commonly used techniques for the identification of proteinaceous paint media, and they generally give more accurate and reliable results than other methods due to their high specificity and sensitivity [5,11,67].

These techniques are also not affected by the constraint of having small samples and are sensitive to the kind of proteinaceous material, even if the latter is present in mixtures with other organic materials. These techniques are said to be destructive as they necessarily require the destruction of the sample that cannot be recovered and used for another type of analysis. Nevertheless, for all practical purposes, regarding the very low amount of sample needed and the high specificity of information achieved, they can be considered as micro-invasive.

By coupling GC with MS as the detection system (either ion trap or quadrupole mass spectrometer), structural information can be obtained regarding unknown or unexpected components. Another advantage of using mass spectrometric detection is that it can distinguish analytes tagged with stable isotopes, offering the possibility to use them as

internal standards for quantification. Using MS can have a great effect on the specificity and sensitivity of detection [5,11,68], and can be further enhanced whenever a derivatisation reaction is applied in the chromatographic protocol. This unique aspect of the detection specificity and sensitivity, together with the increased availability of low cost affordable systems, makes it clear why these techniques are so frequently used.

In the following sections, common features of gas chromatographic procedures applied to proteinaceous material identification in paint are discussed such as sample pretreatments and data analysis. Finally, a section is devoted to the recognition of the amino acid racemisation in ancient proteins encountered mostly in archaeological contexts.

## 9.2 Sampling

Sampling is the first and a crucial step in an analytical procedure. This step becomes extremely important whenever proteinaceous materials have to be characterised in paint. Actually, in order to safeguard the integrity of works of art, the number of samples and their sizes must be reduced as much as possible. That is why it is important to plan these operations in collaboration with restorers and conservators in order to minimise the damage and in the meantime to take micro-samples that are as representative as possible of the work of art [4,5]. Non-invasive techniques (those not requiring the removal of original material) represent a useful tool to obtain the preliminary information by 'scanning' the overall paint to identify the richest areas in organic content. Once the decision of the sampling locations has been taken, several methods of sampling are available, as summarised:

- Scalpels, lancets, brushes, syringes, or logging instruments [69] are the most commonly used tools for mechanical paint sampling. Collected samples are heterogeneous with materials coming from the different adjacent layers of varying composition and thicknesses. Samples need to be carefully subdivided under the microscope to separate the different layers into subsamples so that information on the composition of the various layers may be achieved. The challenge resides in the selective separation of the layers, especially whenever the paint layer is thin or the amount of organic binder is rather low. Contamination from support layers is very frequent such as from the plaster in wall painting samples. A microdrilling method providing 100–200  $\mu\text{m}$  diameter bore samples has been suggested [70]. This method is particularly well suited for the study of multi-layered structures. Samples are separated with a microtome into 10  $\mu\text{m}$  thick subsamples, and as a result, each distinct layer may be analysed more easily. Further technological advancements in sampling such as this, combined with the increasing sensitivities of analytical techniques, promise a future potential for analysing multi-layered objects of precious artistic and historical value.
- Mechanical sampling of artwork can be done by the ablation of material on a microscope glass slide using a pulsed Er:YAG laser system [71] operating at 2.94  $\mu\text{m}$  and is typically used to clean paintings. Using this method the sample is recovered on a microscope glass slide. This system allows many materials from wall, easel and wooden paintings to be safely and effectively ablated. As a result, samples may contain from 1 to 80  $\mu\text{g}$  of organic material, according to the energy delivered. Research is still in progress to develop new techniques to selectively collect paint layers from all kinds of painted surfaces, such as textiles, paper, and walls [72].

### 9.3 Sample Pretreatment

GC requires low molecular weight molecules, and the macromolecular nature of proteinaceous materials (made up of 21 amino acids covalently condensed) means that they are typically too large to be readily identifiable and time consuming pretreatments of the sample are required. In order to free the amino acids, hydrolysis is required. Subsequent steps of purification to eliminate pigment interferences are also often necessary. Consequently sample pretreatments must be carefully carried out to reduce the risk of loss and/or contamination of the sample.

#### 9.3.1 Hydrolysis

Chemical, thermal, or enzymatic treatments are required to obtain analysable samples. Two typical methods used to achieve the hydrolysis of peptidic bonds are enzymatic and chemical catalysis [73]. The reaction times for enzymatic hydrolysis are long and typically lie in the range of 4–8 h [47]. Additionally, they demand purification procedures to get rid of the excess enzyme that could interfere in the protein identification. Due to these drawbacks, this method of hydrolysis finds limited use in the conservation science field.

Alkaline or acidic hydrolysis has shown to be a very effective and suitable approach with reaction times between 1 h and 24 h:

1. Acidic hydrolysis using 6 M HCl at a temperature of 110°C is a well established method for hydrolysing proteins and peptides in paint samples [15,30,46,49,56]. The process is carried out in vacuum or in an inert nitrogen or argon atmosphere for several hours. Different experimental conditions yield an amino acid recovery which is a compromise between an efficient hydrolysis of the most stable peptide bonds (ile-ile, val-val, ala-ala, ile-ala) and the minimum losses of the less stable amino acids (phe, arg, thr, tyr, ser), while tryptophan, cystine, cysteine, and methionine undertake total or partial degradation in the acidic environment. The total content of cystine and cysteine may be achieved by the addition of performic acid which oxidises them into cysteic acid [74–76], an estimation of the amount of tryptophan (trp) may be done using additives, such as mercaptoethanol and tryptamine, by performing hydrolysis with organic acids such as mercaptoethanesulfonic acid and methanesulfonic acid [74,75]. During the hydrolysis process, glutamine and aspartine are converted into glutamic acid (glu) and aspartic acid (asp), respectively. Hydrolysis in the vapour phase has often been adopted as a tool for decreasing the chances of contamination related to the addition of HCl solution into the sample [14,15,42,47]. Microwave assisted hydrolysis using 6 M HCl under nitrogen atmosphere, at 8 atm and 160°C for 40 min (250 W) [47] or using 10 M HCl at 240 W for 90 min [77] has greatly improved the results of vapour acidic hydrolysis leading to either comparable or enhanced yields to those recovered with the classical HCl hydrolysis conditions (6 N HCl, 110°C, 24 h) while dramatically reducing the digestion time. The additional electromagnetic energy improves the efficiency of the hydrolysis of peptide bonds and reduces the amino acid losses due to oxidation and degradation which are characteristic of methods which require longer reaction times. Another concern arises because, in addition to the protein content in the paint samples, sugars and polysaccharides (e.g. vegetal gums, starch, or honey)



are often simultaneously present and interfere with the amino acids during the hydrolysis. Artefacts arise through Maillard reactions: condensation reactions between the aldehyde functions of sugars and amino acids [29,30]. This often leads to the formation of humins at the expense of amino acid content. A method has been suggested in the literature [16,55] to overcome this type of interference. It relies on a mild hydrolysis, performed under vacuum at 110°C for 24 h, in the presence of a strongly acidic ion exchange resin (suspended in water/ethanol solution) that acts as a catalyser. In this way, once the peptide linkages have been hydrolysed, the amino acids and cations from pigments are bound to the cation exchange resin, whereas polysaccharides remain in solution. Amino acids are further recovered after elution with 7 N ammonia solution.

2. Alkaline hydrolysis has the advantage of permitting the recovery of tryptophan [74,75]. Samples (25 mg) are weighed in Pyrex glass tubes with Teflon-lined screw-caps used as the hydrolysis vessel. Three millilitres of 4.2 M sodium hydroxide are then added to the glass tubes and the contents mixed in an ultrasonic bath for 2 min. Air is removed with nitrogen. Subsequently, the samples are hydrolysed by heating at 120°C for 4 h and cooled in an ice bath. Then, the pH is adjusted to 9 with concentrated hydrochloric acid. The resulting solution needs to be vacuum-filtered through Whatman paper (no. 41). The filtrate is diluted to 50 ml with a borate buffer in a volumetric flask. Then, 5 µl of the final solution is injected for analysis [78]. Others propose the use of 1 M barium hydroxide at 108°C for 48 h [79].

### 9.3.2 Sample Purification

Beyond the interference due to the presence of polysaccharidic gums, also widely used as binders and adhesives in art works, the determination of the proteins may be hindered by the loss of amino acids during natural ageing usually undergone by the organic binders (oxidation, cross-linking, condensation, and dehydration). These disadvantages are even more prominent in samples coming from wall paintings where very high amounts of salts are present.

As mentioned in the previous sections, an important interfering agent in the protein analysis in paint samples is the presence of pigments. In fact, the analytical methods may suffer due to pigments that may continuously interact with the medium through the formation of strong complexes [8,9,11–13,30,39,40,42,45]. For example, copper ions in pigments such as azurite have a great affinity for complexing amino acids. Other metal ions, including  $\text{Hg}^{2+}$ ,  $\text{Fe}^{3+}$ ,  $\text{Ni}^{2+}$ ,  $\text{Ca}^{2+}$  and  $\text{Mg}^{2+}$ , from pigments that may be present in paintings, can act in the same way as copper ions. In addition, amino acids differ in their susceptibility to forming metal complexes, and consequently proteins subjected to ageing will react differently relative to the type of pigments present. The above-mentioned interactions with cations may selectively subtract some amino acids from the analysis or give rise to interferences during the analytical pretreatment and thus may hamper the correct identification of the proteinaceous binder [7]. In fact, a decrease in the total recovery of proteins from paint layers has been related to the presence of these inorganic cations and this may be due to the reduced solubility of the organic materials because of cross-linking reactions where cations may be active as catalysers or the formation of stable complexes with the amino acids [11–16]. It has been reported that the recovery of egg protein significantly decreases when gypsum, calcium oxalate or both are present [80].



**Table 9.1** Sample purification methods

Purification method		Notes	Reference
Extraction	NaOH solution	—	42
	Water, 1 N NaOH (80°C, 3 h) and 1 N HCl	100% animal glue, 80% egg but not well adapted to GC due to the high concentration of sodium ions remaining in the hydrolysate	14
	Na <sub>2</sub> EDTA 0.2 M in ammonia buffer at pH = 9	Good recovery for animal glue and casein. Additional dilution of the sample increasing risks of contamination and loss	9,41,44
	Ammonia extraction with NH <sub>3</sub> 2.5 M in a sonicator	100% animal glue, 96% casein, 89% egg. Low recoveries when copper ions present in the sample	8
Ion exchange chromatography	Protonated strong cation exchange resin	Recovery not reported	54
	Small home-made column packed with a cation-exchange resin (DOWEX)	Nearly quantitative	8
	C <sub>18</sub> tip	Very well adapted to all metal ions interferences but low recoveries. Studies in progress for use of C <sub>4</sub> tip	10
	Addition of barium chloride 0.5 M to the acid hydrolysate	Suppression of sulfates	81,82

For the reasons discussed so far, the identification of organic paint constituents and in particular proteinaceous paint media is still a real challenge. One of the main difficulties in the protein analysis lies in the isolation of the proteins from a very heterogeneous sample.

In order to suppress interferences due to the presence of inorganic species and reliably determine the proteinaceous composition of the sample, a clean-up step has often been introduced in the analytical procedure. This step may include the extraction of the proteinaceous matter by an ammonia solution [8], the use of a cation-exchange resin [8,55], a chelating agent [9,41,44], the use of a C<sub>18</sub> resin or the use of barium chloride solution to suppress sulfates [10,81,82]. Table 9.1 reports the methods used to overcome such problems.

## 9.4 Derivatisation Methods

A GC analysis of amino acids requires a derivatisation step to increase the volatility of the amino acids. Generally, norleucine and/or norvaline are the internal standards added to the hydrolysate to check the derivatisation yield. According to the experimental method applied, the limits of detection (LOD) vary in the range 10–100 pg for each amino acid. Regarding the chromatographic columns, as most of the derivatives are esters – barely polar compounds – the most commonly used are fused-silica capillary columns with a low

**Table 9.2** Derivatisation methods for the GC analysis of protein hydrolysates from paint samples

Derivatising agent	Determined amino acids	Reference
Trifluoroacetamide + methanol	ala, val, gly, ile, leu, thr, met, ser, pro, asp, glu, phe, lys, hyp	30
Trifluoroacetamide + isopropyl alcohol	ala, val, gly, ile, leu, thr, ser, pro, asp, glu, phe, hyp	49,50,54
Trifluoroacetamide + butanol	ala, val, gly, ile, leu, thr, met, ser, pro, asp, glu, phe, lys, hyp, tyr	16
<i>N,O</i> -bis(trimethylsilyl)acetamide	ala, val, gly, ile, leu, thr, ser, pro, asp, glu, phe, hyp, tyr	55
<i>N-tert</i> -butyldimethylsilyl- <i>N</i> -methyltrifluoroacetamide	ala, val, gly, ile, leu, thr, met, ser, pro, asp, glu, phe, lys, hyp, arg, his, tyr	47,48,85
Methylchloroformate, ethylchloroformate	ala, val, gly, ile, leu, thr, met, ser, pro, asp, glu, phe, lys, his, hyp, tyr, cis	9,56

Adapted from reference [5].

bleed stationary phase such as 5% phenyl/95% methylpolysiloxane. They allow an enhanced sensitivity and a low baseline drift during temperature programming. Other more polar stationary phases (i.e. polyethylene glycol) are also in use.

Table 9.2 summarises the derivatisation methods most used for the analysis of amino acids in paint hydrolysate. In particular:

- Transformation of amino acids into their *N*-trifluoroacetyl methyl esters [30], their corresponding propyl esters [83], butyl esters [16,55] or *N*-pentafluoropropionyl *n*-propyl esters [84] requires two distinct reaction steps. First, methanol, propanol, butanol, or *n*-propanol is used for the esterification of the acidic functions, and subsequently the reagents and solvents are evaporated. Next, trifluoroacylation or pentafluoropropionylation of the amine group is carried out. A drying step to eliminate all water is required in both of these steps. While the *N*-trifluoroacetyl function is characterised by good stability, *O*-trifluoroacetyl easily undergoes hydrolysis. This means that amino acids with OH functions, such as hydroxyproline, provide only qualitative results. One advantage of this type of derivatisation is the presence of fluorine in the molecule allowing an ideal detection of these derivatives by negative-ion chemical ionisation mass spectrometry or by means of electron capture detection (ECD). ECD allows the determination of amino acid content in as low as the picogramme range.
- Silylation with formation of trimethylsilyl (TMS) derivatives [55,75] or *tert*-butyldimethylsilyl (TBDMS) derivatives [47,48,85–87] has the advantage of the simultaneous derivatisation of acidic and aminic functions. However, the absence of humidity is critical also in this method; indeed, water would degrade the silylating reagent. This is why it is important to make sure that the amino acidic hydrolysate is well dried. These types of derivatisation are widespread in GC-MS methods as complementary mass spectrometric characteristics may be obtained. In fact, detailed fingerprints are provided:  $\alpha$ -amino acids may be selectively detected by monitoring the significant fragment at  $m/z$  218 [TMS-NH<sub>2</sub>CH-COOTMS<sup>+</sup>]. In addition, TBDMS derivatives are quite stable compounds. The fragmentation pattern is rather simple. Dominating the resulting pattern, the ions with  $m/z$  equal to [M-57]<sup>+</sup> (loss of a *tert*-butyl group)

may enable molecular weight determination and are very appropriate for quantitative analysis by selected ion monitoring (SIM). Only in the case of proline or hydroxyproline does a more difficult fragmentation occur, and two derivatised products are obtained.

- Finally, the derivatisation with alkyl chloroformates in ethanol/water/pyridine [88] occurs in a single step, only requires a few seconds, and acts on both amino and hydroxyl groups. Mainly, derivatisations with methyl and ethyl chloroformates have been used in the analyses of binders presenting the advantage of being unaffected by the presence of water, and thus being directly applicable to the hydrolysate. However, the simplicity of working with aqueous solutions is slightly complicated by requiring strict pH control in order to carry out an efficient derivatisation and by a partial loss of amino acids which remain unreacted and present in the aqueous phase as salts [89]. These constraints together with an extensive fragmentation of ethyl chloroformate derivatives make this method less effective for quantitative determination using acquisition in SIM mode. Recently, novel fluoroalkyl chloroformates with three and four carbon atoms were investigated for the immediate conversion of amino acids into hydrophobic derivatives in water-containing media [90]. These derivatising agents seem very promising due to the high reactivity toward amino acids in aqueous media, even without the addition of alcohol, while creating highly volatile derivatives with molecular weights <850 Da. In general, it has to be stressed, that upon working with chloroformates, precautions should be taken into account because of the toxic reagents used and corrosion effects.

## 9.5 Analysis and Quantitation

Chromatographic procedures applied to the identification of proteinaceous paint binders tend to be rather detailed consisting of multiple analytical steps ranging from solvent extractions, chromatography clean up, hydrolysis, derivatisation reactions, and measurement to data analysis. Knowledge of the error introduced at each step is necessary to minimise cumulative uncertainty. Reliable results are consequently obtained when laboratory and field blanks are carefully characterised. Additionally, due to the small amounts of analyte and the high sensitivity of the analysis, the instrument itself must be routinely calibrated with amino acid standards along with measurements of certified reference proteins. All of these factors must be taken into account because many times there is only one chance to take the measurement.

The laboratory blank is achieved by performing all the steps of the analytical procedures without any actual samples. In this way, the analytes examined at the end of the procedure should contain all possible contaminants from laboratory glassware, solvents, reagents, and any other chemicals used during the analytical protocol. The laboratory blanks need to be seriously considered because they contribute to the limit of detection of the applied procedure. Amino acids such as alanine and glycine, but also fatty acids and phthalates represent the most common source of contamination from the laboratory environment. Simple strategies such as rigid cleaning procedures, using analytical or pesticide grade solvents and reagents, and routinely performing chromatographic runs of solvents to monitor memory effects are often implemented to combat these variables.

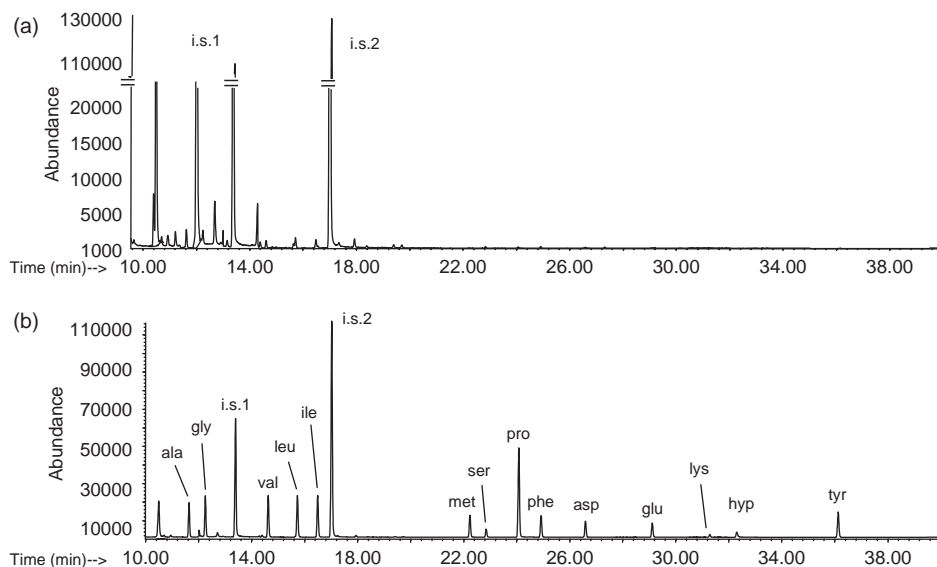


**Figure 9.1** GC-MS chromatograms acquired in the SIM mode of a laboratory blank (a) and an amino acid standard solution with concentrations at the quantitation limit (b). *i.s.1*, Hexadecane internal standard; *i.s.2*, norleucine internal standard

As a general rule, running blanks of the procedure highlights the level of contamination of amino acids. The evaluation of amino acid contamination (expressed in  $\mu\text{g g}^{-1}$  or  $\text{mol}^{-1}$ ) is possible by using calibration curves: an estimation of three times this blank level may be considered as the lower limit to make a positive identification of protein content in an unknown sample.

Figure 9.1a reporting GC-MS results taken on laboratory blank in a GC-MS procedure [87] shows negligible amino acid contamination. Indeed, quantitating a protein as the sum of 14 amino acids, a value of about 200 ng is the minimum required threshold to positively consider the protein identification. Figure 9.1b reports the chromatogram of an amino acid standard solution acquired in the SIM mode and corresponds to the quantitation limit that is a content of about 700 ng in the sample at a confidence level of 95%. This seems amenable when working at the trace level.

Additionally, field blanks quantify a different form of contamination, i.e. environmental factors attributable to storage conditions can add artefacts to a measurement. Over time, particulates could have been accreted or adsorbed on surfaces. Samples collected from surfaces close to the painting (e.g. from the wooden frame) have also been known to show traces of lipids and proteins from human skin cells (possibly resulting from excessive handling), bacteria, and other environmental pollutants. Squalene, a marker compound for skin cells, together with some fatty acids highlights human contamination [91]. Generally, amino acid field blanks exhibit patterns completely different from those of glue, milk, and egg protein and contain small amounts of amino acids; however, this low content can lead to erroneous conclusions.

Calibrations made using certified amino acid sources are of the utmost importance. The evaluation of the content of amino acids in laboratory and field blanks implies a quantitative

analysis of amino acids. Using commercially available certified amino acid standards, linear or quadratic [85] calibration curve fits, with correlation coefficients better than 0.99, can be achieved. Results, which are also a function of the concentration range, are given in mol% [14,15,39,56] or wt% [8,47]. Since the response may change for the different amino acids depending on the analytical procedure, results based upon calculation of the peak areas should be discouraged because these data, obtained under different conditions, cannot be used in intra- and inter-laboratory comparisons. Moreover, quantitative analysis provides data on the amount of protein contained in the samples and in the blanks, thus decisions can be made on the actual presence of proteinaceous binders in paint samples. In fact, the protein 'detected/not detected' decision should still be based on the threshold value of the detection limit.

A very common obstacle encountered in the application of chromatographic diagnostic techniques to works of art is a lack of reference materials. Reference materials such as unused paint samples from paint manufacturing companies, can ensure the quality of the data. Over the last few years several museums, laboratories, and restoration centres around the world have produced collections of reference paint materials such as that stored at the Opificio delle Pietre Dure of Florence (Italy)<sup>1</sup> or the Tintori Collection.<sup>2</sup> Proper characterisation of these samples can obviously improve our capabilities to identify proteinaceous binders in artwork. The reference gives insight into the chemical composition of the artwork when it was freshly finished. They can also be used in different simulated ageing experiments. In a controlled manner, the effects of very many different variables such as the paint's response to temperature, light, and different pollutants can be studied. Different research projects on large collections of reference paint replicas have been done [92] or are still in progress [4]. Such a study has the additional advantage of being able to improve current paint media to be less susceptible to these types of degradations.

## 9.6 Proteinaceous Binder Identification

The identification of the proteinaceous binder is done by the evaluation of the amino acid patterns obtained: generally egg, casein, animal glue and garlic (garlic being used in gildings [93]) are reported. The amino acid profiles have been processed by different methods and several strategies have been developed to obtain the final identification:

1. Comparison of the amino acid profile of unknown samples with amino acid data of reference proteinaceous substances; this is a simple and very subjective method [94]. The mean amino acid profile of the three main proteinaceous paint materials is reported in Chapter 1.
2. Use of characteristic amino acid ratio values which best differentiate the three main animal proteinaceous media [5,11]. The amino acids chosen for the ratios may vary, but

<sup>1</sup> In 1997 a collection of reference samples was prepared at the Opificio delle Pietre Dure of Florence by painting many glasses and wall specimens following Cennini's recipes using different pigments and proteinaceous binders.

<sup>2</sup> Leonetto Tintori (1908–2000), sculptor, painter, and wall paintings conservator, made hundreds of wall paintings replicas simulating different techniques and material combinations. In the past 20 years, over 500 wall painting replicas were produced representing therefore over 5,000 combinations of pigments (mineral, natural, artificial), binders (mainly egg, animal glue, casein, milk, and oil) and phases of application (a fresco over a fresh plaster, *su intonaco stanco* over semi-drier plaster, and a *secco* over dry plaster). This collection has been studied during the research project "Organic Materials in Wall Paintings" coordinated by the Getty Conservation Institute ([http://www.getty.edu/conservation/science/omwp/omwp\\_component1.html](http://www.getty.edu/conservation/science/omwp/omwp_component1.html), 2003–2006) [4,13,96].

all methods exploit the fact that animal glue contains substantially higher amounts of glycine with respect to egg and milk, while casein contains higher amounts of glutamic acid with respect to egg. The use of only a few amino acid ratio means that identification is based on the measure of only a few amino acids, and that not all the information contained in overall amino acid composition is used. Consequently, the identification is often not reliable, especially when mixtures are present.

3. Use of amino acid ratio flow charts using amino acid ratio values [95]; again not all the information contained in overall amino acid composition is utilised.
4. Use of correlation coefficients between amino acid profile data in order to efficiently quantify the degree of similarity between unknown samples and reference proteinaceous materials [7]. The method processes quantitative amino acid concentrations either as per cent relative content ( $\mu\text{g g}^{-1} \%$ ) or per cent molar content ( $\text{mol } \%$ ). A match of more than 0.9 is necessary to ensure a reliable identification of the proteinaceous binder. Table 9.3 reports results obtained on samples coming from the Tintori Collection analysed with two different analytical procedures showing a good correlation with the egg-based binder [96].
5. Use of multivariate statistical analysis such as principal components analysis (PCA) to compare large data sets composed of many reference samples of known composition with unknown samples [5,48,51,83,93,97]. This method also processes quantitative amino acid concentrations. Basically, PCA analysis, a very powerful technique for pattern recognition, is the preferred multivariate method and allows the reduction of redundant information contained in the  $n$ -dimensional amino acidic pattern to two or three variables (the principal components) with a limited loss of variance. As an example, Figure 9.2 reports the score plot using a reference data set of samples containing egg, casein, and animal glue belonging to the paint samples from the collections of the Opificio delle Pietre Dure and of Tintori (series OL17bis). In particular, the PCA is performed, using XLSTAT 6.0 (Addinsoft, France), on the correlation matrix of the data. The first two components account for at least 70% of the total variance of the data. Since PCA is only a projection but not a classification technique, it is possible to assess a close similarity between samples and to highlight any outliers; actually, in the case of protein mixtures, only partial information is achieved.

**Table 9.3** *Results of the amino acid analysis of OL17\_bis series samples from the Tintori Collection*

Sample	Binders	Method reference	Best match of the correlation coefficient method		
			Casein	Egg	Glue
OL17bis_A1	Egg (8.1%) + Linseed oil (10.4%)	87	0.54	0.96	0.53
		86	0.32	0.93	−0.37
OL17bis_A4	Egg (8.1%) + Linseed oil (10.4%)	87	0.55	0.92	0.63
		86	0.35	0.97	−0.32
OL17bis_C1	Egg (8.1%) + Linseed oil (10.4%)	87	0.60	0.94	0.60
		86	0.32	0.91	−0.07
OL17bis_C4	Egg (8.1%) + Linseed oil (10.4%)	87	0.66	0.93	0.68
		86	0.07	0.96	0.36

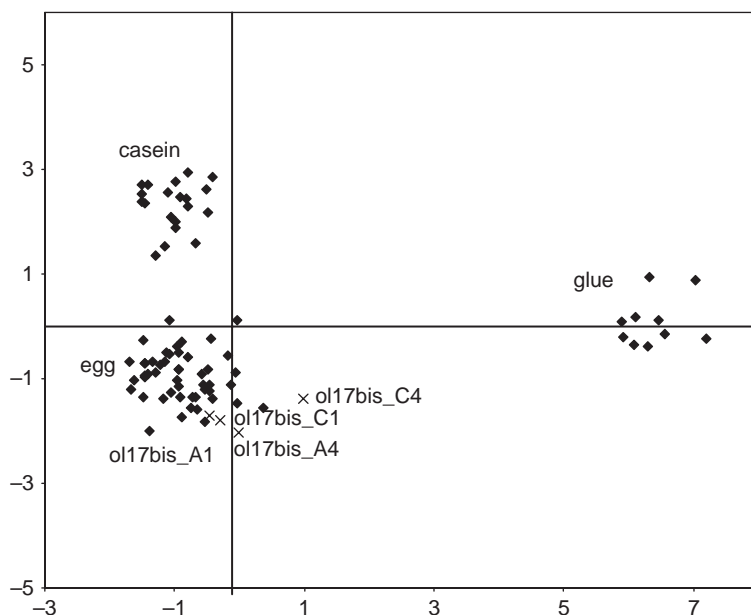


**Figure 9.2** PCA score plot of amino acid profiles obtained in the GC/MS analysis of samples from the collection of paint reference materials of Opificio delle Pietre Dure (◆), containing egg, casein and animal glue as binders, and of samples from the OL17bis series (×) from the Leonetto Tintori Collection [10]

6. Use of multivariate approaches based on classification modelling based on cluster analysis, factor analysis and the SIMCA technique [98,99], and the Kohonen artificial neural network [100]. All these methods, though rarely implemented, lead to very good results not achievable with classical strategies (comparisons, amino acid ratios, flow charts) and, moreover it is possible to know the confidence level of the classification carried out.

## 9.7 Amino Acid Racemisation and Dating

Recently, efforts in the field have focused on amino acid racemisation and dating. The following section provides a brief background regarding the amino acid racemisation analysis, and a review of the applications of this method in paintings. Chemical dating methods, such as amino acid racemisation dating, are based on predictable chemical changes that occur over time. Amino acid racemisation has been used mainly in an archaeological context for about 40 years to determine relative dates of biological materials such as bones, shells and teeth. A number of significant results [54,101–103] have been generated, but many have been questioned and the technique remains controversial. In spite of this, the possibility of reliable amino acid racemisation dating remains attractive.

Amino acids are the building blocks of protein. Except for glycine, all amino acids come into two different chiral forms, *laevorotatory* (L) and *dextrorotatory* (D); these forms are called enantiomers. In living organisms, the amino acids in protein are almost exclusively

L and the D/L ratio approaches zero. After the death of the living organism, proteins start to spontaneously break down. An inter-conversion of the amino acids occurs from one chiral form (L) to a mixture of D- and L- forms following protein degradation; this process is called amino acid racemisation. The extent of racemisation is measured by the ratio of D/L isomers and increases as a function of time and temperature. The longer the racemisation process continues the closer to 1 the ratio between the D- and L-forms becomes. If the D/L ratio is  $< 1$  it may be possible to use it to estimate age. The D/L ratio of aspartic acid and isoleucine are the most widely used for this dating technique [104]. Dates have been obtained as old as 200 000 years. However, it has been used mainly to date samples in the 5000–100 000 year range. Recent studies [105] mention an estimation of the method accuracy to be around 20%.

Racemisation is a chemical reaction, and its rate is different for each type of amino acid. An important fact is that this process is affected by many factors that influence the rate of change of the amino acids stereochemistry [106]. The main parameters affecting the racemisation process include the amino acid structure, the sequence of amino acids in peptides, the bound state versus the free state of the amino acids, the pH in the environment, the concentration of buffer compounds, the contact of the sample with clay surfaces

**Table 9.4** Recent applications of GC/MS procedures to determine proteins in artworks

Painting	Identification of protein and notes	Reference
<i>Qin Shihuang's Terracotta Army</i> , Xian (China)	Egg as paint binder	115
<i>Madonna col Bambino e S. Giovannino</i> by Sandro Botticelli, in the Museo Civico di Piacenza (Italy)	Egg as pigment binder and animal glue for the ground (gypsum, anhydrite)	116
<i>Sixteenth century wall paintings</i> in Spilamberto (Italy)	The pigment was applied directly on the plaster using a egg binder	117
<i>Sarcophagus of Amazons</i> , Florence (Italy)	Egg was used as pigment binder and animal glue in the plaster	118
<i>Wall paintings of Protaton church</i> , Mount Athos (Northern Greece)	Egg and animal glue as binding medium and in the preparation of the plaster	119
<i>Domus de Janas necropolis</i> , Sardinia (Italy)	Egg was used as binder	120
<i>Crypt of the Cathedral</i> of Siena (Italy)	Egg and animal glue	10
<i>Church of the Assumption</i> in Cephalonia (Ionian Island, Greece)	Egg as binding medium, animal glue from the ground preparation and coating layer, casein in the ground	121
<i>Spanish Renaissance panel painting</i> attributed to Bartolomé Bermejo (1468–1495)	Egg white as binding medium	122
<i>Wall paintings at Qusayr Amra</i> , Amman (Jordan)	Egg as binder	123
<i>Church of Agios Sozomenos</i> in Galata (Cyprus)	Casein as binder	124
<i>Mural paintings at the Kariye Museum</i> in Istanbul (Turkey)	Casein as painting binder and animal glue in the plaster	125
<i>St Stephen's wall paintings at Meteora</i> (Greece)	Egg as binder	126



(catalytic effect), the presence of metallic cations, the water concentration in the environment and the temperatures the sample was exposed to. Of these, temperature is generally thought to play the most significant role in determining the racemisation rate [107,108]. The potential variation in the racemisation rate has led some palaeoanthropologists to consider this dating technique relative rather than chronometric. To establish the technique as a dating method, the kinetics and mechanisms of the racemisation (or epimerisation where more than one chiral centre is present) process of free and peptide bound amino acids need to be established. To this end, various scientists in the late 1960s and the 1970s studied free amino acids in solution and carried out laboratory simulations of post mortem changes in the amino acids present in bone [109] and shell [110,111]. Attempts have also been made to correlate the kinetics of free amino acids with those in short polypeptides as well as the proteins in various archaeological samples [112,113].

Considering all the above factors for amino acid racemisation rates, this technique cannot be used as an absolute dating technique. To overcome the problem of uncertainty, the amino acid racemisation method must be calibrated against other more reliable techniques.

In paintings, amino acid racemisation depends upon the presence of albuminous binders, such as blood or egg white. The ability to apply this technique is based on the observation that the number of amino acids present in proteins decreases over time. Decay curves are constructed of paint samples of known age. Moreover, amino acid decay rates are also dependant upon micro-organisms (whose enzymes can digest various types of proteins) and environmental conditions [114].

## 9.8 Conclusions

New chromatographic technologies are widespread in the scientific laboratories of museums and collections, so that there are increasing numbers of publications aimed at the characterisation of proteins in art. Table 9.4 lists some of the most recent applications in the field but it is not exhaustive as lots of works are presented at conferences and workshops.

The data in the literature highlight that proteins are relatively stable to oxidation and that most of the alterations are ascribable to the action of humidity and to the effect of aggressive restoration practice.

## References

1. F. Cappitelli, Y. Shashoua, E. Vassallo (Eds) *Macromolecules in Cultural Heritage*, Macromolecular Symposia 238, Wiley-VCH, Weinheim (2006).
2. R.J. Gettens, G.L. Stout, *Painting Materials – A Short Encyclopaedia*, Dover Publications, Inc., New York (1966).
3. C. Cennini, *Il Libro dell'Arte* (XIV sec.), edited by R. Simi, R. Carabba, Editore, Lanciano (1932).
4. F. Casadio, I. Giangualano, F. Piqué, Organic Materials in Wall Paintings: the Historical and Analytical Literature, *Reviews in Conservation*, **5**, 63–80 (2004).
5. M.P. Colombini, F. Modugno, Characterisation of Proteinaceous Binders in Artistic Paintings by Chromatographic Techniques, *Journal of Separation Science*, **27**, 147–160 (2004).

6. J.J. Boon, S. Peulvé, O.F. van den Brink, M.C. Duursma, D. Rainford, Molecular Aspects of Mobile and Stationary Phases in Ageing Tempera and Oil Paint Films, in *Early Italian Paintings, Techniques and Analysis*, edited by T. Bakkenist, R. Hoppenbrouwers, H. Dubois, Limburg Conservation Institute, Maastricht, 35–56 (1996).
7. M.R. Schilling, H.P. Khanjian, Gas Chromatographic Analysis of Amino Acids as Ethyl Chloroformate Derivatives. II. Effects of Pigments and Accelerated Aging on the Identification of Proteinaceous Binding Media, *Journal of the American Institute of Conservation*, **35**, 123–144 (1996).
8. M.P. Colombini, F. Modugno, A. Giacomelli, Two Procedures for Suppressing Interference from Inorganic Pigments in the Analysis by Gas Chromatography-Mass Spectrometry of Proteinaceous Binders in Paintings, *Journal of Chromatography, A*, **846**, 101–111 (1999).
9. J. de la Cruz-Cañizares, M.T. Doménech-Carbó, J.V. Gimeno-Adelantado, R. Mateo-Castro, F. Bosch-Reig, Suppression of Pigment Interference in the Gas Chromatographic Analysis of Proteinaceous Binding Media in Paintings with EDTA, *Journal of Chromatography, A*, **1025**, 277–285 (2004).
10. G. Gautier, M.P. Colombini, GC-MS Identification of Proteins in Wall Painting Samples: A Fast Clean-up Procedure to Remove Copper-based Pigment Interferences, *Talanta*, **73**, 95–102 (2007).
11. S.L. Vallance, Applications of Chromatography in Art Conservation: Techniques Used for the Analysis and Identification of Proteinaceous and Gum Binding Media, *Analyst*, **122**, 75R–81R (1997).
12. M.P. Colombini, R. Fuoco, A. Giacomelli, B. Muscatello, N. Fanelli, Characterisation of Proteinaceous Binders in Samples of the Giudizio Universale Wall Paintings at Florence Cathedral, *Science and Technology for Cultural Heritage*, **7**(1), 49–58 (1998).
13. A. Andreotti, M.P. Colombini, G. Gautier, *Proceedings of the Organic Materials in Wall Paintings Project Workshop*, Prato/Florence (Italy), 17 June (2003).
14. J. Wouters, M. Van Bos, K. Lamens, Baroque Stucco Marble Decorations. I. Preparation of Laboratory Replicas and Establishment of Criteria for Analytical Evaluation of Organic Materials, *Studies in Conservation*, **45**, 106–116 (2000).
15. M.R. Schilling, H.P. Khanjian, L.A.C. Souza, Gas Chromatographic Analysis of Amino Acids as Ethyl Chloroformate Derivatives. Part 1, Composition of Proteins Associated with Art Objects and Monuments, *Journal of the American Institute for Conservation*, **35**, 45–59 (1996).
16. E. Kenndler, K. Schmidt Beiw, F. Mairinger, M. Pöhm, Identification of Proteinaceous Binding Media of Easel Paintings by Gas Chromatography of the Amino Acid Derivatives after Catalytic Hydrolysis by a Protonated Cation Exchanger, *Fresenius Journal of Analytical Chemistry*, **342**, 135–141 (1992).
17. P. Tiano, Biodegradation of Cultural Heritage: Decay Mechanisms and Control Methods, *Science and Technology for Cultural Heritage*, **7**, 19–38 (1998).
18. O. Ciferri, Microbial Degradation of Paintings, *Applied and Environmental Microbiology*, **65** (3), 879–885 (1999).
19. E. Bock, W. Sand, The Microbiology of Masonary Biodeterioration, *Journal of Applied Bacteriology*, **74**, 503–514 (1993).
20. K. Lal Garg, S. Dhawan, J. Singh (Eds), *Building Mycology: Management of Decay and Health in Buildings*, Chapman & Hall, London, 239–259 (1994).
21. B.M. Feilden, Insects and Other Pests as Causes of Decay, in *Conservation of Historic Buildings*, Butterworth Scientific, London, 139–156 (2003).
22. T. Dornieden, A.A. Gorbushina, W.E. Krumbein, Biodecay of Cultural Heritage as a Space/Time-Related Ecological Situation – an Evaluation of a Series of Studies, *International Biodeterioration & Biodegradation*, **46**, 261–270 (2000).
23. N. Karpovich-Tate, N.L. Rebrikova, Microbial Communities on Damaged Frescoes and Building Materials in the Cathedral on the Nativity of the Virgin in the Pafnutii-Borovskii Monastery, Russia, *International Biodeterioration*, **27**, 281–296 (1990).
24. L.L. Varonina, O.N. Nazarova, U.P. Petushkova, N.L. Rebrikova, Damage of Parchment and Leather Caused by Microbes, ICOM Committee for Conservation, 6th Triennial Meeting, Ottawa, 21–25 September (1981).

25. C.Urzi, Microbes and Art: the Role of Microbial Communities in the Degradation and Protection of Cultural Heritage – A Report on the International Conference on Microbiology and Conservation, *Environmental Microbiology*, **1**, 551–553 (1999).
26. A.A. Gorbushina, J. Heyrman, T. Dornieden, M. Gonzalez-Delvalle, W.E. Krumbein, L. Laiz, K. Petersen, C. Saiz-Jimenez, J. Swings, Bacterial and Fungal Diversity and Biodeterioration Problems in Mural Painting Environments of St. Martins Church (Greene-Kreienzen, Germany), *International Biodeterioration & Biodegradation*, **53**(1), 13–24, (2004).
27. A.A. Gorbushina, K. Petersen, Distribution of Microorganisms on Ancient Wall Paintings as Related to Associated Faunal Elements, *International Biodeterioration & Biodegradation*, **46**(4), 277–284 (2000).
28. P. Messier, Protein Chemistry of Albumen Photographs, *Topics in Photographic Preservation*, **4**, 124–135 (1991).
29. A. Karpowicz, Ageing and Deterioration of Proteinaceous Media, *Studies in Conservation*, **26**, 153–160 (1981).
30. R. White, The Characterization of Proteinaceous Binders in Art Objects, *National Gallery Technical Bulletin*, **8**, 5–14 (1984).
31. R. Pancella, R. Bart, Identification des Liants Organiques dans les Couches Picturales par Chromatographie en Phase Gazeuse, *Zeitschrift für Kunsttechnologie*, **3**, 101–111 (1989).
32. R.H. De Silva, The Problem of the Binding Medium Particularly in Wall Painting, *Archaeometry*, **6**, 56–65 (1963).
33. M. Hey, The Analysis of Paint Media by Paper Chromatography, *Studies in Conservation*, **3**, 183–188 (1958).
34. M.F. Striegel, J. Hill, *Thin Layer Chromatography for Binding Media Analysis (Scientific Tools for Conservation)*, Getty Trust Publication, Los Angeles (1996).
35. L. Masschelein-Kleiner, An Improved Method for the Thin-Layer Chromatography of Media in Tempera Paintings, *Studies in Conservation*, **1**, 207–211 (1974).
36. J. Tomek, D. Pechova, A Note on the Thin-Layer Chromatography of Media in Paintings, *Studies in Conservation*, **37**, 39–41 (1992).
37. S. Keck, T. Peters, Identification of Protein-Containing Paint Media by Quantitative Amino Acid Analysis, *Studies in Conservation*, **14**, 75–82 (1969).
38. V.J. Birstein, On the Technology of Central Asian Wall Paintings: the Problem of Binding Media, *Studies in Conservation*, **20**, 8–19 (1975).
39. S.M. Halpine, A New Amino Acid Analysis System for Characterizing Small Samples: Identification of Egg Tempera and Distemper in a Painting by Cosimo Tura, *Studies in Conservation*, **37**, 22–38 (1992).
40. S.M. Halpine, Investigation of Artists' Materials Using Amino Acid Analysis: Introduction of the One Hour Extraction Procedure, *Conservation Research*, **51**, 28–69 (1995).
41. C.M. Grzywacz, Identification of Proteinaceous Binding Media in Paintings by Amino Acid Analysis Using 9-Fluorenylmethyl Chloroformate Derivatization and Reversed-Phase High-Performance Liquid Chromatography, *Journal of Chromatography, A*, **676**, 177–183 (1994).
42. F. Ronca, Protein Determination in Polychromed Stone Sculptures, Stuccoes and Gesso Grounds, *Studies in Conservation*, **39**, 107–120 (1994).
43. M.P. Colombini, R. Fuoco, A. Giacomelli, B. Muscatello, C. Baracchini, G. Caponi, Pulitura a Tergo di Affreschi: Caratterizzazione Chimica del Materiale Proteico, *Scienza e Beni Culturali: La Pulitura delle Superfici dell'Architettura*, **XI**, 227–236 (1995).
44. S.L. Vallance, B.W. Singer, S.M. Hitchen, J. Townsend, The Analysis of Proteinaceous Artists' Media by High Performance Liquid Chromatography, *Liquid Chromatography-Gas Chromatography International*, **15**, 48–53 (1997).
45. J. Wouters, M. Van Bos, K. Lamens, Baroque Stucco Marble Decorations. II. Composition and Degradation of the Organic Materials in Historical Samples and Implications for their Conservation, *Studies in Conservation*, **45**, 169–179 (2000).
46. W. Nowik, Acides Amines et Acides Gras sur un Mêmes Chromatogramme: un Autre Regard sur l'Analyse des Liants en Peinture, *Studies in Conservation*, **40**, 120–126 (1995).

47. M.P. Colombini, R. Fuoco, A. Giacomelli, B. Muscatello, Characterization of Proteinaceous Binders in Wall Painting Samples by Microwave-Assisted Acid Hydrolysis and GC-MS Determination of Amino Acids, *Studies in Conservation*, **43**, 33–41 (1998).
48. M.P. Colombini, F. Modugno, M. Giacomelli, S. Francesconi, Characterisation of Proteinaceous Binders and Drying Oils in Wall Painting Samples by Gas Chromatography-Mass Spectrometry, *Journal of Chromatography, A*, **846**, 113–124 (1999).
49. A. Casoli, P. Mirti, G. Palla, Characterization of Medieval Proteinaceous Painting Media Using Gas Chromatography and Gas Chromatography – Mass Spectrometry, *Fresenius Journal of Analytical Chemistry*, **352**, 372–379 (1995).
50. A. Casoli, P.C. Musini, G. Palla, Gas Chromatographic-Mass Spectrometric Approach to the Problem of Characterizing Binding Media in Paintings, *Journal of Chromatography, A*, **731**, 237–246 (1996).
51. J.V. Gimeno-Adelantado, R. Mateo-Castro, M.T. Doménech-Carbó, F. Bosch-Reig, A. Doménech-Carbó, J. De la Cruz-Cañizares, M.J. Casas-Catalan, Analytical Study of Proteinaceous Binding Media in Works of Art by Gas Chromatography using Alkyl Chloroformates as Derivatizing Agents, *Talanta*, **56**, 71–77 (2002).
52. M.T. Doménech-Carbó, M.J. Casas-Catalán, A. Doménech-Carbó, R. Mateo-Castro, J.V. Gimeno-Adelantado, F. Bosch-Reig, Analytical Study of Canvas Painting Collection from the Basilica de la Virgen de los Desamparados using SEM/EDX, FT-IR, GC and Electrochemical Techniques, *Fresenius Journal of Analytical Chemistry*, **369**, 571–575 (2001).
53. A. Derieux, S. Rochut, M.C. Papillon, C. Pepe. Identification des Colles Protéiques Présentes dans les Oeuvres d'Art par Couplage CG/SM à Trappe Ionique, *Comptes Rendus de l'Académie des Sciences, Séries IIC, Paris, Chimie*, **4**, 295–300 (2001).
54. L. Castellani, P. Ferrantelli, M. Sinibaldi, G. Vigliano, Identification of Proteinaceous Adhesives in the Wooden Backing of Piero della Francesca's Painting Pala of Saint Bernardino: a Gas Chromatographic Study, *Journal of Cultural Heritage*, **2**, 209–215 (2001).
55. U. Schneider, E. Kenndler, Identification of Plant and Animal Glues in Museum Objects by GC-MS, After Catalytic Hydrolysis of the Proteins by the Use of a Cation Exchanger, with Simultaneous Separation from the Carbohydrates, *Fresenius Journal of Analytical Chemistry*, **371**, 81–87 (2001).
56. P. Přikryl, L. Havlíčková, V. Pacáková, J. Hradilova, K. Stulik, P. Hofta, An Evaluation of GC-MS and HPLC-FD Methods for Analysis of Protein Binders in Paintings *Journal of Separation Science*, **29**, 2653–2663 (2006).
57. R.M. Castro, M.T. Doménech Carbó, V.P. Martínez, J.V. Gimeno-Adelantado, F. Bosch-Reig, Study of Binding Media in Works of Art by Gas Chromatographic Analysis of Amino Acids and Fatty Acids Derivatized with Ethyl Chloroformate, *J. Chromatography, A*, **778**, 373–381 (1997).
58. A. Ballistreri, M. Fichera, P. Fifi, G. Musumarra, Characterization of Vasari and Zuccari Binding Media by Direct Pyrolysis in the Mass Spectrometer, *Science and Technology for Cultural Heritage*, **7**, 27–30 (1998).
59. G. Chiavari, G. Galletti, G. Lanterna, and R. Mazzeo, The Potential of Py-GC/MS in the Recognition of Ancient Painting Media, *Journal of Analytical and Applied Pyrolysis*, **24**, 227–242 (1993).
60. G. Chiavari, P. Bocchini, G. Galletti, Rapid Identification of Binding Media in Painting Using Simultaneous Pyrolysis Methylation Gas Chromatography, *Science and Technology for Cultural Heritage*, **1**, 153–158 (1992).
61. J.M. Challinor, Review: the Development and Applications of Thermally Assisted Hydrolysis and Methylation Reactions, *Journal of Analytical and Applied Pyrolysis*, **61**, 3–34 (2001).
62. X. Zang, J.C. Brown, J.D.H. van Heemst, A. Palumbo, P.G. Hatcher, Characterization of Amino Acids and Proteinaceous Materials using Online Tetramethylammonium Hydroxide (TMAH) Thermochemolysis and Gas Chromatography-Mass Spectrometry Technique, *Journal of Analytical and Applied Pyrolysis*, **61**, 181–193 (2001).
63. I. Bonaduce, M.P. Colombini, Gas Chromatography/Mass Spectrometry for the Characterization of Organic Materials in Frescoes of the Momumental Cemetery of Pisa (Italy), *Rapid Communications in Mass Spectrometry*, **17**, 2523–2527 (2003).
64. P. Bocchini, P. Traldi, Organic Mass Spectrometry in our Cultural Heritage, *Journal of Mass Spectrometry*, **33**, 1053–1062 (1998).

65. M. Carhini, R. Stevanato, M. Rovea, P. Traldi, D. Favretto, Curie-Point Pyrolysis/GC/MS in the Art Field. 2 – The Characterization of Proteinaceous Binders, *Rapid Communications in Mass Spectrometry*, **10**, 1240–1242 (1996).
66. G. Chiavari, N. Gandini, P. Russo, D. Fabbri, Characterisation of Standard Tempera Painting Layers Containing Proteinaceous Binders by Pyrolysis/(Methylation)-Gas Chromatography/Mass Spectrometry, *Chromatographia*, **47**, 420–426 (1998).
67. E. Kaal, H.G. Janssen, Extending the Molecular Application Range of Gas Chromatography, *Journal of Chromatography, A*, **1184**(1–2), 43–60 (2008).
68. J.S. Mills, R. White, *The Organic Chemistry of Museum Objects*, Butterworth-Heinemann, Oxford (1994).
69. C. Lalli, G. Lanterna, Il campionamento e il prelievo: fasi critiche per la corretta impostazione di una campagna analitica, *Kermes*, **16**, 3–11 (1993).
70. T.J. Wess, M. Drakopoulos, A. Snigirev, J. Wouters, O. Paris, P. Fratzl, M. Collins, J. Hiller, K. Nielsen, The Use of Small-Angle X-Ray Diffraction Studies for the Analysis of Structural Features in Archaeological Samples, *Archaeometry*, **43**, 117–129 (2001).
71. A. Andreotti, M.P. Colombini, G. Lanterna, M. Rizzi, A Novel Approach for High Selective Micro-Sampling of Organic Painting Materials by Er:YAG Laser Ablation, *Journal of Cultural Heritage*, **4**, 355–361 (2003).
72. A. Andreotti, M. P. Colombini, S. Conti, A. deCruz, G. Lanterna, L. Nussio, K. Nakahara, F. Penaglia, Preliminary Results of the Er:YAG Laser Cleaning of Textiles, Paper and Parchment, *Lasers in the Conservation of Artworks*, **116**, 213–220 (2007).
73. L. Hill, Hydrolysis of Proteins, *Advances in Protein Chemistry*, **20**, 37 (1965).
74. M.V. Pickering, P. Newton, Amino Acid Hydrolysis: Old Problems, New Solutions, *LC-GC International*, **3**(11), 22–26 (1990).
75. I. Molnar-Perl, Advances in the High-Performance Liquid Chromatographic Determination of Phenylthiocarbamyl Amino Acids, *Journal of Chromatography, A*, **661**, 43–50 (1994).
76. J. Csapó, Z. Csapó-Kiss, T.G. Martin, S. Folestad, O. Orwar, A. Tivesten, S. Némethy, Age Estimation of Old Carpets Based on Cystine and Cysteic Acid Content *Analytica Chimica Acta*, **300**, 313–320 (1995).
77. A. Jurado-Lopez, M.D. Luque de Castro, Optimisation of Focused Microwave Digestion of Proteinaceous Binders Prior to Gas Chromatography, *Talanta*, **65**, 1059–1062 (2005).
78. D.I. Sánchez-Machado, B. Chavira-Willys, J. López-Cervantes, High-Performance Liquid Chromatography with Fluorescence Detection for Quantitation of Tryptophan and Tyrosine in a Shrimp Waste Protein Concentrate, *Journal of Chromatography, B*, **863**(1), 88–93 (2008).
79. D.A. Slatter, N.C. Avery, A.J. Bailey, Collagen in its Fibrillar State is Protected from Glycation, *The International Journal of Biochemistry & Cell Biology*, **40**(10), 2253–2263 (2008).
80. L. Rampazzi, A. Andreotti, I. Bonaduce, M.P. Colombini, C. Colombo, L. Toniolo, Analytical Investigation of Calcium Oxalate Films on Marble Monuments, *Talanta*, **63**(4), 967–977 (2004).
81. U. Bartolucci, M.P. Colombini, L. Dei, F. Giambi, Problemi di Conservazione delle Pitture Murali del Cortile di Michelozzo in Palazzo Vecchio (Firenze), *Scienza e Beni Culturali*, **XXI**, 677–685 (2005).
82. M.P. Colombini, U. Bartolucci, Protocollo Analitico per la Conoscenza dello Stucco. Tecniche Cromatografiche e Spettrometriche, in *L'Arte dello Stucco*, New Press, Como, 139–148 (2006).
83. R. Aruga, P. Mirti, A. Casoli, G. Palla, Classification of Ancient Proteinaceous Painting Media by the Joint Use of Pattern Recognition and Factor Analysis on GC/MS Data, *Journal of Analytical Chemistry*, **365**, 559–566 (1999).
84. B. Singer, R. McGuigan, The Simultaneous Analysis of Proteins, Lipids, and Diterpenoid Resins Found in Cultural Objects, *Annali di Chimica*, **97**, 405–417 (2007).
85. D.A. Scott, M. Dennis, J. Keeney, N. Khandekar, D. Carson, Technical Examination of an Egyptian Cartonnage of the Greco-Roman Period, *Studies in Conservation*, **48**, 41–56 (2003).
86. M.R. Schilling, *Workshop on Binding Media Identification in Art Objects*, LabSTECH European Infrastructure Cooperation Network, 24–26 March, Amsterdam (2003).
87. A. Andreotti, I. Bonaduce, M.P. Colombini, G. Gautier, F. Modugno, E. Ribecchini, Combined GC-MS Analytical Procedure for the Characterization of Glycerolipid, Waxy, Resinous, and



- Proteinaceous Materials in a Unique Paint Microsample, *Analytical Chemistry*, **78**, 4490–4500 (2006).
88. P. Husek, Chloroformates in Gas Chromatography as General Purpose Derivatizing Agents, *Journal of Chromatography, B*, **717**, 57–91 (1998).
  89. P. Husek, P. Matucha, P. Simek, Smooth Esterification of Di- and Tricarboxylic Acids with Methyl and Ethyl Chloroformates in Gas Chromatographic Profiling of Urinary Acidic Metabolites, *Chromatographia*, **58**, 623–630 (2003).
  90. P. Husek, P. Simek, P. Hartvich, H. Zahradnickova, Fluoroalkyl Chloroformates in Treating Amino Acids for Gas Chromatographic Analysis, *Journal of Chromatography, A*, **1186**, 391–400 (2008).
  91. D. Saunders, Pollution and the National Gallery, *National Gallery Technical Bulletin*, **21**, 77–94 (2000).
  92. R. Arbizzani, U. Casellato, E. Fiorin, L. Nodarib, U. Russob, P.A. Vigato, Decay Markers for the Preventative Conservation and Maintenance of Paintings, *Journal of Cultural Heritage*, **5**, 167–182 (2004).
  93. I. Bonaduce, M.P. Colombini, S. Diring, Identification of Garlic in Old Gildings by Gas Chromatography–Mass Spectrometry, *Journal of Chromatography, A*, **1107**, 226–232 (2006).
  94. S.M. Halpine, An Investigation of Artists Materials using Amino-Acid-Analysis + Selected Results from Technical Investigations of Paintings Undergoing Conservation Treatment – Introduction of the One-hour Extraction Method, *Studies in the History of Art*, **51**, 28–69 (1995).
  95. A. Casoli, P.C. Musini, G. Palla, Characterization of Binding Media from Ancient Polychrome Sculptures by means of GC/MS, *Chromatographia*, **42**, 421–430 (1996).
  96. G. Gautier, A Reliable Analytical Procedure for the Characterisation and Identification of Proteinaceous Media in Wall Paintings, PhD Thesis, University of Pisa (2006).
  97. M.P. Colombini, I. Bonaduce, G. Gautier, Molecular Pattern Recognition of Fresh and Aged Shellac, *Chromatographia*, **58**, 357–364 (2003).
  98. G. Musumarra, M. Fichera, Chemometrics and Cultural Heritage, *Chemometrics and Intelligent Laboratory Systems*, **44**, 363–372 (1998).
  99. R. Checa-Moreno, E. Manzano, G. Mirón, L.F. Capitan-Vallvey, Comparison between Traditional Strategies and Classification Technique (SIMCA) in the Identification of Old Proteinaceous Binders, *Talanta*, **75** (3), 697–704 (2008).
  100. R. Lletí, L.A. Sarabia, M.C. Ortiz, R. Todeschini, M.P. Colombini, Application of the Kohonen Artificial Neural Network in the Identification of Proteinaceous Binders in Samples of Panel Painting using Gas Chromatography–Mass Spectrometry, *Analyst*, **128**, 281–286 (2003).
  101. E. Willerslev, E. Cappellini, W. Boomsma, R. Nielsen, M.B. Hebsgaard, T.B. Brand, M. Hofreiter, M. Bunce, H.N. Poinar, D. Dahl-Jensen, S. Johnsen, J. Peder Steffensen, O. Bennike, J.-L. Schwenninger, R. Nathan, S. Armitage, C.-J. de Hoog, V. Alfimov, M. Christl, J. Beer, R. Muscheler, J. Barker, M. Sharp, K.E.H. Penkman, J. Haile, P. Taberlet, M.T.P. Gilbert, A. Casoli, E. Campani, M.J. Collins, Ancient Biomolecules from Deep Ice Cores Reveal a Forested Southern Greenland, *Science* **317**, 111–114 (2007).
  102. F. Mori, R. Ponti, A. Messina, M. Flieger, V. Havlicek, M. Sinibaldi, Chemical Characterization and AMS Radiocarbon Dating of the Binder of a Prehistoric Rock Pictograph at Tadrart Acacus, Southern West Libya, *Journal of Cultural Heritage*, **7**, 344–349 (2006).
  103. A. Casoli, S. Negria, G. Palla, Presence of D,L Amino Acids in Oxalate Patinas on a Stone Monument, in *Proceedings of the 9th International Congress on Deterioration and Conservation of Stone*, edited by V. Fassina, Elsevier, 553–556 (2000).
  104. B.J. Johnson, G.H. Miller, Archaeological Applications of Amino Acid Racemisation, *Archaeometry*, **39**(2), 265–287 (1997).
  105. D. Kaufman, Dating Deep-Lake Sediments by Using Amino Acid Racemization in Fossil Ostracodes, *Geology*, **31**, 1049–1052 (2003).
  106. N.W. Rutter, B. Blackwell, Amino Acid Racemization Dating, in *Dating Methods for Quaternary Deposits*, edited by N.W. Rutter, N.R. Catto, Geological Association of Canada, Newfoundland, 125–164 (1995).

107. J. Robins, M. Jones, E. Matisoo-Smith, *Amino Acid Racemization Dating in New Zealand: An Overview*, Auckland University (2001).
108. E. Fernández, J.E. Ortiz, A. Pérez-Pérez, E. Prats, D. Turbón, T. Torres, E. Arroyo-Pardo, Aspartic Acid Racemization Variability in Ancient Human Remains: Implications in the Prediction of Ancient DNA Recovery, *Journal of Archaeological Science*, **36**, 965–972 (2009).
109. J.L. Bada, The Dating of Fossil Bones using the Racemization of Isoleucine, *Earth and Planetary Science Letters*, **15**, 223–231 (1972).
110. P.E. Hare, P.H. Abelson, Racemization of Amino Acids in Fossil Shells, *Carnegie Institution of Washington Year Book*, **66**, 526–528 (1967).
111. P.E. Hare, R.M. Mitterer, Laboratory Simulation of Amino-Acid Diagenesis in Fossils, *Carnegie Institution of Washington Year Book*, **67**, 205–208 (1969).
112. J.L. Bada, Racemization of Amino Acids in Nature, *Interdisciplinary Science Reviews*, **7**(1), 30–46 (1982).
113. G.G. Smith, R.C. Evans, The Effect of Structure and Conditions on the Rate of Racemization of Free and Bound Amino Acids, in *Biogeochemistry of Amino Acids*, edited by P.E. Hare, T.C. Hoering, J. King, John Wiley & Sons, Ltd, New York, 257–282 (1980).
114. A.I. Thackeray, Dating the Rock Art of South Africa. in *New Approaches to Southern African Rock Art*, edited by J.D. Lewis-Williams, South African Archaeological Society, Cape Town, 21–26 (1983).
115. I. Bonaduce, C. Blaensdorf, P. Dietemann, M.P. Colombini, The Binding Media of the Polychromy of Qin Shihuang's Terracotta Army, *Journal of Cultural Heritage*, **9**, 103–108 (2008).
116. D. Bersani, P.P. Lottici, A. Casoli, D. Cauzzi, Pigments and Binders in ‘‘Madonna col Bambino e S. Giovannino’’ by Botticelli Investigated by Micro-Raman and GC/MS, *Journal of Cultural Heritage*, **9**, 97–102 (2008).
117. F. Ospitali, A. Rattazzi, M.P. Colombini, A. Andreotti, G. di Leonardo, XVI century wall paintings in the ‘Messer Filippo’ Cell of the Tower of Spilamberto: Microanalyses and Monitoring, *Journal of Cultural Heritage*, **8**, 323–327 (2007).
118. A. Andreotti, I. Bonaduce, M.P. Colombini, F. Modugno, Il Sarcofago delle Amazzoni, in *Le componenti organiche della pittura*, edited by A. Bottini, E. Setari, Electa, Milan, 157–162 (2007).
119. S. Daniilia, A. Tsakalof, K. Bairachtari, Y. Chrysoulakis, The Byzantine Wall Paintings from the Protaton Church on Mount Athos, Greece: Tradition and Science, *Journal of Archaeological Science*, **34**, 1971–1984 (2007).
120. L. Rampazzi, L. Campo, F. Cariati, G. Tanda, M. P. Colombini, Prehistoric Wall Paintings: the Case of the Domus de Janas Necropolis (Sardinia, Italy), *Archaeometry*, **49**, 559–569 (2007).
121. E. Kouloumpi, P. Vandenabeele, G. Lawson, V. Pavlidis, L. Moens, Analysis of Post-Byzantine Icons from the Church of the Assumption in Cephalonia, Ionian Islands, Greece: a Multi-Method Approach, *Analytica Chimica Acta*, **598**(1), 169–179 (2007).
122. A. Rodríguez-López, N. Khandekar, G. Gates, R. Newman, Materials and Techniques of a Spanish Renaissance Panel Painting, *Studies in Conservation*, **52**, 81–100 (2007).
123. S. Bianchin, U. Casellato, M. Favaro, P.A. Vigato, Painting Technique and State of Conservation of Wall Paintings at Qusayr Amra, Amman, Jordan, *Journal of Cultural Heritage*, **8**, 289–293 (2007).
124. A. Nevin, J. Loring Melia, I. Osticioli, G. Gautier, M.P. Colombini, The Identification of Copper Oxalates in a 16th Century Cypriot Exterior Wall Painting using Micro FTIR, Micro Raman Spectroscopy and Gas Chromatography-Mass Spectrometry, *Journal of Cultural Heritage*, **9**, 154–161 (2008).
125. S. Bianchin, U. Casellato, M. Favaro, P.A. Vigato, M.P. Colombini, G. Gautier, Physico-Chemical and Analytical Studies of the Mural Paintings at Kariye Museum of Istanbul, *Journal of Cultural Heritage*, **9**, 179–183 (2008).
126. S. Daniilia, E. Minopoulou, K.S. Andrikopoulos, A. Tsakalof, K. Bairachtari, From Byzantine to Post-Byzantine Art: the Painting Technique of St Stephen's Wall Paintings at Meteora, Greece, *Journal of Archaeological Science*, **35**, 2474–2485 (2008).





# 10

## SPME/GC-MS in the Characterisation of Terpenic Resins

*Jean Bleton and Alain Tchapla*

### 10.1 Introduction

Solid phase microextraction (SPME) was first introduced by Pawliszyn and co-workers [1, 2]. It is a simple, rapid, solventless sample preparation technique based on the partition of an analyte between the sample matrix and the coating on a fused silica fibre [3]. This technique combines sampling and preconcentration in a single step and is therefore very sensitive. It can be used with a wide variety of matrices (gas, liquid and solid) and a wide range of analytes, from volatile to semi-volatile compounds, and has become very popular. SPME has been successfully applied in different areas [4], such as in environmental applications [5], foods [6, 7], natural products [8], pharmaceutical applications [9], biological matrices [10, 11] and toxicology [12, 13]. Some applications have been developed in a cultural heritage context. The first published application was devoted to the identification of organic chemicals deposited on the surface of stone monuments [14] and was later followed by another dealing with the identification of secondary metabolites in lichens deposited on stone monuments [15]. SPME was also utilised to estimate the emission of carboxylic acids (acetic and formic) from construction materials in museum displays or storage areas [16–18], and to identify the volatile organic compounds emitted by naturally or artificially aged books [19, 20], magnetic tape coatings [21] and wax objects in museums [22].

Few papers deal with the use of SPME in the characterisation of terpenic resins in archaeological or museum objects [23–26].

An interesting field of application is the study of mummification balms and unguents of Ancient Egypt. According to ancient papyrus and hieroglyphs on the walls inside temples, the recipe of these balms is elaborate and needs many constituents with their own ritual significance: vegetable oils, animal fats, pitches, waxes, honey, gums, resins and gum resins [27, 28]. Among these different substances, resins take pride of place, due to their adhesive, medical and aromatic properties. Most of them are complex mixtures of mono-, sesqui-, di- or triterpenes. Gum resins like olibanum (frankincense) or myrrh have supplementary polysaccharidic components.

Good results have been obtained in the characterisation of mummification balms, by GC/MS, after solvent extraction and fractionation of the samples according to different polarities [29–31] but the methods are relatively complex. Alternatively, GC/MS, after direct treatment of the sample by acid methanolysis and trimethylsilylation [28, 32–35], permits the characterisation, in a single step, of fats, waxes, tannins and gums but fails for some classes of resins. SPME was therefore tested as a fast screening and sensitive preliminary sampling mode in order to detect the presence of terpenes, among other constituents, in an archaeological sample. The method does not alter the initial sample that can be used thereafter for complementary investigations.

The first results encouraged the authors to analyse, by headspace SPME, substances mentioned in ancient texts or hieroglyphics as components of embalming fluids [true resins such as mastic, labdanum and pine resin or pine pitch and gum resins such as olibanum, myrrh and galbanum] [27, 28] with the aim of finding characteristic chemical compounds for each type of resin or gum resin.

In this chapter, we first provide general considerations on the SPME process and important parameters affecting the quality of the results. In Sections 3 and 4 we present the results obtained with different reference substances and archaeological samples.

## 10.2 Analytical Methodology

The SPME process, adapted for solid or viscous matrix, is shown in Figure 10.1. A fused silica fibre, coated with a polymer, is installed inside a stainless steel hollow needle. In the first step, the needle is introduced in the sample vial through the septum. The fibre is then exposed to the headspace above the sample and the organic analytes adsorb to the coating of the fibre. After a variable sampling time, the fibre is drawn into the needle and the needle is withdrawn from the sample vial. Finally, in the same way, the fibre is introduced into the chromatograph injector where the analytes are thermally desorbed.

In many cases, SPME does not allow the exhaustive extraction of most analytes in a sample matrix and is considered as an equilibrium sampling method. Equilibria are established among the concentrations of an analyte in the sample, in the headspace above the sample and in the polymer coating on the fibre. The amount of analyte adsorbed by the fibre depends on the thickness of the polymer coating and on the distribution constant for the analyte. The extraction time is determined by the length of time required to obtain precise extractions for the target analytes with the highest distribution constants. The distribution constant generally increases with increasing the molecular weight and boiling point of the analytes.

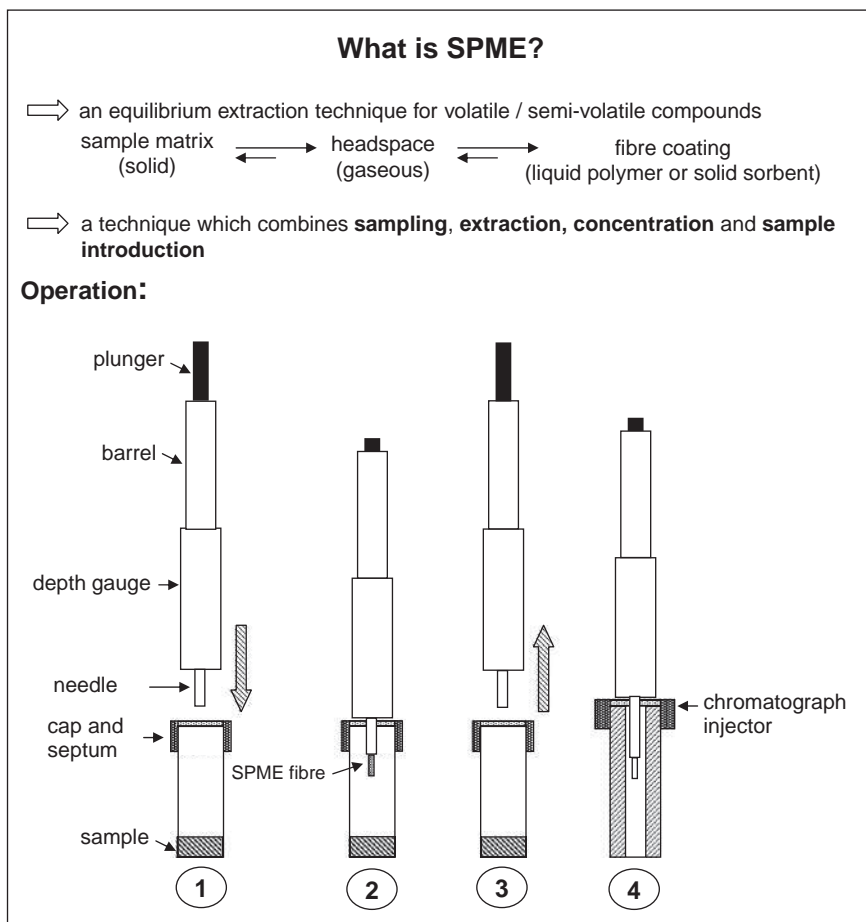


**Figure 10.1** Solid phase microextraction process

Selectivity can be altered by changing the type of polymer coating on the fibre, or the coating thickness, to match the characteristics of the target analytes. Several coatings are commercially available and the needed selectivity is based on polarity and volatility differences among molecules. Poly(dimethylsiloxane) (PDMS) coatings are nonpolar, whilst polyacrylate (PA) and carbowax (CW) coatings are strongly polar. The addition of adsorbent materials like carboxen (CAR) or divinylbenzene (DVB) particles in PDMS or CW coatings improves the extraction of small molecules. The fibre coatings commonly used are PDMS (7, 30 or 100  $\mu\text{m}$ ), PA (85  $\mu\text{m}$ ) and mixed phase PDMS/DVB (60 or 65  $\mu\text{m}$ ), CAR/PDMS (75 or 85  $\mu\text{m}$ ), DVB/CAR/PDMS (50 or 30  $\mu\text{m}$ ) and CW/DVB (65  $\mu\text{m}$ ).

SPME can be used to extract organic compounds from a solid matrix as long as target compounds can be released from the matrix into the headspace. For volatile compounds, the release of analytes into the headspace is relatively easy because analytes tend to vaporise once they are dissociated from their matrix. For semi-volatile compounds, the

low volatility and the relatively large molecular size may slow the mass transfer from the matrix to the headspace and limit the speed of extraction, resulting in a long extraction time. An efficient way to overcome this limitation is to heat the sample to higher temperatures, which increases the vapour pressure of analytes and provides the energy necessary for analytes to be dissociated from the matrix [36, 37]. However, at high temperature, coating headspace partition coefficients decrease and the optimum extraction temperature is determined by the interactions among the analytes, coating and matrix.

Three factors have thus to be optimised in order to obtain consistent results with SPME on a solid or viscous matrix: polarity and thickness of the coating on the fibre, sampling time and temperature. An example of optimisation will be described in Section 3.

### 10.3 Analyses of Reference Substances

#### 10.3.1 Results Obtained with a PDMS Fibre [25]

Six reference resinous substances were analysed using SPME with a 100  $\mu\text{m}$  PDMS fibre using different sampling times and at different temperatures [25]. The temperature increase favoured the extraction of less volatile compounds allowing a better characterisation of the substances but the higher temperature was fixed at 80°C in order to avoid sample deterioration and loss of thermolabile analytes [38]. A sampling time of 40 min allowed good results to be obtained for each substance. The chromatograms were qualitatively similar to those obtained after extraction with methylene chloride in the elution zone of the mono- and sesquiterpenes. The total ion current chromatograms are presented Figure 10.2 and the major extracted compounds are summarized in Table 10.1 with their relative peak area. The chromatographic profiles are different for each resin and should permit their differentiation.

For olibanum, six characteristic diterpenes were observed: cembrene A (**94**), cembrene C (**98**), isoincense acetate (**104**), a dimer of  $\alpha$ -phellandrene (**86**) and two unidentified compounds (**92**) and (**103**).

Among the characteristic furanosesquiterpenes of myrrh trapped by headspace SPME, curzerene (**65**) (= isofuranogermacrene), furanoeudesma-1,3-diene (**80**) and lindestrène (**81**) were predominant.

The volatile extract obtained from galbanum was principally composed of  $\alpha$ -pinene (**1**),  $\beta$ -pinene (**4**), fenchyl acetate (**30**),  $\gamma$ -cadinene (**66**), guaïol (**77**) and *cis*-guaï-9-en-11-ol (**82**).  $\beta$ -dihydroagarofuran (**64**) and epi-ligulyl oxide (**72**) could represent potential biomarkers [39]. However, due to their very low concentration, it will be difficult to detect them by headspace SPME in complex archaeological mixtures.

The major compounds extracted from labdanum were dihydrocinnamic acid (**39**), which is not found in other resins or gum resins and the relatively uncommon aromadendr-1-ene (**51**) and ledene (**61**). Three minor diterpenes are also characteristic [40].

For the mastic, the widespread  $\alpha$ -pinene (**1**) was the main constituent trapped by headspace SPME. Two unidentified diterpenes (**93**) and (**96**) seem to be characteristic.

Limonene (**10**) was the major extracted compound from pine resin (*Pinus pinea*). Since it occurs in other resins or plants it cannot be a biomarker. Longifolene (**49**), present in a lower amount, is more characteristic of a conifer resin. This sesquiterpene is particularly

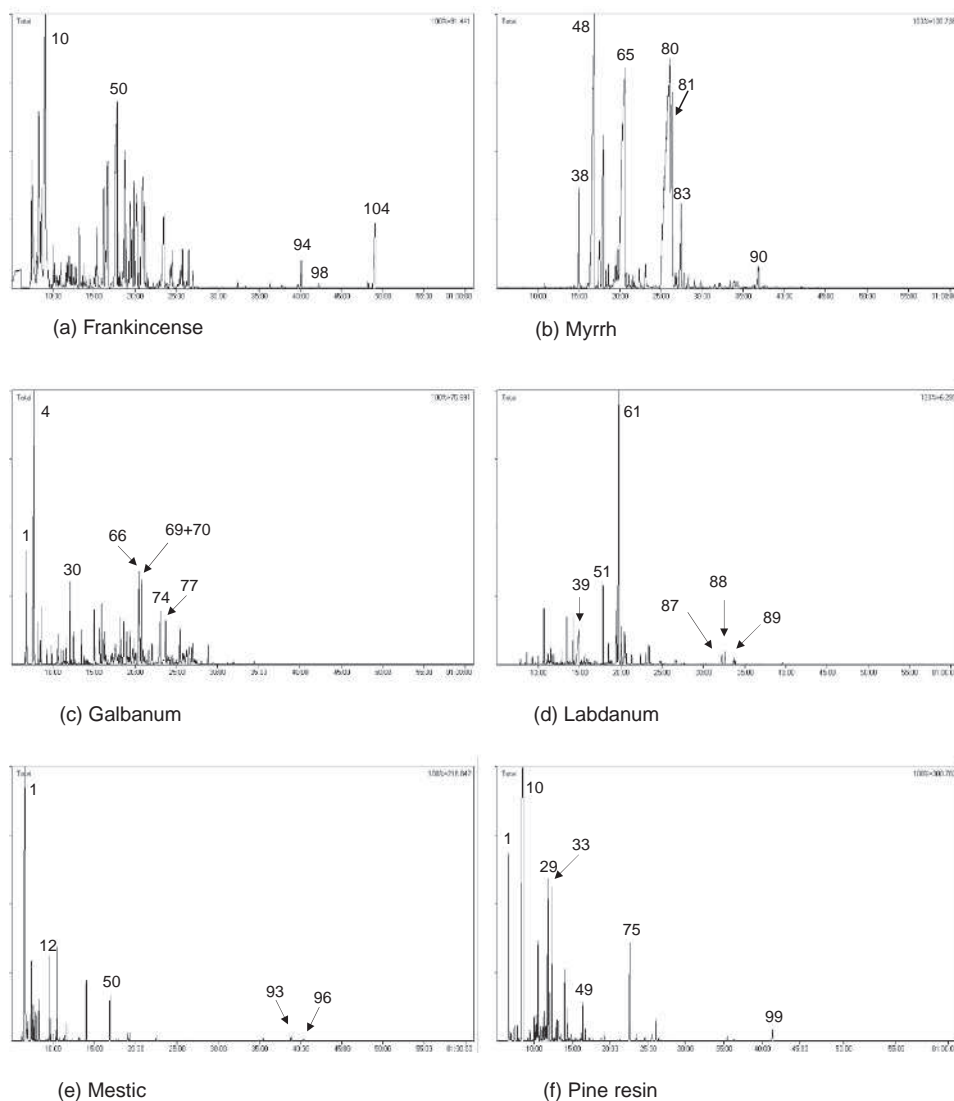


**Figure 10.2** Total ion current chromatograms obtained for modern resins and gum resins after headspace SPME. Peak labels correspond to compound identification given in Table 10.1. Reproduced from S. Hamm, J. Bleton, A. Tchaplé, *J. Sep. Sci.*, **27**, 235–243 (2004). Copyright Wiley-VCH Verlag GmbH & Co. KGaA. Reproduced with permission

abundant in certain pine resins [41, 42]. It has been observed in relatively high amount in colophony and seems to resist ageing well [43].

The method allowed the authors to characterise a pine pitch (viscous ‘tar’ derived from the distillation of wood of pine trees). The main constituents detected by headspace SPME result from the pyrolysis of the lignin, guaiacol (**11**) and its *p*-*n*-alkyl derivatives [methyl

**Table 10.1** Compounds trapped by headspace SPME from different resins, gum resins and archaeological samples, presented by increasing retention indices, with the corresponding relative peak areas (%) for each substance

Peak no.	Compound	RI <sup>a</sup>	Olibanum	Myrrh	Galbanum	Labdanum	Mastic	Resin of <i>Pinus pinea</i>	Pine pitch	Pitch from Fayoum	Sample 1485	Sample 1627	Sample 1625
1	$\alpha$ -Pinene	942	4.6		6.1		59.4	2.9			12.5	28.2	18.2
2	Camphene	949	tr				0.5	tr	0.3		6.5	2.1	0.7
3	4-Methylene-1-(1-methylethyl)-bicyclo[3.1.0]hex-2-ene	952					1.1	0.5			0.9	2.3	
4	$\beta$ -Pinene	966	0.4		24.0		3.7	0.6			0.1	1.6	1.5
5	$\beta$ -Myrcene	994	5.5				1.7						
6	$\alpha$ -Phellandrene	1003	2.4										
7	$\delta$ -3-Carene	1006			1.1								
8	<i>o</i> -Methylanisole	1005	tr				1.4						
9	<i>p</i> -Cymene	1014	1.7		0.4	0.1	0.1		1.7	0.2	4.6	5.2	3.5
10	Limonene	1020	14.4		1.5	tr	2.0	34.1	0.3		3.5	5.4	2.8
11	Guaiacol	1074							4.6	0.2			
12	Linalool	1077	0.8				4.9						
13	Unidentified compound	1111										4.0	
14	Fenchol	1117								0.2	1.0	0.2	
15	$\alpha$ -Campholenal	1119	tr				0.3	0.2			0.3	1.4	0.1
16	(-)- <i>trans</i> -Pinocarveol	1129	0.1		1.0	tr	0.5	0.5			1.1	5.0	4.0
17	( <i>S</i> )- <i>cis</i> -Verbenol	1131	0.2				0.9	5.5				5.5	4.0
18	Camphor	1132								0.1	1.7		
19	Pinocamphone	1170				0.8					0.4	2.0	3.0
20	Borneol	1176				tr				0.8	3.9	0.5	1.7
21	(-)-4-Terpineol	1182	0.1		0.5	1.2						0.4	
22	<i>p</i> -Cymen-8-ol	1187	tr								0.6	1.3	4.0
23	2-Methylacetophenone	1188											4.0
24	<i>p</i> -Methylguaiacol	1191							10.9	0.7	1.2		
25	(+)- $\alpha$ -Terpineol	1193	0.2			1.3	tr				1.2	1.2	0.6
26	Myrtanal	1197			1.0		1.1				0.7	2.0	2.6

27	Myrtenol	1198										0.9	
28	Verbenone	1221	0.1			0.5	0.8	2.5			2.4	15.5	5.5
29	<i>trans</i> -Carveol	1225	0.3					6.7			0.5	0.7	1.0
30	Fenchyl acetate	1226		2.1					0.3	0.3			
31	1,3,3-Trimethyl-2-oxabicyclo[2.2.2]octan-6-ol	1227									0.6		
32	<i>cis</i> -Carveol	1230	0.2					2.5					
33	Carvone	1237	0.3					7.6			0.2	1.0	0.9
34	3,5-Dimethoxytoluene	1264	0.9										
35	<i>p</i> -Ethylguaiaicol	1270							6.9	1.0	0.9		
36	Bornyl acetate	1275	0.3	0.9	2.4			0.9	1.0	0.7	0.1		0.7
37	1-Methyl-4-(1-methylethenyl)-1,2-cyclohexanediol	1321						1.4			0.2	0.1	
38	$\delta$ -Elemene	1339	0.2	2.1									
39	Dihydrocinnamic acid	1343			11.0								
40	Terpinyl acetate	1344	0.3	2.1									
41	Isomer of $\alpha$ -longipinene	1347						0.3				0.2	0.7
42	$\alpha$ -Cubebene	1347	1.5	tr	0.6	tr							
43	<i>p</i> -Propylguaiaicol	1352							8.1	2.5	0.4		
44	Cyclosativene	1360	0.2		1.9	1.1					1.9		
45	Longicyclene	1380									0.9		
46	$\alpha$ -Copaene	1383	2.6	tr	2.3	tr					1.0		
47	$\beta$ -Bourbonene	1388	0.4	0.5	1.1	tr						0.1	
48	$\beta$ -Elemene	1393	5.2	15.5	1.3						6.4		
49	Longifolene	1416						1.3		0.3	16.4		
50	$\beta$ -Caryophyllene	1426	11.6	0.5	0.3		3.5	0.4					
51	Aromadendr-1-ene	1445				6.5							
52	Unidentified sesquiterpene	1450			1.9								
53	$\alpha$ -Caryophyllene	1454	5.0	0.3	0.5		0.2	0.1					
54	Alloaromadendrene	1456	1.0			1.8							
55	(+)- <i>epi</i> -Bicyclosesquiphellandrene	1471			2.0								
56	$\gamma$ -Muurolene	1475	2.6		1.4						0.6		

(continued overleaf)

**Table 10.1** (continued)

[illegible]



82	<i>cis</i> -Guai-9-en-11-ol	1678		1.1				
83	Oxygenated sesquiterpene	1679		3.1				
84	1,4-Dimethoxy-2,3,5,6-tetrachlorobenzene	1721					6.1	
85	Isoledene	1723		1.1				
86	Dimer of $\alpha$ -phellandrene	1795	0.1					
87	15-nor-Labd-8(17)ene	1793			1.0			
88	15-nor-Labd-8-ene	1812			1.4			
89	15-nor-Labd-7ene	1835			0.7			
90	2-Acetoxyfuranodiene	1884		0.8				
91	2-Methylantracene	1905				0.5	1.2	0.2
92	Diterpene	1945	0.1					
93	Diterpene	1946			1.0			
94	Cembrene A	1959	0.8					
95	19-Norabieta-8,11,13-triene	1969				7.1	9.3	0.3
96	Diterpene	1982			0.3			
97	Diterpene	1983				1.2	3.7	0.1
98	Cembrene C	2002	0.1					
99	13-epi-Manoyl oxide	2005			0.8			
100	18-Norabieta-8,11,13-triene	2007				8.6	12.0	0.4
101	3,6-Dimethylphenanthrene	2027				0.7	1.8	0.1
102	10,18-Bisnorabieta-5,7,9(10),11,13-pentaene	2082				1.7	10.4	0.1
103	Diterpene	2141	0.2					
104	Isoincensole acetate	2152	3.0					
105	Retene	–				1.7	11.1	0.4
106	Methyldehydroabietate	–				0.4	5.0	0.1

tr, compound at trace level (<0.1%).

<sup>a</sup>Retention indices relative to C<sub>9</sub>–C<sub>22</sub> alkanes obtained on DB5 column.

Reproduced from S. Hamm, J. Bleton, A. Tchaplal, *J. Sep. Sci.*, **27**, 235–243 (2004). Copyright Wiley-VCH Verlag GmbH & Co. KGaA. Reproduced with permission.

(**24**), ethyl (**35**) and propyl (**43**)] or the less or more important degradation of diterpenoid acids, namely 19-norabieta-8,11,13-triene (**95**), 18-norabieta-8,11,13-triene (**100**) [44], 10,18-bisnorabieta-5,7,9(10),11,13-pentaene (**102**) [45] and retene (**105**). Small amounts of methyldehydroabietate (**106**) were also observed.

### 10.3.2 Example of Optimisation of Headspace SPME [24]

Frankincense, also called olibanum, is a natural oleo gum resin that exudes from incisions in the bark of *Boswellia* trees [46, 47]. Diterpenes like incensole or isoincensole and their oxide or acetate derivatives (see Figure 10.3) are characteristic biomarkers of olibanum [48]. Although diterpenoid hydrocarbons possessing the cembrene skeleton have been isolated from a variety of terrestrial and marine organisms, their occurrence and particularly that of cembrenes A and C (see Figure 10.3) is supplementary proof of the presence of olibanum in a sample. Optimisation of the SPME conditions was done with the aim of trapping these low volatile diterpenes.

#### 10.3.2.1 Choice of the Best Sampling Temperature

The sampling time of the preliminary experiments was arbitrarily fixed at 40 min. This time was sufficiently long to permit the diterpenes to be trapped. Four extraction temperatures were tested: 20°C, 40°C, 60°C and 80°C. The SPME fibre was the commonly used 100 µm PDMS. Results obtained for three classes of terpenes are presented in Figure 10.4.

The three classes of terpenes have different temperature profiles. These differences can be related to their boiling points, which are related to their molecular weight and their number of carbons [49]. Monoterpenes are highly volatile compounds (limonene: bp<sub>763</sub>

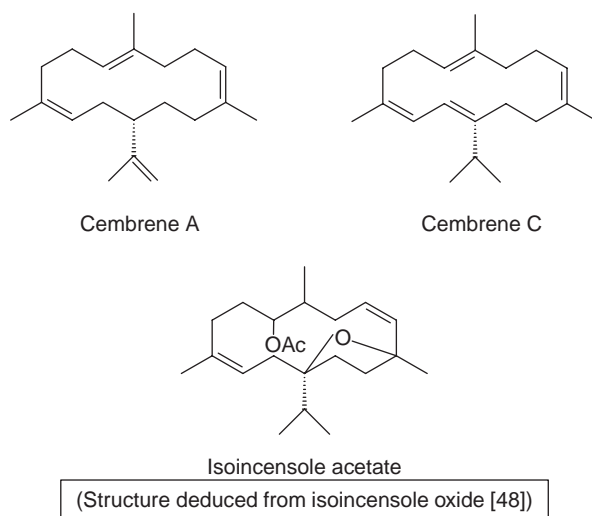


**Figure 10.3** Structure of cembrene A, cembrene C and isoincensole acetate. Reproduced from S. Hamm, E. Lesellier, J. Bleton, A. Tchaplal, *J. Chromatogr., A*, **1018**, 73–83. Copyright 2003 Elsevier Limited

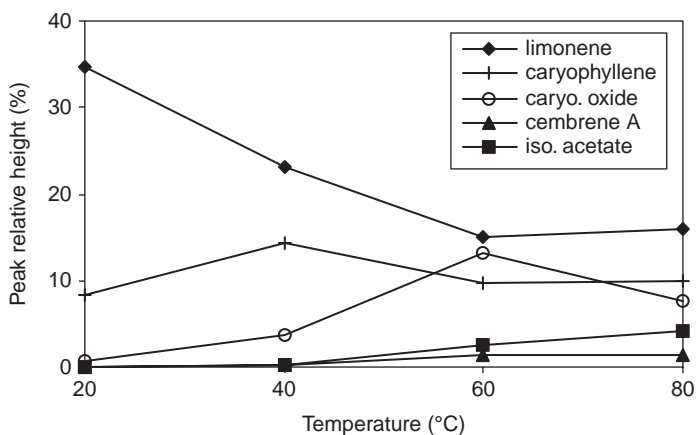


**Figure 10.4** Temperature profiles for three classes of analytes: monoterpenes (limonene); sesquiterpenes [ $\beta$ -caryophyllene, caryophyllene oxide (caryo. oxide)]; and diterpenes [cembrene A, isoincense acetate (iso. acetate)]. PDMS fibre, sampling time 40 min. Reproduced from S. Hamm, E. Lesellier, J. Bleton, A. Tchaplá, J. Chromatogr., A, **1018**, 73–83. Copyright 2003 Elsevier Limited

175.5–176.5°C) and leave the solid matrix very quickly. An increase in temperature does not favour their vaporisation from the matrix to the gaseous phase, but causes their desorption from the fibre to the gaseous phase, which then becomes the major process [50, 51].

The behaviour of sesquiterpenes, which are less volatile ( $\beta$ -caryophyllene: bp<sub>760</sub> 262°C), is quite different. Initially their migration from the matrix to the gaseous phase is predominant but beyond a certain temperature, which depends on the boiling point, the migration from the fibre to the gaseous phase predominates. For example, the optimal trapping temperature is lower (40°C) for  $\beta$ -caryophyllene than for its oxide derivative (60°C).

For the diterpenes, which are the less volatile compounds, the migration from the matrix to the gaseous phase predominates even at 80°C. They do not reach their optimal trapping temperature. In order to better observe diterpenes on the chromatograms, a sampling temperature of 80°C was chosen.

#### 10.3.2.2 Effect of the Sampling Time and Comparison of Different Fibres

Five SPME fibre coatings (PDMS, PDMS/DVB, CAR/PDMS, DVB/CAR/PDMS and CW/DVB) and four sampling times (20, 40, 60 and 80 min) were tested. The sampling temperature was 80°C.

The influence of the sampling time on the amount of extracted terpenes by the different fibre coatings can be observed in Figure 10.5. The sampling profile seems to be only dependent on the volatility of the studied compound. For mono- and sesquiterpenes, independently of the nature of the fibre coating, the extraction optimum is reached in about 20 min. However, for the less volatile diterpenes, 80 min are not enough to extract them completely from the matrix, with the optimal extraction time being longer. Such behaviour is well known and well documented [38, 52–54].

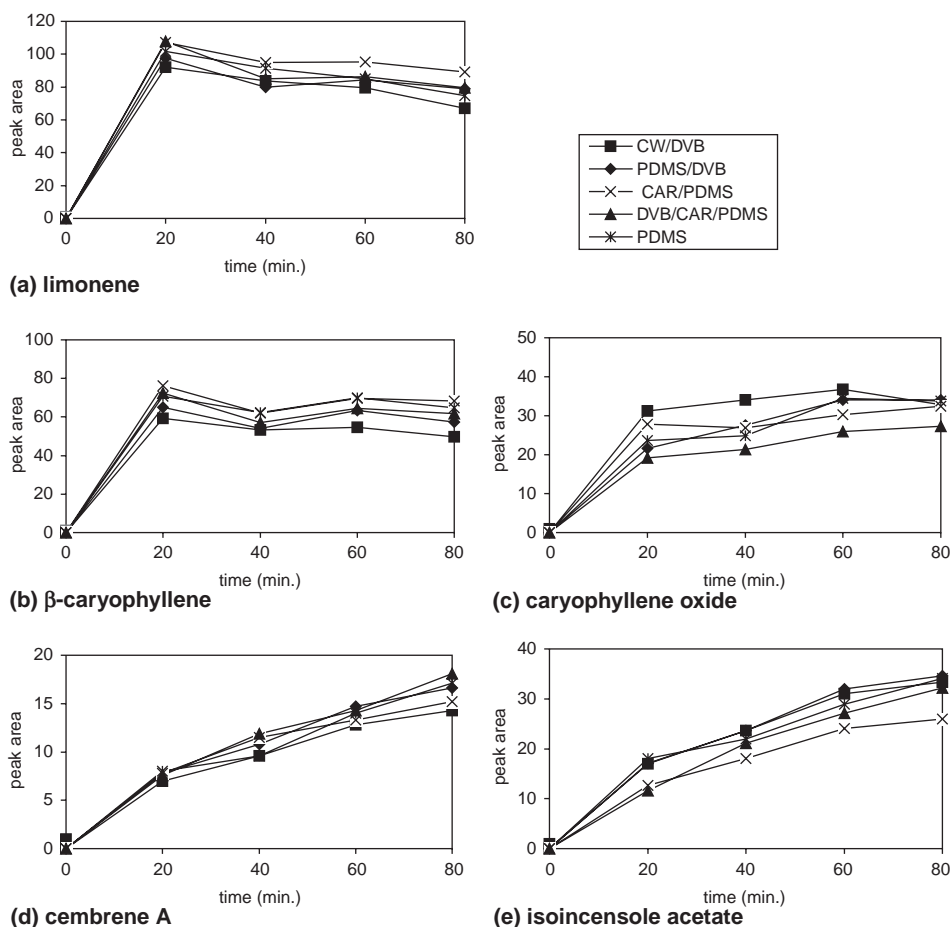


**Figure 10.5** Sampling time profiles for five terpenes with five different fibres. Sampling temperature 80°C. Reproduced from S. Hamm, E. Lesellier, J. Bleton, A. Tchaplal, *J. Chromatogr., A*, **1018**, 73–83. Copyright 2003 Elsevier Limited

For monoterpenes a slight decrease in peak area was observed when increasing the sampling time. In the case of multicomponent systems, a competition occurs for the ‘active places’ of the coating of the SPME fibre. By increasing extraction time the higher-boiling point compounds might displace the previously sorbed lower-boiling ones [55–57].

Diterpenes require more than 80 min to reach equilibrium. This is expected for compounds that exhibit low vapour pressure in combination with a high partition coefficient between the fibre coating and the gaseous phase. During headspace SPME the amount of such compounds present in the gaseous phase is absorbed by the fibre coating at a much faster rate than their release from the matrix, thus the amount of mass in the headspace at any time is small and a long time is required to reach equilibrium [58].

In order to avoid experiments which are very long, the sampling time was fixed at 60 min. In these conditions, the partition equilibrium for diterpenes extraction is not achieved and SPME does not have maximum sensitivity. However, peak intensities are sufficiently high to detect the presence of diterpenes in a sample. Moreover, a proportional relationship exists between the amount of analyte adsorbed by the SPME fibre and its initial concentration in the sample matrix before reaching partition equilibrium [5, 59]. SPME quantifications are then feasible if necessary, by rigorously reproducing the experimental conditions.

However, it was observed that, for each compound, the sampling profile was the same for the five fibre coatings. It could be deduced that the quantity of terpene trapped is independent of the nature of the fibre coating. This behaviour can be explained easily, as the interactions between compounds and fibres are not specific. This is not very surprising because of the nature of the terpenes studied, which are principally composed of carbon and hydrogen.

A mathematical selection based on the criterion function  $F_{ij}$  has been used in order to better discriminate the various fibre coatings [60]. Results are summarised in Table 10.2. The values are very close for the five fibre coatings. Nevertheless, we can note that the CW/DVB fibre gave the worst results for mono- and sesquiterpenes and the CAR/PDMS fibre the worst results for diterpenes. This has been explained by the nature of the two fibre coatings. The CW/DVB coating is polar and therefore is more suitable for polar compounds and less effective in recovering the nonpolar ones [57, 61]. CAR/PDMS is composed of porous carbon better adapted for adsorption of small molecules. Moreover, the CAR/PDMS fibre has been shown to rearrange some monoterpenes to *p*-cymene during headspace SPME, giving erroneous results [62]. In order to obtain the maximum information on an archaeological sample, these two fibres have been eliminated. Among the three remaining fibres, PDMS/DVB gave the best result for diterpenes and good results for mono- and sesquiterpenes.

### 10.3.2.3 Comparison between Headspace SPME and Solvent Extraction

In order to ensure that headspace SPME allows extraction of almost all the volatile or semi-volatile compounds of frankincense, a classical extraction with dichloromethane was performed. Although the two modes of extraction do not give exactly the same chromatogram, headspace SPME gives a good image of the terpenoid composition of olibanum. The two chromatograms can be seen in Figure 10.6.

**Table 10.2** Values of the criterion function  $F_{ij}$  calculated for five different fibre coatings

Fibre coating	$F_{ij}$ for monoterpenes	$F_{ij}$ for sesquiterpenes	$F_{ij}$ for diterpenes
PDMS	1.04	1.06	1.01
CAR/PDMS	1.13	1.07	0.88
CAR/PDMS/DVB	1.04	1.04	0.98
PDMS/DVB	0.95	1.03	1.10
CW/DVB	0.84	0.80	1.03

Sampling time 60 min; extraction temperature 80°C. Monoterpenes:  $\alpha$ -pinene,  $\beta$ -myrcene,  $\alpha$ -phellandrene and limonene; sesquiterpenes:  $\alpha$ -cubebene,  $\alpha$ -copaene,  $\beta$ -elemene,  $\beta$ -caryophyllene,  $\alpha$ -humulene,  $\gamma$ -muurolene,  $\beta$ -eudesmene and caryophyllene oxide; diterpenes: cembrene A and isoincense acetate.

Reproduced from S. Hamm, E. Lesellier, J. Bleton, A. Tchaplal, *J. Chromatogr., A*, **1018**, 73–83. Copyright 2003 Elsevier Limited.

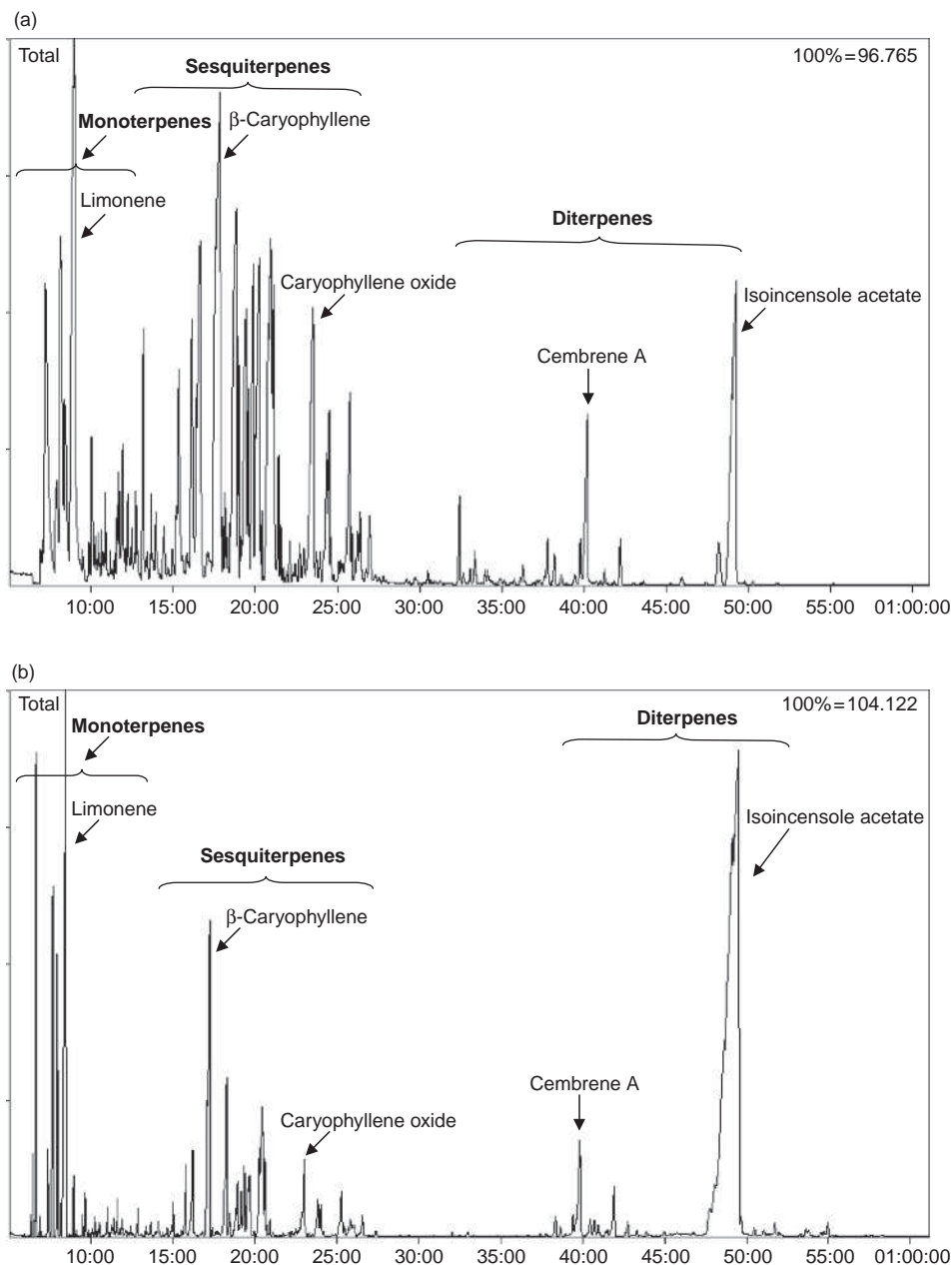


**Figure 10.6** Total ion chromatograms obtained for frankincense showing comparison between (a) SPME and (b) dichloromethane extraction. Reproduced from S. Hamm, E. Lesellier, J. Bleton, A. Tchaplal, *J. Chromatogr., A*, **1018**, 73–83. Copyright 2003 Elsevier Limited

### 10.3.3 Application to Research on Olibanum [26]

As a first step, the authors built a database of the volatile terpenes for six olibanum samples with certified botanical origin and derived characteristic signatures associated with the botanical origin. In the second step they used these signatures to define the species of samples of different origin (commercial societies or markets from various countries of the Middle East) and to recognise the markers of olibanum in a mixture with other plants substances.

#### 10.3.3.1 SPME of Olibanum of Certified Botanical Origin

The main compounds detected by headspace SPME in six olibanum samples are given in Table 10.3. Qualitative results obtained by headspace SPME were identical to those obtained by classical extraction with dichloromethane, except for the triterpenes.

The first observation is the similarity between the chemical compositions of both the *Boswellia carteri* and *Boswellia sacra*. For these three olibanum samples,  $\alpha$ -pinene (**2**),  $\beta$ -myrcene (**8**) and limonene (**14**) are the predominant monoterpenes.  $\beta$ -Caryophyllene (**73**) is the major sesquiterpene besides  $\alpha$ -copaene (**65**),  $\alpha$ -humulene (also called  $\alpha$ -caryophyllene) (**78**) and caryophyllene oxide (**95**). The characteristic olibanum compounds isoincense and isoincense acetate (**128**) together with cembrene A (**120**) are the main diterpenes.

*Boswellia serrata* olibanum has a chemical composition close to that of both the *B. carteri* and of *B. sacra*, but contains compounds that are absent in those from other *Boswellia* and could be used as markers: methylchavicol (**38**), *p*-anisaldehyde (**47**), methyleugenol (**70**), isocaryophyllene (**82**), sesquiterpene **91**, elemicin (**92**) and an unidentified diterpene (**124**) eluting between cembrene C (**123**) and verticilla-4(20),7,11-triene (**125**). It is devoid of  $\beta$ -caryophyllene (**73**),  $\alpha$ -humulene (**78**), caryophyllene oxide (**95**) and bornyl acetate (**50**).

*B. frereana* and *B. papyrifera* olibanum have very different terpenic composition from the others. *B. frereana* olibanum contains the same monoterpenes as olibanum from *B. carteri*, *B. sacra* or *B. serrata*, but is very poor in sesquiterpenes and contains none of the diterpenic biomarkers cited before. Two unidentified compounds (**55** and **56**) seem to be specific and the main diterpenes, present in high level, are four dimers of  $\alpha$ -phellandrene. Dimer 3 (**113**) is the major component. On account of its absence in the other olibanum samples, it can be considered as characteristic of *B. frereana* olibanum.

The chemical composition of *B. papyrifera* olibanum is markedly different from that of other *Boswellia*, with small amounts of monoterpenes and sesquiterpenes, large amounts of *n*-octanol (**18**) and *n*-octylacetate (**40**), with the latter being the major compound, and the presence of particular diterpenes [incense (**127**), incense acetate (**129**), incense oxide (**130**) and incense oxide acetate (**131**)] and the absence of both isoincense and isoincense acetate (**128**). Linear carboxylic acids from hexanoic acid (**10**) to lauric acid (**93**) were also identified in *B. papyrifera* olibanum exclusively.

**Table 10.3** Main components detected by headspace SPME/GC-MS in the six reference olibanum samples with certified botanical origin and in three olibanum samples without botanical origin

Peak no.	Compound	RI <sup>a</sup>	<i>B. carteri</i> Somalia	<i>B. carteri</i> Aden	<i>B. frereana</i> Somalia	<i>B. papyrifera</i> Ethiopia	<i>B. sacra</i> Oman	<i>B. serrata</i> India	Somalia (Wolf)	Somalia (Asie Concept)	Eritrea (Wolf)
1	$\alpha$ -Thujene	916	–	0.1	<b>9.8</b>	–	2.0	<b>11.7</b>	0.1	0.2	–
2	$\alpha$ -Pinene	942	<b>23.2</b>	<b>6.3</b>	<b>12.4</b>	0.5	<b>13.9</b>	3.4	<b>3.9</b>	<b>4.7</b>	2.2
3	4-Methylene-1-(1-methylethyl)- bicyclo[3.1.0]hex-2-ene	946	0.1	0.1	0.4	–	0.2	0.3	–	–	–
4	Camphene	949	0.6	0.2	0.6	–	0.8	0.1	0.9	0.4	–
5	Isomer of 4-methylene-1-(1- methyl-ethyl)- bicyclo[3.1.0]hex-2-ene	952	0.2	0.2	0.6	–	0.7	tr	–	1.2	–
6	Sabinene	963	2.2	0.3	3.2	–	2.1	3.0	0.3	0.6	–
7	$\beta$ -Pinene	966	1.5	0.4	1.4	–	0.9	0.5	0.3	0.6	–
8	$\beta$ -Myrcene	994	<b>4.5</b>	<b>4.4</b>	0.3	–	<b>5.2</b>	<b>7.0</b>	<b>4.0</b>	<b>0.4</b>	–
9	$\alpha$ -Phellandrene	1003	2.1	0.3	1.1	–	0.8	0.9	0.5	–	–
10	<i>n</i> -Hexanoic acid	1003	–	–	–	<b>0.2</b>	–	–	–	–	<b>1.8</b>
11	<i>o</i> -Methylanisole	1005	–	0.2	–	–	–	–	1.2	0.5	–
12	$\delta$ -3-Carene	1006	–	–	–	–	–	0.2	–	–	–
13	<i>p</i> -Cymene	1014	2.5	1.5	<b>7.8</b>	0.2	<b>5.5</b>	<b>4.7</b>	1.2	1.7	–
14	Limonene	1020	<b>22.4</b>	<b>10.2</b>	1.7	0.1	<b>6.9</b>	2.6	<b>7.1</b>	<b>3.3</b>	<b>5.2</b>
15	Eucalyptole	1022	–	–	1.7	0.1	–	–	0.9	–	–
16	Thujol	1049	0.1	tr	0.6	–	0.2	0.4	–	–	–
17	$\gamma$ -Terpinene	1054	tr	–	0.1	–	0.1	0.2	tr	–	–
18	<i>n</i> -Octanol	1063	–	–	–	<b>13.9</b>	–	–	–	–	<b>11.7</b>
19	<i>cis</i> -Linalool oxide	1073	–	tr	tr	0.2	–	–	–	–	–
20	<i>n</i> -Heptanoic acid	1076	–	–	–	<b>tr</b>	–	–	–	–	<b>1.8</b>
21	Linalool	1077	0.2	0.9	1.5	0.2	1.2	1.6	1.0	–	0.5
22	Oxygenated monoterpene	1108	0.3	0.8	2.7	–	2.1	tr	–	0.9	–
23	Thujone	1111	0.1	–	0.8	–	0.6	1.0	–	–	–
24	<i>trans-p</i> -Mentha-2,8-dienol	1113	0.3	0.3	–	–	0.3	–	0.1	0.2	–
25	Octyl formiate	1117	–	–	–	<b>tr</b>	–	–	–	–	<b>1.5</b>
26	$\alpha$ -Campholenal	1119	0.4	0.2	0.7	tr	0.8	0.1	–	0.2	–
27	<i>trans-p</i> -2,8-Menthadien-1-ol	1123	0.1	0.3	–	–	–	–	0.2	0.1	–



28	<i>trans</i> -Pinocarveol	1129	0.9	0.5	1.7	0.1	1.9	0.2	0.4	0.6	–
29	<i>cis</i> -Verbenol	1131	1.5	1.1	3.5	–	3.5	0.7	0.1	1.0	–
30	<i>cis</i> -Sabinol	1170	0.5	–	1.5	–	0.3	0.9	–	–	–
31	4-Terpineol	1182	0.1	tr	2.8	–	0.6	0.1	0.1	–	–
32	Methyl-acetophenone	1186	tr	tr	0.2	–	0.2	–	–	0.2	–
33	<i>p</i> -Cymen-8-ol	1187	1.1	0.9	0.3	–	0.7	0.4	0.3	1.1	–
34	$\alpha$ -Terpineol	1193	0.3	0.4	0.9	–	0.2	–	0.4	0.2	–
35	Myrtenal	1197	–	0.6	0.7	–	0.8	–	–	0.3	–
36	<i>n</i> -Octanoic acid	1197	–	–	–	<b>0.8</b>	–	–	–	–	<b>2.3</b>
37	Myrtenol	1198	0.7	–	0.3	–	0.4	–	–	0.4	–
38	Methylchavicol	1200	–	–	–	–	–	<b>8.9</b>	–	–	–
39	2-Methyl-5-(1-methylethyl)- 1,3-cyclohexadiene monoepoxide	1202	0.9	–	1.0	–	–	0.2	0.6	–	–
40	<i>n</i> -Octyl acetate	1220	–	–	–	<b>64.6</b>	0.3	–	–	0.4	<b>36.8</b>
41	Verbenone	1221	1.4	0.9	3.1	–	3.0	0.2	0.1	1.2	–
42	<i>trans</i> -Carveol	1225	1.3	1.4	0.9	0.3	1.4	0.6	0.4	1.3	2.5
43	<i>cis</i> -Carveol	1230	0.4	0.4	–	–	0.2	–	0.1	0.3	0.6
44	Cumaldehyde	1235	0.3	0.1	0.5	–	0.3	0.1	0.1	0.1	–
45	Carvone	1237	1.0	0.8	0.1	0.3	0.7	0.1	0.3	0.6	1.6
46	$\alpha$ -Cyclogeranyl acetate	1241	–	–	2.2	–	–	–	–	–	–
47	<i>p</i> -Anisaldehyde	1242	–	–	–	–	–	<b>0.5</b>	–	–	–
48	3,5-Dimethoxy-toluene	1264	0.7	1.1	–	–	0.5	–	1.5	0.3	–
49	Nonanoic acid	1265	–	–	–	<b>0.5</b>	–	–	–	–	<b>1.2</b>
50	Bornyl acetate	1275	0.9	0.3	3.8	0.2	1.3	–	0.3	0.5	0.4
51	<i>m</i> -Thymol	1276	0.5	0.1	tr	–	tr	0.2	–	–	–
52	Cuminol	1276	tr	0.1	0.3	–	0.2	tr	0.1	0.3	–
53	Carvacrol	1281	tr	–	1.9	–	0.3	0.2	0.2	0.2	–
54	Perillol	1282	tr	0.3	–	–	tr	0.2	0.1	0.1	–
55	Unidentified compound	1312	–	–	<b>1.9</b>	–	–	–	–	–	–
56	Unidentified compound	1314	–	–	<b>2.0</b>	–	–	–	–	–	–
57	1-Methyl-4-(1-methyl-ethenyl)- 1,2-cyclohexanediol	1321	0.6	0.3	–	tr	0.4	–	–	–	0.8

(continued overleaf)

**Table 10.3** (continued)

Peak no.	Compound	RI <sup>a</sup>	<i>B. carteri</i> Somalia	<i>B. carteri</i> Aden	<i>B. frereana</i> Somalia	<i>B. papyrifera</i> Ethiopia	<i>B. sacra</i> Oman	<i>B. serrata</i> India	Somalia (Wolf)	Somalia (Asie Concept)	Eritrea (Wolf)
58	Terpinyl acetate	1344	0.3	–	–	–	tr	0.1	0.4	–	–
59	$\alpha$ -Cubebene	1347	0.2	0.8	–	–	0.6	0.1	1.8	3.0	–
60	3,4-Dimethoxystyrene	1354	0.1	0.6	0.5	–	0.1	–	tr	–	–
61	Cyclosativene	1360	–	–	–	–	tr	0.1	–	–	–
62	$\alpha$ -Ylangene	1362	–	–	–	–	–	0.1	tr	–	–
63	Decanoic acid	1367	–	–	–	<b>0.1</b>	–	–	–	–	<b>1.4</b>
64	Neryl acetate	1375	–	–	–	0.1	–	–	–	–	1.0
65	$\alpha$ -Copaene	1383	<b>1.6</b>	<b>5.5</b>	0.9	–	<b>4.0</b>	1.1	<b>2.7</b>	<b>2.6</b>	–
66	<i>n</i> -Hexyl hexanoate	1387	–	–	–	<b>0.9</b>	–	–	–	–	<b>0.2</b>
67	$\beta$ -Bourbonene	1388	0.1	–	0.2	–	0.3	4.2	0.9	–	–
68	$\beta$ -Cubebene	1390	–	1.1	–	–	0.4	–	–	–	–
69	$\beta$ -Elemene	1393	0.9	–	2.7	–	1.6	–	5.5	5.6	–
70	Methyl-eugenol	1394	–	–	–	–	–	<b>3.7</b>	–	–	–
71	<i>n</i> -Decyl acetate	1406	–	–	–	<b>0.9</b>	–	–	–	–	<b>1.9</b>
72	(Z)-Caryophyllene	1418	–	–	–	–	–	–	–	–	–
73	$\beta$ -Caryophyllene	1426	<b>6.9</b>	<b>16.9</b>	–	–	<b>4.7</b>	–	<b>12.0</b>	<b>5.5</b>	–
74	$\beta$ -Gurjunene	1427	–	–	–	–	tr	–	1.0	–	–
75	Z- $\alpha$ -trans-bergamotene	1428	–	–	–	–	tr	0.2	–	1.1	–
76	$\alpha$ -Guaiene	1441	–	tr	–	–	tr	–	0.2	0.1	–
77	Aromadendrene	1444	–	–	–	–	–	0.2	0.3	–	–
78	$\alpha$ -Humulene	1454	<b>1.1</b>	<b>5.2</b>	tr	–	<b>3.1</b>	–	<b>5.1</b>	<b>3.3</b>	–
79	allo-Aromadendrene	1456	0.2	0.6	–	–	0.6	0.1	1.2	1.1	–
80	$\gamma$ -Muurolene	1475	0.4	1.0	–	–	1.1	0.4	3.0	3.2	–
81	Germacrene D	1479	0.2	0.2	–	–	0.8	1.5	1.4	–	–
82	Isocaryophyllene	1480	–	–	–	–	–	<b>1.7</b>	–	–	–
83	$\beta$ -Eudesmene	1483	0.6	0.1	0.1	–	0.5	–	3.2	2.9	–
84	2-Isopropenyl-4a,8-dimethyl- 1,2,3,4,4a,5,6,8a- octahydronaphthalene	1485	0.5	1.6	–	–	1.4	–	2.0	–	–
85	$\alpha$ -Muurolene	1501	1.0	0.6	–	–	0.6	0.1	2.6	1.1	–

86	δ-Guaiene	1503	–	tr	–	–	–	–	0.3	0.3	–
87	γ-Cadinene	1509	0.1	0.2	–	–	1.9	0.2	2.9	1.3	–
88	1-Hydroxy-1,7-dimethyl-4-isopropyl-2,7-cyclodecadiene	1511	1.9	5.7	–	–	2.4	–	0.9	9.6	–
89	δ-Cadinene	1524	1.0	2.0	0.1	–	2.2	0.3	1.9	1.6	–
90	1,2,3,4,6,8a-Hexahydro-1-isopropyl-4,7-dimethyl-naphthalene	1528	tr	0.1	–	–	tr	–	0.6	1.2	–
91	Oxygenated sesquiterpene	1529	–	–	–	–	–	<b>8.0</b>	–	–	–
92	Elemicin	1533	–	–	–	–	–	<b>0.9</b>	–	–	–
93	Lauric acid	1572	–	–	–	<b>0.3</b>	–	–	–	–	<b>1.5</b>
94	Hexyl caprylate + another ester	1579	–	–	–	<b>1.2</b>	–	–	–	–	<b>0.7</b>
95	Caryophyllene oxide	1582	<b>2.0</b>	<b>13.1</b>	0.1	–	<b>4.9</b>	–	<b>4.6</b>	<b>11.0</b>	–
96	Ledol	1587	–	–	–	–	2.0	–	0.3	0.4	–
97	Ethyl laurate	1597	–	–	–	–	–	–	–	–	0.4
98	Oxygenated sesquiterpene	1605	–	–	–	–	0.2	–	0.8	–	–
99	1,5,5,8-Tetramethyl-12-oxabicyclo[9.1.0]dodeca-3,7-diene	1607	0.2	2.4	0.2	–	1.8	–	0.6	5.4	–
100	γ-Eudesmol	1609	0.5	–	–	–	0.2	0.6	–	–	–
101	τ-Cadinol	1634	1.2	0.1	–	–	2.7	–	1.6	1.8	–
102	δ-Cadinol	1636	–	tr	–	–	–	–	0.3	0.2	–
103	α-Eudesmol or β-Eudesmol	1649	0.2	–	tr	–	tr	–	0.1	0.9	–
104	α-Cadinol	1651	–	tr	–	–	0.2	–	0.3	0.6	–
105	Oxygenated sesquiterpene	1653	–	0.3	–	–	0.1	–	0.5	1.5	–
106	Oxygenated sesquiterpene	1661	–	1.0	–	–	0.4	–	0.6	2.2	–
107	(E)-9-dodecen-1-ol acetate	1700	–	–	–	–	–	–	–	–	0.4
108	Dimer of α-phellandrene 1	1732	tr	–	0.6	–	–	–	–	–	–
109	Benzyl benzoate	1761	–	–	–	–	–	–	–	–	0.3
110	Octyl caprylate	1779	–	–	–	–	–	–	–	–	0.3
111	Dimer of α-phellandrene 2	1795	1.5	–	–	–	0.3	1.0	0.8	–	–
112	Ethyl myristate	1797	–	–	–	–	–	–	–	–	0.3

(continued overleaf)

**Table 10.3** (continued)

Peak no.	Compound	RI <sup>a</sup>	<i>B. carteri</i> Somalia	<i>B. carteri</i> Aden	<i>B. frereana</i> Somalia	<i>B. papyrifera</i> Ethiopia	<i>B. sacra</i> Oman	<i>B. serrata</i> India	Somalia (Wolf)	Somalia (Asie Concept)	Eritrea (Wolf)
113	Dimer of $\alpha$ -phellandrene 3	1810	–	–	<b>15.6</b>	–	–	–	–	–	–
114	Dimer of $\alpha$ -phellandrene 4	1815	0.2	–	1.6	–	–	0.1	–	–	–
115	Dimer of $\alpha$ -phellandrene 5	1837	0.2	–	2.4	–	–	–	0.1	–	–
116	Unidentified diterpene	1865	–	–	tr	–	–	–	tr	–	–
117	Dimer of $\alpha$ -phellandrene 6	1904	0.4	–	tr	–	–	–	0.4	–	–
118	Dimer of $\alpha$ -phellandrene 7	1918	0.2	–	tr	–	tr	–	0.3	–	–
119	Unidentified diterpene	1945	0.1	0.1	–	–	0.1	1.9	0.3	tr	0.3
120	Cembrene A	1959	0.3	0.7	–	1.7	0.3	2.5	2.0	0.5	0.7
121	Cembrene?	1964	–	–	–	–	–	–	–	–	0.7
122	Unidentified diterpene	1981	tr	–	–	–	tr	0.7	0.1	–	–
123	Cembrene C	2002	tr	0.1	–	tr	tr	tr	0.4	0.1	0.5
124	Unidentified diterpene	2003	–	–	–	–	–	<b>0.1</b>	–	–	–
125	Verticilla-4(20),7,11-triene	2004	0.1	0.1	–	–	0.1	0.3	–	–	1.6
126	Unidentified diterpene	2141	<b>0.1</b>	<b>0.1</b>	–	–	<b>0.1</b>	<b>1.1</b>	<b>0.7</b>	<b>0.2</b>	–
127	Incensole	2150	–	–	–	<b>1.0</b>	–	–	–	–	<b>5.0</b>
128	Isoincensole + isoincensole acetate	2152	<b>1.4</b>	<b>2.1</b>	–	–	<b>1.4</b>	<b>6.9</b>	<b>8.0</b>	<b>2.5</b>	–
129	Incensole acetate	2189	–	–	–	<b>10.8</b>	–	–	–	–	<b>9.4</b>
130	Incensole oxide <sup>b</sup>	–	–	–	–	<b>0.4</b>	–	–	–	–	<b>0.4</b>
131	Incensole oxide acetate <sup>b</sup>	–	–	–	–	<b>0.1</b>	–	–	–	–	<b>0.2</b>

Components are presented by increasing retention indices, with their corresponding relative peak area (%). Values in bold correspond to compounds in high level or characteristic of an olibanum.

tr, traces (<0.1%).

<sup>a</sup>Retention indices relative to C<sub>9</sub>–C<sub>22</sub> alkanes obtained on a DB5 column.

<sup>b</sup>Retention indices of these compounds were not calculated because their retention times were higher than that of the last alkane used (C<sub>22</sub>).

Reproduced from S. Hamm, J. Bleton, J. Connan, A. Tchaplai, *Phytochemistry*, **66**, 1499–1514. Copyright 2005 Elsevier Limited.

### 10.3.3.2 SPME of Olibanum of Unknown Botanical Origin

Eight olibanum samples of unknown botanical origin have been analysed [26]. The chemical compositions are summarized in Table 10.3 for three of them. Both the olibanum coming from Somalia and that from a market in Ta'izz (Yemen) have been attributed to *Boswellia carteri* or *sacra* on the basis of the occurrence of the characteristic diterpenes isoincense and isoincense acetate (**128**) together with diterpene **126**. The absence of methylchavicol (**38**), oxygenated sesquiterpene **91** and diterpene **124** and the presence in relatively large amount of  $\beta$ -caryophyllene (**73**),  $\alpha$ -humulene (**78**) and caryophyllene oxide (**95**) excluded the hypothesis of a *B. serrata* sample.

The samples coming from Eritrea, Jerusalem and Liban could be undoubtedly attributed to *B. papyrifera*, because of their characteristic constituents: octanol (**18**), octyl acetate (**40**), linear caboxylic acids (**10**, **20**, **36**, **49**, **63**), incense (**127**) and its acetate and oxide derivatives (**129–131**).

Samples purchased on markets in Sa'da and San'a in Yemen comprise no diterpenes from the incense family but large amounts of dimers of  $\alpha$ -phellandrene, in particular dimer 3 (**113**), and of both compounds **55** and **56**. This pattern identifies them as *B. frereana* olibanum.

### 10.3.3.3 SPME of Present Day Traditional Incenses

In traditional incenses, olibanum is often mixed with other ingredients. The analysis of two traditional mixtures of the present day are reported: Greek incense and a recreation of an ancient Egyptian recipe.

The GC-MS chromatogram, obtained after SPME of the traditional incense from a monastery of Mount Athos, is presented in Figure 10.7a. The occurrence of octanol (**18**), octyl acetate (**40**), incense (**127**), incense acetate (**129**), incense oxide (**130**) and incense oxide acetate (**131**), allowed the identification of a *B. papyrifera* olibanum (Figure 10.7b) in a mixture with other substances, most probably Damask rose and jasmine.

The analysed Kyphi is a recreation of an ancient Egyptian mixture burnt in temples. Kyphi recipes are inscribed on the walls of the ancient temples of Edfu and Philae. It could include saffron, frankincense, mastic, benzoin, cardamon seeds, galangal root, lemongrass, sandalwood, aloeswood, rose petals, raisins, red wine, honey and other herbs. The GC-MS chromatogram obtained for this mixture is presented in Figure 10.8a. Analysis of the overall information and comparison with GC-MS chromatograms of reference substances confirm that Kyphi contains an olibanum coming from *B. sacra* (Figure 10.8b) rather than from *B. carteri*. Some characteristic compounds of myrrh could be recognised: curzerene (**c**), furanoeudesma-1,3-diene (**d**), lindenstrene, 2-methoxyfuranodiene (**f**) and 2-acetoxymethoxyfuranodiene.

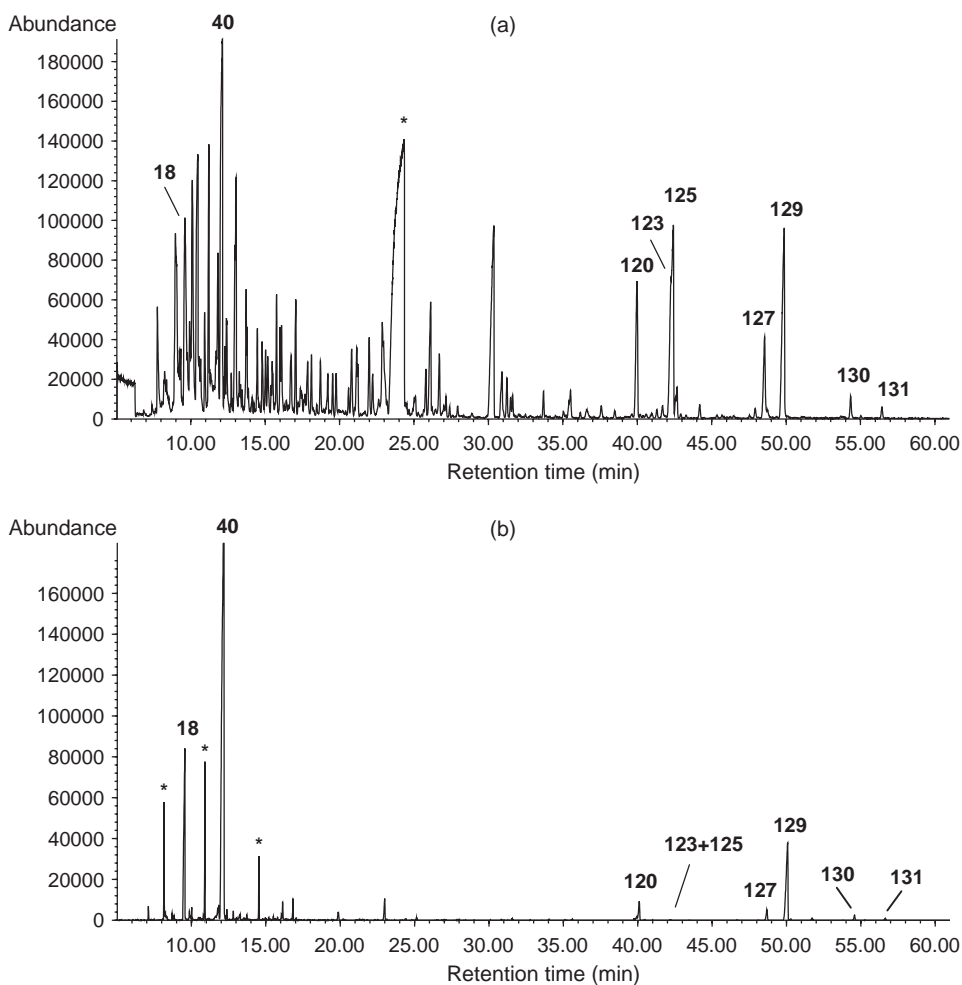


**Figure 10.7** Total ion current chromatograms obtained after headspace SPME for (a) incense from Mount Athos and (b) *B. papyrifera* olibanum. Peak labels correspond to compound identification given in Table 10.3. The occurrence of the following biomarkers of *B. papyrifera* olibanum in the incense from Mount Athos are a clear indication of its botanical origin: *n*-octanol (**18**), *n*-octylacetate (**40**), incensole (**127**), incensole acetate (**129**), incensole oxide (**130**) and incensole oxide acetate (**131**). \*Artefacts. Reproduced from S. Hamm, J. Bleton, J. Connan, A. Tchaplá, *Phytochemistry*, **66**, 1499–1514. Copyright 2005 Elsevier Limited

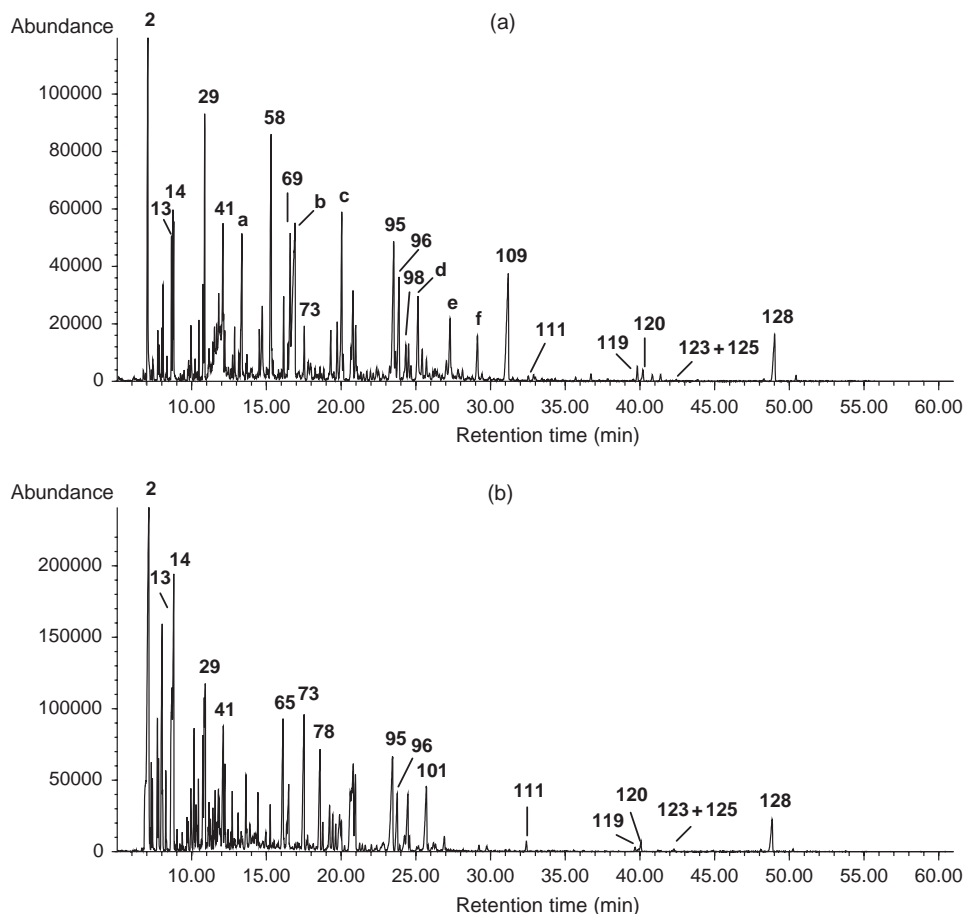


**Figure 10.8** Total ion current chromatograms obtained after headspace SPME for (a) Kyphi and (b) *B. sacra olibanum*. Peak labels correspond to compound identification given in Table 10.3. The occurrence of isoincense acetate (**128**) as well as the occurrence of the oxygenated sesquiterpene **98** and of dimer 2 (**111**) in Kyphi are clear fingerprints of the botanical origin of the olibanum used. Peaks labelled by letters correspond to the following compounds: **a**, cinnamaldehyde; **b**, vanilline; **c**, curzerene; **d**, furanoeudesma-1,3-diene; **e**,  $\alpha$ -santalol; **f**, 2-methoxyfuranodiene. Reproduced from S. Hamm, J. Bleton, J. Connan, A. Tchaplal, *Phytochemistry*, **66**, 1499–1514. Copyright 2005 Elsevier Limited

## 10.4 Application of the Method to Archaeological Samples

### 10.4.1 Results Obtained with the PDMS Fibre at Ambient Temperature

In this section, we present unpublished results with the aim of increasing the number of examples attesting the usefulness of SPME.

The first attempt to identify the volatile compounds in an archaeological sample was motivated by the sample's strong empyreumatic odour. Sample 1998 (Thebes, twenty-fifth dynasty) was from the collections of the Guimet Museum in Lyon (France) and was a bright black sticky substance contained in a glass bottle sealed with a cork. The results obtained by GC-MS after SPME with a PDMS fibre at ambient temperature are presented in Figure 10.9. Peak identification is given in Table 10.4. In the first part of the chromatogram, the clearly identified compounds are aromatic derivatives such as cresols and gaiacols (2-methoxy-phenols), acetophenones and sesquiterpenes. The phenolic derivatives are probably lignin degradation products originating from the pyrolysis of wood. In the second part of the chromatogram, after 18 min., most of the compounds are unidentified sesquiterpenoids formed during the heating process. The characteristic ions of the corresponding spectra are given in the Table 10.5. A similar result has been obtained by Koller *et al.* [63] with the methanolic extract from an unused embalming material from the eighteenth dynasty (1500 BC).

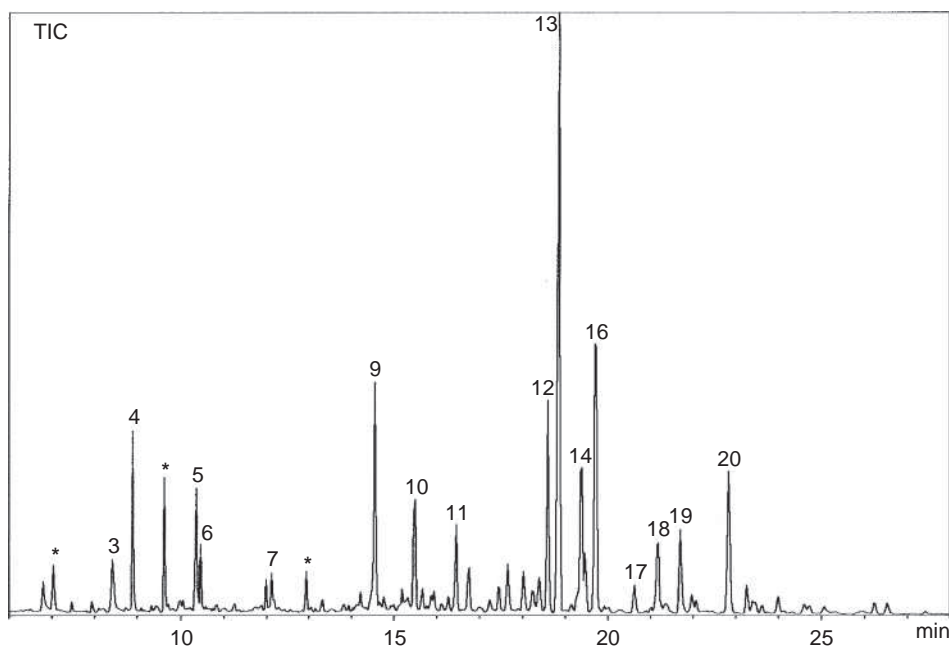


**Figure 10.9** Total ion current chromatogram obtained for sample 1998 after headspace SPME. Peak labels correspond to compound identification given in Table 10.4



**Table 10.4** List of compounds detected by headspace SPME/GC-MS in samples 1998 and 1400

Peak no.	Name	MW
1	Dichlorobenzene	146
2	Acetophenone	120
3	Cresol	108
4	Unidentified	140
5	Methylacetophenone	134
6	Methylguaiacol	138
7	Ethylguaiacol	152
8	Longicyclene	204
9	Unidentified	204
10	Longifolene	204
11	Dihydrocurcumene	204
12	Cuparene	202
13	Unidentified sesquiterpenoid	200
14	Unidentified sesquiterpenoid	200
15	Unidentified	222
16	Unidentified sesquiterpenoid	202
17	Unidentified sesquiterpenoid	216
18	Unidentified sesquiterpenoid	198
19	Unidentified sesquiterpenoid	218
20	Unidentified sesquiterpenoid	220
21	Unidentified sesquiterpenoid	202
*	Siloxanes (artefacts)	

**Table 10.5** Mass spectrometric data obtained for unidentified compounds detected in samples 1998 and 1400

Peak no.	MW	Characteristic fragments: $m/z$ (%)
4	140	85(100), 56(93), 140(22), 125(20), 55(19), 69(18)
9	204	119(100), 43(42), 161(39), 176(34), 91(24), 105(23), 117(17), 120(11), 118(11)
13	200	157(100), 185(61), 200(45), 143(39), 142(29), 141(26), 128(22), 115(16), 129(15)
14	200	185(100), 157(90), 171(66), 200(65), 170(47), 143(43), 142(37), 128(36), 158(32)
15	222	85(100), 109(68), 124(26), 55(26), 69(19), 81(17), 67(14), 95(13), 93(10), 53(10)
16	202	187(100), 145(91), 131(56), 202(43), 128(24), 132(19), 129(19), 115(19), 146(18)
17	216	173(100), 158(77), 133(77), 159(46), 148(28), 160(26), 157(26), 145(25), 128(25)
18	198	183(100), 168(37), 198(38), 82(24), 155(21), 153(21), 141(17), 184(15), 152(14)
19	218	119(100), 57(64), 85(22), 91(18), 161(15), 105(15), 218(14), 203(14), 118(12)
20	220	138(100), 110(58), 137(54), 109(53), 55(50), 41(50), 43(43), 120(40), 69(39)
21	202	159(100), 145(38), 144(36), 202(33), 134(33), 115(29), 91(20), 69(17), 187(15)

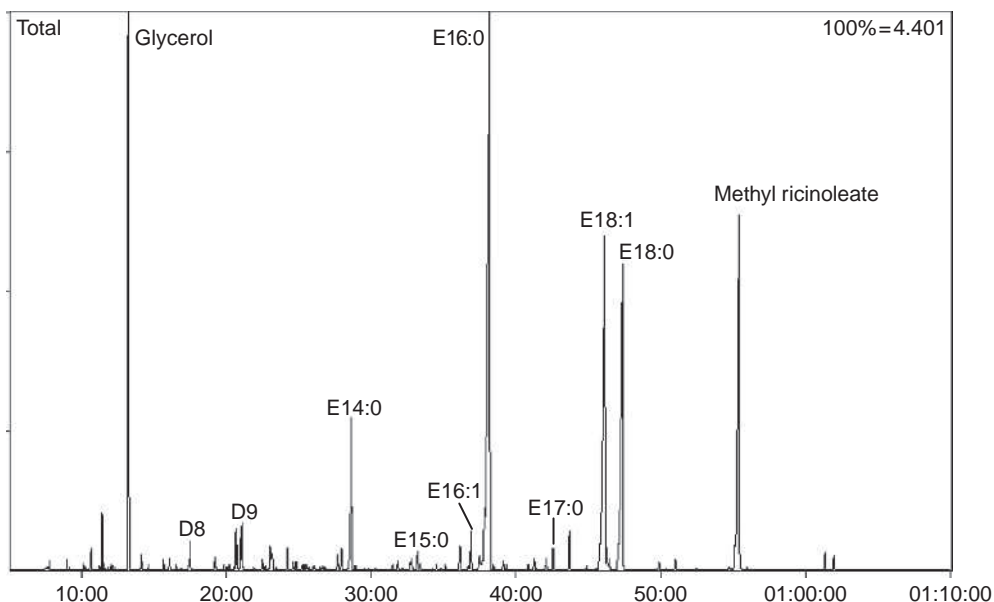


**Figure 10.10** Total ion current chromatogram obtained for sample 1998 after acid methanolysis and trimethylsilylation. Dx, methyl ester of diacid with x carbon atoms. Ex:y, methyl ester of acid with x carbon atoms and y double bonds

The GC-MS chromatogram obtained with the same substance after acid methanolysis and silylation is presented in Figure 10.10. The major compounds are fatty acid methyl esters corresponding to a mixture of an animal fat (attested by the presence of E15:0 and E17:0 with ante and iso isomers) and castor oil (attested by the presence of methyl ricinoleate: E18:1,12OH) [32]. Diterpenoid or triterpenoid resin components are not observed.

The result obtained by GC-MS, with the same SPME conditions, from the black thick balm of a crocodile mummy (sample 1400, Musée Guimet, Lyon, France) is presented in Figure 10.11. The composition of the extract is close to that of sample 1998 but phenolic compounds were not detected. The GC-MS chromatogram obtained with the same substance after acid methanolysis and silylation is presented in Figure 10.12. Except for the sesquiterpenoids eluted between 10 min and 22 min, the observed compounds originate from a beeswax. The biomarkers of this substance are hexadecanoic acids hydroxylated in position 14 or 15 and long chain hydrocarbons, acids and alcohols eluted between 50 min and 90 min. Diterpenoid or triterpenoid resin components are not observed.

These two examples demonstrate clearly the usefulness of SPME to detect volatile compounds in complex mixtures. Among the few sesquiterpenes identified in the SPME extract for the two samples, longifolene can be considered as a biomarker of a substance originating from a conifer tree. The absence of abietane or pimarane diterpenoids is indicative of the use of parts of the tree with low resin content.

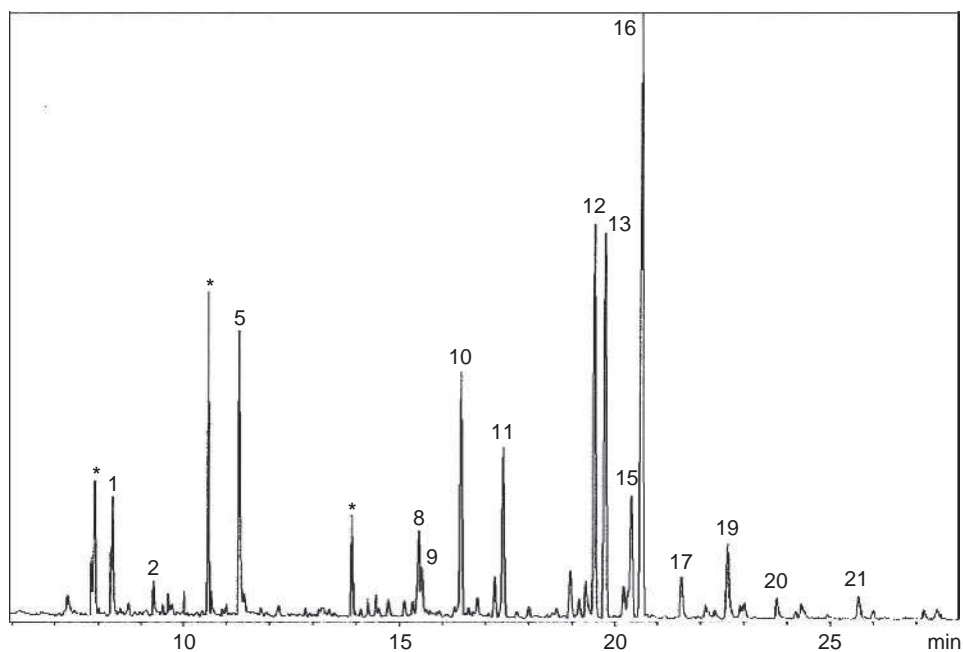


**Figure 10.11** Total ion current chromatogram obtained for sample 1400 after headspace SPME. Peak labels correspond to compound identification given in Table 10.4

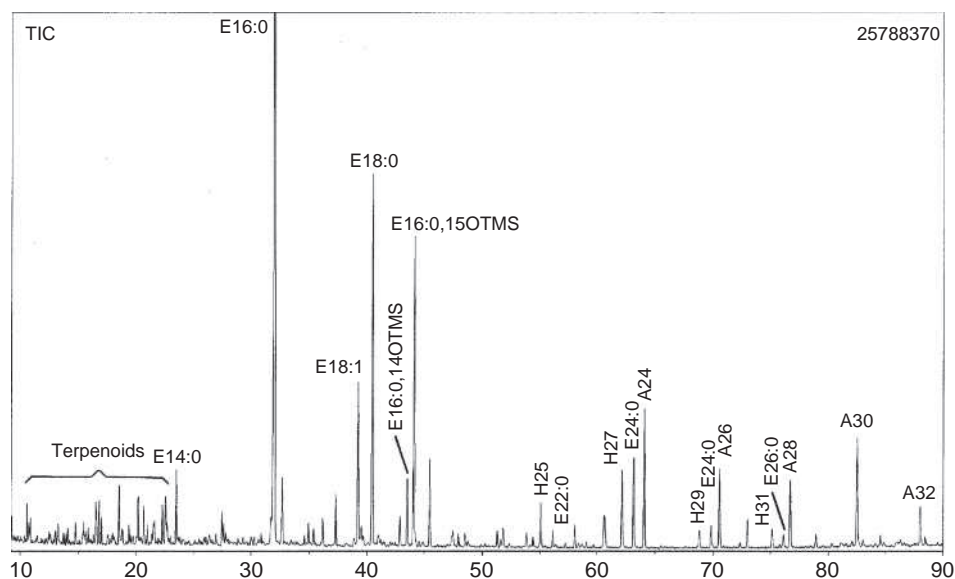


**Figure 10.12** Total ion current chromatogram obtained for sample 1400 after acid methanolysis and trimethylsilylation. Ex:y, methyl ester of acid with x carbon atoms and y double bonds. Hx, alkane with x carbon atoms. Ax, alcohol with x carbon atoms

Four other promising samples coming from the Guimet Museum were also analysed in the same SPME conditions. They come from the digs of de Morgan in Dachour, Egypt [64] and correspond to four of the nine oils cited in the ritual of mouth opening [65]. All were found, in alabaster pots, inside the tomb of Khnoumit, a princess in the reign of Amenemhat II (1929–1892 BC). Numerous volatile terpenes have been extracted from samples 1480 and 1485. The corresponding GC-MS chromatograms are presented Figures 10.13 and 10.14. They are overall very similar. Peak identification is given in Table 10.6. In sample 1480, compound no. 15, 3-methoxy-*p*-cymene (better known in the literature as thymol methyl ether) is very abundant. This compound is usually present in different essential oils but never in such a large amount and it is difficult to determine its origin. Owing to the presence of longifolene among the sesquiterpenes, the two samples should contain a substance originating from conifer trees. In sample 1480,  $\alpha$ -cedrene is also very abundant and clearly accompanied by  $\alpha$ -cedrol. These compounds are biomarkers of a substance coming from a tree of the *Juniperus* species [66]. For samples 1492 and 1484, the extracted terpenes were much less abundant (Figures 10.15 and 10.16). For sample 1492, the major detected sesquiterpene is longifolene. In sample 1484, the major detected sesquiterpene is  $\alpha$ -cedrol. A lot of degradation compounds of a fatty matter [67] were also observed: fatty acids (A6–A9), ketones (K9 and K10) and methyl dodecanoate (E12:0). The origin of the long chain hydrocarbons (H14:1, H14:0, H15:0) detected in the two samples is not known.

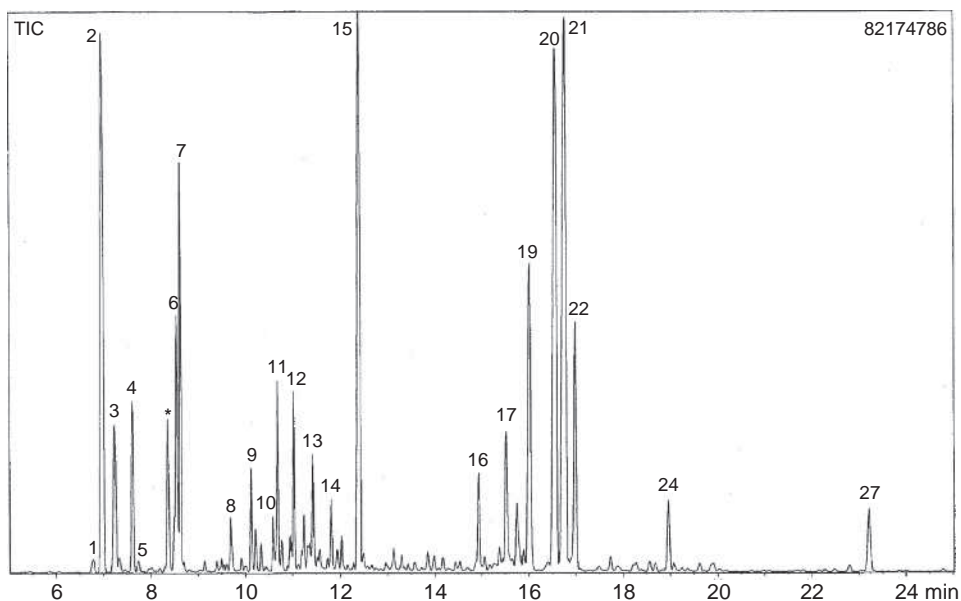


**Figure 10.13** Total ion current chromatogram obtained for sample 1480 after headspace SPME. Peak labels correspond to compound identification given in Table 10.6

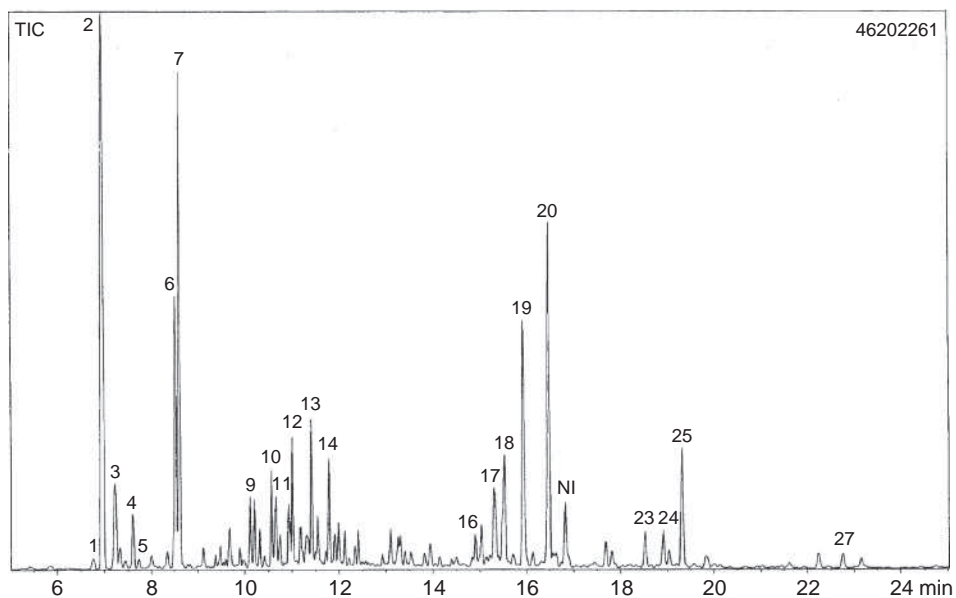


**Figure 10.14** Total ion current chromatogram obtained for sample 1485 after headspace SPME. Peak labels correspond to compound identification given in Table 10.6

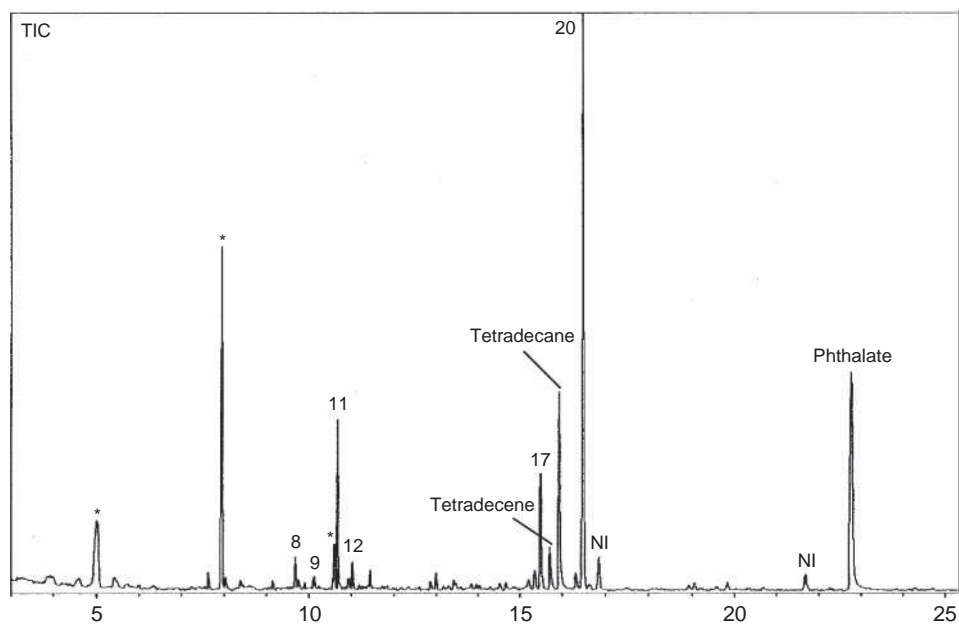


**Figure 10.15** Total ion current chromatogram obtained for sample 1492 after headspace SPME. Peak labels correspond to compound identification given in Table 10.6

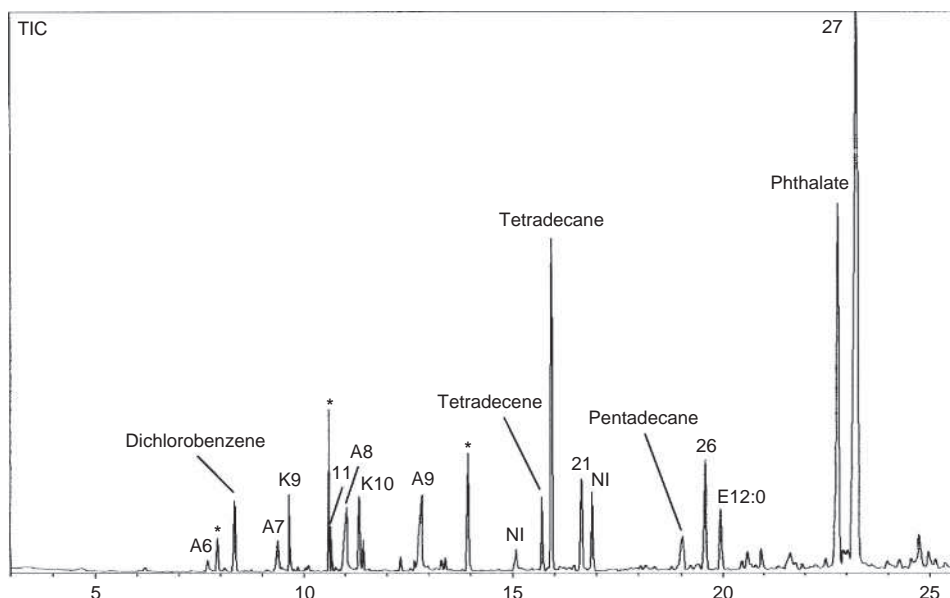


**Figure 10.16** Total ion current chromatogram obtained for sample 1484 after headspace SPME. Peak labels correspond to compound identification given in Table 10.6. Ax, acid with *x* carbon atoms. Kx, ketone with *x* carbon atoms

The results obtained for these four samples by high temperature gas chromatography (HTGC), after extraction with methylene chloride and trimethylsilylation, are presented in Figures 10.17–10.20. Peak identification, according to K. J. van den Berg [68], is given in Table 10.7. In Figures 10.17 and 10.18, the major compounds are silylated derivatives of resin acids. The derivatives of pimaric, isopimaric, dehydroabietic and abietic acids are still observed which means that the resin is relatively well preserved. In Figure 10.9, it is also possible to observe longifolene and  $\alpha$ -cedrene but the other volatile compounds were lost during the evaporation of the silylating reagent or eluted with the solvent. In Figures 10.19 and 10.20, the resin acids are more oxidised which indicates a difference in the preparation of the sample or in the ageing process. In sample 1492, the fatty matter is well preserved. In sample 1484, the fatty matter is completely hydrolysed and the observed trimethylsilyl esters correspond to an animal fat. The relative amount of diterpenoids is low.

The four samples are mixtures of conifer resin and fatty matter, in different relative amounts and different states of conservation, which is not always in agreement with the interpretation of the hieroglyphs engraved on the caps of the alabaster pots.

The results obtained for these four samples highlighted the usefulness of SPME to get complementary information allowing a better characterisation of resinous substances. It is indeed possible to detect many non degraded mono- and sesquiterpenes in well preserved samples such as samples 1480 and 1485 and to detect some characteristic compounds in degraded samples such as sample 1484.

**Table 10.6** Terpenes detected by headspace SPME/GC-MS in four samples from the tomb of Khnoumit (Dachour, Egypt)

Peak no.	Compound	MW	1480	1484	1485	1492
1	Tricyclene	136	+		+	
2	$\alpha$ -Pinene	136	+		+	
3	Camphene	136	+		+	
4	<i>m</i> -Cymene	134	+		+	
5	$\beta$ -Pinene	136	+		+	
6	<i>p</i> -Cymene	134	+		+	
7	Limonene	136	+		+	
8	Fenchone	152	+			+
9	Fenchol	154	+		+	+
10	(-)- <i>trans</i> -Pinocarveol	152	+		+	
11	Camphor	152	+	+	+	+
12	Borneol	154	+		+	+
13	(+)- $\alpha$ -Terpineol	154	+		+	
14	Verbenone	150	+		+	
15	Thymol methyl ether <sup>a</sup>	164	+			
16	Isomer of $\alpha$ -longipinene	204	+		+	
17	Longicyclene	204	+		+	+
18	$\alpha$ -Copaene	204			+	
19	$\beta$ -Elemene	204	+		+	
20	Longifolene	204	+		+	+
21	$\alpha$ -Cedrene	204	+	+		
22	$\beta$ -Caryophyllene	204	+		+	
23	Alloaromadendrene	204			+	
24	$\beta$ -Eudesmene	204	+		+	
25	$\alpha$ -Muurolene	204			+	
26	Cuparene	202		+		
27	$\alpha$ -Cedrol	222	+	+	+	

<sup>a</sup>3-Methoxy-*p*-cymene.

#### 10.4.2 Results Obtained with the PDMS Fibre at 80°C

Twenty-five archaeological samples from ancient Egypt were also analysed with the PDMS fibre, at 80°C, over 1 h [25]. The samples were from the collections of the Guimet Museum in Lyon and are either balms sampled on different mummies or oils or unguents found in containers inside tombs. The best results were obtained when the samples were compact materials able to be ground just before SPME sampling. The five following examples are taken from the literature [25].

The first sample, dating from the Ptolemaic period (~300 BC), was found in a container from a tomb from Fayoum. The volatile compounds observed in this sample (see Table 10.1, column 11) were very similar to those of pine pitch. The two chromatograms are presented in Figure 10.21. The major compounds are guaiacol (**11**) and its *para-n*-alkyl derivatives (**24**, **35**, **43**) and the degradation products of diterpenic acids: 19-norabieta-8,11,13-triene (**95**), 18-norabieta-8,11,13-triene (**100**), 10,18-bisnorabieta-5,7,9(10),11,13-pentaene (**102**), retene (**105**) and methyldehydroabietate (**106**). The major compounds observed after

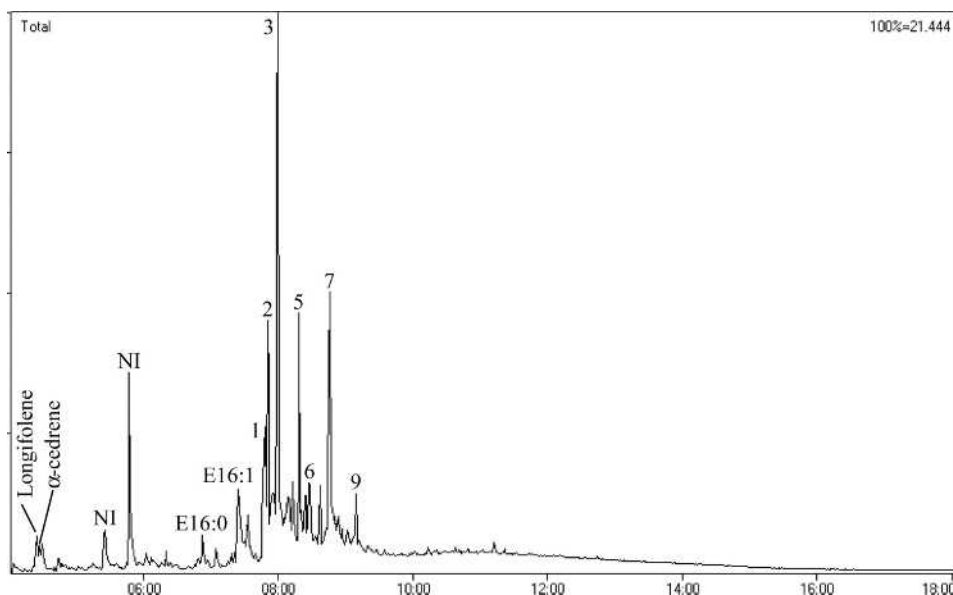


**Figure 10.17** Total ion current chromatogram obtained for sample 1480, by HTGC, after extraction with dichloromethane and trimethylsilylation. Peak labels correspond to compound identification given in Table 10.7. Ex:y, trimethylsilyl ester of acid with x carbon atoms and y double bonds

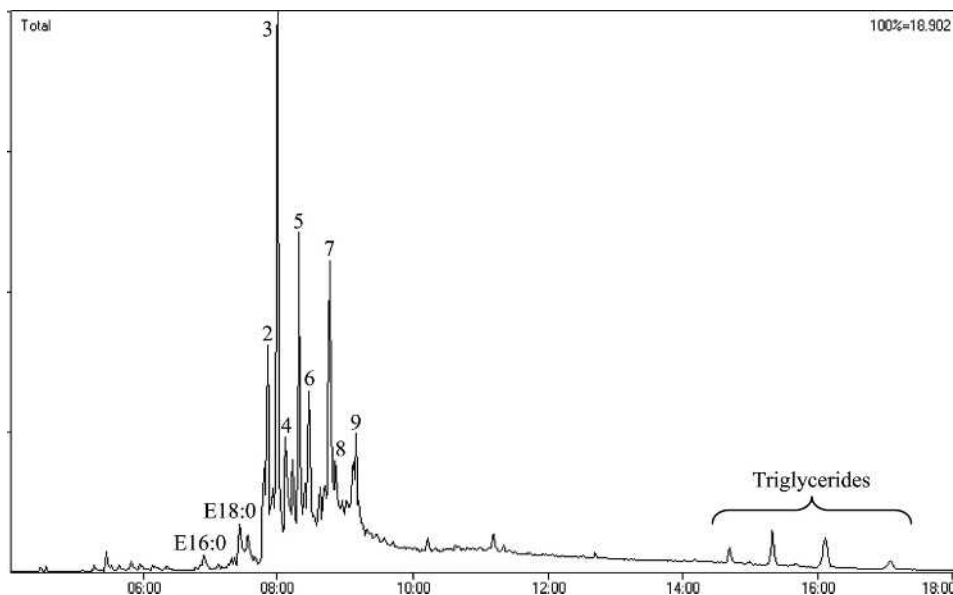


**Figure 10.18** Total ion current chromatogram obtained for sample 1485, by HTGC, after extraction with dichloromethane and trimethylsilylation. Peak labels correspond to compound identification given in Table 10.7. Ex:y, trimethylsilyl ester of acid with x carbon atoms and y double bonds



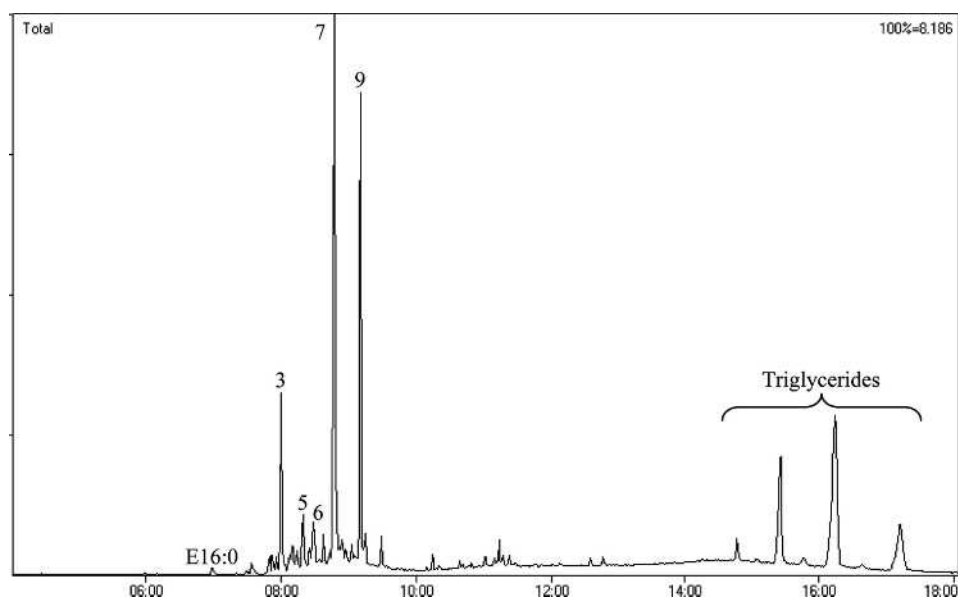


**Figure 10.19** Total ion current chromatogram obtained for sample 1492, by HTGC, after extraction with dichloromethane and trimethylsilylation. Peak labels correspond to compound identification given in Table 10.7. Ex:y, trimethylsilyl ester of acid with x carbon atoms and y double bonds

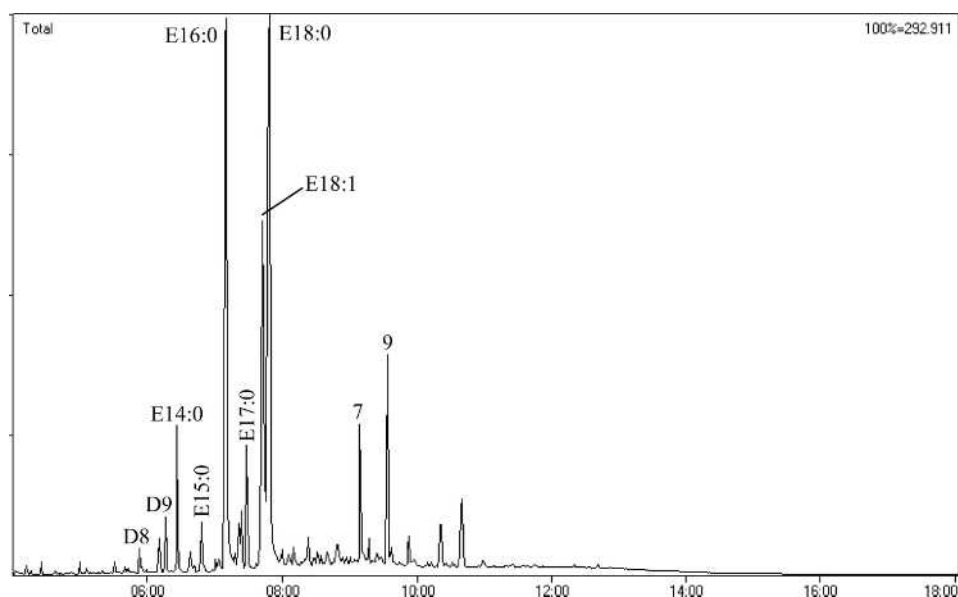


**Figure 10.20** Total ion current chromatogram obtained for sample 1484, by HTGC, after extraction with dichloromethane and trimethylsilylation. Peak labels correspond to compound identification given in Table 10.7. Dx, trimethylsilyl ester of diacid with x carbon atoms. Ex:y, trimethylsilyl ester of acid with x carbon atoms and y double bonds

**Table 10.7** *Compounds appearing in their trimethylsilylated form in Figures 10.9–10.12*

Peak no.	Compound
1	Pimaric acid
2	Isopimaric acid
3	Dehydroabietic acid
4	Abietic acid
5	Unidentified (MW 460); <i>m/z</i> (%): 73(100), 237(64), 191(40), 75(35), 155(16), 445(14), 252(13), 238(13), 147(13), 197(11)
6	15-Hydroxy-dehydroabietic acid
7	7-Oxo-dehydroabietic acid
8	7,15-Dihydroxy-dehydroabietic acid
9	7-Oxo-15-hydroxy-dehydroabietic acid

extraction with methylene chloride were retene and derivatives of dehydroabietic acid. This sample certainly corresponds to a conifer pitch obtained by direct heating of the wood.

The results obtained with sample 1485 in these SPME conditions are given Table 10.1, column 12. They are very similar to those obtained at ambient temperature but less volatile compounds, eluted after  $\alpha$ -cedrol, could be observed. Except for the polychlorinated compound (**84**) of unknown origin, they are degradation products of resin acids resulting from ageing and their presence, even in small amounts, is indicative of a conifer resin.

Sample 1627, from the necropolis of Dachour, is a fragment of a resin bed, on which the body of a princess was lying. The chromatogram obtained is presented in Figure 10.22 and peak identification is given Table 10.1, column 13. The major trapped compounds are monoterpenes. Numerous oxygenated compounds (**16**, **17**, **19**, **26**, **28**) were observed, resulting certainly from the oxidation of  $\alpha$ -pinene or  $\beta$ -pinene [69, 70]. These monoterpenes are common to mastic and pine resin. Therefore it was difficult to choose between these two resins but the absence of degradation products of resin acids spoke in favour of the mastic resin. Observation of the characteristic triterpenic acids after extraction by methylene chloride and methylation with trimethylsilyl diazomethane confirmed the presence of mastic [25]. Characteristic diterpenic acids were not found. As no biomarker of a fatty matter was found it was concluded that mastic resin is the only constituent of the sample.

The same conclusion was drawn for sample 1625, which is a fragment of a resin bed from Monkeys' Valley (mountain of Thebes; see Table 10.1, column 14).

Sample 2013 is an orange-brown fragment of a mummified heart found in a blue-glazed faience jar on exhibition in the Louvre Museum [29]. The SPME GC-MS chromatogram obtained for this sample is shown in Figure 10.23. Except for the cuparene, the sesquiterpenoids are not clearly identified. The characteristic ions of the corresponding spectra are given in Table 10.8. Surprisingly, extraction of this sample by methylene chloride revealed the presence of characteristic triterpenic acids of mastic and other unidentified triterpenes [25]. The authors could not determine the origin of the sesquiterpenoids trapped by SPME.

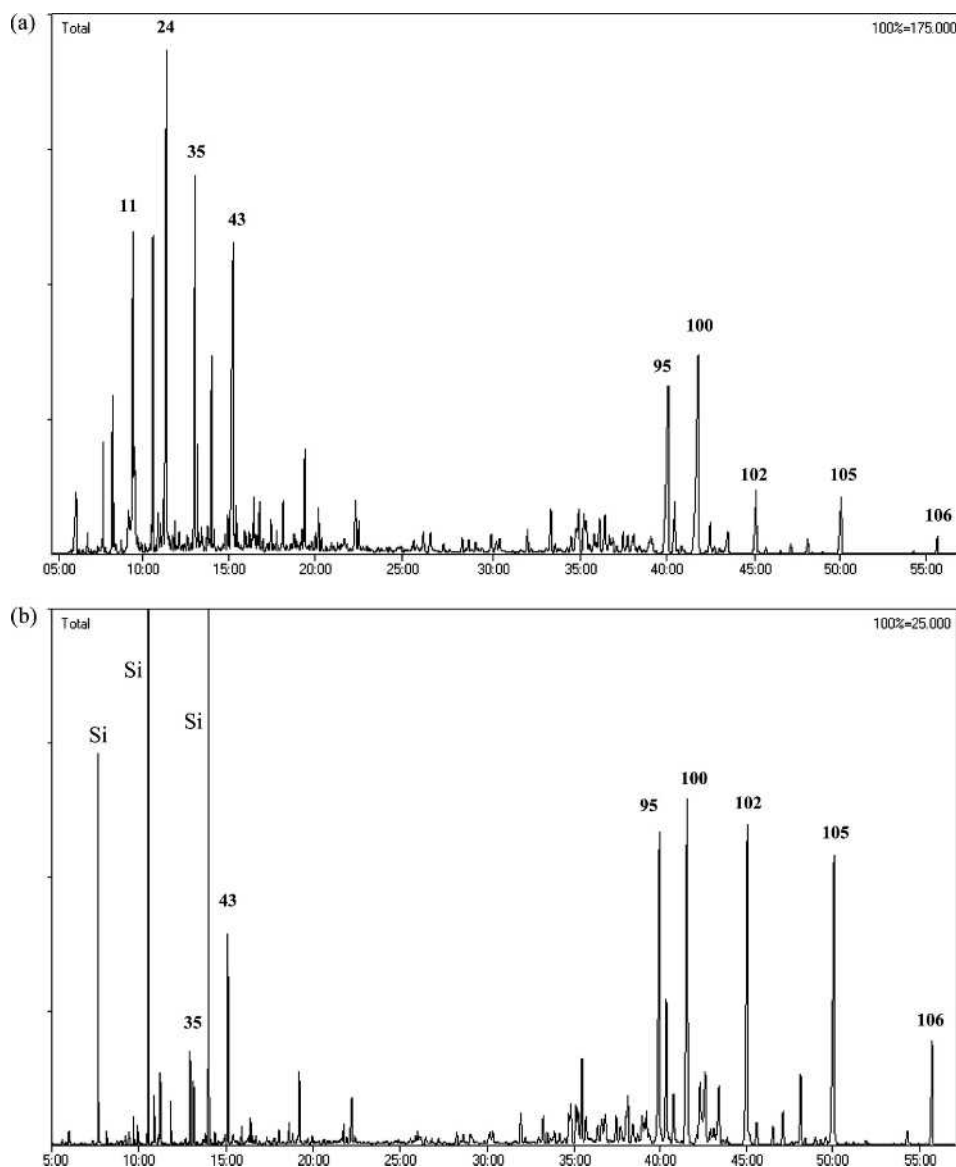


**Figure 10.21** Total ion current chromatograms obtained after headspace SPME for (a) a pine pitch and (b) an archaeological pitch from Fayoum. Peak labels correspond to compound identification given in Table 10.1. Si, siloxanes (artefacts). Reproduced from S. Hamm, J. Bleton, A. Tchaplal, *J. Sep. Sci.*, **27**, 235–243 (2004). Copyright Wiley-VCH Verlag GmbH & Co. KGaA. Reproduced with permission

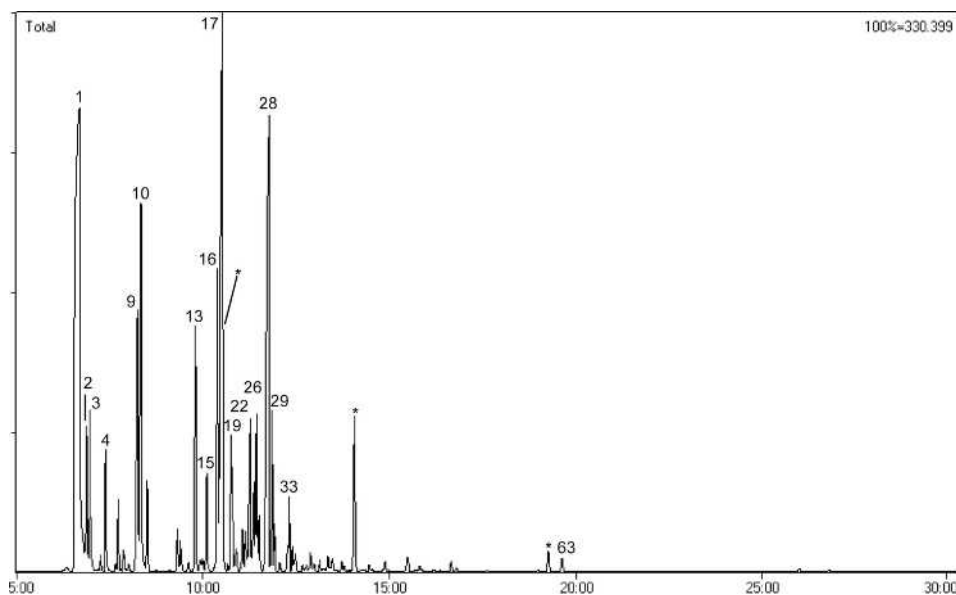


**Figure 10.22** Total ion current chromatogram obtained for sample 1627 after headspace SPME. Peak labels correspond to compound identification given in Table 10.1

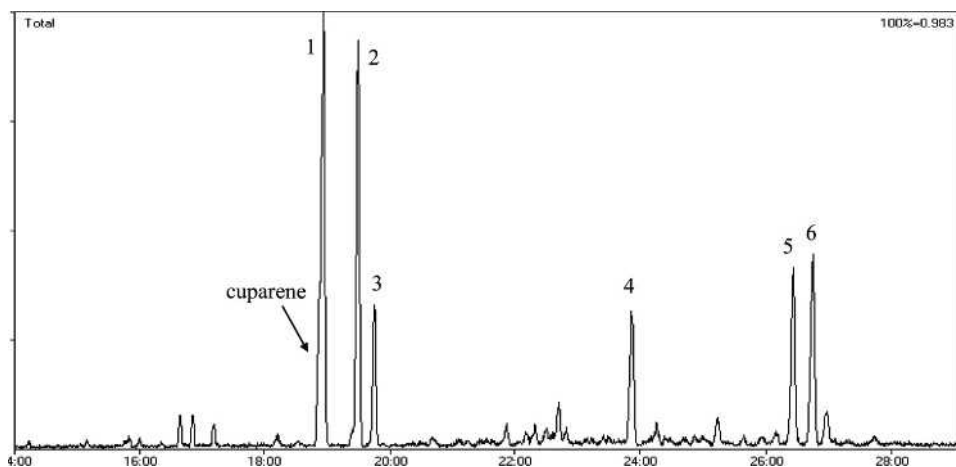


**Figure 10.23** Total ion current chromatogram obtained for the mummified heart (sample 2013) after headspace SPME. Peak labels correspond to compound identification given in Table 10.8. Reproduced from S. Hamm, J. Bleton, A. Tchaplá, *J. Sep. Sci.*, **27**, 235–243 (2004). Copyright Wiley-VCH Verlag GmbH & Co. KGaA. Reproduced with permission

**Table 10.8** Mass spectrometric data obtained for unknown compounds detected in sample 2013

Peak no.	MW	Characteristic fragments of unknown compounds: $m/z$ (%)
1	200	157(100), 185(61), 200(45), 143(39), 142(29), 141(26), 128(22), 115(16), 129(15)
2	200	185(100), 157(90), 171(66), 200(65), 170(47), 143(43), 142(37), 128(36), 158(32)
3	202	187(100), 145(91), 131(56), 202(43), 128(24), 132(19), 129(19), 115(19), 146(18)
4	?	173(100), 55(95), 41(40), 29(38), 99(37), 43(30), 42(27), 45(25), 56(21), 39(21)
5	218	203(100), 43(51), 157(37), 41(21), 119(19), 105(19), 143(18), 145(16), 69(15)
6	210	195(100), 210(40), 180(25), 165(25), 196(15), 178(13), 179(12), 159(9), 115(8)

### 10.4.3 Results Obtained with the PDMS/DVB Fibre at 80°C

The archaeological sample (first to fourth century AD, sample 1286) was stocked in an amphora bearing the inscription ‘incense’ in a warehouse (sector 6) at the Bir Ali site (Yemen). The authors’ objective was to confirm whether it really was frankincense [26].

The GC-MS chromatogram obtained after SPME with the PDMS/DVB fibre, at 80°C, over 1 h, is shown in Figure 10.24a. (The chromatogram obtained for the *B. Carteri* olibanum from Somalia is given in Figure 10.24b for comparison). Twenty-seven monoterpenes and sesquiterpenes were detected in the archaeological sample as well as in modern olibanum samples but the most characteristic compounds are dimer 2 (**111**), cembrene A (**120**) and isoincensole acetate (**128**). These three diterpenes confirm that the sample is olibanum. Their occurrence yields an important piece of information, as they demonstrate that this old incense is an olibanum coming from a *B. carteri* or *B. sacra* tree (Table 10.3). Recently, identification of the triterpenoids in an archaeological sample of the same origin led Mathe *et al.* to the same conclusion [71]. Some compounds were characterised in the archaeological sample whereas they are lacking in modern olibanum, mainly pinocamphone (**a**), borneol (**b**), calamenene (**c**) and cadalene (**d**). The last two compounds are certainly degradation products [72, 73].

## 10.5 Conclusion

These results demonstrate clearly that headspace SPME/GC-MS is well adapted to the detection of volatile or semi-volatile terpenes from resins or gum resins. The method is rapid and simple. A moderate heating (80°C) of the sample allows the extraction of less volatile compounds such as particular diterpenes or diterpenoids which are more specific.

Good results have been obtained with the PDMS fibre (the first marketed and most popular). Other fibres were tested later and the PDMS/DVB fibre seemed to be a bit more

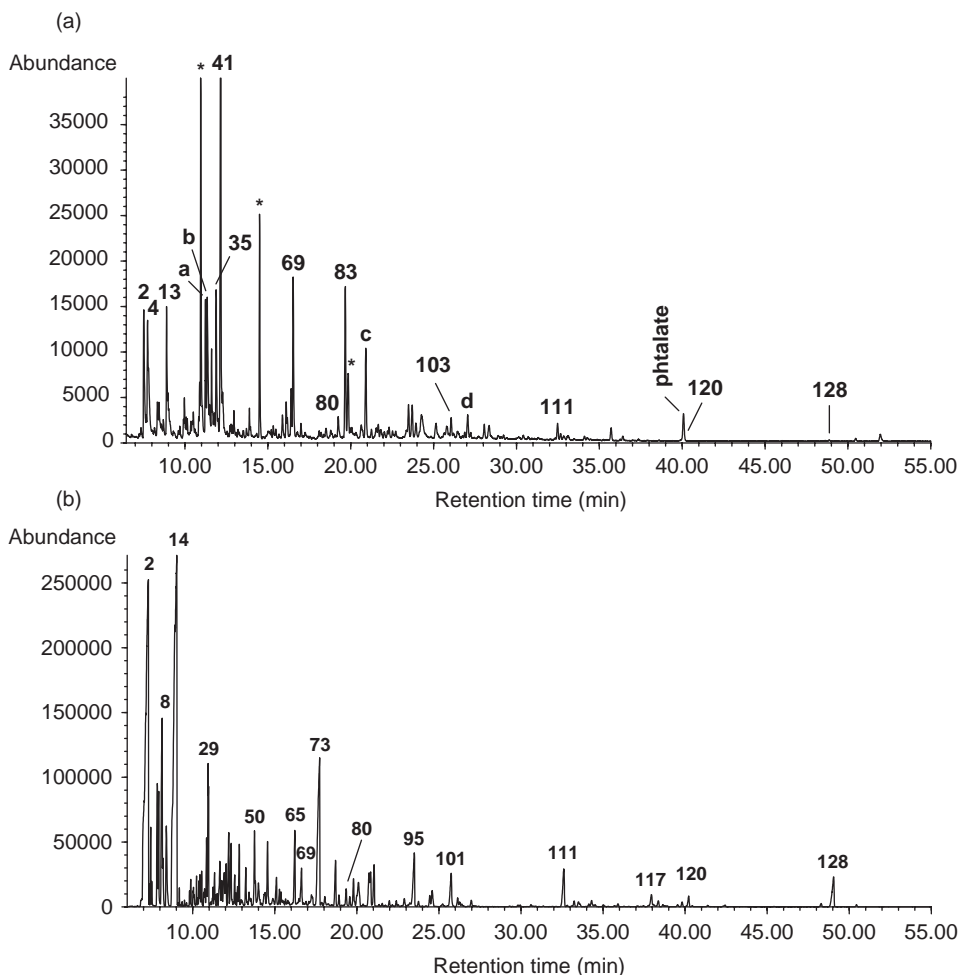


**Figure 10.24** Total ion current chromatograms obtained after headspace SPME for (a) the archaeological incense and (b) *B. carteri* olibanum. Peak labels correspond to compound identification given in Table 10.3. Peaks labelled by letters correspond to the following compounds: **a**, pinocamphone; **b**, borneol; **c**, calamenene; **d**, cadalene. Among other fingerprints, the occurrence of dimer 2 (**111**), cembrene A (**120**) and isoincense acetate (**128**) confirm that this sample is olibanum and attributes its botanical source to *B. carteri* or *B. sacra*. Reproduced from S. Hamm, J. Bleton, J. Connan, A. Tchaplal, *Phytochemistry*, **66**, 1499–1514. Copyright 2005 Elsevier Limited

efficient. The optimised extraction conditions allowed the terpenic composition characteristic of five main species of *Boswellia* (*carteri*, *sacra*, *frereana*, *papyrifera* and *serrata*) and other resins or gum resins to be established. Identification of the studied reference substances is possible either by means of specific markers or by examination of the whole chromatogram.

SPME/GC/MS is an efficient technique to reveal the presence of resinic substances in archaeological samples. Indeed, volatile terpenes are still present in very old archaeological samples (4000 years old), particularly in the case of compact matrixes, and can be trapped by the SPME fibre. In comparison with methylene chloride extraction, SPME is very specific and allows the direct analysis of the volatile terpenes content in complex mixtures including oils, fats or waxes. For this reason, headspace SPME is the first method to use when analysing an archaeological sample: it will either allow the identification of the resin or indicate further sample treatment in order to detect characteristic triterpenes. The method is not really 'nondestructive' because it uses a little of the sample but the same sample can be used for several SPME extractions and then for other chemical treatments.

For the studied archaeological samples, different cases have been observed. For some of them, the extracted terpenes are well preserved and the difference with the corresponding modern substances is essentially due to the partial removal of the most volatile terpenes. For others, known oxidation products are also present in different proportions, probably resulting from natural ageing. For the latter, the major detected compounds are unknown terpenoids. In this case, the archaeological samples are embalming materials and the terpenic substances have certainly been subjected to a heating step. A thorough comparison with geochemical data could provide a better interpretation of the results.

## References

1. R. P. Belardi, J. Pawliszyn, The application of chemically modified fused silica fibers in the extraction of organics from water matrix samples and their rapid transfer to capillary columns, *Water Pollut. Res. J. Can.*, **24**, 179–191 (1989).
2. C. L. Arthur, J. Pawliszyn, Solid phase microextraction with thermal desorption using fused silica optical fibers, *Anal. Chem.*, **62**, 2145–2148 (1990).
3. J. Pawliszyn, *Solid Phase Microextraction. Theory and Practice*, Wiley-VCH, New York, 1997.
4. SPME Applications Guide, Bulletin 925E, Supelco, Bellefonte, PA, 2007.
5. W. Wardencki, J. Curylo, J. Namiesnik, Trends in solventless preparation techniques for environmental analysis, *J. Biochem. Biophys. Methods*, **70**, 275–288 (2007).
6. H. Kataoka, H. L. Lord, J. Pawliszyn, Applications of solid-phase microextraction in food analysis, *J. Chromatogr. A*, **880**, 35–62 (2000).
7. K. Ridgway, S. P. D. Lalljie, R. M. Smith, Sample preparation techniques for the determination of trace residues and contaminants in foods, *J. Chromatogr. A*, **1153**, 36–53 (2007).
8. E. E. Stashenko, J. R. Martinez, Sampling volatile compounds from natural products with headspace/solid-phase micro-extraction, *J. Biochem. Biophys. Methods*, **70**, 235–242 (2007).
9. Y. F. Sha, S. Chen, G. L. Duan, Rapid determination of tramadol in human plasma by headspace solid-phase microextraction and capillary gas chromatography–mass spectrometry, *J. Pharm. Biomed. Anal.*, **37**, 143–147 (2005).
10. G. A. Mills, V. Walker, Headspace solid-phase microextraction procedures for gas chromatographic analysis of biological fluids and materials, *J. Chromatogr. A*, **902**, 267–287 (2000).
11. S. Ulrich, Solid-phase microextraction in biomedical analysis, *J. Chromatogr. A*, **902**, 167–194 (2000).
12. N. H. Snow, Solid-phase microextraction of drugs from biological matrices, *J. Chromatogr. A*, **885**, 445–455 (2000).
13. H. Lord, J. Pawliszyn, Microextraction of drugs, *J. Chromatogr. A*, **902**, 17–63 (2000).
14. F. De Angelis, A. Di Tullio, G. Mellerio, R. Quaresima, R. Volpe, Investigation by solid-phase micro-extraction and gas chromatography/mass spectrometry of organic films on stone monuments, *Rapid Commun. Mass Spectrom.*, **13**, 895–900 (1999).

15. F. De Angelis, R. Ceci, R. Quaresima, S. Reale, A. Di Tullio, Investigation by solid-phase microextraction and gas chromatography/mass spectrometry of secondary metabolites in lichens deposited on stone monuments, *Rapid Commun. Mass Spectrom.*, **17**, 526–531 (2003).
16. M. van Bommel, B. van Elst, F. Broekens, Emission of organic acids from wooden construction materials in a small test chamber; preliminary results of optimisation of the solid phase microextraction technique, 4th Meeting of the Indoor Air Pollution Working Group, Copenhagen, 2001.
17. M. Ryhl-Svendsen, J. Glastrup, Acetic acid and formic acid concentrations in the museum environment measured by SPME-GC/MS, *Atmos. Environ.*, **36**, 3909–3916 (2002).
18. A. F. L. Godoi, L. van Vaecck, R. vanGrieken, Use of solid-phase microextraction for the detection of acetic acid by ion-trap gas chromatography-mass spectrometry and application to indoor levels in museums, *J. Chromatogr. A*, **1067**, 331–336 (2005).
19. A. Lattuati-Derieux, S. Bonnassies-Termes, B. Lavédrine, Identification of volatile organic compounds emitted by a naturally aged book using solid-phase microextraction/gas chromatography/mass spectrometry, *J. Chromatogr. A*, **1026**, 9–18 (2004).
20. A. Lattuati-Derieux, S. Bonnassies-Termes, B. Lavédrine, Characterisation of compounds emitted during natural and artificial ageing of a book. Use of headspace-solid-phase microextraction/gas chromatography/mass spectrometry, *J. Cult. Her.*, **7**, 123–133 (2006).
21. B. Thiébaud, A. Lattuati-Derieux, M. Moira, L. B. Vilmon, Application of headspace SPME-GC-MS in characterisation of odorous volatile organic compounds emitted from magnetic tape coatings based on poly(urethane-ester) after natural and artificial ageing, *Polym. Testing*, **26**, 243–256 (2007).
22. A. Lattuati-Derieux, S. Thao, J. Langlois, M. Regert, First results on headspace-solid phase microextraction-gas chromatography/mass spectrometry of volatile organic compounds emitted by wax objects in museums, *J. Chromatogr. A*, **1187**, 239–249 (2008).
23. M. Regert, V. Alexandre, N. Thomas, A. Lattuati-Derieux, Molecular characterisation of birch bark tar by headspace solid-phase microextraction gas chromatography-mass spectrometry: A new way for identifying archaeological glues, *J. Chromatogr. A*, **1101**, 245–253 (2006).
24. S. Hamm, E. Lesellier, J. Bleton, A. Tchaplá, Optimization of headspace solid phase microextraction for gas chromatography/mass spectrometry analysis of widely different volatility and polarity terpenoids in olibanum, *J. Chromatogr. A*, **1018**, 73–83 (2003).
25. S. Hamm, J. Bleton, A. Tchaplá, Headspace solid phase microextraction for screening for the presence of resins in Egyptian archaeological samples, *J. Sep. Sci.*, **27**, 235–243 (2004).
26. S. Hamm, J. Bleton, J. Connan, A. Tchaplá, A chemical investigation by headspace SPME and GC-MS of volatile and semivolatile terpenes in various olibanum samples, *Phytochemistry*, **66**, 1499–1514 (2005).
27. A. Lucas, J. R. Harris, *Ancient Egyptian Materials and Industries*, Histories and Mysteries of Man Ltd, London, 1962.
28. A. Tchaplá, J. Bleton, S. Goursaud, P. Méjanelle, Contribution à la connaissance des substances organiques utilisées en Egypte ancienne, in *Encyclopédie religieuse de l'Univers végétal. Croyances phytoreligieuses de l'Egypte ancienne*, S. H. Aufrère (Ed.), Vol. 1, Orientalia Monspeliensa X, Montpellier, 1999, pp.445–487.
29. A. Charrié-Duhaut, J. Connan, N. Rouquette, D. Adam, C. Barbotin, M. F. de Rozières, A. Tchaplá, P. Albrecht, The canopic jars of Rameses II: real use revealed by molecular study of organic residues, *J. Archaeol. Sci.*, **34**, 957–967 (2007).
30. S. A. Buckley, R. P. Evershed, Organic chemistry of embalming agents in Pharaonic and Graeco-Roman mummies, *Nature*, **413**, 837–841 (2001).
31. M. P. Colombini, F. Modugno, F. Silvano, M. Onor, Characterization of the balm of an Egyptian mummy from the seventh century B.C., *Stud. Conserv.*, **45**, 19–29 (2000).
32. P. Méjanelle, Contribution à l'étude de substances organiques mises en oeuvre pour la réalisation d'objets d'art et d'archéologie: caractérisation par couplage chromatographie en phase gazeuse-spectrométrie de masse, PhD Thesis, Paris 6 University, 1996.
33. P. Méjanelle, J. Bleton, S. Goursaud, A. Tchaplá, Identification of phenolic acids and inositols in balms and tissues from an Egyptian mummy, *J. Chromatogr. A*, **767**, 177–186 (1997).
34. A. Tchaplá, J. Bleton, S. Goursaud, P. Méjanelle, M.-A. Stenger, R. Mourer, Contribution à l'étude des onguents et fards rituels, in *Encyclopédie religieuse de l'Univers végétal. Croyances*



- phytoreligieuses de l'Egypte ancienne*, S. H. Aufrère (Ed.), Vol. 1, Orientalia Monspeliensa X, Montpellier, 1999, pp. 517–532.
35. A. Tchaplal, P. Méjanelle, J. Bleton, S. Goursaud, Characterisation of embalming materials of a mummy of the Ptolemaic era. Comparison with balms from mummies of different eras, *J. Sep. Sci.*, **27**, 217–234 (2004).
  36. Z. Zhang, J. Pawliszyn, Analysis of organic compounds in environmental samples using headspace solid phase microextraction, *J. High Resol. Chromatogr.*, **16**, 689–692 (1993).
  37. Z. Zhang, M. J. Yang, J. Pawliszyn, Solid phase microextraction: a solvent-free alternative for sample preparation, *Anal. Chem.*, **66**, 844A–853A (1994).
  38. J. A. Field, G. Nickerson, D. D. James, C. Heider, Determination of essential oils in hops by headspace SPME, *J. Agric. Food Chem.*, **44**, 1768–1772 (1996).
  39. A. F. Thomas, M. Ozainne, New sesquiterpene alcohols from galbanum resin; the occurrence of C (10)-epi-sesquiterpenoids, *Helv. Chim. Acta*, **61**(8), 2874–2880 (1978).
  40. P. Weyerstahl, H. Marschall, M. Weirauch, K. Thefeld, H. Surburg, Constituents of commercial Labdanum oil, *Flavour Fragr. J.*, **13**, 295–318 (1998).
  41. C. Arrabal, M. Cortijo, B. Fernandez de Simon, M. C. GarciaVallejo, E. Cadahia, Differentiation among five Spanish *Pinus pinaster* provenances based on its oleoresin terpenic composition, *Biochem. Syst. Ecol.*, **33**, 1007–1016 (2005).
  42. Z. Song, Z. Liang, X. Liu, Chemical characteristics of oleoresins from Chinese pine species, *Biochem. Syst. Ecol.*, **23**, 517–522 (1995).
  43. D. Scalarone, M. Lazzari, O. Chiantore, Ageing behaviour and pyrolytic characterisation of diterpenic resins used as art materials: colophony and Venice turpentine, *J. Anal. Appl. Pyrol.*, **64**, 345–361 (2002).
  44. B. R. T. Simoneit, Diterpenoid compounds and other lipids in deep-sea sediments and their geochemical significance, *Geochim. Cosmochim. Acta*, **41**, 463–476 (1977).
  45. P.-A. Hyniing, M. Remberger, A. H. Neilson, P. Stanley, Identification and quantification of 18-nor- and 19-norditerpenes and their chlorinated analogues in samples of sediment and fish, *J. Chromatogr. A*, **643**, 439–452 (1993).
  46. A. O. Tucker, Frankincense and myrrh, *Economic Botany*, **40**, 425–433 (1986).
  47. G. Khan, M. I. H. Farooqi, Chemical characterisation of resins sold in Indian markets. Part I. Luban and Kundur, *Int. J. Pharmacognosy*, **29**, 302–305 (1991).
  48. S. Basar, A. Koch, W. A. König, A verticillane-type diterpene from *Boswellia carterii* essential oil, *Flavour Fragr. J.*, **16**, 315–318 (2001).
  49. T. Watanabe, A. Namera, M. Yashiki, Y. Iwasaki, T. Kojima, Simple analysis of local anaesthetic in human blood using headspace SPME and GC-MS-electron impact ionization selected ion monitoring, *J. Chromatogr. B*, **709**, 225–232 (1998).
  50. D. Y.-H. Yeung, T. Lee, G. Grant, M. Ma, E. Kwong, A SPME–GC procedure for monitoring peppermint flavor in tablets, *J. Pharm. Biomed. Anal.*, **30**, 1469–1477 (2003).
  51. B. Schäfer, P. Hennig, W. Engewald, Analysis of monoterpenes from conifer needles using SPME, *J. High Resolut. Chromatogr.*, **18**, 587–592 (1995).
  52. D. Zabaraz, S. G. Wyllie, Quantitative analysis of terpenoids in the gas phase using headspace solid-phase microextraction (HS-SPME), *Flavour Fragr. J.*, **16**, 411–416 (2001).
  53. A. J. Matich, D. D. Rowan, N. H. Banks, Solid phase microextraction for quantitative headspace sampling of apple volatiles, *Anal. Chem.*, **68**, 4114–4118 (1996).
  54. D. A. Vereen, J. P. McCall, D. J. Butcher, Solid phase microextraction for the determination of volatile organics in the foliage of Fraser fir (*Abies fraseri*), *Microchem. J.*, **65**, 269–276 (2000).
  55. A. Keszler, K. Heberger, Influence of extraction parameters and medium on efficiency of SPME sampling in analysis of aliphatic aldehydes, *J. Chromatogr. A*, **845**, 337–347 (1999).
  56. K. G. Furton, J. Bruna, J. R. Almirall, A simple, inexpensive, rapid, sensitive and solventless technique for the analysis of accelerants in fire debris based on SPME, *J. High Resolut. Chromatogr.*, **18**, 625–629 (1995).
  57. W. M. Coleman III, A study of the behaviour of polar and nonpolar SPME fibers, *J. Chromatogr. Sci.*, **35**, 245–258 (1997).
  58. Z. Zhang, J. Pawliszyn, Headspace solid phase microextraction, *Anal. Chem.*, **65**, 1843–1852 (1993).

59. J. Ai, Headspace solid phase microextraction. Dynamics and quantitative analysis before reaching a partition equilibrium, *Anal. Chem.*, **69**, 3260 (1997).
60. D. Zuba, A. Parczewski, M. Reichenbacher, Optimization of solid-phase microextraction conditions for gas chromatographic determination of ethanol and other volatile compounds in blood, *J. Chromatogr. B*, **773**, 75–82 (2002).
61. M. E. Miller, J. D. Stuart, Comparison of gas-sampled and SPME-sampled static headspace for the determination of volatile flavor components, *Anal. Chem.*, **71**, 23–27 (1999).
62. D. Zabarás, S. G. Wyllie, Rearrangement of *p*-menthane terpenes by carboxen during HS-SPME, *J. Sep. Sci.*, **25**, 685–690 (2002).
63. J. Koller, U. Baumer, Y. Kaup, M. Schmid, U. Weser, Ancient materials: analysis of a pharaonic embalming tar, *Nature*, **425**, 784 (2003).
64. J. de Morgan, Fouilles à Dachour 1894–1895, Vienna, 1903.
65. S. H. Aufrère, A propos des résultats obtenus sur les échantillons conservés au Museum d'histoire naturelle de Lyon, in *Encyclopédie religieuse de l'Univers végétal. Croyances phytoreligieuses de l'Egypte ancienne*, S. H. Aufrère (Ed.), Vol. 1, Orientalia Monspeliensa X, Montpellier, 1999, pp. 533–547.
66. W. M. Coleman III, B. M. Lawrence, A comparison of selected analytical approaches to the analysis of an essential oil, *Flavour Fragr. J.*, **12**, 1–8 (1997).
67. E. N. Frankel, *Lipid Oxidation*, 2nd ed., Oily Press Lipid Library, **18**, The Oily Press, Bridgwater, 2005.
68. K. J. van den Berg, J. J. Boon, I. Pastorova, L. F. M. Spetter, Mass spectrometric methodology for the analysis of highly oxidized diterpenoid acids in Old Master paintings, *J. Mass Spectrom.*, **35**, 512–533 (2000).
69. M. Lindmark-Henriksson, D. Isaksson, T. Vanek, I. Valterova, H.-E. Högberg, K. Sjödin, Transformation of terpenes using a *Picea abies* suspension culture, *J. Biotechnol.*, **107**, 173–184 (2004).
70. P. A. Robles-Dutenhefner, M. J. da Silva, L. S. Sales, E. M. B. Sousa, E. V. Gusevskaya, Solvent-free liquid-phase autooxidation of monoterpenes catalysed by sol-gel Co/SiO<sub>2</sub>, *J. Mol. Catal. A*, **217**, 139–144 (2004).
71. C. Mathe, J. Connan, P. Archier, M. Mouton, C. Vieillescazes, Analysis of frankincense in archaeological samples by gas chromatography-mass spectrometry, *Annal. Chim.*, **97**, 433–445 (2007).
72. B. R. T. Simoneit, J. O. Grimalt, T. G. Wang, R. E. Cox, P. G. Hatcher, A. Nissenbaum, Cyclic terpenoids of contemporary plant detritus and of fossil woods, ambers and coals, *A. Org. Geochem.*, **10**, 877–889 (1986).
73. B. R. T. Simoneit, Cyclic terpenoids of the geosphere, in *Biological Markers in the Sedimentary Record*, R. B. Johns (Ed.), Elsevier, Amsterdam, 1986, pp.43–99.

# 11

## Py-GC/MS of Organic Paint Binders

*Ilaria Bonaduce and Alessia Andreotti*

### 11.1 Introduction

With the exception of the fresco technique, where pigments are applied on a fresh plaster, and subsequently entrapped in the forming calcium carbonate, all other painting techniques involve using an organic binder to disperse pigments and ensure their cohesion into the paint layers and adhesion to the support. A good organic binder must meet some physico-chemical requirements

- be fluid when mixed with pigments, forming an impasto stable, which is homogeneous and easy to apply;
- be compatible with pigments, dispersing but not making them soluble;
- be transparent and colourless;
- have filming properties: when applied, the binder must dry, giving rise to a resistant solid layer, elastic, but not sticky;
- be stable to ageing.

Over the centuries the natural organic materials that have best met these requirements are proteinaceous materials (egg, animal glue and casein or milk), polysaccharide gums

(arabic, tragacanth and fruit tree gums), drying oils (linseed, walnut and poppy seed oils) and beeswax. Depending on the binder used, the painting techniques have different names:

- proteinaceous tempera, where the binder is a proteinaceous material, most of all egg;
- polysaccharide tempera, where the binder is a polysaccharide material (in watercolours pigments are dispersed in a plant gum, and in gouache technique in addition to the plant gum inorganic thickeners are added to the pigment);
- oil painting, where the binder is a vegetable drying oil;
- tempera grassa, where the binder is a mixture of a vegetable oil and a proteinaceous material;
- encaustic technique, where the pigment is dispersed in hot beeswax or Punic wax (beeswax partially hydrolysed by means of a base, to favour its solubilisation).

Each painter had his own technique: the binding medium was thus prepared using different additives, giving rise to a variety of recipes for each technique. For example, it is believed that fig latex (a white liquid exuded by the fig tree) was commonly added to the egg tempera, and that animal or plant resins were added to oil- and wax-based binders. On account of their adhesive properties, these materials were used not only as paint binders, but also as consolidants in restorations, as ingredients in varnishes used to finish paintings, and as ingredients of mordants to apply metallic leaf decorations.

Most of these organic materials are characterised by a macromolecular nature: in some cases they are natural polymers (such as proteins or plant gums), others undergo oligomerisation or cross-linking reactions as an effect of exposure to light and air (such as natural resins or drying oils). Due to their macromolecular nature, analytical pyrolysis is a fast and efficient approach for identifying such organic materials in samples from works of art. Directly coupling of the pyrolyser to the injection port of a GC/MS is the most straightforward configuration for the pyrolysis system. In fact, coupling the diagnostic power of mass spectrometry with the separation capability of the gas chromatographic system enhances the potential of pyrolytic methods. Although the chemical structures of the molecules originally present in the sample are not always straightforwardly related to the final pyrolysis products, pyrolysis is a valid fingerprinting technique [1]. Some materials, such as sandarac and amber, mainly consist of a polymeric fraction, which cannot be detected by GC/MS [2]. In these cases, pyrolysis is thus strongly recommended, as discussed in Chapter 12.

In addition to natural materials, synthetic polymers might also be present in works of art. Since the end of the nineteenth century, synthetic polymers have been produced and used in the field of cultural heritage, to restore works of art [3], but also as paint binders, such as alkyd resins and acrylic water dispersions. Most synthetic polymers can be detected by GC/MS only through thermal degradation followed by GC/MS [4,5] (Chapter 12 deals with the characterisation of synthetic resins in detail).

One of the main problems of the pyrolysis technique is related to the low volatility of pyrolysis products arising from natural and some synthetic macromolecules. In fact, the polar acidic, alcoholic and aminic moieties are not really suitable for gas chromatographic analysis. Their poor volatility and their polarity cause a rather low reproducibility of the pyrograms, low sensitivity for specific compounds, and strong memory effects. Memory effects need to be borne in mind when the pyrolysis of polar molecules is performed. Polar pyrolysis products may not be completely eluted by the gas chromatographic column, and

may be retained in cold areas of the pyrolyser and the transfer line system. When assembling the instrumentation, dead spaces and cold spots must be avoided. This is also fundamental for avoiding the discrimination of high molecular weight pyrolysis products, which are often extremely diagnostic [6].

When natural macromolecules are pyrolysed, a very high fragmentation of the original molecules occurs. This gives rise to pyrograms which are quite difficult to interpret due to the high amount of unspecific compounds formed.

To overcome problems related to the formation of polar pyrolysis products and unspecific compounds, the most common approach is to use thermally assisted reactions, where the sample is pyrolysed in the presence of a suitable reagent, which transforms polar functionalities into less polar moieties. Thermally assisted hydrolysis and methylation (THM) and thermally assisted silylation are the most commonly used [7,8].

Tetramethylammonium hydroxide (TMAH) is one of the most commonly used reagents for online methylation of acidic and alcoholic moieties. Pyrolysis in the presence of TMAH gives rise to the hydrolysis of ester bonds, followed by the formation of tetramethylammonium salts, which are subsequently subjected to thermal dissociation, leading to the formation of the corresponding methyl derivatives [9,10]. The experimental conditions, such as temperature, reagent concentration, and solvent, may strongly influence the mechanisms of the reactions involved. Although the TMAH thermochemolysis (TMH) method has been extensively applied to the characterisation of materials used in the realisation and restoration of works of art, the strong alkalinity of TMAH may cause problems in the interpretation of pyrograms. The main limitations of this technique are related to decarboxylation reactions undergone by carboxylic acids, the isomerisation of polyunsaturated fatty acids, the formation of dehydration products, and the  $\alpha$ -methylation of acidic moieties [11,12]. TMAH can also induce decomposition of the stationary phase of the gas chromatographic column.

To overcome these problems other derivatising agents have been used, such as trimethylsulfonium hydroxide [13], tetramethylammonium acetate [14], or silylating agents such as *N,O*-bis(trimethylsilyl)trifluoroacetamide (BSTFA) [15] and hexamethyldisilazane (HMDS). HMDS has been used to characterise organic materials in samples from works of art, showing its potential with respect to the strongly alkaline TMAH reagent.

A deactivated silica pre-column is also a fundamental tool when pyrolysis is performed, since it partially helps in avoiding the contamination of the analytical column with underivatised polar compounds. Blanks (that is the pyrolysis of the derivatising agent without sample) must be run between analyses to ensure the absence in the chromatograms of any signals that do not belong to the sample.

Pyrolysis data interpretation is based on the analysis of both chromatographic profiles and the recognition of molecular markers. However, interpreting pyrograms is critical and requires experience. The simultaneous occurrence of different organic materials, the relative abundance of one material with respect to the others, the presence of inorganic matter, sample morphology, and many other factors can contribute in different ways to the resulting pyrograms. For each material there are a variety of molecular markers and pyrolytic profiles suggested. This is due to several factors:

- pyrolysis temperature;
- types of pyrolyser. The most commonly used are: microfurnace (the microfurnace rapidly raises the temperature of the sample until the pyrolysis temperature is reached and then maintains this temperature for the desired pyrolysis time), Curie-point (the

sample is rapidly heated using a high frequency induction coil) and resistively heated filament (the sample is heated through an initial pulse at a high voltage producing a current through the metallic filament);

- instrumental set-up; this involves the sample introduction technique (the sample can be introduced in a quartz tube of various dimensions, or can be directly placed onto the metallic wire, etc.), the pyrolyser geometry and the GC/MS interface (including temperature and dimensions of connections between the pyrolyser and the GC injection port);
- sample composition; the simultaneous occurrence of more than one material in the sample, both organic and inorganic, can become involved in the formation of the final pyrolysis products, affecting marker formation, chromatographic profiles and, in some cases the derivatisation yield.

However, pyrolysis is rapid, avoids sample wet chemical workup, avoiding sample loss and contamination, and has a low sample requirement. It allows the determination, in a single step, of polymeric materials (with *in situ* hydrolysis of the hydrolysable polymers and thermal decomposition of the nonhydrolysable polymers) and low molecular weight components [16]. As a result, pyrolysis is a relatively fast and inexpensive technique, especially if compared with the classical wet analytical procedures that are required prior to GC/MS analyses.

Furthermore, the major disadvantages encountered in GC/MS, i.e. undetectability of synthetic polymers and unpredictable interferences due to their presence, may be avoided using the Py-GC/MS technique. All these aspects strongly suggest how useful, and in some cases fundamental, analytical pyrolysis is in the analysis of complex samples, such as those collected from works of art, to implement and support results obtained with wet chemical pretreatment followed by GC/MS analysis.

The following sections discuss in detail the Py-GC/MS of proteinaceous materials, oils and fats, and then briefly plant and animal resins, polysaccharide materials, and beeswax. Particular attention is given to the application of this analytical technique to characterise samples from works of art. At the end of the chapter four case studies are presented.

## 11.2 Proteinaceous Materials

The pyrolysis of proteinaceous materials gives rise to the formation of complex fragmentations. Very simple and unspecific molecules such as water, ammonia, short chain aldehydes, ketones, amides, and nitriles are obtained, as well as cyclic oligomers and nitrogenous heterocycles, arising from rearrangements, cyclisation and other secondary reactions. The amino acids recovery is very low [17–19]. Thermally assisted reactions coupled to GC/MS have been used for the analysis of amino acids and polypeptides in the presence of both TMAH [20,21] and HMDS [22]. These studies have demonstrated that, although the behaviour of amino acids in the presence of a derivatising agent is quite simple, polypeptides and proteins still undergo rearrangement reactions. The identification of proteinaceous media in old samples from works of art by means of pyrolysis without a derivatising agent [1,23,24], with TMAH [25,26] or HMDS [27–30], arises from the recognition of specific molecular markers in the pyrograms. The molecular markers reported in the literature for the identification of proteinaceous binding media are listed in Table 11.1.

**Table 11.1** Molecular markers suggested in the literature for the identification of proteinaceous binding media

Proteinaceous material	Derivatising agent	Marker	Ref.
Animal glue	None	Pyrrole	1, 23, 73
Animal glue	TMAH	Pyrrole >50%	1
Animal glue	HMDS	Pyrrole, alkyl pyrroles, benzeneacetonitrile and benzenepropanenitrile	28
Animal glue	HMDS	Pyrrole ( <i>main peak</i> ), alkyl pyrroles, benzeneacetonitrile, benzenepropanenitrile, indole ( <i>in lower amounts than benzeneacetonitrile</i> )	29, 30
Animal glue	HMDS	Pyrrole-2- carboxamide, diketodipyrrole, pyrrole[1,2- <i>a</i> ]piperazine-3,6-dione	28
Animal (deer) glue	TMAH	Pyrrole, diketopyrrole	31
Egg yolk	None	Palmitic and oleic acid	73
Egg glair	None	Indole, methyl indole	23, 23
Egg yolk	TMAH	Palmitic and oleic acid methyl esters	73
Egg yolk	TMAH	Palmitic and stearic acids methyl esters (>60%); azelaic acid methyl esters (<10%) and pyrrole (<50%)	1
Whole egg and egg yolk	HMDS	Hexadecanenitrile, octadecanenitrile, cholesterol derivatives (TMS derivative)	28, 29, 30
Whole egg	HMDS	2,5-Diketopiperazines, fatty acids, trimethylsilyl esters	27
Calcium caseinate	None	Pyrroline, 2,5-diketopiperazine	23, 73
Calcium caseinate	TMAH	Pyrrole <50%, palmitic and oleic acid methyl esters <60%	1
Casein	HMDS	Indole	28
Casein	HMDS	Pyrrole, alkyl pyrroles, benzeneacetonitrile, benzenepropanenitrile, indole ( <i>main peak</i> )	29, 30
Milk	HMDS	2,5-Diketopiperazines, silylated and underivatised fragments deriving from carbohydrates	27

The diversity of markers that are reported in the literature for the three proteinaceous binders, even when the same derivatising agent is used, highlights how several aspects come together to determine the final pyrolysis products. Animal glue for example, when pyrolysed at 600°C in the presence of HMDS, gives rise to different markers depending on the pyrolyser and instrumental set-up used:

- Pyrrole, alkyl pyrroles, benzeneacetonitrile and benzenepropanenitrile. Pyrolyser: continuous mode micro furnace pyrolysing injection system Pyrojector (SGE, Austin, Texas, USA); furnace pressure: 14 psi; purge flow: 0.5 ml min<sup>-1</sup> [28].
- Pyrrole (*main peak*), alkyl pyrroles, benzeneacetonitrile, benzenepropanenitrile, indole (*in lower amounts than benzeneacetonitrile*). Pyrolyser: CDS Pyroprobe 5000 series (CDS Analytical Inc, Oxford, USA); pyrolyser interface: 180°C; transfer line: 300°C; valve oven: 290°C [29, 30].



- Pyrrole-2-carboxamide, diketodipyrrole, pyrrole [1,2-*a*]piperazine-3,6-dione. Pyrolyser: CDS pyroprobe 1000 (Chemical Data Systems, Oxford, USA) [27].

For these reasons, when the pyrolysis of samples from works of art is undertaken for the first time, as well as when a new device or a new instrumental set-up is introduced in a laboratory, it is very important to build one's own libraries of chromatographic profiles, based on the analysis of reference materials.

### 11.3 Oils and Fats

The pyrolysis of glycerolipid materials requires the use of a suitable derivatising agent, in order to increase the detectability of fatty acids and dicarboxylic acids, which may be present in a mature paint film as free acids, metal soaps, as well as esterified with glycerol. The oils and fats commonly used in samples from works of art have been analysed by means of pyrolysis using TMAH [12,23,25,26,32–38], and HMDS [37,39].

As described in Chapter 1, drying oils can be distinguished from non-drying oils and animal fats on the basis of the high content of polyunsaturated fatty acids. Unsaturated and mainly polyunsaturated compounds are subject to oxidation reactions. These are responsible for the formation of a cross-linked fraction and oxidation products, which are partially lost by evaporation. In particular, the uptake of oxygen by double bonds leads to the formation of new oxygen containing functional groups and to the oxidative cleavage of fatty acid hydrocarbon chains. As a result, diacids, such as pimelic (heptanedioic), suberic (octanedioic), azelaic (nonanedioic) and sebacic (decanedioic) acids are formed, with azelaic acid being the most abundant [32,40]. For these reasons aged drying oils can be distinguished from non-drying fats on the basis of the high content of dicarboxylic acid with respect to saturated long chain acids. A mature drying oil normally shows an azelaic content that is higher or at least equal to that of palmitic acid. The ratio of palmitic acid over stearic acid, which are both saturated fatty acids and thus less subject to degradation upon ageing, has been used to identify the source of the oil [41]. All these aspects can be easily evaluated with GC/MS based procedures, after the glycerides have been hydrolysed. However, the behaviour in pyrolysis of these materials is complex, because side reactions such as unspecific fragmentation of triglycerides and of the polymeric network, isomerisation of double bonds, and  $\alpha$ -methylation of acidic moieties (when TMAH is used) become involved in changing the fatty acid profile.

To demonstrate these aspects, the different pyrograms obtained from the pyrolysis of aged linseed oil samples using different derivatising agents and different pyrolysers are shown.

Figure 11.1 shows the pyrogram of lead white pigmented linseed oil paint obtained at 610 °C with a Curie-point pyrolyser, with on-line methylation using 2.5% methanolic TMAH. The pyrolyser was a Curie-point pyrolysis system FOM 5-LX, specifically developed at FOM Amolf Institute (Amsterdam, the Netherlands), to reduce cold spots to a minimum. This means that the sample can be flushed before pyrolysis in a cold zone, and it also ensures optimum pressure condition within the pyrolysis chamber, thus guaranteeing an efficient transport to the GC injection system [12].

In the pyrogram obtained in the presence of TMAH,  $\alpha$ -methylated fatty and diacids are observed, due to the strong alkalinity of the reagent (as explained above).



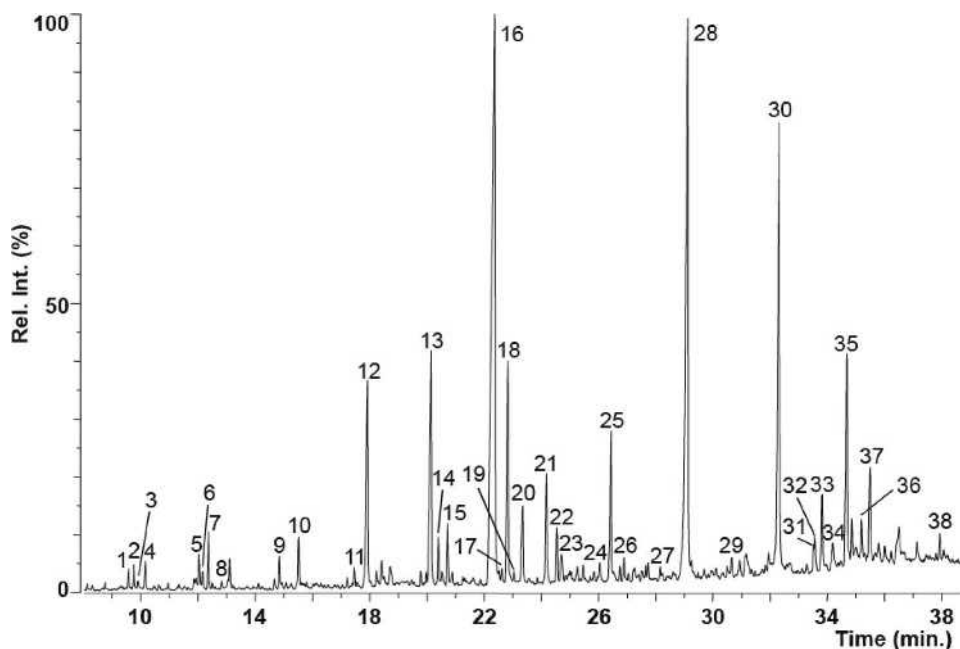


**Figure 11.1** Py/methylation-GC/MS chromatograms of lead white pigmented linseed oil paint after 610 °C Curie-point pyrolysis assisted with on-line methylation using 2.5% methanolic TMAH (the sample and TMAH solution was applied onto a rotating Curie-point wire; pyrolysis time 6 s, interface 180 °C). 1, heptenoic acid, methyl ester; 2, heptanoic acid, methyl ester; 3, butenedioic acid, dimethyl ester; 4, butanedioic acid, dimethyl ester; 5, octenoic acid, methyl ester; 6, octanoic acid, methyl ester; 7, pentenedioic acid, dimethyl ester; 8, pentanedioic acid, dimethyl ester; 9, nonanoic acid, methyl ester; 10, hexanedioic acid, dimethyl ester; 11, decanoic acid, methyl ester; 12, heptanedioic acid, dimethyl ester; 13, octanedioic acid, dimethyl ester; 14, 1,2-benzenedicarboxylic acid, dimethyl ester; 15,  $\alpha$ -methyl octanedioic acid, dimethyl ester; 16, nonanedioic acid, dimethyl ester; 17,  $\alpha$ -methoxy octanedioic acid, dimethyl ester; 18,  $\alpha$ -methyl nonanedioic acid, dimethyl ester; 19,  $\alpha,\alpha$ -dimethyl nonenedioic acid, dimethyl ester; 20a,  $\alpha$ -methyl nonenedioic acid, dimethyl ester; 20b,  $\alpha,\alpha$ -dimethyl nonanedioic acid, dimethyl ester; 21, decanedioic acid, dimethyl ester; 22,  $\alpha$ -methoxy nonanedioic acid, dimethyl ester; 23,  $\alpha$ -methyl decanedioic acid, dimethyl ester; 24, undecanedioic acid, dimethyl ester; 25,  $\alpha$ -methoxy decanedioic acid, dimethyl ester; 26, pentadecanoic acid, methyl ester; 27, dodecanedioic acid, dimethyl ester; 28, hexadecanoic acid, methyl ester; 29, heptadecanoic acid, methyl ester; 30, octadecanoic acid, methyl ester; 31, 8-methoxy-9-octadecenoic acid, methyl ester; 32, 11-methoxy-9-octadecenoic acid, methyl ester; 33, 9-methoxy-10-octadecenoic acid and 10-methoxy-8-octadecenoic acid; 34, 9-oxo-octadecanoic acid, 10-oxo-octadecanoic acid; 35, 9-epoxy-octadecanoic acid; 36, eicosanoic acid, methyl ester; 37, 9,10-dimethoxy-octadecanoic acid, methyl ester; 38, docosanoic acid, methyl ester. Reprinted from J. Anal. Appl. Pyrol., **61**, 1–2, van den Berg and Boon, 19, Copyright 2001, with permission from Elsevier

**Table 11.2** Transmethylation yield of azelaic and palmitic acids using TMAH solution in combination with 610 °C Curie-point Py-GC/MS [12]

Amount of TMAH solution (2.5%) (μl)	Solvent	Azelaic acid dimethyl ester (recovery%)	Palmitic acid methyl ester (recovery%)
2	Water	65	66
2	Methanol	79	78
4	Water	99	98
4	Methanol	60	63
8	Water	100	99
8	Methanol	48	51

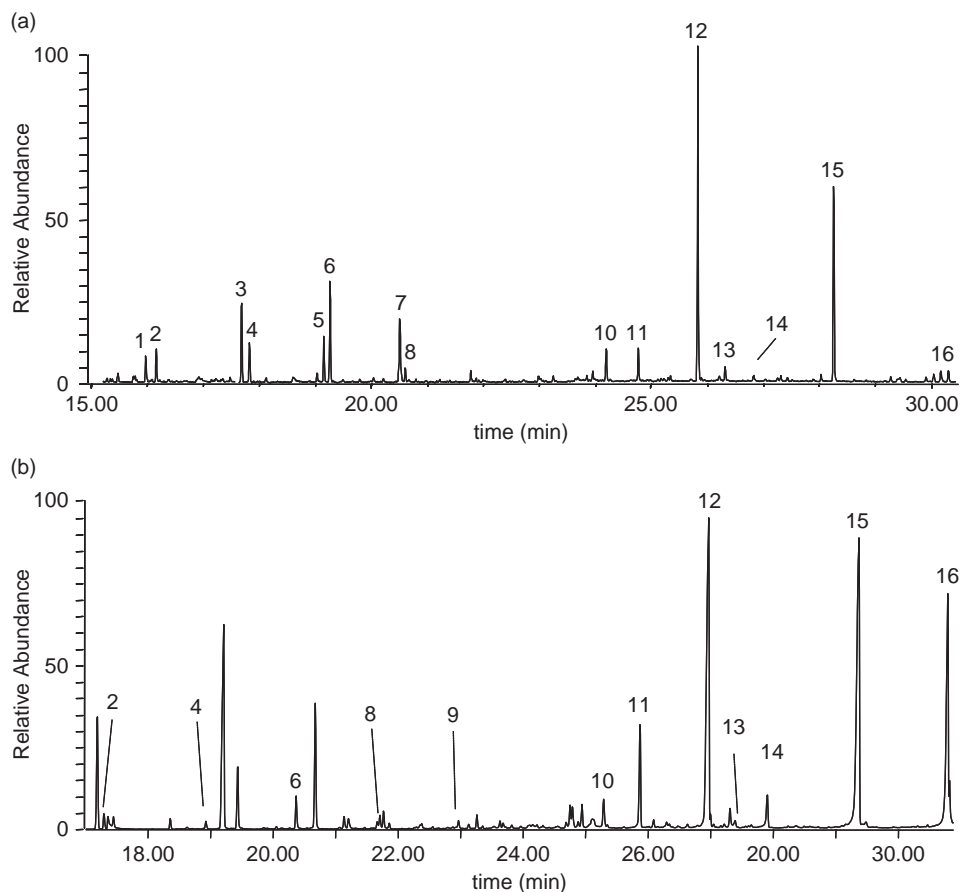
It has been proven that the concentration of the reagent and the solvent used can become involved in the final yield of side reactions, as shown in Table 11.2. The use of water as a solvent and high concentrations of TMAH ensure better yields of the transmethylation reaction. This has been explained on the basis of the co-ordination chemistry, the solvent–analyte mixture determines the reactivity of TMAH with respect to the reactants [12].

Figure 11.2 shows the pyrograms obtained from an aged linseed oil paint layer obtained with different pyrolysers in the presence of HMDS. Figure 11.2a was obtained with a continuous mode microfurnace pyrolysing injection system Pyrojector (SGE, Austin, Texas, USA) and Figure 11.2b with a CDS Pyroprobe 5000 series (CDS Analytical Inc., Oxford, USA).

As far as the silylating agent is concerned, interpreting the pyrolytic profile is somewhat more complex. HMDS is not a strong alkaline reagent, thus both derivatisation after thermal breakdown and transesterification can occur. Moreover, the yield of one process with respect to the other very much depends on the instrumental set-up. This is clearly indicated by the comparison between the chromatograms. The pyrogram obtained with the microfurnace (Figure 11.2a) shows that derivatisation after thermal breakdown is quite significant, as inferred from the high amount of short chain fatty acids produced. The pyrogram obtained with the resistively heated filament (Figure 11.2b) highlights how transesterification is clearly the main phenomenon, with the peaks of azelaic, palmitic and stearic acid trimethylsilyl esters being the most abundant in the chromatogram.

It is important to underline that both when pyrolysis/methylation and pyrolysis/silylation are used, short chain fatty acids (saturated and unsaturated) are generated from the pyrolytic fragmentation of the cured network formed upon ageing and the fatty acids themselves: both saturated and unsaturated forms are observed.

A mature drying oil is normally distinguished from a non-drying oil and a fat from animal origin on the basis of the relative amount of azelaic acid (A) with respect to palmitic acid (P): an  $A/P > 1$  is characteristic for a drying oil, while  $A/P < 1$  is characteristic of egg [41]. The palmitic acid/stearic acid (P/S) ratio indicates the source of the fat: for example, linseed oil:  $P/S \approx 1$ ; walnut oil:  $2.2 < P/S < 2.8$ ; poppy seed oil:  $P/S > 3$ ; egg:  $P/S > 2$  [41]. Although the chromatograms shown in Figure 11.1 and Figure 11.2b seem to fulfil the expected A/P and P/S values for a mature linseed oil, care must be taken in the



**Figure 11.2** Py/silylation-GC/MS chromatograms of aged linseed oil pyrolysed in the presence of HMDS. (a) Pyrogram obtained with a microfurnace pyrolyser; pyrolysis temperature: 600 °C; furnace pressure: 14 psi; purge flow: 0.5 ml min<sup>-1</sup>. (b) Pyrogram obtained with a resistively heated filament pyrolyser; pyrolyser interface: 180°C; transfer line: 300°C; valve oven: 290°C. 1, Hexenoic acid, trimethylsilyl ester; 2, hexanoic acid, trimethylsilyl ester; 3, heptenoic acid, trimethylsilyl ester; 4, heptanoic acid, trimethylsilyl ester; 5, octenoic acid, trimethylsilyl ester; 6, octanoic acid, trimethylsilyl ester; 7, nonenoic acid, trimethylsilyl ester; 8, nonanoic acid, trimethylsilyl ester; 9, decanoic acid, trimethylsilyl ester; 10, lauric acid, trimethylsilyl ester; 11, suberic acid, trimethylsilyl diester; 12, azelaic acid, trimethylsilyl diester; 13, myristic acid, trimethylsilyl ester; 14, sebacic acid, trimethylsilyl diester; 15, palmitic acid, trimethylsilyl ester; 16, stearic acid, trimethylsilyl ester

evaluation of these ratios when a paint sample is analysed. The pyrolysis and derivatisation yields can be strongly influenced when other materials, especially inorganic ones, are simultaneously present. This aspect is highlighted when pyrolysis/methylation and pyrolysis/silylation of mature linseed oil samples are performed in the presence of different pigments as shown in Figure 11.3 [37]. Chromatograms were obtained with a CDS 1000 pyroprobe resistively heated filament pyrolyser (Chemical Data System, Oxford, USA) at

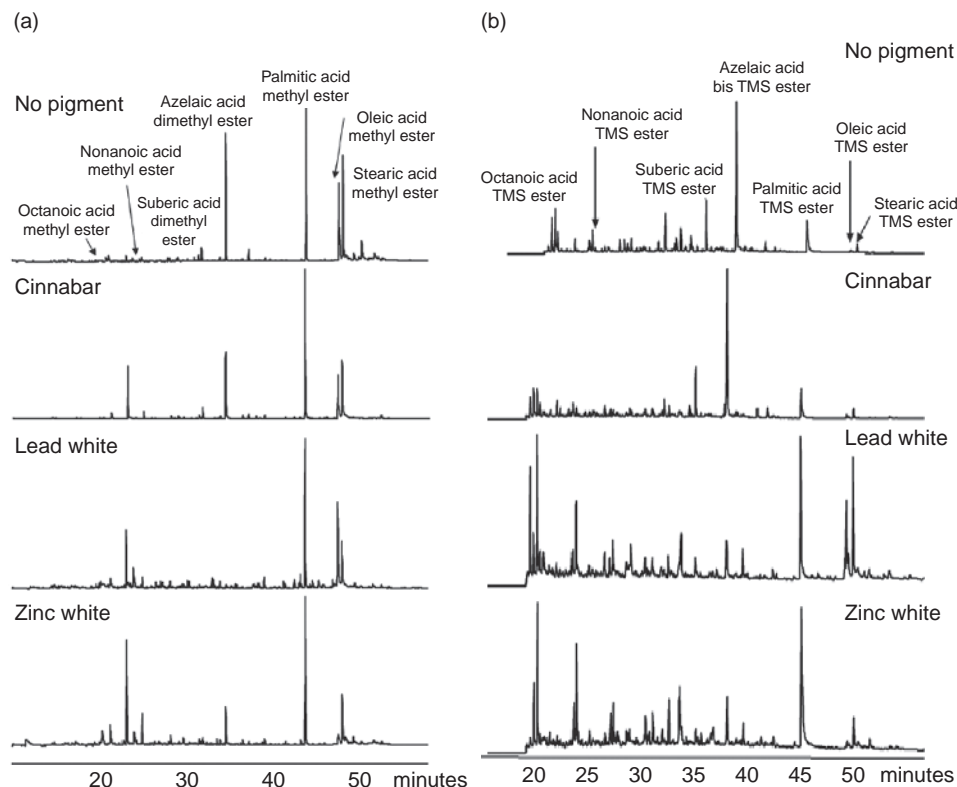


**Figure 11.3** Chromatograms of linseed oil mature films some of which contain pigments, obtained after (a) pyrolysis/methylation and (b) pyrolysis/silylation, at 600°C with a resistively heated filament pyrolyser. Reprinted from *J. Anal. Appl. Pyrol.*, **74**, Chiavari et al., 6, Copyright 2005 with permission from Elsevier

600°C; the sample was inserted in a prepyrolysed quartz tube and admixed with 5  $\mu$ l of derivatising agent, i.e. HMDS or TMAH 25% aqueous solution.

The chromatograms reported in Figure 11.3 clearly show different values for A/P and P/S, some of which are more similar to the expected values for egg tempera rather than linseed oil.

Moreover, the diversity of results obtained for the aged linseed oil-lead white paint samples shown in Figure 11.1 and Figure 11.3a, highlights the important role played by reagent concentration and instrumental set-up.

The inorganic materials are sometimes even capable of hindering derivatisation, as shown in the chromatogram of Figure 11.4, which was obtained from a mature linseed oil paint sample containing high amounts of sulfates: only underderivatised acids are observed. The pyrolyser was a CDS Pyroprobe 5000 series (CDS Analytical Inc, Oxford, USA); pyrolyser interface: 180°C; transfer line: 300°C; valve oven: 290°C. Pyrolysis was performed in the presence of HMDS at 600°C.

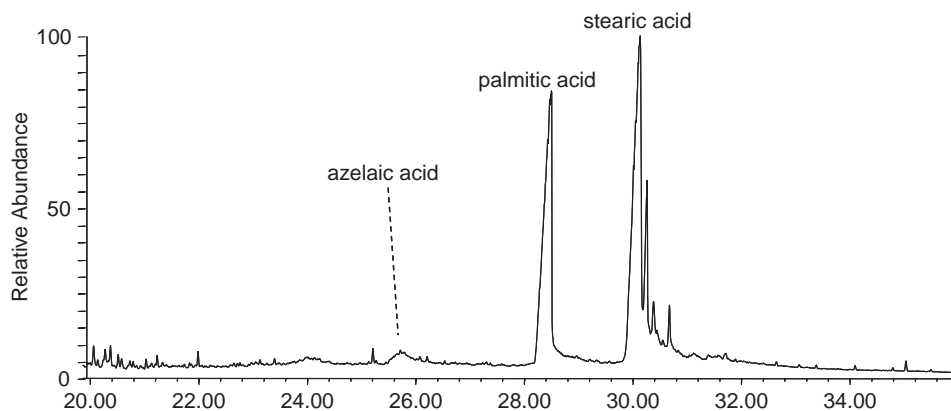


**Figure 11.4** Chromatogram relative to a mature linseed oil paint sample containing a high amount of sulfates, obtained by pyrolysis/silylation with a resistively heated filament pyrolyser at 600°C

## 11.4 Plant Resins

Plant resins are discussed in detail in Chapter 12. Since plant resins were once common additives for paint binders, this section briefly reviews the literature, focusing on the use of different derivatising agents.

Fresh plant resins have been characterised by means of pyrolysis coupled to GC/MS without the use of a derivatising agent. However, many markers used for the identification of resins in samples from works of art are often not cogent, and moreover they disappear during ageing [42].

Pyrolysis in the presence of tetramethylammonium hydroxide (THM)-GC/MS allowed the identification of high- and low-molecular weight components in manila Copal and sandarac fresh and artificially aged samples. The pyrograms showed signals due to the polymer fraction and to free diterpenoids [43]. THM-GC/MS has also been used to determine the molecular composition of *Pinaceae* resins, allowing the study of fresh, naturally and artificially aged samples [16, 44–46].

The strong alkalinity of TMAH can produce problems related to the interpretation of the resulting pyrograms. One of the disadvantages of this technique, especially if compared with conventional GC, is the large number of substances that originate from the pyrolysis process. Free diterpenoid acids easily undergo secondary pyrolysis reactions such as fragmentation, isomerisation and recombination, resulting in the appearance of a large number of peaks. Moreover, TMAH is successful in methylating carboxylic acids, but rather ineffective for hydroxyl groups. This prevents the detection of some phenols, such as totarol, torulosol, manol and sugiol, which are reported to be present in sandarac resins [43]. Moreover, in abietane molecules the methylation of tautomeric forms has been reported, giving rise to an increased complexity in the pyrograms [16].

Py-GC/MS characterisation of diterpenoid resins using online trimethylsilylation with HMDS has been performed on fresh *Pinaceae* resins, manila Copal, sandarac, and Copaiba

balsam commercial products [47–49]. Derivatisation with HMDS reduces the number of side reactions that complicate the interpretation of results [50]. Unlike TMAH, HMDS can discriminate between originally methylated molecules from the derivatisation products, as in the case of the mono methyl ester of agathic acid [47]. However, the yield of HMDS derivatives may be not quantitative.

### 11.5 Animal Resin: Shellac

Due to the macromolecular nature of shellac, GC/MS analysis requires preliminary chemo-lysis or pyrolysis pretreatments [51,52]. As a result, the constituting esters are transformed into more volatile components. The complexity of the fragmentation induced by pyrolysis/silylation presents several problems in obtaining reliable information: the short chain fatty acids arising from the fragmentation of aleuritic acid are a poor diagnostic tool for identifying shellac [48] since these products can also be produced by the pyrolysis of glycerolipid materials. Pyrolysis/silylation (HMDS) with a microfurnace pyrolyser has been used to characterise fresh and naturally aged shellac samples, showing that despite the high fragmentation observed to the detriment of aleuritic acid and the sesquiterpenoid acids, butolic acid is preserved and can thus be used as a molecular marker [53]. Reliable results have also been obtained by applying the thermally assisted hydrolysis and methylation technique to pure shellac samples [54], so that characteristic aliphatic and sesquiterpene acids can be detected.

### 11.6 Polysaccharide Materials

Although the pyrolysis of some classes of polysaccharide materials has been studied quite extensively in the food, petrol and tobacco industry, very little has been published specifically on polysaccharide binders (arabic gum, tragacanth gum, fruit tree gum, honey and starch). The pyrolysis of glucane based polymers, especially cellulose, has been studied in detail [6,55], highlighting how anhydrosugars and furan derivatives are the main pyrolysis products, together with one-, two- and three-carbon aldehydes and acids.

A recent study extensively investigated the pyrolysis of polysaccharide binders, with and without a silylating agent [56]. Some of the main results relative to the pyrolysis silylation of sugars and polysaccharide binders can be summarised as follows [56–59]:

- Free sugars naturally occurring in plant gums all give rise to the formation of furancarboxyaldehydes, which are also formed when plant gums are pyrolysed.
- Glucose, galactose, xylose and arabinose give rise to the formation of the corresponding anhydrosugars.
- When silylation of simple sugars and polysaccharide gums is performed, in addition to persilylated and partially silylated sugars, uronic acids and anhydrosugars, furancarboxyaldehydes are observed together with persilylated and partially silylated cyclopentenones, pyranones and furanones. The relative abundance of one pyrolysis product with respect to others depends on, in addition to the chemical composition of the binder, the strength of the silylating agent.

It can be concluded that polysaccharide binders can be identified in a sample from a work of art when pyrolysis is performed both with or without silylating agents, when

sugars, uronic acids, anhydrosugars, furancarboxyaldehydes, cyclopentenones, pyranones and furanones are observed in the pyrogram (eventually partially or fully silylated) [31,56,60]. Although pyrograms obtained with different gums are distinct, it is often difficult to distinguish between one polysaccharide binder and the other in a paint sample. Both pyrolysis and thermally assisted silylation of sugars and polysaccharide materials give rise to a variety of products. In fact, the high number of alcoholic moieties and the nature of the glycosidic bonds are responsible for the several possible pathways of thermal degradation observed. Moreover, glycosidic bonds do not react quantitatively in a unique way with the derivatising agent, and the silylation yield for alcoholic moieties is strongly dependent on the chemical environment, and seldom quantitative. Identifying the source of a polysaccharide binder in a paint sample is thus currently very difficult if only Py-GC/MS is used, and batch techniques followed by GC/MS are still the most suitable [61].

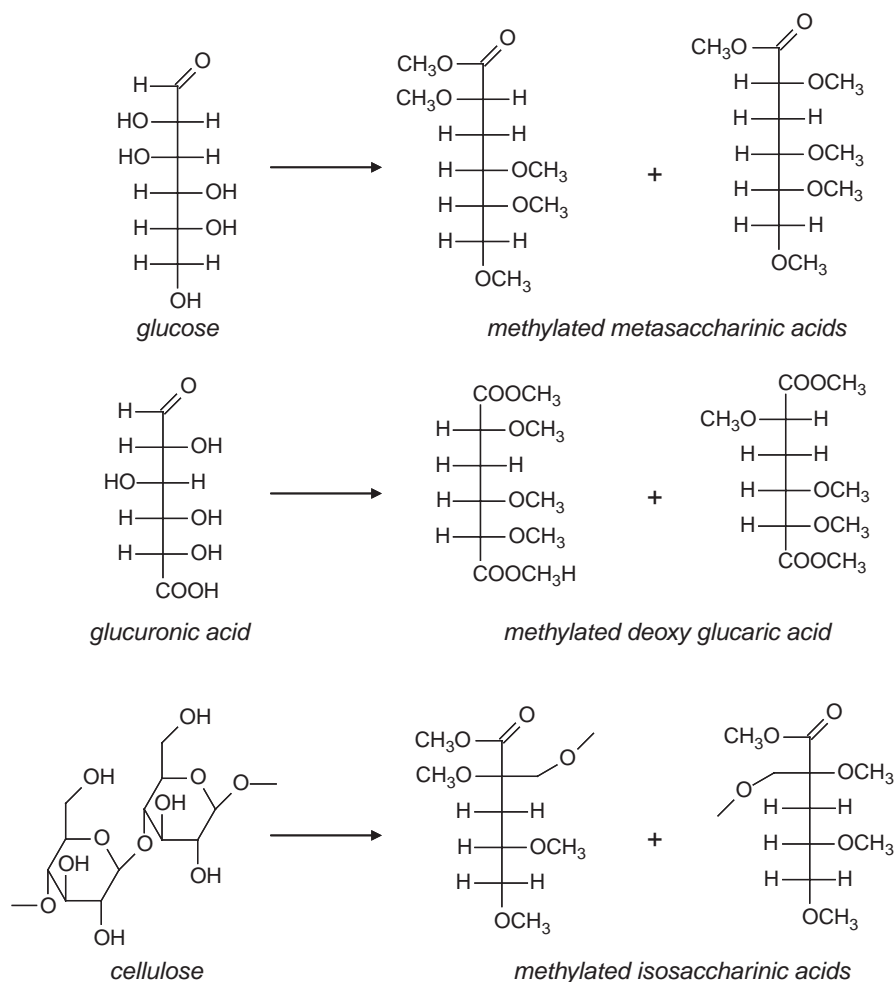


**Figure 11.5** Formation of methylated saccharinic acids from glucose and cellulose, and methylated deoxyglucaric acid from glucuronic acid [66,68]

In the literature there are a few studies regarding the characterisation of some simple sugars and polysaccharides through thermally assisted hydrolysis and methylation reactions [62–67]. It has been shown that reducing sugars form methylated saccharinic acid (deoxyaldonic acid) methyl esters under THM conditions, while 1,4-linked polysaccharides produce methylated isosaccharinic acids (2-hydroxymethyl-pentonic acids) instead of methylated hexonic acids. Due to the reaction mechanisms involved, each carbohydrate yields two isomers of saccharinic acid. Consequently carbohydrates, which differ in the stereochemistry of positions 2 and 3 only, yield the same pair of isomers of saccharinic acids. THM reactions of glucuronic acid and galacturonic acids have been studied as well, showing that they give rise to the formation of epimers of methylated deoxyglucaric acid and deoxygalactaric acid, respectively [68]. The behaviours of these acids when they are part of polymers, depends, as shown for reducing sugars, on the linkages involved, indicating that deoxyglucaric acid and deoxygalactaric acid are not always formed. The formation of methylated saccharinic acids from glucose and cellulose, as well as methylated deoxyglucaric acid from glucuronic acid, under THM conditions is shown in Figure 11.5.

## 11.7 Beeswax

The long chain esters that characterise beeswax, as well as the low volatile and long chain acids, hydroxyacids and alcohols, require some kind of pretreatment prior to GC/MS

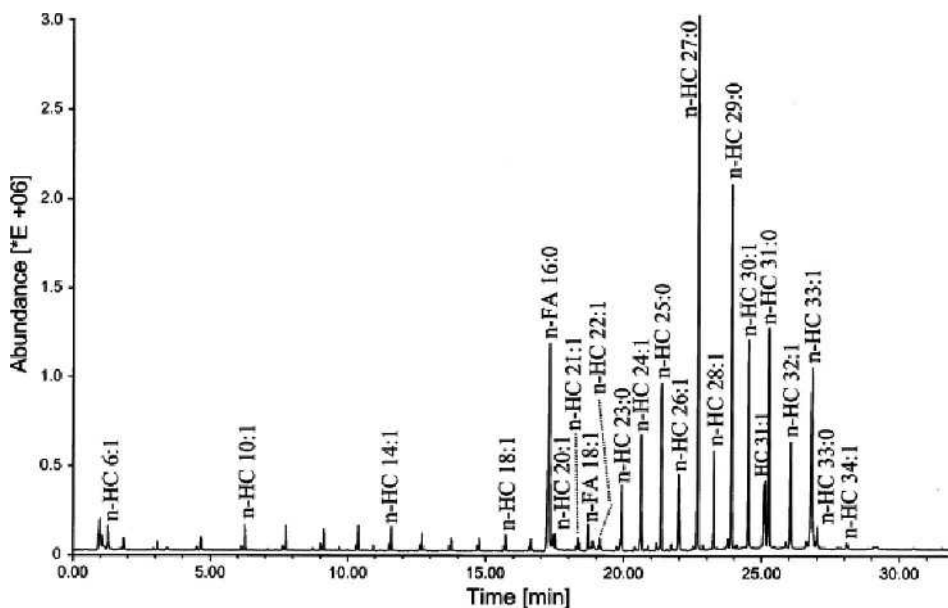


**Figure 11.6** Total ion current pyrogram obtained from 30 µg of bleached beeswax with a resistively heated pyrolyser at 800°C. FA, fatty acid; HC, hydrocarbon; X:Y, chain length X with Y double bonds. Reprinted from *J. Anal. Appl. Pyrol.*, **50**, Asperger et al., 2, 13, Copyright 1999 with permission from Elsevier



analysis. A successful approach to solve the problem of beeswax characterisation that avoids wet chemical pretreatments is pyrolysis, followed by GC coupled with MS. This technique has been used for characterising raw materials [69], also in samples from works of art [1,23]. Chromatograms obtained in this way are characterised by specific *n*-hydrocarbon (saturated and unsaturated) patterns, arising from the thermal fragmentation of long chain constituents (Figure 11.6). Most acids and alcohols naturally occurring in beeswax are not detected in the chromatogram. Although the chromatographic profiles of linear hydrocarbons generated by beeswax pyrolysis without a derivatising agent are quite diagnostic, the simultaneous occurrence of other organic and inorganic materials could prevent the correct interpretation of the pyrogram. In fact other materials, such as glycerolipids (commonly encountered in samples from works of art), can give rise to similar pyrolysis products with a different chromatographic profile. Strong memory effects may also occur.

Pyrolysis with *in situ* derivatisation with HMDS has been proposed [70]. Although the chromatograms are still quite complex, due to the very high degree of thermal fragmentation, all polar compounds are derivatised, thus avoiding the contamination of the column and strong memory effects. The chromatographic profiles of alcohols, fatty acids and hydrocarbons (Figure 11.7), in addition to the occurrence of 15-hydroxyhexadecanoic

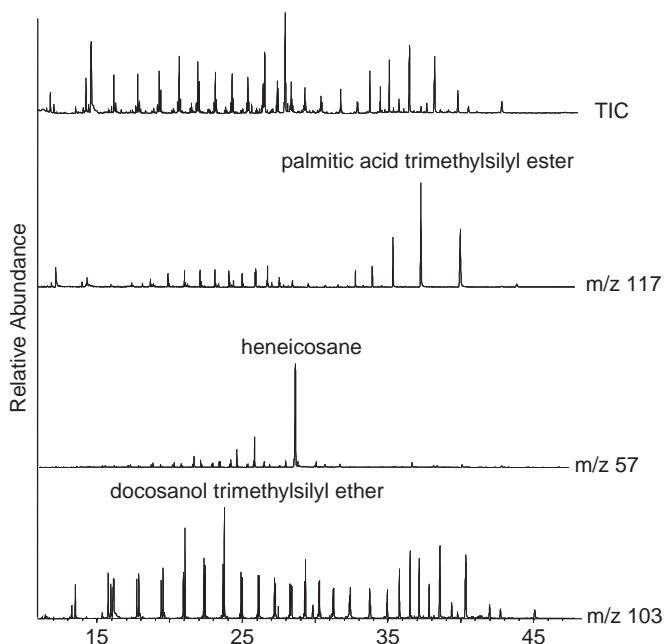


**Figure 11.7** Pyrogram of a beeswax sample obtained with a microfurnace pyrolyser at 600°C, in the presence of HMDS. TIC: total ion current; m/z 117: profile of carboxylic acid trimethylsilyl esters, showing a maximum with palmitic acid; m/z 57: profile of hydrocarbons, showing a maximum with heneicosane; m/z 103: profile of alcohol trimethylsilyl ethers, showing a maximum with docosanol. For the identification of all peaks, see Bonaduce and Colombini [70]

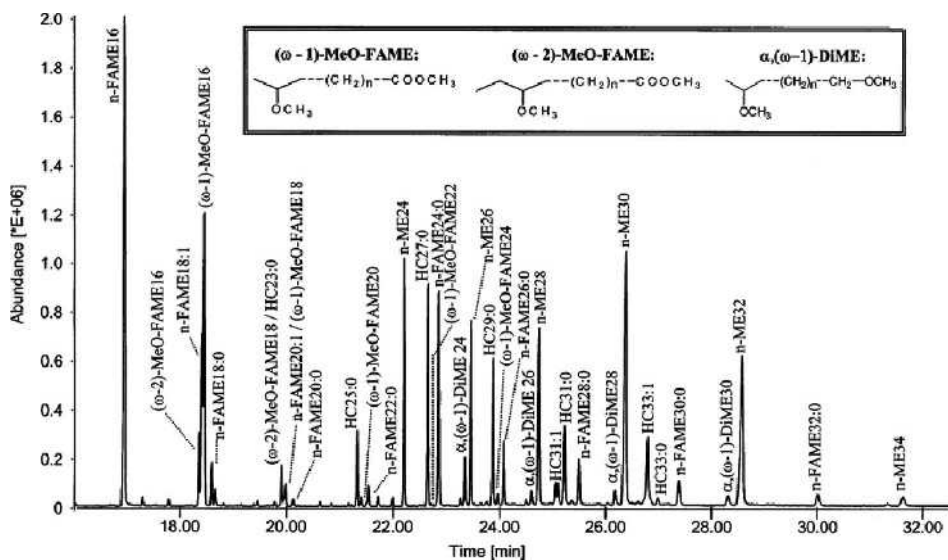


**Figure 11.8** THM-GC trace of bleached beeswax. FAME, fatty acid methyl ester obtained with a resistively heated filament pyrolyser at 550°C; MeO-FAME, methyl ester of methoxy fatty acid; ME, alkyl methyl ether; DiME, dimethoxyalkane; HC, hydrocarbon; X:Y, carbon chain length: number of double bonds. Reprinted from *J. Anal. Appl. Pyrol.*, **52**, Asperger et al., 1, 13, Copyright 1999 with permission from Elsevier

acid, can be used to identify beeswax in samples from works of art, as it has been shown for a sample from a ceroplastic sculpture ('The Plague' by Gaetano Zumbo, seventeenth century), where beeswax and a *Pinaceae* resin were identified [70].

Better results in the analysis of beeswax have been obtained using pyrolysis with thermally assisted hydrolysis and methylation [71–73]. In this way mono- and polyesters are quantitatively hydrolysed, and acids and alcohols are transformed into the corresponding methyl esters and ethers, respectively (Figure 11.8). This approach gives highly specific chromatographic profiles, avoiding the thermal fragmentation of the sample constituents into rather non-specific products, thus improving the interpretation of chromatographic profiles as well as detection limits.

## 11.8 Case Studies

Four case studies are presented in this section, with the aim of showing:

- how pyrolysis can be used to determine the organic composition of a paint sample. This can be achieved without sample pretreatment, permitting, in some cases, the determination of more than one material in one single run (Case Studies 1, 2 and 3);

- the importance of using, when possible, more than one analytical technique, to overcome unpredictable interferences that can occur in the analyses of such complex samples as those collected from painted works of art (Case Study 4).

### 11.8.1 Case Study 1: Characterisation of the Paint Binder of Sixteenth Century Wall Paintings in the “Messer Filippo” Cell of the Tower in Spilamberto, Italy [74]

Figure 11.9 shows the pyrogram of a paint sample collected from the sixteenth century wall paintings in the “Messer Filippo” cell of the tower in Spilamberto, Italy. Pyrolysis was performed with a microfurnace pyrolyser, at 600°C, in the presence of HMDS. On the basis of the pyrolysis products found, egg and a carbohydrate material were identified.

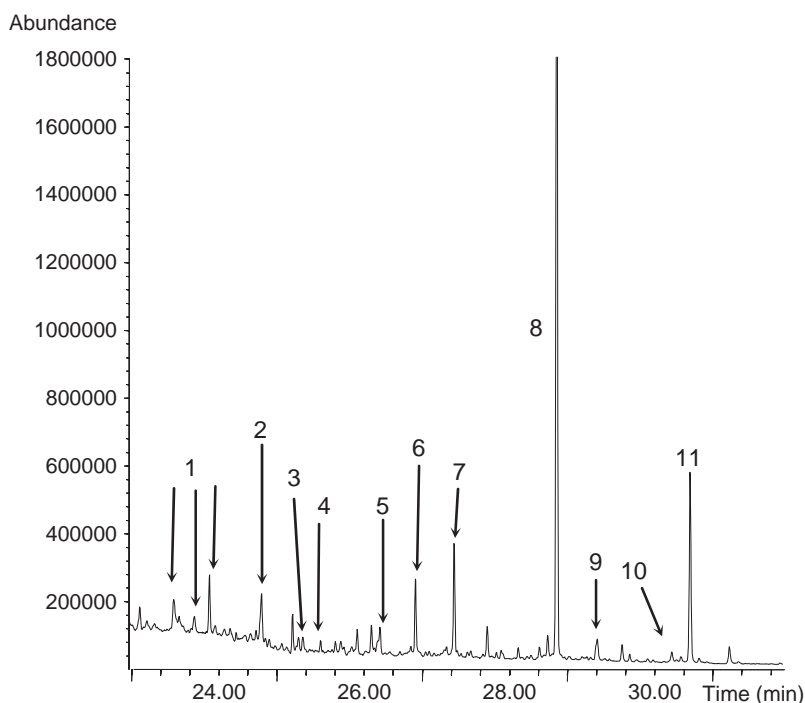


**Figure 11.9** Pyrogram of a paint sample collected from sixteenth century wall paintings in the ‘Messer Filippo’ cell of the tower in Spilamberto, Italy. Pyrolysis was performed with a micro-furnace pyrolyser, at 600°C, in the presence of HMDS. 1, Carbohydrate pyrolysis products\*; 2, lauric acid\*; 3, suberic acid\*; 4, levoglucosane\*; 5, azelaic acid\*; 6, miristic acid\*; 7, hexadecanenitrile; 8, palmitic acid\*; 9, octadecanenitrile; 10, oleic acid\*; 11, stearic acid\*. \*TMS derivative [74]

### 11.8.2 Case Study 2: Characterisation of Carbohydrate Material on the Paint Surfaces of Mural Paintings by Bonamico Buffalmacco (Fourteenth Century), in the Monumental Cemetery of Pisa, Italy [30]

The mural paintings in the Monumental Cemetery of Pisa were detached in a restoration after the Second World War, and were later restored on several occasions. They showed an advanced state of degradation. In Figure 11.10 the pyrograms of two samples collected from the paint surfaces (CSG 13bis from 'Universal Judgement' and CSA 5b from 'Stories of Holy Fathers') are compared with the pyrograms of nitrocellulose, starch and arabic gum.

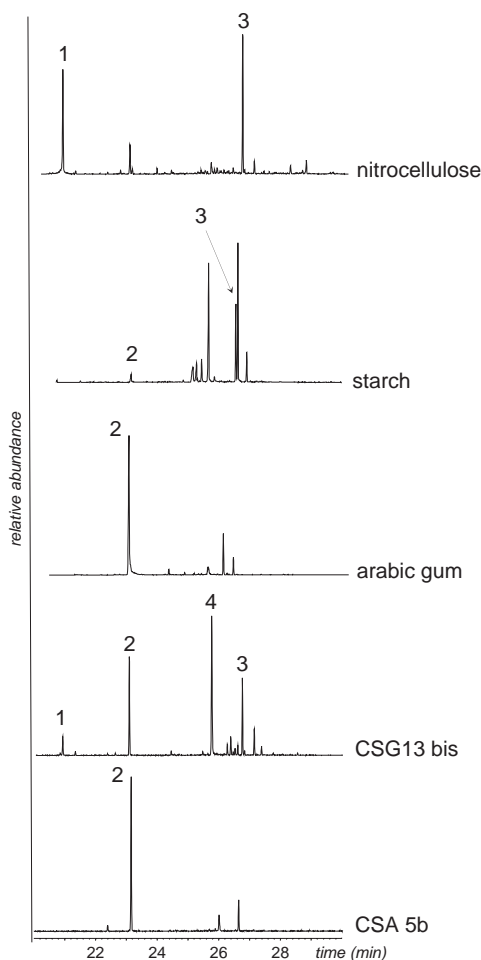


**Figure 11.10** Comparison of extracted ion pyrograms of fragment ion  $m/z$  217 of two samples collected from the paint surfaces of 'Universal Judgement' and 'Stories of Holy Fathers' (Monumental Cemetery of Pisa, Italy, painted by Buffalmacco, fourteenth century) with nitrocellulose, starch and arabic gum. 1, Unidentified compound; 2, 1,2,3,5-tetrakis-(O-TMS)-xylofuranose; 3, tri-(O-TMS)-levoglucosane; 4, isomer of 1,2,3,5-tetrakis-(O-TMS)-xylofuranose. Pyrogram obtained with a resistively heated filament at 600°C in the presence of HMDS [30]

The comparison helped to identify the simultaneous occurrence of nitrocellulose and a polysaccharide gum in sample CSG 13bis, and of a polysaccharide gum in sample CSA 5b.

### 11.8.3 Case Study 3: Characterisation of the Hydrophobic Organic Materials on a Mural Painting by Bonamico Bulffalmacco (Fourteenth century), in the Monumental Cemetery of Pisa, Italy [27]

The sample was collected from a decorative frame of the ‘Universal Judgement’ and, as in Case Study 2, was detached during restoration. It had a completely waterproof surface, due to materials used in a past restoration treatment, preventing any further intervention. In the same sample several organic materials were identified (Figure 11.11):

- animal glue and casein: their use as glues had been documented in past restorations;
- acrylic resins: little residues of synthetic glues used to restore the painting when the impermeability of the surface was ascertained;
- poly(vinyl acetate) (most likely Mowilith ABC): an undocumented glue used in a past restoration, present underneath the paint surface;
- phenol formaldehyde resin: possibly an unwanted product of a reaction between formaldehyde used as a biocide and the proteinaceous materials and poly(vinyl acetate) present. The phenol formaldehyde resin was responsible for the impermeability of the paint surface.

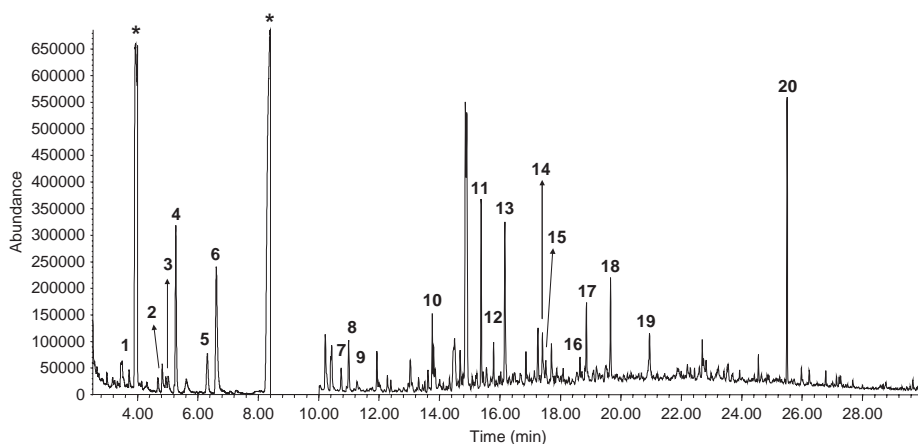


**Figure 11.11** Pyrogram of a paint sample collected from a decorative frame of the ‘Universal Judgement’ by Bonamico Buffalmacco (fourteenth century, Monumental Cemetery of Pisa, Italy). Pyrolysis was performed with a microfurnace pyrolyser, at 600°C, in the presence of HMDS. 1, Benzene; 2, ethyl acrylate; 3, methyl methacrylate; 4, acetic acid, trimethyl silyl ester; 5, pyrrole; 6, toluene; 7, 2-methylpyrrole; 8, 3-methylpyrrole; 9, crotonic acid; 10, benzaldehyde; 11, phenol; 12, 2-methylphenol; 13, 4-methylphenol; 14, 2,4-dimethylphenol; 15, benzyl nitrile; 16, 3-phenylpropionitrile; 17, indole; 18, phthalate; 19, phthalate; 20, benzyl benzoate; \*HMDS pyrolysis products [27]

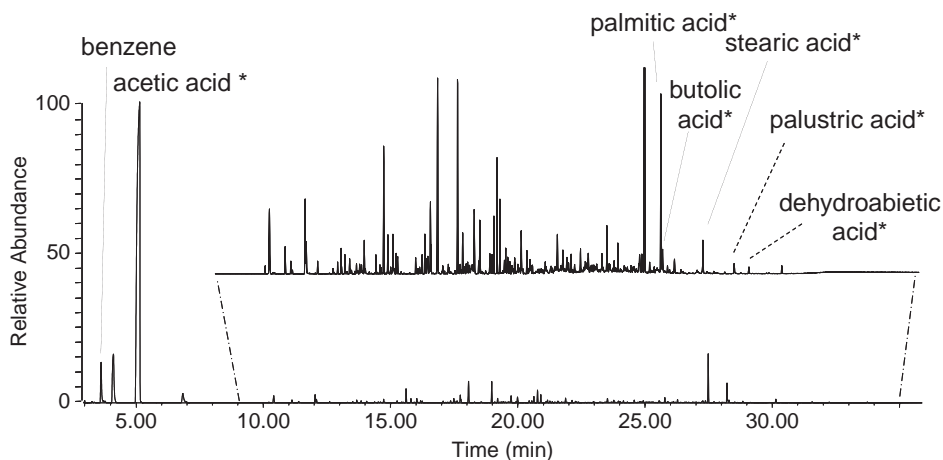


**Figure 11.12** Pyrogram of a gilding sample collected from a fifteenth century mural painting “The Longobardian Ambassadors Returning to Italy” from Teodolinda’s Chapel (Duomo of Monza, Italy) painted by the Zavattari brothers. Pyrolysis was performed with a microfurnace pyrolyser, at 600°C, in the presence of HMDS. The figure shows the whole chromatogram. The inset shows a magnification of the chromatogram between 8 min and 35 min. \*Trimethylsilyl ester [53]

#### 11.8.4 Case Study 4: Characterisation of the Organic Binders in a Mordant Gilding from the Fifteenth Century Mural Paintings of Teodolinda’s Chapel (Duomo of Monza, Italy) [53]

The sample was collected from a gilding of the fifteenth century mural painting “The Longobardian Ambassadors Returning to Italy” from Teodolinda’s Chapel (Duomo of Monza, Italy) painted by the Zavattari brothers. The sample was collected from an area that had recently been restored. The sample was subjected to saponification, silylation and GC/MS analysis, and the analysis revealed the occurrence of egg lipids. No other organic material was identified in this way. Figure 11.12 shows the pyrogram obtained with a microfurnace pyrolyser, at 600°C, in the presence of HMDS, with the assignment of some significant peaks. The pyrolysis of the sample identified, in addition to egg lipids, a poly(vinyl acetate) based glue and a *Pinaceae* resin and shellac. The latter natural resins are normally identified by GC/MS analytical procedures, but in this case the occurrence of poly(vinyl acetate) unpredictably caused some interference, so that the natural resins could not be identified in the sample on the basis of GC/MS analyses alone.

## References

1. P. Bocchini and P. Traldi, Organic mass spectrometry in our cultural heritage, *J. Mass Spectrom.*, **33**, 1053–1062 (1998).
2. J.S. Mills, R. White, *The Organic Chemistry of Museum Objects*, 2nd Edition, Butterworth Heinemann, Oxford, 1994.

3. C.V. Horie, *Materials for Conservation. Organic Consolidants, Adhesives and Coatings*, Butterworth Heinemann, Oxford, 1987.
4. E. Jablonski, T. Learner and J.H.M. Golden, Conservation concerns for acrylic emulsion paints, *Rev. Conserv.*, 1–13 (2003).
5. T. Learner, The analysis of synthetic paints by pyrolysis gas chromatography, mass spectrometry (PyGCMS), *Stud. Conserv.*, **46**, 225–241 (2001).
6. J.J. Boon, Analytical pyrolysis mass spectrometry: new vistas opened by temperature-resolved in-source PYMS, *Int. J. Mass Spectrom.*, **118/119**, 755–787 (1992).
7. G. Chiavari and S. Prati, Analytical pyrolysis as diagnostic tool in the investigation of works of art, *Chromatographia*, **58**, 543–554 (2003).
8. K.L. Sobeih, M. Baron and J. Gonzalez-Rodriguez, Recent trends and developments in pyrolysis–gas chromatography, *J. Chromatogr., A*, **1186**, 51–66 (2008).
9. J. M Challinor, The scope of pyrolysis methylation reactions, *J. Anal. Appl. Pyrol.*, **20**, 15–24 (1991).
10. J.M. Challinor, Review: the development and application of thermally assisted hydrolysis and methylation reactions, *J. Anal. Appl. Pyrol.*, **61**, 3–34 (2001).
11. A. Joll, T. Huynh and A. Heitz, Off-line tetramethylammonium hydroxide thermochemolysis of model compound aliphatic and aromatic carboxylic acids: decarboxylation of some ortho- and/or para-substituted aromatic carboxylic acids, *J. Anal. Appl. Pyrol.*, **70**, 151–167 (2003).
12. J.D.J. van den Berg and J.J. Boon, Unwanted alkylation during direct methylation of fatty (di)acids using tetramethylammonium hydroxide reagent in a Curie-point pyrolysis unit, *J. Anal. Appl. Pyrol.*, **61**, 45–63 (2001).
13. Y. Ishida, S. Wakamatsu, H. Yokoi, H. Ontani and S. Tsurge, Compositional analysis of polyunsaturated fatty acid oil by one-step thermally assisted hydrolysis and methylation in the presence of trimethylsulfonium hydroxide, *J. Anal. Appl. Pyrol.*, **49**, 267–276 (1999).
14. H.-L. Hardell and N.-O. Nilvebrant, A rapid method to discriminate between free and esterified fatty acids by pyrolytic methylation using tetramethylammonium acetate or hydroxide, *J. Anal. Appl. Pyrol.*, **32**, 1–14 (1999).
15. K.-I. Kuroda, Pyrolysis-trimethylsilylation analysis of lignin: preferential formation of cinnamyl alcohol derivatives, *J. Anal. Appl. Pyrol.*, **56**, 79–87 (2000).
16. I. Pastorova, L.F.M. Spetter, K.J. van der Berg, J.J. Boon and J.W.J. Verhoeven, Analysis of oxidised diterpenoid acids using thermally assisted methylation with TMAH, *J. Anal. Appl. Pyrol.*, **43**, 41–57 (1997).
17. V.A. Basiuk, Pyrolysis of valine and leucine at 500°C: identification of less-volatile products using gas chromatography-Fourier Transform infrared spectroscopy-mass spectrometry, *J. Anal. Appl. Pyrol.*, **47**, 127–143 (1998).
18. J. Doua and V.A. Basiuk, Pyrolysis of amino acids, recovery of starting materials and yields of condensation products, *J. Anal. Appl. Pyrol.*, **56**, 113–121 (2000).
19. V.A. Basiuk and J. Doua, Pyrolysis of poly-glycine and poly-l-alanine: analysis of less volatile products by gas chromatography/Fourier Transform infrared spectroscopy/mass spectrometry, *J. Anal. Appl. Pyrol.*, **55**, 235–236 (2000).
20. X. Zang, J.C. Brown, J.D.H. van Heemst, A. Palumbo and P.G. Hatcher, Characterisation of amino acids and proteinaceous materials using online tetramethylammonium hydroxide (TMAH) thermochemolysis and gas chromatography-mass spectrometry technique, *J. Anal. Appl. Pyrol.*, **61**, 181–193 (2001).
21. N. Gallois, J. Templier and S. Derenne, Pyrolysis-gas chromatography-mass spectrometry of the 20 protein amino acids in the presence of TMAH, *J. Anal. Appl. Pyrol.*, **80**, 216–230 (2007).
22. G. Chiavari, D. Fabbri and S. Prati, Gas chromatographic-mass spectrometry analysis of products arising from pyrolysis of amino acid in the presence of hexamethyldisilazane, *J. Chromatogr., A*, **922**, 235–241 (2001).
23. G. Chiavari, G.C. Galletti, G. Lanterna and R. Mazzeo, The potential of pyrolysis gas chromatography mass spectrometry in the recognition of ancient painting media, *J. Anal. Appl. Pyrol.*, **24**, 227–242 (1993).

24. M. Carbini, R. Stevanato, M. Rovea, P. Traldi and D. Favretto, Curie-point pyrolysis-gas chromatography/mass spectrometry in the art field. 2. The characterization of proteinaceous binders, *Rapid Commun. Mass Spectrom.*, **10**, 1240–1242 (1996).
25. G. Chiavari, D. Fabbri, S. Prati, R. Mazzeo, D. Bikiaris, S. Daniilia and Y. Chrussoulakis, Analytical pyrolysis: application to the characterisation of Byzantine painting layers, *Proceedings of 6th International Conference on Non Destructive Testing and Microanalysis for the Diagnostics and Conservation of the Cultural and Environmental Heritage* (Eds M. Marabelli and C. Parisi), Euroma, Rome, 1999, pp. 1145–1162.
26. G. Chiavari, N. Gandini, P. Russo and D. Fabbri, Characterization of standard tempera painting layers containing proteinaceous binders by pyrolysis (/methylation)-gas chromatography-mass spectrometry, *Chromatographia*, **47**, 420–426 (1998).
27. G. Chiavari, G. Lanterna, C. Luca, M. Matteini, S. Prati and I.C.A. Sandu, Analysis of proteinaceous binders by in-situ pyrolysis and silylation, *Chromatographia*, **57**, 645–648 (2003).
28. I. Bonaduce and M.P. Colombini, Gas chromatography/mass spectrometry for the characterization of organic materials in frescoes of the Monumental Cemetery of Pisa (Italy), *Rapid Commun. Mass Spectrom.*, **17**, 2523–2527 (2003).
29. A. Andreotti, I. Bonaduce, M.P. Colombini, F. Modugno and E. Ribechini, The diagnosis of the yellowing of the marble high-reliefs and the black decorations in the chapel of the tomb of Saint Anthony (Padua-Italy), *Int. J. Mass Spectrom.*, **284**, 123–130 (2009).
30. A. Andreotti, C. Baracchini, I. Bonaduce, A. Caleca, M.P. Colombini and A. Paolucci, Saving the medieval paintings by the Master Painter of the Triumph of Death in Pisa, *Proceedings of 2008 ICOM-CC Triennial Conference* (Eds J. Boon, V. Daniel, B. Elhoj, F. Hanssen-Bauer, Y. Shashoua and T. van Oosten), Allied Publishers, New Delhi, pp. 825–832.
31. H. Ling, N. Maiqian, G. Chiavari and R. Mazzeo, Analytical characterization of binding medium used in ancient Chinese artworks by pyrolysis–gas chromatography/mass spectrometry, *Microchem. J.*, **85**, 347–353 (2007).
32. J.D.J. van den Berg, *Analytical chemical studies on traditional linseed oil paints*, PhD Thesis, University of Amsterdam, 2002.
33. F. Cappitelli, T. Learner and O. Chiantore, An initial assessment of thermally assisted hydrolysis and methylation-gas chromatography/mass spectrometry for the identification of oils from dried paint films, *J. Anal. Appl. Pyrol.*, **63**, 339–348 (2002).
34. J.D.J. van den Berg, K.J. van den Berg and J.J. Boon, Identification of non-cross-linked compounds in methanolic extracts of cured and aged linseed oil-based paint films using gas chromatography-mass spectrometry, *J. Chromatogr. A*, **950**, 195–211 (2002).
35. D. Scalarone, M. Lazzari and O. Chiantore, Thermally assisted hydrolysis and methylation-pyrolysis-gas chromatography: mass spectrometry of light-aged linseed oil, *J. Anal. Appl. Pyrol.*, **58–59**, 503–512 (2001).
36. A. Piccirillo, D. Scalarone and O. Chiantore, Comparison between off-line and on-line derivatisation methods in the characterisation of siccative oils in paint media, *J. Anal. Appl. Pyrol.*, **74**, 33–38 (2005).
37. G. Chiavari, D. Fabbri and S. Prati, Effect of pigments on the analysis of fatty acids in siccative oils by pyrolysis methylation and silylation, *J. Anal. Appl. Pyrol.*, **74**, 39–44 (2005).
38. S. Prati, S. Smith and G. Chiavari, Characterization of siccative oils, resins and pigments in art works by thermochemolysis coupled to thermal desorption and pyrolysis GC and GC/MS, *Chromatographia*, **59**, 227–231 (2004).
39. G. Chiavari, D. Fabbri and S. Prati, In-situ pyrolysis and silylation for analysis of lipid materials used in paint layers, *Chromatographia*, **53**, 311–314 (2001).
40. J.D.J. van den Berg, K.J. van den Berg and J.J. Boon, Determination of the degree of hydrolysis of oil paint samples using a two-step derivatisation method and on-column GC/MS, *Prog. Org. Coat.*, **41**, 143–155 (2001).
41. M.P. Colombini, F. Modugno, R. Fuoco and A. Tognazzi, A GC/MS study on the deterioration of lipidic paint binders, *Microchem. J.*, **73**, 175–185 (2002).



42. G. Chiavari, D. Fabbri, R. Mazzeo, P. Bocchini and G.C. Galletti, Pyrolysis gas chromatography-mass spectrometry of natural resin used for artistic objects, *Chromatographia*, **41**, 273–281 (1995).
43. D. Scalarone, M. Lazzari and O. Chiantore, Ageing behaviour and analytical pyrolysis characterisation of diterpenic resins used as art materials: Manila copal and sandarac, *J. Anal. Appl. Pyrol.*, **68–69**, 115–136 (2003).
44. D. Scalarone, M. Lazzari and O. Chiantore, Ageing behaviour and pyrolytic characterisation of diterpenic resins used as art materials: colophony and Venice turpentine, *J. Anal. Appl. Pyrol.*, **64**, 345–361 (2002).
45. K.J. van den Berg, J. van der Horst, J.J. Boon, N. Shibayama and E.R. de la Rie, Mass spectrometry as a tool to study ageing processes of diterpenoid resins in works of art: GC- and LC-MS studies, *Adv. Mass Spectrom.*, **14**, 563–573 (1998).
46. K.J. van den Berg, J.J. Boon, I. Pastorova and L.F.M. Spetter, Mass spectrometric methodology for the analysis of highly oxidized diterpenoid acids in old master paintings, *J. Mass Spectrom.*, **35**, 512–533 (2000).
47. L. Osete-Cortina and M.T. Domenech-Carbo, Analytical characterization of diterpenoid resins present in pictorial varnishes using pyrolysis-gas chromatography-mass spectrometry with on line trimethylsilylation, *J. Chromatogr., A*, **1065**, 265–278 (2005).
48. G. Chiavari, D. Fabbri and S. Prati, Characterisation of natural resins by pyrolysis-silylation, *Chromatographia*, **55**, 611–616 (2002).
49. J. de la Cruz-Canizares, M.T. Domenech-Carbo, J.V. Gimeno-Adelantado, R. Mateo-Castro and F. Bosch-Reig, Study of Burseraceae resins used in binding media and varnishes from artworks by gas chromatography-mass spectrometry and pyrolysis-gas chromatography-mass spectrometry, *J. Chromatogr., A*, **1093**, 177–194 (2005).
50. K.B. Anderson and R.E. Winans, Nature and fate of natural resins in the geosphere. I. Evaluation of pyrolysis-gas chromatography mass spectrometry for the analysis of natural resins and resinates, *Anal. Chem.*, **63**, 2901–2908 (1991).
51. A.N. Singh, A.B. Upadhye, V.V. Mhaskar and Sukh Dev, Chemistry of lac resin-VI. Components of soft resin, *Tetrahedron*, **30**, 867–874 (1974).
52. R.G. Khurana, A.N. Singh, A.B. Upadhye, V.V. Mhaskar and Sukh Dev, Chemistry of lac resin-III. Lac acids (part 3): an integrated procedure for their isolation from hard resin; chromatography characteristics and quantitative determination, *Tetrahedron*, **26**, 4167–4175 (1970).
53. M.P. Colombini, I. Bonaduce and G. Gautier, Molecular pattern recognition of fresh and aged shellac, *Chromatographia*, **58**, 357–364 (2003).
54. L. Wang, Y. Ishida, H. Ohtani and S. Tsuge, Characterisation of natural resin shellac by reactive pyrolysis-gas chromatography in the presence of organic alkali, *Anal. Chem.*, **71**, 1316–1322 (1999).
55. G.R. Ponder and G.N. Richards, A review of some recent studies on mechanisms of pyrolysis of polysaccharides *Biomass Bioenerg.*, **7**, 1–24 (1994).
56. C. Riedo, Pirolisi Analitica di Gomme Polisaccaridiche in Presenza di Agenti Sibilanti, tesi di laurea a/a 2005-2006, [http://aperto.unito.it/bitstream/2318/103/1/tesi\\_laurea\\_fulltext.pdf](http://aperto.unito.it/bitstream/2318/103/1/tesi_laurea_fulltext.pdf).
57. D. Fabbri and G. Chiavari, Analytical pyrolysis of carbohydrates in the presence of hexamethyldisilazane, *Anal. Chim. Acta*, **449**, 271–280 (2001).
58. E.B. Sanders, A.I. Goldsmith and J.I. Seeman, A model that distinguishes the pyrolysis of D-glucose, D-fructose, and sucrose from that of cellulose. Application to the understanding of cigarette smoke formation, *J. Anal. Appl. Pyrol.*, **66**, 29–50 (2003).
59. D. Fabbri, G. Chiavari, S. Prati, I. Vassura and M. Vangelista, Gas chromatography/mass spectrometric characterisation of pyrolysis/silylation products of glucose and cellulose, *Rapid Commun. Mass Spectrom.*, **16**, 2349–2355 (2002).
60. Y. Keheyani and L. Giulianelli, Identification of historical ink ingredients using pyrolysis-GC/MS. A novel study, *E-PS*, **3**, 5–10 (2008).
61. I. Bonaduce, H. Brecoulaki, M.P. Colombini, A. Lluveras, V. Restivo and E. Ribechini, Gas chromatographic-mass spectrometric characterisation of plant gums in samples from painted works of art, *J. Chromatogr., A*, **1175**, 275–282 (2007).

62. D. Fabbri and R. Helleur, Characterization of the tetramethylammonium hydroxide thermo-chemolysis products of carbohydrates *J. Anal. Appl. Pyrol.*, **49**, 277–293 (1999).
63. C. Schwarzing, I. Tanczos and H. Schmidt, Pyrolysis–gas chromatography/mass spectrometry and thermally assisted hydrolysis and methylation (THM) analysis of various cellulose esters, *J. Anal. Appl. Pyrol.*, **58–59**, 513–523 (2001).
64. C. Schwarzing, I. Tanczos and H. Schmidt, Levoglucosan, cellobiose and their acetates as model compounds for the thermally assisted hydrolysis and methylation of cellulose and cellulose acetate, *J. Anal. Appl. Pyrol.*, **62**, 179–196 (2002).
65. G. Chiavari, S. Montalbani, S. Prati, Y. Keheyan and S. Baroni, Application of analytical pyrolysis for the characterisation of old inks, *J. Anal. Appl. Pyrol.*, **80**, 400–405 (2007).
66. C. Schwarzing, On the mechanism of thermally assisted hydrolysis and methylation of carbohydrates: the contribution of aldol and retroaldol reactions, *J. Anal. Appl. Pyrol.*, **68–69**, 137–149 (2003).
67. C. Schwarzing, Identification of methylated saccharinolactones and partially methylated saccharinic acids in the thermally assisted hydrolysis and methylation of carbohydrates, *J. Anal. Appl. Pyrol.*, **71**, 501–514 (2004).
68. I. Tanczos, C. Schwarzing, H. Schmidt and J. Balla, THM-GC/MS analysis of model uronic acids of pectin and hemicelluloses, *J. Anal. Appl. Pyrol.*, **68–69**, 51–162 (2003).
69. A. Asperger, W. Engewald and G. Fabian, Analytical characterization of natural waxes employing pyrolysis-gas chromatography-mass spectrometry, *J. Anal. Appl. Pyrol.*, **50**, 103–115 (1999).
70. I. Bonaduce and M.P. Colombini, Characterisation of beeswax in works of art by gas chromatography-mass spectrometry and pyrolysis-gas chromatography-mass spectrometry procedures, *J. Chromatogr., A*, **1028**, 297–306 (2004).
71. A. Asperger, W. Engewald and G. Fabian, Advances in the analysis of natural waxes provided by thermally assisted hydrolysis and methylation (THM) in combination with GC/MS, *J. Anal. Appl. Pyrol.*, **52**, 51–63 (1999).
72. A. Asperger, W. Engewald and G. Fabian, Thermally assisted hydrolysis and methylation - a simple and rapid on line derivatization method for gas chromatographic analysis of natural waxes, *J. Anal. Appl. Pyrol.*, **61**, 91–109 (2001).
73. G. Chiavari, P. Bocchini and G. C. Galletti, Rapid identification of binding media in paintings using simultaneous pyrolysis methylation gas chromatography, *Sci. Technol. Cult. Herit.*, **1**, 153–158 (1992).
74. F. Ospitali, A. Rattazzi, M.P. Colombini, A. Andreotti and G. Lonardo, XVI century wall paintings in the ‘Messer Filippo’ cell of the tower of Spilamberto: microanalyses and monitoring, *J. Cult. Herit.*, **8**, 323–327 (2007).

# 12

## Py-GC/MS of Natural and Synthetic Resins

*Dominique Scalarone and Oscar Chiantore*

### 12.1 Introduction

Natural and synthetic resins are organic compounds easily found in art objects either as varnishes and protective coatings or binding media, adhesives, consolidants and finishing layers. They are mainly used in manufacturing paintings, but also in pottery, furniture and wooden objects, sculptures, musical instruments and works on paper. In addition, natural and synthetic resins have widespread use as conservation materials.

Natural resins have been known and used from very ancient times. The presence of mastic and pine resins was revealed in coatings applied by Egyptians to mummy cases, wooden funerary objects and embalming materials, while sandarac and amber were found in Phoenician mummies [1,2]. Rosin, together with polysaccharide gums and waxes, has been identified by Py-GC/MS in Egyptian cartonnages dated back to ca. 2000 BC [3].

The importance of natural resins in the cultural heritage field lies principally in the preparation of varnishes. Varnishes were and are still used to protect paintings and other colourful decorated surfaces from impacts, abrasions, dust, humidity and light. Especially in dealing with paintings, varnishes also have an important aesthetic function, which is to increase the brightness of the surface and enhance the colour saturation without changing the original hues of the painted layers. For that purpose paint varnishes must be transparent and colourless. Moreover, a varnish must be reversible, which means it should be easily removed and substituted when it has become too degraded.

Natural resins are exudates from living trees, fossil plants or insects. Chemically, they are formed by complex mixtures of molecules having different molecular structures and molar masses, and they may be quite different from each other in terms of composition and their physico-chemical properties. The resins more widely used in the cultural heritage field belong to the common family of terpenic structures, diterpenic and triterpenic, and form the basis of natural varnishes. The term varnish comes from the greek word βερνίκη or βερνίκη. In ancient times *Beronice* or *Berenice* was used to indicate amber. The name appears to be connected with the legend of Queen Berenice of Cyrene, whose amber-coloured hair was transformed in the homonymous constellation [4]. A different interpretation is offered which again makes reference to the Queen of Cyrene: in ancient times sandarac resin was called *berenice* and exported from that African coast, hence *berenice* and sandarac soon became equivalent terms [5]. From then on, in many places and for many centuries, identification and names of natural resins were often ambiguous or confusing, with attribution of the same name and properties to different substances. In particular, amber was confused with sandarac and later even with copal, up to the point that in Arab countries the word sandarac was used indistinctly for the different resins. *Berenice* in Latin became *vernix*, and in the Middle Ages this term took the meaning of sandarac and, more generally, of resin [4].

This also explains the origin of the term *vernice liquida*, occurring frequently in the early Italian recipes and mentioned by Cennini [6]: the solid resin (*vernix*) was dissolved in hot linseed oil to finally give a liquid formulation which was used not only as a varnish for paintings and metals, but also as ingredient for pigment binding.

Varnishes and lacquers prepared with plant resins dissolved in oils were known in China, India and Persia even before the time of Greek civilization, and it is likely that from the exchanges with those populations the Greeks learned about varnish application and properties. For a first historical reference, however, we must wait until the famous description by Pliny of the transparent varnish (*atramentum*) invented by Apelles for controlling the brilliance of colours and protecting the paintings from 'dust and dirt' [7]. Strangely enough, the secret of this process was not transmitted and there are no other mentions in Roman times about the use of varnishes in works of art, notwithstanding the fact that resins dissolved in vegetal oils were widely employed for pharmaceutical and cosmetic purposes.

Starting from the eighth century, historical records about resins and their use in varnish making appear in recipes collected from a number of manuscripts from the Middle Ages. It is not always possible to understand the exact nature of the resins mentioned in these ancient recipes, because the terms amber, mastic and sandarac were used indiscriminately, together with other names not in use today. Turpentine and different types of pine balsams were also available, and African copals were starting to reach the Mediterranean markets. Dating from the twelfth century and later the manuscripts contain recipes for preparation of the *vernice liquida*, which is mentioned by Cennini as universally adopted in Italy, and originally composed of sandarac dissolved in hot linseed oil, with other resins like colophony or incense occasionally added. Various modifications are found in the historical manuscripts, with description of the *vernice comune*, whose name was intended to differentiate it from *vernice liquida*. In all cases the principle was the same, still used today, for preparation of an oil varnish. Varnishes always consisted of a soluble resin, either sandarac or mastic or

colophony (*pece greca*, greek pitch), or two of them, dissolved in siccative oil, either linseed or nut [8]. With time, better appreciation of the effects of the different resins developed among users, and this may be one reason for the variety in the recipes. At the beginning of their use the oil-resin varnishes had quite dark colours which were considered in their use. The classical *vernice liquida*, sandarac in linseed oil, produced a reddish-brown coating which tended to be brittle and darkening with age. Addition of turpentine or of colophony was found to improve the varnish in several ways: dissolution of sandarac was facilitated, brittleness reduced, colour was less dark and appearance more brilliant. The search for colourless, or at least light-coloured varnish formulations, favoured the use of other resins, mastic in particular from which the so-called *white varnish* was produced. Mastic gives varnishes which are light-coloured, glossy and more elastic than those of sandarac. Again, improvements in the coating properties and in durability were often achieved with the addition of colophony. In some documents the name *white varnish* was used to indicate a varnish made by colophony alone, but among oil varnishes those based on mastic were probably the most widely used. Their better quality was so much recognized as to overcome the higher cost of the resin, which was about three times more than that of sandarac [1].

In Germany and in Flemish countries amber was initially the principal ingredient of oil varnishes. The northern part of Germany was the principal region of origin of amber, and this facilitated its use. Amber varnishes produced smooth and hard coatings, excellent resistance to humidity, and brilliant colour appearance. In the practice of Flemish painters amber was considered the most resistant among the varnishes which could be mixed with pigments dispersed in oil; the qualities of such varnishes were soon spread throughout different countries and Leonardo da Vinci wrote about the use of nut-oil and amber varnish [9]. The invention of oil painting by van Eyck, as described by Vasari in his famous book, derives from the search of a better varnish formulation, colourless and more siccative, which was subsequently found to be good for mixing colours to obtain a brilliant and waterproof binder [10].

In the eighteenth century spirit varnishes appear: the resins are dissolved in turpentine or natural naphtha, and later in alcohol. Recipes used by Flemish painters speak of Venice turpentine dissolved in spirits of turpentine, with occasional addition of sandarac, mastic, and oils [11]. Spirit-varnish resins with shellac became appreciated for their smooth finish and high polish. Treatises on varnish formulations blossomed in the eighteenth century due to increasing applications and market opportunities. The spirit varnishes find their optimal use on wooden manufactured goods, particularly in musical instruments, furniture, decorative objects, and even for treatment of natural science collections and archaeological findings. In addition, growing interest for the painted wooden panels imported from China and the spread of collections of Chinese objects brought attention to the techniques employed for such artworks [12]. Thenceforth trials for reproducing the secrets of *Chinese varnish* are countless and always based on natural resins dissolved in spirits and oils, often mixed with plant gums (arabic, adraganth, plum tree, cherry and others).

In the nineteenth century dammar, a soft resin derived from trees of southern Asia was introduced in Europe and used for making colourless varnish. Mixed with oil of turpentine it has become the preferred varnish for oil painting, due to its superior optical properties and better ageing stability than the other natural resins.

Thanks to their excellent optical, adhesive and protective properties, natural resins are still used by artists and restorers and are also frequently used as additives in the formulations of industrial paints or adhesives. However, the introduction of synthetic paints, starting from nitrocellulose (*pyroxylin*) lacquers, made available to the twentieth century artists a wide range of new materials which they have used as binding media, coatings and adhesives. Many types of synthetic varnishes were introduced, mostly composed of ketone or acrylic resins dissolved in mineral spirits. Advantages of such varnishes are their inherent higher stability compared with those based on natural resins. However, synthetic polymers may show poorer optical characteristics, and this has been attributed to the higher solution viscosities due to the high molecular weights of the polymers involved [13].

## 12.2 Py-GC/MS Characterization of Terpenoid Resins and Varnishes

### 12.2.1 Chemical Composition of Terpenoid Resins

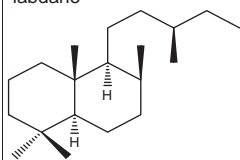
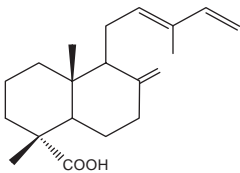
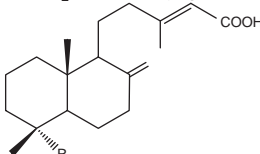
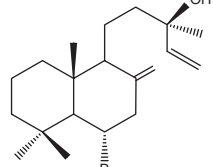
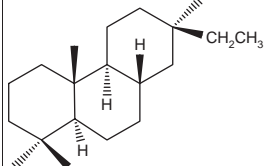
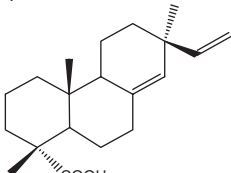
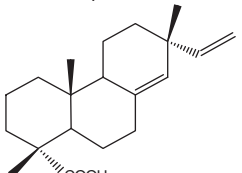
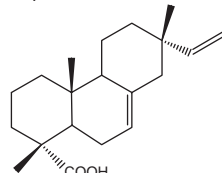
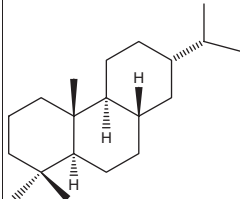
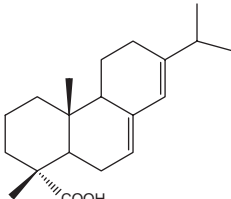
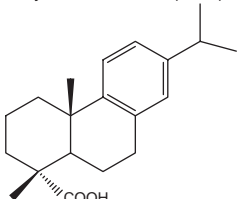
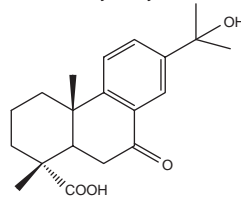
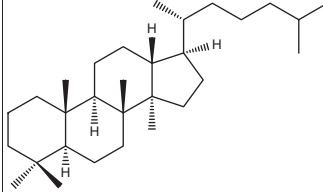
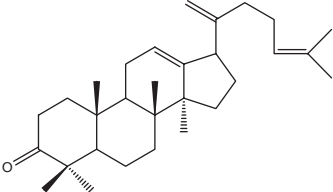
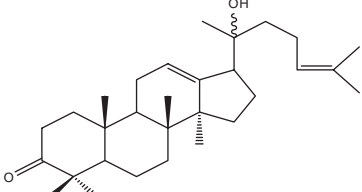
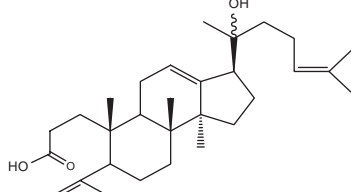
Most natural resins are complex mixtures of apolar terpenes, polar terpenoids and high molecular weight compounds. From a molecular point of view di- and triterpenes consist of four and six isoprene units, respectively. The terpenic skeleton can have extra functional groups resulting in a great variety of di- and triterpenoids which differ in the degree of unsaturation and in the number of oxygen atoms [14]. The structures of terpenic molecules have already been illustrated in Chapter 1, and may be seen here in Table 12.1. Diterpenoids can be classified into two main groups: labdanes which are bicyclic molecules with a highly reactive unsaturated C<sub>6</sub> side chain; and pimaranes and abietanes which are tricyclic acids (Table 12.1). The triterpenic fraction of natural resins mainly consists of compounds with dammarane, lanostane, oleanane and ursane type skeletons, whose chemical structures are reported in Table 12.1. Dammaranes and lanostanes are tetracyclic molecules with a C<sub>8</sub> aliphatic side chain, whilst oleanane and ursane type molecules are based on a pentacyclic aliphatic structure.

The characterization of natural resins is difficult not only because of their chemical heterogeneity, but also due to the different reactivity and ageing behaviour of the resin components. During ageing, the chemical composition of natural resins changes qualitatively and quantitatively because of oxidation, polymerization, isomerization and cleavage reactions. Furthermore, interactions with other painting materials, especially pigments, can influence the behaviour of varnishes and their degradation mechanisms.

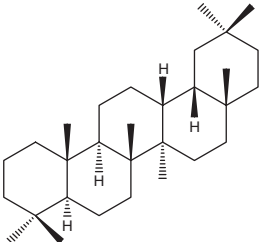
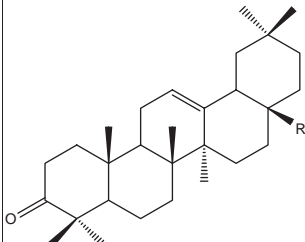
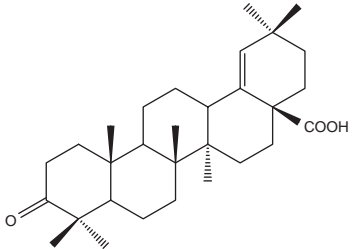
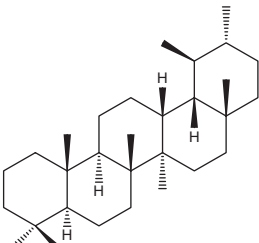
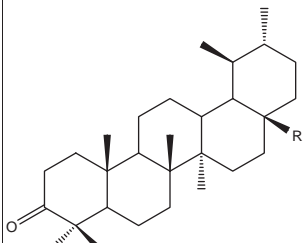
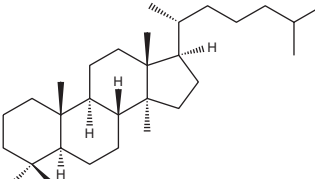
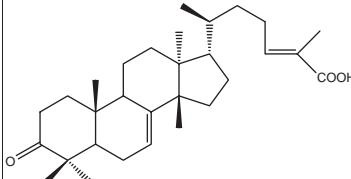
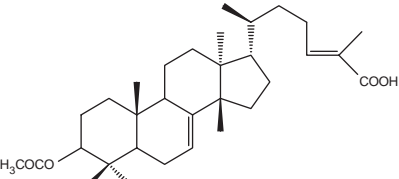
In the last few decades the composition and degradation of natural resin varnishes have been extensively investigated. Combined studies, carried out with different analytical techniques [15–18], have allowed the identification of a number of marker compounds, and several ageing processes, which fit the experimental results well, have been proposed [19–22]. Oxidation, proceeding via autoxidative radical chain reactions [23], has turned out to be one of the most important processes of degradation, causing darkening, yellowing, poor solubility, cracking and detachment.

The analytical technique of choice for the identification of low molecular weight terpenes and terpenoids is GC/MS, assisted by off-line methylation or silylation reactions. However, comparable results in terms of sensitivity and response specificity

**Table 12.1** Chemical structures of di- and triterpenoid components of natural resin varnishes

Basic terpene skeleton	Examples of terpenoid components of natural resins		
<p>labdane</p> 	<p><i>trans</i>-communic acid</p> 	<p>R = COOH agathic acid R = CH<sub>2</sub>OH agatholic acid R = CH<sub>2</sub>OAc acetoxyagatholic acid</p> 	<p>larixol R = OH larixyl acetate R = OAc</p> 
<p>pimarane</p> 	<p>pimaric acid</p> 	<p>sandaracopimaric acid</p> 	<p>isopimaric acid</p> 
<p>abietane</p> 	<p>abietic acid</p> 	<p>dehydroabietic acid (DHA)</p> 	<p>7-oxo-15-hydroxy-DHA</p> 
<p>dammarane</p> 	<p>dammaradienone</p> 	<p>hydroxydammarenone</p> 	<p>dammarenic acid</p> 

**Table 12.1** (continued)

<p>oleanane</p> 	<p>R = CHO oleanonic aldehyde R = COOH oleanonic acid</p> 	<p>moronic acid</p> 
<p>ursane</p> 	<p>R = CHO ursonic aldehyde R = COOH ursonic acid</p> 	
<p>lanostane</p> 	<p>(iso)masticadienonic acid</p> 	<p>3-O-acetyl-3-(iso)masticadienolic acid</p> 



can be achieved by thermally assisted hydrolysis and methylation (THM)-GC/MS that also, as additional advantages, does not need any sample pretreatment and is a well suited technique for the analysis of nonvolatile, polymeric and cross-linked components. The latter can result from cross-linking reactions of the original components or they can be already present in the native material as polymeric fractions. In effect, terpenoid resins can also contain natural polymers in different proportions depending on their botanical and geographical origin. The poly( $\beta$ -myrcene) fraction of mastic [24], for instance, can be detected only after separation from the raw resin, as its percentage is very low. Other resins, such as sandarac and copals, are almost entirely composed of polymeric material.

Numerous studies carried out in the last decade on fresh, artificially and naturally aged resins and varnishes have demonstrated that by means of THM-GC/MS a number of di- and triterperpenoids can be identified and, among them, the marker compounds that can be unequivocally used for resin recognition in real pictorial samples.

### 12.2.2 Analytical Pyrolysis Characterization of Fresh and Aged Di- and Triterpenic Resins

The terpenoid resins commonly used as artists' materials were colophony, Venice turpentine, mastic, dammar, copals and sandarac, and most of the scientific literature concerning the identification of Old Master varnishes and the study of their degradation focuses on these resins.

Colophony, also known as Greek pitch, is the solid residue obtained after distillation of resins of *Pinus* species and consists almost entirely of abietane and pimarane acids. The abietane type molecules, having conjugated double bonds, easily undergo oxidation reactions [25], while pimarane acids, lacking conjugated double bonds, are stable towards oxidation and isomerization. Characteristic marker compounds, especially in the aged resins, are the oxidation products of abietic acid, such as dehydroabietic acid (DHA), 7-oxo-DHA, 7-hydroxy-DHA, 15-hydroxy-DHA and 7-oxo-15-hydroxy-DHA. According to the ageing mechanism proposed by Pastorova *et al.* [19,26] oxidation starts on the double bonds of abietane diterpenoids to form DHA and continues by further incorporation of oxygen.

The THM-GC/MS traces of fresh and aged colophony are shown in Figure 12.1. Mono- and sesquiterpenoids, that are eluted in the first part of the pyrograms, are followed by various compounds of diterpenic nature, that can be ascribed to secondary pyrolysis products of the main diterpenoid acids and, for seriously degraded resins [27], to fragments resulting from photochemical or oxidation reactions. According to the various GC/MS procedures reported in the literature the most significant resinous acids (pimaric, sandaracopimaric, palustric, isopimaric, abietic and neoabietic acids) are eluted in the final part of the analysis. They are well separated and identified, except for laevopimaric acid, which easily isomerizes when it is heated or light irradiated [28,29]. In the same range of retention times the pyrogram of aged colophony shows additional peaks due to dehydrogenation (peaks 11 and 14 in Figure 12.1) and oxidation products of DHA (peaks 15, 17, 18 and 19 in Figure 12.1).

The composition of colophony is very similar to that of Venice turpentine, a resin exuded by *Larix* species; thus, in both cases the THM procedure is advisable in order to

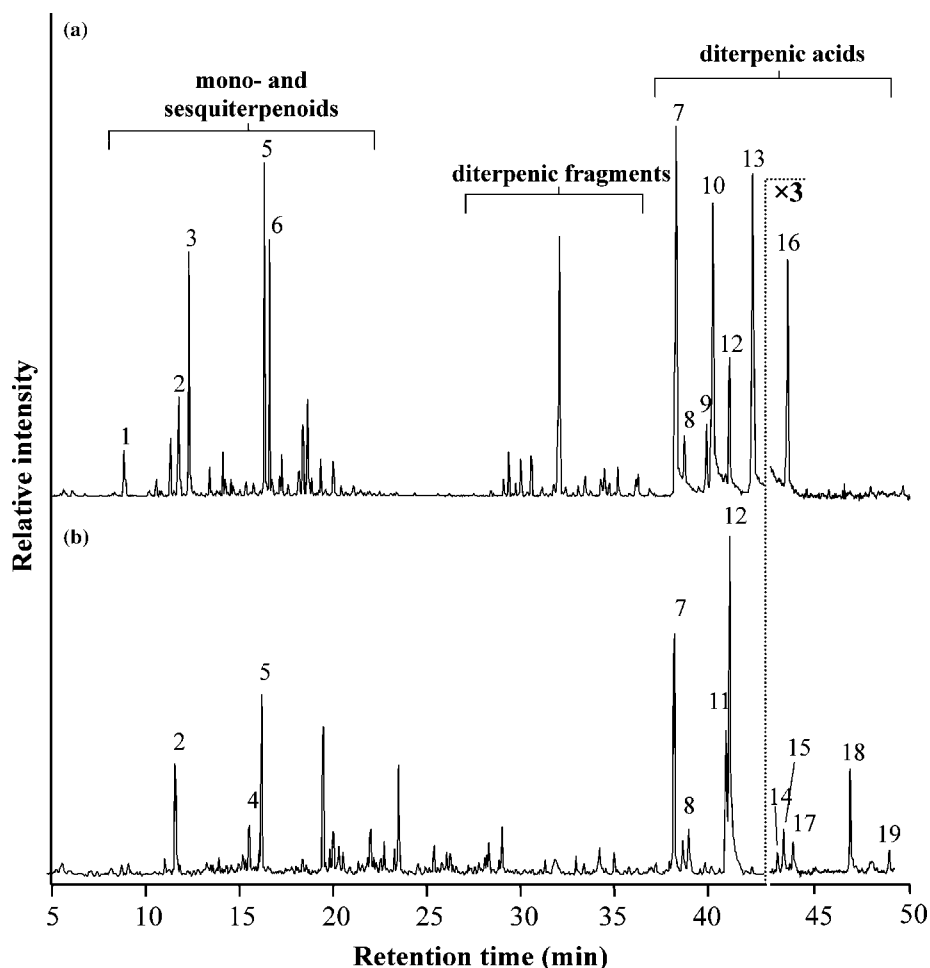


**Figure 12.1** THM-GC/MS curves of unaged (a) and naturally aged colophony (b). Peak assignments: 1, *p*-cymene; 2, norchrysantemic acid methyl ester; 3,  $\alpha$ -terpineol; 4, longicyclene; 5, longifolene; 6, caryophyllene; 7 pimaric acid methyl ester; 8, sandaracopimaric acid methyl ester; 9, palustric acid methyl ester; 10, isopimaric acid methyl ester; 11, 1,2,3,4,4a,10a-hexahydro-1,4a-dimethyl-7-(1-methylethyl)-phenanthrenecarboxylic acid methyl ester; 12, dehydroabietic acid (DHA) methyl ester; 13, abietic acid methyl ester; 14 1,2,3,4,4a-hexahydro-1,4a-dimethyl-7-(1-methylethenyl)-phenanthrenecarboxylic acid methyl ester; 15, 7-methoxy-DHA methyl ester; 16, neoabietic acid methyl ester; 17, 15-methoxy-DHA methyl ester; 18, 7-oxo-DHA methyl ester; 19, 7-oxo-15-hydroxy-DHA methyl ester. Reprinted from *J. Anal. Appl. Pyrol.*, **64**, Scalarone et al., 17, 2, Copyright 2002, with permission from Elsevier

transform acidic and alcoholic functionalities in the more volatile methyl ester derivatives. Venice turpentine, being a semiliquid resin, is composed of many mono- and sesquiterpenoids that are progressively lost during ageing. The diterpenic fraction is composed of abietane and pimarane acids, together with smaller amounts of labdane alcohols. As to be

expected on the basis of its chemical composition, Venice turpentine undergoes oxidation processes similar to colophony. The main effects of ageing are the decrease of the volatile fraction and the formation of oxidized diterpenoids such as 7-oxo-DHA, 7-hydroxy-DHA, 15-hydroxy-DHA and 7-oxo-15-hydroxy-DHA.

Characteristic markers of Venice turpentine are larixol and larixyl acetate, but in many cases they may remain undetected, as larixyl acetate hydrolyses and the methylation of hydroxyl groups is not as effective as for carboxylic acids. On-line derivatization with tetramethylammonium hydroxide (TMAH) is, for instance, scarcely effective on hydroxyl groups and involves a number of secondary reactions (isomerization, dehydration and cleavage of hydrolysable bonds) due to the strong alkalinity of the TMAH solution. When the experimental conditions are such that THM of labdanes occurs larixol and larixyl acetate are detected as a single peak since in the derivatization process larixyl acetate is hydrolysed to larixol [29].

Sandarac and copals are fossil resins which, apart from free diterpenoids, consist of a highly polymerized fraction of polycommunic acid or communic acid copolymerized with communol. They can be mixed with oils only after heating and subsequent decarboxylation and depolymerization of polycommunic acid. In particular, the popularity of copal varnishes increased in the second half of the nineteenth century when they were extensively used for varnishing coaches, woodwork and in general all articles requiring a tough coating. The main problems connected with the use of 'hard' varnishes, especially if dissolved in drying oils, are the yellowing and the inability to remove them properly.

Though the use of copals and sandarac as painting materials is documented in a number of historical sources, it is extremely difficult to detect them experimentally. The main factors complicating the recognition of such resins in real paint samples are their insolubility, the fact that they were often used in combination with other natural products, the high temperatures required for the preparation of oil varnishes and the degradation processes occurring during ageing.

GC/MS has given poor results in the analysis of copals and sandarac because using this technique only the low molecular weight fraction, which is mainly composed of labdane type molecules and sandaracopimaric acid, can be identified. To determine the nature and composition of the cross-linked fraction analytical pyrolysis is required [30,31]. The most important pyrolysis products of Manila copal and sandarac include both free diterpenoids and pyrolysis fragments of the polycommunic acid fraction. Among free diterpenoids the most abundant ones are sandaracopimaric acid, agathic acid and its monomethyl ester, agathalic acid and acetoxyl agatholic acid. Free *cis*- and *trans*-communic acids are only in traces, as demonstrated by comparison with GC/MS data [32] (Figure 12.2a). The main pyrolysis products of polycommunic acid include the monomer, communic acid, and bicyclic acids, such as 1,4a,6-trimethyl-1,2,3,4,4a,7,8,8a-octahydro-naphthalencarboxylic acid, 1,4a,6-trimethyl-5-methylene-1,2,3,4,4a,5,8,8a-octahydro-naphthalencarboxylic acid, 1,4a,5,6-tetramethyl-1,2,3,4,4a,7,8,8a-octahydro-naphthalencarboxylic acid, 5-ethyl-1,4a,6-trimethyl-1,2,3,4-tetrahydro-naphthalencarboxylic acid and 5-(3-methyl-but-2-enyl)-6-methylene-1,4a,6-trimethyl-decahydro-naphthalencarboxylic acid, generated by breakage and loss of the unsaturated side chain of communic acid (Figure 12.2b). These fragments, which are produced in considerable amount, can be used as markers for both resins.

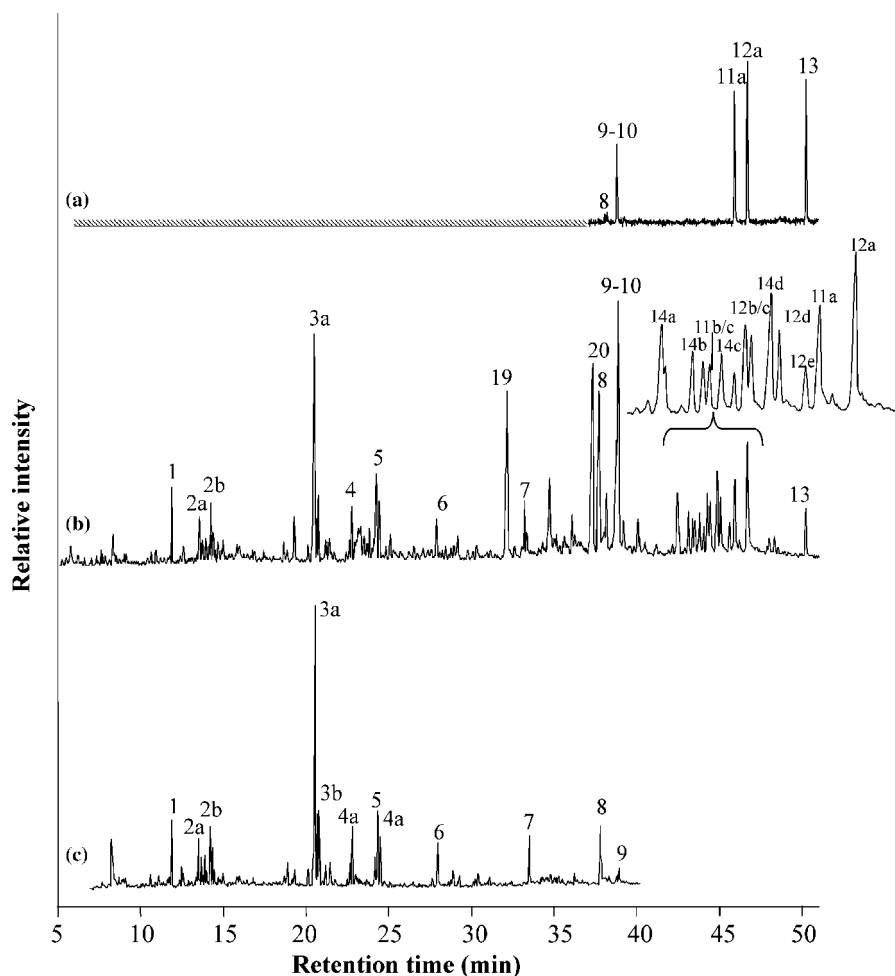


**Figure 12.2** (a) GC/MS curve of the soluble fraction of Manila copal obtained after methylation with TMS-diazomethane; (b) THM-GC/MS curve of Manila copal resin; (c) THM-GC/MS curves of the polymer fraction isolated from Manila copal. Peak assignments: 1, 1,3-dimethyl-cyclohexa-2-en-carboxylic acid methyl ester; 2a,b, 1,2,3-trimethyl-cyclohexa-2-en-carboxylic acid methyl ester and isomer; 3a,b, 1,4a,6-trimethyl-1,2,3,4,4a,7,8,8a-octahydro-naphthalen-carboxylic acid methyl ester and isomer; 4, 1,4a,6-trimethyl-1,2,3,4,4a,5,8,8a-octahydro-naphthalen-carboxylic acid methyl ester; 5, 1,4a,5,6-tetramethyl-1,2,3,4,4a,7,8,8a-octahydro-naphthalen-carboxylic acid methyl ester; 6, 5-ethyl-1,4a,6-trimethyl-1,2,3,4- tetrahydro-naphthalen-carboxylic acid methyl ester; 7, 5-(3-methyl-but-2-enyl)-6-methylene-1,4a,6-trimethyl-decahydro-naphthalen-carboxylic acid methyl ester; 8, *cis*-communic acid methyl ester; 9, *trans*-communic acid methyl ester; 10, sandaracopimaric acid methyl ester; 11a–c, agathalic acid methyl ester and isomers; 12a–e, agatholic acid dimethyl ester and isomers; 13, acetoxo agatholic acid methyl ester; 14a–d, 5-(5-methoxymethyl-5,8a-dimethyl-2-methylene-decahydro-naphthalen-1-yl)-3-methyl-pent-2-enoic acid methyl ester and isomers. Reprinted from *J. Anal. Appl. Pyrol.*, **68–69**, Scalarone et al., 22, 2, Copyright 2003 with permission from Elsevier

By THM-GC/MS high and low molecular weight components can be identified simultaneously. The pyrogram in Figure 12.2c show signals due to free diterpenoids and the polymer fraction. The main disadvantage of this technique, especially if compared with conventional GC, is the large number of substances that originate from the pyrolysis process. Free diterpenoid acids easily undergo secondary pyrolysis reactions, such as fragmentation, isomerization and recombination reactions that result in the appearance of a large number of peaks.

As an alternative, a two-step Py-GC/MS technique can be applied allowing the identification of volatile diterpenoids in the first step and of the polymeric fraction in the second step [33]. The procedure involves an on-line derivatization at 250°C with TMAH, followed by the pyrolysis of the remaining high molecular weight fraction.

In light-aged sandarac and copal varnishes, the amount of free diterpenoids is largely reduced, but some additional diterpenoids appear: 19-norlabda-8(20),13-dien-15-oic acid, that might derive from agathalic and agathic acids by loss of the aldehydic and carboxylic groups in C4, 19-norlabda-4,8(20),13-trien-15-oic acid, that is the dehydrogenation product of 19-norlabda-8(20),13-dien-15-oic acid, that is reasonably the hydrolysis product of acetoxy agatholic acid [32]. As for the polycommunic acid component, in the pyrograms of the light-aged resins the relative intensity of communic acids decreases and they totally disappear after a long artificial ageing, while the intensity of the smaller pyrolysis fragments of the polymer fraction remain unchanged. This result has been attributed to the formation of a highly cross-linked network of interconnected bicyclic units and alkyl bridges, similar to the maturation process of polylabdanoids in fossil resins [34–36].

As regards triterpenic resins, the most important ones used as art materials are mastic and dammar. The latter, in particular, is still used by many contemporary artists and restorers.

Dammar is produced by trees belonging to the Dipterocarpaceae family. It is mainly composed of triterpenoids, but it also contains a polymeric fraction based on polycadinene, a polysesquiterpene [37,38]. The main components of the triterpene fraction are compounds with a dammarane type skeleton and oleanane/ursane type molecules [39,40].

The potentialities of THM-GC/MS in the analysis of triterpenic resins are limited when compared with conventional GC/MS procedures. Sensitivity is low and a number of interference peaks, especially in the range of retention times of triterpenoid molecules, complicate the interpretation of the pyrograms. The situation is particularly critical when aged resins are analysed; oxidized terpenoids, being polar and low volatile, are partially trapped in the pyrolysis chamber, thus lowering the signal to noise ratio (Figure 12.3). In particular, the three characteristic oxidation products of hydroxydammaranone, 20,24-epoxy-25-hydroxy-3,4-seco-4(28)-dammaran-3-oic acid, 20,24-epoxy-25-hydroxy-dammaran-3-one and 3-oxo-25,26,27-trisnor-dammarane-20,24-lactone, are hardly detected when pyrolysis is coupled with GC/MS. This may be ascribed to the pyrolytic cleavage of the substituted tetrahydrofuran and  $\gamma$ -lactone side groups and to dehydration of the sterically hindered OH group in ocotillone type molecules when alkaline reagents are present. This last reaction also occurs with hydroxydammaranone and dammaranolic acid [41] and explains the lower GC/MS response of the two compounds when THM is applied. Despite these problems THM-GC/MS as a whole is sensitive enough to identify dammar in complex multicomponent samples and to differentiate dammar from other triterpenic resins and especially from mastic.

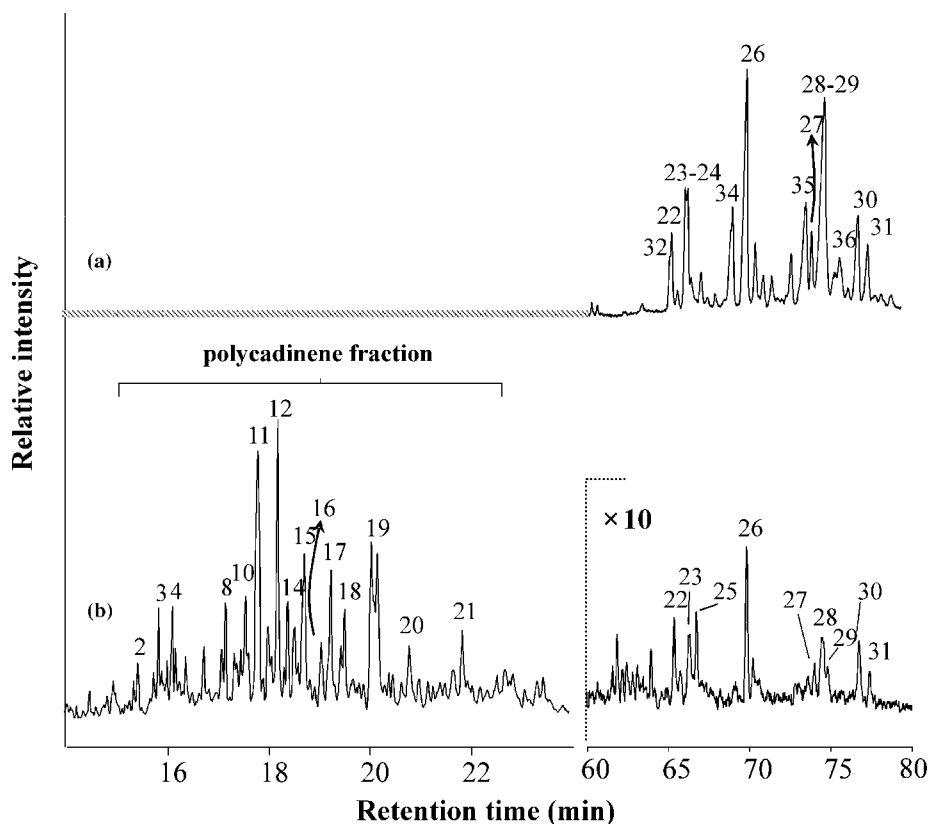


**Figure 12.3** GC/MS (a) and THM-GC/MS (b) curves of aged dammar. Peak assignments: 2,  $\alpha$ -cubebene; 3, copaene; 4,  $\beta$ -bourbonene; 8,10–12, cadinane type pyrolysis fragments; 14–16, cadinene type pyrolysis fragments; 17, calamanene type pyrolysis fragments; 18–21, unidentified sesquiterpenoids; 22, dammaradienone; 23, dammaradienol; 24, nor- $\alpha$ -amyrene; 25, 28-nor-olean-17-en-3-one; 26, dammarenolic acid methyl ester; 27, oleanonic acid; 28, hydroxydammarenone; 29, oleanonic aldehyde; 30, ursonic acid methyl ester; 31, ursonic aldehyde; 32, nor- $\beta$ -amyrene; 34, 20,24-epoxy-25-hydroxy-3,4-seco-4(28)-dammaren-3-oic acid methyl ester; 35, 20,24-epoxy-25-hydroxy-dammaren-3-one; 36, dammaradienol

Under pyrolysis conditions the polycadinene fraction, if not eliminated during the manufacturing of the varnish, undergoes depolymerization. Pyrolytic decomposition of polycadinene proceeds through the cleavage of bonds in the allylic position, resulting in the formation of  $C_{15}$ ,  $C_{30}$  and  $C_{45}$  fragments. The main pyrolysis products identified by THM-GC/MS are molecules with a cadinane type skeleton and with one to four double bonds (Figure 12.3). By direct temperature mass spectrometry (DTMS) of raw dammar cadinene monomers, dimers, trimers and tetramers have been detected, as well as oxidized oligomers when light aged samples were analysed [38].

The composition of mastic is similar to that of dammar. Experimental data obtained by THM-GC/MS (Figure 12.4) indicate that mastic is mainly composed by oleanonic

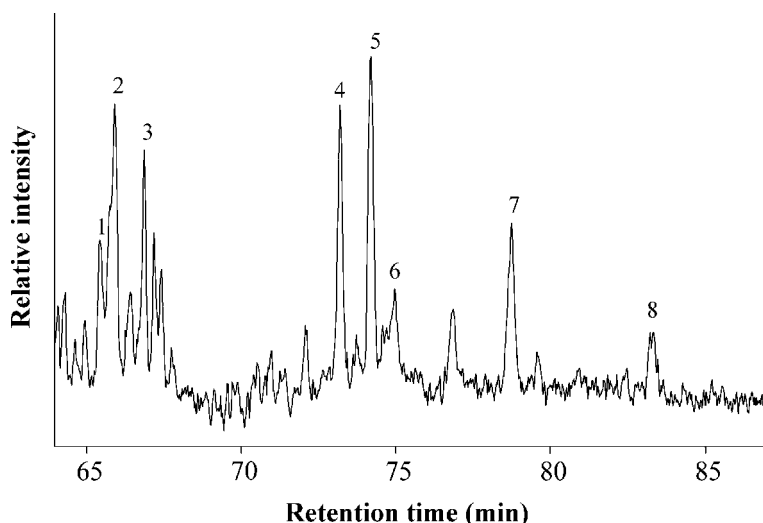


**Figure 12.4** THM-GC/MS curve of mastic resin. Peak assignments: 1, *nor-β-amyrone*; 2, *(8R)-3-oxo-hydroxypolipoda-13E,17E,21-triene*; 3, *nor-28-olean-18-en-3-one*; 4, *moronic acid methyl ester*; 5, *oleanonic acid methyl ester*; 6, *oleanonic aldehyde*; 7,8, *(iso)masticdienonic acid methyl ester*

aldehyde, moronic, oleanonic and masticdienonic acids. The dammarane compounds, hydroxydammarone (6) and its oxidation products, remain undetected.

Several studies have dealt with the problem of discriminating between mastic and dammar, and three marker compounds of mastic have been identified: moronic, masticdienonic and acetyl masticdienonic acids [42]. The chemical structure of (iso)masticdienonic acid and 3-*O*-acetyl-3-*epi*-(iso)masticdienonic acid is characterized by a side chain, as for dammarane molecules, but with a carboxylic acid end group (Table 12.1). Under pyrolysis conditions this side chain is susceptible to cleavage as demonstrated by the presence, among the pyrolysis products of mastic, of 2-methyl-pent-2,4-dienoic acid, that perfectly matches with the chemical structure of the side chain end. In addition 3-*O*-acetyl-3-*epi*-(iso)masticdienonic acid also loses the acetyl group and, in contrast to masticdienonic acid, is not detected at all.

### 12.2.3 On-line Derivatization Methods and Reagents for Py-GC/MS

In the last decade modifications to the pyrolysis process have been developed to improve analytical efficiency and increase detectability. In the same way as in conventional GC, derivatization reagents may be used to improve the chromatographic separation and response of polar compounds. In order to reduce the time required for the analysis, the risk of contamination and of losing part of the sample, on-line derivatization methods should be preferred and those based on quaternary ammonium hydroxides are certainly the most widely used.

THM using TMAH has been applied successfully to a variety of samples ranging from natural organic substances to synthetic polymers [43,44]. The method is based on the high

temperature reaction of the quaternary alkylammonium hydroxide with molecules containing functional groups, carboxylic acids, ethers and esters especially, which are susceptible to hydrolysis and methylation. According to the reaction scheme proposed by Kossa *et al.* [45] the thermally assisted methylation of acidic groups involves deprotonation of the acids by the reagent and formation of the quaternary ammonium salts of the acidic groups that immediately thermally decompose into the corresponding methyl esters and tertiary amines. With esters or ethers high-temperature hydrolysis by reaction of the basic TMAH precedes the formation of tetra-alkylammonium salts that then undergo thermal fragmentation to methyl derivatives [46].

Despite its utility the THM process employing TMAH also shows some defects. Measurements are less specific, especially from a quantitative point of view, as the effectiveness of the methylation reaction varies according to the chemical structure of the analytes, the solvent chosen for the TMAH solution and the pyrolysis temperature used [47]. Recombination of the pyrolysis products can also occur, together with the formation of differently methylated isomers and the degradation of alkaline-sensitive compounds. The formation of trans–trans polyunsaturated isomers in oils, for example, has been attributed to base catalysed and thermally induced isomerization of unsaturated fatty acids [48]. The base catalysed isomerization is believed to be caused by excess TMAH and the high temperature required during THM. This can be reduced by adding acetic acid or methyl acetate that react with the excess TMAH, or by reducing the pyrolysis temperature. When TMAH is used to methylate terpenoid acids containing ketone groups, the methylated enol tautomer can form resulting in extra chromatographic peaks whose number and intensity may vary depending on the applied experimental conditions [19].

In the last 10 years, alternative derivatization reagents have been tested and proved to give good results in very specific applications. Less alkaline tetramethylammonium compounds, such as tetramethylammonium acetate (TMAAc) and tetramethylsulfonium hydroxide (TMSH) were found to successfully methylate free fatty acids and to reduce unwanted isomerization reactions [49,50]. The low basicity of (*m*-trifluoromethylphenyl) trimethylammonium hydroxide (TFTMTH) and the lower temperature required for methylation were reported to reduce considerably the isomerization of polyunsaturated fatty acids [51], even if this conclusion cannot be extended to terpenoid resins. de la Rie and Watts [41] have compared TMAH and TFTMTH on-line methylation within the pyrolysis interface, applied to the analysis of triterpenoid standards and dammar. In general, with quaternary ammonium hydroxide reagents the derivatization of OH groups is difficult, especially when the OH is sterically hindered as in the dammarane side chain. In this respect, TFTMTH, being a weaker base than TMAH, is less efficient in methylating samples. Moreover, underivatized hydroxyl groups easily dehydrate and isomerize and this results in additional derivatization products besides the fully methylated ones. As already discussed for TMAH in the previous section, the detection of the marker compounds in aged dammar varnish is a problematic task with TFTMTH on-line methylation. Characteristic ageing products with ocotillone structure and methyl ursonate have been identified, but the corresponding chromatographic peaks are not very intense and sometimes they are poorly resolved from additional unidentified compounds. These problems, together with low reproducibility of the results, limit the applicability of quaternary ammonium



hydroxides to the pyrolysis of triterpenoid resins, although further and more systematic work is necessary and desirable in order to optimize the procedure.

Another common derivatization method applied to GC is silylation. Silylation reduces the polarity of the compound, as well as hydrogen bonding, and consists of the replacement of active hydrogens by silyl groups. Silylated derivatives are thus more volatile and stable than the corresponding underivatized precursors, and detection is enhanced. The trimethylsilyl group is the most popular one for gas chromatographic applications and the two preferred reagents for trimethylsilylation are hexamethyldisilazane (HMDS) and *N,O*-bis(trimethylsilyl)trifluoroacetamide (BSTFA).

First attempts to combine pyrolysis with *in situ* HMDS silylation of organic art materials were reported by Chiavari *et al.*, who were successful in obtaining trimethylsilyl derivatives of fatty acids [52], amino acids [53] and carbohydrates [54]. The same authors also applied pyrolysis-silylation to the analysis of different kinds of natural resins and for each of them diagnostic silylated compounds were identified, even if many were difficult to assign precise structures [55].

HMDS is a mild reagent compared with the stronger alkaline TMAH. However, the pyrograms obtained with HMDS on-line silylation show a higher number of peaks compared with the runs without derivatization. The effect of HMDS appears to be that of transforming many pyrolysis products into volatile molecules, but also of inducing more fragmentation. In addition, decarboxylation and partial silylation, especially in the presence of hindered hydroxyl groups, further increase the number of pyrolysis products [56]. Another problem in on-line pyrolysis-silylation with HMDS is the memory effect. It was found that using HMDS, whose boiling point is 125°C, the optimum interface temperature for avoiding fast volatilization of the reagent and enabling thermal extraction of trimethylsilyl (TMS) derivatives is 150°C, instead of the 250–280°C set in standard pyrolysis methods. However, under these conditions low volatile fragments, for instance high molecular weight, polar or partially silylated compounds, may be trapped in the interface and then released in the following runs.

More recently on-line pyrolysis with HMDS has been performed successfully even if the pyrolysis interface was kept at 250°C. In fact, Doménech-Carbó and colleagues [57,58] have obtained very good results on a variety of art materials and on real paint samples as well. They have applied Py-GC/MS with on-line trimethylsilylation to the characterization of diterpenoid resins and, in contrast to previous literature data, the derivatization method enabled not only the identification of resinous carboxylic acids in the form of TMS esters, but also an efficient conversion of hydroxyl groups to TMS ethers.

Although HMDS seems to promote dehydration more than TMAH, the number of side reactions occurring upon methylation of diterpenoids is reduced by using trimethylsilylation and as a consequence more simplified chromatograms are obtained. This is in addition to a general improvement in sensitivity and better resolution of some representative peaks.

In Pinaceae resins, for instance, fully trimethylsilylated derivatives of 7-hydroxy-DHA, 15-hydroxy-DHA and 15-hydroxy-7-oxo-DHA have been identified, as well as all the other abietadiene and pimaradiene acids present in these resins. The derivatization was ineffective on some labdane alcohols such as larixyl acetate, a marker compound for Venice turpentine, but in general labdane compounds have been identified in their trimethylsilylated form. Labdane acids, such as communic, agathic, agathalic, agatholic and acetoxy agatholic acids, that are among the most important constituents of sandarac

and Manila copal, have been successfully silylated and also the acidic fragments resulting from the pyrolysis of polycommunic acid, according to the pathway proposed by Scalarone *et al.* [38], have been detected as TMS esters.

The use of HMDS as a derivatization reagent in the analysis of triterpenoid resins has been less explored. The TMS derivatives of triterpenoids bearing hydroxyl groups [ $\alpha$ -amyrine,  $\beta$ -amyrine and hop-22(29)-en-3 $\beta$ -ol] have been identified in the triterpenic fraction of Burseraceae resins, thus demonstrating that HMDS combined with Py-GC/MS is effective in the derivatization of triterpenoid compounds [59]. However, the range of structures that can be fully derivatized and detected must be extended and, in order to get comprehensive results comparable with those coming from the well assessed off-line GC/MS procedures, general improvements in the on-line trimethylsilylation-pyrolysis method are needed.

At present on-line trimethylsilylation with HMDS in the presence of trimethylchlorosilane (TMCS) as a catalyst is under investigation and preliminary results show a great improvement in the conversion of OH groups in multihydroxylic molecules to the corresponding pertrimethylsilyl derivatives [60]. The use of TMCS in combination with HMDS is already recommended in off-line derivatization for GC because it increases the silylating power of the reagent on account of the chlorine atom, which is a good leaving group in the nucleophilic derivatization process. The catalytic effect of TMCS facilitates the silylation of primary, secondary and tertiary alcohols in order, and that of hindered hydroxyls which would not be completely derivatized by HMDS alone.

BSTFA is considered a reagent particularly efficient for silylation of –OH groups prior to gas chromatographic analysis [61]. In comparison with HMDS, the main advantage for pyrolysis and on-line derivatization should be its high boiling point which allows the pyrolysis interface to be set at 280°C without any risk of losing the reagent before the derivatization and thus making easier the transfer of high molecular mass fragments to the GC column. BSTFA has been used in the on-line trimethylsilylation and pyrolysis of phenolic and alcoholic hydroxyl groups in lignin [62]. Recent studies on analytical pyrolysis of monosaccharides in the presence of BSTFA [60] show that the silylating efficiency decreases with increasing number of hydroxyl groups in the molecule.

The goal for the future is to set and optimize on-line silylation methods with improved silylation efficiency. As silylated derivatives are expected to be more volatile and stable, detection should be enhanced making this method of great potential interest in the cultural heritage field where tiny amounts of sample are available.

### 12.3 Py-GC/MS of Modern Polymer Paint Varnishes

As discussed in the previous sections, natural resins undergo photo-oxidation processes that increase their polarity and, depending on the specific type of resin, cause cross-linking or breakage of chemical bonds, with possible loss of volatile fragments and changes in molecular weight. The consequences from the point of view of the conservation practise are the reduced solubility and reversibility of old varnishes, yellowing, darkening and brittleness.

It is obvious that natural resins did not satisfy the requirements an 'ideal' varnish should have. This is why at the beginning of the twentieth century, when synthetic polymers reached the market and were acknowledged as stable materials compared with natural organic substances, they soon attracted the attention of both artists and restorers.

The first synthetic polymers to be used as paint varnishes were acrylic and vinylic resins. Poly(vinyl acetate) (PVAc), commercialized under the name Mowilith by Hoechst and Vinylite by Union Carbide, has been used in conservation as an adhesive since 1932 and in 1937 it was proposed as a picture varnish by Stout and Cross [63]. PVAc was soon rejected as a varnish because, despite its light stability and good solubility in organic solvents, it demonstrated poor optical properties in terms of colour saturation and the tendency to pick up dirt due to its low glass transition temperature.

Under pyrolysis PVAc degrades through a side-group elimination mechanism. Side-group elimination is a two-stage process. The loss of acetic acid, leaving an unsaturated polymer chain, is followed by further degradation of the resulting polyene, essentially through scission and aromatization reactions. The pyrogram of a Mowilith 30 sample in Figure 12.5 shows that acetic acid, aromatic compounds (benzene, styrene) and polycyclic aromatic hydrocarbons (naphthalene, biphenyl, indene, fluorene, anthracene) are the most characteristic pyrolysis products of PVAc.

Poly(butyl methacrylate) (PBMA) began to be used as a picture varnish in the early 1930s. It encountered a considerable success because of its resistance to yellowing, adequate flexibility, no dirt pick-up and good solubility in nonpolar hydrocarbon solvents. Products based on PBMA, such as Elvacite 2044 and Elvacite 2045 by Du Pont, were abandoned when it was discovered that under light exposure they cross-link to an unexpected extent becoming insoluble [64]. From this point of view acrylic copolymers based on methyl and ethyl acrylates/methacrylates show a much better long-term stability.

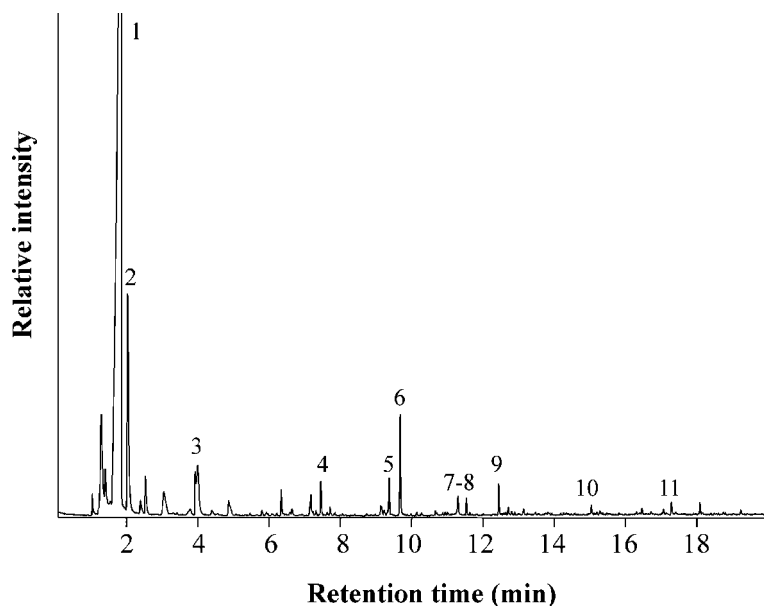


**Figure 12.5** Pyrogram of Mowilith 30, a vinyl acetate polymer used in conservation. Peak assignments: 1, acetic acid; 2, benzene; 3, styrene; 4, indene; 5, 1,2-dihydro-naphthalene; 6, naphthalene; 7, 2-methyl-naphthalene; 8, 1-methyl-naphthalene; 9, biphenyl; 10, fluorene; 11, anthracene

Methacrylic polymers in general can be easily identified by Py-GC/MS because at temperatures higher than 400°C they degrade by unzipping, a mechanism of depolymerization in which the polymer essentially reverts to monomers [65]. Thus the main pyrolysis product of Elvacite 2044 is BMA.

Under the same conditions acrylate polymers degrade to monomers and oligomers. The presence of tertiary hydrogen atoms prone to radical abstraction results in the formation of free radicals along the polymer chain and then in the production of oligomers. It follows that in acrylate-methacrylate copolymers, where the two described degradation processes are combined, the main pyrolysis products are the corresponding acrylic and methacrylic monomers, but oligomers of different length are also released [66,67]. The characteristic pyrolysis fragments of Paraloid B72 (Rohm & Haas), a poly(ethyl methacrylate-*co*-methyl acrylate) (EMA-*co*-MA), are MA and EMA (Figure 12.6). Besides the monomer peaks, the pyrogram in Figure 12.6 shows relatively intense peaks assigned to secondary pyrolysis products of the monomeric units (i.e. MMA). At higher retention times sesquimers and dimers are eluted, followed by six peaks of trimers.

Despite their good performance in terms of stability, acrylic coatings change the appearance of a painting. Gloss and colour saturation are reduced in comparison with traditional resin varnishes due to the increased light scattering at the surface. This effect has been studied in detail by de la Rie [68,69] who has demonstrated that the key parameter affecting the surface appearance is the molecular weight of the varnish. In general, the lower the molecular weight of a resin, the better is its capability of reducing surface roughness and light scattering.

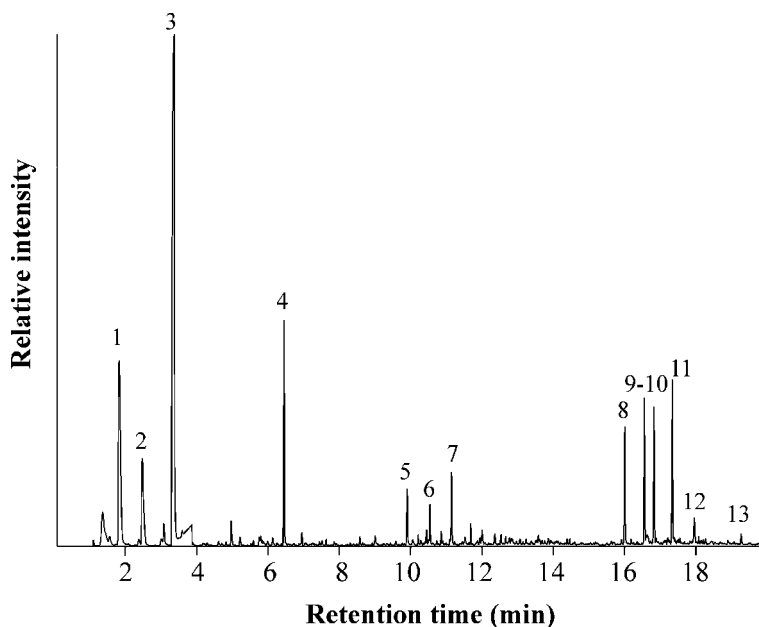


**Figure 12.6** Pyrogram of Paraloid B72. Peak assignments: 1, MA; 2, MMA; 3, EMA; 4, BMA; 5, MA dimer; 6, EMA-MA sesquimer; 7, EMA-MA dimer; 8, MA trimer; 9–11, MA-MA-EMA or MA-EMA-MA or EMA-MA-MA trimers; 12, EMA-MA-EMA trimer; 13, EMA trimer

From this point of view low molecular weight (LMW) synthetic resins are able to mimic natural resins better than the acrylic ones. Another point in favour of LMW resins is that cross-linking does not have a great influence on their solubility. The search for LMW resins with high refractive indexes and good solubility in aliphatic hydrocarbon solvents ended with the selection of some suitable products for use in picture varnish. Ketone or polycyclohexanone resins [AW2 (BASF), MS2 (Laport Industries), Ketone Resin N (BASF), Laropal K80 (BASF)], generally sold as additives to improve the gloss and hardness of industrial paints and coatings, have been used to varnish paintings since the 1950s [70]. Reduced ketone resins (MS2A and MS2B by Laport Industries), in which the ketone group is reduced to hydroxyl, were introduced in the 1960s. These were more photochemically stable than ketone resins, but also more brittle because of the increased hydrogen bonding.

Py-GC/MS of Laropal K80 results in a number of intense oligomeric fragments, while smaller fragments are minor pyrolysis products [71]. Cyclohexene, cyclohexanol, cyclohexanone, methyl-cyclohexanone and methylene-cyclohexanone can be attributed to secondary pyrolysis products of the monomeric units (Figure 12.7). The most intense

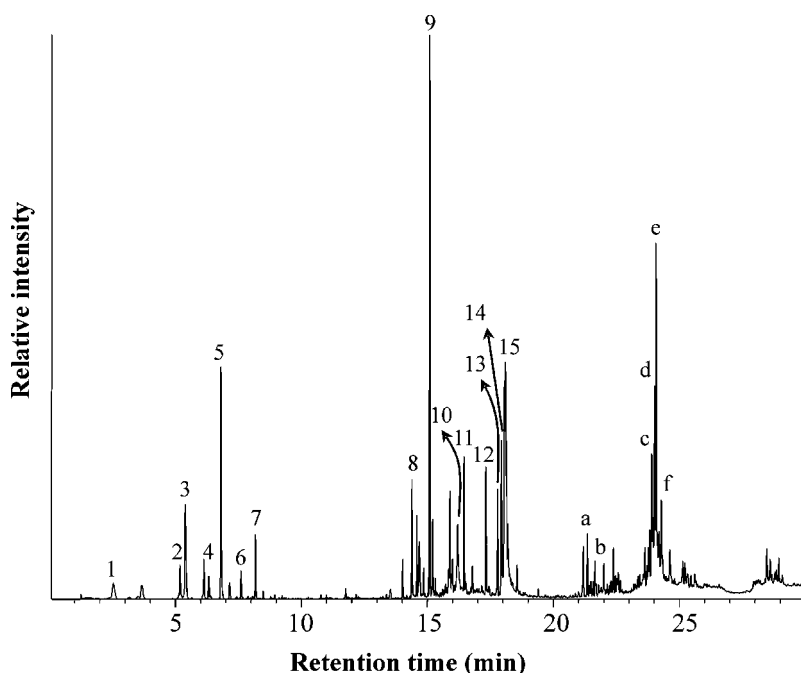


**Figure 12.7** Pyrogram of Laropal K80. Peak assignments: 1, cyclohexene; 2, cyclohexanol; 3, cyclohexanone; 4, 2-methyl-cyclohexanone; 5, 2-methylene-cyclohexanone; 6, 2-methyl-6-methylene-cyclohexanone; 7, 2,6-dimethylene-cyclohexanone; 8, cyclohexenyl-cyclohexanol; 9, cyclohexenylmethyl-cyclohexanone; 10, cyclohexanolmethyl-cyclohexanone; 11, 2-methylene-6-cyclohexenylmethyl-cyclohexanone; 12, 13, 2,2'-methylenebiscyclohexanone; 14, 15, 2,2'-methylenebiscyclohexanol. Peaks labelled with letters, and having mass spectra with molecular ions  $m/z=302$  and  $m/z=304$ , have been assigned to tricyclic cyclohexanone based molecules

peak of the Py-GC/MS trace of Laropal K80 has been identified as (cyclohexenylmethyl)-cyclohexanone. In the same range of retention times other dicyclic ketone fragments have been identified (2,2'-methylenebiscyclohexanone and 2-methylene-6-cyclohexylmethyl-cyclohexanone) and other peaks have been tentatively assigned to cyclohexanol derivatives (cyclohexenyl-cyclohexanol, cyclohexanolmethyl-cyclohexanone, 2,2'-methylenebiscyclohexanol). The higher oligomeric segments, eluted at higher retention times, are difficult to identify because they often co-elute and their mass spectra are unknown. However, analysis of their mass spectra suggests that most of them are isomers and fragments with similar chemical structure. Compounds labelled a–f in Figure 12.7 are probably tricyclic cyclohexanone based molecules.

In the 1990s another type of LMW resins, hydrogenated hydrocarbon resins, was produced and in a short time it became extensively used for varnishing because of its excellent stability. These resins were obtained by oligomerization of unsaturated hydrocarbons or by oligomerization of  $\alpha$ -methyl styrene and its isomers, followed by hydrogenation, in order to remove residual double bonds. Figure 12.8 shows the pyrogram obtained from Regalrez 1094 (Eastman). It is characterized by three groups of peaks; the first group includes a variety of alkyl substituted cyclohexane and cyclohexene molecules, whilst the second and the third groups include bigger molecules, not fully identified, but possibly ascribed to dimers and higher oligomeric fragments of the hydrogenated hydrocarbon resin.

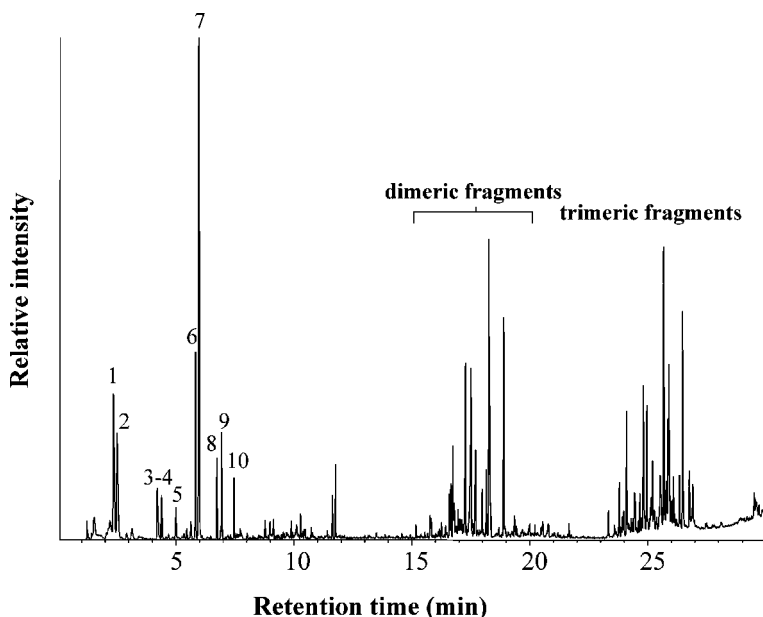


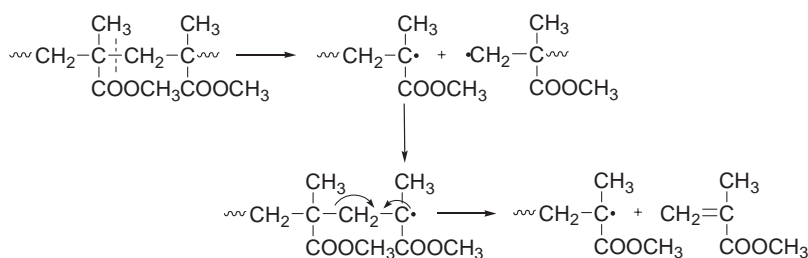
**Figure 12.8** Pyrogram of Regalrez 1094. Peak assignments: 1, cyclohexane; 2, cyclohexene; 3, ethenyl-cyclohexane; 4, ethyl-cyclohexane; 5, ethylidene-cyclohexane; 6, 1-methylethyl-cyclohexane; 7, 1-methylethyl-cyclohexene; 8, 1-methylethylidene-cyclohexane; 9, 1,1-dimethylethyl-cyclohexane; 10, 1,2-propadienyl-cyclohexane

## 12.4 Py-GC/MS Applied to the Analysis of Synthetic Polymers used in Art and Conservation

The application of analytical pyrolysis to the study of polymer materials is traditionally devoted to compositional characterization. This may be dated back to the historical experiments of Michael Faraday, who in 1826 determined the hydrocarbon composition of natural rubber by dry distillation of caoutchouc [72], and of Greville Williams, who 30 years later named isoprene the lightest product of natural rubber thermal decomposition concluding that the caoutchouc hydrocarbon is an isoprene polymeric compound [73].

Pyrolysis products of synthetic polymers are in most cases complex mixtures of substances reflecting the original chemical structures in ways which depend on the specific decomposition mechanisms of the compounds. The following three main categories of thermal degradation processes may be envisaged for polymer systems [74]:

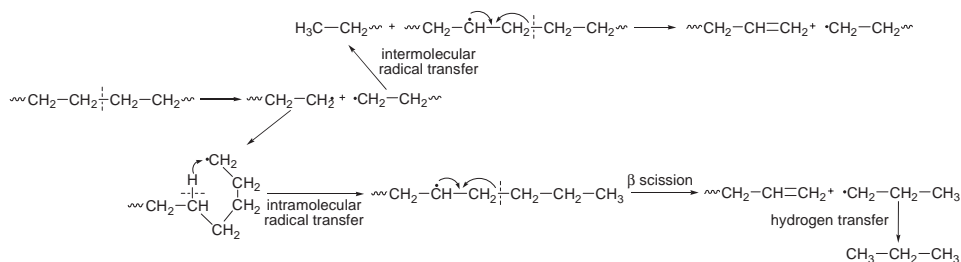
### 1. Unzipping



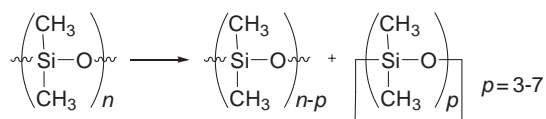
Unzipping is a free radical mechanism where the polymer essentially reverts to a monomer. Homolytic cleavage of the polymer chain and formation of two macroradicals are the first steps of the degradation process. Each radical undergoes scission in the  $\beta$ -position to produce the unsaturated monomer molecule and another of the same free radical which propagates this depolymerization reaction. The degradation proceeds until complete depolymerization of all molecules is achieved. A good example of a polymer whose thermal degradation occurs by unzipping is poly(methyl methacrylate) (PMMA).

### 2. Chain scission

Chain scission results from degradation of the polymer skeleton to smaller fragments, typically oligomers with different chain lengths.

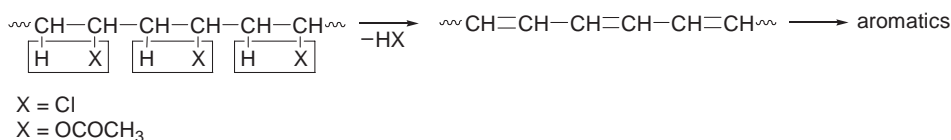


Polyethylene, and polyolefins in general, are good examples. Thermal degradation proceeds through extraction of a radical hydrogen and formation of a free radical on the polymer backbone. Bond scission in the  $\beta$ -position produces a terminal unsaturated fragment and a new macroradical that immediately transforms into a saturated molecule by hydrogen extraction or by combination with another free radical. Since scission occurs randomly along the polymer molecules, a wide range of chain lengths is produced.



In polysiloxanes the random scission mechanism is combined with cyclization reactions, and oligomeric cycles with a number of structural units ranging from 3 to 7 are formed in large amounts.

### 3. Side-group elimination



Side-group elimination is a two-stage process. Side groups are initially removed through a concerted mechanism involving two adjacent carbon atoms for production of an unsaturated polymer chain. The subsequent side-group elimination proceeds through the neighbouring units, promoted by the allylic intermediate radicals, with formation of polyene structures along the chains. Further degradation occurs through scission and aromatization reactions. This mechanism typically occurs in poly(vinyl chloride) (PVC) and PVAc with loss of HCl and acetic acid, respectively, followed by scission of the unsaturated backbone to form aromatic compounds and small unsaturated hydrocarbons.

Condensation polymers such as polyesters or polyamides undergo more complex thermal degradation processes where the resulting pathway is a combination of different reactions including scission, elimination and cyclization [75].

It must be also considered that the reaction rates of different thermal processes which can occur simultaneously are influenced by the treatment conditions (temperature, heating rate, pressure, static or dynamic atmosphere). This will affect the relative quantities of the products formed and in some cases also their nature, when recombination reactions give rise to secondary degradation products. On account of its sensitivity and resolution power Py-GC/MS will also provide useful information on minor components present in a material, including low molecular weight additives and pigments.

A few reviews have dealt with the identification of synthetic polymers by Py-GC/MS [76]. In addition to compositional studies, applications of pyrolysis to synthetic polymers include sequence length characterization in copolymers [77] and tacticity measurements in stereoregular homopolymers [78].



Synthetic polymers are extensively used in art and conservation in two different ways: as materials for conservation, i.e. as consolidants, adhesives or protective coatings, and as art materials for paintings, sculptures, and all kinds of artistic objects or installations. This means that almost any type of polymer structure may be found in historical and modern artworks, either added in some conservation treatment or as constituent materials. In particular, synthetic binders were chosen by artists as painting materials because they required short drying times and exhibited excellent optical properties, flexibility and good resistance to light, humidity and heat. Furthermore, industrial polymers were also employed in the form of sheets, laminates and foams as construction materials for sculptures, three-dimensional works and design objects [79]. The analysis of synthetic polymers is therefore an essential step for a complete knowledge of the constituents in such works of art, and Py-GC/MS has been applied with success in many cases.

Polymer materials in works of art undergo environmental ageing, and this must be taken into account when interpreting the results of analysis. Chemical ageing produces modifications in chemical composition and structures, while physical ageing processes manifest with loss of additives and low molecular weight components. The identification of constituent polymeric structures and of the additives functional to the material in the artwork is necessary for any choice regarding conservation needs and related restoration treatments. There are very few reports in the literature on the analysis of products used in restoration treatments, although it is common knowledge in the field that synthetic resins of different origins and structures have been extensively used in past restorations. One typical example is that related to the characterization of synthetic polymers found on Giotto's mural paintings on the Scrovegni Chapel, achieved by Py-GC/MS [80].

The principal field of application for synthetic polymers as art materials is that of paint binders, which developed in the second half of the twentieth century when manufacturers of artists' paints and varnishes realized the potential of synthetic resins used in the decorative household and industrial paint market [81]. The most important families of synthetic artists' paints are the acrylics, the vinyl acetate resins, and the alkyds, and Py-GC/MS has been used to identify all these types of modern paints.

A number of solid acrylic resins, all known under the commercial name of Paraloid, are used in art conservation, dissolved in organic solvents, as consolidants, coatings, or in varnish formulations; these resins are generally copolymers formed by two acrylic/methacrylic monomers [82]. Paraloid B-72 is the most widely used acrylic resin in conservation, and is formed by a methyl acrylate/ethyl methacrylate (MA/EMA) copolymer with molar composition 70/30.

Acrylic paints were first available in the 1940s under the name of Magna paints, and were used as turpentine solutions. The polymeric binder was poly(*n*-butyl methacrylate) which in the pyrolysis stage undergoes complete depolymerization, thus giving only the monomer peak. The EI mass spectrum of *n*-butyl methacrylate contains the same fragments as iso-butyl methacrylate, which is the monomer component of a different acrylic resin often used in acrylic varnish formulations. As in the pyrograms there are no other peaks; the two different resins can be only distinguished by their different retention times [83].

Acrylic emulsions, or better referred to as waterborne dispersion acrylic paints, were introduced in the 1950s and soon became the most used artists' media because of their

more friendly environmental formulations and application characteristics. Acrylic emulsion paints were initially mostly produced with ethyl acrylate/methyl methacrylate copolymers, poly(EA-co-MMA), but later preferred formulations on the market appeared to be based on *n*-butyl acrylate/methyl methacrylate, poly(nBA-co-MMA). Furthermore, more complex media were also produced such as poly(nBA-co-/MMA/styrene) and butyl methacrylate/2-ethylhexyl acrylate/styrene, poly(BMA-co-2EHA-co-S), terpolymers [81]. Emulsion paint formulations contain a number of additives including surfactants, protective colloids, stabilizers, and the dispersed pigments, which may affect the results of their characterization.

A selection of acrylic emulsion paints produced in the 1990s from different companies, were investigated by Py-GC/MS and other techniques [84]. For each brand the pure binding medium and a range of different colours were analysed. Identification of the polymeric binder relies not only on the presence of the monomers in the pyrograms but more particularly on the analysis of the oligomeric fragments which can elute from the column. The paints based on poly(EA-co-MMA) binder, for instance, give on pyrolysis the two monomers, but also lower intensity peaks of MA and EMA which are secondary products formed in the copolymer thermal decomposition (Figure 12.9). At higher retention time sesquimers, dimers and higher oligomers appear, and the structure assignment allows confirmation of the copolymer composition. The mass spectra of the oligomeric fragments do not contain molecular ions, and in addition EA and MMA have the same molar mass. Interpretation must be therefore based on the fragment ions obtained either by loss of an ethoxy or of a methoxy group.

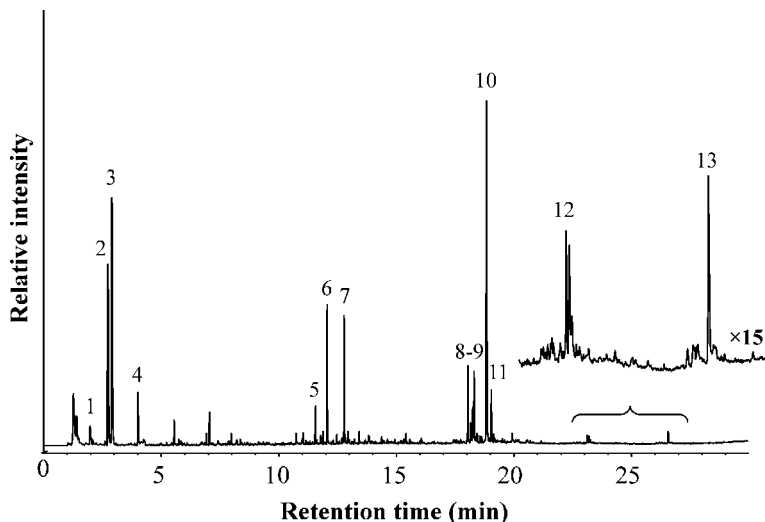


**Figure 12.9** Pyrogram of a poly(EA-co-MMA) waterborne binder. Peak assignments: 1, MA ; 2, EA ; 3, MMA ; 4, EMA ; 5, EA-MMA sesquimer ; 6, EA sesquimer ; 7, EA dimer ; 8, EA-EA-MMA trimer ; 9, EA-MMA-MMA trimer ; 10, EA-MMA-EA trimer ; 11, EA trimer ; 12, tetramers ; 13, pentamers. Reprinted from *J. Sep. Sci.*, 27, 263–274, Scalapone and Chiantore, Copyright 2004, with permission from Wiley VCH

A similar approach must be used for identification of paints based on poly(nBA-co-MMA). The monomer peaks are the more intense ones, but MA, n-BMA and butanol are found as secondary products. The structural assignment of the oligomeric fragments is again necessary to confirm the copolymer composition. In contrast to poly(EA-co-MMA), MMA and nBA have different molar masses and sesquimers and dimers are unequivocally recognized by characteristic fragment ions formed by scission of a methoxy or a butoxy group. Other fragmentation paths must be considered to assign the chemical structures of the four trimer peaks appearing in the pyrogram: the first two eluting trimers are nBA-nBA-MMA sequences differing in the double bond location; they are followed by a nBA-MMA-nBA sequence, and the last is the nBA trimer [84].

Acrylic resins are generally well characterized by Py-GC/MS without the need for any derivatization reaction. However, in waterborne polymer dispersions it is common to have minor amounts of acrylic and/or methacrylic acid monomers added in the copolymerization to help the stability of the final latex. These monomers can also appear in the pyrolysis products, and it has been shown that with on-line derivatization they can be more efficiently revealed [85].

Apart from composition of the polymeric component, Py-GC/MS can provide information on other organic molecules present in emulsion paints. In particular, the pyrolytic fragmentation of synthetic pigments belonging to the families of azo and anthraquinone compounds has been described [83]. In Figure 12.10 the pyrograms of acrylic waterborne paints containing different organic pigments, indicated by their Colour Index names [86], are shown, with numbers indicating the marker peaks of the pigments and the corresponding structures; the marker peaks are well separated from each other and from the other paint components, making it possible to simultaneously identify more than one pigment. This aspect is particularly important when dealing with samples from works of art, especially if the resulting colour is the combination of two or more different paints mixed to obtain a new hue.

Py-GC/MS makes also possible the identification of surfactants present in waterborne paint formulations, even if they are present in lower amounts than pigments or other additives. Recent emulsion paint formulations include non-ionic type surfactants with a polyethoxylated structure. Mass spectra of hydroxy-terminated polyethylene glycols and of their pyrolysis fragments are characterized by fragment ions at  $m/z$  45, 89, 133 and 177. With alkylaryl polyethoxylates marker compounds are alkylphenols, for instance octyl phenol ( $m/z$  135, 206) is formed from octyl phenol polyethoxy ethanol. Depending on the paint composition, marker peaks of polyethoxylates may be partially or totally overlaid by other components. If not evident from the total ion current chromatogram, the presence of pyrolysis fragments of these non-ionic surfactants can be enhanced by plotting the corresponding single ion mass profiles [87].

PVAc ('vinyl') paints were introduced in the late 1940s finding successful application as household emulsion paints. As artists' paints, vinyl emulsions became available from some manufacturers in the 1960s, but their use was not widespread and only a very few of them remained on the market. Notwithstanding, vinyl binders have been detected in a number of works of important American and European artists who began to use the cheap vinyl house paints for preparing their colours [81]. Pyrolysis of PVAc takes place through the side-group elimination mechanism, and the most characteristic products are acetic acid and aromatic compounds formed by cyclization of the polymer

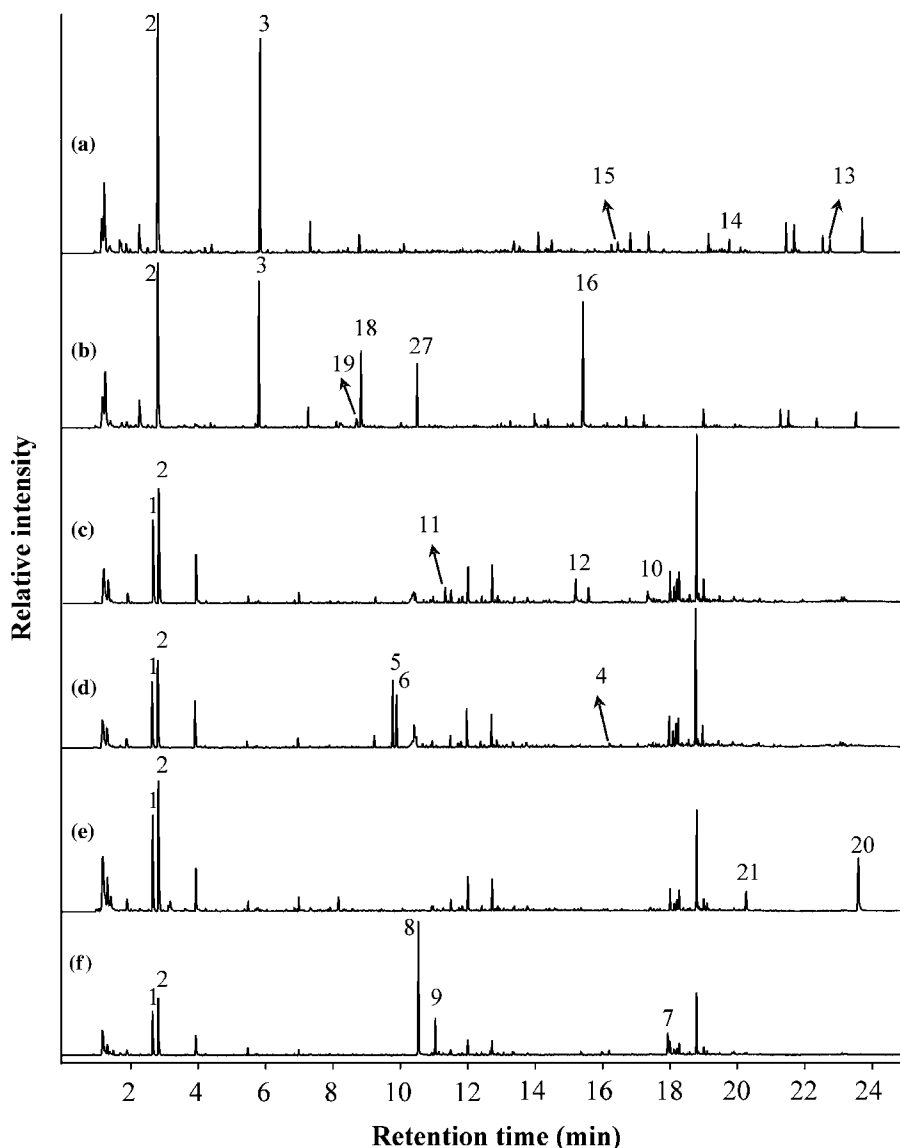


**Figure 12.10** Pyrogram of acrylic emulsion paints containing different organic pigments: (a) PR5; (b) PR112; (c) PR4; (d) PY3; (e) PR 251; (f) PY74. Peak assignments: 1, EA; 2, MMA; 3, nBA; 4, 4-chloro-2-nitro-benzenamine; 5, 2-chloro-benzenamine; 6, 1-chloro-2-isocyanato-benzene; 7, 2-methoxy-4-nitro-benzenamine; 8, 2-methoxy-benzenamine; 9, 1-isocyanato-2-methoxy-benzene; 10, 1-chloro-4-nitro-benzenamine; 11, 1-chloro-2-nitro-benzene; 12, 2-naphthalenol; 13, 3-amino-4-methoxy-N,N-diethyl-benzenesulfonamide; 14, 4-methoxy-N,N-diethyl-benzenesulfonamide; 15, 5-chloro-2,4-demethoxy-benzenamine; 16, 2,4,5-trichloro-benzenamine; 17, 1,3,4-trichloro-benzene; 18, 2-methyl-benzenamine; 19, 1-isocyanato-2-methyl-benzene; 20, 1-amino-9,10-anthracenedione; 21, 9,10-anthracenedione. Reprinted from *J. Sep. Sci.*, 27, 263–274, Scalapone and Chiantore, Copyright 2004, with permission from Wiley VCH

fragments. PVAc resins often contain plasticizers which are used to improve film flexibility, and in the pyrolysis the fragments from those components may be found, helping to identify the paint formulation. Plasticizers may be external, like dibutyl- and dioctyl phthalate which are added to the base polymer, or internal in the form of monomers such as nBA or 2-ethylhexyl acrylate, which enter in the polymer chains. As preferred plasticizing comonomers highly branched C<sub>9</sub> and C<sub>10</sub> vinyl esters, known as VeoVa resins, have been mostly used [88].

Figure 12.11 shows the pyrograms of vinyl paints from two monochromes by the Italian artist Piero Manzoni. The two paints are clearly different in composition: acetic acid (peak 1) and benzene (peak 2) are present as common markers of the PVAc binder in both cases, but sample (a) contains dibutyl phthalate (peak 6) as external plasticizer. Peak 5 was recognized as bis(2-methylpropyl)-phthalate which is formed from dibutylphthalate isomerization, while butyl acetate (peak 3) and butyl benzoate (peak 4) are secondary products of recombination reactions occurring during the pyrolysis. Sample (b), however,

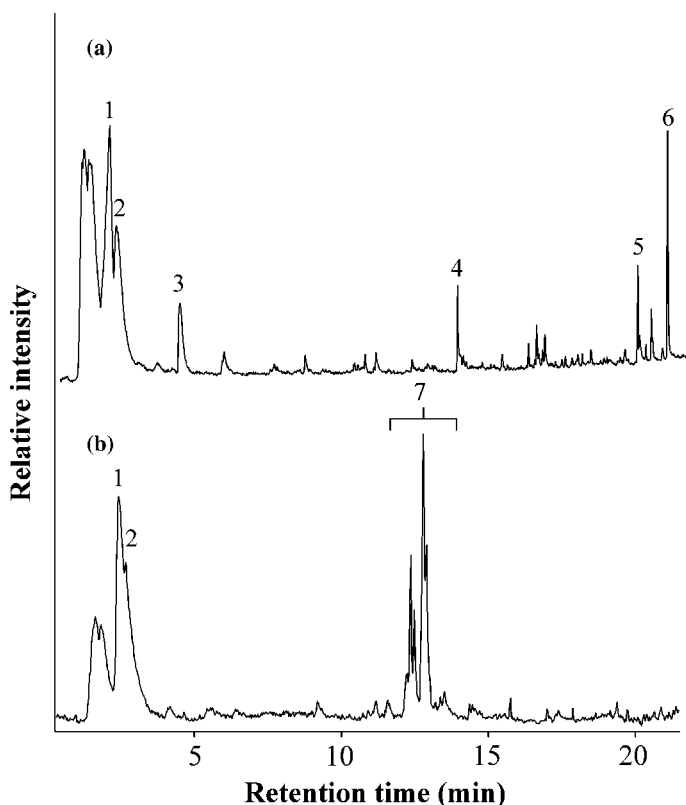


**Figure 12.11** Pyrograms of a PVAc paint containing external plasticizers (a). and of a vinyl acetate/VeoVa copolymer (b). Peak assignments: 1, acetic acid, 2, benzene, 3, butyl acetate, 4, butyl benzoate, 5, bis(2-methylpropyl)-phthalate, 6, dibutylphthalate, 7, branched acrylates ranging from C<sub>7</sub> to C<sub>9</sub>

contains a number of branched acrylates ranging from C<sub>7</sub> to C<sub>9</sub>, and can be considered to be a copolymer similar to a PVAc/VeoVa resin.

Alkyd paints are synthetic polyesters formed by polycondensation of polyhydric alcohols with polybasic acids and anhydrides in the presence of unsaturated fatty acids or of siccative oils. Glycerol, pentaerythritol and phthalic anhydride are common precursors, together with the fatty acids or with drying or semi-drying oils. The paints dry in a similar way to the auto-oxidative process occurring in oil paints, with the oxygen attack on the fatty acid chains inducing the cross-linking reactions. In alkyd resins the siccative oils traditionally used in paintings, such as linseed, walnut and safflower, are used together with other oil types, namely soya, hydrogenated castor, fish and coconut oil. Other modifiers may be also present in the alkyd resin formulations: styrene and vinyl toluene to improve hardness and alkali resistance, rosin to increase brilliance and adhesion, and silicone to impart heat and water resistance. The analysis of alkyd resins with Py-GC/MS is properly done with on-line thermally assisted hydrolysis and derivatization of the hydroxy and carboxylic groups present in the resin components and fragments. A suitable derivatization method is thermally assisted hydrolysis and methylation (THM) using tetramethyl ammonium hydroxide (TMAH), with the same approach successfully developed for the chemical characterization of oil paintings [89].

The alkyd paint compositions which are encountered in works of art may be quite different from each other, not only because of the variations in recipes within the few available commercial artists' paints but also due to the frequent use by modern artists of household alkyd paints. In the characterization of such paints pyrograms comparison is not straightforward, and detailed peak analysis is required. In Figure 12.12 the pyrogram of an artist alkyd colour is shown in comparison with an alkyd sample taken from a work of the artist Lucio Fontana ('Concetto spaziale', 1961). The components of an oil modified alkyd paint based on glycerol and pentaerythritol are recognized: peaks 1, 2 and 3 are pyrolysis products of glycerol, and peaks 5 and 7 derive from pentaerythritol. The presence of the same pyrolysis product with different degrees of methylation is due to incomplete methylation of –OH groups in complex molecules. Glycerol is a reagent in the polyester synthesis but it can also derive from fragmentation of triglycerides constituting the oil component. Peak 12, dimethyl phthalate, comes from phthalic acid, whose decarboxylation may explain the presence of benzoic acid methyl ester. Benzoic acid, however, can be also present in the resin as a terminal chain length modifier [90] and this must be the case in the Fontana's paint where peak 23 is very high. Peaks 13–19 and peak 25 reveal the presence of fatty acids, detected as methyl esters, while peaks 4, 6 and 8 derive from the organic yellow pigment. The differences between the two alkydic paints are noteworthy: in the Winsor & Newton paint the high intensity of azelaic acid dimethyl ester (peak 13) attests an important amount of siccative oil, whereas in the Fontana sample the resin is an alkyd resin with low oil content, modified with adipic acid (peak 24), styrene (peak 20), and possibly added with diterpenic resin components revealed by the low intensity peaks 26–28. The alcohol component of the polyester formulation is seen in the pyrogram only in the form of peaks 21 and 22, due to fragments not giving precise identification.

Other examples of alkyd resins with variations in binder compositions across the different colours have been found in samples from a painting by Jackson Pollock analysed with Py-GC/MS and on-line TMAH derivatization [91].

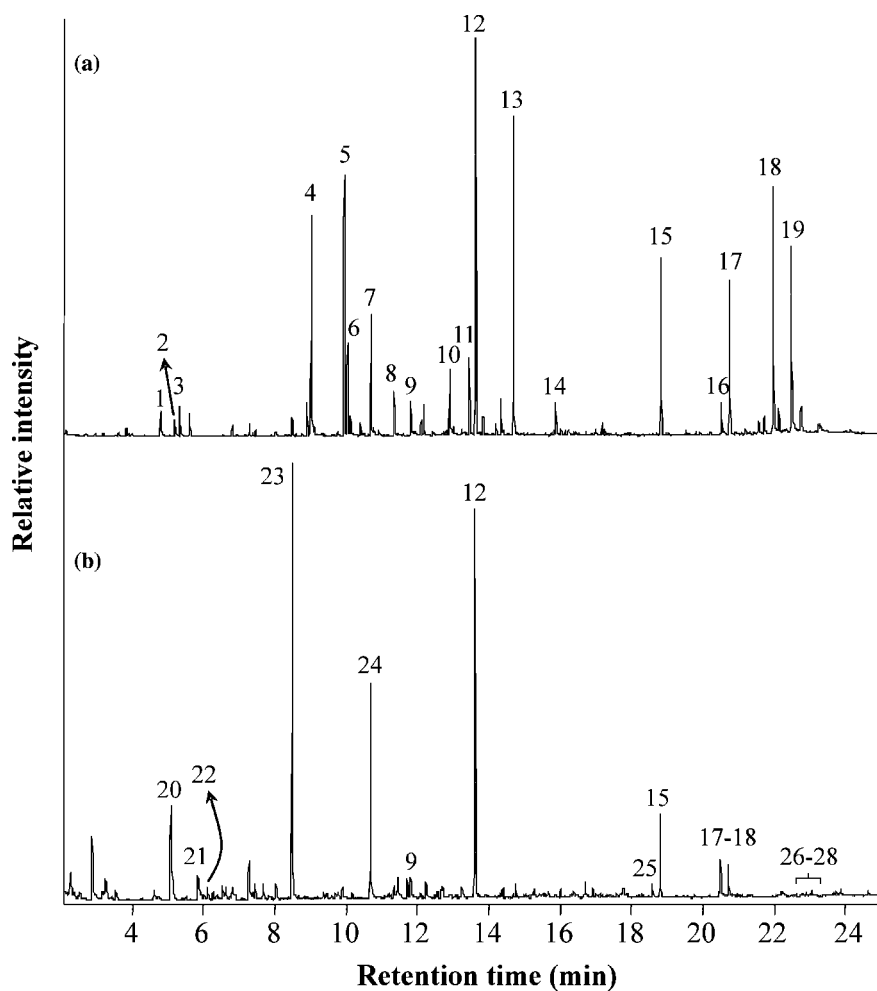


**Figure 12.12** THM-GC/MS curves of a Winsor & Newton lemon alkyd paint (a) and of an alkyd sample taken from Fontana's work 'Concetto spaziale' (1961) (b). Peak assignments: 1, 1,3-dimethoxy-2-propanol; 2, 1,2,3-trimethoxy-propane; 3, 3-methoxy-1,2-propandiol; 4, 4-chloro-benzenamine; 5, 3-methoxy-2,2-bis(methoxymethyl)-1-propanol; 6, 3-chloro-N-methyl-benzenamine; 7, 3-methoxy-2-methoxymethyl-1-propanol; 8, 4-chloro-N-methyl-benzenamine; 9, phthalic anhydride; 10, 3-chloro-4-methoxy-benzenamine; 11, suberic acid dimethyl ester; 12, dimethyl phthalate; 13, azelaic acid dimethyl ester; 14, sebacic acid dimethyl ester; 15, palmitic acid methyl ester; 16, oleic acid methyl ester; 17, stearic acid methyl ester; 18, 12-hydroxy stearic acid methyl ester; 19, 12-methoxy stearic acid methyl ester; 20, styrene; 21, 2-(2-methoxyethoxy)-ethanol; 22, 1,1'-oxybis(2-methoxy-ethane); 23, benzoic acid methyl ester; 24, adipic acid dimethyl ester; 25, hexadecenoic acid methyl ester; 26, dihydroisopimaric acid methyl ester; 27, dehydroabietic acid methyl ester; 28, 4-epidehydroabietol

In the characterization of alkyd resin formulations the palmitic acid to stearic acid (P/S) ratio, often used to identify the type of oil in a binder, cannot be applied as many different oils other than the traditional ones are commonly employed in industrial formulations. Moreover, they are often in mixtures, with the additional complication that fatty acids are also sometime added to the vegetable oils, thus making it impossible to rely on measured P/S values. In any case it is important to always derivatize the samples if Py-GC/MS is used and an alkyd is suspected. Phthalic anhydride will be detected also in an underivatized alkyd pyrogram; however, isophthalic acid will not, leading to confusion and the possibility of uncorrected identification [92].

Other polymeric binders, natural and synthetic, may be found as paints or varnishes in modern artworks and installations. Artists very easily adopt resins developed as industrial coatings or for specialized applications, and use them according to their creative needs. Natural rubber latex is a water dispersion of 1,4-*cis*-polyisoprene particles where pigments can be added to give coloured paints. By means of Py-GC/MS the presence of these paints can be easily assessed. As shown in Figure 12.13, the principal marker peaks in the pyrogram are those of isoprene, limonene and other cyclic dimers.

Silicone paints are formed by controlled hydrolysis and condensation of alkyl alkoxysilanes, and may be encountered either alone or in formulations with other synthetic resins. The typical structural unit in the polymer chain is dimethyl siloxane, and pyrolysis of such resins takes place with random chain scission and the extended formation of stable cyclic fragments. In Figure 12.14 the pyrogram of a silicone resin is shown, with cyclic siloxane oligomers eluting at the shorter retention times, followed by the linear siloxane fragments.

In conclusion, it may be stated that Py-GC/MS is the method of choice for chemical characterization of synthetic polymers used in artworks or as conservation materials. The chemical information is generally specific for the individual component, and the amount of sample required is practically negligible, thus allowing application of the technique even

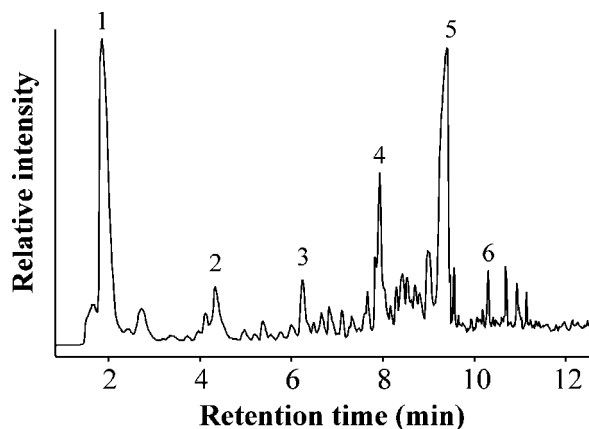


**Figure 12.13** Pyrogram of a natural rubber latex paint. Peak assignments: 1, isoprene; 2, toluene; 3, xylene; 4, 4-ethenyl-1,4-dimethyl-cyclohexene; 5, limonene; 6, dehydro-*p*-cymene



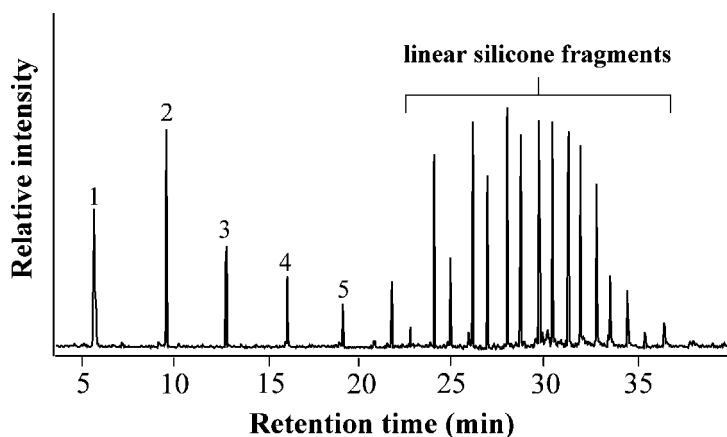


**Figure 12.14** Pyrogram of the silicone coating from Mello's 'Tavolo erba'. Peak assignments: 1, hexamethyl-cyclotrisiloxane; 2, octamethyl-cyclotetrasiloxane; 3, decamethyl-cyclopentasiloxane; 4, dodecamethyl-cyclohexasiloxane; 5, tetradecamethyl-cyclooctasiloxane

in the most difficult cases when sampling is the main obstacle. Depending on the type of pyrolysis products which are formed, the method can be optimized for overcoming the gas chromatographic elution difficulties raised by very polar compounds. In such cases, on-line derivatization techniques can be applied, and high quality separations obtained. In many cases the on-line sample treatment is not necessary, but with unknown samples the recommended procedure is to first perform the analysis with TMAH treatment, in order to obtain the methylation of the hydroxyl groups eventually present and to be certain not to lose evidence of a component. In fact, it is not uncommon to have more than one type of paint binder or varnish in works of art, and the pyrolysis products can have different behaviours in the gas chromatographic elution.

## References

1. T.H. Barry, *Natural Varnish Resins*, Ernest Benn, Ltd., London (1932).
2. S.A. Buckley and R.P. Evershed, Organic chemistry of embalming agents in Pharaonic and Graeco-Roman mummies, *Nature*, **413**, 837–841 (2001).
3. M.M. Wright and B.B. Wheals, Pyrolysis mass spectrometry of natural gums, resins, and waxes and its use for detecting such materials in ancient Egyptian mummy cases (cartonnages), *J. Anal. Appl. Pyrol.*, **11**, 195–211 (1987).
4. C.L. Eastlake, *Materials for a History of Oil Painting*, Longman, Brown, Greene and Longmans, London (1847).
5. A.P. Laurie, *The Materials of the Painter's Craft*, J.B. Lippincott Co., Philadelphia (1911).
6. C. Cennini, *Il libro dell'arte*, Neri Pozza, Vicenza (2004).
7. Pliny, *Naturalis Historia*, **XXXV**, 97.
8. M.P. Merrifield, *Medieval and Renaissance Treatises on the Arts of Painting*, Dover Publications, London (1967).
9. Leonardo da Vinci, *Trattato della pittura*, Carabba Editore, Lanciano (1947).
10. G. Vasari, *Le vite de più eccellenti pittori, scultori et architetti*, Newton & Compton, Roma (2001).

11. D. Fels, *Lost Secrets of Flemish Masters. Including the First Complete English Translation of the De Mayerne Manuscript, B.M. Sloane 2052*, Alchemist, London (2001).
12. V. Gheroldi, *Le vernici al principio del Settecento, Studi sul Trattato di Filippo Bonanni*, Turriz Editrice, Cremona (1995).
13. R.S. Berns and E.R. de la Rie, Exploring the optical properties of picture varnishes using imaging techniques, *Stud. Conserv.* **48**, 73–82 (2003).
14. J.S. Mills and R. White, *The Organic Chemistry of Museum Objects*, Butterworth-Heinemann, Oxford (1994).
15. E.R. de la Rie, Photochemical and thermal degradation of films of dammar resin, *Stud. Conserv.*, **33**, 53–70 (1988).
16. M.R. Derrick, D. Stulik and J.M. Landry, *Infrared Spectroscopy in Conservation Science*, The Getty Conservation Institute, Los Angeles (1999).
17. P. Vandenabeele, B. Wohling, L. Moens, H. Edwards, M. De Ren and G. van Hooydonk, Analysis with micro-Raman spectroscopy of natural organic binding media and varnishes used in art, *Anal. Chim. Acta*, **407**, 261–274 (2000).
18. D. Scalarone, M.C. Duursma, J.J. Boon and O. Chiantore, MALDI-TOF mass spectrometry on cellulosic surfaces of fresh and photo-aged di- and triterpenoid varnish resins, *J. Mass Spectrom.*, **40**, 1527–1535 (2005).
19. I. Pastorova; K.J. van der Berg; J.J. Boon and J.W. Verhoeven, Analysis of oxidized diterpenoid acids using thermally assisted methylation with TMAH, *J. Anal. Appl. Pyrol.*, **43**, 41–57 (1997).
20. G.A. van der Doelen and J.J. Boon, Artificial ageing of varnish triterpenoids in solution, *J. Photochem. Photobiol., A*, **134**, 45–57 (2000).
21. G.A. van der Doelen, *Molecular studies of fresh and aged triterpenoid varnishes*, Molart Report 1, PhD thesis, University of Amsterdam (1999).
22. P. Dietemann, M. Kälén, S. Zumbühl, R. Knochenmuss, S. Wülfert and R. Zenobi, A mass spectrometry and electron paramagnetic resonance study of photochemical and thermal aging of triterpenoid varnishes, *Anal. Chem.*, **73**, 2087–2096 (2001).
23. R.L. Feller, *Accelerated Ageing, Photochemical and Thermal Aspects*, The Getty Conservation Institute, Los Angeles (1994).
24. K.J. van der Berg, J. van der Horst, J.J. Boon and O.O. Sudmeijer, Cis-1,4-poly- $\beta$ -myrcene; the structure of the polymeric fraction of mastic resin (*Pistacia lentiscus* L.) elucidated, *Tetrahedron Lett.*, **39**, 2645–2648 (1998).
25. J.S. Mills and R. White, Natural resins of art and archaeology. Their sources, chemistry and identification, *Stud. Conserv.*, **22**, 12–31 (1977).
26. K.J. van der Berg, J. van der Horst, J.J. Boon, N. Shibayama and E.R. de la Rie, Mass spectrometry as a tool to study ageing processes of diterpenoid resins in works of art: GC- and LC-MS studies, *Adv. Mass Spectrom.*, **14**, 563–573 (1998).
27. D. Scalarone, M. Lazzari and O. Chiantore, Pyrolytic characterisation and ageing behaviour of diterpenic resins used as art materials: colophony and Venice turpentine, *J. Anal. Appl. Pyrol.*, **64**, 345–361 (2002).
28. J.S. Mills and R. White, Natural resins of art and archaeology. Their sources, chemistry and identification, *Stud. Conserv.*, **22**, 12–31 (1977).
29. K.J. van den Berg, J.J. Boon, I. Pastorova and L.F.M. Spetter, Mass spectrometric methodology for the analysis of highly oxidized diterpenoid acids in Old Master paintings, *J. Mass. Spectrom.*, **35**, 512–533 (2000).
30. K.B. Anderson, R.E. Winans and R.E. Botto, The nature and fate of natural resins in the geosphere-II. Identification, classification and nomenclature, *Org. Geochem.*, **18**, 829–841 (1992).
31. K.J. van den Berg, J. Ossebaer and H. van Keulen, Analysis of copal resins in 19th century oil paints and resin/oil varnishes, in *Art 2002*, R. van Grieken, P. Janssens, K. van't Dack and L. Meersman (Eds), University of Antwerp, Antwerp (2002).
32. D. Scalarone, M. Lazzari and O. Chiantore, Ageing behaviour and pyrolytic characterisation of diterpenic resins used as art materials: Manila copal and sandarac, *J. Anal. Appl. Pyrol.*, **68–69**, 115–136 (2003).

33. K.J. van den Berg, J. van der Horst and J.J. Boon, Recognition of copals in aged resin/oil paints and varnishes, in *Preprints of the ICOM-CC 12th Triennial Meeting, Lyon, 29 August–3 September*, J. Bridgland and J. Brown (Eds), James and James, London 855–861 (1999).
34. D.J. Clifford and P.H. Hatcher, Structural transformations of polylabdanoid resinites during maturation, *Org. Geochem.*, **23**, 407–418 (1995).
35. K.B. Anderson, New evidence concerning the structure, composition, and maturation of Class I (polylabdanoid) resinites, in *Amber, Resinite and Fossil Resins*, K.B. Anderson and J.C. Crelling (Eds), vol. **617**, American Chemical Society, Washington, DC 105–129 (1995).
36. K.B. Anderson and R.E. Winans, Nature and fate of natural resins in the geosphere. 1. Evaluation of pyrolysis-gas chromatography/mass spectrometry for the analysis of natural resins and resinites, *Anal. Chem.*, **63**, 2901–2908 (1991).
37. B.G.K. van Aarssen, J.W. de Leeuw, M. Collinson, J.J. Boon and K. Goth, Occurrence of polycadinene in fossil and recent resins, *Geochim. Cosmochim. Acta*, **58**, 223–229 (1994).
38. D. Scalarone, J. van der Horst, J.J. Boon and O. Chiantore, Direct-temperature mass spectrometric detection of volatile terpenoids and natural terpenoid polymers in fresh and artificially aged resins, *J. Mass Spectrom.*, **38**, 607–617 (2003).
39. G.A. van der Doelen, K.J. van der Berg and J.J. Boon, Comparative chromatographic and mass-spectrometric studies of terpenoid varnishes: fresh material and aged samples from paintings, *Stud. Conserv.*, **43**, 249–264 (1998).
40. G.A. van der Doelen, K.J. van der Berg, J.J. Boon, N. Shibayama, E.R. de la Rie and W.J.L. Geniut, Analysis of fresh triterpenoid resins and aged triterpenoid varnishes by high-performance liquid chromatography-atmospheric pressure chemical ionisation (tandem) mass spectrometry, *J. Chromatogr., A*, **809**, 21–37 (1998).
41. E.R. de la Rie and S. Watts, GCMS analysis of terpenoid resins: in situ derivatization procedures using quaternary ammonium hydroxides, *Stud. Conserv.*, **47**, 257–272 (2002).
42. V.P. Papageorgiou, M.N. Bakola-Christianopoulou, K.K. Apazidou and E.E. Psarros, Gas chromatographic-mass spectrometric analysis of the acidic triterpenic fraction of mastic gum, *J. Chromatogr., A*, **769**, 263–267 (1997).
43. J.M. Challinor, Review: the development and applications of thermally assisted hydrolysis and methylation reactions, *J. Anal. Appl. Pyrol.*, **61**, 3–34 (2001).
44. J.M. Challinor, A pyrolysis-derivatisation-gas chromatography technique for the structural elucidation of some synthetic polymers, *J. Anal. Appl. Pyrol.*, **16**, 323–333 (1989).
45. W.C. Kossa, J. MacGee, S. Ramachandran and A.J. Webber, Pyrolysis methylation/gas chromatography: a short review, *J. Chromatogr. Sci.*, **17**, 177–187 (1979).
46. J.M. Challinor, On the mechanism of high temperature reactions of quaternary ammonium hydroxides with polymers, *J. Anal. Appl. Pyrol.*, **29**, 223–224 (1994).
47. Y. Ishida, H. Othani and S. Tsuge, Effects of solvents and inorganic salts on the reactive pyrolysis of aromatic polyester in the presence of tetramethylammonium hydroxide studied by pyrolysis-gas chromatography/mass spectrometry, *J. Anal. Appl. Pyrol.*, **33**, 167–180 (1995).
48. J.M. Challinor, A rapid simple pyrolysis derivatisation gas chromatography-mass spectrometry method for profiling of fatty acids in trace quantities of lipids, *J. Anal. Appl. Pyrol.*, **37**, 185–197 (1996).
49. H.-L. Hardell and N.-O. Nilvebrandt, A rapid method to discriminate between free and esterified fatty acids by pyrolytic methylation using tetramethylammonium acetate or hydroxide, *J. Anal. Appl. Pyrol.*, **52**, 1–14 (1999).
50. Y. Ishida, S. Wakamatsu, H. Yokoi, H. Othani and S. Tsuge, Compositional analysis of polyunsaturated fatty acid oil by one-step thermally assisted hydrolysis and methylation in the presence of trimethylsulfonium hydroxide, *J. Anal. Appl. Pyrol.*, **49**, 267–276 (1999).
51. K.R. Sutherland, *Solvent extractable components of oil paint films*, PhD thesis, University of Amsterdam (2001).
52. G. Chiavari, D. Fabbri and S. Prati, In-situ pyrolysis and silylation for analysis of lipid materials used in paint layers, *Chromatographia*, **53**, 311–314 (2001).
53. G. Chiavari, D. Fabbri and S. Prati, Gas chromatographic-mass spectrometric analysis of products arising from pyrolysis of amino acids in the presence of hexamethyldisilazane, *J. Chromatogr., A*, **922**, 235–241 (2001).

54. D. Fabbri and G. Chiavari, Analytical pyrolysis of carbohydrates in the presence of hexamethyldisilazane, *Anal. Chim. Acta*, **449**, 271–280 (2001).
55. G. Chiavari, D. Fabbri and S. Prati, Characterisation of natural resins by pyrolysis – silylation, *Chromatographia*, **55**, 611–616 (2002).
56. D. Fabbri, G. Chiavari, S. Prati, I. Bassura and M. Vangelista, Gas chromatography/mass spectrometric characterisation of pyrolysis/silylation products of glucose and cellulose, *Rapid Commun. Mass Spectrom.*, **16**, 2349–2355 (2002).
57. M.J. Casas-Catalan and M.T. Doménech-Carbó, Identification of natural dyes used in works of art by pyrolysis-gas chromatography/mass spectrometry combined with in situ trimethylsilylation, *Anal. Bioanal. Chem.*, **382**, 259–268 (2005).
58. L. Osete-Cortina and M.T. Doménech-Carbó, Analytical characterization of diterpenoid resins present in pictorial varnishes using pyrolysis-gas chromatography-mass spectrometry with on line trimethylsilylation, *J. Chromatogr., A*, **1065**, 265–278 (2005).
59. J. De la Cruz-Cañizares, M.-T. Doménech-Carbó, J.-V. Gimeno-Adelantado, R. Mateo-Castro and F. Bosch-Reig, Study of Burseraceae resins used in binding media and varnishes from artworks by gas chromatography-mass spectrometry and pyrolysis-gas chromatography-mass spectrometry, *J. Chromatogr., A*, **1093**, 177–194 (2005).
60. D. Scalarone, O. Chiantore and C. Riedo, Gas chromatographic/mass spectrometric analysis of on line pyrolysis-silylation products of monosaccharides, *J. Anal. Appl. Pyrol.*, **83**, 157–164 (2008).
61. R.P. Evershed, Advances in silylation, in *Handbook of Derivatives for Chromatography* (2nd ed.), K. Blau and J. Halket (Eds), John Wiley & Sons, Ltd, New York 51–108 (1993).
62. K.-I. Kuroda, Pyrolysis-trimethylsilylation analysis of lignin: preferential formation of cinnamyl alcohol derivatives, *J. Anal. Appl. Pyrol.*, **56**, 79–87 (2000).
63. G.L. Stout and H.F. Cross, Properties of surface films, *Tech. Stud. Fine Arts*, **5**, 241–249 (1937).
64. C.V. Horie, *Materials for Conservation*, Butterworth-Heinemann, Oxford (1987).
65. W.J. Irwin, *Analytical Pyrolysis: A Comprehensive Guide*, Marcel Dekker, New York (1982).
66. T. Learner, The analysis of synthetic paints by pyrolysis-gas chromatography-mass spectrometry (PyGCMS), *Stud. Conserv.*, **46**, 225–241 (2001).
67. D. Scalarone and O. Chiantore, Chromatographic separation techniques in the analysis of synthetic emulsion paints, *J. Sep. Sci.*, **27**, 263–274 (2004).
68. E.R. de la Rie, The influence of varnishes on the appearance of paintings, *Stud. Conv.*, **32**, 1–13 (1987).
69. R.S. Berns and E.R. de la Rie, The effect of the refractive index of a varnish on the appearance of oil paintings, *Stud. Conv.*, **48**, 251–262 (2003).
70. E.R. de la Rie and A.M. Shedrinsky, The chemistry of ketone resins and the synthesis of derivative with increased stability and flexibility, *Stud. Conv.*, **34**, 9–19 (1989).
71. H. Mestdagh, C. Rolando, M. Sablier and J.-P. Rioux, Characterization of ketone resins by pyrolysis-gas chromatography/mass spectrometry, *Anal. Chem.*, **64**, 2221–2226 (1992).
72. M. Faraday, *Q. J. Sci. Lit. Arts*, **21**, 19 (1826).
73. C. G. Williams, *Philos. Trans. R. Soc. London*, **150**, 241 (1860).
74. N. Grassie and G. Scott, *Polymer Degradation and Stabilisation*, Cambridge University Press, Cambridge (1985).
75. H. Othani and S. Tsuge, Degradation mechanisms of condensation polymers, in *Applied Pyrolysis Handbook*, T.H. Wampler (Ed.), Marcel Dekker, New York, 97–124 (1999).
76. J.K. Haken, Pyrolysis gas chromatography of synthetic polymers – a bibliography, *J. Chromatogr., A*, **825**, 171–187 (1998).
77. F.C.-Y. Wang and P.B. Smith, Quantitative analysis and structure determination of styrene/methyl methacrylate copolymers by pyrolysis gas chromatography, *Anal. Chem.*, **68**, 3033–3037 (1996).
78. S. Tsuge and H. Othani, Structural characterization of polymeric materials by pyrolysis-GC/MS, *Polym. Degrad. Stab.*, **58**, 109–130 (1997).
79. T. van Oosten, Y. Shashoua and F. Waentig (Eds), *Plastic in Art, History, Technology, Preservation*, Siegl, Munich (2002).

80. G. Chiavari, M. Ioele, S. Prati and S. Santopadre, Py-GC-MS of the synthetic polymers used in past restorations on Giotto's mural paintings at the Scrovegni Chapel (Padova), *Chromatographia*, **56**, 763–767 (2002).
81. J. Crook and T.J.S. Learner, *The Impact of Modern Paints*, Tate Publishing, London (2000).
82. O. Chiantore and M. Lazzari, Characterization of acrylic resins, *Int. J. Polym. Anal. Char.*, **2**, 395–408 (1996).
83. T.J.S. Learner, The analysis of synthetic paints by pyrolysis gas chromatography - mass spectrometry (Py-GC-MS), *Stu. Conserv.*, **46**, 225–241 (2001).
84. D. Scalarone and O. Chiantore, Separation techniques for the analysis of artists' acrylic emulsion paints, *J. Sep. Sci.*, **27**, 263–274 (2004).
85. L. Osete-Cortina and M.T. Doménech-Carbó, Characterization of acrylic resins used for restoration of artworks by pyrolysis-silylation-gas chromatography/mass spectrometry with hexamethyldisilazane, *J. Chromatogr., A*, **1127**, 228–236 (2006).
86. Colour Index, *The Society of Dyers and Colourists*, Bradford (1971).
87. R.P. Lattimer, Tandem mass spectrometry of poly(ethylene glycol) proton- and deuterium-attachment ions, *Int. J. Mass Spectrom. Ion Processes*, **116**, 23–36 (1992).
88. M.M.C. Slinckx and H.P.H. Scholten, VeoVa9/(meth)acrylates, a new class of emulsion copolymers, *Surf. Coat. Int.*, **77**, 107–112 (1994).
89. G. Chiavari, P. Bocchini and G.C. Galletti, Rapid identification of binding media in paintings using simultaneous pyrolysis methylation gas chromatography, *Sci. Technol. Cult. Herit.*, **1**, 153–158 (1992).
90. J.M. Challinor, Structure determination of alkyd resins by simultaneous pyrolysis methylation, *J. Anal. Appl. Pyrol.*, **18**, 233–244 (1991).
91. F. Cappitelli, THM-GCMS and FTIR for the study of binding media in *Yellow Islands* by Jackson Pollock and *Break Point* by Fiona Banner, *J. Anal. Appl. Pyrol.*, **71**, 405–415 (2004).
92. R. Ploeger, D. Scalarone and O. Chiantore, The characterization of commercial artists' alkyd paints, *J. Cult. Herit.*, **9**, 412–419 (2008).



# **Part IV**

## **Liquid Chromatography/Mass Spectrometry**





# 13

## Characterization of Organic Natural Dyes by Electrospray Mass Spectrometry Coupled with HPLC and/or Capillary Electrophoresis

*Katarzyna Lech, Katarzyna Połec-Pawlak and Maciej Jarosz*

### 13.1 Introduction

Identification and quantification of natural dyes need high performance analytical techniques, appropriate for the analysis of materials of complicated matrices containing a small amount of coloured substances. This requirement perfectly fits coupling of modern separation modules (usually high performance liquid chromatography in reversed phase mode, RPLC, but also capillary electrophoresis, CE) with selective detection units (mainly mass spectrometer).

For the last several years, mass spectrometry with atmospheric pressure chemical ionization (APCI) and electrospray ionization (ESI) have determined the trends in the analysis of dyes. Since 1987, various variants of ESI have been used in which droplet formation was assisted by compressed air,[1,2] temperature (e.g. 'Turbo Ion Spray') or ultrasound, and they were able to handle flow rates up to 1–2 ml min<sup>-1</sup>. This made a combination of analytical RPLC and ESI easily and widely used. The reason why it often was (and is) used instead of a traditional UV-Vis detector is the better sensitivity and selectivity of MS in comparison with spectrophotometric detection. Apart from these advantages, MS offers easily interpretable structural information. However, various

compounds are ionized to a different degree, and quality and purity of the chromatogram can be very poor when mass spectra are scanned over a wide mass range (full scan mode). For that reason, a good solution is to create one analytical system by coupling two detectors: UV-Vis, which allows compounds eluted and registered as chromatographic peaks to be distinguished as well as leaves them intact when they pass the detection cell; and MS, which provides information about molecular mass and structure.

Elaboration of the method for the identification of colour compounds by RPLC-MS should comprise four steps: (1) spectral characterization of reference materials (standards) and subsequent optimization of detection parameters, as well as those of their chromatographic separation; (2) analysis of natural dyestuffs used as colouring materials in historical objects; (3) analysis of model samples (dyed fibres, paintings) prepared according to old recipes; (4) application of the acquired knowledge to identification of colourants present in historical objects.

The C18 stationary phase is the one that is the most often used in analysis of natural dyes and their colourants.[3,4] However, analyses carried out with C4, C8, and NH<sub>2</sub> columns have showed that the use of other fillings with the proper choice of mobile phase could also give satisfactory separation.[5-7] The proper selection of both phases plays a key role in the effectiveness of the process, as they are responsible for retention times of separated compounds, the shape of chromatographic peaks, and the time of analysis, as well as influencing the intensity of MS signals. Due to better selectivity and efficiency in comparison with isocratic elution, gradient elution is generally performed with binary solvent systems, with water containing methanol (MeOH) or acetonitrile (ACN) as organic modifier. Being more polar and less toxic, methanol is recommended more often than acetonitrile. Separation of polar colourants usually requires the use of mobile phases rich in water. However, in order to conform to the requirements of chromatographic and detection systems, the eluate from the column often has to be enriched with organic solvents or other additives.

In many analyses keeping the pH in the optimal range plays a crucial role. Acidic or alkaline additives can sharpen elution bands obtained with the use of a modified silica column. The presence of a small amount of acid in the mobile phase allows the acid-base equilibria occurring between forms of the solvated compounds to be controlled.[8] In acidic solutions, most of the separated compounds are present in neutral forms. However, it is known that the mobile phase containing a strong acid such as trifluoroacetic acid (TFA) may suppress ESI due to ion pairing and surface tension effects. Other modifiers such as formic (FA) or acetic acid (AcOH) are recommended as an alternative for TFA. At the same time inorganic buffers widely used for keeping the pH in the proper region in HPLC-UV-Vis must be avoided, when ESI MS serves as the detector. For instance, non-volatile phosphate buffers should be replaced by ammonium acetate (AcONH<sub>4</sub>) or ammonium formate.[9]

CE, another high performance separation technique, was also proved to be a powerful tool and an alternative for HPLC in the analysis of natural dyestuffs, even if its application in this field is still considerably limited. It could play an important role especially in the analysis of artworks, as it requires a very small volume of a sample solution (a few dozen nanolitres). In CE[10-14] separation of charged species is based on their different migration properties along the capillary tube which is in a constant electric field. Two platinum electrodes and both ends of a narrow bore (i.d. 25-100  $\mu$ m) flexible fused silica capillary (usually 60-100 cm long) filled with a suitable conducting buffer are immersed in two

vials. After the sample has been injected into the capillary, a high potential difference (20–30 kV) is applied across the electrodes and induces the electro-osmotic flow (EOF). EOF is a bulk flow of liquid in the capillary, which occurs as a consequence of the surface charge on the inner capillary wall. A unique feature of EOF in the capillary is its flat profile, in contrast with the parabolic profile characteristic of pressure driven or laminar flows (observed in LC systems). Separation in CE depends mainly on the electrophoretic mobility of migrating species, which is proportional to their mass to charge ratio,  $m/z$ . CE has been used in the identification of some polar colourants, such as anthraquinones or flavonoids, mostly with a spectrophotometric diode array detector.[15–18] The separation is performed under alkaline conditions (pH 8–9) for negatively charged components of the analysed mixture.

Coupling of CE with MS is a difficult task, because of the incompatibility of the EOF (100–500 nl min<sup>-1</sup>) and optimal ESI ionization conditions. Moreover, a stable current for reproducible electrophoretic separations must be ensured. Fortunately, both these problems can be solved by adding make-up solution (10–100  $\mu$ l min<sup>-1</sup>), which also ensures an electric connection between the nebulizer and the tip of a capillary.

Statistical evaluation of HPLC–UV–MS[19] and CE–UV–MS[20] methods proves that MS detection of anthraquinone dyes is more sensitive than UV, especially in the case of chromatographic analysis of laccaic acids (almost 20 times) and purpurin (almost 40 times). However, detection limits of HPLC–ESI MS determination of alizarin and purpurin (0.03  $\mu$ g ml<sup>-1</sup>) are about 20 times lower than those of CE–ESI MS (0.52–0.58  $\mu$ g ml<sup>-1</sup>).

It has to be stressed that selectivity of both separation methods depends on the matrix effect and the additives used, which can strongly influence chromatographic or electrophoretic equilibria. For that reason proper sample preparation plays a crucial role in the analytical process.

## 13.2 Sample Preparation

Extraction or rather leaching of colourants is the first and a very important step in the analytical procedure for the analysis of natural dyes. The chemical composition of extracts from historical materials depends on many factors, such as the source of natural dyes, the technological procedure of their production, storage conditions over the centuries, ageing processes and extraction conditions. The choice of the extraction method depends on the properties of the components and the matrix from which they are isolated, as well as on the mechanism of dyeing with the particular dyestuff. In this regard, they are usually divided into three groups: direct, vat and mordant dyestuffs.

The main representatives of direct dyes are turmeric, annatto, saffron, and orchil. They are directly bound to fibres. Most of the colourants present in these dyestuffs can be easily extracted by water or alcohols.

Vat dyes (the best known are Tyrian purple, indigo and woad) are insoluble in water. Before dyeing, they must be reduced into water-soluble leucoforms. After impregnation of the textile, dyestuffs are again oxidized into colour forms. As far as their extraction is concerned, aprotic solvents are usually recommended, e.g. pyridine, dimethylformamide or dimethylsulfoxide.

Mordant dyes form the widest group of natural materials. Their colouring agents are mainly flavonoids (e.g. in weld, old and young fustic, sawwort, dyer's broom) or anthraquinones (cochineal, madder, lac dye, kermes). The process of dyeing with mordant dyes has two stages: mordanting, which consists of treating the textile with metal salt solution; and dyeing the textile in a water extract of the dyestuff. As a result, metal ions (e.g. aluminium, iron, tin, chromium, copper) bound to fibres form complexes with organic colour molecules, fixing them to the ground. Their further extraction can be performed only with the use of aggressive agents (mainly solutions of strong acids).

However, other problems arise when dyes or art objects contain components which can be extracted together with colourants. Three strategies can be chosen for leaching: (1) selective extraction of colourants exhibiting specific polarity; (2) sequential extraction of polar and nonpolar colourants performed in two or three steps; or (3) total extraction of all components (Figure 13.1).

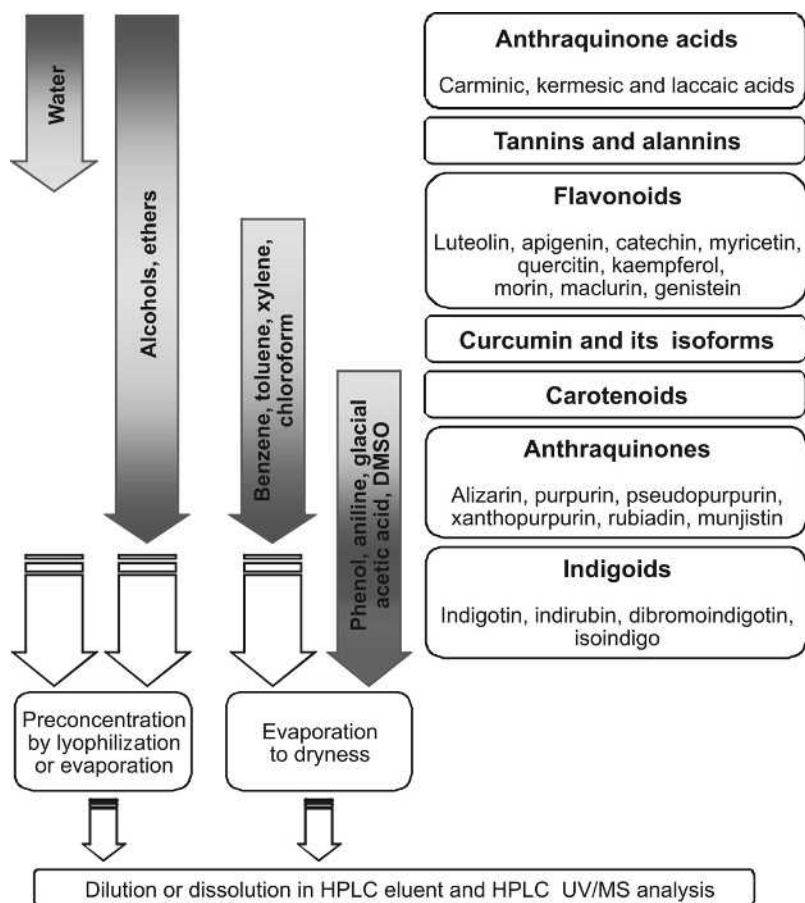


**Figure 13.1** Typical procedures and solvents used for extraction of organic colouring compounds

Antraquinones and flavonoids are present in plants mostly as polar glycosides; for these colouring agents classical extraction with hot aqueous methanol[19–21] or ethanol[21] was proved to be the most appropriate. Other water-soluble dyestuffs, such as turmeric or saffron, are also extracted mainly with methanol.[22–26] However, in the case of fibre analysis, bonds between colourant and metal ion or ground must be destroyed, and the extraction procedure has to be combined with acid hydrolysis in order to improve recovery. As a result, glycosides of anthraquinones and flavonoids are decomposed forming less polar aglycones. Chemical hydrolysis is usually performed at elevated temperatures (80–100°C) or by refluxing with hydrochloric acid,[6–8,27–37] occasionally with sulfuric acid,[38–40] hydrofluoric acid,[41] or even in the presence of enzymes.[42] Such a procedure is not an optimal solution, as it may cause loss of some information about the source of dyes, as well as it demands evaporation of strong inorganic acids. Consequently, organic acids, e.g. ethylenediaminetetraacetic (EDTA),[6] formic[6,7,38] or trifluoroacetic (TFA) acid,[42] were tested for extraction of mordant dyes. The last two, being more volatile, were found to be efficient leaching agents suitable for ESI MS conditions. In these cases evaporation to dryness is not required and only dilution of concentrated sample is necessary. The final extraction after hydrolysis can also be performed with polar organic solvents, e.g. *n*-amyl alcohol.[20] Unfortunately, this procedure can interfere in chromatographic separation, as *n*-amyl alcohol can suppress hydrophobic interactions of analytes with the stationary phase.

Indigoids, nonpolar colourants (insoluble in acidic solvents), are usually leached with aprotic polar reagents, such as pyridine,[32] dimethylformamide (DMF),[43] or dimethylsulfoxide (DMSO).[44,45] The obtained extracts are usually analysed with the use of APCI MS or HPLC–APCI MS. Such detection is more suitable for small, nonpolar compounds than ESI MS. However, indigoids could also be identified by ESI MS after their isolation from DMSO (which strongly interfere in MS analysis, when ESI is used) by HPLC.[44] Among non-typical procedures worthy of mention is extraction of dyes from old maps which is carried out with the use of a brush imbibed with sodium dodecyl sulfate (SDS) solution modified with acetic acid in order to dissolve indigotin.[5,18] Isolation of indigo precursors from woad leaves is performed by using a mixture of acetone and acetic acid.[46] Nonpolar alkannins from *Alkanna* roots are separated as hexane extracts by using Soxhlet apparatus.[47] Solid-phase extraction (SPE) is seldom recommended;[48,49] it is sometimes used e.g. for the analysis of tannins or flavonoid glycosides present in saffron.

### 13.3 Analysis of Red Dyes

In the world of red colourants, anthraquinones, which are obtained from plants or animals, are the largest group. They can be separated by RPLC due to diverse polarity caused by the presence of various polar groups in their structure. However, forms of identified compounds depend mostly on extraction and hydrolysis conditions.

RPLC separation with spectrophotometric detection is often applied to the identification of the anthraquinone colour components of cochineal, lac dye and madder.[28,40,41,50–53] In particular the latter, containing many colourants, is the object of many research studies. Due to the large number of anthraquinones isolated from plants of the *Rubiaceae* family, their unambiguous identification solely by UV-Vis detection is not always possible,

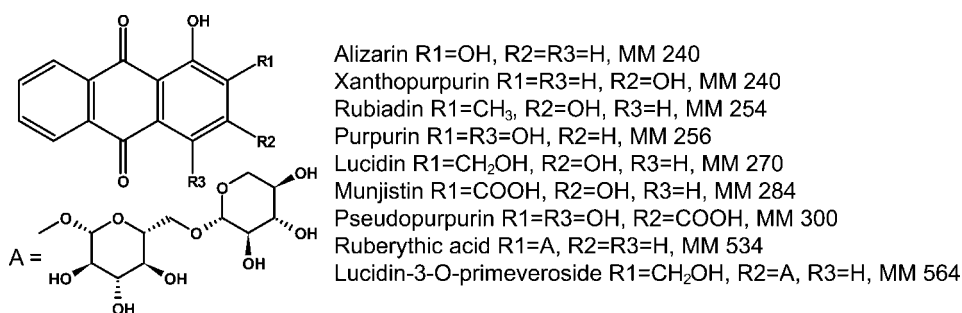


**Figure 13.2** Structures of colour components present in plants of the Rubiaceae family. A, 6-O-β-D-xylopyrosyl-D-glycosyl

especially without appropriate standards. This is why both RPLC–DAD and RPLC–MS methods are used to provide information for the identification of anthraquinone glycosides and aglycones present in madder roots extract.[8,19,34,38,42,54]

For the extraction of colourants from *Rubia tinctorum* (Figure 13.2) roots, mostly methanol,[42] water-methanol (with the addition of *n*-amyl alcohol in the case of lake extraction)[19,20] or water-ethanol solutions[38] are used. Additional hydrolysis can be performed with hydrochloric acid[8,19,20,34] and trifluoroacetic acid,[42] but also with madder root enzymes,[42] responsible for cleavage of anthraquinone glycosides into the corresponding aglycones and sugars.

In the identification of anthraquinones, both positive (PI) and negative (NI) ionization can be applied (Table 13.1), but when ESI MS is used, mostly the NI mode is recommended. In the analysis of water-ethanol extract from *Rubia tinctorum* roots, the intensity of the negative ions is tenfold higher than that of positive ones.[38,39] The addition of EDTA (30 mg l<sup>-1</sup>) to the ammonium formate-formic acid-acetonitrile mobile phase, improves the peak shape of basic compounds. This procedure requires post-column supplying of eluate with ammonia, which deprotonates the examined molecules and improves signal intensity for RPLC–NI ESI MS. In the PI mode, the main registered peak corresponds to the ammonium adduct [M+NH<sub>4</sub>]<sup>+</sup>, where M represents the anthraquinone glycoside. In the NI mode, in the case of lucidin primeveroside the following ions were registered: [M–H]<sup>–</sup> at *m/z* 563.0, [2M–H]<sup>–</sup> at *m/z* 1126.9, [3M–H]<sup>–</sup> at *m/z* 1691.7, [M+HCOOH–H]<sup>–</sup> at *m/z* 608.7, and ions formed by the loss of primeverose at *m/z* 269.2. On the mass spectrum of ruberythric acid, the ions observed were as follows: [M–H]<sup>–</sup> at *m/z* 533.1, [2M–H]<sup>–</sup> at *m/z* 1066.8, [3M–H]<sup>–</sup> at *m/z* 1600.7, [M+HCOOH–H]<sup>–</sup> at *m/z* 578.4, and also ions formed by the loss of primeverose at *m/z* 239.3.

LC–ESI MS allows also the identification of other anthraquinones in madder preparations. Based on structural information obtained by NI mass spectra and specific retention times (signals corresponding to quasi-molecular ions [M–H]<sup>–</sup> and fragment ions [M–CO<sub>2</sub>–H]<sup>–</sup>), pseudopurpurin (peaks at *m/z* 299.1 and 255.3) and munjistin (at *m/z* 283.1 and 239.3) are found in the natural material. Alizarin glycoside is identified by deprotonated quasi-molecular ions at *m/z* 401.1 and ions formed by the loss of glucose at *m/z* 239.1. Similar ions are found to be characteristic of lucidin

**Table 13.1** Identification of anthraquinones by liquid chromatography-electrospray mass spectrometry (and/or UV-Vis)

Sample	Anthraquinones	Extraction/ hydrolysis agents	Eluents	Detection wavelength/ ionization mode	Remarks	Ref.
<i>Rubia tinctorum</i> roots	Alizarin, alizarin glucoside, purpurin, pseudopurpurin, lucidin glucoside, lucidin primeveroside, munjistin, ruberythric acid	EtOH/H <sub>2</sub> O, H <sub>2</sub> SO <sub>4</sub>	<b>A:</b> ACN; <b>B:</b> ammonium formate/FA with EDTA	250, 254 nm/ESI (±)	Post-column modification of eluent (5% NH <sub>3</sub> in H <sub>2</sub> O) for NI mode	38
Madder lake, lac dye, cochineal	Alizarin, purpurin, ruberythric acid, lucidin, laccaic acid A, carminic acid	HCl/H <sub>2</sub> O, <i>n</i> -amyl alcohol, MeOH	H <sub>2</sub> O/MeOH with AcOH	250, 280 nm/ESI (–)	HPLC optimization	19
Madder, Armenian cochineal, lac dye; historical samples – pigment and wall painting	Alizarin, munjistin, purpurin, xanthopurpurin, rubiadin, laccaic acid A, laccaic acid B, carminic acid, kermesic acid, flavokermesic acid	HCl/MeOH/ H <sub>2</sub> O	<b>A:</b> H <sub>2</sub> O; <b>B:</b> ACN with TFA	275 nm/ESI (–)	HPLC optimization	34
<i>Rubia tinctorum</i> roots	Alizarin, munjistin, purpurin, pseudopurpurin, lucidin, nordamnacanthal (as glycosides or aglycones)	MeOH/H <sub>2</sub> O, TFA, HCl, H <sub>2</sub> O (enzymatic hydrolysis)	ACN/AcONH <sub>4</sub>	254 nm/ESI (+)	Hydrolysis optimization, characterization of root components	42
Wool dyed with <i>Rubia tinctorum</i> and <i>Galium verum</i>	Alizarin, quinalizarin, purpurin, xanthopurpurin, purpuroxanthin dimethyl ether, munjistin, rubiadin, nordamnacanthal, anthragallol, kermesic acid, hystazarin, emodin, quinizarin	HCl/MeOH/ H <sub>2</sub> O	<b>A:</b> H <sub>2</sub> O; <b>B:</b> ACN with AcOH or FA	250 nm/ESI (–)	HPLC optimization	8



glycoside, registered at  $m/z$  431.0 and 269.1, respectively, accompanied by signals at  $m/z$  476.7 and 862.8, recognized as  $[M+HCOOH-H]^-$  and  $[2M-H]^-$ . In the spectrum registered in PI mode[42] mainly protonated  $[M+H]^+$  and sodiated  $[M+Na]^+$  quasi-molecular ions are observed, when water-acetonitrile eluent modified by ammonium acetate is used as the mobile phase. Apart from the aforementioned anthraquinones, nordamnacanthal is also found and quantified in the analysed material.

Detailed examination of another madder preparation proved that the sample can be pre-mordanted with alum.[19] After hydrolysis performed with hydrochloric acid and extraction with *n*-amyl alcohol, only four colourants are found: alizarin, purpurin, and probably lucidin and ruberythric acid. Additionally, signals at  $m/z$  525 and 539 are observed in the mass spectrum. Analysis of the preparation by inductively coupled plasma mass spectrometry (ICP MS) shows that aluminium and calcium are the main inorganic components of the sample. This is why it was suggested that the signal at  $m/z$  539 can be attributed to the complex of aluminium with alizarin, and the second one, observed at  $m/z$  525, to an aluminium-calcium cluster.

The same extracts can be analysed using other techniques, namely CE.[20] It was the first time that coupling of CE and ESI MS had been applied to the investigation of natural dyes. Separation of dyes is performed using a fused-silica capillary. Its end is introduced into the nebulizer steel capillary in the ESI interface. Ammonium carbonate solution (pH 9.0) is used as an electrolyte in CE ESI MS, while spectrophotometric detection is carried out with sodium phosphate buffer (pH 8.5). In the obtained electropherogram for madder lake only two main peaks, corresponding to alizarin and purpurin, are registered (Figure 13.3). No alizarin complex is detected.

Cochineal and lac dye can be studied by HPLC with spectrophotometric and NI ESI MS detection.[34] In cochineal, carminic acid appears as a dominant colouring agent. In lac dye extracts, the signal at  $m/z$  536 corresponding to a quasi-molecular ion of laccaic acid A is observed as the dominant one.[19]

A similar analysis of cochineal can be performed with the use of CE with ESI MS detection. The results are similar to those obtained with HPLC-MS.[20] In the lac dye extract, the signal of laccaic acid A is found in the mass spectrum as the dominant one at  $m/z$  536. However, a second peak is observed on the electropherogram, and the eluted substance can be identified as laccaic acid E, on account of the mass spectrum which consists of the following signals: at  $m/z$  494  $[M-H]^-$ , 476  $[M-H_2O-H]^-$  and 450  $[M-CO_2-H]^-$ .

HPLC-ESI MS is also a useful tool in the analysis of non-anthraquinone red dyestuffs. The use of this technique allows the identification of carthamin as the main colour component of safflower.[34] Ten species of the genus *Alkanna* are extracted with hexane, and dissolved in water-methanol solution after evaporation.[47] Ammonium formate buffer (pH 3.0) was used as the mobile phase modifier. In the preparations, alkannin and many hydroxynaphthoquinones (alkannin derivatives) were identified by comparison of retention times, as mass spectra (in the NI mode) for all compounds consisted only of quasi-molecular peaks.

Analysis of dyed fibres allows identification of real colouring components of natural dyestuffs taking part in the dyeing process. Wool threads dyed with madder (*Rubia tinctorum*) as well as Our Lady's bedstraw (*Galium verum*), were studied by HPLC-DAD-ESI MS<sup>n</sup> (SIM mode).[8] Chromatograms of the extracts from wool dyed with madder



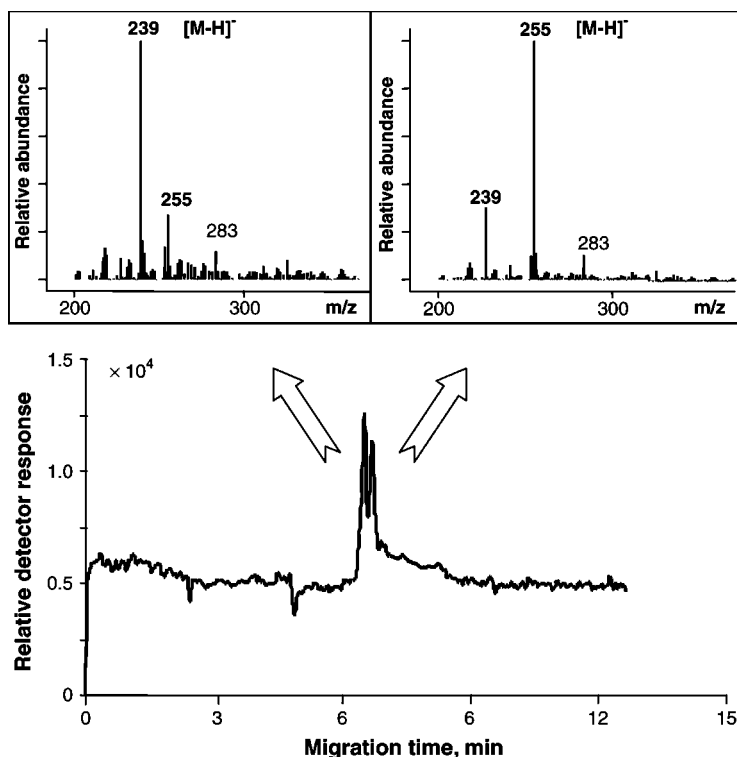


**Figure 13.3** Electropherogram (total ion current) of the madder lake extract and ESI mass spectra taken at the apex of the peaks. Identified colourants: alizarin,  $m/z$  239; purpurin,  $m/z$  255. Reproduced from M. Puchalska, M. Orlińska, M.A. Ackacha, K. Połec-Pawlak and M. Jarosz. *J. Mass Spectrom.*, **38**, 1252–1258 (2003). By permission of John Wiley & Sons, Ltd

showed the presence of many components (Table 13.1) at trace level. Even kermesic acid, probably contamination from another dye, was found. The most intense signals corresponding to anthraquinones were registered for deprotonated molecules  $[M-H]^-$ . The structures of four compounds from this class (rubiadin, munjistin, purpuroxanthin dimethyl ether and nordamnacanthal) were identified by  $MS^n$ . Essential daughter ions were formed as a result of successive fragmentations of quasi-molecular ions. For most of the anthraquinones, ions formed by the loss of CO (28 amu), CO<sub>2</sub> (44 amu) and H<sub>2</sub>C=O (30 amu) were observed. Unfortunately, the comparison of retention times of standards was required, since several compounds were of the same molecular mass and almost of the same  $MS^3$  fragmentation patterns. Additional information could be obtained by the proper selection of the acidic modifier of the mobile phase. The replacement of formic by acetic acid allows two forms of acidic munjistin to be found in equilibrium registered as a large forked peak (Figure 13.4).

In the threads dyed with *Galium verum*, purpurin and rubiadin were identified as the main components.

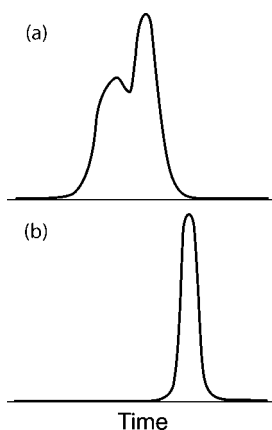


**Figure 13.4** Chromatographic signals of munjistin registered for mobile phases containing acetic acid (a) and formic acid (b)

HPLC–ESI MS was applied in the analysis of artworks of historical value, e.g. Philippe de Cuapaigne’s painting ‘Cardinal Richelieu’ (painted around 1637). Red paint sample from the Cardinal’s cloak was examined by the coupled technique.[54] Sample was extracted with boron trifluoride-methanol solution. Protonated ions of laccaic acid A observed at  $m/z$  538 were identified. Its methyl ester was recognized due to the signals at  $m/z$  552  $[M+CH_2+H]^+$  and 567  $[M+2CH_2+H]^+$ . The quasi-molecular ions at  $m/z$  497 corresponding to the laccaic acid B were also found. Finally, the pigment present in the red paint was identified as lac dye. From the analyses performed, other conclusions were also drawn. Careful interpretation of the registered spectra allowed it to be stated that laccaic acids can form multiply charged clusters (containing even 56 protonated molecules of laccaic acid A), as well as daughter ions.

It has to be noted that mass spectra of anthraquinones obtained by HPLC–MS usually consist of only a few specific signals, which makes the identification of their structures difficult or even impossible (especially in the case of isomers). Retention time is an additional and useful parameter, allowing verification of their identity, but proper interpretation of obtained results still poses a considerable challenge for analysts. Moreover, tiny samples often turn out to be insufficient for the isolation of the satisfactory amount of colourants for spectrometric analyses; this is why wide experience and careful planning are necessary.

### 13.4 Analysis of Yellow and Brown Dyes

Yellow dyes are obtained only from plants and can generally be divided into two classes, i.e. flavonoids and others among which there are mainly carotenoids and diarylheptanoids. Most are water-soluble, and procedures for their extraction are similar to those recommended for red colourants. Although they were popular as textile colourants, analytical

methods for their identification were elaborated on mainly because of their properties which were beneficial to health.[27,55–58]

For the characterization of compounds extracted from plants, wool and dye baths, acquisition in the NI mode is used. The main signals in the mass spectra of each colourant are attributed to deprotonated molecular ions  $[M-H]^-$ . More detailed studies can be performed by ESI MS<sup>n</sup> with a quadrupole ion trap mass analyzer, and such a set-up was used e.g. for the investigation of photo-oxidation processes of components of weld and onion skins.[29]

Products of the oxidation of flavonols are also identified using a C8 column coupled with a ESI triple quadrupole MS.[37] The fragmentation of quasi-molecular ions of hydroxybenzoic acids is performed both for positively and negatively charged ions. A typical fragmentation pattern for carboxylic acids (sequential loss of neutral molecules of H<sub>2</sub>O, CO or CO<sub>2</sub>) is observed in the PI mode for 3,4-dihydroxybenzoic acid ( $m/z$  155) and 4-hydroxybenzoic acid ( $m/z$  139). The fragmentation of isomeric 2,4-dihydroxybenzoic acid takes place without the loss of CO<sub>2</sub>. Although slight differences in the mass spectra obtained for isomeric hydroxybenzoic acids are observed, multiple reaction monitoring (MRM) is recommended in such procedures because of the unique selectivity required, especially for compounds eluted close to the void volume of the HPLC column.

Flavonoids bonded to fibres undergo photodegradation over the course of time; their identification in historic textiles is thus often difficult. The analysis of a wool orange fibre (from a nineteenth century Aubusson tapestry) dyed with alum mordant and quercetin enabled the presence of quercetin (at  $m/z$  301) and its decomposition products, 3,4-dihydroxybenzoic acid (at  $m/z$  153) and methyl 3,4-dihydroxybenzoate (at  $m/z$  167), to be confirmed.[30] The samples were hydrolysed with hydrochloric acid and analysed with RPLC–MS.

Silk fibres dyed with onion skin and pagoda tree buds were extracted with hydrochloric, formic and EDTA acids in order to compare the efficiency of the procedures.[6] The obtained extracts were analysed with the use of a C4 column and two detection modes (spectrophotometric within visible range and the NI mode ESI MS). When hydrochloric acid was used, the extracts of silk dyed with pagoda tree buds and onion skins were indistinguishable. Due to hydrolysis of all glycosides, only quercetin and kaempferol were detected (Table 13.2). Much more information was obtained for the fabrics extracted with mild reagents (weak formic acid or EDTA), which hydrolyse only bonds between metal ions and colourant molecules, and do not destroy the glycoside structure of the latter. By the use of these reagents different flavonoid glycosides were isolated from fibres dyed with each dye. Chromatograms of the pagoda tree extracts allowed the identification of rutin (at  $m/z$  609) and kaempferol-3,7-diglycoside (also at  $m/z$  609) as well as their isomers, while the onion extract contained quercetin-4'-glycoside (at  $m/z$  463). Such identification was confirmed by different retention times of compounds of the same molecular mass, e.g. rutin, its isomers and kaempferol-3,7-diglycoside.

Mild extraction was also found to be effective in the analysis of extracts of *Flaveria haumanii*,[7] in which quercetin, kaempferol, isorhamnetin as well as their glycosides and sulfate esters were identified. The obtained results were useful in the identification of the colourants from fibres from pre-Columbian Andean textiles extracted with the use of water-methanol solution with formic or hydrochloric acid. The components of each extract were separated on a reversed phase HPLC column and the eluates were monitored at

**Table 13.2** Identification of yellow colourants by liquid chromatography-electrospray mass spectrometry

Sample	Colourants	Extraction/hydrolysis reagents	Eluents	Detection wavelength/ionization mode	Remarks	Ref.
Silk dyed with <i>Reseda luteola</i> , <i>Sophora japonica</i> and <i>Allium cepa</i>	Rutin, quercetin, kaempferol, kaempferol-3,7-diglucoside, quercetin-4'-glucoside, luteolin	HCl/MeOH/H <sub>2</sub> O, HCOOH/MeOH, H <sub>2</sub> EDTA/ACN/MeOH	<b>A:</b> H <sub>2</sub> O; <b>B:</b> ACN; <b>C:</b> H <sub>2</sub> O with HCOOH	350, 450, 490 nm/ESI (–)	Column C4	6
<i>Flaveria haumanii</i> , <i>Cotinus coggygria</i> , <i>Coreopsis</i> spp. and pre-Columbian Andean textiles	Okanine, luteolin, butein (as aglycones, glycosides or as methyl ethers), quercetin, isorhamnetin (as sulfate esters), sulfuretin, fisetin, hydroxybenzoic acids	HCl/MeOH/H <sub>2</sub> O, HCOOH/MeOH	<b>A:</b> H <sub>2</sub> O; <b>B:</b> ACN; <b>C:</b> H <sub>2</sub> O with HCOOH	254, 350 nm/ESI (±)	Column C4	7
Greek saffron	Picrocrocin, safranal, crocins, kaempferol diglucoside	MeOH/H <sub>2</sub> O	<b>A:</b> MeOH; <b>B:</b> H <sub>2</sub> O with AcOH	250, 308, 440 nm/ESI (+)	ESI interface	22
<i>Curcuma longa</i>	Curcumin, demethoxycurcumin, bisdemethoxycurcumin	MeOH	<b>A:</b> ACN; <b>B:</b> H <sub>2</sub> O with AcOH	250 nm/ESI (±)		23
Standards, fresh turmeric rhizomes	Curcumin, demethoxycurcumin, bisdemethoxycurcumin, dihydrocurcumin, dihydrodemethoxycurcumin, dihydrobisdemethoxycurcumin	MeOH	<b>A:</b> ACN; <b>B:</b> H <sub>2</sub> O with ammonium formate/HCOOH	230, 425, 550 nm/ESI (±)	MS/MS (ion trap)	25, 26

350 nm. The identified colourants included glycosidic derivatives of butein, okanine, luteolin and even sulfuretin, which suggested that fibres were dyed with a chalcone plant. In other threads, derivatives of quercetin, kaempferol and isorhamnetin were found, which suggested the use of flavonol dyes obtained from *Flaveria* species. Fibres dyed with heartwood of *Cotinus coggygria* were also found, which was confirmed by the identification of fisetin and sulfuretin.

Carotenoids belong to diarylheptanoids, which are responsible for the biological and medicinal activity of turmeric. The main colouring carotenoids in this dyestuff are curcumin, demethoxycurcumin and bisdemethoxycurcumin. A turmeric rhizome was examined with the use of HPLC–DAD–ESI MS in both PI and NI modes,[23,25,26] but the PI was reported as more sensitive. The three main colourants of *Curcuma longa* were successfully separated and identified in a fresh turmeric extract using a C18 column and water-acetonitrile containing an acetic acid mobile phase.[23] The mass spectra of each peak showed main signals of protonated quasi-molecular ions  $[M+H]^+$  at  $m/z$  369, 339 and 309, less intense sodiated ions  $[M+Na]^+$  at  $m/z$  391, 361 and 331, and dimeric ions  $[2M+Na]^+$  at  $m/z$  759, 699 and 639, corresponding to curcumin, demethoxycurcumin and bisdemethoxycurcumin, respectively. In the NI mode only deprotonated quasi-molecular ions (ion A) were present in the mass spectra of these three curcuminoids, at  $m/z$  367, 337 and 307.[25,26] Their MS/MS fragmentation occurred through just a few channels producing simple spectra. Curcumin and demethoxycurcumin gave signals mainly at  $m/z$  217 (ion B) and 173 (ion D), whereas ions at  $m/z$  187 and 143 were observed for bisdemethoxycurcumin as a result of the lack of any methoxy group on aromatic rings (Figure 13.5). The fragmentation spectra allowed the identification of unknown curcuminoids and demonstrated that these compounds, as a group, have the same fragmentation pathway (Figure 13.6). The formation of the product ion B could proceed via a  $\beta$ -hydrogen shift (reaction 2) to the double bond of the diketone form of the respective precursor ion A, leading to the loss of a neutral moiety. Alternatively ion B could be formed from the keto-enol form of the phenolate A via reaction 3. Ion C could be formed by a ring-closure reaction from A (reaction 5), while ion D involved rearrangement of B and a loss of one molecule of  $CO_2$  (reaction 4). Product ion E could be produced from either ion A or A' (reaction 2 or 6). Moreover, ion E could be formed from either the diketone or the keto-enol form of A, but with the ionization of the opposing phenolic hydroxyl group (next to R1).

A careful interpretation of the spectra allowed the identification of monoacetate and diacetate derivatives of curcumin[26] in the turmeric extract, as well as of nineteen other diarylheptanoids, including twelve not reported until that time.[25]

Saffron, the dried stigmas of *Crocus sativus* L., is valued for its intense colouring properties. The dyeing components of saffron are crocins, a family of water-soluble carotenoids – mono- and diglycosyl esters of crocetin (Figure 13.7). The main colourant in saffron is digentiobiosyl ester of crocetin ( $Gnt = \beta$ -D-glc-1 $\rightarrow$ 6- $\beta$ -D-glc), called  $\alpha$ -crocins. Crocins exhibit characteristic spectra in the visible region with two maxima between 400 nm and 500 nm, and in the UV region between 320 nm and 340 nm. However, the analysis of saffron performed with HPLC–UV–Vis[24,59] turns out to be insufficient for the identification of all detected crocins and their isomers, and only HPLC–ESI MS (in the PI mode) allows recognition of compounds extracted with a mixture of methanol and water.[22] Crocetin di( $\beta$ -D-gentiobiosyl) ester (molecular mass 976) was registered as a

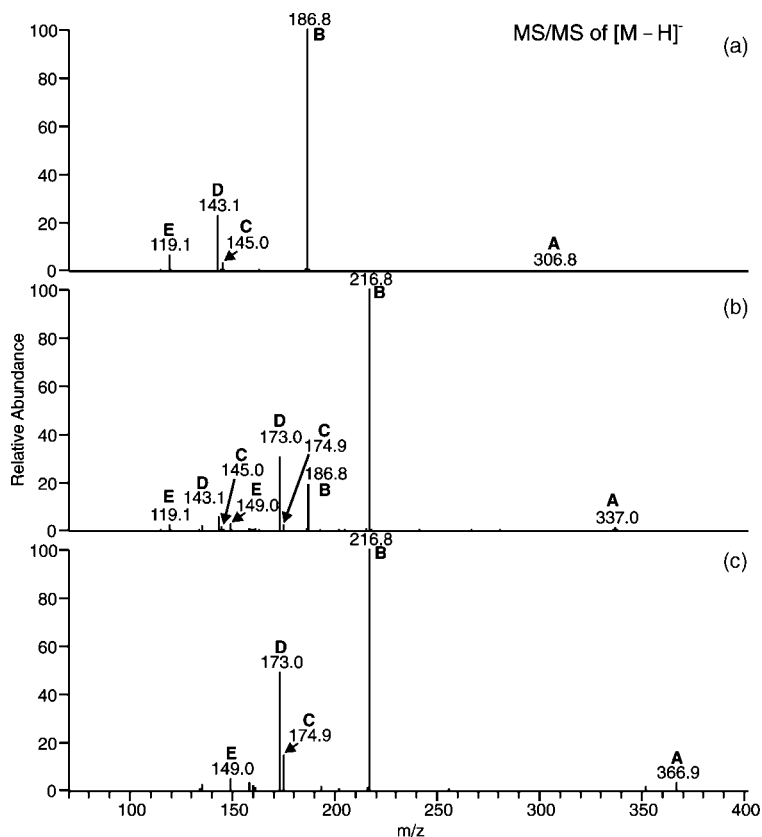


**Figure 13.5** Product ion spectra of curcuminoids (NI HPLC–ESI MS/MS). Product ion labels correspond to fragments depicted in Figure 13.6: (a) bisdemethoxycurcumin; (b) demethoxycurcumin; (c) curcumin. Reproduced from H. Jiang, A. Somogyi, N.E. Jacobsen, B.N. Timmermann and D.R. Gang. *Rapid Commun. Mass Spectrom.*, **20**, 1001–1012 (2006). By permission of John Wiley & Sons, Ltd

sodiated quasi-molecular ion at  $m/z$  999  $[M+Na]^+$ . Other identified signals included the one at  $m/z$  511  $[M+2Na]^{2+}$  and those at  $m/z$  675  $[M+Na-Gnt]^+$  and 329  $[M+H-2Gnt]^+$  related to the loss of gentiobiosyl groups. Reconstruction of the chromatograms for the ions at  $m/z$  1161, 837, 675 and 513 allowed the identification of crocetin penta-, tri-, di- and mono-glycosylates. Double charged ion  $[M+2Na]^{2+}$  at  $m/z$  592 confirmed the presence of crocetin pentaglycoside. Monitoring of its quasi-molecular ion  $[M+Na]^+$  at  $m/z$  1161 showed at least four isomers for each trans and cis form.

Polyphenols, as one of the largest and most widespread class of plant compounds, are also present in saffron stigma. In the mass spectrum of the flavonoid fraction of the methanolic extract from saffron there were ions at  $m/z$  611 and 633 which may be attributed to protonated and sodiated quasi-molecular ions of kaempferol diglycoside.[22] Flavonoids from the water extract can be isolated and concentrated

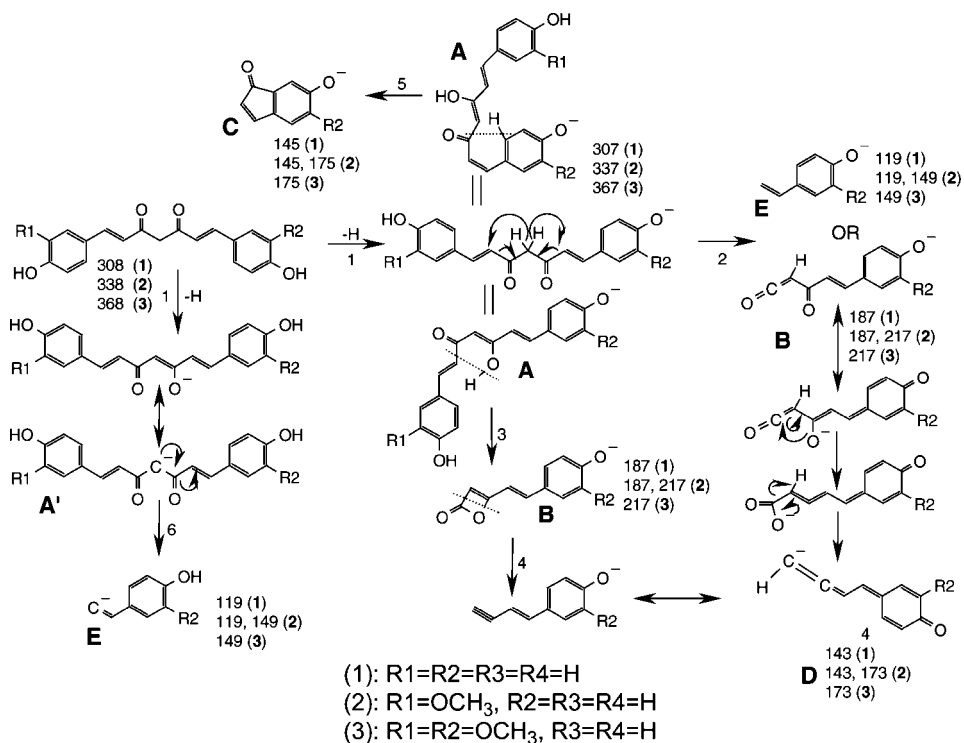


**Figure 13.6** ESI MS/MS fragmentation of curcuminoids; NI mode. Reproduced from H. Jiang, A. Somogyi, N.E. Jacobsen, B.N. Timmermann and D.R. Gang. *Rapid Commun. Mass Spectrom.*, **20**, 1001–1012 (2006). By permission of John Wiley & Sons, Ltd

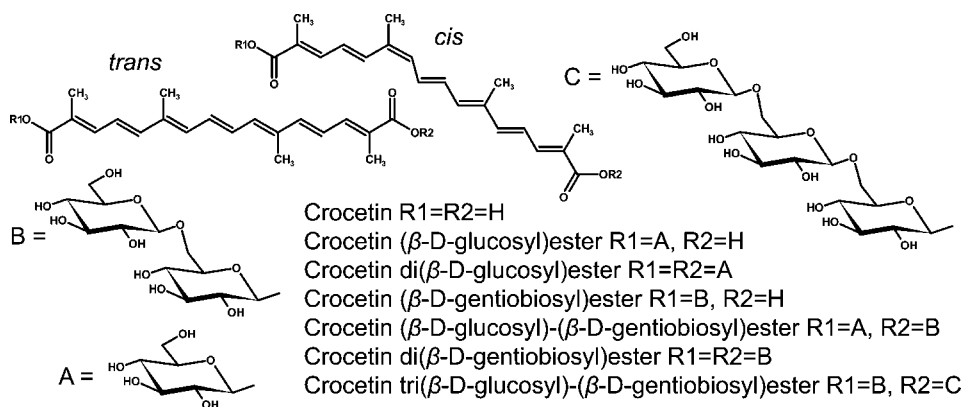


**Figure 13.7** Glycosyl esters of *trans*- and *cis*-crocetin: (A)  $\beta$ -D-glycosyl; (B)  $\beta$ -D-gentiobiosyl; (C) three  $\beta$ -D-glucosyl

on a C18 solid-phase SPE cartridge and eluted with acetonitrile.[49] The MS spectra registered in the NI mode of two major compounds consisted of signals of deprotonated quasi-molecular ions at  $m/z$  771 and 609 and ions at  $m/z$  285, corresponding to aglycones. Acidification of the solution caused their full hydrolysis, after which the only compound observed was identified as kaempferol aglycone. Therefore, the two major compounds were identified as 3-sophoroside-7-glycoside and 3-sophoroside of kaempferol. Also kaempferol-3,7,4'-triglycoside ( $m/z$  771  $\rightarrow$  609  $\rightarrow$  429, 285, 256) and other hexosides of kaempferol were recognized.

### 13.5 Analysis of Blue-violet Dyes

Indigo is considered as one of the most important dyes. Its preparations are usually analysed by HPLC with UV-Vis[46,60] or APCI MS detection.[61,62] Separation of the colouring components of indigo extracted with DMSO is usually performed with the use of a C18 column. Spectrophotometric detection of blue indigotin is performed at 617 nm, red indirubin at 540 nm, and brown isoindigo at 365 and 490 nm. As mobile phases, mixtures of methanol or acetonitrile and water with the addition of TFA or formic acid are used to ensure compatibility with the requirements of the APCI source.

RPLC-APCI MS is used for the identification of colourants in extracts of the *Isatis indigotica* plant. RPLC separation of isomeric indigotin and indirubin is necessary for proper colourant identification, since in their spectra only positive quasi-molecular ions are observed at  $m/z$  263.[61,62] Coupling of RPLC with APCI allows the identification of tryptanthrin ( $m/z$  249) and isatan B as other specific components that can be extracted from the plants which are indigo sources. Due to the low polarity of indigoids, APCI seems to be the best technique for MS studies. However, RPLC-ESI MS also allowed results to be obtained for indigoids.[44] Due to the structure of the molecule, which allows the formation of two internal hydrogen bonds, indigotin can be protonated more easily than deprotonated (Figure 13.8). The dominating peak in the PI spectrum of indigotin and indirubin can be attributed to the quasi-molecular one (at  $m/z$  263), but also a few other signals originating from fragment ions are observed:  $[M+H-CO]^+$ ,  $[M+H-CONH_2]^+$  and  $[M+H-CO-HCO]^+$ , at  $m/z$  235, 219 and 206, respectively. Only in the case of indigotin are doubly charged quasi-molecular ion  $[M+2H]^{2+}$  at  $m/z$  132 also observed due to the specific symmetry of the molecule.

In the case of indirubin or isoindigo, where one or two protons are not blocked by hydrogen bonds, deprotonation is possible (signal at  $m/z$  261), and in the NI mode the intensity of the registered signals is even higher than in the PI mode. In this mode only small chromatographic peaks of indigotin are observed.[45]

HPLC-UV-Vis-ESI MS was used to identify indigoid dyes in blue fibre extracts taken from a Japanese tapestry (nineteenth century). Two main colourants were recognized as indigotin and Methylene Blue,[44] a thiazine cationic dye first synthesized at the end of the nineteenth century, commonly used for silk and cotton dyeing (Figure 13.9).

Indigoid species are also present in another dyestuff, Tyrian Purple, extracted from molluscs from the *Muricidae* family. It owes its specific red shade to the presence of bromoindigoids. In the extract of the dyestuff, after chromatographic separation of its components,[44] in addition to indigotin, indirubin and isoindigo, 6,6'-dibromoindigotin is



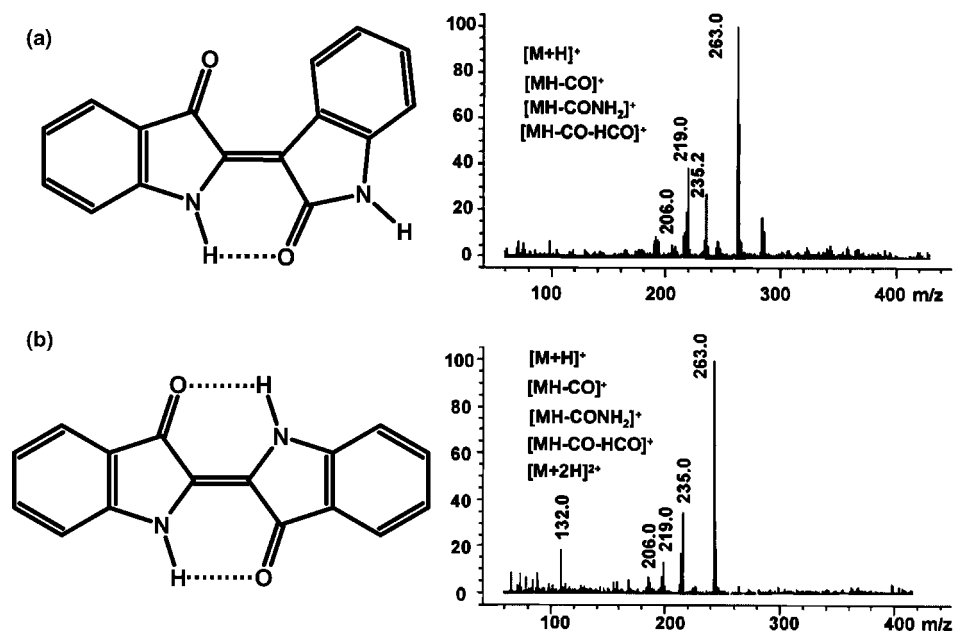


**Figure 13.8** Structures and ESI mass spectra of (a) indirubin and (b) indigotin. Reproduced from M. Puchalska, K. Połec-Pawlak, I. Zadrozna, H. Hryszko and M. Jarosz. *J. Mass Spectrom.*, **39**, 1441–1449 (2004). By permission of John Wiley & Sons, Ltd

also isolated and identified by ESI MS. The presence of ions in the region of  $m/z$  419–423 reflects the isotopic pattern of the quasi-molecular ion  $[M+H]^+$  of 6,6'-dibromoindigo with two bromine atoms. Additionally, the fragment ion at  $m/z$  205 is observed due to elimination of bromine and CO  $[M-2Br-2CO+H]^+$ .

RPLC–MS can also be successfully applied in the analysis of less popular blue dye-stuffs, namely logwood and elderberry.[45] The main colourant in logwood is hematein, which is obtained by oxidation of hematoxylin. Methanolic solutions of logwood colour compounds eluted from a C18 column were monitored by UV–Vis spectrophotometry at 280, 445, 520 and 600 nm, and an MS analysis was performed with ESI. Only quasi-molecular ions were observed in the NI mode ( $m/z$  299 and 301 for hematein and hematoxylin, respectively), but signals of low intensity corresponding to deprotonated dimers were also found at  $m/z$  599 and 603. Mass spectra registered for positively charged ions consisted of more signals. In the hematoxylin spectrum there were observed peaks corresponding to sodiated ions  $[M+Na]^+$  at  $m/z$  325, protonated ions  $[M+H]^+$  at  $m/z$  303, and fragment ions at  $m/z$  285, 177 and 149 obtained by the loss of  $H_2O$ , resorcinol and CO. The mass spectrum of more hydrophobic hematein registered in the same mode consisted of the main signal at  $m/z$  301  $[M+H]^+$  and  $[M-CO+H]^+$ ,  $[2M+H]^+$  and  $[2M+H_2O+H]^+$  observed at  $m/z$  273, 601 and 619, respectively.

Hematein and hematoxylin are known as the main components of logwood, but other characteristic colourants are also present in its preparations, e.g. tannins and

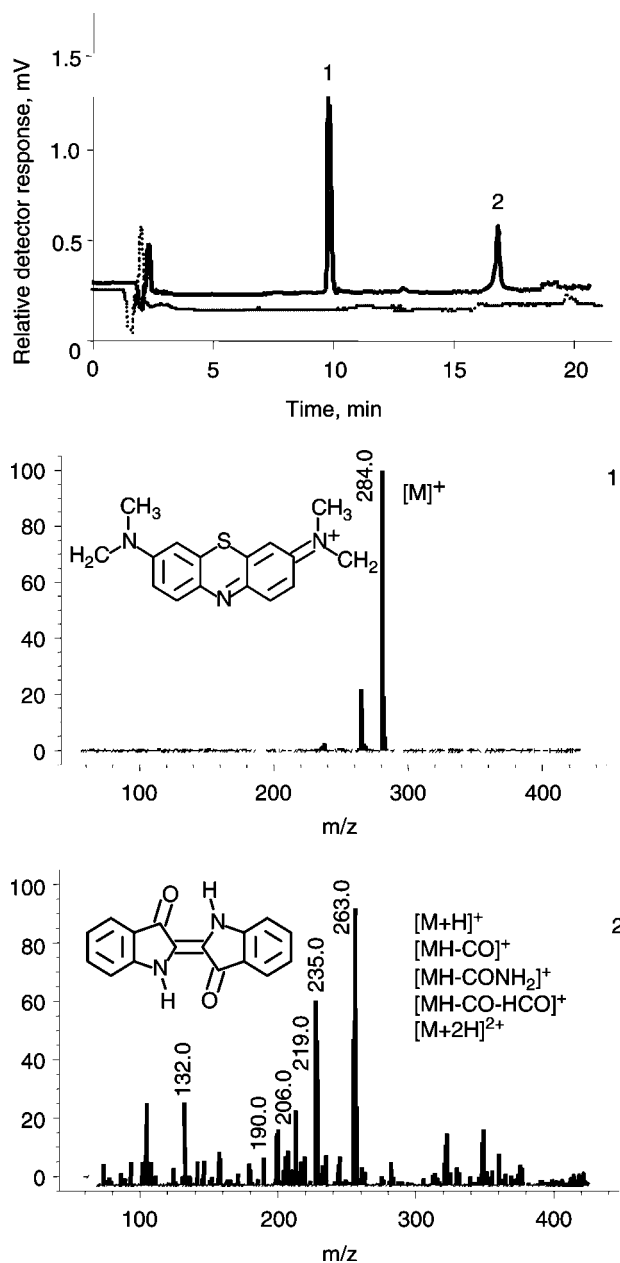


**Figure 13.9** Chromatogram obtained for extract of blue fibre from a Japanese tapestry and ESI mass spectra of the compounds eluted in the chromatographic peaks: (1) Methylene Blue; (2) indigotin. Reproduced from M. Puchalska, K. Połec-Pawlak, I. Zadrożna, H. Hryszko and M. Jarosz. *J. Mass Spectrom.*, **39**, 1441–1449 (2004). By permission of John Wiley & Sons, Ltd

gallotannins. A methanolic solution of tannic acid, a natural polymer composed of many glucose molecules and gallic acid (GA) fragments, was analysed using the same procedure as for logwood colourants.[45] The solvent used was able to cleave the polymer into pentagalloyl-glucose units (molecular mass 940),[63,64] which were observed as a quasi-molecular ion. When the same compound was analysed as a methanolic extract of standard, seven peaks were registered on the RPLC chromatogram. The mass spectra taken at the apex of the peaks show that decomposition of pentagalloyl-glucose takes place in the liquid phase. The following signals, corresponding to the loss of galloyl units, are dominant in the mass spectra of separated chromatographic peaks:  $[M-H_2O+H]^+$  (at  $m/z$  923),  $[M-GA+H]^+$  (771),  $[M-GA-(GA-H_2O)+H]^+$  (619),  $[M-GA-(GA-H_2O)_2+H]^+$  (467),  $[M-GA-(GA-H_2O)_2-H_2O+H]^+$  (449),  $[GA+H]^+$  (171) and  $[GA-H_2O+H]^+$  (153). In the NI mode similar results are obtained, and the mass spectra contain: quasi-molecular ions  $[M-H]^-$  (at  $m/z$  939) and fragment ions  $[M-(GA-H_2O)-H]^-$  (787),  $[M-(GA-H_2O)_2-H]^-$  (635),  $[M-(GA-H_2O)_3-H]^-$  (483),  $[M-(GA-H_2O)_4-H]^-$  or  $[2GA-H_2O-H]^-$  (321) and  $[GA-H]^-$  (169). Retention times, over a wide range from 16 to 22 min, increase with  $m/z$  value of the eluted compounds. Tannins can also be analysed with the use of RPLC coupled with ESI MS/MS. The fragmentation carried out with triple quadrupole MS allows specific fragmentation pathways to be found.[48]

Rich in anthocyanins (mainly cyanidin-3,5-diglycoside and cyanidin-3-glycoside), elderberry is another mordant dye that was considered as a potential dyestuff, analysed by RPLC-ESI MS.[45] In the mass spectra registered in the NI and PI mode, signals of monoglycosidic ions at  $m/z$  447 and 449 and of aglycones at  $m/z$  285 and 287, respectively, were found. In addition, in the spectra of diglycoside small signals of quasi-molecular ions are also observed at  $m/z$  609 (NI) and 611 (PI).

The optimized RPLC-UV-Vis-ESI MS method for all typical blue colourants (indigoids, hematein, tannins, anthocyanins and selected flavonoids) was used for the identification of dyes extracted from a thread taken from an 'Italian' tapestry of unknown origin from the collection of the National Museum in Warsaw (Poland). It was found that to obtain the red-blue colour of the fibre a mixture of dyestuffs was probably used. The presence of indigotin, tannic and ellagic acid (at  $m/z$  301, NI), as well as carminic acid, suggested the use of indigo and cochineal. *Reseda luteola* could also have been used due to the presence of luteolin and apigenin.

### 13.6 Conclusions

In the contemporary investigation of artworks and especially in the identification of natural organic dyestuffs the applicability of HPLC-MS cannot be questioned. This technique allows recognition of almost all common colourants 'in one run', which decreases the probability of losing specific information (Table 13.3). In comparison with GC-MS, HPLC-MS has wider application, as it is not limited by the presence of polar and nonvolatile compounds, and therefore it usually does not require the derivatization step. The number of published papers, which has doubled in the last 3 years in comparison with the period 2000-2004, proves that HPLC-MS performs a pivotal role in the analysis of the colourants discussed.

**Table 13.3** Identification of colourants in work arts by liquid chromatography-electrospray mass spectrometry

Sample	Colourants	Extraction/hydrolysis agents	Eluents	Detection wavelength/ionization mode	Remarks	Ref.
Silk and wool fibres of Coptic textiles – from fourth to twelfth century	Carminic acid, laccaic acids A, B, C and E, xantholaccaic acid A, purpurin, xanthopurpurin, alizarin, monochloroalizarin, dichloroalizarin, ellagic acid, luteolin, apigenin, rhamnetin, indirubin	HCl/EtOH, pyridine	<b>A:</b> ACN; <b>B:</b> H <sub>2</sub> O with TFA	278, 350 nm/ESI (±)		31, 32
Standards, red-blue 'Italian' tapestry	Indigotin, indirubin, hematein, hematoxylin, gallic acid, ellagic acid, tannic acid, cyanidine-3,5-diglucoside, cyanidine-3-glucoside, apigenin, luteolin, fisetin, myricetin, quercetin, kaempferol, rutin, carminic acid	MeOH or DMSO (solvents), HCl/DMSO	<b>A:</b> MeOH; <b>B:</b> H <sub>2</sub> O with HCOOH	280, 445, 520, 600 nm/ESI (±)	SIM mode	45
Standards, Aubusson tapestry – from nineteenth century	Gallic acid, dihydroxybenzoic acids, carminic acid, alizarin, purpurin, xanthopurpurin, quinizarin, emodin, morin, quercetin, luteolin, apigenin, rhamnetin, hystazarin, anthragallool	HCl/MeOH/H <sub>2</sub> O, DMSO	<b>A:</b> ACN; <b>B:</b> H <sub>2</sub> O with HCOOH	256 nm/ESI (±)	SIM mode	37

A great advantage of the universal LC–MS method is the possibility to also observe the degradation products of dyes. Such complementary information is valuable in archaeometry, as it allows the recognition of dyestuffs originally used by artists, even when they underwent complete degradation over time, due to weather conditions, and so on (e.g. indigotin is degraded to isatin[44] and flavonols are photo-oxidized to hydroxybenzoic acids).[28,30] However, the applicability of the developed methods will always depend on the knowledge of their users, namely the analysts and art historians.

## References

1. A.P. Bruins, T.R. Covey and J.D. Henion, Ion spray interface for combined liquid chromatography/atmospheric pressure ionization mass spectrometry, *Anal. Chem.*, **59**, 2642–2646 (1987).
2. G. Hopfgartner, T. Wachs, K. Bean and J. Henion, High-flow ion spray liquid chromatography/mass spectrometry, *Anal. Chem.*, **65**, 439–446 (1993).
3. I. Zadrozna, K. Połec-Pawlak, I. Gluch, M.A. Ackacha, M. Mojski, J. Witowska-Jarosz and M. Jarosz, Old master paintings – a fruitful field of activity for analysts: targets, methods, outlook, *J. Sep. Sci.*, **26**, 996–1004 (2003).
4. E. Rosenberg, Characterisation of historical organic dyestuffs by liquid chromatography-mass spectrometry, *Anal. Bioanal. Chem.*, **391**, 33–57 (2008).
5. R. Blanc, T. Espejo, A. López-Montes, D. Torres, G. Crovetto, A. Navalón and J.L. Vélchez, Sampling and identification of natural dyes in historical maps and drawings by liquid chromatography with diode-array detection, *J. Chromatogr. A*, **1112**, 105–113 (2006).
6. X. Zhang and R.A. Laursen, Development of mild extraction methods for the analysis of natural dyes in textiles of historical interest using LC-diode array detector-MS, *Anal. Chem.*, **77**, 2022–2025 (2005).
7. X. Zhang, R. Boytner, J.L. Cabrera and R. Laursen, Identification of yellow dye types in pre-Columbian Andean textiles, *Anal. Chem.*, **79**, 1575–1582 (2007).
8. L. Rafaëly, S. Héron, W. Nowik and A. Tchaplá, Optimisation of ESI-MS detection for the HPLC of anthraquinone dyes, *Dyes and Pigments*, **77**, 191–203 (2008).
9. J.K. Prasain, C.H. Wang and S. Barnes, Mass spectrometric methods for the determination of flavonoids in biological samples, *Free Radic. Biol. Med.*, **37**, 1324–1350 (2004).
10. S.F.Y. Li, *Capillary Electrophoresis: Principles, Practice and Applications*, Elsevier, Amsterdam (1992).
11. P. Jandik and G. Bonn, *Capillary Electrophoresis of Small Molecules and Ions*, VCH Publishers, New York (1993).
12. R. Weinberger, *Practical Capillary Electrophoresis*, Academic Press, San Diego (1993).
13. S.C. Beale, Capillary electrophoresis, *Anal. Chem.*, **70**, 279R–300R (1998).
14. P. Schmitt-Kopplin, *Capillary Electrophoresis. Methods and Protocols*, Humana Press, Neuherberg (2008).
15. M. Trojanowicz, L. Wójcik and K. Urbaniak-Walczak, Identification of natural dyes in historical Coptic textiles by capillary electrophoresis with diode array detection, *Chem. Anal. (Warsaw)*, **48**, 607–620 (2003).
16. M. Zougagh, B.M. Simonet, A. Ríos and M. Valcárcel, Use of non-aqueous capillary electrophoresis for the quality control of commercial saffron samples, *J. Chromatogr., A*, **1085**, 293–298 (2005).
17. Y. Li, S. Qi, X. Chen and Z. Hu, Separation and determination of the anthraquinones in *Xanthophyllum atropensis pierre* by nonaqueous capillary electrophoresis, *Talanta*, **65**, 15–20 (2005).
18. A. López-Montes, R.B. García, T. Espejo, J.F. Huertas-Perez, A. Navalón and J.L. Vélchez, Simultaneous identification of natural dyes in the collection of drawings and maps from The Royal Chancellery Archives in Granada (Spain) by CE, *Electrophoresis*, **28**, 1243–1251 (2007).

19. M.A. Ackacha, K. Połec-Pawlak and M. Jarosz, Identification of anthraquinone coloring matters in natural red dyestuffs by high performance liquid chromatography with ultraviolet and electrospray mass spectrometric detection, *J. Sep. Sci.*, **26**, 1028–1034 (2003).
20. M. Puchalska, M. Orlińska, M.A. Ackacha, K. Połec-Pawlak and M. Jarosz, Identification of anthraquinone coloring matters in natural red dyes by electrospray mass spectrometry coupled to capillary electrophoresis, *J. Mass Spectrom.*, **38**, 1252–1258 (2003).
21. D. Cristea, I. Bateau and G. Vilarem, Identification and quantitative HPLC analysis of the main flavonoids present in weld (*Reseda luteola* L.), *Dyes and Pigments*, **57**, 267–272 (2003).
22. P.A. Tarantilis, G. Tsoupras and M. Polissiou, Determination of saffron (*Crocus sativus* L.) components in crude plant extract using high-performance liquid chromatography-UV-visible photodiode-array detection-mass spectrometry, *J. Chromatogr. A*, **699**, 107–118 (1995).
23. X.G. He, L.Z. Lin, L.Z. Lian and M. Lindenmaier, Liquid chromatography-electrospray mass spectrometric analysis of curcuminoids and sesquiterpenoids in turmeric (*Curcuma longa*), *J. Chromatogr. A*, **818**, 127–132 (1998).
24. P. Lozano, M.R. Castellar, M.J. Simancas and J.L. Iborra, Quantitative high-performance liquid chromatographic method to analyse commercial saffron (*Crocus sativus* L.) products, *J. Chromatogr. A*, **830**, 477–483 (1999).
25. H. Jiang, B.N. Timmermann and D.R. Gang, Use of liquid chromatography-electrospray ionization tandem mass spectrometry to identify diarylheptanoids in turmeric (*Curcuma longa* L.) rhizome, *J. Chromatogr. A*, **1111**, 21–31 (2006).
26. H. Jiang, A. Somogyi, N.E. Jacobsen, B.N. Timmermann and D.R. Gang, Analysis of curcuminoids by positive and negative electrospray ionization and tandem mass spectrometry, *Rapid Commun. Mass Spectrom.*, **20**, 1001–1012 (2006).
27. S. Häkkinen and S. Auriola, High-performance liquid chromatography with electrospray ionization mass spectrometry and diode array ultraviolet detection in the identification of flavonol aglycones and glycosides in berries, *J. Chromatogr. A*, **829**, 91–100 (1998).
28. P. Novotná, V. Pacáková, Z. Bosáková and K. Štulík, High-performance liquid chromatographic determination of some anthraquinone and naphthoquinone dyes occurring in historical textiles, *J. Chromatogr. A*, **863**, 235–241 (1999).
29. E.S.B. Ferreira, A. Quye, H. McNab, A.N. Hulme, J. Wouters and J.J. Boon, Development of analytical techniques for the study of natural yellow dyes in historic textiles, *Dyes in History and Archaeology*, **16/17**, 179–186 (2001).
30. E.S.B. Ferreira, A. Quye, H. McNab and A.N. Hulme, Photo-oxidation products of quercetin and morin as markers for the characterisation of natural flavonoid yellow dyes in ancient textiles, *Dyes in History and Archaeology*, **18**, 63–72 (2002).
31. B. Szostek, J. Orska-Gawryś, I. Surowiec and M. Trojanowicz, Investigation of natural dyes occurring in historical Coptic textiles by high-performance liquid chromatography with UV-Vis and mass spectrometric detection, *J. Chromatogr. A*, **1012**, 179–192 (2003).
32. M. Trojanowicz, J. Orska-Gawryś, I. Surowiec, B. Szostek, K. Urbaniak-Walczak, J. Kehl and M. Wróbel, Chromatographic investigation of dyes extracted from Coptic textiles from the National Museum in Warsaw, *Stud. Conserv.*, **49**, 115–130 (2004).
33. G.G. Balakina, V.G. Vasiliev, E.V. Karpova and V.I. Mamatyuk, HPLC and molecular spectroscopic investigations of the red dye obtained from an ancient Pazyryk textile, *Dyes and Pigments*, **71**, 54–60 (2006).
34. I. Karapanagiotis and Y. Chrysoulakis, Investigation of red natural dyes used in historical objects by HPLC-DAD-MS, *Annal. Chim.*, **96**, 75–84 (2006).
35. I. Surowiec, A. Quye and M. Trojanowicz, Liquid chromatography determination of natural dyes in extracts from historical Scottish textiles excavated from peat bogs, *J. Chromatogr. A*, **1112**, 209–217 (2006).
36. I. Karapanagiotis, L. Valianou, S. Daniilia and Y. Chrysoulakis, Organic dyes in Byzantine and post-Byzantine icons from Chalkidiki (Greece), *J. Cult. Herit.*, **8**, 294–298 (2007).
37. I. Surowiec, B. Szostek and M. Trojanowicz, HPLC-MS of anthraquinoids, flavonoids, and their degradation products in analysis of natural dyes in archeological objects, *J. Sep. Sci.*, **30**, 2070–2079 (2007).

38. G.C.H. Derksen, H.A.G. Niederländer and T.A. van Beek, Analysis of anthraquinones in *Rubia tinctorum* L. by liquid chromatography coupled with diode-array UV and mass spectrometric detection, *J. Chromatogr. A*, **978**, 119–127 (2002).
39. G.C.H. Derksen, M. Naayer, T.A. van Beek, A. Capelle, I.K. Haaksman, H.A. van Doren and Æ. Groot, Chemical and enzymatic hydrolysis of anthraquinone glycosides from madder roots, *Phytochem. Anal.*, **14**, 137–144 (2003).
40. G.C.H. Derksen, G.P. Lelyveld, T.A. van Beek, A. Capelle and Æ. Groot, Two validated HPLC methods for the quantification of alizarin and other anthraquinones in *Rubia tinctorum* cultivars, *Phytochem. Anal.*, **15**, 397–406 (2004).
41. J. Sanyova and J. Reisse, Development of a mild method for the extraction of anthraquinones from their aluminum complexes in madder lakes prior to HPLC analysis, *J. Cult. Herit.*, **7**, 229–235 (2006).
42. I. Boldizsár, Z. Szűcs, Z. Füzfai and I. Molnár-Perl, Identification and quantification of the constituents of madder root by gas chromatography and high-performance liquid chromatography, *J. Chromatogr. A*, **1133**, 259–274 (2006).
43. I. Karapanagiotis, Identification of indigoid natural dyestuffs used in art objects by HPLC coupled to APCI-MS, *Am. Lab.*, **38**, 36–40 (2006).
44. M. Puchalska, K. Połec-Pawlak, I. Zadrożna, H. Hryszko and M. Jarosz, Identification of indigoid dyes in natural organic pigments used in historical art objects by high-performance liquid chromatography coupled to electrospray ionization mass spectrometry, *J. Mass Spectrom.*, **39**, 1441–1449 (2004).
45. K. Pawlak, M. Puchalska, A. Miszczak, E. Rosłonec and M. Jarosz, Blue natural organic dyestuffs – from textile dyeing to mural painting. Separation and characterization of coloring matters present in elderberry, logwood and indigo, *J. Mass Spectrom.*, **41**, 613–622 (2006).
46. T. Maugard, E. Enaud, P. Choisy and M.D. Legoy, Identification of an indigo precursor from leaves of *Isatis tinctoria* (Woad), *Phytochemistry*, **58**, 897–904 (2001).
47. A.N. Assimopoulou, I. Karapanagiotis, A. Vasiliou, S. Kokkini and V.P. Papageorgiou, Analysis of alkannin derivatives from *Alkanna* species by high-performance liquid chromatography/photodiode array/mass spectrometry, *Biomed. Chromatogr.*, **20**, 1359–1374 (2006).
48. J.P. Salminen, V. Ossipov, J. Loponen, E. Haukioja and K. Pihlaja, Characterisation of hydrolysable tannins from leaves of *Batula pubescens* by high-performance liquid chromatography-mass spectrometry, *J. Chromatogr. A*, **864**, 283–291 (1999).
49. M. Carmona, A.M. Sánchez, F. Ferreres, A. Zalacain, F. Tomás-Barberán and G.L. Alonso, Identification of the flavonoid fraction in saffron spice by LC/DAD/MS/MS: comparative study of samples from different geographical origins, *Food Chem.*, **100**, 445–450 (2007).
50. G.C.H. Derksen, T.A. van Beek, Æ. Groot and A. Capelle, High-performance liquid chromatographic method for the analysis of anthraquinone glycosides and aglycones in madder root (*Rubia tinctorum* L.), *J. Chromatogr. A*, **816**, 277–281 (1998).
51. J. Wouters, The dye of *Rubia peregrina*, *Dyes in History and Archaeology*, **16/17**, 145–157 (2001).
52. J. Méndez, M. González, M.G. Lobo and A. Carnero, Color quality of pigments in cochineals (*Dactylopius coccus* Costa). Geographical origin characterization using multivariate statistical analysis, *J. Agric. Food Chem.*, **52**, 1331–1337 (2004).
53. M. González, M.G. Lobo, J. Méndez and A. Carnero, Detection of colour adulteration in cochineals by spectrophotometric determination of yellow and red pigment groups, *Food Control*, **16**, 105–112 (2005).
54. R. White and J. Kirby, Preliminary research into lac lake pigments using HPLC/electrospray mass spectrometry, *Dyes in History and Archaeology*, **16/17**, 167–178 (2001).
55. F.L. Liu, C.Y.W. Ang, T.M. Heinze, J.D. Rankin, R.D. Beger, J.P. Freeman and J.O. Lay Jr, Evaluation of major active components in St. John's Wort dietary supplements by high-performance liquid chromatography with photodiode array detection and electrospray mass spectrometric confirmation, *J. Chromatogr. A*, **888**, 85–92 (2000).
56. V. Carbone, P. Montoro, N. de Tommasi and C. Pizza, Analysis of flavonoids from *Cyclanthera pedata* fruits by liquid chromatography/electrospray mass spectrometry, *J. Pharmaceut. Biomed.*, **34**, 295–304 (2004).

57. M.-J. Dubber, V. Sewram, N. Mshicileli, G.S. Shephard and I. Kanfer, The simultaneous determination of selected flavonol glycosides and aglycones in Ginkgo biloba oral dosage forms by high-performance liquid chromatography-electrospray ionization-mass spectrometry, *J. Pharmaceut. Biomed.*, **37**, 723–731 (2005).
58. S. Kazuno, M. Yanagida, N. Shindo and K. Murayama, Mass spectrometric identification and quantification of glycosyl flavonoids, including dihydrochalcones with neutral loss scan mode, *Anal. Biochem.*, **347**, 182–192 (2005).
59. N. Li, G. Lin, Y.W. Kwan and Z.D. Min, Simultaneous quantification of five major biologically active ingredients of saffron by high-performance liquid chromatography, *J. Chromatogr. A*, **849**, 349–355 (1999).
60. J. Wouters and N. Rosario-Chirinos, Dye analysis of pre-Columbian Peruvian textiles with high-performance liquid chromatography and diode array detection, *J. Am. Inst. Conserv.*, **31**, 237–255 (1992).
61. K.G. Gilbert, D.J. Hill, C. Crespo, A. Mas, M. Lewis, B. Rudolph and D.T. Cooke, Qualitative analysis of indigo precursors from woad by HPLC and HPLC-MS, *Phytochem. Anal.*, **11**, 18–20 (2000).
62. B.C. Liao, T.T. Jong, M.R. Lee and S.S. Chen, LC-APCI-MS method for detection and analysis of tryptanthrin, indigo, and indirubin in daqingye and banlangen, *J. Pharm. Biomed. Anal.*, **43**, 346–351 (2007).
63. A.R.S. Ross, M.G. Ikononou and K.J. Orians, Characterization of dissolved tannins and their metal-ion complexes by electrospray ionization mass spectrometry, *Anal. Chim. Acta*, **411**, 91–102 (2000).
64. Y.Y. Soong and P.J. Barlow, Isolation and structure elucidation of phenolic compounds from longan (*Dimocarpus longan* Lour.) seed by high-performance liquid chromatography-electrospray ionization mass spectrometry, *J. Chromatogr. A*, **1085**, 270–277 (2005).



# **Part V**

## **Other MS-based Techniques**



# 14

## Compound-specific Stable Isotopes in Organic Residue Analysis in Archaeology

*Richard P. Evershed*

### 14.1 Introduction

One of the major advances of the past 30 years of study of the chemistry of organic materials of archaeological origin has been recognition of the value of exploring their compositions at the molecular level (Evershed 1993, 2008). As a result of such investigations it is now established that the biomolecular components of organic materials associated with human activity survive in a wide variety of locations and deposits at archaeological sites, i.e. pottery, human and animal remains, soils, art objects, various hoards and amorphous residues. The archaeological information contained in organic residues is represented by the biomolecular components of the natural products that contribute to the formation of a given residue. As shown elsewhere in this volume by applying appropriate separation (chromatographic) and identification (mass spectrometric) techniques the preserved, and altered, biomolecular components of such residues can be revealed. Once identified the structure of a given biomolecule or suite of biomolecules (the 'chemical fingerprint') can be related to the compositions of organisms exploited by man in the past. Sometimes the structure of a single component is sufficient to define the origin of a constituent of an organic residue, e.g. di- and triterpenoid components of plant resins offer a robust means of assigning their presence as components of organic residues, sometimes to the botanical species or genus level (Hayek *et al.* 1990;

Charters *et al.* 1993; Evans and Heron 1993; Evershed *et al.* 1997a; Grunberg 2002; Urem-Kotsou *et al.* 2002; Regert *et al.* 2003). Further examples include plant and insect waxes, particularly beeswax, which are readily recognised due to the characteristic aliphatic components they contain (Evershed *et al.* 1991; Heron *et al.* 1994; Charters *et al.* 1995; Evershed *et al.* 1997b, 2003a; Reber and Evershed, 2004a,b; Reber *et al.* 2004; Regert *et al.* 2005).

However, the most commonly occurring organic residues encountered in archaeology are those preserved in archaeological pottery and human remains. The major components of organic residues in archaeological pottery are fatty acids and related acyl lipids, i.e. mono-, di- and triacylglycerols, which are rather non-specific biomarkers and thus present considerable challenges to identifying their origins (Condamine *et al.* 1975; Passi *et al.* 1981; Rottländer and Schlichtherle 1983; Patrick *et al.* 1985; Rottländer 1990; Evershed *et al.*, 1991). In skeletal and soft tissue remains the major organic component is the structural protein collagen, which occurs together with lower concentrations of cholesterol and its various derivatives (Kuksis *et al.* 1978; Evershed and Connolly 1994; Evershed *et al.* 1995), and a wide range of fatty acyl components deriving from structural and storage lipids (Evershed and Connolly 1987; Gülaçar *et al.* 1989, 1990; Evershed 1990, 1992; Mayer *et al.* 1997; Corr *et al.* 2008). While collagen is widely exploited for its bulk stable isotope signature in the reconstruction of ancient human diet there is now considerable evidence that additional information exists in its constituent amino acids (Tuross *et al.* 1998; Corr *et al.* 2005, 2009; Fogel and Tuross 2003; Jim *et al.*, 2006). Moreover, the co-occurring lipid constituents of skeletal and soft tissues hold considerable untapped potential to enhance studies of ancient diet (Stott and Evershed 1996; Howland *et al.* 2003; Jim *et al.* 2004; Corr *et al.* 2008).

The aims of this contribution are to: (i) consider the theoretical principles underlying the use of compound-specific stable isotope analysis in archaeology; (ii) consider the practical aspects of undertaking compound-specific stable isotope analyses; and (iii) demonstrate the value of linking the structures of amino acids, fatty acids and/or sterols, to their compound-specific stable isotope values to achieve new insights into variations in metabolism and environment in order to enhance archaeological interpretations.

## 14.2 Stable Isotopes in the Environment

### 14.2.1 Definition

Isotope ratios are reported using the delta ( $\delta$ ) notation in parts per thousand or per mil (‰):

$$\delta^N X = (R_{\text{sample}} - R_{\text{standard}}) \times 1000 / R_{\text{standard}}$$

where  $R_x$  is the ratio of heavy to light isotope e.g.  $^{13}\text{C}/^{12}\text{C}$ ,  $^{15}\text{N}/^{14}\text{N}$ . The  $\delta$  value is 10 times the per cent difference in the isotope ratio of a sample relative to a standard (Table 14.1). The more positive the  $\delta$  value, the more enriched the sample is with respect to the heavier isotope. The factors controlling the isotopic composition of the most studied elements, carbon and nitrogen, in the biogeosphere are discussed below.

**Table 14.1** Relative abundances of the stable isotopes of hydrogen, carbon, nitrogen, oxygen and sulfur (Hoefs 1996; Schoeller 1999)

Element	Isotope	Fractional abundance	1‰ change	International standard
Hydrogen	<sup>1</sup> H	0.999844		Standard Mean Ocean Water (SMOW)
	<sup>2</sup> H	0.000156	0.000000156	
Carbon	<sup>12</sup> C	0.98889		PeeDee Belemnite limestone (PDB)
	<sup>13</sup> C	0.01111	0.00001123	
Nitrogen	<sup>14</sup> N	0.99634		Air
	<sup>15</sup> N	0.00366	0.00000367	
Oxygen	<sup>16</sup> O	0.99755		Standard Mean Ocean Water (SMOW)
	<sup>17</sup> O	0.00039	0.00000039	
	<sup>18</sup> O	0.00206	0.00000207	
Sulfur	<sup>32</sup> S	0.9502		Canyon Diablo Iron meteorite (CDT)
	<sup>33</sup> S	0.0075		
	<sup>34</sup> S	0.0421	0.0000450045	
	<sup>36</sup> S	0.0002		

### 14.2.2 Isotopic Fractionation

Isotopic fractionation is a consequence of the different reaction rates associated with the isotopes. The expression of isotopic discrimination will depend on whether the bias is large enough to introduce a measurable difference and whether the yield is less than 100%. If a reaction proceeds to completion, with no branching, there is no scope for isotopic fractionation. All biochemical and physical transformations are subject to isotope fractionation. Isotopic discrimination is greatest for the atoms directly involved in bond breaking and bond making and is of the order of a few per mil for carbon and nitrogen. If the discrimination is against the heavy isotope, the  $\delta$  value of the product (P) will be lower (or more negative) than the original reactant. Hence, the  $\delta$  value of the remaining reactant (R) will be higher. Discrimination factors are conventionally expressed using either  $\varepsilon$  or  $\alpha$ , where:

$$\varepsilon_{P-R} = 1 - \alpha \left[ \frac{\delta^N X_P + 1000}{\delta^N X_R + 1000} - 1 \right] \times 1000 \approx \delta^N X_P - \delta^N X_R \quad (14.1)$$

Figure 14.1 illustrates two physiological conditions (Hayes 1993; Schoeller 1999; Brenna 2001):

- (1) If the system is in a steady state (i.e. the absence of measurable change), the isotope ratio of the analyte ( $R_{\text{Analyte}}$ ) is determined by the relative contributions of the external world to its precursors, inputs 1A, 1B, 2A and 2B.
- (2) At constant external input,  $R_{\text{Analyte}}$  is governed by the inputs (1 and 2) and outputs (3 and 4) within the system (i.e. the physiological state of the organism). Constant input means that the dietary supply does not change, while environmental factors that affect physiology may vary.

Hence,  $R_{\text{Analyte}}$  can change due to variations in external inputs (e.g. diet) or due to changes in physiology (e.g. pregnancy), or both.

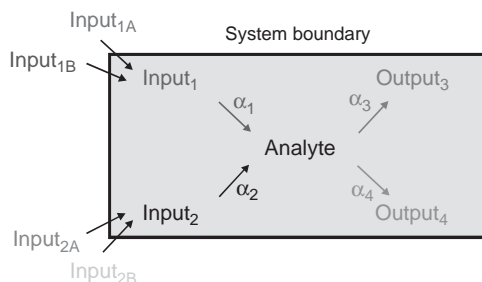


**Figure 14.1** Stylised diagram illustrating the inputs and outputs that determine analyte isotope ratios. The analyte can be a compound, a position in a compound, or a bulk mixture. Inputs 1 and 2 and outputs 3 and 4 are internal to the system (e.g. an organism). Inputs 1A, 1B, 2A, and 2B are external contributors to inputs 1 and 2, respectively. The isotope ratios of inputs 1 and 2 depend on relative flux (e.g. diet) from the outside.  $\alpha_x$  are fractionation factors between precursors and products. The isotope ratio of the analyte ( $R_{Analyte}$ ) is a composite of the relative contributions of inputs 1 and 2 and degradation to outputs 3 and 4. Adapted from Brenna (2001)

### 14.2.3 Distribution of Carbon and Nitrogen Isotopes in the Biogeosphere

The use of natural abundance variations in stable isotopes as tracers relies on the fractionations that occur during chemical, physical and biological processes (Ambrose 1993). Differences in fractionation during these processes lead to distinct isotopic signatures for biological materials, such as in foods exploited by humans in antiquity.

#### 14.2.3.1 Carbon Isotopic Fractionation during Photosynthesis

The largest mechanistic causes of variation in the isotopic composition of plant tissues are differences between plant photosynthetic pathways (for a review see Bruognoli and Farquhar 2000). Terrestrial plants can be divided into three groups on the basis of distinctions in photosynthesis and anatomy:  $C_3$  (Calvin-Benson cycle; temperate shrub, trees and some grasses),  $C_4$  (Hatch-Slack cycle; herbaceous tropical, arid-adapted grasses) and Crassulacean acid metabolism (CAM; succulents).  $C_4$  plants are thought to have evolved a number of times in the last 7–5 million years in response to decreased atmospheric levels of  $CO_2$ , and increased levels of  $O_2$  (Gröcke 2002). Several species of succulent plants fix carbon using the CAM mechanism, which is effectively a hybrid of  $C_3$  and  $C_4$  metabolism. This pathway is thought to have resulted from the biological and physiological adaptation of plants to counter water stress.

Atmospheric  $CO_2$  currently has a  $\delta^{13}C$  value of ca.  $-8\text{‰}$ , although anthropogenic burning of fossil fuels has resulted in a ca.  $1\text{‰}$  depletion during the last 200 years (Hoefs 1996). The three classes of plant exhibit varying degrees of isotopic fractionation with respect to atmospheric  $CO_2$  and hence have distinct  $\delta^{13}C$  values (Figure 14.2):  $C_3$  plants  $-23$  to  $-34\text{‰}$  (average  $-27\text{‰}$ ),  $C_4$  plants  $-8$  to  $-16\text{‰}$  (average  $-13\text{‰}$ ; O'Leary 1981). The carbon isotope ratios of CAM plants display intermediate  $\delta^{13}C$  values (Hoefs 1996).

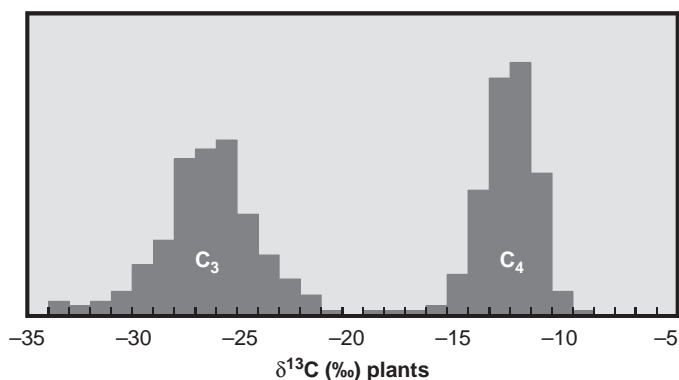


**Figure 14.2**  $\delta^{13}\text{C}$  values of modern terrestrial plants (O'Leary 1981)

#### 14.2.3.2 Nitrogen Isotopes in Plants

Plants do not fractionate nitrogen isotopes when absorbing soil nitrate from fertile soils (Garten 1993), but variations in the  $\delta^{15}\text{N}$  values of soil nitrate will result in differences in plant  $\delta^{15}\text{N}$  values (Handley and Raven 1992). Plants that fix atmospheric nitrogen (legumes) have  $\delta^{15}\text{N}$  values similar to their source because their symbiotic root bacteria do not significantly fractionate nitrogen isotopes in  $\text{N}_2$  (Delwiche and Steyn 1970). Soil  $\delta^{15}\text{N}$  values tend to be positive due to denitrification, and hence plants that fix atmospheric  $\text{N}_2$  can have lower  $\delta^{15}\text{N}$  values than non- $\text{N}$ -fixing plants at the same site (Shearer and Kohl 1986). In exceptional circumstances  $\delta^{15}\text{N}$  values of less than  $-15\text{‰}$  have been recorded as a result of increased isotopic fractionation during nitrogen assimilation in slow growing plants (McKee *et al.* 2002). As shown in Figure 14.3 there is a ca.  $3\text{‰}$  increase in  $\delta^{15}\text{N}$  value with each trophic level in a food web (DeNiro and Epstein 1981). Such shifts have been used widely in archaeological investigations to infer dietary preferences, however, a recent investigation of the  $\delta^{15}\text{N}$  values of modern cereals derived from long-term agricultural experiments have shown that manuring can increase the  $\delta^{15}\text{N}$  values of cultivated plants by ca.  $3\text{‰}$  (Bogaard *et al.* 2007). The results suggest that the Neolithic human collagen  $\delta^{15}\text{N}$  values from individuals consuming manured cereals could resemble those from a largely animal based diet. The elevated  $\delta^{15}\text{N}$  values are believed to derive from the loss of isotopically light nitrogen during denitrification.

#### 14.2.3.3 Marine Ecosystems

The isotopic composition of marine food webs tends to be more enriched in both  $^{13}\text{C}$  and  $^{15}\text{N}$  than terrestrial  $\text{C}_3$  or freshwater ecosystems (Hobson 1999). During photosynthetic fixation of dissolved  $\text{CO}_2$  into organic matter, algae discriminate against  $^{13}\text{C}$  (Hoefs 1996). Consequently, marine phytoplankton has lower  $\delta^{13}\text{C}$  values relative to dissolved  $\text{CO}_2$ . Although marine plants almost exclusively use the  $\text{C}_3$  pathway for carbon fixation, they have distinct  $\delta^{13}\text{C}$  values from terrestrial  $\text{C}_3$  plants because terrestrial plants utilise atmospheric  $\text{CO}_2$  as a carbon source as opposed to the aqueous  $\text{CO}_2$  exploited by marine plants. The carbon isotopic composition of marine algae is a function of the carbon isotopic

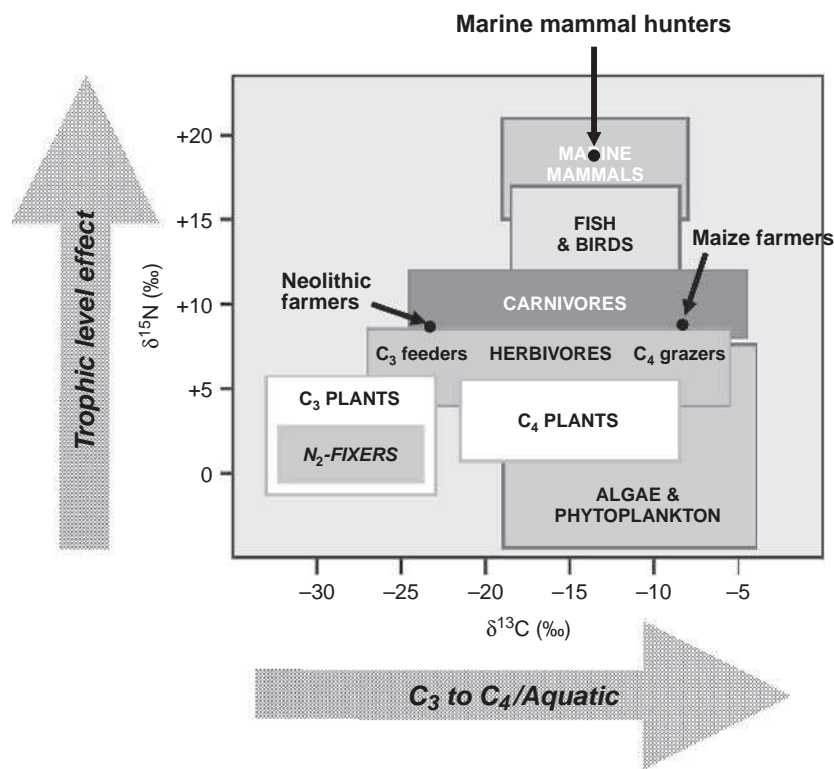


**Figure 14.3** Isotopic 'map' of terrestrial and marine food webs (adapted from O'Connell 1996)

composition of inorganic dissolved carbon, surface water [ $\text{CO}_{2(\text{aq})}$ ], cellular growth rate, cellular geometry and possibly irradiance and nitrate concentration (Pagani 2002). The  $\delta^{15}\text{N}$  values of marine plants are about 4‰ higher than those of terrestrial plants. This relative enrichment is due to the elevated  $\delta^{15}\text{N}$  values of dissolved inorganic seawater nitrogen (>5‰) at the base of the food chain and the many trophic levels in marine ecosystems.

### 14.3 Stable Isotopes in Archaeology

The first stable isotope studies in the field of archaeology used the  $\delta^{13}\text{C}$  values of bone collagen to assess the introduction of maize into North America (Vogel and van der Merwe 1977) and the Mesolithic Neolithic transition in Denmark (Tauber 1981). The inspiration for these investigations was provided by the variations observed in collagen  $\delta^{13}\text{C}$  values during  $^{14}\text{C}$  dating. Since then numerous investigators have utilised both  $\delta^{13}\text{C}$  and  $\delta^{15}\text{N}$  analyses of fossil and modern animal tissues to study diet. Around the same time organic residues in archaeological pottery began to be investigated by bulk isotopic analysis (e.g. Hastdorf and DeNiro 1985; Morton



and Schwarcz 1988). While the bulk stable isotope analysis of skeletal remains has been used widely in archaeology and palaeoecology, the application of bulk stable isotope analysis in archaeology pottery has been much more limited. The difference in the trajectories of application of stable isotope analysis in the two areas is due to the contrasting nature of the materials involved. The primary target analyte in skeletal studies is the structural protein collagen which appears to be well preserved in many fossil bones, affording robust carbon and nitrogen isotope signatures upon combustion to  $\text{CO}_2$  and  $\text{N}_2$  and stable isotope analysis. In contrast, organic residues occurring in archaeological pottery have more complex compositions and less well-defined origins, such that interpretations of their stable isotope values carry with them many uncertainties that have inevitably limited the utility of stable isotope analysis in their widespread investigation.

There are a number of compelling reasons for considering employing compound-specific stable isotope approaches (rather than more traditional bulk measurements), namely that: (i) different biochemical components, even those within a single organism, can possess different stable isotope values, e.g.  $\delta^{13}\text{C}$  values of amino acids deriving from different biochemical pathways; (ii) structurally similar biochemical components can derive from a range of sources potentially exhibiting different stable isotopic signatures, e.g. fatty acids in archaeological cooking pots can derive from a wide range of animals and plants; (iii) biogenic organic matter, either living or dead, is chemically complex such that changes in the bulk stable isotope value may occur as a result of changes in chemical composition, i.e. loss or gain of components with stable isotope values that differ from the bulk (mean) stable isotope value may be erroneously interpreted as fractionation phenomena, e.g. preferential degradation of isotopically heavy components would lead to an overall lowering of bulk stable isotope values; (iv) the complementary use of structurally diagnostic biomarkers together with their compound-specific stable isotope values provides metabolic process or biochemical pathway-based information inaccessible through bulk stable isotope analyses; (v) different biochemical components, and even identical components within different pools, of an organism can possess significantly different turnover times that would be undetectable in bulk analyses and may even lead to erroneous interpretations of trends seen in recorded stable isotope values, especially in temporal studies, e.g. essential and non-essential components or structural versus storage substances; and (vi) where genuine kinetic isotope based fraction effects exist their source can only be determined through stable isotopic assessments at the level of the biochemical component and specific pathway.

It is therefore essential that in order to use light stable isotopes effectively in archaeology a mechanistic understanding of the biochemical factors that underpin stable isotope signals be developed. Figure 14.4 compares the bulk and molecular schemes for the metabolic fate of macronutrient components between diet and consumer tissues. Even at this simplistic level it is clear how determining the stable isotope values of individual biochemical components of clearly defined biochemical origins will greatly enhance archaeological interpretations. This principle applies no matter what stable isotope or combination of isotopes is being employed or what archaeological material or region is under investigation. Unless we strive for a level of understanding that links biochemistry to stable isotope composition it is

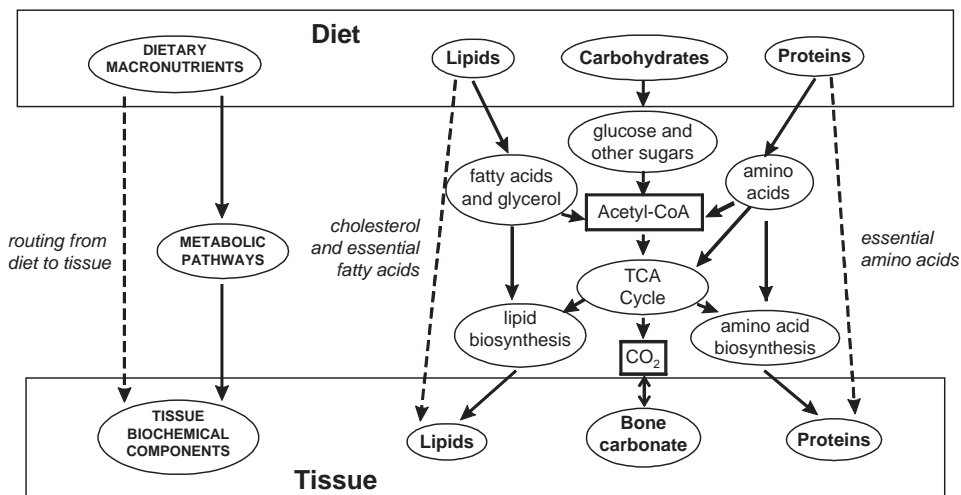


**Figure 14.4** Schematic diagram comparing the bulk and molecular schemes for the metabolic fate of macronutrient components between diet and consumer tissues

unlikely that we can ever rigorously interpret the results of bulk stable isotopes or exploit the use of light stable isotopes in archaeological research to their fullest potential.

## 14.4 Analytical Considerations

Figure 14.5 summarises schematically the instrument configurations used to determine stable isotope compositions of environmental materials. The original approach, in which samples were oxidised off-line in sealed tubes, has largely been superseded by the use of elemental analysers which allow samples to be combusted, gases separated and analysed on-line followed by isotope ratio mass spectrometry (IRMS). Both these approaches yield bulk isotope compositions for complex materials which integrate the stable isotopic compositions of all components present. While the isotopic compositions of individual compounds can be obtained by prior purification the major breakthrough in compound-specific stable isotope analysis came with the development and then commercial production of the gas chromatograph-combustion-isotope ratio mass spectrometer (for GC-C-IRMS) in the early 1990s (Barrie *et al.* 1984; Hayes *et al.* 1990; Merritt *et al.* 1994, 1995). Further impetus has been given to the compound-specific stable isotope approach through the recent development of a workable interface that allows high-performance liquid chromatography to be linked to IRMS (the technical aspects of such instruments are discussed in detail below).

Compound-specific stable isotope analyses are more complex to undertake than bulk stable isotope analyses and require careful consideration to be given to sample

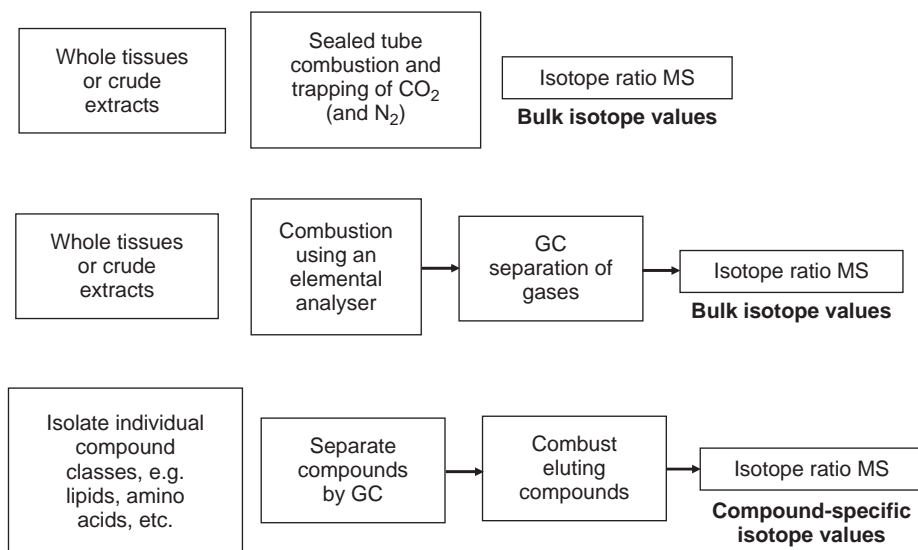


**Figure 14.5** Schematic diagram of instrumental variants of stable isotope analysis providing either bulk or compound-specific stable isotope values

preparation protocols. Such factors that need to be considered are: (i) the identity of the target compound(s); (ii) whether the target compounds exist in more than one physical or chemical state within a complex extract of an archaeological material; (iii) whether the target compounds are amenable to GC analysis directly or will require derivatisation; (iv) the most suitable derivatising agent for GC-C-IRMS analysis; this is not necessarily the most appropriate derivative if only GC analysis was intended (the specific considerations for GC derivative selection are given later); (v) the most suitable GC column (stationary phase and column dimensions); and (vi) whether the target compound(s) are fully separable from other eluting compounds, i.e. can baseline resolution be achieved? Each of the latter factors will be dealt with in the following sections.

The overall aim of any compound-specific stable isotope analysis is to provide accurate stable isotope value(s) for a specific component(s) of what is likely to be a biochemically complex matrix containing many tens, hundreds or even thousands of components of widely varying chemical and physical state. Thus, the aim will be to purify that compound avoiding, or accounting for, protocol induced isotope effects such that the recorded stable isotope value will be comparable, within reasonable analytical error, with that of the compound in its natural state. Given that the primary means of obtaining compound-specific stable isotope values will be via GC-C-IRMS, then sample preparation schemes will comprise the following steps: (i) extraction; (ii) separation; and (iii) derivatisation (in the case of functionalised compounds). General and specific features of such schemes are presented in turn below (Figures 14.6 and 14.7).

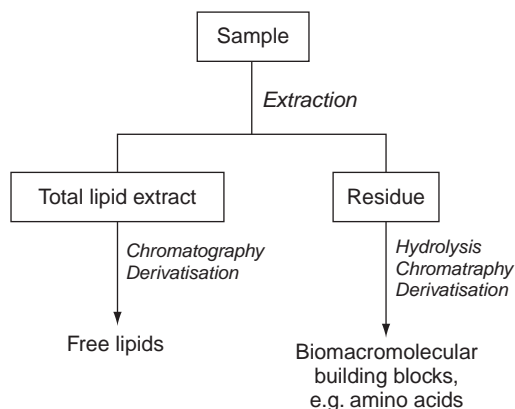


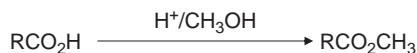
**Figure 14.6** Generalised analytical protocol for the compound-specific stable isotope analysis of free and building block components of complex archaeological materials

### Trimethylsilylation



BSA = N,O-bis(trimethylsilyl)acetamide

### Esterification



### Esterification-acylation (two step)

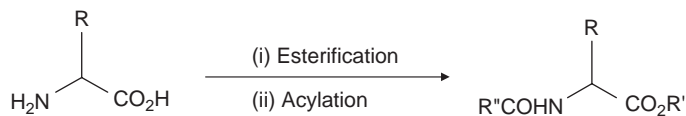


**Figure 14.7** Principal derivatisation strategies for the GC-C-IRMS of lipids [trimethylsilylation (cholesterol) and esterification (fatty acids)] and amino acids (esterification-acylation)

## 14.5 Sample Preparation

Figure 14.6 shows a typical protocol for the isolation of the most common compounds targeted for compound-specific stable isotope analysis. Before extraction, samples are dried and crushed to ensure homogeneity and increase the effectiveness of solvent penetrating the sample matrix. No matter which extraction method is employed the resulting total lipid extract (TLE) is then further separated into different compound classes using various chromatographic methods. Occasionally, a single chromatographic

technique does not yield baseline resolved peaks in the GC-C-IRMS determination and a combination of separation techniques is required. Whichever technique(s) is selected it is important to verify whether or not aspects of the analytical protocol will introduce an isotopic fractionation effect by analysis of reference compounds of known stable isotope composition. Many important components of archaeological materials cannot be analysed directly by GC. For example, complex lipids require chemical cleavage, to yield GC amenable components, i.e. commonly occurring triacylglycerols or wax esters are saponified and methylated to generate fatty acid methyl esters (FAMES; Mottram *et al.* 1999). Likewise, solvent insoluble biopolymers, such as proteins, must be chemically or enzymatically cleaved to their biochemical building blocks (Docherty *et al.* 2001). Care must be taken to ensure that such cleavage reactions are complete, since incomplete reactions may result in kinetic isotope effects (Jim *et al.* 2003a).

## 14.6 Derivatisations for Compound-specific Stable Isotope Analysis

GC-C-IRMS instrumentation enables the compound-specific isotope analysis of individual organic compounds, for example, *n*-alkanes, fatty acids, sterols and amino acids, extracted and purified from bulk organic materials. The principle caveat of compound-specific work is the requirement for chemical modification, or derivatisation, of compounds containing polar functional groups primarily to enhance their volatility prior to introduction to the GC-C-IRMS instrument. Figure 14.7 summarises the most commonly employed procedures for derivatisation of polar, nonvolatile compounds for compound-specific stable isotope analysis using GC-C-IRMS.

The addition of a derivative group (or several derivative groups in the case of polyfunctionalised compounds, such as amino acids) introduces exogenous carbon which ultimately alters the  $\delta^{13}\text{C}$  value of the compound of interest. Derivatisation of fatty acids and sterols, to FAMES and sterol trimethylsilyl ethers, respectively, is relatively straightforward since the resulting sample-to-derivative carbon molar ratio is high, resulting in minimal analytical error. Additionally, derivatisation reactions, such as esterification and silylation are typically rapid and quantitative thereby precluding kinetic isotope effects (Rieley 1994).

In contrast, derivatisation of low molecular weight, polyfunctional compounds, such as amino acids, presents a more complex analytical challenge. The preferred procedure for derivatisation of amino acids for GC analysis involves esterification of the carboxylic acid group with an acidified alcohol and acylation of amino, hydroxyl and thiol groups with an anhydride, to form N(O,S)-acyl alkyl esters (Demmelmair and Schmidt 1993; Metges *et al.* 1996; Macko *et al.* 1997; Metges and Daenzer 2000; Docherty *et al.* 2001; O'Brien *et al.* 2002; Jim *et al.* 2003a; Corr *et al.* 2005, 2007a,b). A perceived shortcoming of the acylation approach is the kinetic isotope effect (KIE) associated with the procedure, which precludes the direct calculation of compound-specific  $\delta^{13}\text{C}$  values via a simple mass balance equation. However, because such reactions have been shown to be quantitative and reproducible for each amino acid, the KIE can be accounted for by employing empirical correction factors ( $\delta^{13}\text{C}_{\text{corr}}$ ) to calculate the 'effective'  $\delta^{13}\text{C}$  value of the reagent where fractionation occurs (Demmelmair and Schmidt 1993; Rieley 1994; Docherty *et al.* 2001; Corr *et al.* 2007a,b). Hence, three acylation procedures, in combination with esterification, are now routinely employed for amino acid  $\delta^{13}\text{C}$  measurements: acetylation

(+2C; Demmelmair and Schmidt 1993; Metges *et al.* 1996), trifluoroacetylation (+2C; Macko *et al.* 1997; Docherty *et al.* 2001; O'Brien *et al.* 2002; Howland *et al.* 2003; Jim *et al.*, 2003a) and pivaloylation (+5C; Metges *et al.* 1996; Metges and Petzke 1997; Metges and Daenzer 2000). *N*-trifluoroacetyl iso-propyl (NTFA-IP) esters are extensively employed in the stable carbon isotope analysis of amino acids due to their excellent chromatographic properties compared with *N*-acetyl iso-propyl (NAIP) esters (Figure 14.8). However, their compatibility with GC-C-IRMS is now uncertain because the fluorine liberated on combustion of fluorinated derivatives irreversibly poisons the platinum catalyst, forming extremely stable  $\text{CuF}_2$  and  $\text{NiF}_2$  products with associated reduction in oxidation efficiency (Meier-Augenstein 1999). This shortcoming has, nevertheless, recently been resolved by analysing amino acid NAIP esters on a high-polarity stationary phase to prevent the previously reported poor chromatography and co-elution problems identified for these derivatives on the traditionally employed nonpolar/low-polarity phases (Corr *et al.* 2007a,b).

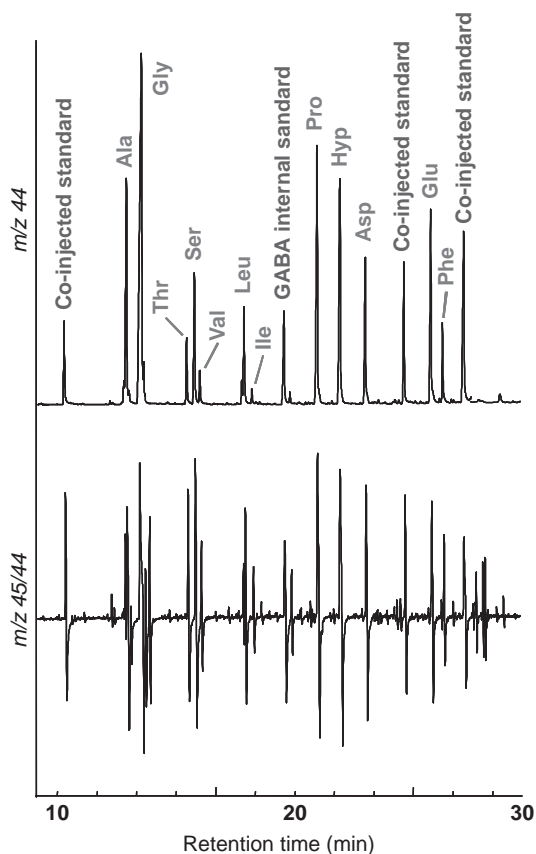


**Figure 14.8** Partial  $m/z$  44 and  $m/z$  45/44 traces obtained by GC-C-IRMS analysis of commonly occurring amino acids (as their trifluoroacetyl-isopropyl ester derivatives) together with a range of co-injected internal standards

## 14.7 Instrumental Aspects of Compound-specific Stable Isotope Determinations

### 14.7.1 Determining the $\delta^{13}\text{C}$ , $\delta^{15}\text{N}$ , $\delta\text{D}$ and $\delta^{18}\text{O}$ Values of Individual Compounds

GC-C-IRMS was first demonstrated by Matthews and Hayes (1978). However, it was somewhat later that Barrie and others (Barrie *et al.*, 1984) coupled a GC, via a combustion interface, to a dual collector mass spectrometer to produce the forerunner of today's GC-C-IRMS instruments. Even so, true determinations of  $\delta^{15}\text{N}$  values of individual compounds by GC-C-IRMS remained elusive until finally demonstrated by Hayes and co-workers (Merritt and Hayes, 1994). More recently the precision of GC-C-IRMS instruments has been improved further still with uncertainties in  $\delta^{13}\text{C}$  values as small as  $\pm 0.5\text{‰}$  for samples containing 5 pmol C and  $\pm 0.1\text{‰}$  for 100 pmol samples having been demonstrated (Merritt and Hayes 1994). Instruments available commercially today, from several manufacturers, all conform to the same general principles of design.

Figure 14.9 depicts a generalised schematic of a GC-C-IRMS instrument configured for determinations of  $\delta^{13}\text{C}$  (or  $\delta^{15}\text{N}$ ) values of individual compounds. Briefly, mixtures of compounds are separated by high resolution capillary GC then individually combusted online over a catalyst ( $\text{CuO/Pt}$ , 850 °C or  $\text{CuO/NiO/Pt}$ , 940 °C; Merritt *et al.* 1995) generating  $\text{CO}_2$  and  $\text{H}_2\text{O}$ . For the determination of  $\delta^{15}\text{N}$  values or  $\delta^{13}\text{C}$  values of compounds containing nitrogen ( $\text{N}_2\text{O}$  is generated and causes isobaric interference with  $m/z$  44 and 45; Metges and Daenzer 2000) the effluent is then passed through a second reactor where nitrogen oxides are catalytically ( $\text{Cu}$ , 600 °C) reduced to  $\text{N}_2$  (Brand *et al.* 1994).  $\text{H}_2\text{O}$  is removed by a water separator, typically comprising a length of water permeable Nafion<sup>TM</sup> tubing, thereby avoiding the formation of  $\text{HCO}_2^+$  ions that would otherwise result in isobaric interference with  $^{13}\text{CO}_2$  (Leckrone and Hayes 1998) it should be noted that the efficiency of this process is temperature dependent (Leckrone and Hayes 1997).

For determination of  $\delta^{13}\text{C}$  values the remaining  $\text{CO}_2$  is introduced into a mass spectrometer equipped with a triple collector comprising three Faraday cups monitoring simultaneously  $m/z$  44, 45 and 46 corresponding to the ions of the three isotopomers  $^{12}\text{C}^{16}\text{O}_2$ ,  $^{13}\text{C}^{16}\text{O}_2$  and  $^{12}\text{C}^{18}\text{O}^{16}\text{O}$ , respectively. For the determination of  $\delta^{15}\text{N}$  values, the eluting  $\text{CO}_2$  is retained in a cryogenic trap to avoid the production of isobaric  $\text{CO}^+$  resulting from the unimolecular decomposition of  $\text{CO}_2^+$  ions (Brand *et al.* 1994). The remaining  $\text{N}_2$  is then introduced in an identical manner but this time monitoring simultaneously  $m/z$  28 and 29 using the first two Faraday cups corresponding to the isotopomers  $^{14}\text{N}^{14}\text{N}$  and  $^{15}\text{N}^{14}\text{N}$ . The resultant output currents are then amplified, digitised and recorded by computer which then integrates each signal and calculates the corresponding stable carbon or nitrogen isotope ratio, represented by the signal, relative to either co-injected standards or a gas standard, returning it as a  $\delta$ -value (Merritt *et al.* 1994; Ricci *et al.* 1994).

The single most important requirement in performing a valid and robust determination of the isotope value of an individual compound by GC-C-IRMS is good chromatographic separation of the target compound(s) as shown in Figure 14.8, achieved by optimisation of the GC operating conditions and judicious column selection. Peaks that are not fully resolved (up to 25% co-elution) can still be integrated separately as long as a minimum estimate of analytical error is gained by running the sample at different concentrations

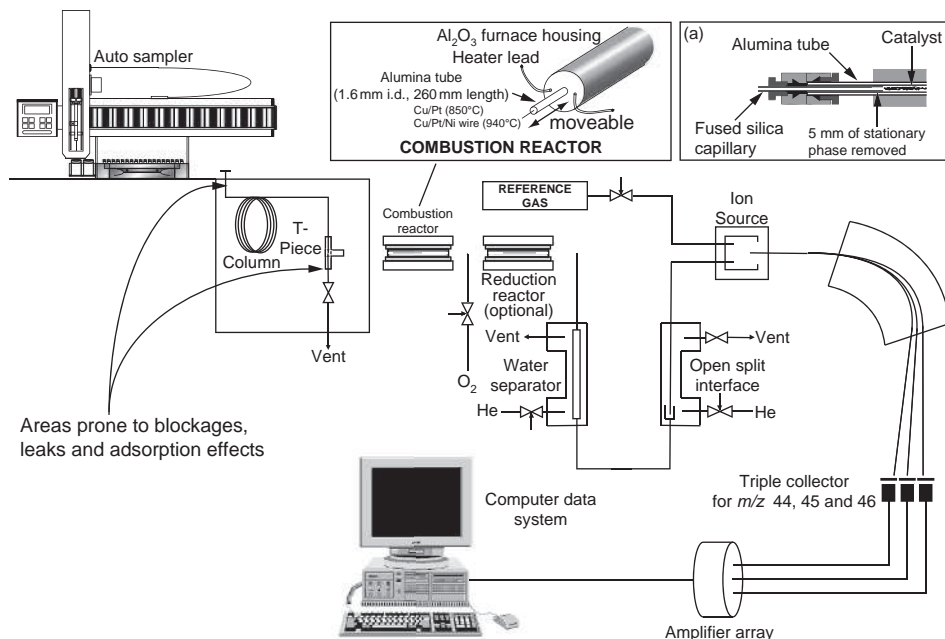


**Figure 14.9** Schematic diagram of a GC-C-IRMS instrument configured for the determination of  $\delta^{13}\text{C}$  values of organic compounds. In order to configure the instrument for determining the  $\delta^{15}\text{N}$  values of N-containing compounds the Faraday cup collector systems would have to be changed to detect *m/z* 28 and 29 in addition to using a cryogenic trap to remove  $\text{CO}_2$ . Determinations of  $\delta\text{D}$  and  $\delta^{18}\text{O}$  values would require fundamental changes to the interface and Faraday cup collectors as described in the text

(Ricci *et al.* 1994). For any larger overlap, co-eluting peaks must be integrated as one peak using the integration software, although the errors associated with such determinations may be substantial.

In addition to the reference gas calibrant it is important that the performance of the GC-C-IRMS instrument be constantly monitored using a suite of compounds of known relative stable isotopic composition. Such references should ideally belong to the same compound class as the target compounds since the performance of the instrument for one particular class of compounds cannot necessarily replicate that of a different class of compounds (Meier-Augenstein *et al.* 1996). In addition, a range of homologues should be utilised as a standard mixture thereby assessing the performance of the instrument across the entire temperature range utilised by GC. By doing this factors such as leaks and/or blockages at varying temperatures can be quickly identified and resolved.

In addition to the potential problem of isobaric interference from  $\text{CO}^+$  (*m/z* 28) ions there are a number of additional factors that should be considered when attempting compound specific  $\delta^{15}\text{N}$  analysis. First, the actual abundance of N in an organic compound is typically  $<10\%$  (cf. C  $>60\%$ ), in a gas sample 1 molecule of  $\text{N}_2$  contains two N atoms (only 1 C in  $\text{CO}_2$ ), the natural abundance of  $^{15}\text{N}$  is 0.732% (cf. 1.08%  $^{13}\text{C}$ ) and  $\text{N}_2$  has an



ionisation efficiency of 70% relative to that of CO<sub>2</sub>. All of these factors result in the average N containing organic compound requiring, for  $\delta^{15}\text{N}$  analysis, a minor isotope abundance around 50 times that required for the corresponding  $\delta^{13}\text{C}$  analysis (Brand *et al.* 1994). This problem may be partially overcome by using shorter GC columns (e.g. 30 m) with both a smaller internal diameter (e.g. 0.25 mm) and thicker stationary phase (e.g. 0.4  $\mu\text{m}$ ) thereby generating a higher signal to noise ratio and enabling a higher sample loading. An increase in the sensitivity of the mass spectrometer (e.g. a higher accelerating voltage, optimised tuning) will also help alleviate this problem. The second major drawback relating to compound specific  $\delta^{15}\text{N}$  analyses results from the fact that the atmosphere comprises >78% N<sub>2</sub>. The risk of introducing atmospheric N<sub>2</sub> into the ion source either by inadequate sample handling or leaks in the flow path of the GC-C-IRMS instrument and thereby compromising the accuracy of determined  $\delta^{15}\text{N}$  values is particularly high. Those parts of the GC-C-IRMS instrument exposed to repetitive changes in temperature, i.e. those parts associated with the GC oven, are particularly prone to leaking and should be regularly checked and made gas tight if necessary. There can be no doubt that, despite its undeniable value in a wide range of applications,  $\delta^{15}\text{N}$  analysis of individual compounds still remains a non-trivial methodology, which probably accounts for the current paucity of communications reporting the use of the technique.

The main difference between compound specific  $\delta\text{D}$  or  $\delta^{18}\text{O}$  analysis and the analytical techniques outlined above lies in the method by which the analyte gas is generated. For both  $\delta\text{D}$  and  $\delta^{18}\text{O}$  analyses organic compounds are converted online to produce  $^1\text{H}^1\text{H}$ ,  $^2\text{H}^1\text{H}$ ,  $^{12}\text{C}^{16}\text{O}$ ,  $^{13}\text{C}^{16}\text{O}$  and  $^{12}\text{C}^{18}\text{O}$ . Several methods have been adopted by different manufacturers and researchers to achieve this chemical conversion including reduction using a chromium metal catalyst at 1050 (e.g. Gehre *et al.* 1996) and pyrolysis in a graphitised alumina reactor at 1450 °C (Begley and Scrimgeour 1997; Tobias and Brenna 1997); only the latter technique shall be considered here.

In GC-C-IRMS instruments configured for compound specific  $\delta\text{D}$  analysis the combustion reactor is replaced with a thermal conversion reactor (the term 'thermal conversion' is used since there is currently no consensus of how to refer to this reaction and terms such as quantitative pyrolysis or calcination are too specific), which comprises an empty alumina tube maintained at a working temperature of 1450 °C. At this temperature compounds eluting from the gas chromatograph into the reactor are quantitatively converted to H<sub>2</sub>, CO and their corresponding isotopomers (after Burgoyne and Hayes 1998). Since the reaction produces no water the Nafion<sup>TM</sup> water trap can be omitted. The analyte gases are introduced to the mass spectrometer via an open split and the ion beams corresponding to  $m/z$  2 and 3 are monitored by two Faraday cups for a simultaneous determination of H<sub>2</sub> and HD, respectively. An electrostatic filter is placed inline with the Faraday cup measuring the HD ion beam to remove the effect of the disperse  $^4\text{He}^+$  ion beam that would otherwise superimpose and corrupt the measurement of the small HD beam (Hilkert *et al.* 1999). The resulting ion currents are recorded and converted to  $\delta\text{D}$  values in a process similar to that detailed above. One crucial difference is the need to determine the effect that protonation reactions occurring in the ion source have on the determination of  $\delta\text{D}$  values. Such reactions result in the formation of H<sub>3</sub><sup>+</sup> ions. Since the abundance of H<sub>3</sub><sup>+</sup> is proportional to the square of the hydrogen pressure a correction factor, termed an 'H<sub>3</sub>-factor', may be determined based on the peak area information obtained from a series of reference gas pulses of different magnitude. The calculation of H<sub>3</sub>-factors and associated

corrections have been reviewed previously in detail (Sessions *et al.*, 2001a,b). Another vital factor for the determination of accurate  $\delta D$  values is the need to ensure that the alumina reactor in the thermal conversion interface has been suitably graphitised prior to performing any analyses. Burgoyne and Hayes (1998) reported that such treatment resulted in better peak shapes and reproducibility. This 'conditioning' may be achieved by the direct injection of *n*-hexane or alternatively Bilke and Mosandl (2002) reported that conditioning the reactor by backflushing  $CH_4$  resulted in greater stability over the ensuing sampling period. In addition, the accuracy of  $\delta D$  values may also be improved by the use of a concentrated 'sacrificial' compound that elutes prior to the compound(s) of interest; this is a particularly useful method by which the accuracy of  $\delta D$  values determined for early eluting components may be improved. Finally, the flow through the reactor should ideally be fairly low, e.g.  $\sim 0.8 \text{ ml min}^{-1}$  and certainly no greater than  $1.2 \text{ ml min}^{-1}$ , since an overly short residence time in the central  $\sim 10 \text{ cm}$  zone of optimum performance can result in non-quantitative thermal conversion.

Determinations of compound-specific  $\delta^{18}O$  values utilise an instrument configuration very similar to that used for  $\delta D$  analyses. No applications of this methodology currently exist in the field of archaeology. The main point of divergence between the two techniques is in the design of the thermal conversion reactor. The empty alumina reactor is replaced by an alumina reactor containing a Pt tube that also contains Ni wire. The function of the Pt tube is to prevent any exchange of oxygen between the CO formed during thermal conversion and the alumina ( $Al_2O_3$ ) reactor; the Ni is required as a support for graphitised carbon since carbon is not retained by the surface of the Pt tube. Eluting CO is introduced into a mass spectrometer equipped with a triple collector comprising three Faraday cups monitoring simultaneously  $m/z$  28, 29 and 30 corresponding to the ions of the three isotopomers  $^{12}C^{16}O$ ,  $^{13}C^{16}O$  and  $^{12}C^{18}O$ , respectively (Hener *et al.*, 1998).  $\delta^{18}O$  values are calculated in an analogous fashion to the methods outlined above.

## 14.8 Data treatment: Correcting for Derivative Groups and KIEs

As discussed above, account must be taken of exogenous atoms added to the analyte molecule during analysis. In addition, any potential derivatisation reaction must be evaluated for fractionation resulting from KIEs. Bonds involving heavier isotopes have a higher potential energy which can result in different reaction rates in reactions involving different isotopic species (Melander and Saunders 1980). For derivatisation the most significant isotopic fractionation is the primary KIE that occurs at a specific molecular position causing an alteration in the  $\delta$ -value at that position. Hence, if the rate determining step of a derivatisation reaction involves the making or breaking of a bond to the atom under consideration, then the reaction involving that atom may be non-quantitative and any KIE must be quantified. If the KIE is reproducible, a correction can be made.

If no KIE is present, the contribution of the derivative atom to the measured  $\delta$ -value of the derivatised compound can be calculated using a simple mass balance equation (14.2), where  $n$  is number of moles of the isotope of interest,  $F$  is the fractional abundance of the isotope of interest,  $c$  refers to the compound of interest,  $d$  refers to the derivative group and

cd refers to the derivatised compound (Rieley 1994). For compounds at natural abundance,  $F$  can be replaced with the corresponding  $\delta$ -value (14.3):

$$n_{cd}F_{cd} = n_cF_c + n_dF_d \quad (14.2)$$

$$n_{cd}\delta_{cd} = n_c\delta_c + n_d\delta_d \quad (14.3)$$

The application of these equations requires the isotope value of the derivatising molecule to be established. If all the atoms of interest in the derivatising reagent are transferred to the analyte, the contribution can be measured directly offline. However, if this is not the case or if the reagent is purchased in numerous small batches thereby precluding off-line analysis, the contribution of the derivatising group can be measured indirectly by derivatising a compound of known isotope value. However, this will have implications for the errors associated with the measurement, as discussed below.

If the observed  $\delta$ -values for derivatised analytes do not equal those predicted by Equation (14.2), then a kinetic isotope effect is present. Correction for the KIE can be made through the use of correction factors, as long as the KIE is proved to be reproducible across a range of analyte concentrations. These correction factors are defined as the 'effective' stable isotope composition of the derivative carbon introduced during derivatisation taking into account the isotopic fractionation associated with the reaction. Correction factors are determined indirectly by measuring the  $\delta$ -value of an underivatised standard of the compound of interest (by off-line IRMS), the value of the standard after derivatisation (by GC-C-IRMS), and using a rearranged Equation (14.3) to determine  $\delta_d$ . The  $\delta_d$  term can then be replaced with  $\delta_{corr}$  to represent the correction factor for the molecule of interest (Silfer *et al.* 1991; Macko *et al.* 1998).

Where no KIE is present, the measurement of the  $\delta$ -value is a result of two measurements, each with their own associated precision. During correction for the added derivative carbon, where  $\sigma$  is the standard deviation associated with a given  $\delta$  determination, the errors propagate according to Equation (14.4).

$$\sigma_c^2 = \sigma_{cd}^2 \left( \frac{n_c + n_d}{n_c} \right)^2 + \sigma_d^2 \left( \frac{n_d}{n_c} \right)^2 \quad (14.4)$$

In derivatisation reactions with a KIE correction factors are first calculated; this calculation introduces another step where errors propagate. The propagation of errors under these circumstances is calculated using Equation (14.5), where subscript s stands for the standard used in correction factor determination and sd stands for the derivatised standard. The magnitude of the errors associated with the correction factors themselves can be calculated using Equation (14.4), along with the precisions for each determination (Docherty *et al.* 2001).

$$\sigma_c^2 = \sigma_s^2 \left( \frac{n_s}{n_c} \right)^2 + \sigma_{sd}^2 \left( \frac{n_s + n_d}{n_c} \right)^2 + \sigma_{cd}^2 \left( \frac{n_c + n_d}{n_c} \right)^2 \quad (14.5)$$

The precision associated with the determination of  $\delta$ -values is derived from the errors associated with the correction factors and is also dependent on the molar ratio of the element of interest between the sample and derivative. Therefore in order to minimise the final error it is preferable to employ a derivatisation reaction with no associated KIE and to minimise the amount of derivative atoms added.

## 14.9 Applications of Compound-specific Stable Isotope Analysis in Archaeology

### 14.9.1 Compound-specific Stable Carbon Isotope Analysis of Bone and Tissue Biochemical Components

The use of bone in palaeodietary reconstruction was motivated by the variations in collagen  $\delta^{13}\text{C}$  values observed during  $^{14}\text{C}$  dating, and light stable isotopes were first used in archaeology in the late 1970s (Vogel and van der Merwe 1977). Since then dietary analysis through both carbon and nitrogen isotopes has been applied extensively to archaeological studies (Koch 2007; Lee-Thorp 2008). The reconstruction of ancient diets is possible because  $\delta^{13}\text{C}$  and  $\delta^{15}\text{N}$  values of fossil bone reflect the isotopic signatures of the local environment, specifically the plants that lie at the base of the food chain (Gannes *et al.* 1998). Very extensive investigations of human diet in the past have been undertaken using the stable isotopic signals recorded in collagen and hydroxyapatite in bones, with important evidence also coming from teeth. As shown below there is an increasing trend towards the compound-specific stable carbon isotope analysis of bone components such as cholesterol, fatty acids and individual collagen amino acids to palaeodietary reconstruction.

### 14.9.2 Cholesterol in Archaeological Bone and Soft Tissues

The use of cholesterol as a palaeodietary indicator is a relatively recent development. Archaeological human and animal bones have been found to contain free cholesterol and cholesteryl fatty acyl esters, and diagenetic products ( $5\alpha$ - and  $5\beta$ -cholestan-3-one,  $5\alpha$ - and  $5\beta$ -cholestanol and cholest-5-en-7-one- $3\beta$ -ol; Evershed *et al.* 1995; Stott *et al.* 1997a). The cholesterol found in bone may derive from either the remnants of the original blood-borne lipid (in the case of vascular bones), the fat component of bone marrow that would have been present at the time of death of the organism or a component of cellular lipids present in bone forming cells (Stott *et al.* 1997b). The use of cholesterol as a palaeodietary indicator has been extensively investigated (Stott and Evershed 1996; Stott *et al.* 1997b, 1999; Jim *et al.* 2004). The  $\delta^{13}\text{C}$  values of cholesterol are readily recorded by GC-C-IRMS as its trimethylsilyl (TMS) ether derivative (Figures 14.10 and 14.11) and were constant across different skeletal members for a given individual (Stott and Evershed 1996). Assessment of  $\delta^{13}\text{C}$  values for cholesterol from animals raised on isotopically distinct diets (Stott *et al.* 1997a; Jim 2000; Jim *et al.* 2001, 2003b, 2004; Corr 2003) indicate that: (i) cholesterol is a strong indicator of whole diet; (ii) neosynthesis of cholesterol is more significant than assimilation in determining the  $\delta^{13}\text{C}$  value of cholesterol; and (iii) bone cholesterol  $\delta^{13}\text{C}$  values respond to changes in the isotopic composition of whole diet more rapidly than collagen and apatite such that cholesterol is an indicator of short-term diet (Stott *et al.* 1997a; Jim 2000).

The  $\delta^{13}\text{C}$  values of cholesterol have been investigated, alongside collagen and apatite analysis, to address archaeological questions relating to the diets of a range of ancient populations (Stott *et al.* 1999; Jim 2000; Jones 2002; Corr 2003; Howland 2003; Copley *et al.* 2004). For example, Figure 14.12 shows the results of a range of dietary proxies, being used in parallel to assess the progress of introduction of maize agriculture in the

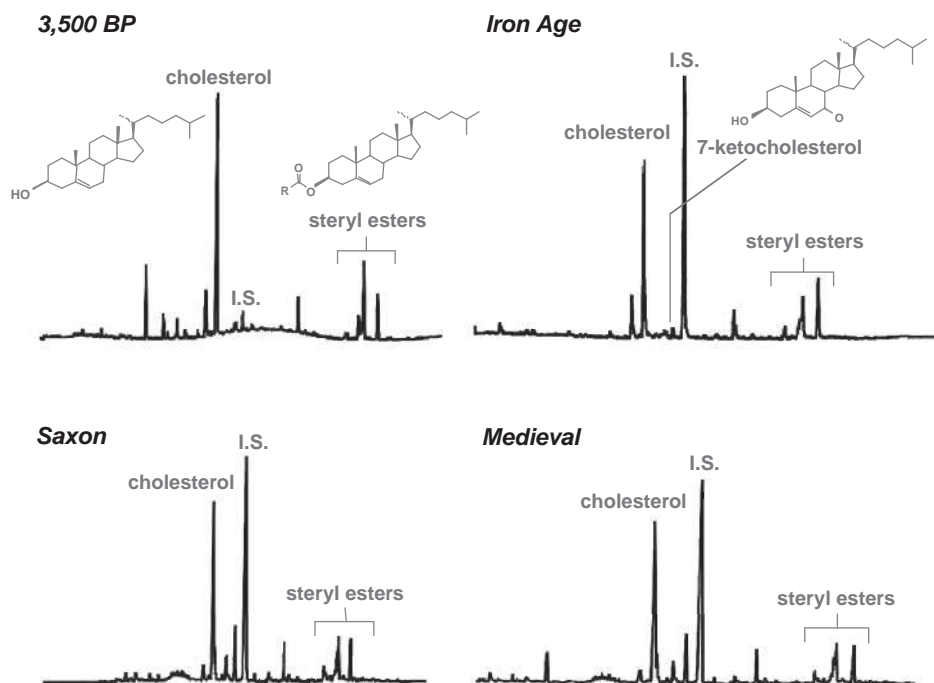


**Figure 14.10** GC profiles of total lipid extracts of archaeological bones showing the widespread survival of lipids, in particular cholesterol and its derivatives

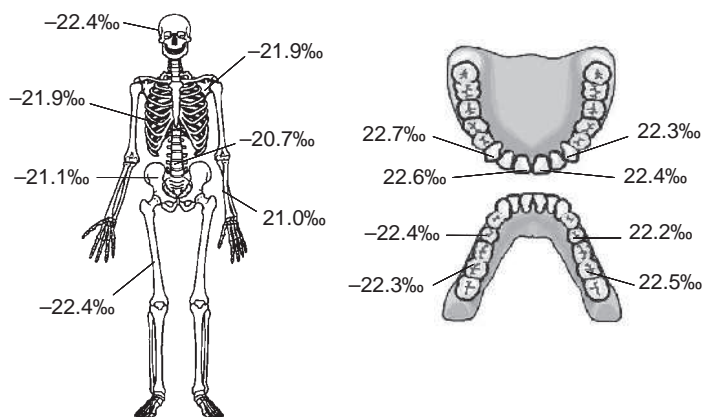


**Figure 14.11**  $\delta^{13}\text{C}$  values of cholesterol recorded by GC-C-IRMS from a wide range of skeletal members and teeth confirming the consistency of the signals and potential utility for palaeo-dietary reconstruction

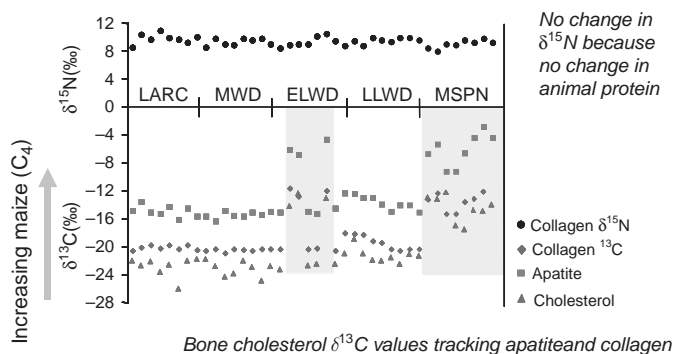


**Figure 14.12** Trends through time in the bulk stable isotope values of collagen ( $\delta^{13}\text{C}$  and  $\delta^{15}\text{N}$ ), apatite ( $\delta^{13}\text{C}$ ) and compound-specific  $\delta^{13}\text{C}$  values of cholesterol recorded from a number of individuals from the Illinois River Valley, USA, showing contiguous fluctuations in carbon stable isotope composition consistent with differing contributions of maize to the diet (Jim, Ambrose and Evershed unpublished data)

Illinois River Valley. A number of advantages of such a multi-proxy approach are clearly evident. Most notably, all of the carbon proxies, i.e. collagen, cholesterol and apatite, show parallel trends lending greater confidence to interpretations than would exist if only a single proxy was used.

### 14.9.3 Fatty Acids in Archaeological Skeletal and Soft Tissue Remains and Experimental Animals

As alluded to above, and will be discussed in detail below, fatty acids have been used as biomarkers for animal fats in the study of lipid residues in archaeological pottery sherds. However, the analysis of fatty acids from archaeological bone has been much less explored (Evershed *et al.* 1995). This is mainly due to the apparently low survival rates of bone fatty acids in the archaeological record; fatty acids only seem to be preserved in significant abundances under exceptional burial environments, for example arid, waterlogged and frozen sites (Evershed and Connolly 1987; Mayer *et al.* 1997; Copley *et al.* 2004; Corr *et al.* 2008). Fatty acids present in bone most likely originate from bone marrow fat (Evershed *et al.* 1995). Studies on rats and pigs raised on isotopically controlled diets have shown that bone fatty acid  $\delta^{13}\text{C}$  values are  $^{13}\text{C}$ -depleted by up to 3.4 ‰ with respect to whole diet (Jim 2000; Jim *et al.* 2001, 2003b; Howland *et al.* 2003). This phenomenon results from a KIE occurring during the oxidation of pyruvate by pyruvate dehydrogenase to acetyl CoA, the common precursor in lipid biosynthesis (DeNiro and Epstein 1977; Hayes 1993). The  $\delta^{13}\text{C}$  values of bone fatty acids have recently been used together with those of individual amino acids and apatite as indicators of trends in the management of domesticated animals in Egypt (Copley *et al.* 2004).

In a recent study (Corr *et al.* 2008, 2009) the male remains of a preserved ice body recovered from a retreating glacier in the Tatshenshini–Alsek Park, British Columbia in August 1999 were investigated. Despite the remote location 80 km inland, bulk bone collagen stable isotope analysis indicated that the individual spent much of his life in a region rich in marine foods ( $\delta^{13}\text{C}$ :  $-13.7\text{‰}$  and  $\delta^{15}\text{N}$ :  $+17.9\text{‰}$ ; Richards *et al.* 2008). To probe how long



he spent in this remote location prior to his death, the more rapidly remodelled lipid components of his tissues were analysed to determine whether a marine or terrestrial diet could be inferred. Molecular fingerprinting and compound-specific carbon isotope analysis were performed on individual lipids extracted from his bone (turnover  $\approx \geq 1$  year) and skin (turnover  $\approx$  several weeks). A considerable abundance of endogenous fatty acids (FAs;  $C_{12:0}$ ,  $C_{14:0}$ ,  $C_{16:0}$ ,  $C_{16:1}$ ,  $C_{18:0}$ ,  $C_{18:1}$  FAs), cholesterol and hydroxy FAs, including the unusual long-chain hydroxy FAs (LCHFAs), 10- and 12-hydroxyeicosanoic acid and 10- and 12-hydroxydocosanoic acid, were detected in the bone. The origin of these hydroxy acids was assigned to microbially activated hydration of the double bonds of  $C_{20:1}$  and  $C_{22:1}$  FAs, the latter likely originating from the consumption of a largely marine-based diet. The marine biomarker trilogy of isoprenoidal compounds, phytanic acid, pristanic acid and 4,8,12-trimethyltetradecanoic (TMTD) acid, were also detected. In contrast, the skin lipid composition was dominated by  $C_{16:0}$  FA with only trace amounts of the marine LCHFAs and isoprenoidal compounds, suggesting less reliance on coastal marine foods in the last period of life. This theory is consistent also with the more marine dietary signal observed in the bone than skin FA  $\delta^{13}\text{C}$  values, determined using GC-C-IRMS. Figure 14.13 summarises the results of compound-specific carbon isotope analysis of bone and skin FAs and cholesterol as their methyl esters and TMS ethers, respectively.  $\delta^{13}\text{C}$  values were obtained for FAs which achieved baseline chromatographic resolution:  $C_{14:0}$  FA,  $C_{16:0}$  FA,  $C_{16:1}$  FA,  $C_{18:0}$  FA and  $C_{18:1}$  FA. The pattern observed in the Kwäday Dän Ts'inchí individual's bone (Figure 14.13), where  $C_{18:0}$  FA ( $-23.2\text{‰}$ ) =  $C_{18:1}$  FA ( $-23.2\text{‰}$ ) >  $C_{16:1}$  FA ( $-24.0\text{‰}$ ) >  $C_{14:0}$  FA ( $-24.2\text{‰}$ ) >  $C_{16:0}$  FA ( $-24.6\text{‰}$ ) is similar to that reported in the bone of pigs reared on isotopically controlled diets (Stott *et al.*, 1997a; Howland *et al.*, 2003), and in the adipose tissue of the redhead duck (Hammer *et al.* 1998). In terms of dietary input, there is little to reference these FA  $\delta^{13}\text{C}$  values to since there are few published human FA  $\delta^{13}\text{C}$  values for tissues other than plasma/serum (Binnert *et al.* 1995; Meier-Augenstein 1999). Interestingly, in a metabolic tracer study Metges and co-workers (Metges *et al.* 1994) reported serum FA  $\delta^{13}\text{C}$  values of  $-28.0$  and  $-31.0\text{‰}$  for  $C_{16:0}$  FA and  $C_{18:0}$  FA, respectively, for humans consuming  $C_3$  diets. The mean  $\delta^{13}\text{C}$  value for Kwäday Dän Ts'inchí's bone FAs ( $-23.8 \pm 0.6\text{‰}$ ) is substantially higher than this, which is consistent with a diet more enriched in marine foods. Kwäday Dän Ts'inchí individual's FA  $\delta^{13}\text{C}$  values are also remarkably congruent with the adipose tissue ( $-24.7\text{‰}$ ,  $n = 12$ ) of Arctic polar bears with predatorial relationships with ringed seals (Ramsay and Hobson 1991). There is, in addition, a high degree of similarity between the FA  $\delta^{13}\text{C}$  values and those extracted from the bones of laboratory rats fed on a diet of 70% tuna/30%  $C_3$  carbohydrates (Jim 2000; Jim *et al.* 2003b; see also Figure 14.13). It can be seen that the bone FA  $\delta^{13}\text{C}$  values of Kwäday Dän Ts'inchí individual and the rats raised on the 70% marine diet diverge significantly from those of rats raised on the baseline  $C_3$  diet.

The skin FA  $\delta^{13}\text{C}$  values were similar to those of the bone with little difference observed between the two with respect to mean FA  $\delta^{13}\text{C}$  values ( $-23.8 \pm 0.6\text{‰}$  and  $-24.0 \pm 0.3\text{‰}$ , respectively; Figure 14.13). This is not in agreement with the differences observed in lipid compositions, where the bone showed a more marine dietary fingerprint. However, it has been shown that pigs reared on long-term isotopically controlled diets have skin FA  $\delta^{13}\text{C}$  values  $2.7 \pm 0.4\text{‰}$  higher than observed for bone, possibly arising from tissue biosynthetic differences (Mukherjee 2004). If the present skin FA  $\delta^{13}\text{C}$  values are corrected for this difference, the mean skin FA value becomes  $2.7\text{‰}$  lower than that of the bone, indicating the input of significantly less carbon from marine foods to Kwäday Dän

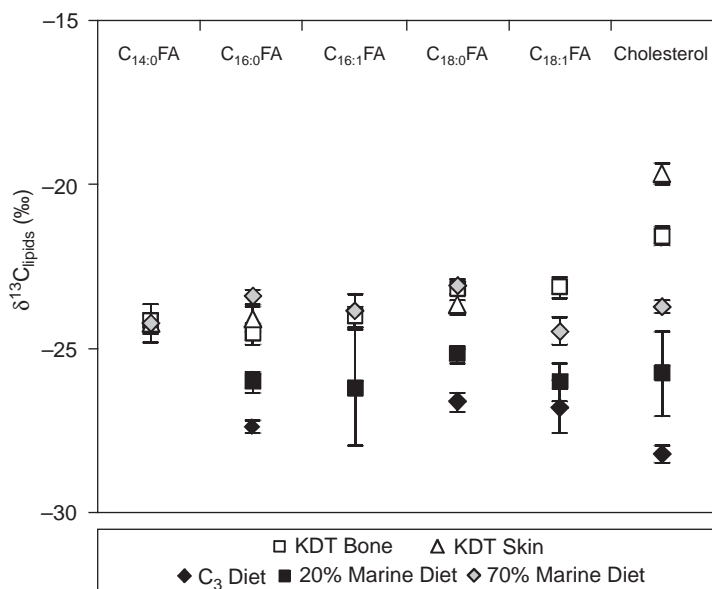


**Figure 14.13**  $\delta^{13}\text{C}$  values of the most abundant FAs and cholesterol in the Kwäḍay Dän Ts'inchí bone and skin samples (determined by GC-C-IRMS) compared with  $\delta^{13}\text{C}$  values determined for the same compounds in individual's bone extracted from rats subjected to a pure  $\text{C}_3$  terrestrial diet, a 20% marine protein (tuna) diet and a 70% marine (tuna) diet (Jim, unpublished data)

Ts'inchí individual's skin than bone. Thus, the isotopic data indicate a divergence from an almost exclusive marine diet in the last months of life.

#### 14.9.4 Amino Acids in Archaeological Bones and Those of Experimental Animals

Compound-specific stable isotope analyses of the building blocks of complex biopolymers are essential to unravelling the stable isotope signals expressed in bulk signals (Abelson and Hoering 1961). The exploitation of individual collagenous amino acids has great potential in palaeodietary reconstruction. However, surprisingly only a handful of studies have determined the  $\delta^{13}\text{C}$  values of amino acids from ancient bone collagen (Hare and Estep 1983; Tuross *et al.*, 1988; Hare *et al.* 1991; Fogel and Tuross 2003; Copley *et al.* 2004; Corr *et al.* 2005, 2009). Amino acids are difficult to isolate for isotopic analysis. Ion exchange liquid chromatography has been used but is slow and the reproducibility of retention times is poor (Hare and Estep 1983; Macko *et al.* 1983, 1987; Tuross *et al.* 1988; Hare *et al.* 1991). Moreover, van Klinken (1991) has reported that isotopic fractionation is a major disadvantage with this technique.

GC-C-IRMS enables amino acids to be separated by GC, combusted on-line, for stable isotopic analysis; thereby avoiding manual preparative steps (see Figures 14.5, 14.8 and 14.9). The  $\delta^{13}\text{C}$  values of individual collagen amino acids are highly robust and by



use of mass balance calculations can even be used to reconstruct the bulk  $\delta^{13}\text{C}$  value of whole collagen (Figure 14.14; Jim *et al.* 2003a). A study of pigs raised on six isotopically controlled diets investigated the routing of dietary macronutrients to bone biochemical components (Howland 2003; Howland *et al.* 2003), showing that: (i) the  $\delta^{13}\text{C}$  values of single amino acids accurately predicted the  $\delta^{13}\text{C}$  value of whole collagen; (ii) the  $\delta^{13}\text{C}$  values of nonessential amino acids alanine and glutamate, from bone collagen correlated well with whole diet; and (iii) the essential amino acids leucine and phenylalanine showed little isotopic fractionation between diet and bone collagen. More recently a feeding experiment involved rats fed on diets where the  $\delta^{13}\text{C}$  values of the major dietary macronutrients were switched between  $\text{C}_3$  and  $\text{C}_4$  enabling quantitative assessment to be made of the carbon sources used in the *de novo* synthesis of non-essential amino acids (Jim *et al.* 2006).

Applying these techniques to archaeological populations has demonstrated the wider utility of compound-specific stable isotope analysis of individual bone collagen amino acids to distinguish between high marine protein and terrestrial consumers (Corr *et al.* 2005). This was previously shown to be problematic in extremely arid environments using bulk collagen  $\delta^{15}\text{N}$  values alone (Heaton *et al.*, 1986; Heaton 1987; Sealy 1997; Schwarcz *et al.*, 1999) since herbivore bone collagen  $\delta^{15}\text{N}$  values overlap with the range for marine species (Heaton *et al.* 1986; Sealy 1997). Due to their contrasting metabolic pathways,  $\delta^{13}\text{C}$  values of the essential amino acid phenylalanine and the non-essential amino acid glycine in bone collagen (Figure 14.15; Beynon 1998) preserve different palaeodietary signals and this difference ( $\delta^{13}\text{C}_{\text{Glycine-Phenylalanine}}$ ) can be exploited to distinguish between high marine protein and terrestrial consumers (Figure 14.16). This new proxy provided further palaeoforensic evidence for the dietary activities of the Kwäday Dän Ts'ínchí individual. The lower  $\delta^{13}\text{C}_{\text{Glycine-Phenylalanine}}$  value for the individual's skin (fast turnover) compared with the bone (slow turnover) was consistent with the divergence away from marine resources in the last months of his life (Corr *et al.* 2009).

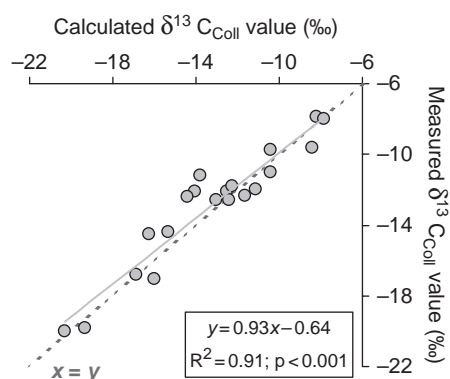


**Figure 14.14** Linear correlations between calculated, based upon individual amino acids determined by GC-C-IRMS and measured, bulk collagen  $\delta^{13}\text{C}$  values (dotted line represents  $x = y$ )

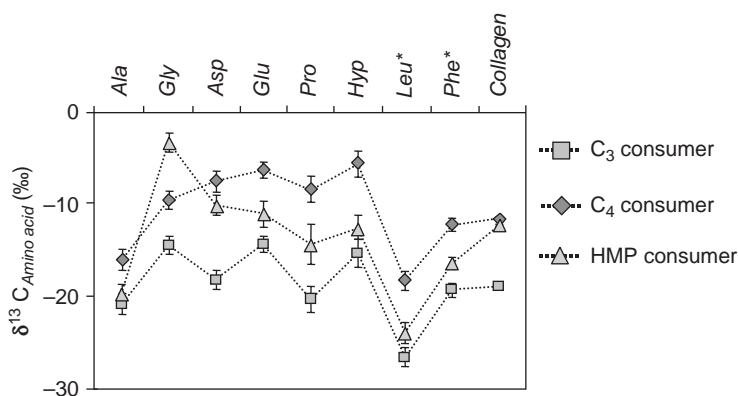


**Figure 14.15** Comparison of bulk collagen and individual amino acid  $\delta^{13}\text{C}$  values for high marine protein,  $\text{C}_3$  and  $\text{C}_4$  consumer later Stone Age humans from the Western Cape of South Africa (adapted from Corr et al. 2005)

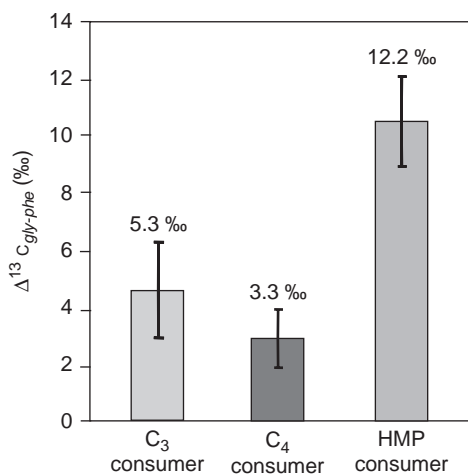


**Figure 14.16** Comparison of  $\Delta^{13}\text{C}$  values for high marine protein,  $\text{C}_3$  and  $\text{C}_4$  consumer later Stone Age humans from the Western Cape of South Africa (adapted from Corr et al. 2005)

In summary, the recent investigations discussed above now mean that a range of bone based biochemical proxies exists for investigating: (i) whole diet; (ii) specific elements of the diet e.g. protein and energy components; and (iii) long- and short-term dietary variation within such proxies, and as such are highly applicable to the investigation of ancient diet. The next few years will undoubtedly see an expansion in the range of applications of the above techniques in archaeology and palaeoecology. A recent major development has been the first reported applications of an operational HPLC-IRMS instrument. The new HPLC-IRMS method appears to offer a useful

addition to the armoury of techniques available for undertaking compound-specific carbon isotope analyses, particularly for functionalised compounds, such as amino acids. Analytes separated by aqueous based HPLC are quantitatively converted to  $\text{CO}_2$  in a reactor containing ammonium peroxodisulfate (Figure 14.17). Preliminary analyses have shown that amino acids can be analysed directly on such HPLC-IRMS systems to provide accurate  $\delta^{13}\text{C}$  values (Krummen *et al.* 2004; McCullagh *et al.* 2006). Analytical precisions reported for a range of amino acids are ca.  $\pm 0.2$  to  $0.3\%$  for 100 to 300 ng amino acid injected. Notable disadvantages compared with GC-C-IRMS is the larger amounts of sample required for the high precision analyses and the current lack of an effective HPLC-IRMS interface for nitrogen isotope determinations. In spite of this, there is every indication that a step change is occurring in the use of compound-specific stable isotope analyses in this area.

### 14.9.5 Organic Residues in Archaeological Pottery

Early work in the use of stable isotopes in archaeological pottery involved bulk isotopic analysis (e.g. Hastdorf and DeNiro 1985; Morton and Schwarcz 1988; Sherriff *et al.* 1995). Compound-specific stable isotope analysis was first applied to archaeological potsherds in 1994 (Evershed *et al.* 1994), confirming that an extract with lipid distribution consistent with wild type *Brassica* species was of a  $\text{C}_3$  plant origin. This was followed by its application to the identification of degraded beeswax in Minoan Lamps (Evershed *et al.* 1997b). The major advantage of applying compound-specific stable isotope analysis via GC-C-IRMS to lipid residues in archaeological pottery is the greater specificity achievable than is possible with bulk analyses, since the structures of diagnostic (biomarker) components of complex mixtures can be unambiguously linked to their stable isotope values. Most importantly the compound-specific  $\delta^{13}\text{C}$  values record the biochemical history of preserved biomarkers, which are of particular value in distinguishing the sources of specific compounds even when chemical structures are identical.

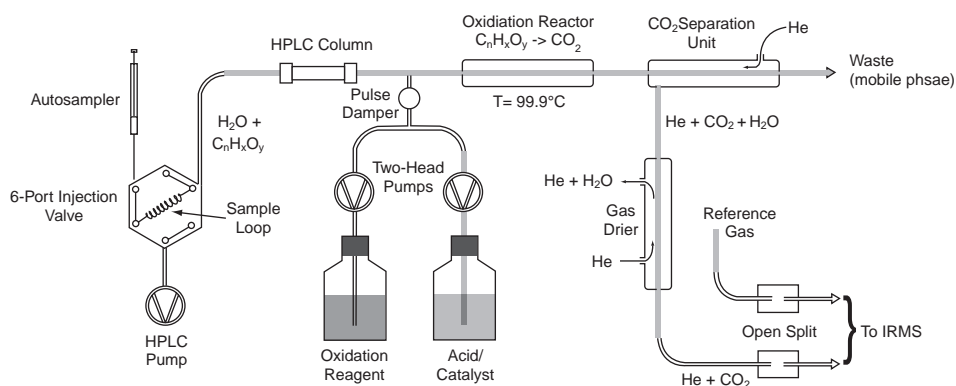


**Figure 14.17** Schematic diagram of the ThermoElectron liquid chromatography-isotope ratio mass spectrometry chemical oxidation reactor

### 14.9.6 Compound-specific Carbon Isotope Values and the Origins of Animal Fats

GC-C-IRMS has proven to be especially powerful in resolving the origins of *n*-alkanoic acids, i.e. FAs, which is the most commonly observed class of lipid residue observed in archaeological pottery. Compound-specific  $\delta^{13}\text{C}$  values are readily determined for FAs derivatised to FAMES and studies of the stable isotopic properties of fats from the major old world domesticates have revealed the  $\delta^{13}\text{C}$  values of FAs of ruminant (e.g. sheep/goat and cattle) and porcine (pig) adipose fats are readily distinguishable (Figure 14.18; Evershed *et al.* 1997c, 2003b). In the first application of this approach the  $\delta^{13}\text{C}$  values of the  $\text{C}_{16:0}$  and  $\text{C}_{18:0}$  FAs in Medieval pottery were compared with modern reference fats

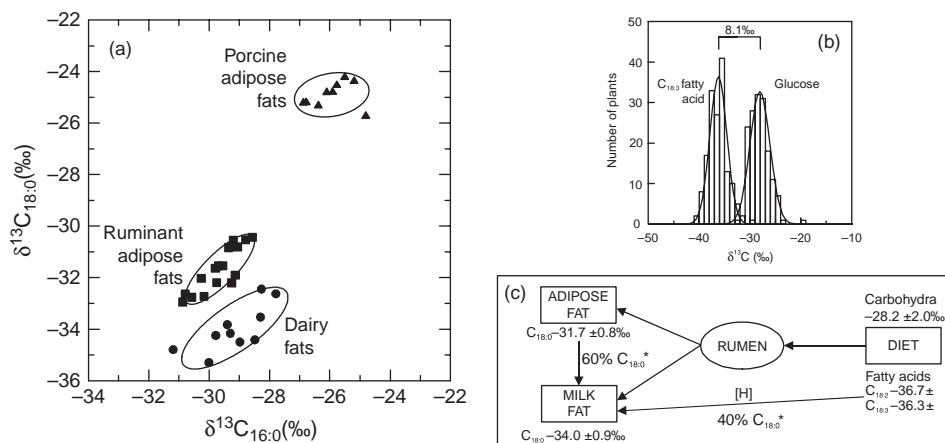


**Figure 14.18** (a) Plot of the  $\delta^{13}\text{C}$  values of the major saturated fatty acid components ( $\text{C}_{16:0}$  and  $\text{C}_{18:0}$ ) of the lipid extracts from modern reference fats showing the resolution of dairy fats from ruminant and non-ruminant adipose fats. The three fields correspond to 1 SD confidence ellipses calculated for the  $\delta^{13}\text{C}$  values of the domesticates known to comprise the major component of prehistoric economies in Britain. All the animals were raised on  $\text{C}_3$  diets. The  $\delta^{13}\text{C}$  values for the fatty acids have been corrected for post-Industrial Revolution effects of fossil fuel burning, which has led to more depleted atmospheric  $\delta^{13}\text{CO}_2$  values, and has been calculated to be 1.2‰ (Friedli *et al.* 1986). Analytical precision is  $\pm 0.3$ ‰. (b) Histogram of the  $\delta^{13}\text{C}$  values of  $\text{C}_{18:3}$  fatty acids and glucose extracted from plants. The histogram of the  $\delta^{13}\text{C}$  values of the major fatty acids and carbohydrates of 166 modern plants demonstrates that there is an 8.1‰ mean difference in the  $\delta^{13}\text{C}$  values of  $\text{C}_{18:3}$  fatty acid (mean =  $-36.3$ ‰) and glucose (mean =  $-28.2$ ‰) which is the basis of the difference in the  $\delta^{13}\text{C}$  value of the  $\text{C}_{18:0}$  fatty acid in dairy and milk fat. This difference in  $\delta^{13}\text{C}$  value between lipids and carbohydrates is seen in both  $\text{C}_3$  and  $\text{C}_4$  plants. (c) Diagram showing the routing of dietary fatty acids and carbohydrates in the rumen, adipose tissue and mammary gland of the ruminant animal. Note, 60% of the  $\text{C}_{18:0}$  in ruminant milk is rerouted from adipose tissue and is comprised of carbon originating from dietary glucose and fatty acids, and the remaining 40% (McDonald *et al.* 1988) is directly incorporated from the diet following biohydrogenation of unsaturated fatty acids in the rumen (shown by asterisk), and reflects the inability of the mammary gland to biosynthesise  $\text{C}_{18:0}$  (Christie 1981; Byers and Schelling 1988). The 2.3‰ mean difference in the  $\delta^{13}\text{C}$  values of  $\text{C}_{18:0}$  in ruminant adipose tissues and dairy fats can be seen graphically in (a) (Copley *et al.* 2003)

revealing that ruminant fat had been used as fuel in the lamps, whereas porcine fat was collected in the dripping dishes, disproving the theory that fat was collected from spit-roasting and recycled as lamp fuel (Evershed *et al.* 1997c; Mottram *et al.* 1999). The  $\delta^{13}\text{C}$  values exhibited by these animals reflect their different diets and variations in their metabolisms and physiologies (Evershed *et al.* 1999).

Subsequent research showed that ruminant adipose and dairy fats can also be distinguished by the  $\delta^{13}\text{C}$  values of their FAs (Dudd and Evershed 1998). The  $\text{C}_{18:0}$  FA in dairy fat is significantly more depleted in  $^{13}\text{C}$  ( $>2.3\%$ ; Copley *et al.* 2003). FAs in ruminant adipose are mainly synthesised from acetate (as acetyl CoA), originating predominately from the fermentation of dietary carbohydrate in the rumen. The mammary gland is incapable of synthesising the  $\text{C}_{18:0}$  FA; instead, it is obtained via the remobilisation of adipose FAs and directly from the dietary  $\text{C}_{18}$  FAs, after biohydrogenation in the rumen (Moore and Christie 1981). The difference between the  $\text{C}_{18:0}$  FAs from ruminant adipose and dairy fat can be explained by the fact that lipids are more depleted in  $^{13}\text{C}$  than carbohydrates (DeNiro and Epstein 1977) and c. 60% of the  $\text{C}_{18:0}$  FA in dairy fat are derived via biohydrogenation of dietary unsaturated  $\text{C}_{18}$  FAs (i.e.  $\text{C}_{18:1}$ ,  $\text{C}_{18:2}$  and  $\text{C}_{18:3}$ ) in the rumen. The  $\delta^{13}\text{C}$  values of the contributors to the  $\text{C}_{18:0}$  FA in dairy fat are summarised in Figure 14.18.

GC-C-IRMS analysis of remnant animal fats of archaeological origin has now been extensively used to address some key questions concerning animal husbandry in prehistory, for example the earliest evidence for dairying in prehistoric Britain (Dudd and Evershed 1998; Copley *et al.* 2003, 2005a,b,c; Berstan *et al.* 2004), and the exploitation of pigs in late Neolithic Britain (Mukherjee *et al.* 2005, 2007, 2008).  $\delta^{13}\text{C}$  values of FAs extracted from potsherds have also been used to identify prehistoric dairying activities in the Western Isles of Scotland (Craig *et al.* 2005) and Switzerland (Spangenberg *et al.* 2006).

The  $\delta^{13}\text{C}$  values of the individual FAs are affected by a range of environmental variables which increase the range of carbon isotope for FAs depending upon climatic influences and the presence of plants of varying  $\delta^{13}\text{C}$  value, e.g.  $\text{C}_3$  versus  $\text{C}_4$ , etc. (Mukherjee *et al.* 2005). Whilst these influences might seem to complicate classifications of fats plotting  $[\Delta^{13}\text{C}_{18:0-16:0}]$  values removes the bulk of the environmental variability expressed in the raw  $\delta^{13}\text{C}$  values and emphasises the differences between fat types. The subtraction gives a numeric that is a reflection of the biochemical and physiological origins of the specific fat types, which is independent of the photosynthetic pathways of the plants at the base of the food chain in any terrestrial ecosystem. Critical to the success of this proxy is the *difference* between the  $\delta^{13}\text{C}$  values of the FAs and carbohydrates produced by the plants that the animals consume and use in fat biosynthesis. This major aspect of plant biochemistry, expressed as a difference of ca. 5–8‰, is fundamental to *all* plants and results from the fractionation involved in the enzymatic oxidation of pyruvate  $\rightarrow$  acetyl CoA (DeNiro and Epstein 1977; Deines 1980; Dungait *et al.* 2008 and references therein). It is the differing balances between the amount of plant carbohydrate and FA derived carbon used in mammalian FA biosynthesis that gives rise to the separations between fat types expressed in the plots of  $\Delta^{13}\text{C}$  values. This ability to decouple the proxy from the  $\text{C}_3/\text{C}_4$  and other environmental influences is a very powerful feature of the proxy, which appears to make it globally applicable. The robustness of the proxy is emphasised in Figure 14.19 for reference fat data sets collected in the UK and the Eurasian Steppe. While the absolute

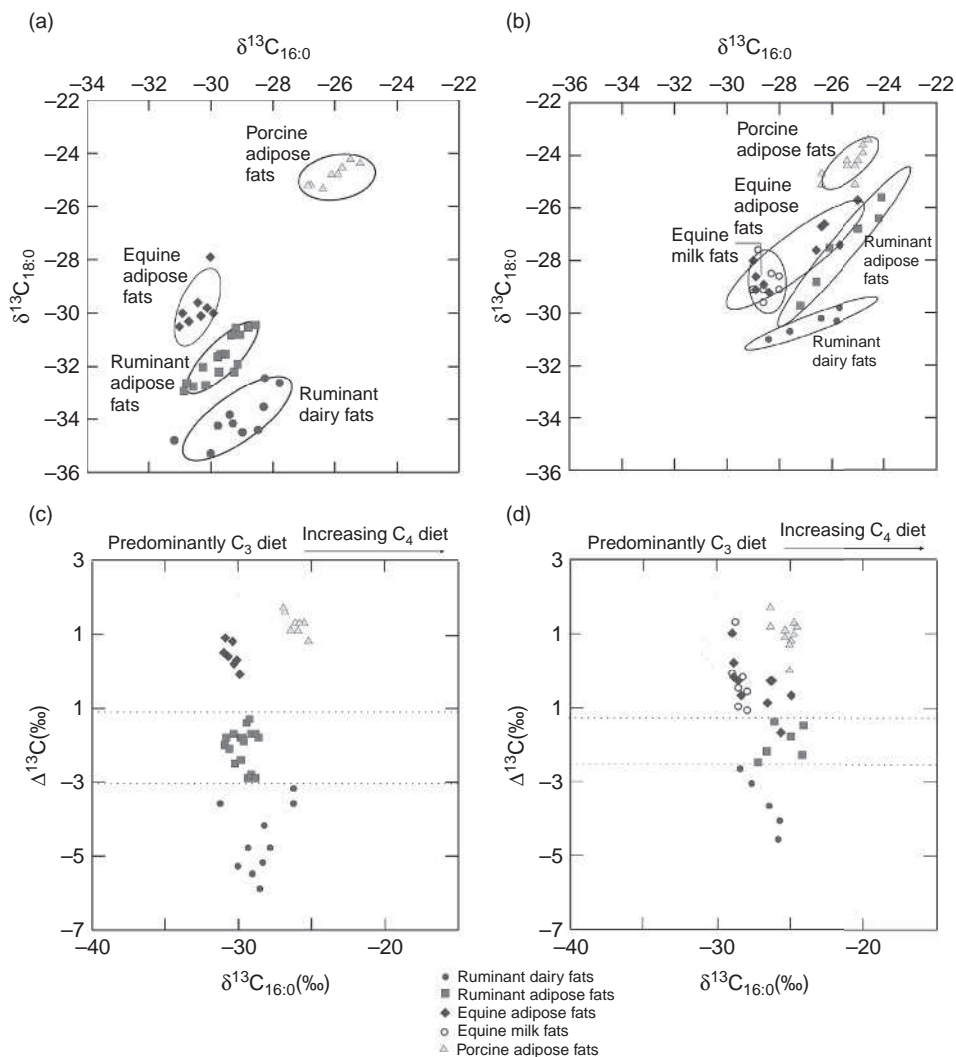


**Figure 14.19** Scatterplots comparing (a) the  $\delta^{13}\text{C}$  values of the fatty acids of the modern British reference animal fats with (b) the  $\delta^{13}\text{C}$  values of the fatty acids of the modern Kazakh reference animal fats; and (c) the  $\Delta^{13}\text{C}$  values of the British reference animal fats with (d) the  $\Delta^{13}\text{C}$  values of the Kazakh reference animal fats. (British reference animal fat values taken from Dudd 1999 and Kazakh values from Outram *et al.* 2009)

ranges for the  $\delta^{13}\text{C}$  values are wider in Kazakhstan than the UK the means and ranges for the  $\Delta^{13}\text{C}$  values are virtually identical.

This proxy approach has recently been used to provide the earliest evidence for prehistoric milk use (Evershed *et al.* 2008). A study of the lipid content of >2200 pottery vessels from sites in the Near East and the Balkans dating from the fifth to seventh millennia was carried out. It was shown that milk was in use by the seventh millennium

and that milking was particularly important in north-west Anatolia (Figure 14.20), pointing to regional differences linked with conditions more favourable to cattle compared with other regions, where sheep and goat were relatively common and milk use less important. The latter is supported by correlations between the fat type and animal bone evidence (Evershed *et al.* 2008).

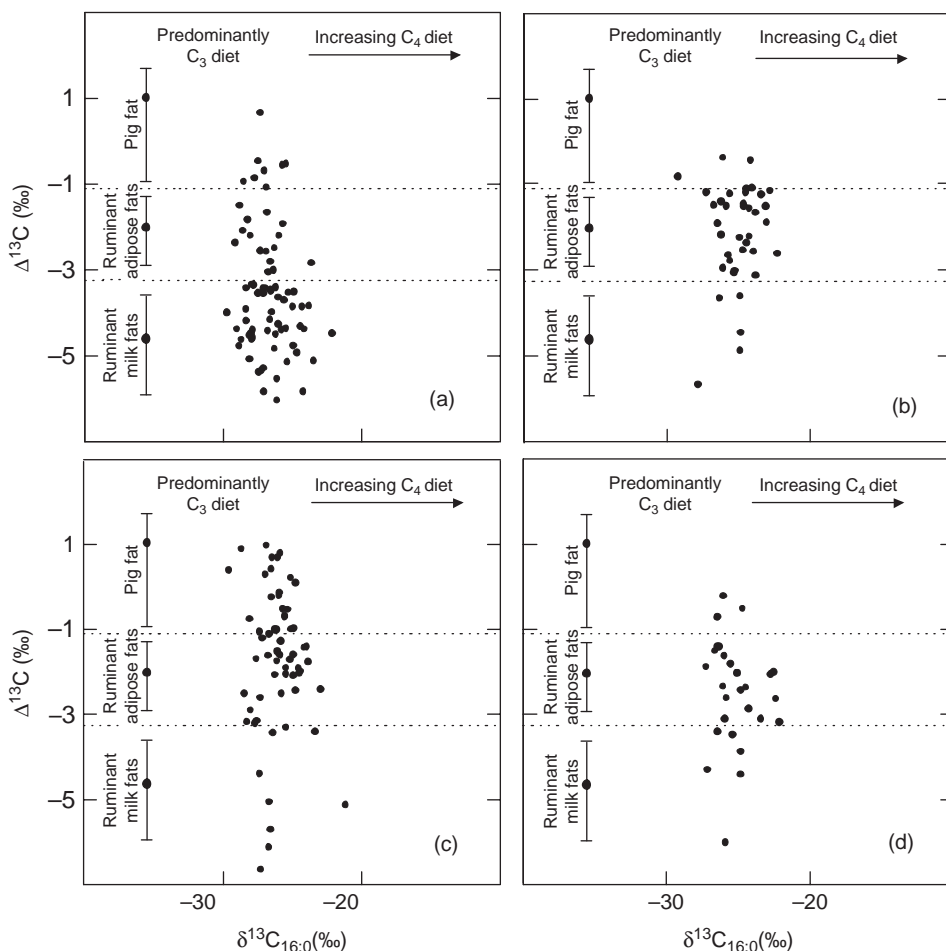


**Figure 14.20** Plot of the  $\Delta^{13}\text{C}$  values for archaeological animal fat residues in pottery showing most intensive milk use in northwestern Anatolia dating back to the seventh millennium BC. Pottery was from: (a) northwestern Anatolia; (b) central Anatolia; (c) southeastern Europe/northern Greece; and (d) eastern Anatolia and the Levant. The  $\Delta^{13}\text{C}$  values ( $= \delta^{13}\text{C}_{18:0} - \delta^{13}\text{C}_{16:0}$ ) for the ruminant dairy fats are more depleted than the ruminant adipose fats; the difference in the means is  $\sim 2.8\text{‰}$  which is highly significant (t-test;  $P < 0.0005$ ). Pig fats have positive  $\Delta^{13}\text{C}$  values which do not exhibit significant variance and the differences in the mean values are also highly significant (ANOVA;  $P < 0.0005$  between all three commodity groups; Bonferroni adjustment applied). (Evershed *et al.* 2008)

### 14.9.7 The Hydrogen Isotopic Composition of Fatty Acids

Considerable scope exists for exploiting the variations in the hydrogen isotopic composition of animal FAs and other biochemical components, preserved at archaeological sites, caused by variations in meteoric waters, along with any inherent variations introduced by biochemical processes within the animal itself, to provide further proxies for palaeodietary reconstruction. Initial investigations performed in our laboratory have focused on the development of a method for the compound-specific hydrogen isotope analysis of FAs using GC-TC-IRMS. Despite GC-TC (thermal conversion)-IRMS being used previously to determine compound-specific hydrogen isotope composition of FAs (e.g. Scrimgeour *et al.* 1999; Sessions *et al.* 2002; Yang and Huang 2003; Chikaraishi *et al.* 2004a,b), the technique is still relatively new (Hilkert *et al.* 1999), and reports often lack explicit experimental details. We have explored methods to: (i) normalise data produced by the GC-TC-IRMS instrument to the VSMOW-SLAP scale (Coplen 1996), by regular comparison with an external standard of 15 homologous *n*-alkanes (Schimmelman 2007); and (ii) correct for the derivatisation of FAs required for GC analysis. As usual FAs were derivatised as methyl esters by the action of 14% w/v boron trifluoride in methanol. Correction was found to be necessary for this derivatisation, in part because the additional methyl hydrogen affects the overall hydrogen isotope composition of the analyte, but also because of some unaccounted fractionation observed during the derivatisation procedure. On account of the extremely labile carboxyl hydrogen of the FA it is not trivial to determine the initial  $\delta D$  value of the fatty acid needed as reference for the correction; the final correction factor is determined as follows:

$$\delta D_{FA} = \frac{(2N_{FA} + 2)\delta D_{FAME}}{(2N_{FA} - 1)} - 0.4N_{FA} + 29 \quad (14.6)$$

where  $\delta D_{FA}$  is the corrected  $\delta D$  value of the fatty acid,  $\delta D_{FAME}$  is the measured value of the FAME and  $N_{FA}$  is the number of carbon atoms in each FA molecule. This correction factor was tested against (the sodium salts of) FAs of unknown hydrogen isotopic content. Overall, no significant alteration was detected in the  $\delta D$  values of FAs during their extraction and preparation for analyses.

### 14.9.8 The Preservation of the Hydrogen Isotopic Composition of Fatty Acids

Hydrogen isotope analysis of these preserved archaeological FAs will only provide useful data if the  $\delta D$  values obtained from FAs recovered after burial are representative of the  $\delta D$  values of the FAs in the original commodity. It was hypothesised that the hydrogen isotope content of FAs preserved in buried clay pottery may alter over time, either by  $\alpha$ -hydrogen exchange in the acidic clay environment (Larcher *et al.* 1986) or through fractionation during dissolution and degradation. Heating FAs to a temperature of 270 °C overnight on deuterium depleted clay powder was found only to induce exchange of the two FA  $\alpha$ -hydrogen atoms (Larcher *et al.* 1986). Despite this potential for hydrogen exchange to occur, it was found that very little significant exchange actually occurred during the cooking and adsorption of animal FAs into the walls of a pottery vessel. Burial for 16 months of sherds taken from a pot in which lamb was repeatedly cooked, resulted



in a loss of 96% of lipid and more than 99% loss of triacylglycerols present in the sherds immediately after cooking. The mean changes in  $\delta D$  value of palmitic and stearic acids of  $+3.5 \pm 13.0$  ‰ and  $-1.6 \pm 4.0$  ‰, respectively, compared with the raw meat prior to cooking and burial was much less than the natural variation in  $\delta D$  values observed in the FAs of animal origin. This can be demonstrated by superimposing a plot of the change in  $\delta D$  value of FAs caused by burial over a plot showing the range of natural variation in the  $\delta D$  values of terrestrial and marine animal FAs. It is clear from Figure 14.21 that any change in the  $\delta D$  values of lamb FAs caused by cooking and burial will not have altered interpretations about the origins of the fat. Even the FAs showing the greatest alteration during processing and burial would still be classed as of ruminant origin based on their  $\delta D$  values. It is therefore possible to conclude that any FA hydrogen exchange caused during processing or burial of animal products is not significant enough to affect the validity of the application of hydrogen isotope analysis of FAs preserved within archaeological pottery.

Investigations of the fats of modern reference animals suggest a relationship between the ratio of  $\delta D$  values of animal stearic and palmitic acids and the trophic level or

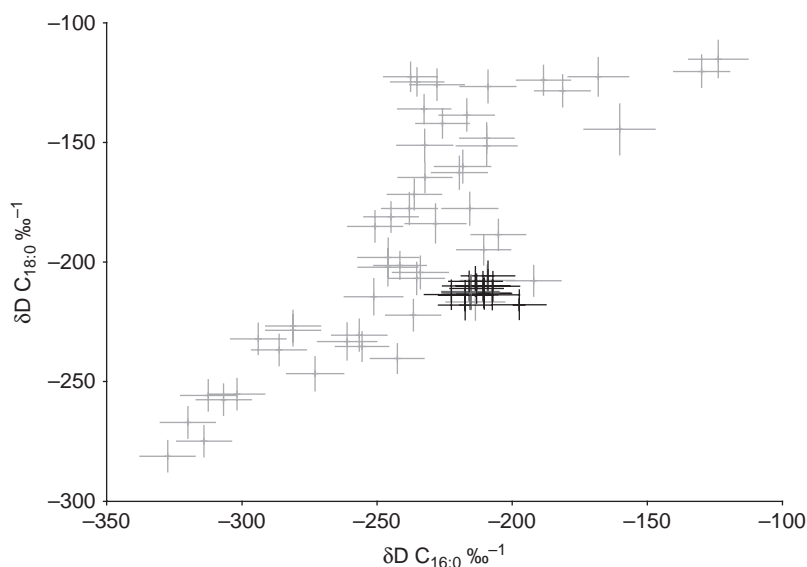


**Figure 14.21** Data from the simulated burial experiment superimposed on a plot of reference animal fatty acid  $\delta D$  values, showing how any change in  $\delta D$  value caused by burial is not significant compared with natural variations in  $\delta D$  values of animal fatty acids. Data from the burial experiment is blue, except for the raw lamb which is red. Reference animal fatty acid  $\delta D$  values are green and correspond to a wide range of terrestrial and marine species drawn from a wide geographical range (see colour Plate 2)

digestive physiology of the organism. Further investigations need to be conducted into the origins and mechanism behind this effect, which may involve feeding experiments of animals with labelled food and water; particularly, carbohydrates and lipids of different hydrogen isotopic composition, to determine relative incorporation rates of hydrogen into animal FAs. The origin of the amount of fractionation between environmental water (and, indeed, body water) and lipids is also not clear, particularly as it is greater than that observed in other animal tissue (e.g. Hobson *et al.* 1999; Sharp *et al.* 2003).

We have begun to apply these compound-specific  $\delta D$  approaches to archaeological questions with promise appearing to exist in the detection of marine FAs in archaeological pottery due to the high values revealed. However, the area of greatest promise revealed up to now has been in exploiting the seasonal signal. This effect has been used in work on early horse domestication in the Eurasian Steppe. Horses give birth during the spring and as such only lactate during the summer (Levine 1999). On account of the large seasonal variations in meteoric water within Kazakhstan (ca. 80 ‰; IAEA 2001; Bowen and Revenaugh), FAs in horse milk produced during the summer are expected to display a more enriched  $\delta D$  value than the seasonal average of horse carcass fat. This has been confirmed via compound-specific  $\delta D$  values recorded for the  $C_{16:0}$  and  $C_{18:0}$  FAs of modern reference animals (Figure 14.22). Subsequent analyses of potsherd residues from the Eneolithic site of Botai have revealed a small proportion of animal fat residues exhibiting relatively enriched  $\delta D$  values consistent with the presence of horse milk. The overall higher  $\delta D$  values compared with the present day agree with known climate trends with the region being more arid compared with the present day. Further evidence of

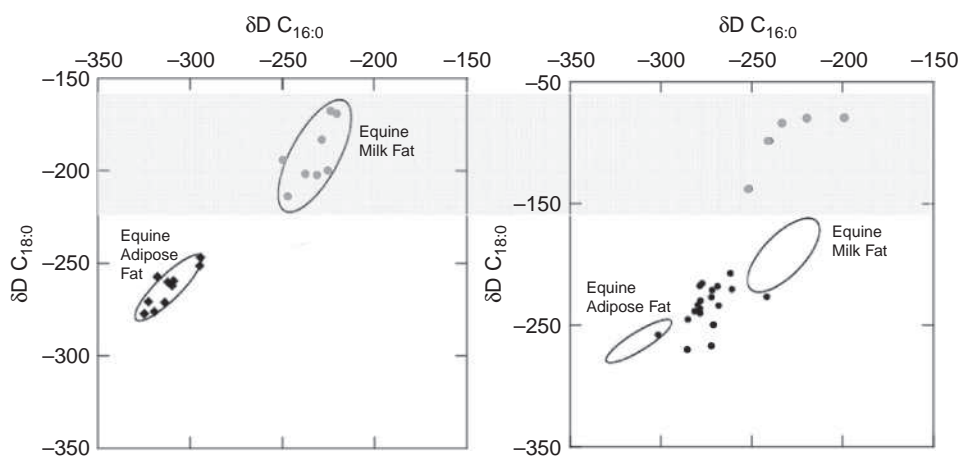


**Figure 14.22** Hydrogen isotope ratios of  $C_{16:0}$  and  $C_{18:0}$  fatty acids in modern horse milk and adipose fat, both from Kazakhstan (a), displaying seasonal influences [ellipses are 68 % ( $1\sigma$ ) confidence intervals], compared (b) with  $\delta D$  values recorded for fatty acids from Eneolithic cooking pot sherds from Botai residues assigned as equine fats based on  $\delta^{13}C$  analysis. Confidence ellipses are  $1\sigma$  and correspond to the modern reference equine fat values (Outram *et al.* 2009)

domestic horses at Botai has been provided by the first identified biting damage on a horse tooth and four mandibular diastema from Botai and metrical evidence that indicates that the Botai horses were more slender than wild horses and were morphologically more similar to modern and Bronze Age domestic horses (Outram *et al.* 2009). Overall, the results provide compelling evidence for the exploitation of domestic horses at the site of Botai indicating that at least a proportion of the horses were domesticated for their secondary products and harnessed for transport.

## 14.10 Conclusion

Major impetus was given to the field of compound-specific stable isotope analysis through the development of the GC-C-IRMS technique and the last decade has provided a number of applications which confirm the powerful synergy that can be achieved in linking biomarker structures to their stable isotope compositions. However, widespread adoption of the approach has been surprisingly slow, possibly due to unfamiliarity of workers with the sample preparation and chromatographic approaches that underpin all applications of compound-specific stable isotope analyses. The major fields of application in the future will likely be skeletal remains and pottery, although investigations of sediments, palaeobotanical and amorphous deposits for the purpose of environmental reconstruction and provenancing may prove to be fertile avenues of application.

There is considerable promise in the use of compound-specific isotope approaches to unravel the stable isotope signature of collagen in archaeological humans and domesticated species to shed light on activities that are intractable to the bulk approaches that have been applied so extensively for the past three decades. Recent studies show that otherwise inaccessible information becomes available via compound-specific studies of the amino acids that comprise collagen (Corr *et al.* 2005). Likewise, new possibilities exist for using largely untapped sources of light stable isotope information contained in such compounds as cholesterol and FAs preserved in human and animal tissues, which reflect different aspects of diet and environment (Jim *et al.* 2004; Corr *et al.* 2009). While instrumentation for the stable isotope analysis of other light isotopes, e.g. N, D and O, is commercially available surprisingly few publications have emerged for compound-specific studies; there is every likelihood that the next few years will see a number of applications emerging using such approaches. For example, the hydrogen isotopic content in lipids other than FAs can be studied by GC-TC-IRMS. Cholesterol is one candidate as it has only one non-carbon bound hydrogen atom per molecule. This extremely labile hydrogen can be removed by acetylation of the alcohol using acetic anhydride and pyridine with little or no fractionation (Sauer *et al.* 2001). Bone cholesterol has a high turnover rate (Jim 2000) and as such will record seasonal differences in hydrogen isotopic ratios. This may prove useful, for example, to determine the season of cull of animals.

The bulk hydrogen isotopic composition of amino acids has been shown to depend on animal trophic level (Birchall *et al.* 2005). Furthermore, compound-specific hydrogen isotopic analyses of amino acids may help elucidate the mechanism behind this enrichment, by determining the differences in  $\delta D$  value between essential and non-essential amino acids, and may also provide a further palaeodietary indicator (e.g. Corr *et al.* 2005). However, amino acids are highly functional, with both amino and carboxyl extremely

labile hydrogen. For compound-specific carbon analysis they require derivatisation twice to form trifluoroacetyl-isopropyl esters, and require the addition of at least seven hydrogen atoms per molecule. For amino acids such as glycine, which only has two 'non-exchangeable' hydrogen atoms per molecule, or asparagine, which only has three but contains increased functionality, derivatisation is likely to result in large errors in the measurement of amino acid  $\delta D$  values.

One of the 'Holy Grails' of the stable isotope analysis field is the routine determination of compound-specific nitrogen isotope analyses of amino acids. Technically such determinations are feasible using the GC-C-IRMS method described above but in practice the determinations are very challenging. We have recently recorded some of the first compound-specific  $\delta^{15}N$  values of archaeological humans and animals by GC-C-IRMS and the trends observed in our values agree with earlier observations made by Hare *et al.* (1991) on modern and fossil animals (Styring *et al.* in press). Such determinations open up a wide range of possibilities of unravelling the nitrogen isotope signal of bone collagen in order to provide new insights into the factors underpinning the trophic level effect and potentially lead to new dietary proxies.

## References

- Abelson, P. H. and Hoering, T. C. (1961) Carbon isotope fractionation in the formation of amino acids by photosynthetic organisms. *Proceedings of the National Academy of Sciences USA* **47**(5), 623–632.
- Ambrose, S. H. (1993) Isotopic analysis of palaeodiets: methodological and interpretive considerations. In *Investigations of Ancient Human Tissue* (Ed. Sandford, M. K.), Gordon & Breach, Langhorne, PA, pp. 59–130.
- Barrie, A., Bricout, J. and Koziat, J. (1984) Gas-chromatography – stable isotope ratio analysis at natural abundance levels. *Biomedical Mass Spectrometry* **11**, 439–447.
- Begley, I. S. and Scrimgeour, C. M. (1997) High-precision  $\delta^2H$  and  $\delta^{18}O$  measurement for water and volatile organic compounds by continuous-flow pyrolysis isotope ratio mass spectrometry. *Analytical Chemistry* **69**, 1530–1535.
- Berstan, R., Dudd, S. N., Copley, M. S., Morgan, E. D., Quyec, A. and Evershed, R. P. (2004) Characterisation of 'bog butter' using a combination of molecular and isotopic techniques. *Analyst* **129**, 270–275.
- Beynon, S. (1998) *Metabolism and Nutrition*. Mosby International Ltd, London.
- Bilke, S. and Mosandl, A. (2002) Measurements by gas chromatography/pyrolysis/mass spectrometry: fundamental conditions in  $^2H/^1H$  isotope ratio analysis. *Rapid Communications in Mass Spectrometry* **16**, 468–472.
- Binnert, C., Laville, M., Pachiaudi, C., Rigalleau, V. and Beylot, M. (1995) Use of gas-chromatography isotope ratio-mass spectrometry to study triglyceride-metabolism in humans. *Lipids* **30**, 869–873.
- Birchall, J., O'Connell, T. C., Heaton, T. H. E. and Hedges, R. E. M. (2005) Hydrogen isotope ratios in animal body protein reflect trophic level. *Journal of Animal Ecology* **74**, 877–881.
- Bogaard, A., Heaton, T. H. E., Poulton P. and Merbach, I. (2007) The impact of manuring on nitrogen isotope ratios in cereals: archaeological implications for reconstruction of diet and crop management practices. *Journal of Archaeological Science* **34**, 335–343.
- Bowen, G. J. and Revenaugh, J. (2003) Interpolating the isotopic composition of modern meteoric precipitation. *Water Resources Research* **39**(10), 1299.
- Brand, W. A., Tegtmeier, A. R. and Hilkert, A. (1994) Compound-specific isotope analysis: extending toward  $^{15}N/^{14}N$  and  $^{18}O/^{16}O$ . *Organic Geochemistry* **21**, 585–594.

- Brenna J. T. (2001) Natural intramolecular isotope measurements in physiology: elements of the case for an effort toward high-precision position-specific isotope analysis. *Rapid Communications in Mass Spectrometry* **15**(15), 1252–1262.
- Brugnoli E. and Farquhar G. D. (2000) Photosynthetic fractionation of carbon isotopes. In *Photosynthesis: Physiology and Metabolism* (Eds Leegood, T. D., Sharkey, T. D. and von Caemmerer, S.), Kluwer Academic, Dordrecht, pp. 399–434.
- Burgoyne, T. W. and Hayes, J. M. (1998) Quantitative production of H<sub>2</sub> by pyrolysis of gas chromatographic effluents. *Analytical Chemistry* **70**, 5136–5141.
- Byers, F. M. and Schelling, G. T. (1988) Lipids in ruminant nutrition. In *The Ruminant Animal: Digestive Physiology and Nutrition* (Ed. Church, D. C.), Prentice-Hall, Englewood Cliffs, pp. 298–310.
- Charters, S., Evershed, R. P., Goad, L. J., Heron, C. and Blinkhorn, P. W. (1993) Identification of an adhesive used to repair a Roman jar. *Archaeometry* **35**, 91–101.
- Charters, S., Evershed, R. P., Blinkhorn, P. W. and Denham, V. (1995) Evidence for the mixing of fat and wax in archaeological ceramics. *Archaeometry*, **37**, 13–28.
- Chikaraishi, Y., Naraoka, H. and Poulson, S. R. (2004a) Carbon and hydrogen isotopic fractionation during lipid biosynthesis in a higher plant (*Cryptomeria japonica*). *Phytochemistry* **65**, 323.
- Chikaraishi, Y., Naraoka, H. and Poulson, S. R. (2004b) Hydrogen and carbon isotopic fractionations of lipid biosynthesis among terrestrial (C3, C4 and CAM) and aquatic plants. *Phytochemistry* **65**, 1369.
- Christie, W. W. (1981) The effects of diet and other factors on lipid composition of ruminant tissues and milk. In *Progress in Lipid Research. Supplement 1. Lipid Metabolism in Ruminant Animals* (Ed. Christie, W. W.), Pergamon Press, Oxford, pp. 193–226.
- Condamin, J., Formenti, F., Metais, M. O., Michel, M. and Blond, P. (1976) The application of gas chromatography to the tracing of oil in ancient amphorae. *Archaeometry* **18**, 195–201.
- Coplen, T. B. (1996) New guidelines for reporting stable hydrogen, carbon, and oxygen isotope-ratio data. *Geochimica et Cosmochimica Acta* **60**, 3359.
- Copley, M. S., Berstan, R., Dudd, S. N., Docherty, G., Mukherjee, A. J., Straker, V., Payne, S. and Evershed, R. P. (2003) Direct chemical evidence for widespread dairying in prehistoric Britain. *Proceedings of the National Academy of the United States of America* **100**, 1524–1529.
- Copley, M. S., Jim, S., Jones, V., Rose, P., Clapham, A., Edwards, D. N., Horton, M., Rowly-Conwy, P. and Evershed, R. P. (2004) Short- and long-term foraging and foddering strategies of domesticated animals from Qasr Ibrim, Egypt. *Journal of Archaeological Science* **31**, 1273–1286.
- Copley, M. S., Berstan, R., Dudd, S. N., Straker, V., Payne, S. and Evershed, R. P. (2005a) Dairying in antiquity. I. Evidence from absorbed lipid residues dating to the British Iron Age. *Journal of Archaeological Science* **32**, 485–503.
- Copley, M. S., Berstan, R., Dudd, S. N., Straker, V., Payne, S. and Evershed, R. P. (2005b) Dairying in antiquity. II. Evidence from absorbed lipid residues dating to the British Bronze Age. *Journal of Archaeological Science* **32**, 505–521.
- Copley, M. S., Berstan, R., Mukherjee, A. J., Dudd, S. N., Straker, V., Payne, S. and Evershed, R. P. (2005c) Dairying in antiquity. III. Evidence from absorbed lipid residues dating to the British Neolithic. *Journal of Archaeological Science* **32**, 523–546.
- Corr, L. T. (2003) *The evaluation of a multi-proxy stable isotope approach to palaeodietary reconstruction*. PhD thesis, University of Bristol.
- Corr, L. T., Sealy, J. L., Horton, M. C. and Evershed, R. P. (2005) A novel marine dietary indicator utilising compound-specific collagen amino acid  $\delta^{13}\text{C}$  values of ancient humans. *Journal of Archaeological Science* **32**, 321–330.
- Corr, L. T., Berstan, R. and Evershed, R. P. (2007a) Development of *N*-acetyl methyl ester derivatives for the determination of  $\delta^{13}\text{C}$  values of amino acids using gas chromatography-combustion-isotope ratio mass spectrometry. *Analytical Chemistry* **79**, 9082–9090.
- Corr, L. T., Berstan, R. and Evershed, R. P. (2007b) Optimisation of derivatisation procedures for the determination of  $\delta^{13}\text{C}$  values of amino acids using gas chromatography-combustion/isotope ratio mass spectrometry. *Rapid Communications in Mass Spectrometry* **21**, 3759–3771.
- Corr, L. T., Richards, M. P., Jim, S., Ambrose, S. H., Mackie, A., Beattie, O. and Evershed, R. P. (2008) Probing dietary change of the Kwäday Dän Ts'inchj individual, an ancient glacier body from British Columbia: I. Complementary use of marine lipid biomarker and carbon

- isotope signatures as novel indicators of a marine diet. *Journal of Archaeological Science* **35**, 2102–2110.
- Corr, T. T., Richards, M. P., Grier, C., Mackie, A., Beattie, O. and Evershed, R. P. (2009) Probing dietary change of the Kwäday Dän Ts'ìnchj individual, an ancient glacier body from British Columbia: II. Deconvoluting whole skin and bone collagen  $\delta^{13}\text{C}$  values via carbon isotope analysis of individual amino acids. *Journal of Archaeological Science* **36**, 12–18.
- Craig, O. E., Taylor, G., Collins, M. J. and Parker Pearson, M. (2005) The identification of prehistoric dairying activities in the Western Isles of Scotland: an integrated biomolecular approach. *Journal of Archaeological Science* **32**, 91–103.
- Deines, P. (1980) The isotopic composition of reduced organic carbon. In *Handbook of Environmental Isotope Geochemistry* (Eds Fritz, P. and Fontes, J. C.), Elsevier, p. 329.
- Delwiche C. C. and Steyn P. L. (1970) Nitrogen isotope fractionation in soils and microbial reactions. *Environmental Science and Technology* **4**, 929–935.
- Demmelmair, H. and Schmidt, H.-L. (1993) Precise  $\delta^{13}\text{C}$ -determination in the range of natural abundance on amino acids from protein hydrolysates by gas chromatography - isotope ratio mass spectrometry. *Isotopenpraxis* **29**, 237–250.
- DeNiro, M. J. and Epstein, S. (1977) Mechanism of carbon isotope fractionation associated with lipid synthesis. *Science* **197**, 261–263.
- DeNiro, M. J. and Epstein, S. (1981) Influence of diet on the distribution of nitrogen isotopes in animals. *Geochimica et Cosmochimica Acta* **45**, 341–351.
- Docherty, G., Jones, V. and Evershed, R. P. (2001) Practical and theoretical considerations in the gas chromatography/combustion/isotope ratio mass spectrometry  $\delta^{13}\text{C}$  analysis of small polyfunctional compounds. *Rapid Communications in Mass Spectrometry* **15**, 730–738.
- Dudd, S. N. (1999) Molecular and isotopic characterization of animal fats in archaeological pottery. *PhD Thesis, University of Bristol*.
- Dudd, S. N. and Evershed, R. P. (1998) Direct demonstration of milk as an element of archaeological economies. *Science* **282**, 1478–1481.
- Dungait, J. A. J., Docherty, G. and Evershed, R. P. (2008) Interspecific variation in bulk tissue, fatty acid and monosaccharide  $\delta^{13}\text{C}$  values of leaves from mesotrophic grassland species. *Phytochemistry* **69**, 2041–2051.
- Evans, K. and Heron, C. (1993) Glue, disinfectant and chewing gum: natural products chemistry in archaeology. *Chemistry and Industry* **12**, 446–449.
- Evershed, R. P. (1990) Preliminary report of the analysis of lipids from samples of skin from seven Dutch bog bodies. *Archaeometry* **32**, 139–153.
- Evershed, R. P. (1992) Chemical composition of bog body adipocere. *Archaeometry* **34**, 253–265.
- Evershed, R. P. (1993) Biomolecular archaeology and lipids. *World Archaeology* **25**, 74–93.
- Evershed, R. P. (2008) Organic residue analysis in archaeology: the archaeological biomarker revolution. *Archaeometry* **50**, 895–924.
- Evershed, R. P. and Connolly, R. C. (1987) Lipid preservation in Lindow Man. *Naturwissenschaften* **75**, 143–145.
- Evershed, R. P. and Connolly, R. C. (1994) Post-mortem transformations of sterols in bog body tissues. *Journal of Archaeological Science* **21**, 577–583.
- Evershed, R. P., Heron, C. and Goad, L. J. (1991) Epicuticular wax components preserved in potsherds as chemical indicators of leafy vegetables in ancient diets. *Antiquity* **65**, 540–544.
- Evershed, R. P., Arnot, K. I., Collister, J., Eglinton, G. and Charters, S. (1994) Application of isotope ratio monitoring gas chromatography-mass spectrometry to the analysis of organic residues of archaeological origin. *Analyst* **119**, 909–914.
- Evershed, R. P., Turner-Walker, G., Hedges, R. E. M., Tuross, N. and Leyden, A. (1995) Preliminary results for the analysis of lipids in ancient bone. *Journal of Archaeological Science* **22**, 277–290.
- Evershed, R. P., van Bergen, P. F., Peakman, T. M., Leigh-Firbank, E. C., Horton, M. C., Edwards, D., Biddle, M., Kjolbye-Biddle, B. and Rowley-Conwy, P. A. (1997a) Archaeological frankincense. *Nature* **390**, 667–668.
- Evershed, R. P., Vaughan, S. J., Dudd, S. N. and Soles, J. S. (1997b) Fuel for thought? Beeswax in lamps and conical cups from Late Minoan Crete. *Antiquity* **71**, 979–985.



- Evershed, R. P., Mottram, H. R., Dudd, S. N., Charters, S., Stott, A. W., Gibson, A. M., Conner, A., Blinkhorn, P. W. and Reeves, V. (1997c) New criteria for the identification of animal fats preserved in archaeological pottery. *Naturwissenschaften* **84**, 402–406.
- Evershed, R. P., Dudd, S. N., Charters, S., Mottram, H., Stott, A. W., Raven, A., van Bergen, P. F. and Bland, H. A. (1999) Lipids as carriers of anthropogenic signals from prehistory. *Philosophical Transactions of the Royal Society of London Series B-Biological Sciences* **354**, 19–31.
- Evershed, R. P., Anderson-Stojanovic, V. R., Dudd, S. N. and Gebhard, E. R. (2003a) New chemical evidence for the use of combed ware pottery vessels as beehives in ancient Greece. *Journal of Archaeological Science* **31**, 1–12.
- Evershed, R. P., Dudd, S. N., Copley, M. S. and Mukherjee, A. J. (2003b) Identification of animal fats via compound specific  $\delta^{13}\text{C}$  values of individual fatty acids: assessments of results for reference fats and lipid extracts of archaeological pottery vessels. In *Documenta Praehistorica, XXIX; 9th Neolithic Studies* (Ed. Budja, M.), Ljubljana, pp. 73–96.
- Evershed, R. P., Payne, S., Sherratt, A. G., Copley, M. S., Coolidge, J., Urem-Kotsu, D., Kotsakis, K., Özdoğan, M., Özdoğan, A., Nieuwenhuys, O., Akkermans, P. M. M. G., Bailey, D., Andeescu, R.-R., Campbell, S., Farid, S., Hodder, I., Yalman, N., Özbaraşan, M., Bıçakcı, E., Garfinkel, Y., Levy, T. and Burton, M. M. (2008) Earliest date for milk use in the Near East and southeastern Europe linked to cattle herding. *Nature* **455**, 528–531.
- Fogel, M. L. and Tuross, N. (2003) Extending the limits of palaeodietary studies of humans with compound specific carbon isotope analysis of amino acids. *Journal of Archaeological Science* **30**, 535–545.
- Friedli, H., Lotscher, H., Oeschger, H., Siegenthaler, U. and Stauffer, B. (1986) Ice core record of the  $^{13}\text{C}/^{12}\text{C}$  ratio of atmospheric  $\text{CO}_2$  in the past two centuries. *Nature* **324**, 237–238.
- Gannes, L. Z., del Rio, C. M. and Koch, P. (1998) Natural abundance variations in stable isotopes and their potential uses in animal physiological ecology. *Comparative Biochemistry and Physiology, A: Molecular and Integrative Physiology* **119**, 725–737.
- Garten, C. T. (1993) Variation in foliar  $^{15}\text{N}$  abundance and the availability of soil-nitrogen on Walker Branch Watershed. *Ecology* **74**, 2098–2113.
- Gehre, M., Hoefling, R., Kowski, P. and Strauch, G. (1996) Sample preparation device for quantitative hydrogen isotope analysis using chromium metal. *Analytical Chemistry* **68**, 4414–4417.
- Gröcke, D. R. (2002) The carbon isotope composition of ancient  $\text{CO}_2$  based on higher-plant organic matter. *Philosophical Transactions of the Royal Society of London Series A-Mathematical Physical and Engineering Sciences* **360**, 633–658.
- Grunberg, J. M. (2002) Middle palaeolithic birch-bark pitch. *Antiquity* **76**, 15–16.
- Gülaçar, F. O., Buchs, A. and Susini, A. (1989) Capillary gas-chromatography mass-spectrometry and identification of substituted carboxylic acids extracted from a 400-year-old Nubian burial. *Journal of Chromatography* **479**, 61–72.
- Gülaçar, F. O., Susini, A. and Koln, M. (1990) Preservation and post-mortem transformations of lipids in samples from a 4000-year-old Nubian mummy. *Journal of Archaeological Science* **17**, 691–699.
- Hammer, B. T., Fogel, M. L. and Hoering, T. C. (1998) Stable carbon isotope ratios of fatty acids in seagrass and redhead ducks. *Chemical Geology* **152**, 29–41.
- Handley, L. L. and Raven, J. A. (1992) The use of natural abundance of nitrogen isotopes in plant physiology and ecology. *Plant Cell and Environment* **15**, 965–985.
- Hare, P. E. and Estep, M. L. F. (1983) Carbon and nitrogen isotopic composition of amino acids in modern and fossil collagens. *Carnegie Institution Washington Yearbook* **82**, 410–414.
- Hare, P. E., Fogel, M. L., Stafford, T. W., Mitchell, A. D. and Hoering, T. C. (1991) The isotopic composition of carbon and nitrogen in individual amino acids isolated from modern and fossil proteins. *Journal of Archaeological Science* **18**, 277–292.
- Hastdorf, C. A. and DeNiro, M. J. (1985) Reconstruction of prehistoric plant production and cooking practice by a new isotopic method. *Nature* **315**, 489–551.
- Hayek, E. W. H., Krenmayr, P., Lohninger, H., Jordis, U., Moche, W. and Sauter, F. (1990) Identification of archaeological and recent wood tar pitches using gas chromatography/mass spectrometry and pattern recognition. *Analytical Chemistry* **62**, 2038–2043.
- Hayes, J. M. (1993) Factors controlling  $^{13}\text{C}$  contents of sedimentary organic compounds - principles and evidence. *Marine Geology* **113**, 111–125.

- Hayes, J. M., Freeman, K. H., Popp, B. N. and Hoham, C. (1990) Compound-specific isotopic analyses: a novel tool for the reconstruction of ancient biogeochemical processes. In *Advances in Organic Geochemistry 1989* (Eds Durand, B. and Behar, F.), Pergamon Press, Oxford, pp. 1115–1128.
- Heaton, T. H. E. (1987) The  $^{15}\text{N}/^{14}\text{N}$  ratio of plants in South Africa and Namibia: relationship to climate and coastal/saline environments. *Oecologia* **74**, 236–246.
- Heaton, T. H. E., Vogel, J. C., von la Chevallerie, G. and Collett, G. (1986) Climatic influence on the isotopic composition of bone collagen. *Nature* **322**, 822–823.
- Hener, U., Brand, W. A., Hilkert, A. W., Juchelka, D., Mosandl, A. and Podebrad, F. (1998) Simultaneous online analysis of  $^{18}\text{O}/^{16}\text{O}$  and  $^{13}\text{C}/^{12}\text{C}$  ratios of organic compounds using GC-pyrolysis-IRMS. *Zeitschrift für Lebensmittel-Untersuchung und –Forschung* **206**, 230–232.
- Heron, C., Nemcek, N. and Bonfield, K. M. (1994) The chemistry of Neolithic beeswax. *Naturwissenschaften* **81**, 266–269.
- Hilkert, A. W., Douthitt, C. B., Schlüter, H. J. and Brand, W. A. (1999) Isotope ratio monitoring gas chromatography/mass spectrometry of D/H by high temperature conversion isotope ratio mass spectrometry. *Rapid Communications in Mass Spectrometry* **13**, 1226–1230.
- Hobson, K. A. (1999) Tracing origins and migration of wildlife using stable isotopes: a review. *Oecologia* **120**, 314–326.
- Hobson, K. A., Atwell, L. and Wassenaar, L. I. (1999) Influence of drinking water and diet on the stable-hydrogen isotope ratios of animal tissues. *Proceedings of the National Academy of Sciences of the United States of America* **96**, 8003–8006.
- Hoefs, J. (1996) *Stable Isotope Geochemistry*. Springer, Berlin.
- Howland, M. R. (2003) *Compound-specific stable isotope investigations of the influence of diet on the stable isotope composition of body tissues*. PhD thesis, University of Bristol.
- Howland, M. R., Corr, L. T., Young, S. M. M., Jones, V., Jim, S., Van der Merwe, N. J., Mitchell, A. D. and Evershed, R. P. (2003) Expression of the dietary isotope signal in the compound-specific  $\delta^{13}\text{C}$  values of pig bone lipids and amino acids. *International Journal of Osteoarchaeology* **13**, 54–65.
- IAEA, GNIP (2001) Maps and animations. Accessible at <http://isohis.iaea.org>, International Atomic Energy Agency, Vienna
- Jim, S. (2000) *The development of bone cholesterol  $\delta^{13}\text{C}$  values as a new source of palaeodietary information: models of its use in conjunction with bone collagen and apatite  $\delta^{13}\text{C}$  values*. PhD thesis, University of Bristol.
- Jim, S., Stott, A. W., Evershed, R. P., Rogers, J. M. and Ambrose, S. H. (2001) Animal feeding experiments in the development of cholesterol as a palaeodietary indicator. In *Archaeological Sciences '97* (Ed. Millard, A.), BAR International Series, Oxford, pp. 68–77.
- Jim, S., Jones, V., Copley, M. S., Ambrose, S. H. and Evershed, R. P. (2003a) Effects of hydrolysis on the delta C-13 values of individual amino acids derived from polypeptides and proteins. *Rapid Communications in Mass Spectrometry* **17**, 2283–2289.
- Jim, S., Ambrose, S. H. and Evershed, R. P. (2003b) Natural abundance stable carbon isotope evidence for the routing and de novo synthesis of bone FA and cholesterol. *Lipids* **38**, 179–186.
- Jim, S., Ambrose, S. H. and Evershed, R. P. (2004) Stable carbon isotopic evidence for differences in the dietary origin of bone cholesterol, collagen and apatite: implications for their use in palaeodietary reconstruction. *Geochimica et Cosmochimica Acta* **68**, 61–72.
- Jim, S., Jones, V., Ambrose, S. H. and Evershed, R. P. (2006) Quantifying dietary macronutrient sources of carbon for bone collagen using natural abundance stable carbon isotope analysis. *British Journal of Nutrition* **95**, 1055–1062.
- Jones, V. (2002) *Investigating the routing and synthesis of amino acids between diet and bone collagen via feeding experiments and applications to palaeodietary reconstruction*. PhD thesis, University of Bristol.
- Koch, P. L. (2007) Isotopic study of the biology of modern and fossil invertebrates. In *Stable Isotopes in Ecology and Environmental Science*, 2nd Edn (Eds Lajtha, K. and Michener, R. H.), Blackwell Scientific, pp. 99–154.
- Krummen, M., Hilkert, A. W., Juchelka, D., Duhr, A., Schluter, H. J. and Pesch, R. (2004) A new concept for isotope ratio monitoring liquid chromatography/mass spectrometry. *Rapid Communications in Mass Spectrometry* **18**, 2260–2266.



- Kuksis, A., Child, P., Myher, J. J., Marai, L., Yousef, I. M. and Lewin, P. K. (1978) Bile acids of a 3200-year-old Egyptian mummy. *Canadian Journal of Biochemistry* **56**, 1141–1148.
- Larcher, A. V., Alexander, R., Rowland, S. J. and Kagi, R. I. (1986) Acid catalysis of alkyl hydrogen exchange and configurational isomerisation reactions: acyclic isoprenoid acids. *Organic Geochemistry* **10**, 1015.
- Leckrone, K. J. and Hayes, J. M. (1997) Efficiency and temperature dependence of water removal by membrane dryers. *Analytical Chemistry* **69**, 911–918.
- Leckrone, K. J. and Hayes, J. M. (1998) Water-induced errors in continuous-flow carbon isotope ratio mass spectrometry. *Analytical Chemistry* **70**, 2737–2744.
- Lee-Thorp, J. A. (2008) On isotopes and old bones. *Archaeometry* **50**, 925–950.
- Levine, M. A. (1999) Origins of horse husbandry. In *Late Prehistoric Exploitation of the Eurasian Steppe* (Eds Levine, M. A., Rassamakin, Y., Kislenko A. and Tatarintseva, N.), McDonald Institute for Archaeological Research, Cambridge, pp. 5–58.
- Macko, S. A., Estep., M. L. F., Hare, P. E. and Hoering, T. C. (1983) Stable nitrogen and carbon isotopic composition of individual amino acids isolated from cultured microorganisms. *Carnegie Institution Washington Yearbook* **82**, 404–410.
- Macko, S. A., Uhle, M. E., Engel, M. H. and Andrusevich, V. (1997) Stable nitrogen isotope analysis of amino acid enantiomers by gas chromatography combustion/isotope ratio mass spectrometry. *Analytical Chemistry* **69**, 926–929.
- Macko, S. A., Ryan, M. and Engel, M. H. (1998) Stable isotopic analysis of individual carbohydrates by gas chromatographic combustion/isotope ratio mass spectrometry. *Chemical Geology* **152**, 205–210.
- Matthews, D. E. and Hayes, J. M. (1978) Isotope-ratio-monitoring gas chromatography-mass spectrometry. *Analytical Chemistry* **50**, 1465–1473.
- Mayer, B. X., Reiter, C. and Bereuter, T. L. (1997) Investigation of the triacylglycerol composition of iceman's mummified tissue by high-temperature gas chromatography. *Journal of Chromatography, B* **692**, 1–6.
- McCullagh, J. S. O., Juchelka, D. and Hedges, R. E. M. (2006) Analysis of amino acid  $^{13}\text{C}$  abundance from human and faunal bone collagen using liquid chromatography/isotope ratio mass spectrometry. *Rapid Communications in Mass Spectrometry* **20**, 2761–2768.
- McDonald, P., Edwards, R. D. and Greenhalgh, J. F. D. (1988) *Animal Nutrition*. Pergamon Press, Colchester.
- McKee, K. L., Feller, I. C., Popp, M. and Wanek, W. (2002) Mangrove isotopic ( $\delta^{15}\text{N}$  and  $\delta^{13}\text{C}$ ) fractionation across a nitrogen vs. phosphorus limitation gradient. *Ecology* **83**, 1065–1075.
- Meier-Augenstein, W. (1999) Applied gas chromatography coupled to isotope ratio mass spectrometry. *Journal of Chromatography, A* **842**, 351–371.
- Meier-Augenstein, W., Watt, P. W. and Langhans, C.-D. (1996) Influence of gas chromatographic parameters on the measurement of  $^{13}\text{C}/^{12}\text{C}$  isotope ratios by gas-liquid chromatography-combustion isotope ratio mass spectrometry. I. *Journal of Chromatography, A* **752**, 233–241.
- Melander, L. and Saunders, W. H. (1980) *Reaction Rates of Isotopic Molecules*. John Wiley & Sons, Ltd, New York.
- Merritt, D. A. and Hayes, J. M. (1994) Nitrogen isotopic analysis by isotope-ratio-monitoring gas-chromatography mass-spectrometry. *Journal of the American Society of Mass Spectrometry* **5**, 387–397.
- Merritt, D. A., Brand, W. A. and Hayes, J. M. (1994) Isotope-ratio-monitoring gas chromatography-mass spectrometry: methods for isotopic calibration. *Organic Geochemistry* **21**, 573–583.
- Merritt, D. A., Freeman, K. H., Ricci, M. P., Studley, S. A. and Hayes, J. M. (1995) Performance and optimisation of a combustion interface for isotope ratio monitoring gas chromatography/mass spectrometry. *Analytical Chemistry* **67**, 2461–2473.
- Metges, C. C. and Daenzer, M. (2000)  $^{13}\text{C}$  gas chromatography-combustion isotope ratio mass spectrometry analysis of *N*-pivaloyl amino acid esters of tissue and plasma samples. *Analytical Biochemistry* **278**, 156–164.
- Metges, C. C. and Petzke, K. J. (1997) Measurement of  $^{15}\text{N}/^{14}\text{N}$  isotopic composition in individual plasma free amino acids of human adults at natural abundance by gas chromatography combustion isotope ratio mass spectrometry. *Analytical Biochemistry* **247**, 158–164.
- Metges, C. C., Petzke, K. J. and Hennig, U. (1996) Gas chromatography combustion isotope ratio mass spectrometric comparison of *N*-acetyl- and *N*-pivaloyl amino acid esters to measure  $^{15}\text{N}$

- isotopic abundances in physiological samples: a pilot study on amino acid synthesis in the upper gastro-intestinal tract of minipigs. *Journal of Mass Spectrometry* **31**, 367–376.
- Metges, C. C., Kempe, K. and Wolfram, G. (1994) Enrichment of selected serum fatty-acids after a small oral dosage of (1-C-13)triolein and (8-C-13)triolein in human volunteers analyzed by gas-chromatography combustion isotope ratio mass-spectrometry. *Biological Mass Spectrometry* **23**, 295–301.
- Moore, J. H. and Christie, W. W. (1981) Lipid metabolism in the mammary gland of ruminant animals In *Progress in Lipid Research Supplement no. 1* (Ed. Christie, W. W.), Pergamon Press, London, pp. 227–276.
- Morton, J. D. and Schwarcz, H. P. (1988) Stable isotope analysis of food residues from Ontario ceramics In *26th International Archaeometry Symposium, Toronto* (Ed. Farquhar, R.), University of Toronto, Toronto, pp. 89–93.
- Mottram, H. R., Dudd, S. N., Lawrence, G. J., Stott, A. W. and Evershed, R. P. (1999) New chromatographic, mass spectrometric and stable isotope approaches to the classification of degraded animal fats preserved in archaeological pottery. *Journal of Chromatography, A* **833**, 209–221.
- Mukherjee, A. J. (2004) The importance of pigs in the later British Neolithic: integrating stable isotope evidence from lipid residues in archaeological potsherds, animal bones, and modern animal tissues. PhD Thesis, University of Bristol.
- Mukherjee, A. J., Copley, M. S., Berstan, R. and Evershed, R. P. (2005) Interpretation of  $\delta^{13}\text{C}$  values of fatty acids in relation to animal husbandry, food processing and consumption in prehistory. In *The Zooarchaeology of Fats, Oils, Milk and Dairying* (Eds Mulville, J. and Outram, A. K.), Oxbow Books, Oxford, pp. 77–92.
- Mukherjee, A. J., Berstan, R., Copley, M. S., Gibson, A. M. and Evershed, R. P. (2007) Compound-specific stable carbon isotope detection of pork consumption applied to the British Late Neolithic. *Antiquity* **81**, 743–754.
- Mukherjee, A. J., Gibson, A. M. and Evershed, R. P. (2008) Trends in pig product processing at British Neolithic Grooved Ware sites traced through organic residues in potsherds. *Journal of Archaeological Science* **35**, 2059–2073.
- O'Brien, D. M., Fogel, M. L. and Boggs, C. L. (2002) Renewable and nonrenewable resources: amino acid turnover and allocation to reproduction in *Lepidoptera*. *Proceedings of the National Academy of Sciences of the United States of America* **99**, 4413–4418.
- O'Connell, T. C. (1996) The isotopic relationship between diet and body proteins: implications for the study of diet in archaeology. DPhil Thesis, Oxford University.
- O'Leary, M.H. (1981) Carbon isotope fractionation in plants. *Phytochemistry* **20**, 552–567.
- Outram, A. K., Stear, N. A., Bendrey, R., Olsen, S., Kasparov, A., Zaibert, V., Thorpe, N. and Evershed, R. P. (2009) The earliest horse harnessing and milking. *Science* **323**, 1333–1335.
- Pagani, M. (2002) The alkenone- $\text{CO}_2$  proxy and ancient atmospheric carbon dioxide. *Philosophical Transactions of the Royal Society of London, Series A* **360**, 609–632.
- Patrick, M., Koning, A. J. and Smith, A. B. (1985) Gas-liquid chromatographic analysis of fatty acids in food residues from ceramics found in the Southwestern Cape. *Archaeometry* **27**, 231–236.
- Passi, S., Rothschildboros, M.C., Fasella, P., Nazzaroporro, M. and Whitehouse, D. (1981) An application of high-performance liquid-chromatography to analysis of lipids in archaeological samples. *Journal of Lipid Research* **22**, 778–784.
- Ramsay, M. A. and Hobson, K. A. (1991) Polar bears make little use of terrestrial food webs - evidence from stable-carbon isotope analysis. *Oecologia* **86**, 598–600.
- Reber, E. A. and Evershed, R. P. (2004a) How did Mississippians prepare maize? The application of compound specific carbon isotopic analysis to absorbed pottery residues from several Mississippi Valley sites. *Archaeometry* **46**, 19–33.
- Reber, E. A. and Evershed, R. P. (2004b) Identification of maize in absorbed organic residues: a cautionary tale. *Journal of Archaeological Sciences* **31**, 399–410.
- Reber, E. A., Dudd, S. N., van der Merwe, N. J. and Evershed, R. P. (2004) Direct detection of maize processing in archaeological pottery through compound-specific stable isotope analysis of *n*-dotriacontanol in absorbed organic residues. *Antiquity* **78**, 682–691.
- Regert, M., Vacher, S., Moulherat, C. and Decavallas, O. (2003) Adhesive production and pottery function during iron age at the site of Grand Aunay (Sarthe, France). *Archaeometry* **45**, 101–120.

- Regert, M., Langlois, J. and Colinart, S. (2005) Characterisation of wax works of art by gas chromatographic procedures. *Journal of Chromatography, A* **1091**, 124–136.
- Ricci, M. P., Merritt, D. A., Freeman, K. H. and Hayes, J. M. (1994) Acquisition and processing of data for isotope-ratio-monitoring mass spectrometry. *Organic Geochemistry* **21**, 561–571.
- Richards, M. P., Greer, S., Corr, L. T., Beattie, O., Mackie, A., Evershed, R. P., von Finster, A. and Southon, J. (2007) Radiocarbon dating and dietary stable isotope analysis of Kwaday Dän Ts'inchí. *American Antiquity* **72**, 719–733.
- Rieley, G. (1994) Derivatization of organic-compounds prior to gas-chromatographic combustion-isotope ratio mass-spectrometric analysis – identification of isotope fractionation processes. *Analyst* **119**, 915–919.
- Rottländer, R. C. A. (1990) Die resultate der modernen Fettanalytik und ihre Anwendung auf die prähistorisches Forschung. *Archaeo-Physika* **12**, 1–354.
- Rottländer, R. C. A. and Schlichtherle, H. (1983) Chemical-analysis of fat residues in prehistoric vessels. *Naturwissenschaften* **70**, 33–38.
- Sauer, P. E., Eglinton, T. I., Hayes, J. M., Schimmelmann, A. and Sessions, A. L. (2001) Compound-specific D/H ratios of lipid biomarkers from sediments as a proxy for environmental and climatic conditions. *Geochimica et Cosmochimica Acta* **65**, 213–222.
- Schimmelmann, A. (2007) H, C, N, O stable isotope reference materials from Indiana University. <http://php.indiana.edu/~aschimme/hc.html>.
- Schoeller D. A. (1999) Isotope fractionation: why aren't we what we eat? *Journal of Archaeological Science* **26**, 667–673.
- Schwarcz, H. P., Dupras, T. L. and Fairgrieve, S. I. (1999)  $^{15}\text{N}$  enrichment in the Sahara: in search of a global relationship. *Journal of Archaeological Science* **26**, 629–636.
- Scrimgeour, C. M., Begley, I. S. and Thomason, M. L. (1999) Measurement of deuterium incorporation into fatty acids by gas chromatography/isotope ratio mass spectrometry. *Rapid Communications in Mass Spectrometry* **13**, 271.
- Sealy, J. (1997) Stable carbon and nitrogen isotope ratios and coastal diets in the Later Stone Age of South Africa: a comparison and critical analysis of two data sets. *Ancient Biomolecules* **1**, 131–147.
- Sessions, A. L., Burgoyne, W. W. and Hayes, J. M. (2001a) Correction of  $\text{H}_3^+$  contributions in hydrogen isotope ratio monitoring mass spectrometry. *Analytical Chemistry* **73**, 192–199.
- Sessions, A. L., Burgoyne, W. W. and Hayes, J. M. (2001b) Determination of the  $\text{H}_3$  factor in hydrogen isotope ratio monitoring mass spectrometry. *Analytical Chemistry* **73**, 200–207.
- Sessions, A. L., Jahnke, L. L., Schimmelmann, A. and Hayes, J. M. (2002) Hydrogen isotope fractionation in lipids of the methane-oxidizing bacterium *Methylococcus capsulatus*. *Geochimica et Cosmochimica Acta* **66**, 3955.
- Sharp, Z. D., Atudoreia, V., Panarellob, H. O., Fernándezb, J. and Douthitt, C. (2003) Hydrogen isotope systematics of hair: archeological and forensic applications. *Journal of Archaeological Science* **30**, 1709.
- Shearer G. and Kohl D. H. (1986)  $\text{N}_2$  fixation in field settings - estimations based on natural  $^{15}\text{N}$  abundance. *Australian Journal of Plant Physiology* **13**, 699–756.
- Sherriff, B. L., Tisdale, M. A., Sayer, B. G., Schwarcz, H. P. and Knyf, M. (1995) Nuclear magnetic resonance spectroscopic and isotopic analysis of carbonized residues from subarctic Canadian prehistoric pottery. *Archaeometry* **37**, 95–111.
- Silfer, J. A., Engel, M. H., Macko, S. A. and Jumeau, E. J. (1991). Stable carbon isotope analysis of amino-acid enantiomers by conventional isotope ratio mass-spectrometry and combined gas chromatography-isotope ratio massspectrometry. *Analytical Chemistry* **63**, 370–374.
- Spangenberg, J. E., Jacomet, J. and Schibler, J. (2006) Chemical analyses of organic residues in archaeological pottery from Arbon Bleiche 3, Switzerland – evidence for dairying in the late Neolithic. *Journal of Archaeological Science* **33**, 1–13.
- Stott, A. W. and Evershed, R. P. (1996)  $\delta^{13}\text{C}$  analysis of cholesterol preserved in archaeological bones and teeth. *Analytical Chemistry* **68**, 4402–4408.
- Stott, A. W., Davies, E., Evershed, R. P. and Tuross, N. (1997a) Monitoring the routing of dietary and biosynthesised lipids through compound-specific stable isotope ( $\delta^{13}\text{C}$ ) measurements at natural abundance. *Naturwissenschaften* **84**, 82–86.

- Stott, A. W., Evershed, R. P. and Tuross, N. (1997b) compound-specific approach to the  $\delta^{13}\text{C}$  analysis of cholesterol in fossil bones. *Organic Geochemistry* **26**, 99–103.
- Stott, A. W., Evershed, R. P., Jim, S., Jones, V., Rogers, J. M., Tuross, N. and Ambrose, S. (1999) Cholesterol as a new source of palaeodietary information: experimental approaches and archaeological applications. *Journal of Archaeological Science* **26**, 705–716.
- Styring, A. K., Sealy, J. C. and Evershed, R. P. (in press) Resolving the bulk  $\delta^{15}\text{N}$  values of ancient human and animal bone collagen via compound-specific nitrogen isotope analysis of constituent amino acids. *Geochimica et Cosmochimica Acta*.
- Tauber, H. (1981)  $^{13}\text{C}$  evidence for dietary habits of prehistoric man in Denmark. *Nature* **292**, 332–333.
- Tobias, H. J. and Brenna, J. T. (1997) On-line pyrolysis as a limitless reduction source for high-precision isotopic analysis of organic-derived hydrogen. *Analytical Chemistry* **69**, 3148–3152.
- Tuross, N., Fogel, M. L. and Hare, P. E. (1988) Variability in the preservation of the isotope composition of collagen from fossil bone. *Geochimica et Cosmochimica Acta* **52**, 929–935.
- Urem-Kotsou, D., Stern, B., Heron, C. and Kotsakis, K. (2002) Birch-bark tar at Neolithic Makriyalos, Greece. *Antiquity* **76**, 962–967.
- van Klinken, G. J. (1991) *Dating and dietary reconstruction by isotopic analysis of amino acids in fossil bone collagen – with special reference to the Caribbean*. PhD thesis, University of Groningen, The Netherlands.
- Vogel, J. C. and van der Merwe, N. J. (1977) Isotopic evidence for early maize cultivation in New York State. *American Antiquity* **42**, 238–242.
- Yang, H. and Huang, Y. (2003) Preservation of lipid hydrogen isotope ratios in Miocene lacustrine sediments and plant fossils at Clarkia, northern Idaho, USA. *Organic Geochemistry* **34**, 413.

# 15

## ToF-SIMS Study of Organic Materials in Cultural Heritage: Identification and Chemical Imaging

*Vincent Mazel and Pascale Richardin*

Secondary ion mass spectrometry (SIMS) is a widespread analytical technique for the study of surfaces in materials science. Mostly used for elemental analyses and depth profiling, it is particularly relevant for many different fields of research including cultural heritage studies. Reviews of its use for the study of ancient glasses or metal artefacts already exist in the literature [Spoto 2000, Darque-Ceretti and Aucouturier 2004, Dowsett and Adriaens 2004, Adriaens and Dowsett 2006, Anderle *et al.* 2006, McPhail 2006], but as only elemental information is obtained, these studies are limited to inorganic materials.

Nevertheless, the introduction of time-of-flight (ToF) analysers for SIMS analyses at the beginning of the 1980s, as well as the recent development of liquid ion sources delivering cluster projectiles now permit the analysis of organic materials with high sensitivity and selectivity. Moreover, thanks to its excellent lateral resolution (in the order of micrometres), and its minimal sample preparation, ToF-SIMS has become the reference technique for chemical imaging by mass spectrometry.

Beside numerous applications for biological samples [Belu *et al.* 2003, Brunelle *et al.* 2005], studies of organic materials from cultural heritage artefacts have been developing since the beginning of the twenty-first century. In this review we show, through some selected examples, the different aspects and possibilities of ToF-SIMS analyses.

First, because ToF-SIMS is not yet a classical technique for cultural heritage studies, we will begin with a brief overview of the physical principle, the instrumentation and sample

preparation. The aim is not to present a complete description of the technique, since this can be found elsewhere [Belu *et al.* 2003, Sodhi 2004], but to give the reader an idea of the specificity and applicability of ToF-SIMS analyses.

## 15.1 Physical Principle, Instrumentation and Sample Preparation

### 15.1.1 Physical Principle

SIMS involves bombarding a material surface with a primary ion beam, with a typical energy in the keV range. Ion impacts on the surface induce a so-called ‘collision cascade’ sputtering process, where the energy of the primary ions is transferred to the surface through nuclear collisions [Brunelle *et al.* 2005].

Part of this energy allows desorption of neutral molecules, positive or negative ions and atoms from the surface when the energy is sufficient to overcome the binding energy [Sodhi 2004]. Close to the impact point, the transferred energy is higher than the bond energy of the molecules, leading to extensive fragmentation of molecules and to desorption of atoms or small fragments. In contrast, far from the collision site, this energy decreases, leading to desorption of larger molecular fragments and even of complete molecular species [Belu *et al.* 2003]. The entities desorbed that are charged (positively or negatively) are called secondary ions (Figure 15.1).

In some publications, ToF-SIMS is also called Static-SIMS (S-SIMS) because ToF-SIMS analyses are performed in static conditions. In this mode, the damage of the surface is very low. Indeed, the primary ion flux is set so that the collisions sites do not overlap with each other. A limit of  $10^{13}$  atoms  $\text{cm}^{-2}$  is generally allowed [Belu *et al.* 2003]. Under these conditions, secondary ions are emitted from the very extreme surface, i.e. from the first few nanometres, and therefore ToF-SIMS is truly a technique for the study of the ultrasurface.

The secondary ion yield depends both on the energy and the nature of the primary ions. It has been demonstrated that the use of clusters instead of monoatomic ions improves the secondary yield. Classical primary ions, like  $\text{Ga}^+$  and  $\text{Cs}^+$ , are increasingly replaced by  $\text{Au}_3^+$ ,  $\text{Bi}_3^+$  or  $\text{C}_{60}^+$  which has permitted great progress in organic ToF-SIMS studies [Kollmer 2004, Touboul *et al.* 2004, Winograd 2005].

### 15.1.2 Instrumentation

#### 15.1.2.1 Apparatus

Figure 15.2 shows the schematic representation of a typical ToF-SIMS device. All the system is placed under high vacuum (typically  $10^{-7}$  torr) to avoid interactions between ions and air molecules. Primary ions are produced by a liquid metal ion gun and then focused on the sample to a spot with a typical size of less than 1  $\mu\text{m}$ . After they impinge the surface, secondary ions are extracted and analysed by the ToF analyser. To synchronize the ToF analyser, the primary ion beam must be in pulsed mode.

One of the specificities of ToF-SIMS is the possibility to switch easily from positive to negative ion mode by reversing the extraction potential. The mass calibration of spectra is internal, using low mass ions ( $\text{H}^+$ ,  $\text{H}_2^+$ ,  $\text{H}_3^+$ ,  $\text{C}^+$ ,  $\text{CH}^+$ ,  $\text{CH}_2^+$  and  $\text{CH}_3^+$  ion peaks in



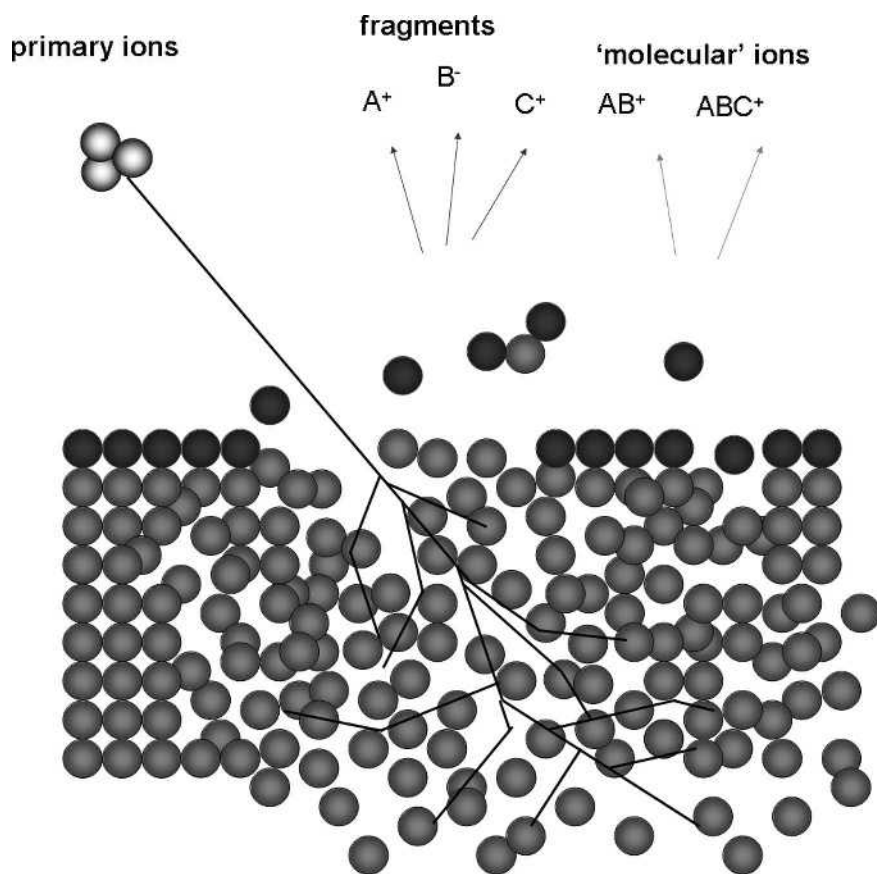


**Figure 15.1** Collision cascade and secondary ion production during ToF-SIMS analysis

positive ion mode and  $\text{H}^-$ ,  $\text{C}^-$ ,  $\text{CH}^-$ ,  $\text{CH}_2^-$ ,  $\text{C}_2^-$ ,  $\text{C}_3^-$ , and  $\text{C}_4^-$  in negative ion mode) that are always present in spectra.

#### 15.1.2.2 Charge Neutralization

Organic materials are insulator materials and they can accumulate charge on their surface during the analysis. This charge build-up can lead to signal suppression. Neutralization of the surface during experiments is achieved using low energy electrons that are flooded to the surface, by a so-called ‘flood gun’ in pulsed mode.

#### 15.1.2.3 Imaging

As the primary ion beam can be focused to less than  $1\ \mu\text{m}$ , ToF-SIMS is well suited to chemical imaging. For this purpose, the beam is rastered by electrostatic fields all over the surface, and a spectrum is recorded for each point. This allows the distribution of a specific ion all over the analysed surface to be mapped, and also to access a mass spectrum

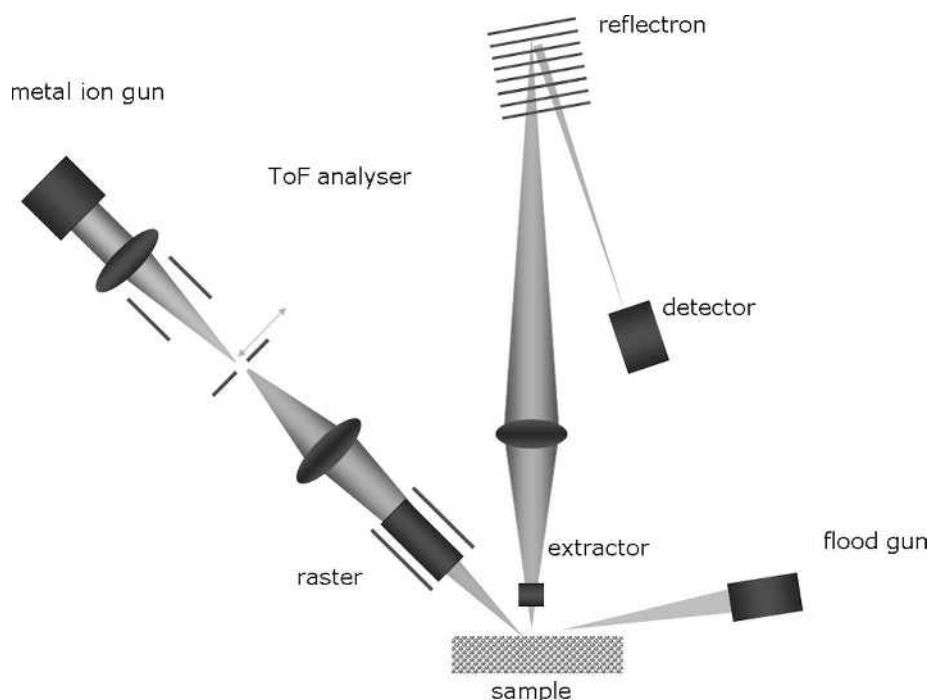


**Figure 15.2** Schematic representation of a ToF-SIMS apparatus

characteristic of an area by summing the spectra of each pixel of this region. Only a few minutes are usually necessary to obtain a  $256 \times 256$  pixels image of an area of generally  $500 \times 500 \mu\text{m}^2$  or less.

### 15.1.3 Sample Preparation

SIMS is one of the only mass spectrometric techniques that allow solid samples to be analysed without any extraction of compounds or matrix addition. Generally, no specific preparation technique is required, and solid samples can directly be analysed if they are small enough to be fixed on the sample holder. In most cases, this means that the sample size must not be more than 1 cm.

In practice, some precautions are necessary. The first arises directly from the physical principle of the technique. As only the first few nanometres of the surface are analysed, ToF-SIMS is greatly affected by surface pollution. A prolonged contact of the sample with the atmosphere can lead to disturbing pollution. Poly(dimethylsiloxane)s are classical pollutants which can be detected in numerous studies [Sodhi 2004]. As a consequence, fresh prepared surfaces are recommended for ToF-SIMS analyses.

The second requirement is related to chemical imaging applications. Very flat samples are required to avoid problems of depth of field. Even if this is common to every imaging technique, it is in this case coupled with surface pollution problems. Sample preparation must then lead to flat surfaces without surface pollution. For cultural heritage samples,



imaging techniques are mostly used for the study of cross-sections. To prepare flat surfaces, two methods are described in the literature. Keune *et al.* [2005] recommended dry-polishing the surface of the sample embedded in resin with fine polishing cloths. Other studies describe the use of microtomy [Saito *et al.* 2008] or ultramicrotomy [Mazel *et al.* 2006] to cut the surface. This allows very flat surfaces to be obtained and avoids contact with possible contaminants from polishing cloths.

#### 15.1.4 Mass Spectra Interpretation

ToF-SIMS mass spectra are generally obtained for  $m/z$  ratio from 1 to 1000 or 2000. However, due to a high fragmentation process, ToF-SIMS mass spectra are generally very complex and the fragmentation/ionization processes are very different compared with other mass spectrometric techniques. The main peaks are generally low mass fragments ( $m/z < 100$ ).

Adduct ions are quite frequent in the mass spectra. In positive ion mode, sodium or potassium cluster ions are commonly found. Mineral compounds often lead to multiple cluster ions. For example, spectra of  $\text{FeCl}_3$  in negative ion mode lead to several peaks from  $m/z$  35 ( $\text{Cl}^-$ ) to  $m/z$  487 ( $[(\text{FeCl}_3)_2\text{FeCl}_3]^-$ ) [Van Ham *et al.* 2004].

Mass spectra interpretation can be very difficult, especially in the case of a complex sample, so the possibility of chemical imaging can help reduce the complexity of the technique. Indeed, instead of using the spectra of the whole sample, specific mass spectra can be recalculated from a precise area giving more specific information. A general method for spectra examination is described in Figure 15.3: from the global spectrum,

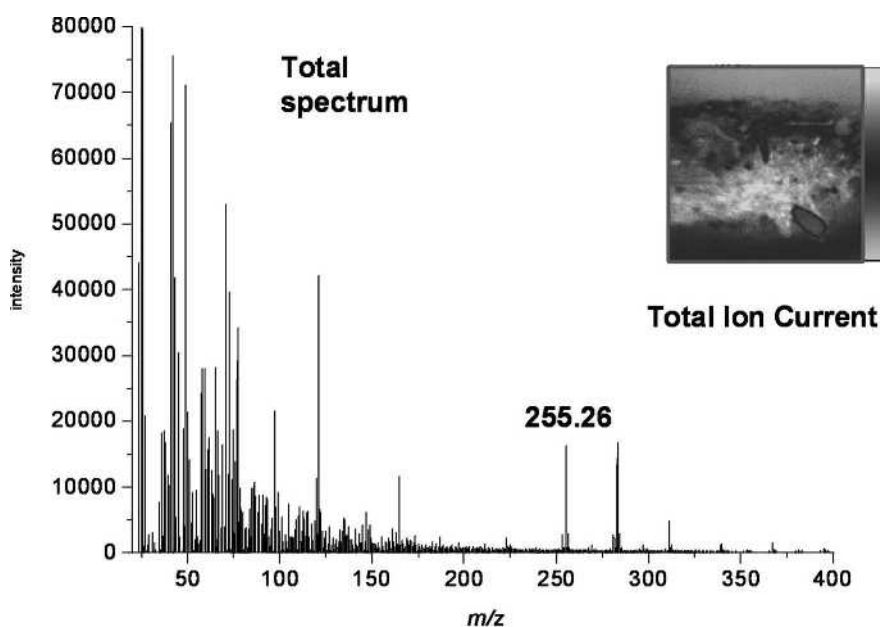


**Figure 15.3** Example of the use of a region of interest (ROI) on ToF-SIMS images to obtain a more specific spectrum. On account of the selected area on the image, signals from fatty acids are emphasized on the selected spectrum (see colour Plate 3)

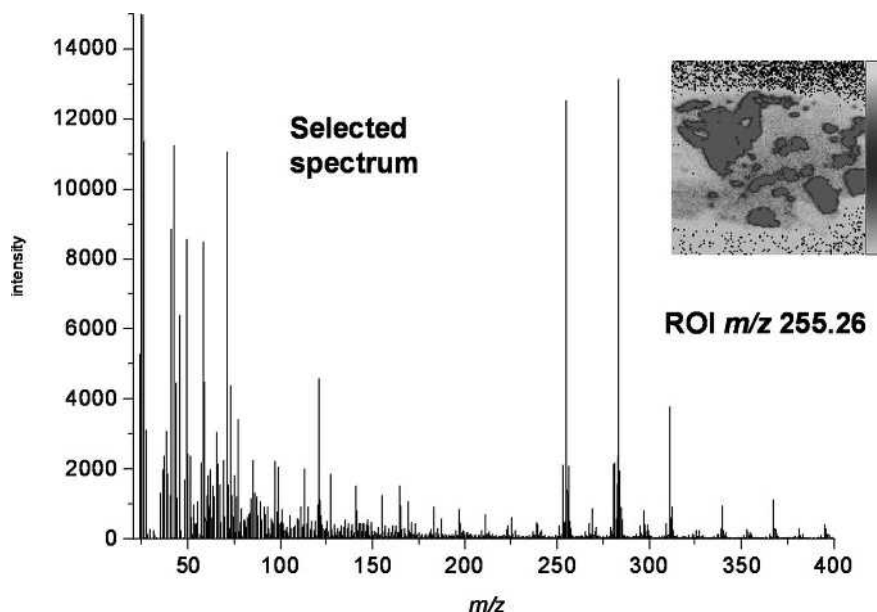


**Figure 15.3** (continued)

peaks that seem interesting are selected and their spatial distribution is drawn. If some of these peaks give a specific spatial distribution with areas of important concentration, spectra from these areas are recalculated. The obtained spectra are then more specific and easier to interpret.

## 15.2 Application in Art and Archaeology

ToF-SIMS is quite a new analytical tool for the study of organic materials from art and archaeological artefacts. Nevertheless, we will see that in the first published studies, its application can cover a great number of subjects and materials.

### 15.2.1 Identification of Organic Materials: Examples of Polymers in Conservation Science

As in any organic mass spectrometric technique, ToF-SIMS first aims to identify organic compounds. As stated earlier,  $m/z$  ratios do not usually exceed 2000 due to the ionization process. Nevertheless, even for large molecules like polymers, interesting information can be obtained.

Synthetic polymers are very important in conservation science because they are commonly used for the conservation and restoration of artworks. Consequently, their chemical characterization must be precise enough to well define their innocuousness for art objects and their long term stability. An example is given in the ToF-SIMS analysis of polymers

used as water repellent in stone protection [Torrìsi *et al.* 2008]. These compounds of the Zonyl™ family all contain fluorinated alkyl chains. They could be used to decrease water adsorption which is a way of delaying the ageing process.

Different categories of Zonyl™ polymers are studied by ToF-SIMS both in the positive and negative ion mode. Studies have shown that, for each polymer, a specific fingerprint is obtained and the peaks corresponding to the specific chemical moieties of each polymer are detected (Figure 15.4). To represent this good selectivity, Principal Component Analysis is performed on the obtained spectra. The result clearly discriminates the different polymers. ToF-SIMS is then suited to the characterization of these materials.

Polymers are also part of cultural heritage artefacts in which they often give rise to conservation problems, due to the poorly known degradation process. ToF-SIMS can therefore be useful for the characterization of these materials and of their degradation. In their study of thermoplastic beads from 1970s jewellery, Abel and Coppiters [2008] first used ToF-SIMS to identify the polymer and its additives. Analyses in both positive and negative mode proved that the material was polystyrene. Peaks observed in positive ion mode at  $m/z$  494, 522 and 550 seem to indicate the presence of dimethyl distearyl ammonium. This compound is often used as an antistatic and antimicrobial agent. These peaks could also be attributed to glycerol trioleate, which is used mainly as a surfactant and plasticizer.

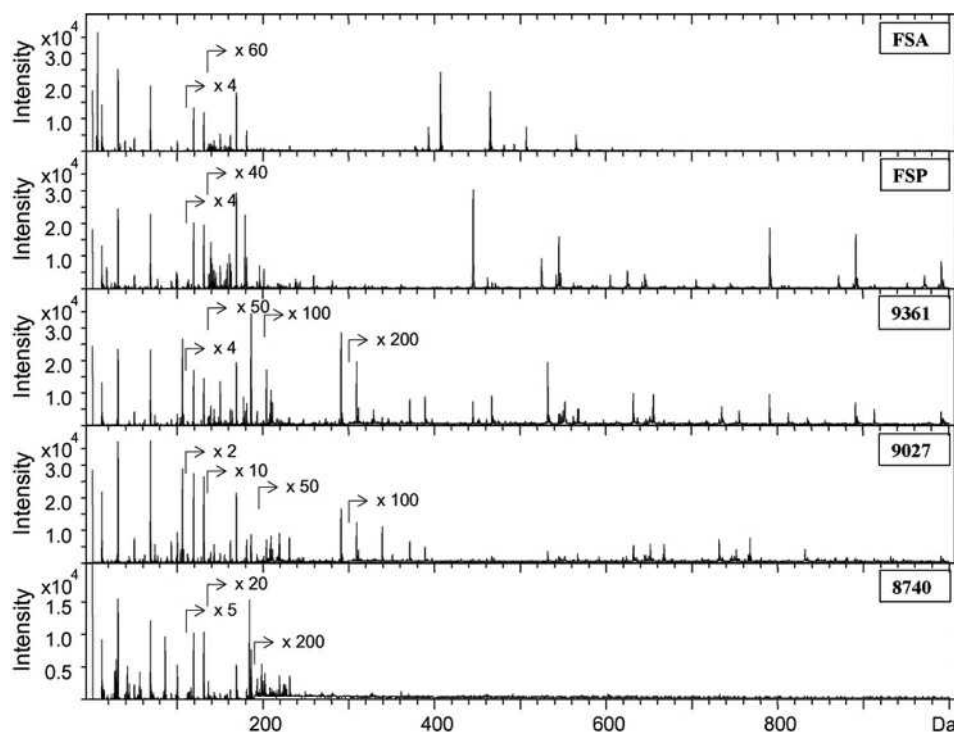


**Figure 15.4** Positive ion ToF-SIMS spectra of five fluorinated compounds. Reproduced from *Applied Surface Science*, Torrìsi *et al.*, Copyright 2008 Elsevier

They tried to understand the role of additives during the degradation process. For this purpose, they studied cross-sections of the beads, and recorded mass spectra at different points of the sample. The higher concentration of additives at the surface, where degradation phenomena occur, suggests that they might be involved in the stress cracking of the beads. Damage of the material could be partially due to the migration of chemicals. This is a good example of the use of ToF-SIMS for compound localization.

### 15.2.2 Surface Interaction and Degradation: Natural Fibre Studies

As ToF-SIMS is a surface analytical technique, it is well suited to the study of surface interaction between a material and its environment or between a material and products applied to it. The surface modifications can then be studied, making it possible to establish links with degradation processes. Published papers on the study of natural fibres related to cultural heritage typically illustrate this aspect of ToF-SIMS analysis.

#### 15.2.2.1 Tapestry Cleaning and Degradation

Different studies have been conducted by the same team of researchers for the analyses of tapestry fibres. The main aim was to study the surface evolution of these fibres, silk or wool, during light ageing or cleaning procedures.

Carr *et al.* [2004] studied the incidence of different cleaning procedures on wool. ToF-SIMS analyses performed on the commercially scoured wool (negative ion mode) showed the presence of 18-methyleicosanoic acid thioester species ( $m/z$  341), attributed to the presence of 18-methyleicosanoic acid (18-MEA) which is normally the predominant compound of the surface layer of wool. Other lipids are also detected. After artificial sunlight exposure, analyses show that 18-MEA disappears from the surface.

Different cleaning procedures are tested with both non-anionic and anionic surfactants. Analyses of samples after these cleaning procedures show the presence of remaining surfactant on the surface (Figure 15.5). Carr *et al.* observe that the amount of remaining surfactant is greater after artificial ageing.

A similar study has been performed on silk [Howell *et al.* 2007]. The ToF-SIMS fingerprint of silk exhibits the presence of different amino acid fragments (positive ion mode). In contrast to wool, the effect of artificial ageing is not obvious and no modification appears in the ToF-SIMS spectra. Nevertheless, the study of the cleaning procedures leads to the same conclusion as that in the case of wool. The amount of remaining surfactant increases with artificial ageing.

In another study on wool, Batcheller *et al.* [2006] explore the effect of the scouring method on greasy wool. Two procedures are used: the first is a modern commercial one; and the second is based on an historic recipe using a stale urine solution.

Spectra of the greasy wool are more complicated than in the previous study. In negative ion mode, different fatty acids, fatty alcohols and alkanes are detected, whereas the positive ion mode shows mainly the presence of cholesterol and the cholesterol oxidation product (Figure 15.6). These ions are attributed to the presence of wool wax on the surface of raw wool.

After the modern cleaning procedure, analyses lead to the same results as those previously presented by Carr *et al.* [2004] with the presence of the 18-MEA signal. This procedure is really effective for the removal of wool wax. In comparison, the urine based

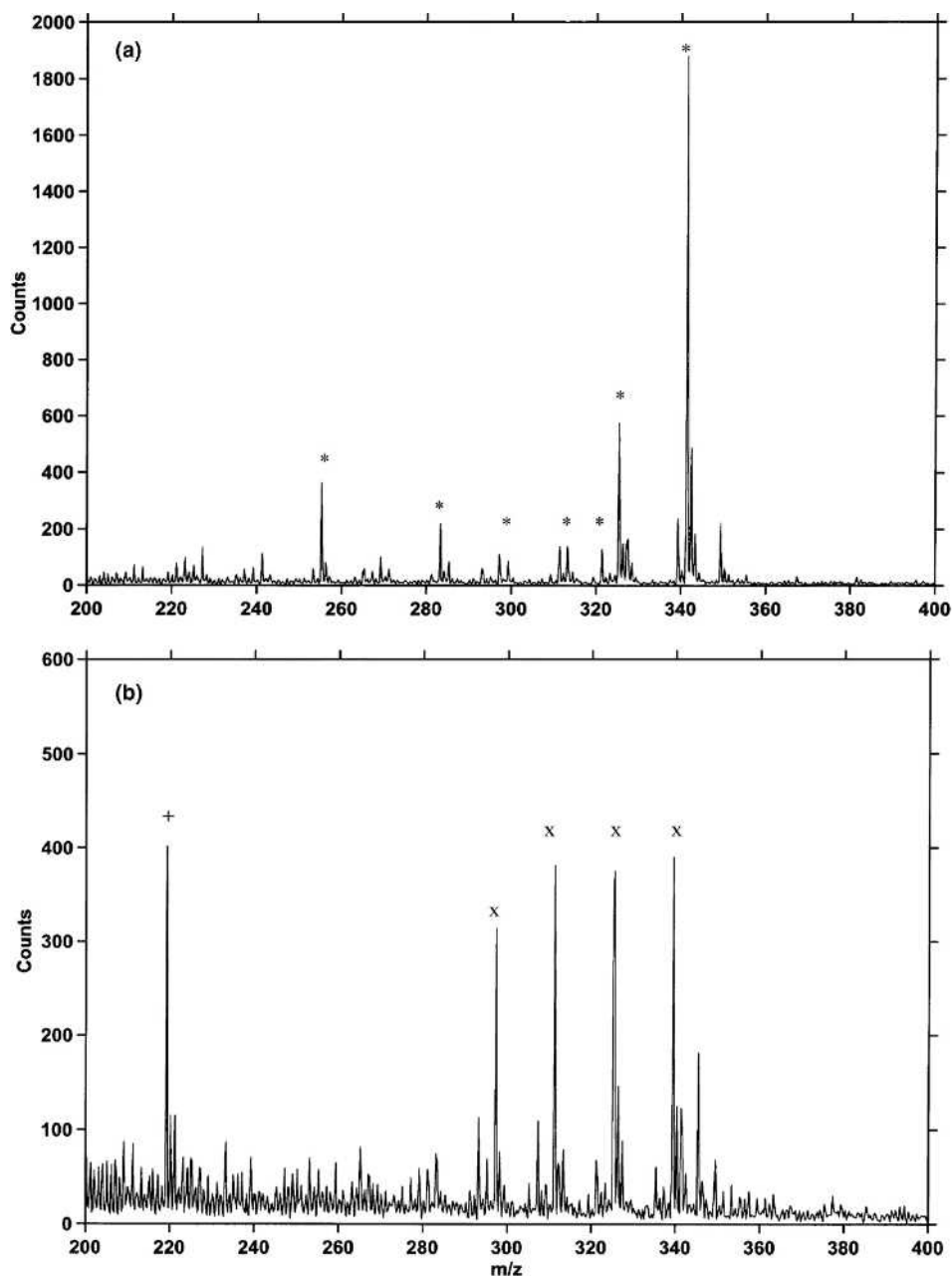


**Figure 15.5** (a) Negative ion ToF-SIMS spectrum of untreated wool (\*, wool surface lipids). (b) Negative ion ToF-SIMS spectrum of photo-oxidized wool washed in an aqueous solution of Syneronic N (+, nonylphenoxide anion; x, linear alkylbenzene sulfonates). With kind permission from Springer Science and Business Media, *Journal of Materials Science*, **39**, Carr, 24, 7317–7325, Copyright 2004

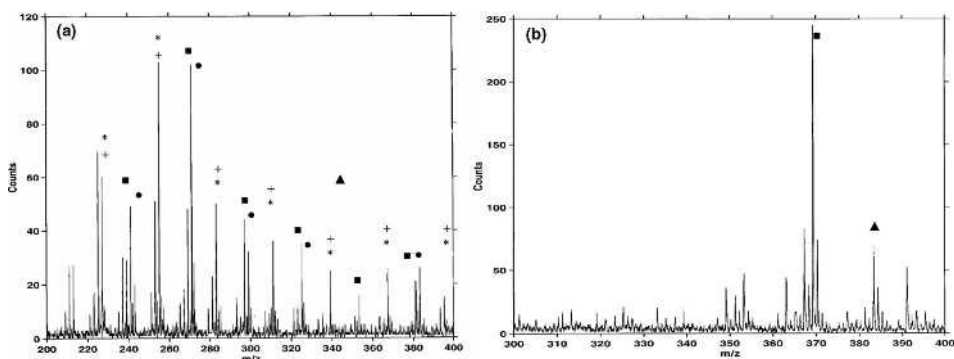


**Figure 15.6** (a) Negative ion ToF-SIMS spectrum of greasy Spanish wool. Homologous series of ions: (\*, +) *n*-alkanoic acids and iso-alkanoic acids, (■) anteisoalkanoic acids, (●) hydroxyalkanoic acids and (▲) 18-methyleicosanoic acid thioester derivative ion. (b) Positive ion ToF-SIMS spectrum of greasy Spanish wool: (■) cholesterol and (▲) cholest-5-en-3-ol-one ions. Reproduced from *Applied Surface Science*, Batcheller *et al.*, Copyright 2006 with permission from Elsevier

cleaning method is less effective, and the wool wax component is still detected on the surface.

Batcheller *et al.* also discuss the influence of the dyeing process on the composition of the fibre's surface. They note that high alkalinity/acidity and extended processing time result in loss of surface lipid. Nevertheless, the dyeing process has limited influence on the ageing process due to light exposure.

#### 15.2.2.2 Identification of Dyes on Textile Fibres

Dye identification is of great interest in textile studies. The classical procedure requires a hydrolysis step and other extraction techniques, followed by identification of the individual compounds present after separation by a chromatographic technique, e.g. high-performance liquid chromatography [Novotna *et al.* 1999, Szostek *et al.* 2003]. However, ToF-SIMS can be an alternative method, avoiding the phase of extraction which is always a time consuming and delicate step because of the possible destruction of the molecular structure of the sample [Ferreira *et al.* 2002]. The development of ToF-SIMS for dye detection has been reported in different studies.

One example is given in the PhD thesis of Sanjova with the characterization of madder derived dyes [Sanjova 2001]. A specific study of alizarin (A), purpurin (P), quinizarin (Q) and their respective lakes (manufactured with aluminium sulfate) is performed. The spectrum of each dye is characterized by ions corresponding to the protonated and deprotonated intact molecules in positive and negative ion mode, respectively. For the lakes, aluminium clusters are also observed in the case of alizarin and quinizarin. For the alizarin complex,  $[(A-H)_2Al]^+$  ( $m/z$  505) is detected in positive ion mode and  $[A_2Al]^-$  ( $m/z$  503) in negative ion mode. These ions derive from the complexation of aluminium ions. Complexation sites are ceto-phenolates in positive ion mode and ceto-phenolates or diphenolates for negative ions. In the case of quinizarin, only ceto-phenolate complexes

are observed. However, in positive ion mode, other clusters are detected, for example  $(\text{HQ-Al-Q-Al-HQ})^+$  at  $m/z$  770, because of the presence of two ceto-phenolate sites on each molecule. In this case, analysis is not limited to dye identification but also includes the interaction phenomena between organic molecules and metallic cations.

This first example shows the possibility of identifying dyes, even if they are prepared as lakes. In another study, Lee *et al.* [2008] demonstrated the possibility of identifying dyes on textile fibres. The different studied dyes were curcumin (tumeric), crocin (gardenia), carthamin (safflower), purpurin (madder), alizarin (madder), brazilin (sapponwood), shikonin (gromwell) and indigo. Analyses in positive ion mode of pure pigments showed that, except for crocin and carthamin,  $[\text{M}+\text{H}]^+$  ions were detected. Moreover, in each case specific fragments were identified.

Lee *et al.* then proved that this detection is also possible in the case of dyed textile. The different dyes were applied on silk and samples were analysed by ToF-SIMS. For textiles dyed with madder, gromwell and indigo,  $[\text{M}+\text{H}]^+$  ions and other specific ions were observed. The background from the textile support does not prevent identification. For safflower and gardenia, informative peaks were also detected. Of course, dyeing processes usually require the use of mordants or fixing agents to bind dye moieties and fibres. Metal ions from mordants (aluminium, tin or copper) can be also detected in the low mass region of spectra.

Finally, two ancient textiles of the sixteenth and seventeenth century were studied. The presence of molecular ion at  $m/z$  263 and fragment ions at  $m/z$  235 and  $m/z$  247 demonstrate that indigo was used (Figure 15.7). No mordant-related peaks were detected. Lee *et al.* explain that indigo has so strong an affinity with the fibres that it could be used without mordant.

### 15.2.2.3 Wood Study for Dendrochronological Approach

The last example of ToF-SIMS analysis of natural fibres is of a structural characterization of wood species for an eventual dendrochronological study [Saito *et al.* 2008]. The aim of this research was to develop a new method to differentiate heartwood and sapwood. In dendrochronology, when bark is not present on the samples, the presence of sapwood is the key to determining felling date. Usually, heartwood and sapwood can easily be differentiated by their colour, with heartwood being much darker. Nevertheless, in the case of

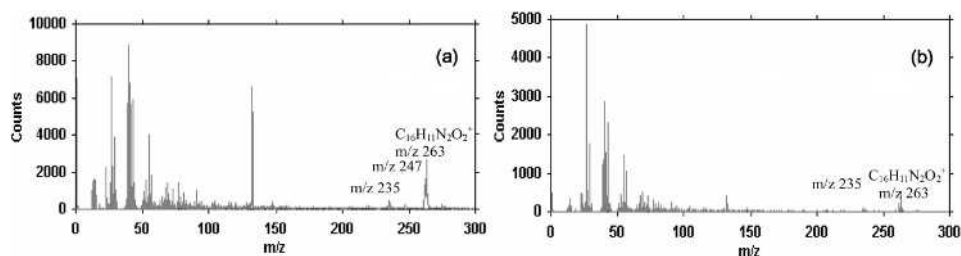


**Figure 15.7** Positive ion ToF-SIMS spectra of the antique textiles known as (a) Kim Wak and (b) Gurye Sonssi. Reproduced from *Applied Surface Science*, Lee *et al.*, Copyright 2007 with permission from Elsevier



very old wood, discolouring might take place, and it becomes impossible to distinguish the two kinds of wood. It is then important to evaluate the distribution of specific markers of sapwood and heartwood. The samples studied were from Hinoki cypress. Two samples came from dated trees recently felled and another one was from the Horyuji Temple which is preserved in the National Museum of Japanese History (Sakura, Japan).

ToF-SIMS spectra were acquired in positive ion mode and four different extractives were identified. The two main peaks were assigned to hinokinin ( $m/z$  353) and hinokiresinol ( $m/z$  252). Lower peaks at  $m/z$  299 and  $m/z$  302 were assigned to hinokione and hinokiol, respectively. These identifications were confirmed by the study of the pure molecules.

The radial distribution of the extractives in the wood from recently felled trees was then studied. It was shown that their concentration is low in the sapwood and increases just before the heartwood/sapwood boundary. Concentrations were then higher in the heartwood. The increase in the concentration of the extractive is then a good means to find the boundary (Figure 15.8a).

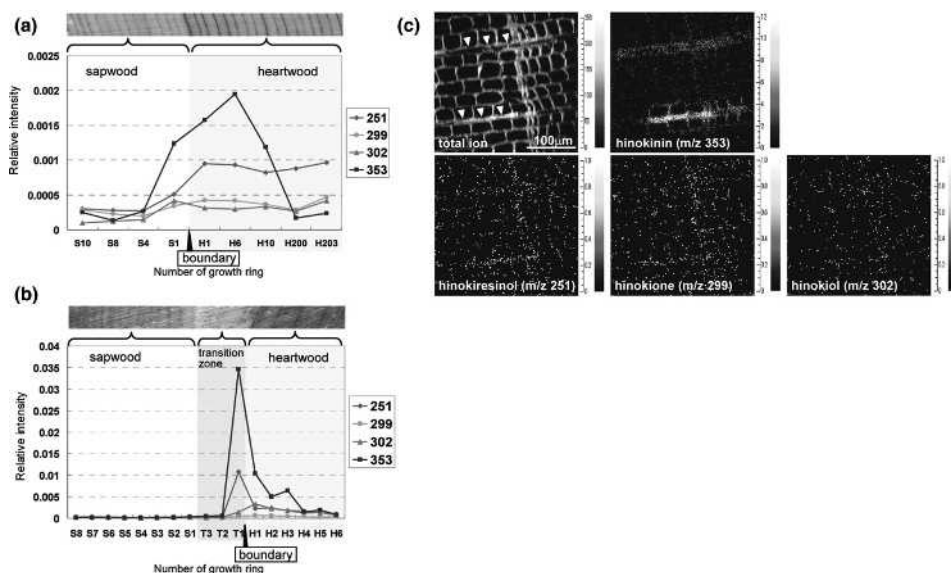


**Figure 15.8** Distribution of relative intensities of extractive ions at  $m/z$  251 for hinokiresinol,  $m/z$  299 for hinokione,  $m/z$  302 for hinokiol and  $m/z$  353 for hinokinin from sapwood to heartwood in Hinoki cypress. The values were obtained from the positive ToF-SIMS spectra of (a) naturally dried 233-year-old and (b) freeze-preserved 31-year-old Hinoki samples. The 'boundary' indicates the boundary between sapwood and heartwood. The growth rings determined were numbered by counting the number of years from the boundary. (c) Positive ion image ( $300 \times 300 \mu\text{m}^2$ ; scale bar,  $100 \mu\text{m}$ ) of the transverse section of the ancient Hinoki wood sample, including the ring boundary between the 44th and 45th rings; the total ion image and selected ion images for hinokinin, hinokiresinol, hinokione and hinokiol are shown. Yellow represents high intensity and black represents low yields. Adapted from *Analytical Chemistry*, **80**, 1552–1557, Saito et al., Copyright 2008 American Chemical Society (see colour Plate 4)



In the study of a discoloured ancient wood from a Buddhist building constructed before or during the eighth century AD, concentrations show the same kind of evolution. Moreover, the levels of extractives in the ancient wood are comparable to those in recently cut wood, meaning that they do not undergo degradation in the ancient wood. The method developed on recently cut wood is then applicable to old discoloured wood.

As ToF-SIMS also allows the mapping of the chemical species inside the sample, distributions of the different extractives in the cross-section of the wood are evaluated. They show clearly that hinokinin is predominantly localized in parenchyma cells; other extractives are distributed randomly in both parenchyma and tracheid cells (Figure 15.8c). This could be very helpful in understanding the heartwood formation mechanism.

### 15.2.3 Studying Organic Materials in Hybrid Mixtures: Painting Materials

In the studies described above, organic matter was the main, and most of the time, the only component of the samples. However, in a lot of cases, analyses must be performed on complex samples, composed of both organic and mineral materials. For this reason, organic compounds are often extracted from samples to be analysed. ToF-SIMS allows samples to be worked on without extraction, allowing the simultaneous study of organic and inorganic compounds and the characterization of their interactions. By way of illustration, we will review articles about the most well known example of hybrid samples in cultural heritage, namely paintings.

#### 15.2.3.1 Study of the Binding Media

In the study of painting layers, the identification of both pigments and binding media is important. For binding media two approaches are generally used. The first consists of the extraction of the organic matter followed by its analysis by chromatographic techniques. This procedure is very effective but has the disadvantage of being destructive for the sample. The other approach is based on microchemical tests on cross-sections of samples. ToF-SIMS can offer an alternative to these techniques.

In an article published in *Analytical Chemistry* in 2004, Keune and Boon [2004a] present the application of ToF-SIMS analysis to a paint cross-section. The sample used was from the panel painting 'The Descent from the Cross' (Museo del Prado, Madrid) by the early Flemish painter Rogier van der Weyden (1399/1400–1464). Scanning electron microscopy with energy dispersive X-ray analysis (SEM-EDX) and infrared microscopy were also used to complete and confirm the results.

The aim of the study was to reveal whether or not egg tempera was mixed with oil as binding media. The cross-section was studied in both positive and negative ion modes. Lead white with linseed oil, tripalmitin, stearic acid and lead white with egg tempera were studied as reference samples.

In positive ion mode, the characteristic peaks representative of the binding media were fatty acids from lead soaps (of palmitic acid at  $m/z$  461–463 and of stearic acid at  $m/z$  489–491). Other peaks corresponding to mono- and diacylglycerol cations, protonated stearic acid or its acylium ions could be found in the spectra of the reference products but not in the paint sample. The spectrum of lead white egg tempera paint exhibits peaks of phosphocholine ( $m/z$  184) and protonated ketocholesterol ( $m/z$  401). These peaks were not found in the spectrum from the cross-section. In negative ion mode, the spectrum of the oil

paint mainly showed deprotonated palmitic and stearic acids. In addition, other peaks attributed to short chain fatty acids (8-, 9- and 10-hydrocarbon chain length) were detected.

The presence of characteristic peaks from palmitic and stearic acids is consistent with the hypothesis of the use of oil as binding media. The lack of any characteristic ions issued from egg tempera means that ToF-SIMS does not allow detection of egg tempera in this sample. However, it could be present but is not detected due to high degradation occurring in very old egg tempera. The presence of short chain fatty acids, which are not detected in the new reference sample, is attributed to oil ageing. The distribution of fatty acid ions in the cross-section is well correlated with the distribution of lead. The ions are not detected in the ground layer (Figure 15.9).

In addition to these numerous results, two other points are discussed by the authors: fatty acid speciation and oil identification. These two aspects are developed in another publication written by the same authors [Keune *et al.* 2005]. The fatty acid speciation is based on the positive ion ToF-SIMS analysis and aims to prove if the fatty acids detected exist as free fatty acids, ester bound fatty acids or metal soaps. On account of the study of different standards, it is shown that when free fatty acids are present, the protonated molecular ion and its acylium ( $[M-OH]^+$ ) ion are detected. In cases of ester-bound fatty acid only the

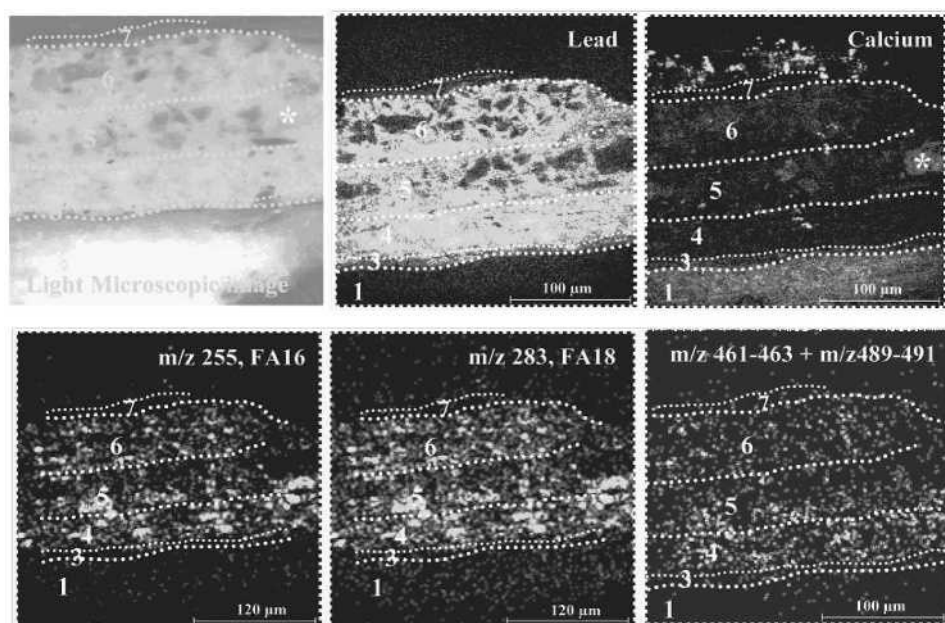


**Figure 15.9** Microscopic image and ToF-SIMS images of the cross-section from the painting 'The Descent from the Cross' (Museo del Prado, Madrid) by van der Weyden. Images of lead, calcium and lead soaps ( $m/z$  461–463 and 489–491) have been acquired in positive ion mode (image size  $250 \times 250 \mu m^2$ ). Images of palmitic ( $m/z$  255) and stearic ( $m/z$  283) acids have been acquired in negative ion mode (image size  $300 \times 300 \mu m^2$ ). Yellow represents high intensity and black represents low yields. The numbers on the images refer to the different layers. Adapted from *Analytical Chemistry*, 76, 1374–1385, Keune *et al.*, Copyright 2004 American Chemical Society (see colour Plate 5)

acylium ion is detected. Finally, for metal soap, spectra exhibit a peak for the molecular ion of clusters of metal ions and carboxylic fatty acid, and a small peak for the protonated fatty acid whereas the acylium ion is absent. Application of this to the sample of van der Weyden's painting shows that fatty acids are mainly present as metal soaps, which are, in this case, lead soaps because of the use of lead white as chemical drier. This explains the correlation between lead and fatty acids observed previously, even if caution has to be taken when interpreting ToF-SIMS imaging of paint layers containing binders and pigments because the ionization yield of organic species can be influenced by the presence of metals [Keune and Boon 2004b].

To identify the kind of oil, Keune *et al.* [2005] used the classical approach based on the palmitic acid/stearic acid (P/S) ratio usually obtained from GC/MS data. Ratios less than 2 correspond to linseed oil, whereas ratios higher than 5 correspond to poppy seed oil. Intermediate values can be attributed to walnut, poppy seed oil or mixtures [Schilling and Khaijan 1996]. Keune *et al.* first show that ionization efficiency is the same for the two fatty acids in negative ion mode permitting the use of ToF-SIMS for the calculation of the P/S ratio. A test on the oil-paint model system shows a ratio of 2.0 for linseed oil and 3.6 for poppy seed oil, which can allow the two oils to be differentiated. Nevertheless, it is important to note that the ratio is not constant all over the cross-section.

Different cross-sections from paintings have been studied. For the previously mentioned van der Weyden painting, P/S ratios varying from 1.3 to 1.8 are found indicating the use of linseed oil. Other examples allowed the identification of linseed oil or walnut/poppy seed oil in painting cross-sections. The same approach is used by Marino *et al.* [2006] to identify the oil used as binding media in the painting 'Plaster Figure of a Female Torso' by Van Gogh. Here the P/S ratios obtained (2.4 and 2.3) are inconclusive with respect to the type of oil used.

To conclude these studies about oil binding media, in another study, Keune and Boon [2004b] has proven that an ultrathin gold coating of the painting cross-sections enhances positive and negative secondary ion yields of lipids. By coating the samples with a 2 nm thick gold layer, the negative secondary ion yield is multiplied by three whereas in positive ion mode factors of two to four have been found. They also show that the fragmentation of the fatty acid is not affected, whereas the dissociation of mineral clusters seems to be reduced.

#### 15.2.3.2 Identification of Organic Pigments: Example of Verdigris

Binding media is not the only organic component of painting layers. For example, varnishes or organic pigments can also be found. No studies of varnishes by ToF-SIMS have been published up to now, but Van ham *et al.* [2005] give an example of organic pigment analysis through the study of verdigris. They have also published other studies on the speciation of mineral pigment [Van Ham *et al.* 2002, 2004].

The potential of ToF-SIMS is well established for inorganic pigment studies, and hybrid pigments (organic and inorganic) are perfectly suited to ToF-SIMS analyses.

Verdigris (copper acetate) is analysed as a pure pigment in both positive and negative ion mode. ToF-SIMS spectra allow verdigris to be easily differentiated from other copper pigments, like malachite (Figure 15.10). The negative ion spectrum exhibits clearly a peak corresponding to acetate ( $\text{CH}_3\text{COO}^-$ ) and other peaks for species containing both copper

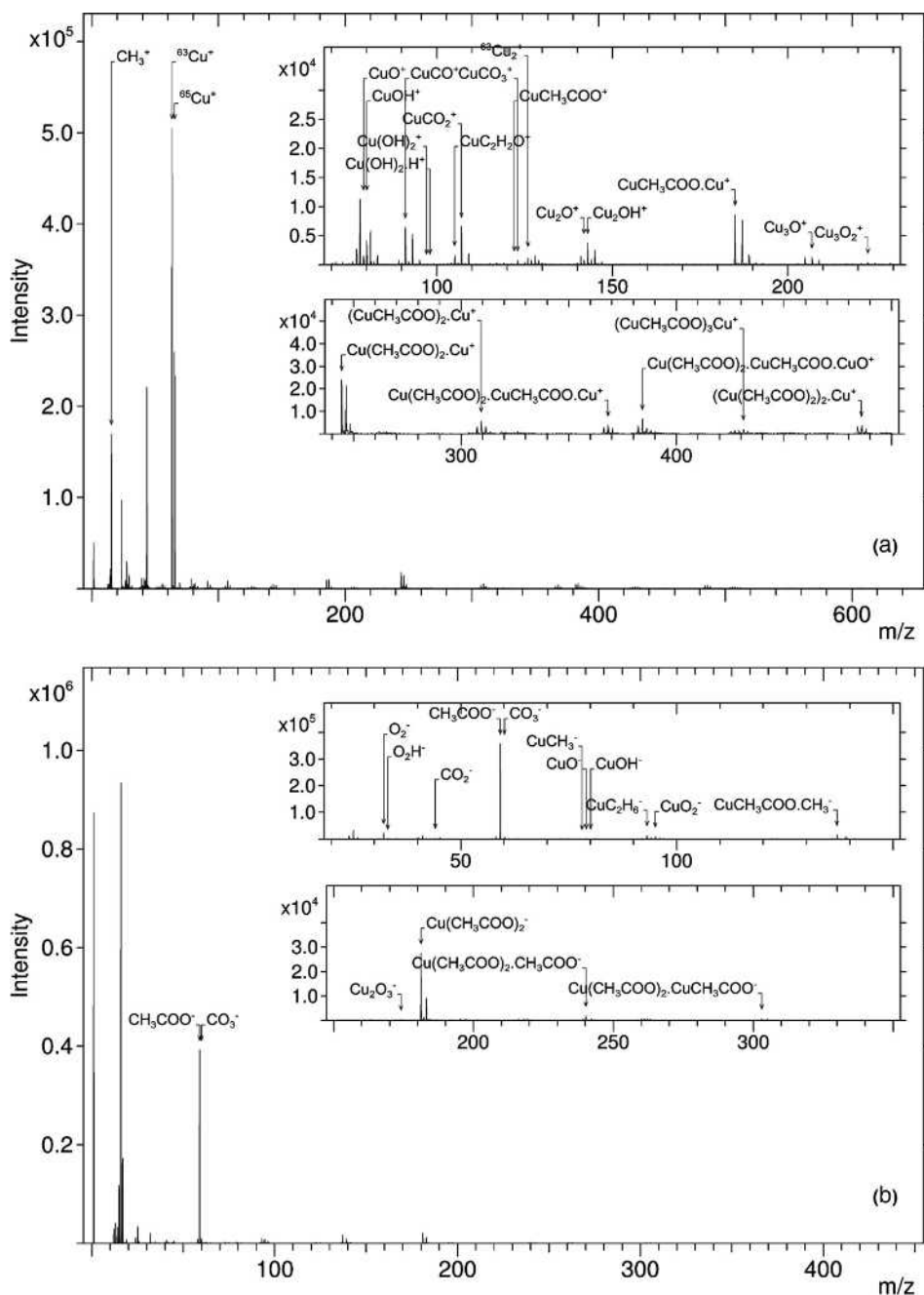


**Figure 15.10** (a) Positive ion and (b) negative ion ToF-SIMS spectra from a pellet of verdigris. With kind permission from Springer Science and Business Media, *Analytical and Bioanalytical Chemistry*, **383**, 991–997, Van Ham, Copyright 2005

and acetate, e.g.  $\text{Cu}(\text{CH}_3\text{COO})_2^-$ . In positive ion mode, copper clusters are also detected, e.g.  $\text{Cu}(\text{CH}_3\text{COO})\text{Cu}^+$  or  $\text{Cu}(\text{CH}_3\text{COO})_2\text{Cu}^+$ . These ions are specific to verdigris pigment. The interactions between organic compounds and inorganic ions are therefore well suited to ToF-SIMS analyses.

#### 15.2.3.3 Interactions between Oils and Inorganic Ions

The problem of interaction between binding media and inorganic ions has already been mentioned in the case of binding media identification [Keune and Boon 2004a]. This problem has been further developed in other research by the same team.

The first case deals with the well known smalt discoloration [Boon *et al.* 2001]. This blue pigment, which is a ground cobalt glass and was used as a substitute for azurite or ultramarine, is known to undergo discoloration when used with oil binding media. Boon *et al.* studied cross-sections of paint layers with partially or totally discoloured smalt particles. The distribution of different ions in these cross-sections indicates the presence of palmitic acid around smalt particles and levels of potassium much higher in coloured areas than in discoloured ones. The presence of potassium in the binding media is interpreted as leaching of potassium out of the smalt particle due to the influence of oil organic compounds. This interaction would then be responsible for smalt discolouring.

Another example of interactions between inorganic ions and the oil component is given by the extended study on lead soap performed by the Amolf team from the Foundation for Fundamental Research on Matter in Amsterdam. Development of such compounds is mainly due to the use of lead white as a drier of oil media but is associated with the ageing process of the paint layer [van der Weerd 2002]. This phenomenon is also responsible of the development of round protruding masses and white efflorescence crust [Boon *et al.* 2005]. A ToF-SIMS study of the cross-section of a sample presenting such a phenomenon shows that monocarboxylic lead soaps are concentrated in the core, while diacids are detected in the rim of the aggregate (Figure 15.11). This separation could be related to the formation process of the crystalline lead soap structure. A more detailed description of these phenomena can be found in Boon *et al.* [2006].

### 15.2.4 Versatility of the Technique: Complex and Biological Samples

The different examples described above have shown that ToF-SIMS is well suited to the study of a large variety of materials, classically found in cultural Heritage analyses. The following will be mainly focused on the versatility of the technique through a large study of African art artefacts. However, we will begin with an example of a complex sample, of biological nature, from an archaeological context.

#### 15.2.4.1 Archaeological Soft Tissues

The main problem with organic analyses from archaeological remains is their state of conservation. The question to be answered is whether any organic materials can be preserved over centuries or millennia. Many authors have proven that in certain conditions, preservation is possible [Evershed *et al.* 1992, Regert *et al.* 2003]. The question is of course very relevant in the case of dinosaur remains. In the case of preservation of organic materials, ToF-SIMS is well suited for such a study, because samples are very small and



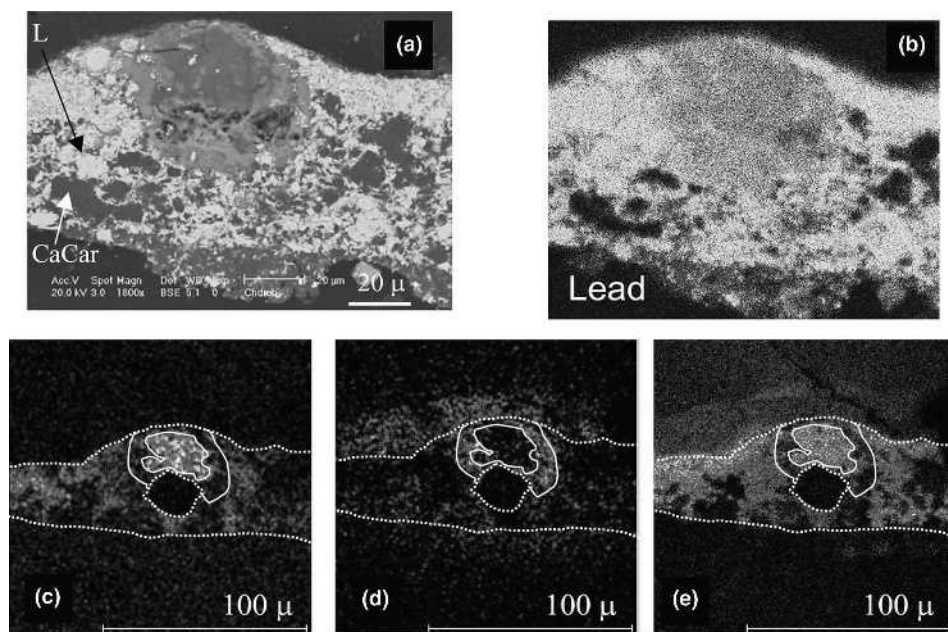


**Figure 15.11** Cross-section of a sample from a painting from the Hudson River School presenting a round protruding mass. (a) SEM image and EDX images of (b) lead, (c) lead soaps, (d) azelaic acid and (e) stearic acid. Reprinted from Boon *et al.*, *Microscopy and Microanalysis*, **11**, Supplement 2, pp. 444–445, 2005, by permission of Cambridge University Press (see colour Plate 6)

precious, and no sample preparation is required and it is a nondestructive technique for the sample.

In the study of the bones of an exceptionally well preserved *Tyrannosaurus rex*, Schweitzer *et al.* [2007] try to determine the remains of original tissues through the presence of preserved proteins from the original collagen. Demineralized samples are submitted to ToF-SIMS analyses. Analysis of proteins by ToF-SIMS has been described in several articles, and leads, in positive ion mode, to short fragments of amino acids [Lhoest *et al.* 2001, Sanni *et al.* 2002, Wagner and Castner 2004]. Using high mass resolution, low mass species can be attributed without ambiguity. Glycine ( $m/z$  30) and alanine ( $m/z$  44) are the main amino acids detected with a relative ratio of 2.6:1. This is comparable with the specific collagen  $\alpha 1$  type 1 from chicken in which the ratio is 2.5:1. Proline ( $m/z$  70), lysine ( $m/z$  84) and leucine/isoleucine ( $m/z$  86) are also detected. These results prove the presence of well conserved proteins in the dinosaur bones.

#### 15.2.4.2 Identification of Blood

The problem of biological remains in cultural heritage studies is also often cited in the case of African art objects through the identification of blood. Indeed, many African art objects are in fact related to ritual ceremonies and are covered with a thick patina formed by

materials spread on their surface during ceremonies where sacrifices may have taken place. In Mali, Dogon wooden statuettes, as well as the *boliv* (complex objects with an internal structure of bamboo and cotton) from Bamana culture, are good examples of this practice.

The identification of blood is generally performed using immunological tests. However, ToF-SIMS can also be used, with a different approach [Mazel *et al.* 2007]. Different objects, Dogon and Bamana, presenting thick patina were studied to prove whether or not blood was employed for making the patina. For each object, a microsample of patina was removed from the surface, and cross-sections were prepared by ultramicrotomy.

In the multistage approach, ToF-SIMS plays an important role and is first used to detect the presence of proteins in museum objects. Indeed, if blood is present in such a state of conservation that it can be recognized through chemical composition, proteins must be present. For this purpose, as described previously, low mass fragments are studied. Since samples are very complex and in order to ensure identification, two-dimensional images of all protein fragments are drawn and compared. Correlation between the different images confirms the presence of proteins.

After this first step, where some samples are eliminated because they are not suited to the protocol, the positive ion mode is used to investigate haem, an iron porphyrin which is a blood marker. Spectra taken of the haem reference show that it can be detected due to  $[M]^+$  and  $[M+H]^+$  ions (respectively, at  $m/z$  616.2 and 617.2), and also due to a large distribution of fragment peaks between  $m/z$  350 and  $m/z$  550 (Figure 15.12a). The same spectrum has also been obtained for haemoglobin leading to the conclusion that the presence of protein does not disturb the detection of haem.

In four samples, all from Bamana sculptures, the signal of haem has been detected. The intensity is different for the diverse samples, which means that the state of conservation of haem is variable depending on each sample. Nevertheless, the two-dimensional mapping

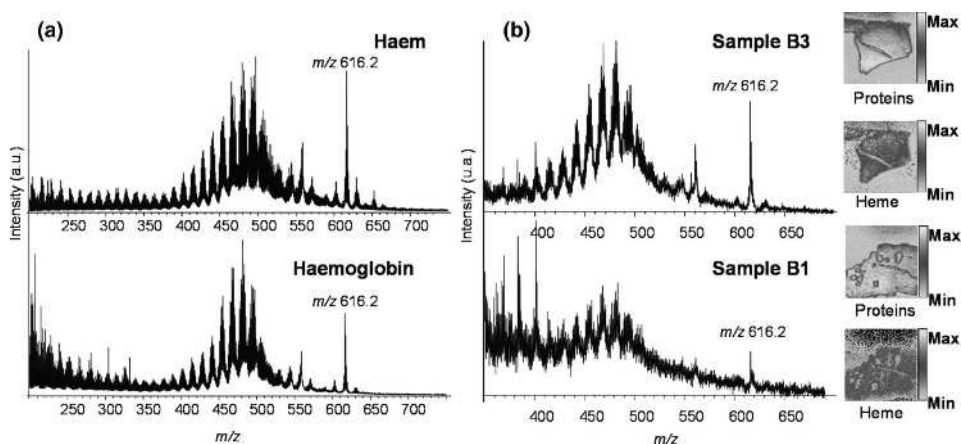


**Figure 15.12** Identification of blood. (a) ToF-SIMS spectra in positive ion mode of hemin and haemoglobin. (b) ToF-SIMS spectra in positive ion mode of two cross-sections of boliv patina (samples B1 and B3) and images of the localization of haem and proteins in the sample (see colour Plate 7)

of haem fragments shows a very good correlation with protein distribution as expected (Figure 15.12b). In the two Dogon samples, no haem has been detected in the protein area, which could mean that it is too degraded to be detected. In these cases, other synchrotron based techniques have been used to assess the presence of blood through detection of iron and studying its chemical environment.

#### 15.2.4.3 *Organic Product Identification and Localization in Complex Mixtures*

Blood is the most often reported component of the patina from African ritual statuettes but other materials are also used. The patina is generally a quite complex mixture of different products from various chemical families. In the study of such complex mixtures, ToF-SIMS offers another great advantage, namely its versatility. Indeed, in a unique analysis, performed in positive and negative ion mode, a great number of different compounds can be detected.

This is well illustrated by the study of a sample from the Dogon statuette 73.1964.3.39 from the Musée du Quai Branly (Paris) [Mazel *et al.* 2006]. A multi-method protocol was performed on complex samples of patina from African art. ToF-SIMS was coupled with infrared microspectrometry and SEM. Different kinds of compounds were found in the sample.

Proteins are detected and localized by ToF-SIMS on account of the detection of amino acid fragments, as described previously. A similar approach is used for polysaccharide residues. Fragments at  $m/z$  45, 59, 71 and 99 are used for their identification and localization (Figure 15.13). The attribution of these small fragments to polysaccharides is ensured

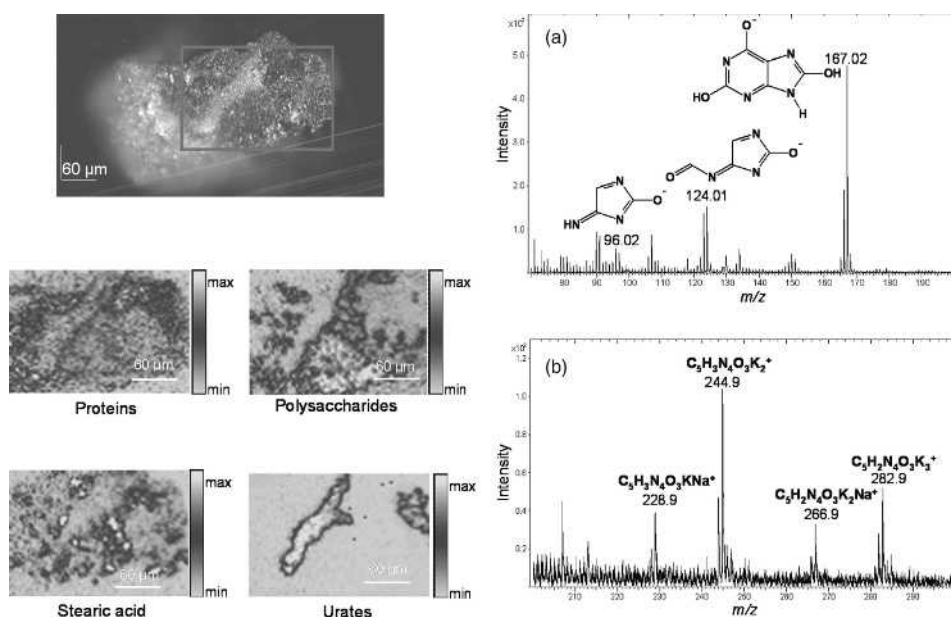


**Figure 15.13** Study of the sample from the Dogon statuette 73.1964.3.39. The area analysed by ToF-SIMS is outlined in red on the optical microphotograph. The spectra have been calculated from the area rich in urates in (a) negative and (b) positive ion mode (see colour Plate 8)



by the fact that all these ions have the same distribution and by the comparison of this distribution with the image of the characteristic glycosidic linkage vibration in polysaccharides obtained by infrared spectroscopy.

Lipids are easily detected in negative ion mode on account of the peaks of deprotonated stearic, palmitic and arachidic acids. In positive ion mode, mono- and diacylglycerol are also detected. All these lipids show the same distribution all over the sample. An interesting point is the predominance of stearic acid. This could be consistent with the use of shea butter or karite in the recipe of the patina, products commonly used in West Africa.

The last compound identified is more surprising and less common in a cultural heritage study. A white area, clearly visible on the microphotograph, contains urate salts. This identification is first based on negative ion mode spectra and images. An intense ion at  $m/z$  167.02 could correspond to deprotonated uric acid ( $C_5H_3N_4O_3^-$ ). This identification is confirmed by the colocalization of this ion with the classical fragments of uric acid found in the literature ( $m/z$  124.01 and 96.01) (Figure 15.13). This result is another example of the use of chemical imaging for the identification of ions, and not only to map their distribution. As in the case of lipids in painting studies, positive ion mode ToF-SIMS analysis is a very promising technique for the speciation of a compound. In the positive ion mode, the protonated molecule, which should appear at  $m/z$  169.03, is mostly absent. This could be due to the presence of urate salts rather than uric acid and this also explains the presence of potassium and sodium cationic forms of potassium urate (Figure 15.13). The white area of the sample is then composed of urate salts, which is confirmed by the presence of characteristic round shaped grains observed by SEM.

Finally, the versatility of the technique and its use as a chemical imaging technique allow retrieval of the structural composition of a sample, in order to understand its complete recipe [Mazel *et al.* 2008]. The composition of a sample from the Dogon statuette 71.1935.105.169 has been studied. Proteins, polysaccharides, lipids and minerals have been found. The distribution of these different chemicals shows that the patina sample can be divided into four different layers (Figure 15.14). Layers 1 and 3 are mainly composed of proteins whereas layer 2 consists of lipids and polysaccharides. Minerals can be found at the interface of layers 1 and 2, and 2 and 3. Finally, layer 4 is the more complex because it contains all the types of compounds. One can suppose that it is in fact composed of different layers that do not appear clearly on the cross-section.

From these results, we can suppose that this patina has been made in several steps, each step corresponding to one layer. The presence of a mineral phase represents mineral deposit on the surface of the object between two uses of the statuette due to environmental pollution. Based on results obtained in previous articles, it can be inferred that proteins come from the use of blood and that polysaccharides correspond to millet mush spread on the object, as described in the ethnological literature [Griaule 1932a,b]. The good correlation between lipids and polysaccharides suggests that the compounds might have been mixed before being poured over the object.

This example highlights the performance of ToF-SIMS analyses. On other samples studied in the same paper, the results are less satisfactory due to the massive quantity of minerals and the degradation of the organic matter. Nevertheless, the information obtained can clearly confirm that there are two different kinds of patina corresponding to two different historical periods. Only the structure of the patina of the recent statuettes is in agreement with the ethnological literature, which suggests a change in ritual practices over time.

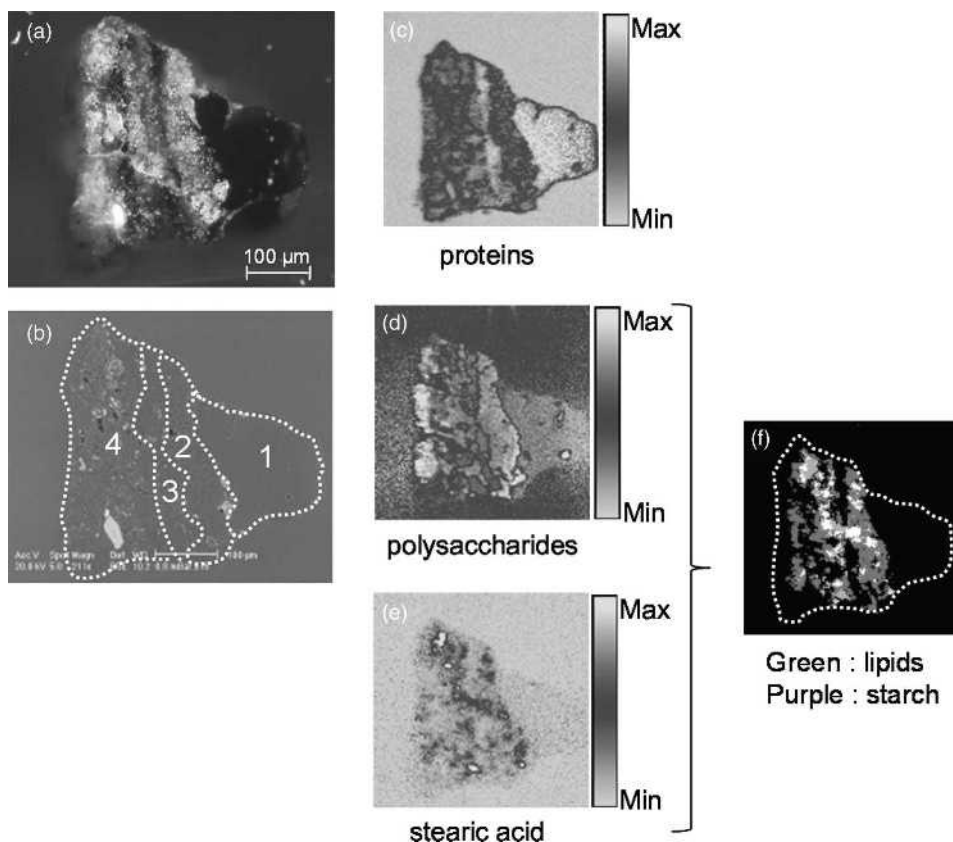


**Figure 15.14** Study of the sample from the Dogon statuette 71.1935.105.169. (a) Optical microphotograph; (b) SEM micrograph showing the layer structure; ToF-SIMS images of (c) proteins, (d) polysaccharides and (e) stearic acid; (f) superposition of the distribution of polysaccharides and stearic acid (see colour Plate 9)

### 15.3 Conclusion

The different examples presented in this review show the large range of possible applications of ToF-SIMS in the cultural heritage field. We have seen that it can be used for the characterization of different kinds of materials such as polymers, fibres and textiles, painting materials or biological samples, but any other material could be considered.

This relatively new method is quite different from other mass spectrometric techniques usually used for this topic. ToF-SIMS presents two main advantages. First, it permits the analysis of solid samples with minimal sample preparation. This avoids the necessity of extractions, and therefore, it can be very useful for small and precious samples.

The second advantage is the possibility of performing chemical imaging analyses. Even if other techniques, such as matrix-assisted laser desorption/ionization, also allow images to be acquired, ToF-SIMS is, for now, the mass spectrometric technique with the best spatial resolution performance.

ToF-SIMS results are sometimes difficult to interpret, but they often allow complementary results to be obtained using a different approach. The different articles referred to in this review have shown examples of the fruitful combination of ToF-SIMS with infrared microscopy or SEM.

Although there are still only a few articles published, the new possibilities offered by this technique are very promising for future applications in cultural heritage.

## References

- M.-L. Abel and C. Coppitters, Conservation of polymers: a view to the future, *Surface Interface Analysis*, **40**, 445–449 (2008).
- A. Adriaens and M. G. Dowsett, Applications of SIMS to cultural heritage studies, *Applied Surface Science*, **252**, 7096–7101 (2006).
- M. Anderle, M. Bersani, L. Vanzetti and S. Pederzoli, State of art in the SIMS (secondary ion mass spectrometry) application to archaeometry studies, *Macromolecular Symposia*, **238**, 11–15 (2006).
- J. Batcheller, A. M. Hacke, R. Mitchell and C. M. Carr, Investigation into the nature of historical tapestries using time of flight secondary ion mass spectrometry (ToF-SIMS), *Applied Surface Science*, **252**, 7113–7116 (2006).
- A. M. Belu, D. J. Graham and D. G. Castner, Time-of-flight secondary ion mass spectrometry: techniques and applications for the characterization of biomaterial surfaces, *Biomaterials*, **24**, 3635–3653 (2003).
- J. J. Boon, K. Keune, J. van der Weerd, M. Geldof and J. de Boer, Imaging microspectroscopic, secondary ion mass spectrometric and electron microscopic studies on discoloured and partially discoloured smalt in cross-sections of 16th century paintings, *Chimia*, **55**, 952–960 (2001).
- J. J. Boon, K. Keune and J. Zucker, Imaging analytical studies of lead soaps aggregating in preprimed canvas used by the Hudson River School painter F. E. Church, *Microscopy and Microanalysis*, **11**(Suppl. 2), 444–445 (2005).
- J. J. Boon, F. Hoogland and K. Keune, Chemical processes in aged oil paints affecting metal soap migration and aggregation, *AIC Annual Meeting*, Providence, Rhode Island, June 16–19, 2006.
- A. Brunelle, D. Touboul and O. Lapr v te, Biological tissue imaging with time-of-flight secondary ion mass spectrometry and cluster ion sources, *Journal of Mass Spectrometry*, **40**, 985–999 (2005).
- C. M. Carr, R. Mitchell and D. Howell, Surface chemical investigation into the cleaning procedures of ancient tapestry materials. Part 1, *Journal of Materials Science*, **39**, 7317–7325 (2004).
- E. Darque-Ceretti and M. Aucouturier, Secondary ion mass spectrometry. Application to archaeology and art objects, in *Non-destructive Analysis of Cultural Heritage Materials*, K. Janssens and R. Van Grieken (eds), Comprehensive Analytical Chemistry XLII, Elsevier BV, Amsterdam, 2004, pp. 397–461.
- M. Dowsett and A. Adriaens, Role of SIMS in cultural heritage studies, *Nuclear Instruments & Methods in Physics Research Section B—Beam Interactions with Materials and Atoms*, **226**, 38–52 (2004).
- R. P. Evershed, C. Heron, S. Charters and L. J. Goad, The survival of food residues: new methods of analysis, interpretation and application, in *New Developments in Archaeological Science*, A. M. Pollard (ed.), Proceedings of the British Academy, vol. 77, Oxford University Press, Oxford, 1992, pp. 187–208.
- E. S. B. Ferreira, A. Quye, H. McNab and A.N. Hulme, Photo-oxidation products of quercetin and morin as markers for the characterisation of natural flavonoid yellow, *Dyes in History and Archaeology*, **18**, 63–72 (2002).
- M. Griaule, La mission Dakar-Djibouti, rapport g n ral (mai 1931–mai 1932), *Journal de la Soci t  des Africanistes*, **II**, 113–122 (1932a).
- M. Griaule, La mission Dakar-Djibouti, rapport g n ral (juin–novembre 1932), *Journal de la Soci t  des Africanistes*, **II**, 229–236 (1932b).

- D. Howell, R. Mitchell and C. M. Carr, Surface chemical investigation into the cleaning procedures of historic tapestry materials. Part 2, *Journal of Materials Science*, **42**, 5452–5457 (2007).
- K. Keune and J. J. Boon, Imaging secondary ion mass spectrometry of a paint cross-section taken from an early Netherlandish painting by Rogier van der Weyden, *Analytical Chemistry*, **76**, 1374–1385 (2004a).
- K. Keune and J. J. Boon, Enhancement of the static SIMS secondary ion yields of lipid moieties by ultrathin gold coating of aged oil paint surfaces, *Surface and Interface Analysis*, **36**, 1620–1628 (2004b).
- K. Keune, E. S. B. Ferreira and J. J. Boon, Characterization and localization of the oil-binding medium in paint cross-sections using imaging secondary ion mass spectrometry, *Preprints of the 14th Triennial Meeting of ICOM-CC Committee for Conservation*, The Hague (Netherlands), **2**, 796–802 (2005).
- F. Kollmer, Cluster primary ion bombardment of organic materials, *Applied Surface Science*, **231–232**, 153–158 (2004).
- Y. Lee, J. Lee, Y. Kim, S. Choi, S.W. Ham and K.-J. Kim, Investigation of natural dyes and ancient textiles from Korea using ToF-SIMS, *Applied Surface Science*, **255**, 1033–1036 (2008).
- J. B. Lhoest, M. S. Wagner, C. D. Tidwell and D. G. Castner, Characterization of adsorbed protein films by time-of-flight secondary ion mass spectrometry, *Journal of Biomedical Materials Research*, **57**, 432–440 (2001).
- B. Marino, J. J. Boon, E. Hendricks, F. Horr  ard and F. Hillion, Imaging ToF-SIMS and NANOSIMS studies of barite-celestite particles in grounds from paintings by Van Gogh, *e-Preservation Science*, **3**, 41–50 (2006).
- V. Mazel, P. Richardin, D. Touboul, A. Brunelle, P. Walter and O. Lapr  v  te, Chemical imaging techniques for the analysis of complex mixtures: new application to the characterization of ritual matters on African wooden statuettes, *Analytica Chimica Acta*, **570**, 34–40 (2006).
- V. Mazel, P. Richardin, D. Debois, D. Touboul, M. Cotte, A. Brunelle, P. Walter and O. Lapr  v  te, Identification of ritual blood in African artifacts using ToF-SIMS and synchrotron radiation microspectroscopies, *Analytical Chemistry*, **79**, 9253–9260 (2007).
- V. Mazel, P. Richardin, D. Debois, D. Touboul, M. Cotte, A. Brunelle, P. Walter and O. Lapr  v  te, The patinas of the Dogon – Tellem statuery: a new vision through physico-chemical analyses, *Journal of Cultural Heritage*, **9**, 347–353 (2008).
- D. S. McPhail, Some applications of SIMS in conservation science, archaeometry and cosmochemistry, *Applied Surface Science*, **252**, 7107–7112 (2006).
- P. Novotna, V. Pacakova, Z. Bosakova and K. Stulik, High-performance liquid chromatographic determination of some anthraquinone and naphthoquinone dyes occurring in historical textiles, *Journal of Chromatography, A*, **863**, 235–241 (1999).
- M. Regert, N. Garnier, O. Decavallas, C. Cren-Oliv   and C. Rolando, Structural characterization of lipid constituents from natural substances preserved in archaeological environments, *Measurement Science and Technology*, **14**, 1620–1630 (2003).
- K. Saito, T. Mitsutani, T. Imai, Y. Matsushita and K. Fukushima, Discriminating the indistinguishable sapwood from heartwood in discolored ancient wood by direct molecular mapping of specific extractives using time-of-flight secondary ion mass spectrometry, *Analytical Chemistry*, **80**, 1552–1557 (2008).
- O. D. Sanni, M. S. Wagner, D. G. Briggs, D. G. Castner and J. C. Vickerman, Classification of adsorbed protein static ToF-SIMS spectra by principal component analysis and neural networks, *Surface and Interface Analysis*, **33**, 715–728 (2002).
- J. Sanyova, Contribution    l’  tude de la structure et des propri  t  s de la laque de garance, PhD Thesis, Brussels, 2001. Downloadable from <http://theses.ulb.ac.be/ETD-db/collection/available/ULBetd-08092006-162429/>.
- M. R. Schilling and H. P. Khaijan, Gas chromatographic determination of fatty acid and glycol content of lipids I. The effect of pigments and ageing on the composition of oil paints, *Preprints of the 11th Triennial Meeting of the ICOM Committee for Conservation*, Edinburgh, **1**, 211–219 (1996).
- M. H. Schweitzer, Z. Suo, R. Avci, J. M. Asara, M. A. Allen, F. T. Arce and J. R. Horner, Analyses of soft tissue from *Tyrannosaurus rex* suggest the presence of protein, *Science*, **316**, 277–280 (2007).
- R. N. S. Sodhi, Time-of-flight secondary ion mass spectrometry (ToF-SIMS): versatility in chemical and imaging surface analysis, *Analyst*, **129**, 483–487 (2004).

- G. Spoto, Secondary ion mass spectrometry in art and archaeology, *Thermochimica Acta*, **365**, 157–166 (2000).
- B. Szostek, J. Orska-Gawrys, I. Surowiec and M. Trojanowicz, Investigation of natural dyes occurring in historical Coptic textiles by high-performance liquid chromatography with UV-vis and mass spectrometric detection, *Journal of Chromatography, A*, **1012**, 179–192 (2003).
- A. Torrisi, N. Tuccitto, G. Maccarrone and A. Licciardello, ToF-SIMS characterization of fluoroalkyl derivatives of possible interest as water repellent for stone protection, *Appl. Surf. Sci.*, **255**, 1527–1530 (2008).
- D. Touboul, F. Halgand, A. Brunelle, R. Kersting, E. Tallarek, B. Hagenhoo and O. Laprévotte, Tissue molecular ion imaging by gold cluster ion bombardment, *Analytical Chemistry*, **76**, 1550–1559 (2004).
- J. van der Weerd, Microspectroscopic analysis of traditional oil paint, PhD Thesis, University of Amsterdam, 2002.
- R. Van Ham, L. Van Vaeck, A. Adriaens, F. Adams, B. Hodges and G. Groenewold, Inorganic speciation in static SIMS: a comparative study between monatomic and polyatomic primary ions, *Journal of Analytical Atomic Spectrometry*, **17**, 753–758 (2002).
- R. Van Ham, L. Van Vaeck, F. C. Adams and A. Adriaens, Systematization of the mass spectra for speciation of inorganic salts with static secondary ion mass spectrometry, *Analytical Chemistry*, **76**, 2609–2617 (2004).
- R. Van Ham, L. Van Vaeck, F. Adams and A. Adriaens, Feasibility of analyzing molecular pigments in paint layers using TOF S-SIMS, *Analytical and Bioanalytical Chemistry*, **383**, 991–997 (2005).
- M. S. Wagner and D. G. Castner, Analysis of adsorbed proteins by static time-of-flight secondary ion mass spectrometry, *Applied Surface Science*, **231–232**, 366–376 (2004).
- N. Winograd, The magic of cluster SIMS, *Analytical Chemistry*, **77**, 143A–149A (2005).



# 16

## Accelerator Mass Spectrometry for $^{14}\text{C}$ Dating

*Mariaelena Fedi*

### 16.1 Introduction

Dating is of crucial importance in art and archaeology. Several different techniques, such as luminescence, dendrochronology, radiocarbon, uranium-series and potassium-argon, have been developed with the aim of covering as wide a range as possible of calendar years, even up to 100 000 years ago.[1] Among the techniques, dating based on the radioactive decay of radiocarbon ( $^{14}\text{C}$ ) is definitely the most well known, employed and, perhaps, also the most reliable technique. All the organic finds that were once part of the biosphere can actually be dated by  $^{14}\text{C}$ : for example, wood, charcoal, bones, textiles, papyri, parchment, paper and, in certain cases, even food residues found in pottery. The main principles of  $^{14}\text{C}$  dating were formulated by the American chemist W. F. Libby and his colleagues in the late 1940s at the University of Chicago.[2,3] The huge impact of the new dating method on archaeology was immediately acknowledged by archaeologists: indeed, many refer to its introduction as a real revolution. Moreover, in 1960, Libby was awarded the Nobel Prize in chemistry and in the presentation speech the Royal Swedish Academy of Sciences recognized that radiocarbon had become ‘indispensable for research work in many fields and in many institutes throughout the world’.[4]

A detailed description of the  $^{14}\text{C}$  dating method goes beyond the scope of this chapter; for those interested, many resources can be found in the literature.[5,6] In the following, only the basics that are fundamental to the understanding of the present topic are illustrated.

$^{14}\text{C}$  is the only 'natural' unstable isotope of carbon. It is mainly produced in the upper layers of the atmosphere by the reaction of thermal neutrons (secondary products of primary cosmic radiation) on  $^{14}\text{N}$  nuclei[7] and it decays via beta emission to  $^{14}\text{N}$ , with a half life  $T_{1/2}$  of  $(5730 \pm 40)$  years.[8] The other two natural carbon isotopes,  $^{12}\text{C}$  and  $^{13}\text{C}$ , are both stable and constitute almost all the carbon on earth. Actually,  $^{12}\text{C}$  and  $^{13}\text{C}$  are 98.9% and 1.1% of the total carbon, respectively, while the  $^{14}\text{C}/^{12}\text{C}$  ratio in the atmosphere is about  $1.2 \times 10^{-12}$ . In the atmosphere,  $^{14}\text{C}$  atoms are rapidly oxidized to  $\text{CO}_2$  and then dissolve in the oceans or enter the biosphere through different mechanisms such as photosynthesis, thus being assimilated by all living organisms (both terrestrial and marine). The times characteristic of carbon mixing in the overall system represented by the atmosphere, oceans and biosphere (often called the carbon exchange reservoir) are smaller than the  $^{14}\text{C}$  half life; the radiocarbon concentration in the reservoir reaches equilibrium and can be considered approximately uniform. This is a key point to use radiocarbon as a chronometer: every living organism has the same  $^{14}\text{C}$  concentration as that in the atmosphere ( $\sim 10^{-12}$   $^{14}\text{C}$  atoms with respect to all carbon atoms); then, when the organism dies, if we consider it as a closed system, this concentration starts to decrease due to radiocarbon decay, which is no longer compensated for by the mechanism of continuous exchange with the reservoir. After a period  $t$  after death, the 'organism' will have a residual radiocarbon concentration  $^{14}R(t)$  given by the law of radioactive decay:

$$^{14}R(t) = ^{14}R_0 e^{-\frac{t}{\tau}} \quad (16.1)$$

where  $^{14}R_0$  is the equilibrium radiocarbon concentration at the moment of death and  $\tau$  ( $=T_{1/2}/\ln 2$ ) is the  $^{14}\text{C}$  mean life. Assuming for  $\tau$  the so-called Libby mean life of 8033 years and choosing a conventional value for  $^{14}R_0$  arbitrarily equal to the  $^{14}\text{C}$  concentration in the atmosphere during 1950, we can define the conventional radiocarbon age  $t_{RC}$  from Equation (16.1) as:[9]

$$t_{RC} = \tau \ln \left[ \frac{^{14}R_0}{^{14}R(t)} \right] \quad (16.2)$$

The radiocarbon age from Equation (16.2) is expressed in years BP, i.e. Before Present, where Present, by convention, is 1950 AD. Actually, 1950 is considered the reference year in radiocarbon dating, especially due to historical reasons. Following the same convention, in Equation (16.2), when measuring  $^{14}R(t)$ , its value is usually normalized to the concentration of a standard material in 1950; the normalized value is expressed in units of pMC (per cent of Modern Carbon), the standard material being 100 pMC.

It is well known that the radiocarbon age does not correspond to the real calendar age of an organism, since Equation (16.2) is based on assumptions that are true only to a first approximation; namely, the hypothesis of a constant value of  $^{14}R_0$  over time in the past.[10] An accurate calibration curve[11,12] has thus to be used to convert the  $t_{RC}$  value of a measured sample into its true age. For a complete discussion on this topic, the already cited literature on radiocarbon dating can be considered for reference. In contrast, the focus of this chapter is on how to measure the radiocarbon age  $t_{RC}$ , i.e. how to measure  $^{14}R(t)$ . Assuming, as explained above,  $^{14}R_0$  and  $\tau$  in Equation (16.2) are known, it is indeed clear that a measurement of  $^{14}R(t)$  allows us to determine the radiocarbon age.



In principle,  $^{14}\text{R}(t)$  might be measured directly using spectrometric techniques: the different carbon isotopes ( $^{14}\text{C}$ ,  $^{12}\text{C}$  and also  $^{13}\text{C}$ ) might be separated and counted according to their mass. However, this approach has a strong limitation owing to the extremely low abundance of radiocarbon in the materials to be dated (as already mentioned,  $\sim 10^{-12}$  in modern samples). Using a traditional mass spectrometer, what is very critical is not the discrimination of mass 14 from mass 12 and from mass 13, but the separation of the rare isotope from isobar elements or molecules with masses that are very close to that of the rare isotope and whose concentrations are higher. In the case of a radiocarbon measurement, the interference of isobars is related to the presence of  $^{14}\text{N}$  (which is the most abundant element in air) and carbon molecules such as  $^{12}\text{CH}_2$  and  $^{13}\text{CH}$ . Some numbers can help in understanding the problem: the relative mass difference  $\Delta m/m$  is only 0.000012 with respect to  $^{14}\text{N}$  and 0.0006 with respect to  $^{13}\text{CH}$ . Such mass differences might be resolved even by traditional spectrometers, pushing their resolution to extreme values (for example, by narrowing the exit slits from the spectrometer), but at the cost of strongly reducing their efficiency. Therefore, this procedure is not compatible with the search for atoms of a rare isotope, where an efficiency as high as possible is clearly needed.[13]

For these reasons, since the pioneering work of Libby the measurement technique used has been different from mass spectrometry and has exploited the characteristics of the process of the radioactive decay. From the law of radioactive decay, the activity of a sample, namely the number of decays per unit time, is proportional to the number of radioactive isotopes (i.e. their concentration in the sample). Indeed, by differentiation, Equation (16.1) becomes:

$$\frac{d^{14}\text{R}(t)}{dt} = -\frac{1}{\tau} {}^{14}\text{R}(t) = -\lambda {}^{14}\text{R}(t) \quad (16.3)$$

where  $\lambda$  is the constant describing the decay probability.

According to Equation (16.3), the concentration of radiocarbon  $^{14}\text{R}(t)$  can thus be calculated from the activity  $\frac{d^{14}\text{R}(t)}{dt}$ , which is measured by counting the particles emitted in the decay (in the case of  $^{14}\text{C}$ ,  $\beta$  particles, i.e. electrons). This is the so-called conventional or radiometric method.[14] In this kind of measurement, in most applications, the sample taken from the find to be dated is converted to a chemical form, typically benzene ( $\text{C}_6\text{H}_6$ ), which is suitable to be mixed with a liquid scintillator that is used to count the emitted electrons. This procedure maximizes counting efficiency. It is evident that such a measurement is destructive,[15] so, especially when dealing with artistic and/or archaeological objects, one should limit the invasiveness of the technique by sampling the smallest possible fragments from the object, thus preserving its integrity. However, there is a minimal sample size required for the measurements in order to acquire the needed level of precision. An example can better illustrate the problem. Let us consider a sample of 1 g of carbon and let us suppose that it is modern, i.e. characterized by a  $^{14}\text{C}/^{12}\text{C}$  ratio[16] of  $1.2 \times 10^{-12}$ : it contains therefore about  $6 \times 10^{10}$  radiocarbon atoms. Since  $\lambda = 1/\tau = 1.2 \times 10^{-4} \text{ year}^{-1} = 3.8 \times 10^{-12} \text{ s}^{-1}$ , its activity is only about 0.23 decays  $\text{s}^{-1}$ . This means that, in order to measure the radiocarbon age with a precision of 1% (which requires accumulation of about 10 000 counts), the measurement should last almost 12 h, even in the optimistic case of 100% detection efficiency, and with no background. When the measured sample is not modern, its activity becomes smaller, so one should wait for an even longer time to achieve the same precision, or perhaps one should select higher mass samples, much bigger than 1 g (and this is not always possible). Typical sample masses[17] used in radiometric measurements are listed in Table 16.1.

**Table 16.1** *Typical sample masses used in radiometric measurements. The quoted masses refer to raw sample material and are only indicative, since the needed amounts depend on the state of preservation of the sample and of the kind of sample itself (a bone for example is composed also of an inorganic fraction that has to be removed before dating)*

Material	Mass (g)
Wood	5
Bone	500
Charcoal	3–5
Paper, textiles	5–10
Hair, skin	5–7
Shell, carbonates	10

Radiometric measurements are still used in radiocarbon laboratories worldwide;[18] however, it is evident that the sample size requirements limit the kind of samples used: for example, would the Turin Shroud ever have been radiocarbon dated, if a 10 g piece (corresponding to some hundreds of square centimetres) had to be sampled?

A new idea to directly measure the amount of residual  $^{14}\text{C}$  in a sample overcoming the difficulties in traditional mass spectrometry and reducing sample sizes needed for radiometric measurements began to emerge from low-energy nuclear physics laboratories in the late 1970s. The new approach dealt with the use of a particle accelerator as an ultra sensitive mass spectrometer. First, Muller from Berkeley proposed to directly measure  $^{14}\text{R}(t)$  using a cyclotron;[19] later in the same year, two different groups, one from the Simon Fraser and McMaster universities in Canada[20] and the other from the universities of Toronto and Rochester, together with the commercial General Ionex Corporation,[21] demonstrated that  $^{14}\text{C}$  can be identified and counted using a Van de Graaff tandem accelerator. From these first experiments, the advantages of coupling a low-medium energy accelerator with mass spectrometric filters were evident: much smaller quantities of carbon were needed with respect to the radiometric method (decreasing by orders of magnitude, from grams to milligrams) and shorter counting times were required to gain the desired good precision. Let us again consider a numeric example to clarify the problem. Let us consider measuring the  $^{14}\text{C}$  concentration in a sample containing 1 mg of modern carbon by such an accelerator; with a good efficiency ion source the beam extracted from the sample is expected to contain about  $5 \times 10^{13}$  stable  $^{12}\text{C}$  ions per second and therefore about 60 radiocarbon ions per second. Assuming a (realistic) beam transmission of about 50%, only 5 min are required to acquire 10 000 radiocarbon counts thus reaching a precision of 1% (the same as obtained with 1 g of modern carbon by a radiometric measurement lasting 12 h).

The impact of this new technique, which was called Accelerator Mass Spectrometry (AMS), on the radiocarbon and archaeologist communities, was immediate and revolutionary. The introduction of AMS is indeed recognized by some as the third revolution in radiocarbon dating[22,23] and it has provided the opportunity to date very precious finds by collecting very small samples. The interest in developing the technique of AMS was so evident that, just few years after the measurements cited above, a first dedicated AMS system (based on a tandem accelerator) was designed and built;[24] then, the first dedicated

laboratories, at Tucson in Arizona, Toronto in Canada and Oxford in the UK, were established in the early 1980s. The potentials of AMS were soon exploited to measure other long-lived radioisotopes[25] in addition to  $^{14}\text{C}$ .

In the following, attention will be focused on the measurement of radiocarbon only. Details about the main components of an AMS system will be given and examples of the importance of AMS in radiocarbon dating will be discussed.

## 16.2 General Features of Accelerator Mass Spectrometry

### 16.2.1 Performance of Accelerator Mass Spectrometry Systems

Mass spectrometry is based on the principle that trajectories of ions can be separated according to their mass-to-charge ratios by passing through magnetic or electrostatic fields. In this way, ions of different masses can be counted in order to have quantitative information on, for example, the isotopic composition of a sample. The sensitivity limits of traditional mass spectrometry in rare isotope measurements, already discussed in the Introduction, are overcome in AMS by coupling the traditional selective elements, such as magnetic and electrostatic analysers, with a particle accelerator. The great advantage is represented by the capability of a very high suppression of isobar interferences, both elemental and molecular. Actually, in AMS systems, the ion source and the accelerator are used as filters to remove isobars. In order to understand how this is achieved in the case of a radiocarbon measurement, the main features of a tandem accelerator – today the most widespread accelerator type used for  $^{14}\text{C}$  – are summarized below (details will be given in Section 16.3):

- the main interfering isobar, the stable nuclide  $^{14}\text{N}$ , does not form stable negative ions[26] and it is as negative ions that particles have to be injected in tandem accelerators;
- the molecular isobars are destroyed at the high voltage terminal through the stripping process peculiar to the tandem acceleration mechanism.

In this kind of facility (see Figure 16.1), negative ions, produced in the source from the sample typically by sputtering with a caesium beam, are first analysed according to their mass-charge-energy ratios, injected into the accelerator and then accelerated to the high voltage terminal that is in the middle of the ion path inside the tandem. Here they are converted to positively charged particles by passing through a stripping medium (either a very thin foil or a weak gas flow maintained in the canal at the high voltage terminal) and they are thus further accelerated to ground potential. Following acceleration, the selected and analysed ions are usually the multiply charged ones, for example  $^{14}\text{C}^{3+}$ . The stripping process acts as a very important filter, since multiply charged molecules are not stable as

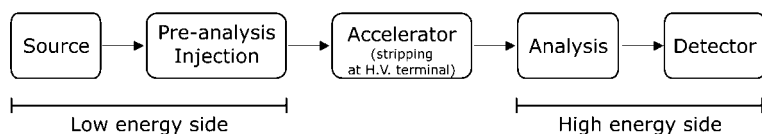


**Figure 16.1** Block diagram of AMS measurements with a tandem accelerator

such, but they are all dissociated into their atomic components, so that they are removed as isobars from the transmitted beam. Finally, the rare isotopes are counted in the detector: the relatively high energies of typical ion beams in AMS allow the use of detector systems that are usually employed in nuclear physics experiments, like, for example,  $\Delta E$ - $E$  telescopes, thus introducing a further possible filter.

In this way, it is possible to reach an extremely high selective sensitivity down to 1 part in  $10^{15}$ , which in  $^{14}\text{C}$  dating corresponds to being able to date samples about 50 000 years old. Moreover, modern systems can measure isotopic ratios in modern carbon, both  $^{14}\text{C}/^{12}\text{C}$  and  $^{13}\text{C}/^{12}\text{C}$ , with an ultimate precision as good as 2‰ and 1‰, respectively. The former value corresponds to determining the conventional radiocarbon age with an absolute error, smaller than in the past, better than  $\pm 20$  years, while the 1‰ precision for the  $^{13}\text{C}/^{12}\text{C}$  allows an adequate correction for isotopic fractionation effects. Even in routine measurements, at least in the case of historical samples, a precision of 5‰ in the  $^{14}\text{C}/^{12}\text{C}$  measured value is standard, corresponding to an uncertainty in the radiocarbon age of  $\pm 40$  years.[27]

### 16.2.2 Properties of Electromagnetic Filters Used in AMS

The most well known filter used in mass spectrometry, and also in AMS, is the magnetic one. The motion of a charged particle in a magnetic field is driven by the Lorentz force: when passing through a uniform magnetic field  $B$  normal to the plane of motion, a particle characterized by a charge  $q$ , a mass  $m$  and an energy  $E$  will follow a circular trajectory with a curvature radius  $r$  equal to:

$$r = \frac{1}{B} \sqrt{\frac{2mE}{q^2}} \quad (16.4)$$

Using such a filter, by fixing the geometry of the magnet, i.e. the dimension  $r$  and the intensity of the magnetic field  $B$ , it is possible to discriminate particles with the same charge and energy according to their mass.

Another kind of filter is based on the transit of the charged particles through a region where a uniform transverse electric field is applied: the electrostatic analyser (ESA). The ESA consists of two concentric cylindrical or spherical electrodes, between which a potential difference is applied. The trajectory of the ions inside the ESA, i.e. the allowed bending radius  $r$ , is of course fixed by the construction geometry; so, changing the applied voltage to the plates (i.e. changing the electric field  $\mathcal{E}$ ), one can select the particles with a certain ratio of energy to charge  $E/q$ . In the simplifying assumption of parallel electrodes, the ion path inside the electrostatic analyser can be described according to the equation:

$$\frac{E}{q} = \frac{1}{2} r \mathcal{E} \quad (16.5)$$

A filter that combines both a magnetic and electric field is the so-called Wien filter (or velocity filter). In this case, charged ions pass through a region characterized by uniform magnetic and electric fields at right angles to each other and to the direction of incident ions: only those particles for which the module of the Lorentz

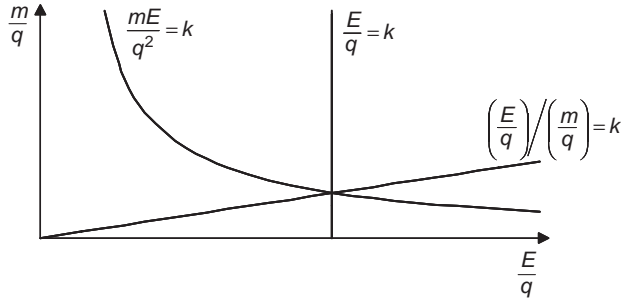


**Figure 16.2** Loci of values of  $\frac{m}{q}$  vs  $\frac{E}{q}$  as determined by different beam filters:  $\frac{mE}{q^2} = k$  identifies the magnetic analyser,  $\frac{E}{q} = k$  the ESA and  $\left(\frac{E}{q}\right) / \left(\frac{m}{q}\right) = k$  the Wien filter

force is equal and opposite to that of the electrostatic force are transmitted in a straight direction beyond this filter. Varying the intensity of the magnetic field  $B$  and the electric field  $\mathcal{E}$ , the transmitted particles are selected according to:

$$\left(\frac{\mathcal{E}}{B}\right)^2 = 2 \frac{E}{m} \quad (16.6)$$

where  $E$  and  $m$  are the energy and the mass of the ions, respectively.

In tandem-based AMS systems, analysis on both low and high energy sides is typically performed by coupling at least two of the described filters. The reason can be easily understood by looking at Figure 16.2, where the loci of values of  $\frac{m}{q}$  vs  $\frac{E}{q}$  as determined by different beam analysers are represented.

Each of the described filters only selects a group of ions with the right combination of mass, charge and energy. Thus, if we want to suppress the presence of interfering components, we can use two different filters at least in order to transmit only those particles with the characteristics represented by the intersection point of the curves drawn in Figure 16.2.

Following this overview on the main features of AMS and the properties of the beam analysers, in the following section the experimental apparatus will be described in detail. In particular, an AMS system based on the use of a tandem accelerator will be considered as reference.

### 16.3 AMS Measurements with a Tandem Accelerator

The general scheme of an AMS beam line installed in a tandem accelerator has already been represented in Figure 16.1. As an example of one of these systems, Figure 16.3 shows the layout of the AMS facility at the LABEC laboratory in Florence,[28] where a 3 MV tandem accelerator by High Voltage Engineering Europe (HVEE) is installed.

The scheme is useful as the starting point for the detailed description of the different components along the beam line.

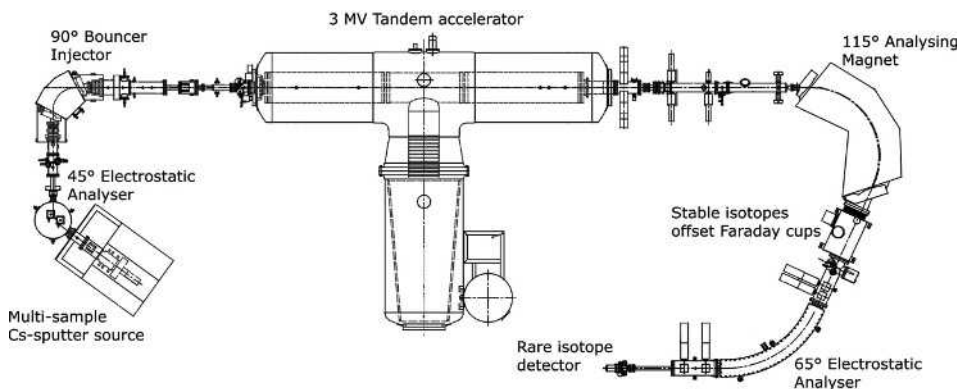


**Figure 16.3** Schematic layout of the AMS beam line at LABEC in Florence. Note that the system is also equipped with two independent ion sources dedicated to Ion Beam Analysis and with a switching magnet with six measurements beam lines (not shown)

### 16.3.1 Ion Source

As already mentioned, particles have to be injected in a tandem accelerator as negative ions. Thus, an ion source suitable for AMS has to produce negative ions, with high intensity and efficiency (since the abundance of the rare isotope is very low), a small emittance (in order to achieve a good transmission along the beam line up to the final detector) and with a low memory effect (since a wide range of rare isotope concentration ratios can be measured in sequence, in different samples, within the same run).[29] The most used source fulfilling the above requirements is a caesium sputtering source,[30,31] where the desired particles (in the case of a  $^{14}\text{C}$  measurement, carbon ions) are extracted from the measured sample by sputtering of low-energy heavy ions, i.e. caesium with energy normally less than 10 keV.

In this kind of source, samples are typically inserted as graphite pellets pressed in aluminium holders. By heating a reservoir containing caesium, caesium vapour is produced; this vapour diffuses into the source and comes into contact with the hot metal surface of the so-called ionizer; by thermal ionization caesium positive ions are formed. The concave (e.g. spherical) shape of the ionizer makes it possible to focus a caesium beam to a small spot on the surface of the sample,[32] which is just in the geometrical centre of the ionizer surface and is kept at a negative voltage with respect to it (for the latter reason the sample will be referred to as a 'cathode' in the following). Caesium ions bombard the sample graphite, sputtering some atoms and molecules that acquire a negative charge when passing the thin caesium layer that in the meanwhile is forming on the graphite surface; then the ions are extracted through a hole in the centre of the ionizer and focused by the appropriate electrostatic optics. The graphite target is at a negative potential to ground, which is the sum of an extraction voltage  $V_{ext}$  and a cathode voltage  $V_{cat}$ .  $V_{ext}$  can be usually adjusted in the range 0 to  $-30$  kV,  $V_{cat}$  in the range 0 to  $-10$  kV. Secondary electrons, mainly produced in the caesium beam bombardment, are suppressed by means of a pair of permanent magnets installed in the source housing.

An AMS ion source must also have the possibility to rapidly switch from one sample to another.[33] This can be achieved by putting all the samples in a wheel contained in a separate chamber of the source (see Figure 16.4). Then, for the measurement, each sample is picked from that wheel by a mechanical arm and pushed into the sputtering position.

Since the beginning of AMS, a possible limitation in the use of a caesium sputtering source for radiocarbon measurements has been considered to be the formation of craters on the sputtered graphite surface which alters the focusing of the extracted beam. This effect can be avoided by mounting the cathode housing on an  $x$ - $y$  movable stage. In this way, during sputtering, one can move the target with respect to the caesium beam and measurements are taken at slightly different positions of the cathode sample, thus also averaging over the whole surface.

In a particular range of applications, i.e. when samples of very small mass are dated, measuring with gaseous  $\text{CO}_2$  samples rather than with solid carbon samples can be advantageous.[34] For this purpose, caesium sputtering ion sources have been redesigned to allow for gaseous samples.[35,36] In these sources,  $\text{CO}_2$  is directly sprayed into vacuum and sputtered by a caesium beam. The required technology is however quite delicate: for example, particular arrangements must be followed to reduce possible cross contaminations and to obtain stable ion currents. Finally, another kind of gaseous ion source has to be mentioned:[37] a gas microwave plasma source fed with  $\text{CO}_2$  (in a mixture with an inert gas like argon). The development of these new gaseous sources is related to the development of a new branch of AMS: coupling gas chromatography with the accelerator, i.e. using the  $\text{CO}_2$  derived from combustion of the sample to feed directly the ion source of a tandem accelerator[38,39] (see also Section 16.4.2). This system is primarily paving the way for developments in environmental and biomedical investigations.



**Figure 16.4** View of the wheel holding several samples to be measured. The photograph is from the HVEE 846b source at the LABEC laboratory in Florence



### 16.3.2 Analysis on the Low Energy Side

After the source, the beam is composed of ions of all the fragments originating from the sputtering process (carbon isotopes, carbon hydride molecules, polyatomic carbon clusters, oxygen ions, etc.). Thus, some beam transport devices that can select the right particles are required:  $^{12}\text{C}$ ,  $^{13}\text{C}$  and  $^{14}\text{C}$  ions[40] with the right charge state and energy must be injected into the tandem accelerator. The filters used are those described in Section 16.2.2.

A typical configuration, often used in general-purpose AMS systems, is shown in Figure 16.3: an electrostatic analyser after the exit of the ion source followed by an injection magnet.

As discussed in the previous section, ions are extracted from the source by applying a potential  $V_{\text{ext}}$ . In principle, considering their charge state as fixed (usually  $q = -1$ ), all the particles should have the same energy  $E_{\text{inj}}$ , since  $E_{\text{inj}}$  is given by  $qV_{\text{ext}}$ . However, in practice, the extracted beam is not exactly monoenergetic: there can be some tails towards lower and higher energies due to the sputtering mechanism and to the break-up of molecules.[41] The ESA is used to suppress these tails, selecting only ions with the right energy by fixing the ratio  $E_{\text{inj}}/q$ .

The analysing magnet then selects the different masses (12, 13 and 14) to be injected into the accelerator, according to Equation (16.4). It is evident that, without changing the magnetic field  $B$ , the trajectories of the three carbon isotopes, having the same energy  $E = E_{\text{inj}}$  and charge  $q$  but different masses, are different. The radius of the trajectory is however fixed by geometry, thus some parameters should be changed to transmit alternatively all the masses. Changing the magnetic field is not convenient, because the operation cannot be very fast due to magnetic hysteresis. A solution to this problem is represented by keeping  $B$  fixed and changing the energy  $E$  of the three isotopes inside the magnet. This can be achieved by applying a proper voltage to the magnet chamber, which is kept electrically insulated with respect to the beam line upstream and downstream. By changing the applied voltage in sequence ('bouncing' system), one can select and inject the desired isotopes one after the other during cycles lasting typically some milliseconds. This is the so-called sequential injection.[42] The transitions between the voltages applied for the different isotope masses to be transmitted are not instantaneous (even though they are much faster than would be necessary to change the magnetic field): they are in the order of 0.1 ms. During transitions, in order to avoid introducing spurious particles into the accelerator, a 'blanking' voltage is usually applied to the beam: in this condition, the beam is completely deflected from the straight path. Time laps for the transmission of the three isotopes are chosen in such a way that  $^{14}\text{C}$  is transmitted for most of the time during each bouncing cycle. Thus, one can also decrease the  $^{12}\text{C}$  and  $^{13}\text{C}$  average beam intensities in the accelerator tubes by injecting these much more abundant masses for very small time intervals. In particular, the mass 12 beam is strongly reduced, being injected only for periods of the order of microseconds. Moreover, typically, a factor of 100 between the time intervals for mass 13 and mass 12 is chosen: in this way, as a consequence of the atomic ratio between the two stable isotopes, the average beam currents measured on the high energy side for  $^{12}\text{C}$  and  $^{13}\text{C}$  are approximately the same.

Another injection system used especially in radiocarbon-dedicated AMS facilities is based on the simultaneous transmission of two or more isotopes.[43] It is called a



recombinator and consists of a succession of analysing magnets: the first separates the different masses, which are finally recombined into one beam for injection into the tandem. Before recombination, the intensity of the most abundant isotopes is reduced by inserting on their path an attenuator such as a rotating slit or a fixed grid. In this configuration, particular attention must be paid to designing the magnets, in order to minimize beam aberrations.[44]

Before describing the next step in particle transmission through the beam line, the accelerator itself, it is worth remembering that, using either a sequential or a simultaneous injection, what is transmitted into the accelerator are not only the carbon isotopes  $^{12}\text{C}$ ,  $^{13}\text{C}$  and  $^{14}\text{C}$ , but also the molecular isobars, e.g.  $^{12}\text{CH}_2$  and  $^{13}\text{CH}$ , when injecting mass 14, and  $^{12}\text{CH}$ , when injecting mass 13. These interferences will be suppressed only at the high voltage terminal within the accelerator.

### 16.3.3 The Tandem Accelerator

A tandem is a kind of electrostatic accelerator where charged particles are accelerated in a static electric field in a process made up of two successive steps.[45] The accelerator tube is divided into two sections; between these two sections, the terminal is kept at high positive voltage (usually in the order of megavolts), while the extremities of the tube are kept at ground potential. In this way, when injected as negative ions, beam particles are accelerated to the high voltage terminal. Then, by passing through a medium like a gas or a foil, they undergo the so-called stripping process: several electrons are removed so that ions change their charge from negative to positive and are further accelerated to ground potential to the end of the accelerator tube. The advantage of using such an accelerator in AMS measurements lies in the fact that, with stripping, molecules are destroyed into their elemental components (especially if we consider final charge states greater than unity). Thus, molecular isobars in the mass-14 beam break into ions of stable isotopes of carbon and hydrogen, which are then accelerated in the second part of the tube as independent fragments. After the exit of the accelerator, they can be then removed by selecting ions of mass 14, a fixed value of charge, and energy given indeed by that value of charge and the terminal voltage.

The total energy  $E_{fin}$  acquired by the particles in a tandem can be written as:

$$E_{fin} = (E_{inj} + eV_T) \frac{m_i}{m_{tot}} + qeV_T \quad (16.7)$$

where  $E_{inj}$  is the energy the particles have before injection into the accelerator,  $e$  is the elementary charge,  $V_T$  is the terminal voltage,  $m_i$  is the mass of the positive ion after stripping, in the charge state  $q$ , and  $m_{tot}$  is the mass of the negative ion initially injected. For elemental ions, for example,  $^{14}\text{C}$  ions, of course  $m_i = m_{tot}$ , while this is not the case for the fragments of the molecular isobars after stripping, and this is the key point to separate them in the analysis at high energy.

The tandem accelerators installed in most of the laboratories worldwide have a maximum terminal voltage ranging from 1 to 8 MV. To keep these high voltages without sparking, accelerator tubes are mounted in a tank filled with high pressure insulating gas, e.g.  $\text{SF}_6$ . Two different systems are used to generate the high voltage at the terminal. One exploits the transmission of charge from ground to the terminal by a rotating belt made

of insulating rubber (as in the old Van de Graaff systems)[46] or, similarly, by a chain of metal pellets connected by insulating nylon links (as in the Pelletron systems[47] from National Electrostatic Corporation, NEC). The other is based on a cascade generator, working on the same principle as the Cockroft-Walton voltage multiplier. In this kind of accelerator (as in the Tandetron from HVEE), a solid-state radio frequency (RF) driver supplies power to an oscillator circuit, which is then capacitively coupled to a stack made of multiple stages of diodes that rectify the RF and multiply the initial signal.[48] In their traditional configuration, the power supply of the Tandetron is mounted in a separate leg of the tandem (see Figure 16.3). In new systems,[49] the solid state power supply has also been constructed around the high energy accelerator tube.

Stripping has been already mentioned as a fundamental process for particle acceleration. In the following some more details about this physical process are given. As a swift ion penetrates a target medium, it undergoes a large series of ion-electron collisions (electron-loss and electron-capture processes). When the medium is thicker than a so-called equilibrium thickness (about  $1 \mu\text{g cm}^{-2}$  in typical conditions for radiocarbon measurements),[50] the net effect is that particles will have lost some electrons, giving rise to a distribution of final charge states that depends on the atomic number and the velocity of the incident ions. For carbon ions with incoming energy at the terminal of 2–3 MeV and in equilibrium conditions, the most probable charge state after stripping ( $\sim 55\%$ ) is  $3+$ . Stripping efficiency can be slightly different whether a gas or solid medium is used. In AMS applications, a gas stripper (usually argon) is normally preferred, since a solid one, like a thin carbon foil, can be quickly damaged by radiation, reducing its thickness and thus changing the properties of the transmitted beam. A gas stripper consists of a narrow gas canal, open on both sides, in which argon gas is allowed to flow; the gas streaming out from the canal is then recirculated by a turbo molecular pump.[51]

Before continuing with the description of beam transport and analysis, the effect of passing through the tandem can be thus summarized in this way. After being accelerated, radiocarbon ions can be separated from fragments originated by break up of molecular isobars; this is possible, on the high energy side of tandem systems, by analysing only those  $^{14}\text{C}$  ions with  $3+$  charge state (the most probable charge state in typical conditions) and with an energy given by Equation (16.7).

### 16.3.4 Analysis on the High Energy Side

Analysis on the high energy side is of course performed by a combination of, at least, two of the already described electromagnetic filters. In Figure 16.3, a configuration consisting of a magnet followed by an electrostatic analyser is illustrated.

First, the magnet transmits  $^{14}\text{C}^{3+}$  ions, thus removing other masses and other charge states from the main beam. However, in the transmitted beam of  $^{14}\text{C}^{3+}$  there can still be a residual background of different atomic species with various combinations of mass, energies and charge states, due to the occurrence of charge-exchange processes outside the high voltage terminal, along the acceleration tubes. In fact, although being not very probable, these ‘undesired’ processes are possible and, involving particles that are much more abundant with respect to radiocarbon itself, lead to a non-negligible residual background in the transmitted beam, which, on the contrary, should nominally be composed of only  $^{14}\text{C}$ . This is the reason for the presence of another filter like the ESA.

The high energy analysing magnet is used also for measuring the abundance of the stable isotopes  $^{12}\text{C}$  and  $^{13}\text{C}$ . Ions of  $^{12}\text{C}$  and  $^{13}\text{C}$  injected during their relative time intervals of the bouncing sequence (see above), and having after the overall acceleration process the same charge and energy of the selected  $^{14}\text{C}^{3+}$  ions, have obviously different trajectories inside the high energy magnet. However, if the exit port of the high energy magnet is wide enough, they can be transmitted and intercepted by offset Faraday cups to measure their current, proportional to their abundances in the sample sputtered in the source.

The final stage in measuring  $^{14}\text{C}$  ions is represented by counting them in a detector, which can be used either as a simple counter, at least in the case of radiocarbon, or as a further filter (e.g. implementing  $\Delta E$ - $E$  measurements). A typical detector used in these applications is an ionization chamber.[52] This detector is constituted by a chamber filled with gas, in which an electric field is applied between two electrodes. After passing through a thin entrance window (either a Mylar or a silicon nitride foil), particles enter the chamber and ionize the gas along their path, thus creating electron-positive ion pairs, that start moving towards, respectively, the anode and cathode. The number of created pairs is proportional to the energy of the incident particle. Collection of electrons at the anode gives rise to a voltage signal, whose amplitude is proportional to the energy of the particle. Signals are then amplified, converted into digital form to be acquired by a PC and represented in a spectrum. Counts in this spectrum represent the number of radiocarbon atoms in the measured sample. Sometimes, ionization chambers used in radiocarbon AMS measurements can have the anode divided into separate sections. In this way, on each anode, a signal corresponding to a fraction  $\Delta E$  of the total energy  $E$  of the ion is acquired. By representing the acquired signal in a plane  $\Delta E$  vs  $E$ , it is possible to discriminate whether residual interfering particles have reached the detector, despite all the previous magnetic and electrostatic analysis.

Figure 16.5 illustrates the suppression efficiency of undesired ions and the typical sensitivity in AMS radiocarbon measurements. In Figure 16.5a, beam currents measured by a Faraday cup before injection in the tandem as a function of the magnetic field set in the injection magnet are reported. We can notice the presence of many components: stable carbon isotopes,  $^{12}\text{C}$  and  $^{13}\text{C}$ , oxygen ( $^{16}\text{O}$ ), different hydrides ( $^{13}\text{CH}$ ,  $^{16}\text{OH}$ ,  $^{24}\text{MgH}$ ), a diatomic carbon cluster ( $^{12}\text{C}_2$ ), and others. In the used scale, the signal of mass 14 is not appreciable. Figure 16.5b shows the results of scanning the magnetic field of the analysing magnet on the high energy side during the injection into the accelerator of only mass 14: currents measured by a Faraday cup on the straight path after the exit of the magnet are reported. The signal due to  $^{14}\text{C}^{3+}$  at the 'right' value of  $B$  is still not detectable due to the low sensitivity of the Faraday cup, but it is interesting to notice the presence of two signals due to  $^{12}\text{C}^{3+}$  and  $^{13}\text{C}^{3+}$  of lower energy, derived from the molecular isobars, injected together with radiocarbon, broken at the tandem terminal. The importance of stripping in drastically reducing molecular isobar interference is thus evident. Finally, Figure 16.5c shows the spectrum obtained by acquiring the  $\Delta E$  signal from an ionization chamber used as detector. The area of the peak in the spectrum represents the number of  $^{14}\text{C}^{3+}$  ions extracted from the sample in the source.

In this example, as in many facilities, the final detector is simply used to count the particles. When this is the case, solid state detectors, like silicon surface barrier ones, can also be used.

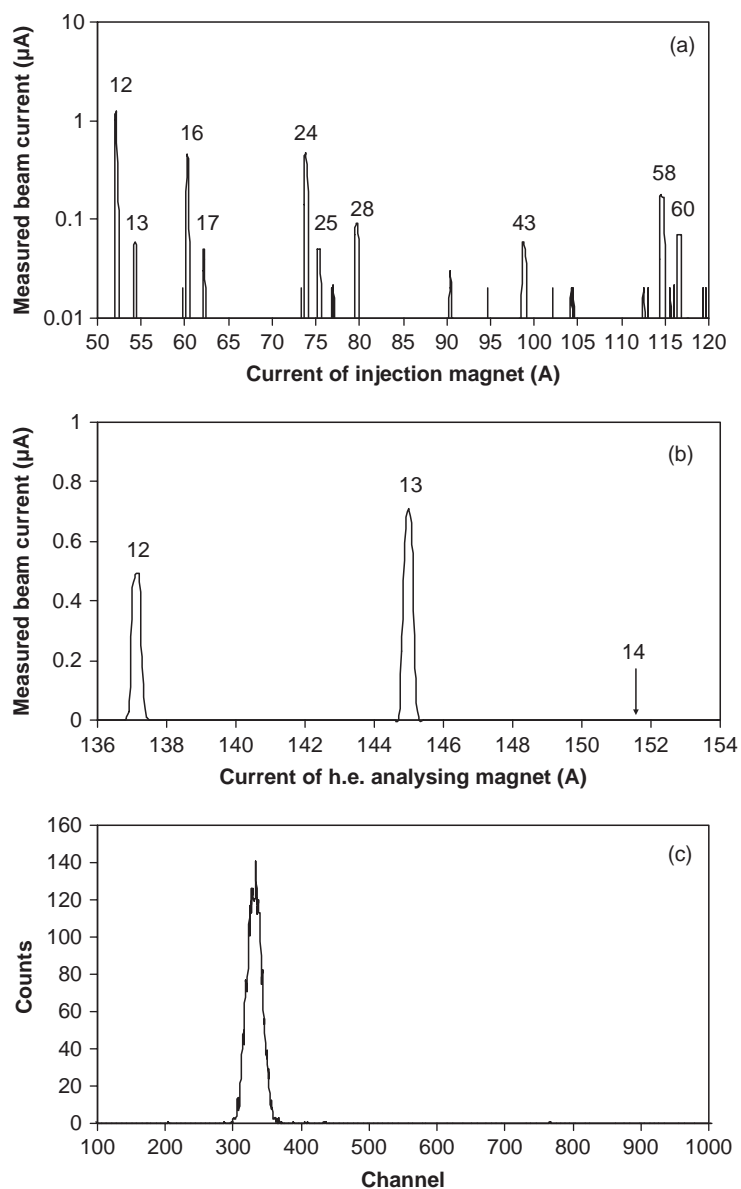


**Figure 16.5** Ion beam components in an AMS radiocarbon measurement: (a) beam currents measured by a Faraday cup before injection in the tandem as a function of the magnetic field set in the injection magnet; transmitted mass is indicated for each of the main peaks; (b) scanning of the magnetic field of the analysing magnet on the high energy (h. e.) side; signals due to fragments of mass-14 molecular isobars are present; (c)  $^{14}\text{C}$  spectrum obtained by acquiring the  $\Delta E$  signal from an ionization chamber used as detector

### 16.3.5 New Perspectives: Low Voltage Machines and ‘Single-stage’ AMS Systems

Many of the radiocarbon AMS laboratories worldwide are based on accelerator systems whose characteristics are the typical ones presented in the previous sections. The most well known,[53] include the 3 MV Tandetron in Oxford, the 3 MV Pelletron at VERA in Vienna,[54] the 2.5 MV Tandetron in Groningen,[55] the 3 MV Tandetron at the Leibniz Labor in Kiel,[56] the 2 MV Tandetron STAR at ANSTO in Sidney,[57] the 2.5 MV Tandetron and the 3 MV Pelletron at the NSF-Arizona AMS laboratory in Tucson,[58] and the two Tandetrons at the Nagoya University Center for Chronological Research in Japan.[59] Other facilities are based on higher terminal voltage accelerators[60].

However, the most significant development in recent years has been represented by the trend towards smaller facilities based on smaller accelerators. The work done at ETH in Zurich on the study of stripping yields, molecular dissociation and detection efficiency at low energies has led to the development of systems based on low voltage tandem machines; they have demonstrated that  $^{14}\text{C}$  measurement is also possible using 500 kV or even 200 kV accelerators.[61,62] The main advantage in the use of dedicated  $^{14}\text{C}$  smaller accelerators is the reduced space requirements:[63] for example, while the 3 MV VERA facility covers an area of  $192\text{ m}^2$ , the compact 500 kV AMS system at the Poznan Radiocarbon Laboratory in Poland covers an area of  $30\text{ m}^2$  and the 200 kV MICADAS system in Zurich only about  $7\text{ m}^2$ .

Another interesting development is represented by the introduction (by NEC) of a new kind of AMS system based on single stage machines:[64] the ion source and low energy side spectrometer are at ground potential, and the stripper and high energy spectrometer are mounted on a 250 kV deck. Actually, in these systems, particles, which are injected as negative ions, are no further accelerated after stripping. The main advantage of these single stage systems is that the high voltage components do not need an insulated tank but are simply mounted on an open air platform. The performance of this kind of facility (5‰ precision in  $^{14}\text{C}/^{12}\text{C}$  measurements and a background of less than 0.5% modern) is a little worse than what is achieved by traditional systems but it is however suitable for routine measurements in many applications.

## 16.4 AMS Radiocarbon Sample Preparation

A radiocarbon AMS measurement cannot occur without previous treatment or preparation of the sample to be dated.

Any possible contamination has to be removed. Carbon is everywhere, so there is always the possibility that the dated find had exchanged carbon with the external environment after the death of the organism. In this way any sample might have a non-endogenous carbon fraction, which might be ‘dead’ (with only stable carbon) or ‘modern’ (rich in  $^{14}\text{C}$ ). Thus the measured age might appear different from the real value, i.e. older in the case of dead carbon contamination or younger in the case of modern carbon contamination. Possible contaminations can be either ‘natural’ or ‘anthropogenic’. As to natural sources, humic acids from the soil can contaminate a buried sample; calcium carbonate, such as limestone, can dissolve in ground water and so be deposited within a sample. A possible

reason for anthropogenic contamination is that historical objects might have been preserved from degradation using organic compounds such as resins and waxes.

Removal of all possible contaminants is not the only reason for sample preparation, since each clean and purified material has then to be converted into the chemical form suitable for the accelerator ion source. In most cases (as explained in the previous section), samples are put into the caesium sputtering source as graphite, solid elemental carbon, and for this reason samples are first burnt and then chemically reduced to graphite.

Radiocarbon sample preparation can thus be divided into three different steps:

- physical and chemical pretreatment;
- combustion, i.e. conversion of the purified sample to gaseous  $\text{CO}_2$ ;
- graphitization, i.e. reduction of the  $\text{CO}_2$  to solid graphite.

In all these processes, however, when manipulating samples, there may be the risk of the operator introducing some spurious carbon. To take this effect into account, samples of certified  $^{14}\text{C}$  concentration[65] and of dead carbon are also prepared and then measured together with the unknown samples, hence making it possible to evaluate and correct for possible systematic errors due to unwanted carbon contamination during sample preparation.

#### 16.4.1 Physical and Chemical Pretreatment of Samples

During the pretreatment phase, contaminants are removed. Moreover, for some kinds of samples, a further treatment is needed: as a matter of fact, in some cases, not all the organic fraction can be used, but the one most suitable for dating has to be extracted. This is the case, for example, for bone.[66] A bone is made of two fractions, both of them including carbon: the organic protein of collagen and an inorganic compound primarily made of hydroxyapatite and calcium carbonate. In principle, the latter component contains carbon originally in equilibrium with the biosphere and might be used for dating; in practice, however, it is completely unsuitable, since it might be contaminated by dead calcium carbonate due to percolating groundwater, and there would be no way to chemically separate this spurious contribution from the overall calcium carbonate content. Thus, in this case, chemical pretreatment aims to separate collagen, or even a particular fraction of the protein.

The choice of the right strategy in sample pretreatment strongly depends on the material, thus it is impossible to describe it here in detail. The idea is however general: first of all, if they are supposed to be contaminated, sample external layers are usually mechanically removed using simple tools such as tweezers or scalpels. Sometimes the sample is then crushed to increase the surface area before further treatment, which involves an appropriate chemical attack by acids and bases. The chemical pretreatment employed usually follows the guidelines of the so-called ABA (acid-base-acid) treatment.[67] Samples are first washed in a diluted aqueous solution of hydrochloric acid to dissolve any spurious carbon, typically present as calcium carbonate; the chemical reaction of  $\text{CaCO}_3$  with  $\text{HCl}$  produces gaseous  $\text{CO}_2$  that simply leaves the solution by bubbling out. Then a diluted sodium hydroxide solution is added to the sample in order to remove possible humic acids. Since, during this bath, atmospheric  $\text{CO}_2$  can dissolve in the solution (and this carbon can also be incorporated into the sample structure as carbonate), hydrochloric acid is then added again

to remove this contamination. The ABA method is applied, for example, in many cases as a pretreatment of charcoal, wood, peat and textiles. In dealing with textiles, a slightly different situation occurs when treating wool samples. The main component of wool is the protein keratin that is partially soluble in alkaline solutions; thus, in this case, ABA treatment has to be modified in order to preserve the integrity of the sample to be dated.

### 16.4.2 Combustion and Graphitization of Samples

After cleaning samples, as already mentioned, the most common approach is to convert the carbon in the samples to  $\text{CO}_2$  by combustion and then to carbon by chemical reaction.

When any organic material is combusted, not only  $\text{CO}_2$  is produced but also nitrogen, water and sulfur compounds, all derived from oxidation of elements present in the samples. Two methods for combustion, 'slow' and 'fast', are used in laboratories. In 'slow' combustion,[68] the sample is inserted in a quartz vial together with grains of pure copper oxide and a silver wire. The vial is then evacuated, sealed and heated in a muffle furnace at about  $900^\circ\text{C}$  for usually 4 h. During heating, the oxygen coming from  $\text{CuO}$  oxidizes carbon in the sample to  $\text{CO}_2$  and the silver wire acts as a binder for the sulfur and the halogens formed in the combustion and that, if still present, may inhibit the following reaction of graphitization. When combustion is completed, gases are transferred to the apparatus used for graphitization. This apparatus is, to a first approximation, a previously evacuated line where the graphitization reaction occurs. The transferred gas is of course a mixture of all the oxides and the elements originating in the combustion and has to be purified to only  $\text{CO}_2$  before going on with graphitization. For this purpose, for example, removing water vapour is possible by using a trap made of dry ice and isopropanol.

The 'fast' combustion method is based on the use of an elemental analyser.[69] In such a system, samples are burnt in a few tenths of a second due to the mechanism of high temperature flash combustion; then  $\text{CO}_2$  is separated from the other gases by exploiting the differences in retention times in passing through a gas chromatographic column. Collection of pure  $\text{CO}_2$  in the graphitization line is thus achieved by connecting the output of the elemental analyser to the input of the line only for the time window during which  $\text{CO}_2$  is flowing out. This system enables us to avoid using different traps to purify the gas from combustion, even though some studies indicate the presence of small, although essentially negligible in many applications, memory effects in the gas chromatographic column.[70] The use of elemental analysers is increasing in radiocarbon laboratories worldwide and is developing a new philosophy for AMS measurements (as mentioned at the end of Section 16.3.1).

The successive step in sample preparation is graphitization. Several different reactions can be used. The most well known is probably the iron-catalysed reduction of the collected  $\text{CO}_2$  by reaction with hydrogen:[71]



The above reaction occurs in two different steps, with carbon monoxide ( $\text{CO}$ ) formed as an intermediate product. Temperature is a very important parameter: at temperatures higher than  $800^\circ\text{C}$ , there can be excess  $\text{CO}$  produced, while at temperatures lower than  $500^\circ\text{C}$ ,  $\text{CH}_4$  and other hydrocarbons are formed. In order to catalyse the reaction, finely powdered iron ( $\sim 10\ \mu\text{m}$ ) is usually used. Unless removed, the water produced may react



back with graphite thus inhibiting further production of graphite. For this reason, a section of the graphitization reactor is typically cooled down to a temperature low enough to condensate  $\text{H}_2\text{O}$  (but not  $\text{CO}_2$ ), either e.g. by Peltier-based cooling devices or mixed dry ice–isopropanol traps. As a result, according to reaction (16.8), carbon is produced over iron powder as filamentous graphite, which is eventually pressed to pellets to be inserted in the ion source.

Another graphitization method is based on the reduction of  $\text{CO}_2$  to CO by reaction with Zn (at high temperature) and the subsequent conversion of CO to carbon again by reaction with hydrogen. In most recent set-ups,[72] hydrogen is not inserted in the reaction vessel in its gaseous form but in a solid form as  $\text{TiH}_2$ . Also, in this case, during the second step of the reaction, graphite is finally deposited over a catalyst (either iron or cobalt powder).

## 16.5 Examples of Applications

The main advantage in measuring radiocarbon by AMS certainly relies on the fact that only very small quantities of material must be ‘sacrificed’ for analysis. To a good approximation, typical sample masses for AMS measurements are in the milligram range, three orders of magnitude less than typical masses needed for radiometric measurements (as reported in Table 16.1).

It is impossible to cite here all the radiocarbon AMS dating projects in which archaeologists, geologists and physicists are involved every year. Out of hundreds or thousands that we might call (of course, not in a pejorative sense) ‘routine’ cases, particular applications have sometimes come to the fore. One example is the case of the Turin Shroud. Three radiocarbon AMS laboratories (Tucson, Oxford and Zurich) were involved in the dating process.[73] A strip of the precious linen (about 150 mg) was sampled from the shroud and divided into three subsamples, which were sent to the three laboratories. Radiocarbon dated the samples to 1260–1390 AD, thus attributing the shroud to a medieval period and not to the period of Christ’s death. It is not the purpose of this chapter to comment on this result. It is however interesting to underline that the intercomparison between the three different laboratories, or even one single measurement, would have been impossible if the radiometric method was the only technique available to measure radiocarbon. The publication of the results caused passionate debates worldwide which are still ongoing.[74]

Another example taken from the archaeological and religious world was the dating of the Dead Sea Scrolls. The first scrolls were discovered in a cave in the Middle East, near Khirbet Qumran, in 1947. By the end of the archaeological campaign, about 800 manuscripts, written on papyrus or parchment, had been recovered. They were written in Hebrew and in Aramaic; palaeographic studies attributed them to the Essenes, one of the major religious movements of Judaism. The question of dating appeared to be of crucial importance from the beginning since the scrolls contained some texts from the Old Testament and also some ‘sectarians’ writings from the Essenes. Libby himself, in 1951, dated a linen wrapping of one of the first discovered scrolls. However, it was only with the introduction of AMS that dating material from the scrolls and not samples associated with them was finally possible.[75,76] Even though a few discrepancies were found, the results of radiocarbon dating essentially confirmed palaeographic considerations. However, also in



this case,  $^{14}\text{C}$  results have led to polemics and discussion.[77] Without entering the debate in depth, it is worthwhile stating that this is a clear example that in many cases, e.g. when manuscripts or works of art like paintings are involved,  $^{14}\text{C}$  can give information on when the support was prepared and not necessarily when it was used to produce the object itself.

The case of Oetzi (or the Iceman), the frozen mummy found in 1991 on the Alps on the border between Austria and Italy and now kept at the Archaeological Museum of Bolzano (Italy), is also well known. AMS radiocarbon measurements from the laboratories of Zurich[78] and Oxford[79] on tissue and bone samples from the Iceman dated him to  $4550 \pm 19$  years BP. When calibrated, this radiocarbon age corresponds to three probable calendar time intervals between 3350 BC and 3100 BC. Consistent measurements were obtained by dating some of his equipment and also botanic remains from the discovery site.[80] In this context, it is important to note that dating of Oetzi represents a good example of the relevance of the behaviour of the calibration curve in the final precision of a radiocarbon measurement. Actually, in this case, despite a very high precision of the radiocarbon age ( $\pm 19$  years), the special trend in the calibration curve around the dated period, i.e. in particular the so-called wiggles, prevents a more exact and unambiguous absolute age determination.

This occurrence is not so unusual in  $^{14}\text{C}$  dating. As an additional example, an application performed at the LABEC laboratory in Florence (see Figure 16.3) can be cited.[81] This example involves both history of art and religion as some of the relics traditionally associated with St Francis (the patron saint of Italy) were dated. Several samples taken from two woollen frocks (one kept in the church of St. Francis in Cortona, Tuscany, Italy, and the other kept in the Basilica of Santa Croce in Florence) and two samples from two of the inner cases of a pillow (also kept in Cortona) were dated. The goal of this study not only focused on the determination of the authenticity of the relics but was also aimed at defining a correct strategy for sampling. Samples were taken following the advice of a textile conservator in order to collect the material from areas safely judged to be representative; even though no darn or patches were present, more pieces were sampled from each frock, since both consisted of several woollen cloths sewn together. In this way, it was possible to compare data from several samples of the same macroscopic object, providing a check of self-consistency and thus reducing the possibility of ambiguities. It should be stressed again that this kind of sampling strategy can be applied due to the small quantities of material needed in AMS measurements (in this case about 10 mg per sample). Samples from the Cortona frock were all consistent with one another, and also with samples from the pillow and with a sample taken from the belt kept with the Santa Croce frock. Samples from the Santa Croce frock were also consistent with one another, but not with those from the Cortona frock. Figure 16.6 summarizes the results: it shows the calibrations of the radiocarbon ages of the two frocks (each calculated as weighted average of the samples taken from that frock). The frock from Cortona, and similarly the pillow and the belt from Santa Croce, are dated to a period that is compatible with the life of St Francis. In contrast, the frock from Santa Croce is dated to a more recent period. It is interesting to note that, also in this case, a very good precision in the determination of the radiocarbon age ( $\pm 18$  years) does not provide a correspondingly accurate calendar date: for the Santa Croce frock, the calibration of the radiocarbon age gives as a result two almost equally probable but well separated calendar ranges, 1285–1300 and 1365–1385, at  $1\sigma$  confidence level. From the data of these measurements, we can conclude that, apart from the merit of the

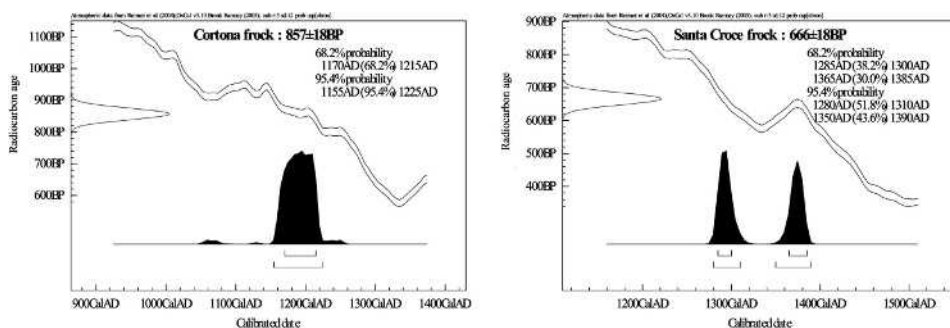


**Figure 16.6** Calibration of the radiocarbon ages of the Cortona and Santa Croce frocks; the software used[83] is OxCal v.3.10. Radiocarbon age is represented on the y-axis as a random variable normally distributed; experimental error of radiocarbon age is taken as the sigma of the Gaussian distribution. Calibration of the radiocarbon age gives a distribution of probability that can no longer be described by a well defined mathematical form; it is displayed in the graph as a dark area on the x-axis

results,  $^{14}\text{C}$  and AMS have helped to study the relics in their historical context. Even the dating of the Santa Croce frock can be valuable for the reconstruction of the history of religion during the Middle Ages.

Besides being used in many applications involving historical problems, as in the examples shown above, radiocarbon has been successfully employed in the study of prehistory, where it represents the main source of time perspective. AMS in particular has helped in extending the possibility of  $^{14}\text{C}$ . For example, radiocarbon dating of single seeds, only possible by AMS, has contributed to the study of the beginnings of agriculture.[82]

The cited examples provide evidence of how strong the connection between  $^{14}\text{C}$  and archaeology and art is and prove that AMS is now a well established (but still developing) technique, not just restricted to the world of physicists and technicians.

## References

1. M.J. Aitken, *Science Based Dating in Archaeology*, Longman, London and New York (1990).
2. J.R. Arnold and W.F. Libby, Age determination by radiocarbon content: check with samples of known age, *Science* **110**, 678–680 (1949).
3. W.F. Libby, Atmospheric helium three and radiocarbon from cosmic radiation, *Phys. Rev.* **69**, 671–672 (1946).
4. Both the presentation speech and the Libby Nobel lecture can be found on the official Nobel Prize web site: <http://nobelprize.org/index.html>.
5. Most of the relevant literature about radiocarbon can be found in the scientific publication *Radiocarbon*, edited by the University of Arizona since 1959 (<http://www.radiocarbon.org>).
6. S. Bowman, *Radiocarbon Dating (Interpreting the Past Series)*, University of California Press and British Museum, London (1990).
7. S.A. Korff and R.B. Mendell, Variations in radiocarbon production in the Earth's atmosphere, *Radiocarbon* **22**, 159–165 (1980).
8. H. Godwin, Half life of radiocarbon, *Nature* **195**, 984 (1962).

9. M. Stuiver and H.A. Polach, Discussion: reporting of  $^{14}\text{C}$  data, *Radiocarbon* **19**, 355–363 (1977).
10. H.E. Suess, Secular variations of cosmogenic  $^{14}\text{C}$  on earth; their discovery and interpretation, *Radiocarbon* **28**, 259–265 (1986).
11. P.J. Reimer, M.G.L. Baillie, E. Bard, A. Bayliss, J.W. Beck, C.J.H. Bertrand, P.G. Blackwell, C.E. Buck, G.S. Burr, K.B. Cutler, P.E. Damon, R.L. Edwards, R.G. Fairbanks, M. Friedrich, T.P. Guilderson, A.G. Hogg, K.A. Hughen, B. Kromer, G. McCormac, S. Manning, C. Bronk Ramsey, R.W. Reimer, S. Remmele, J.R. Southon, M. Stuiver, S. Talamo, F. W. Taylor, J. van der Plicht and C.E. Weyhenmeyer, IntCal04 terrestrial radiocarbon age calibration, 0–26 cal kyr BP, *Radiocarbon* **46**, 1029–1058 (2004).
12. K.A. Hughen, M.G. L. Baillie, E. Bard, J.W. Beck, C.J.H. Bertrand, P.G. Blackwell, C.E. Buck, G.S. Burr, K.B. Cutler, P.E. Damon, R.L. Edwards, R.G. Fairbanks, M. Friedrich, T.P. Guilderson, B. Kromer, G. McCormac, S. Manning, C. Bronk Ramsey, P.J. Reimer, R.W. Reimer, S. Remmele, J.R. Southon, M. Stuiver, S. Talamo, F.W. Taylor, J. van der Plicht and C.E. Weyhenmeyer, Marine04 marine radiocarbon age calibration, 0–26 cal kyr BP, *Radiocarbon* **46**, 1059–1086 (2004).
13. R.C. Finkel and M. Suter, AMS in the Earth Sciences: techniques and applications, *Adv. Anal. Geochem.* **1**, 1–114 (1993).
14. H.A. Polach, Evaluation and status of liquid scintillation counting for radiocarbon dating, *Radiocarbon* **29**, 1–11 (1987); H.A. Polach, Liquid scintillation C-14 spectrometry: errors and assurances, *Radiocarbon* **31**, 327–331 (1989).
15. It is important to keep in mind that a radiocarbon measurement would also be destructive if mass spectrometry was applicable.
16. As mentioned in the Introduction, almost all natural carbon on Earth is represented by the isotope  $^{12}\text{C}$ , thus the concentration  $^{14}\text{R}$  can be defined as the ratio between the number of atoms of  $^{14}\text{C}$  and atoms of  $^{12}\text{C}$ .
17. C. Tuniz, Accelerator mass spectrometry: ultra-sensitive analysis for global science, *Rad. Phys. Chem.* **61**, 317–322 (2001).
18. See for example, from the 19th International Radiocarbon Conference held in 2006: A.G. Hogg, L.K. Fifield, J.G. Palmer, C.S.M. Turney and R. Galbrait, Robust radiocarbon dating of wood samples by high sensitivity liquid scintillation spectroscopy in the 50–70 kyr age range, *Radiocarbon* **49**, 379–391 (2007).
19. R. Muller, Radioisotope dating with a cyclotron, *Science* **196**, 489 (1977).
20. D.E. Nelson, R.G. Korteling and W.R. Stott, Carbon-14: direct detection at natural concentrations, *Science* **198**, 507–508 (1977).
21. C.L. Bennett, R.P. Beukens, M. R. Clover, H.E. Gove, R. B. Liebert, A.E. Litherland, K.H. Purser and W.E. Sondheim, Radiocarbon dating using electrostatic accelerators: negative ions provide the key, *Science* **198**, 508–510 (1977).
22. R.E. Taylor, History of radiocarbon dating, lecture presented at *Radiocarbon in ecology and earth system science* (<http://ecology/botany/ufl/radiocarbon07/>), University of California, Irvine (2006). (The first radiocarbon revolution is represented by the development of the dating method by Libby and his colleagues; the second radiocarbon revolution is considered to be the introduction of calibration.)
23. R.E. Taylor, Fifty years of radiocarbon dating, *Am. Sci.* **88**, 60–64 (2000).
24. K.H. Purser, R.B. Liebert and C.J. Russo, MACS: an accelerator-based radioisotope measuring system, *Radiocarbon* **22**, 794–806 (1980).
25. C. Tuniz, J.R. Bird, D. Fink and G.F. Herzog, *Accelerator Mass Spectrometry: Ultrasensitive Analysis for Global Science*, CRC Press, Boca Raton (1998).
26. R. Middleton, *A Negative Ion Cookbook*, Department of Physics, University of Pennsylvania, Pittsburgh (1990).
27. It is important to remember that sometimes, in spite of the excellent performances of an AMS measurement, the final uncertainty on the true calendar age of a sample is a function of the behaviour of the calibration curve in that time interval: a small error on the radiocarbon age does not necessarily correspond to a small, or a unique, calendar span on the BC/AD axis.
28. M.E. Fedi, A. Cartocci, M. Manetti, F. Taccetti and P.A. Mandò, The  $^{14}\text{C}$  AMS facility at LABEC, Florence, *Nucl. Instrum. Methods B* **259**, 18–22 (2007).

29. L.R. Kilius, W.E. Kieser, A.E. Litherland, X.L. Zhao, J.C. Rucklidge and R.P. Beukens, Ion source design criteria for AMS, *Nucl. Instrum. Methods B* **123**, 5–9 (1997).
30. R. Middleton, A review of ion sources for accelerator mass spectrometry, *Nucl. Instrum. Methods B* **5**, 193–199 (1984).
31. G.D. Alton, Recent advancements in high intensity heavy negative ion sources based on sputter principle, *Nucl. Instrum. and Methods A* **287**, 139–149 (1990).
32. B.X. Han, J.R. Southon, M.L. Roberts and K.F. von Reden, Computer simulation of MC-SNICS for performance improvements, *Nucl. Instrum. Methods B* **261**, 588–593 (2007).
33. I.D. Proctor, J.R. Southon, M.L. Roberts, J.C. Davis, D.W. Heikkinen, T.L. Moore, J.L. Garibaldi and T.A. Zimmerman, The LLNL ion source – past, present and future, *Nucl. Instrum. Methods B* **52**, 334–347 (1990).
34. The reasons will be clearer after Section 16.4, where AMS radiocarbon sample preparation procedures will be described. Now we would simply like to recall that in preparing graphite pellets for the sputtering source, after a physical-chemical cleaning, samples to be dated are usually combusted to obtain CO<sub>2</sub>, which is then converted to graphite by a further step. In this process, the main problem with small samples (a few tens of micrograms) is the possible introduction of contamination.
35. C. Bronk Ramsey and R.E.M. Hedges, Carbon dioxide sputter source development at Oxford, *Nucl. Instrum. Methods B* **92**, 100–104 (1994).
36. C. Bronk Ramsey, P. Ditchfield and M. Humm, Using a gas ion source for radiocarbon AMS and GC-AMS, *Radiocarbon* **46**, 25–32 (2004).
37. M.L. Roberts, R.J. Schneider, K.F. von Reden, J.S.C. Wills, B.X. Han, J.M. Hayes, B.E. Rosenheim and W.J. Jenkins, Progress on a gas-accepting ion source for continuous-flow accelerator mass spectrometry, *Nucl. Instrum. Methods B* **259**, 83–87 (2007).
38. A. Rottenbach, T. Uhl, A. Hain, A. Scharf, K. Kritzer and W. Kretschmer, Development of a fraction collector for coupling gas chromatography with an AMS facility, *Nucl. Instrum. Methods B* **266**, 2238–2241 (2008).
39. K.F. von Reden, M.L. Roberts, W.J. Jenkins, B.E. Rosenheim, A.P. McNichol and R.J. Schneider, Software development for continuous-gas-flow AMS, *Nucl. Instrum. Methods B* **266**, 2233–2237 (2008).
40. The measurement of both <sup>14</sup>C and <sup>12</sup>C is necessary to estimate the radiocarbon age on the basis of the isotopic ratio <sup>14</sup>R; measuring <sup>13</sup>C allows us to evaluate the effects of isotopic fractionation, according to which the measured radiocarbon concentration can be corrected. For details, see Aitken.<sup>1</sup>
41. A.E. Litherland, Accelerator mass spectrometry, *Nucl. Instrum. Methods B* **5**, 100–108 (1984).
42. M. Klein, D.J.W. Mous and A. Gott dang, Fast and accurate sequential injection AMS with gated Faraday cup current measurement, *Radiocarbon* **46**, 77–82 (2004).
43. A. E. Litherland and L. R. Kilius, A recombinator for radiocarbon accelerator mass spectrometry, *Nucl. Instrum. Methods B* **52**, 375–377 (1990).
44. R.J. Schneider, K.F. von Reden and K.H. Purser, A triple-isotope injector for accelerator mass spectrometry, *Particle Accelerator Conference, 1991, Accelerator Science and Technology, Conference Record of the 1991 IEEE*, 878–880 (1991).
45. F. Hinterberger, Electrostatic accelerators, in *Proceedings of CERN Accelerator School and KVI: Specialised CAS Course on Small Accelerator*, D. Brandt (Ed.), CERN, Geneva, CERN 2006-012, 95–112 (2006).
46. R.J. Van de Graaff, K.T. Compton and L.C. Van Atta, The electrostatic production of high voltage for nuclear investigations, *Phys. Rev.* **43**, 149–157 (1933).
47. R.G. Herb, Pelletron accelerators for very high voltage, *Nucl. Instrum. Methods* **122**, 267–276 (1974).
48. D.J. W. Mous, R. Koudijs, P. Dubbelman and H.A.P. van Oosterhout, The HVEE Tandetron Line; new developments and design considerations, *Nucl. Instrum. Methods B* **62**, 421–424 (1992).
49. A. Gott dang, D.J.W. Mous and R.G. Haitsma, The novel HVEE 5 MV Tandetron, *Nucl. Instrum. Methods B* **190**, 177–182 (2002).
50. H. J. Hofmann, G. Bonani, M. Suter and W. Wölfl, Charge state distributions and isotopic fractionation, *Nucl. Instrum. Methods B* **29**, 100–104 (1987).

51. G. Bonani, P. Eberhardt, H.J. Hofmann, Th.R. Niklaus, M. Suter, H.A. Synal and W. Wölfli, Efficiency improvements with a new stripper design, *Nucl. Instrum. Methods B* **52**, 338–344 (1990).
52. G.F. Knoll, *Radiation Detection and Measurement*, John Wiley & Sons, Ltd, New York (2000).
53. The list is not intended to be exhaustive, but it simply gives examples of AMS facilities especially involved in applications of radiocarbon dating to art and archaeology. A complete list of laboratories worldwide can be found at: <http://www.radiocarbon.org>.
54. P. Steier, R. Golser, W. Kutschera, A. Priller, C. Vockenhuber and S. Winkler, VERA, an AMS facility for 'all' isotopes, *Nucl. Instrum. Methods B* **223–224**, 67–71 (2004).
55. J. van der Plicht, S. Wijma, A.T. Aerts, M.H. Pertuisot and H.A.J. Meijer, Status report: The Groningen AMS facility, *Nucl. Instrum. Methods B* **172**, 58–67 (2000).
56. M.J. Nadeau, M. Schleicher, P.M. Grootes, H. Erlenkeuser, A. Gott dang, D.J.W. Mous, J.M. Sarnthein and H. Willkomm, The Leibniz-Labor AMS facility at the Christian-Albrechts University, Kiel, Germany, *Nucl. Instrum. Methods B* **123**, 22–30 (1997).
57. D. Fink, M. Hotchkis, Q. Hua, G. Jacobsen, A. M. Smith, U. Zoppi, D. Child, C. Mifsud, H. van der Gaast, A. Williams and M. Williams, The ANTARES AMS facility at ANSTO, *Nucl. Instrum. Methods B* **223–224**, 109–115 (2004).
58. D. J. Donahue, J. W. Beck, D. Biddulph, G.S. Burr, C. Courtney, P.E. Damon, A.L. Hatheway, L. Hewitt, A.J.T. Jull, T. Lange, N. Lifton, R. Maddock, L.R. McHargue, J.M. O'Malley and L.J. Toolin, Status of the NSF-Arizona AMS laboratory, *Nucl. Instrum. Methods B* **123**, 51–56 (1997).
59. T. Nakamura, E. Niu, H. Oda, A. Ikeda, M. Minami, T. Ohta and T. Oda, High precision  $^{14}\text{C}$  measurements with the HVEE Tandemron AMS system at Nagoya University, *Nucl. Instrum. Methods B* **223–224**, 124–129 (2004).
60. S. Freeman, P. Bishop, C. Bryant, G. Cook, D. Dougans, T. Ertunc, A. Fallick, R. Ganeshram, C. Maden, P. Naysmith, C. Schnabel, M. Scott, M. Summerfield and S. Xu, The SUERC AMS laboratory after 3 years, *Nucl. Instrum. Methods B* **259**, 66–70 (2007).
61. M. Suter, Jacob St. and H. A. Synal, AMS of  $^{14}\text{C}$  at low energies, *Nucl. Instrum. Methods B* **123**, 148–152 (1997).
62. H.A. Synal, M. Döbeli, S. Jacob, M. Stocker and M. Suter, Radiocarbon AMS towards its low-energy limits, *Nucl. Instrum. Methods B* **223–224**, 339–345 (2004).
63. W. Kutschera, Progress in isotope analysis at ultra-trace level by AMS, *Int. J. Mass Spectrom.*, **242**, 145–160 (2005).
64. J.B. Schroeder, T.M. Hauser, G.M. Klody and G.A. Norton, Initial results with low energy single stage AMS, *Radiocarbon* **46**, 1–4 (2004).
65. International standard reference material (Oxalic acid SRM 4990C) is supplied worldwide by the National Institute of Standards and Technology (<http://www.nist.gov>); other reference materials of different certified  $^{14}\text{C}$  concentrations are provided by the International Agency of Atomic Energy (<http://www-naweb.iaea.org/nahu/nmr/nmr2003/index.htm>).
66. I.A. Law and R.E.M. Hedges, A semi-automated bone pretreatment system and the pretreatment of older and contaminated samples, *Radiocarbon* **31**, 247–253 (1989).
67. T. Higham, <http://www.c14dating.com/>.
68. E. Wild, R. Golser, P. Hille, W. Kutschera, A. Priller, S. Puchegger, W. Rom, P. Steier and W. Vycudilik, First  $^{14}\text{C}$  results from archaeological and forensic studies at the Vienna Environmental Research Accelerator, *Radiocarbon* **40**, 273–281 (1998).
69. C. Bronk Ramsey an M.J. Humm, On-line combustion of samples for AMS and ion source developments at ORAU, *Nucl. Instrum. Methods B* **172**, 242–246 (2000).
70. A.T. Aerts-Bijma, J. van der Plicht and H.A.J. Meijer, Automatic AMS sample combustion and  $\text{CO}_2$  collection, *Radiocarbon* **43**, 293–298 (2001).
71. D.C. Lowe and W.J. Judd, Graphite target preparation for radiocarbon dating by accelerator mass spectrometry, *Nucl. Instrum. Methods B* **28**, 113–116 (1987).
72. X. Xu, S.E. Trumbore, S. Zheng, J.R. Southon, K.E. McDuffee, M. Luttgen and J.C. Liu, Modifying a sealed tube zinc reduction method for preparation of AMS graphite targets: reducing background and attaining high precision, *Nucl. Instrum. Methods B* **259**, 320–329 (2007).

73. P.E. Damon, D.J. Donahue, B.H. Gore, A.L. Hatheway, A.J. T. Jull, T.W. Linick, P.J. Sercel, L.J. Toolin, C.R. Bronk, E.T. Hall, R. E. M. Hedges, R. Housley, I. A. Law, C. Perry, G. Bonani, S. Trumbore, W. Woelfli, J. C. Ambers, S. G. E. Bowman, M. N. Leese and M.S. Tite, Radiocarbon dating of the Shroud of Turin, *Nature* **337**, 611–615 (1989).
74. A.J.T. Jull, D.J. Donahue and P.E. Damon, Factors affecting the apparent radiocarbon age of textiles: a comment on 'Effects of fires and biofractionation of carbon isotopes on results of radiocarbon dating of old textiles: the Shroud of Turin', by D.A. Kouznetsov et al. , *J. Archaeol. Sci.* **23**, 157–160 (1996); D.A. Kouznetsov, A.A. Ivanov and P.R. Veletsky, Effects of fires and biofractionation of carbon isotopes on results of radiocarbon dating of old textiles: the Shroud of Turin, *J. Archaeol. Sci.* **23**, 109–121 (1996).
75. G. Bonani, S. Ivy, W. Wolfli, M. Broshi, I. Carmi and J. Strugnell, Radiocarbon dating of fourteen Dead Sea Scrolls, *Radiocarbon* **34**, 843–849 (1992).
76. A.J. Timothy Jull, D.J. Donahue, M. Broshi and E. Tov, Radiocarbon dating of Scrolls and linen fragments from the Judean desert, *Radiocarbon* **37**, 11–19 (1995).
77. J. van der Plicht, Radiocarbon dating and the Dead Sea Scrolls: a comment on 'redating', *Dead Sea Discoveries* **14**, 77–89 (2007); J. Atwill, S. Braunheim and R. Eisenman, Redating the radiocarbon dating of the Dead Sea Scrolls, *Dead Sea Discoveries* **11**, 143–157 (2004).
78. G. Bonani, S. Ivy, I. Hajdas, T.R. Niklaus and M. Suter, AMS  $^{14}\text{C}$  age determinations of tissue, bone and grass samples from the Otztal Ice man, *Radiocarbon* **36**, 247–250 (1994).
79. R.E.M. Hedges, R.A. Housley, C.R. Bronk and G.J. van Klinken, Radiocarbon dates from the Oxford AMS system: Archaeometry datelist 15, *Archaeometry* **34**, 337–357 (1992).
80. W. Kutschera and W. Mueller, 'Isotope language' of the Alpine Iceman investigated with AMS and MS, *Nucl. Instrum. Methods B* **204**, 705–719 (2003).
81. M.E. Fedi, A. Cartocci, F. Taccetti and P.A. Mandò, AMS radiocarbon dating of medieval textile relics: the frocks and the pillow of St. Francis of Assisi, *Nucl. Instrum. Methods B* **266**, 2251–2254 (2008).
82. C. Bronk Ramsey, Development of the radiocarbon calibration program, *Radiocarbon* **43**, 355–363 (2001).
83. A. Long, B.F. Benz, D.J. Donahue, A.J.T. Jull and L.J. Toolin, First direct AMS dates on early maize from Tehuacan, Mexico, *Radiocarbon* **31**, 1035–1040 (1989).



# Index

*Note:* Page numbers in italic type refer to figures. Page numbers in bold type refer to tables.

- A/P ratio 198–9, 207
- ABA treatment 474–5
- Abietane 331
- Abietic acid 14
- Accelerator mass spectrometry (AMS) 462–3
  - applications 476–8
  - electromagnetic filters 464–5
  - high-energy analysis 470–2
  - ion source 466–7
  - isobar removal 463
  - low-energy analysis 468–9
  - low voltage machines 473
  - particle stripping 470
  - performance 463–4
  - sample masses **462**
  - sample preparation
    - graphitisation and combustion 475–6
    - pretreatment 474–5
  - sensitivity 464
  - separation efficiency 472
  - single-stage 473
  - tandem accelerator 469–70
- Acrylic paints 349–51, 352
- Acrylic resins 27
- Adduct ions 47
- Adhesives 117
  - artificial 28
  - GALDI/MS 159
  - see also* Animal glues
- African art objects
  - blood 450–2
  - complex patina mixtures 452–3
- Agathic acid 14
- Agatholic acid 14
- Aline* wax sculpture 118
- Alizarin 442–3
- Alkyd paints 354–6
- Alkyl chloroformates 247
- Aloe resin 147–9, **149**
- Ambers 18–19
- Amiet, Cuno 153–5
- Amino acids 4, 5
  - isotope ratios in bones and experimental animals 412–15
  - makeup of animal products **6**
  - racemisation 251–3
  - see also* Proteomics
- Amphorae 218–22
- $\alpha$ -amyrine 80, 81
- Animal fats 99–100
  - determining origin 416–19
  - distinguishing from vegetable fats 197
  - ESI/MS of triacylglycerols 123, 124–5
  - fatty acid composition 7, 9
  - horse, hydrogen isotope ratios 422
  - sample preparation, electrospray ionisation mass spectrometry **103**
  - see also* Lipids
- Animal glues 167–8
  - graphite-assisted laser desorption/ionisation mass spectrometry 159
  - molecular markers (pyrolysis) **307**
  - in mortars **179**
  - as paint binder 238
  - peptide mass mapping **177**
  - pyrolytic molecular markers **307**
- Animal resins 17–18
- Animal waxes 10–11, 99
- Annatto **25**
- Anthraquinoid dyes **23**, 369–72
- Antinoe 90–1
  - GC/MS of lamp illuminant residue 201–3

- Arabic gum 20  
     composition **21**  
     protein content 168  
 Arabinose, pyrolysis 314  
 Argancy 89  
*Arribidaea chica* 22  
 Asphalt 19–20  
 Atmospheric pressure chemical ionization (APCI) **45**, 50–1  
 AW2 resin 159  
 Azelaic acid 107  
     ratio to glycerol 199  
     ratio to palmitic acid 198–9, 207  
     transmethylation yields from TMAH 310  
  
 Bakelite **27**  
 Bamana sculptures 451  
 Barberry **25**  
 Bark tar, *see* Birch bark tar  
 Beeswax 10–11, 99, **100**, 121  
     ageing 200  
     in archaeological finds 115–17  
     electrospray ionisation mass spectrometry **103**  
     graphite-assisted laser desorption ionisation mass spectrometry 150–1  
     long-chain compounds 123–4  
     mass spectrum 120  
     pyrolysis gas chromatography mass spectrometry 316–18  
     as reference substance 106–8  
 Benzoe resin 17, 228–9, 229  
 Berenice 328  
 Betulin 223, **224**  
 Betulone 223, **224**  
 Binding media, *see* Paints, binding media  
 Birch bark tar 19, 84, 89, 222–7  
 Bitumen **4**, 19–20  
 Black alder **25**  
 Blood 168, 450–2  
 Blue-violet dyes 380–3  
*Boliw* 451  
 Bone 410–11, 412–15, **462**  
 Bonfigli, Benedetto 185  
 Boswellic acids 16, 219  
 Botai 422–3  
 Boucher, François **207**, 208–9  
*Brassicaceae* oils 197, 202  
     *see also* Vegetable oils  
 Brazilwood **25**  
 Brown dyes 374–80  
 BSTFA 217  
 Building materials 169–70, 178, **179**, 182–4  
 Bulffalmacco, Bonamico 320–21  
  
 Calcium caseinate **307**  
 Candelilla wax 11–12, 99, **100**, 113  
 Capillary electrophoresis **43**, 366–7  
     red dyes 372  
     sample preparation 367–9  
 Carbon  
     isotopic fractionation  
         derivatisation and 401  
         marine ecosystems 395–6  
         during photosynthesis 394  
     radiocarbon, *see* Radiocarbon  
     relative isotopic abundance **393**  
         in archaeological bone and tissue 408  
         cholesterol in bone and tissue 408–10, 409  
         fatty acids 417  
         instrumental configuration 403, 404  
*Cardinal Richelieu* 374  
 Carnauba wax 11, 99, **100**, 108–9, 111  
 Carotenoid dyes 377  
 Casein **5**, **6**, 238, **307**  
 Castor oil **7**, 8  
 Cellulose 20  
 Cellulose acetate **27**  
 Ceresine 112  
 Chain scission 347–8  
 Charcoal **462**  
 Charge residue model (CRM) 50  
 Chemical imaging 71–2, 435–6  
 Chemical ionization (CI) **45**, 47–9  
 Chinese varnish 328  
 Chinese wax 11  
 Chirality, amino acids 251–3  
 Cholesterol 408–10, 409, 412  
 Chromatographic techniques 241  
     *see also* Gas chromatography; Reverse-phase liquid chromatography  
*Coccus ceriferus* 11  
 Cochineal **23**, 371  
 Collagen 166  
     amino acid composition **6**  
     isotope ratios 413, 414  
 Colophony 84–7, 86, 145–7, **146**, 329, 333–4, 334  
 Communic acid 14  
 Copaiba balsam **147**  
 Copals 335, 336  
*Copernicia cerifera* 11–12  
 Copper acetate 447–9  
 Cow milk fat 124, 125  
 Crassulacean acid metabolism 394  
 Crocins 377  
*Cruciferae* 9  
 Curcuminoids 376, 378, 379  
 Curd **179**  
     *see also* Milk



- Curie-point pyrolyser 305–6  
 Cyclohexanone resins 156–9  
 Cytochrome c 69, 70
- Dachour 294  
 Dalou, Aime-Jules 119, 122  
*Dama con Liocorno* 209  
 Dammarene, structure 331  
 Dammar resin 17, 138, 139  
   ageing **141**  
   discriminating from mastic 339  
   pyrolysis 337–8, 338
- Databases  
   mass spectral 66–7  
   protein binders 173
- Deconvolution 70–1
- Dehydroabietic acid 220, 230
- Dendrochronology 443–5
- Derivatisation  
   for gas chromatography mass spectrometry  
     lipids 194, 195  
     protein paint binders 245–7  
     resins 216–17, 218, 230  
   15-hydroxy-7-oxodehydroabietic acid 231  
   for isotope ratio mass spectrometry 400,  
     401–2  
     data correction 406–7  
   for pyrolysis gas chromatography mass  
     spectrometry 305  
     beeswax 316–18  
     lipids 308–10  
     plant resins 313–14  
     terpenoid resins 339–42
- Desorption electrospray ionisation (DESI) **45**,  
 52–3
- Deuterium ratio, instrumental  
   configuration 405–6
- Dicarboxylic acids 106, 107, 198–9
- Dietary reconstruction 408–10  
   amino acids 412–15  
   fatty acids 410–12
- Dihydroxycarboxylic acids 201–3
- Direct exposure mass spectrometry  
   (DE-MS) 79  
   case studies 90–3  
   lipids 101–2, 105–6  
   reference materials 80–7
- Direct exposure probe (DEP) 101
- Direct inlet mass spectrometry (DI-MS) 43,  
 78, 79  
   case studies 88–9  
   lipids 101–2, 106
- Direct insertion probe 101
- Direct mass spectrometry, *see* Mass  
 spectrometry
- Direct temperature resolved mass spectrometry  
   (DTMS) 43, 87–8, 93
- Diterpenoid resins 14–16  
   graphite-assisted laser desorption/ionisation  
     mass spectrometry 145–50  
   pyrolysis gas chromatography-mass  
     spectrometry 333–9  
   solid phase microextraction 272–3  
   structures of main constituents 331–2
- Dogon wooden statuettes 451–2, 454
- Drying oils 198–9, 205–7  
   definition 192  
   distinguishing from non-drying oils 310–11
- Dyes 22, 365–7  
   anthraquinone **23**, 369–72  
   carotenoid 377  
   chemical composition **23–5**  
   direct mass spectrometry 145  
   flavonoid **24**, 275–380  
   LC/MS, sample preparation 367–9  
   madder 442–3  
   mordant 368  
   purple **24**  
   red 369–74  
   secondary ion mass spectrometry 442–3  
   yellow and brown 374–80
- Egg 5  
   amino acid composition **6**  
   as binder 167  
   fatty acid composition **7**  
   molecular markers (pyrolysis) **307**  
   in mortars **179**  
   in paint binders 238  
     secondary ion mass spectrometry 445–7  
   peptide mass mapping **176–7**
- Elderberry 381
- Electron ionization (EI) 45–7, **45**  
   data interpretation 66–7  
   lipids 101–2, 102–3, 126
- Electro-osmotic flow 367
- Electrospray ionization  
   (ESI) **45**, 69  
   lipids 102–3, 122–5, 126
- Electrostatic analyser (ESA) 464–5
- Elemi **13**
- Enzyme-linked immunosorbent assay  
   (ELISA) 169
- Epilaccishellolic acid 232
- Epishellolic acid 230, 232
- Epoxy resins, applications **27**  
 20, 24-epoxy-25-hydroxydammar-  
   3-one 232
- Esparto wax 12
- Euphorbia* sp. 11

- Fatty acids 6–9  
   isotope ratios  
     origin determination 416–19  
     preservation of ratios 420–23  
     in skeletal and soft tissue remains 410–12  
   lipid identification and 197
- Fermentation, paint binders 240
- Fibres  
   flavonoid dyes 375  
   secondary ion mass spectrometry 440–5,  
     442–3
- Fig latex 304
- Fish glue 168, **176**
- Flavonoid dyes **24–5**, 275–80, 375–80  
   chemical composition **24**
- Fontana, Lucio 354
- Fossil resins 18–19
- Fossil waxes 12, 99
- Fourier transform mass analyser **55**, 58–60
- Frankincense 16, 83, 264, 329  
   composition **13**  
   gas chromatography mass spectrometry  
     analysis 218  
   solid phase microextraction gas  
     chromatography mass spectrometry  
     analysis 265, **266–9**, 275–81  
   comparison with classical solvent  
     extraction 274
- Fruit tree gum 20, **21**
- Fustic **24**
- Galactose 314
- Galbanum 264, 265
- GALDI, *see* Graphite assisted laser desorption  
   ionisation
- Garlic **5**, **6**
- Gas chromatography 43
- Gas chromatography mass spectrometry  
   analytical procedure 192–6  
   blank runs 248  
   lipids  
     applications 192  
     case studies 201–9  
     contamination 193  
     data interpretation 196–200  
   proteins  
     amino acid racemisation 251–3  
     analysis 247–9  
     pretreatment 243–5  
     sampling 242  
   resins 215–18  
   sample size 193
- Gas phase 39
- Gauguin, Paul 118
- Gelatine 167
- Ghatti **21**
- Glucose, pyrolysis 314, 315
- Glues, *see* Animal glues
- Glycerol 199
- Glycerolipids 4, 6–9
- Graphite-assisted laser desorption ionisation  
   (GALDI) mass spectrometry 131–2  
   adhesives 159  
   aqueous paint binders 159  
   artworks 144–5  
   cyclohexanone resins 156–9  
   detection limits 144  
   natural resins 145–50  
     pure triterpenes 133–8  
     triterpenoid 138–42  
   oils and fats 152–6  
   rubber 149–50  
   waxes 150–2
- Graphitisation 475
- Guar **21**
- Guimet Museum 284, 288
- Gums 20, **21**, 168
- Haem 451
- Hair **462**
- Headspace solid phase microextraction (HS-  
   SPME) 216
- Heartwood 443–4
- Heating  
   resins 19  
   *see also* Pyrolysis
- Hematein 381
- Henna **25**
- Hexamethyldisilazane (HMDS) 341–2
- Hide glue **177**
- High performance liquid chromatography  
   (HPLC)  
   carotenoid dyes 377  
   indigoid dyes 380–1  
   proteins in binders 168  
   red dyes 372  
   resins 217–18  
   reverse phase 366  
     anthraquinone dyes 369–70, **371**  
     flavonoid dyes 375–6  
     indigoid dyes 380–1  
     sample preparation 367–9  
   reverse phase, blue dyes 381–3
- High temperature gas chromatography mass  
   spectrometry 196
- High Voltage Engineering Europe 465
- Hinoki cypress 444–5
- Hodler, Ferdinand 156
- Honey **21**
- Horyuji Temple 444

- Hydrogen  
 isotope ratio mass spectrometry 405–6  
 relative isotopic abundance **393**  
 fatty acids 420
- Hydrolysis, paint binder proteins 243–4
- 15-hydroxy-7-oxodehydroabiatic acid 231
- Hydroxydammarone 135, 136
- Iceman 477
- Incense 12, 281  
 solid-phase microextraction profile 282
- Indigo **23**, 380
- Indigoid dyes **23–4**, 380–1
- Inlet system 42–3
- Instrumentation  
 accelerator mass spectrometry 463, 465–73  
 inlet system 42–3  
 ionization techniques, *see* Ionization techniques  
 isotope ratio mass spectrometry (IRMS) 398–9  
 mass analyser 55–7  
 resolution 53–4  
 overview 41–2  
 resolution 53, 54
- Ion evaporation model (IEM) 50
- Ionization techniques 42–3, **45**  
 accelerator mass spectrometry 466–7  
 atmospheric pressure chemical (APCI) 50–1  
 chemical (CI) 47–9  
 desorption electrospray (DESI) 52–3  
 electrospray (ESI), *see* Electrospray ionization  
 graphite-assisted laser desorption (GALDI) 132–3  
 for inorganic materials 53  
 matrix-assisted laser desorption (MALDI) 51–2, 131–2  
 soft 47, 67–71
- Ions  
 definition 39  
 metastable 60  
 pseudomolecular 48
- Ion trap mass analyser **55**
- Isatis indigotica* 380
- Isinglass 168
- Isobars 463
- Isopimaric acid 14
- Isotope ratio mass spectrometry (IRMS) 392  
 advantages 397  
 analytical considerations 398–9  
 applications  
 amino acids in bones and experimental animals 412–15  
 bone and soft tissues  
 carbon 408  
 cholesterol 408–10  
 fatty acids 410–12  
 carbon ratios in animal fats 416–19  
 fatty acid hydrogen ratios 420–3  
 organic residues in pottery 415  
 compound-specific 403–6  
 instrumentation 398–9  
 for carbon ratio measurement 403  
 sample preparation 400–1
- Isotopes 64–5  
*see also* Isotopic fractionation; Isotope ratio mass spectrometry; Radiocarbon
- Isotopic fractionation 393–6  
*see also* Kinetic isotope effect
- Japan wax **100**, 110–15, 112, 122, 155, **156**
- Keratin **6**
- Ketone Resin N 158
- Ketone resins **27**, 345
- Kinetic isotope effect 406–7  
*see also* Isotopic fractionation
- Kyphi 281, **282–3**
- La Castellina 124
- La Fangade 88–9
- La Semeuse 118
- Labdane 331
- Labdanum 14, 264, 265, **266–9**
- LABEC laboratory 477
- Laccifer lacca* Kerr 17
- Lady's bedstraw **23**, 372
- Lamp residues 201–2
- Lanolin 11
- Lanostane 332
- Lard **7**  
*see also* Animal fats
- Laropal K80 345–6, 345
- Latex paints 356
- Lead soap 449
- Lead white 445–7
- Levopimaric acid 14
- Libby mean life 460
- Light, resin ageing and 142
- Liguria 93
- Linseed oil 152  
 fatty acid composition **7**  
 GALDI mass spectrum 153  
 in paint binder, gas chromatography mass spectrometry  
 trace 205–6  
 pyrogram 309

- Lipids 191–2  
 analytical methodology 100–1  
 archaeological samples 115–17  
 in complex mixtures 453  
 degradation 8  
 derivatisation for gas chromatography mass spectrometry 194, **195**  
 fatty acid composition 197  
 gas chromatography mass spectrometry  
 data interpretation 196–200  
 lipids 205–9  
 ionisation methods  
 electron ionisation 101–2, 126  
 electrospray 102–3, 122–5, 126  
 from marine products 9  
 oxidation 8  
 in paint samples 197–9, 205–9  
*see also* Animal fats; Vegetable oils; Waxes
- Liquid chromatography **43**  
*see also* Capillary electrophoresis; High performance liquid chromatography
- LMW resins 345–6  
 Locust bean 20, **21**  
 Logwood **25**, 381–3  
 Lorentz force 464  
 Lucerne 151  
 Lupenone **223**, **224**  
 Lupeol **224**
- Madder dyes 373  
 chemical composition **23**  
 LC/ESI-MS **371**  
 secondary ion mass spectrometry 442–3
- Madonna con Bambino in Trono e due Angeli* 207
- Mai* mask 156, 157
- Maillard reactions 244
- Makarov, Alexander 58
- Manila copal 336
- Manzoni, Piero 353
- Mass analyser  
 basic principles 54–5  
 detectors 60  
 double focusing 55  
 Fourier transform ion cyclotron resonance 59–60  
 ion traps 57–8  
 Orbitrap 58–9  
 resolution 53, 54  
 time of flight 56–7
- Mass number 64
- Mass spectrometry 36–7, 79  
 advantages and characteristic features 38–9  
 beeswax 106–7, 110, 123–4  
 data interpretation 63–4  
 electron ionization 66–7  
 isotopes 64–5  
 nitrogen rule 66  
 soft ionization 67–71  
 from electron ionization 66–7  
 imaging 71–2  
 information obtainable 40–1  
 instrumentation, *see* Instrumentation  
 ionization techniques, *see* Ionization techniques  
 large molecules 69  
 lipids  
 archaeological samples 115–17  
 electron ionisation mode 101–2  
 electrospray ionisation 102–3  
 reference materials  
 beeswax 106–7, 110  
 candelilla wax 114  
 carnauba wax 109–14, 111  
 palmitic acid 105–6  
 spermaceti 108–9  
 vegetable oils 114–15  
 wax sculptures 117–22  
 mass analyser, *see* Mass analyser  
 nitrogen rule 66  
 for proteomics 172–3  
 separation techniques 43  
 tandem 60–3  
 terpenoid resins  
 case studies 88–93  
 reference samples 80–8
- Mass-to-charge ratio 37–8
- Mastic resin 16, 91, 143  
 ageing 140, **141**  
 composition **13**  
 discriminating from dammar 339  
 GALDI spectrum 140  
 gas chromatography mass spectrometry  
 analysis 227–8  
 mass spectrum 83  
 pyrolysis 338–9  
 solid phase microextraction gas chromatography mass spectrometry  
 analysis **266–9**
- Matrix assisted laser desorption ionization (MALDI) mass spectrometry **45**, 51–2, 131–2  
*see also* Graphite assisted laser desorption ionisation mass spectrometry; Proteomics
- Messer Fillipo cell 319
- Metal ions 168  
 lipids and 449  
 proteins and 239–40, 244
- Metastable ions 60

- Methylation 194, 195  
*see also* Derivatisation
- Methylene blue 380, 382, 383
- Microcrystalline wax 12
- Milk 167  
   cow 124, 125  
   horse, hydrogen isotope ratios 422, 422  
   as paint binder 238  
   pyrolysis, molecular markers **307**
- Molecular ions 46
- Molecular weight 40
- Monocarboxylic acids 105–6
- Monoterpenes 270–1  
*see also* Terpenoid resins
- Montan wax 12
- Mordant dyes, LC/MS, sample preparation 368
- Morinda **23**
- Moringa oil 9
- Mortars  
   organic additives **169**  
   proteomic analysis 178, **179**
- Mowilith 343
- Multivariate analysis, *see* Principal Components Analysis
- Mummification balms 262, 284–6
- Munch, Edvard **180**
- Myrrh **13**, 16  
   solid phase microextraction gas chromatography mass spectrometry analysis 264, 265, **266–9**
- Neoabietic acid 14
- NIST/EPA/NIH Mass Spectral Library 66–7
- Nitrogen  
   isotope ratios, instrumental configuration 404  
   isotopic fractionation 395–6  
   relative isotopic abundance **393**  
   plants 395
- Nitrogen rule 66
- Nonacosan-15-one 68
- Nylons, applications **27**
- Oetzi 477
- Oils, *see* Vegetable oils
- Oil paints 154  
*see also* Paints, binding media, lipids
- Old fustic **24**
- Oleanine, structure 332
- Oleanolic acid 80, 81
- Oleic acid  
   in lamp residues 201–2  
   ratio to stearic acid, paint binder ageing 199
- Olibanum, *see* Frankincense
- Olive oil **7**
- Orbitrap mass analyser **55**, 58–9
- Orchil, chemical composition **24**
- Ouricuri wax 11
- Ovalbumin 238
- Oxidation  
   lipids 8  
   triterpenoid resins 16–17
- 7-oxodehydroabietic acid 82, 85
- Oxygen isotope ratios **393**, 406
- Ozokerite 12, 151
- P/S ratio 199, 207, 447
- Paints  
   binding media 166–8, 237–9, 303–4  
     aqueous 159  
     beeswax 10–11  
     cyclohexanone 156–9  
     gas chromatography mass spectrometry analysis 205–9  
     graphite assisted laser desorption ionisation/MS 152–9  
   identification 249–51  
   lipids 9, 152–6, 192  
     fatty acid composition 197–8  
     linseed oil 205–6  
   proteins 168–9  
     animal glues 238  
     databases 173  
     egg 238, 445–7  
     hydrolysis 243–4  
   reference materials 249  
   sampling 242  
   synthetic 156–9  
     acrylic 349–51  
     alkyd 354–6  
     vinyl 351–4  
   latex 356  
   physico-chemical properties 303–4  
   protein databases 173  
   secondary ion mass spectrometry 445–7, 445–9  
   silicone 356
- Palmitic acid 105–6, 194–5  
   esters 106–8, 123–4  
   glycerol and 199  
   ratio to azelaic acid 198–9, 207  
   ratio to stearic acid 447  
     alkyd paints 356  
     drying oils and 199, 207
- Palmitin 122
- Palustric acid 14
- Paraffin 12, **100**, 122
- Paraloid B72 26, 349

- Peptide mass mapping (PMM) 170–3  
   building materials 178–80, 182–4  
   data analysis 175  
   measurement 175  
   proteolytic cleavage 171–2  
   sample preparation 174–5
- Perrier, Alexander 159
- Persian berries, chemical composition **24**
- Phenolic resins 12, 17
- Photosynthesis 394
- Pigments  
   aloe 147  
   interfering effects in protein binder analysis 244  
   secondary ion mass spectrometry 447–9
- Pimarane, structure 331
- Pimaric acid 14odegradation, proteins 241
- Pine pitch  
   gas chromatography mass spectrometry analysis 218  
   oxidation pathways 221  
   solid phase microextraction gas chromatography mass spectrometry analysis 265, **266–9**
- Pine resin 14–15, 88–9  
   composition **13**  
   diterpenoid compounds 14  
   graphite assisted laser desorption ionisation mass spectrometry 145–6  
   solid phase microextraction 264–70, 265, **266–9**  
   in wax sculptures 121, 122  
   *see also* Terpenoid resins
- Pitch 19, 218–19
- Plants 394, 395
- Plant waxes 11–12
- Plinius 3, 202
- Pollock, Jackson 354
- Polyamides **27**
- Poly(butyl methacrylate) (PBMA) 343–4
- Poly(EA-co-MMA) paints 350
- Poly(ethylene glycols) **27**
- Polymers **4**, 26–8  
   applications **27**  
   degradation 438–40  
   pyrolysis gas chromatography mass spectrometry 342–6  
   secondary ion mass spectrometry 438–40  
   thermal degradation mechanisms 347–8
- Polymethyl methacrylate (PMMA) 26
- Poly(nBA-co-MMA) paints 351
- Polyphenols 378–80
- Polysaccharides **4**, 20–2, 314–16
- Polyurethanes **27**
- Polyvinyl acetate (PVAc) 343, 351–4
- Polyvinyl chloride (PVC), pyrolytic thermal degradation 348
- Poppy seed oil, mass spectrum 114
- The Post House at Oschwand* 154
- Principal Components Analysis (PCA) 250  
   DE-MS data 90–1, 92  
   gas chromatography mass spectrometry of resins 221–2
- Product ion scan 60–1
- Proteases 171–2
- Proteins 4–6, 165–6  
   amino acid racemisation 251–3  
   amino acid sequencing 5  
   artworks 180–1  
   biological degradation 240  
   in building materials 169–70, 178, **179**  
   cleavage 171–2, 174  
   denaturing 4–5  
   environmental 240–2  
   hydrolysis 243–4  
   metal ions and 239–40  
   in paint binders 176–8  
   animal glues 238  
   egg 238, 445–7  
   high-performance liquid chromatography 168  
   identification 249–51  
   pH changes 5  
   pyrolysis 306–8  
   *see also* Amino acids; Peptide mass mapping
- Protonated molecules 48
- Purple dyes, chemical composition **24**
- Pyrolysis direct mass spectrometry 79
- Pyrolysis gas chromatography mass spectrometry 304–6  
   beeswax 316–18  
   case studies 318–22  
     Monumental Cemetery, Pisa 320–21  
     mordant gilding, Teodolinda's chapel 322  
     wall paintings 319  
   lipids 308–12  
   polysaccharides 314–16  
   proteins 306–8  
   synthetic polymers 342–6  
   terpenoid resins 330–3  
   derivatisation methods 339–42
- Quadrupole mass analyser **55, 56**  
   triple 61
- Quercitron bark **24**
- Rabbit glue 168
- Racemisation, amino acids 251–3

- Radiocarbon dating 459–63  
     calibration 460  
     sample preparation 473–4  
     timescale 460  
*see also* Accelerator mass spectrometry  
 Radiometric carbon dating 461  
 Radish oil 202  
 Raffaelli, Jean-Francois 155–6  
 Raffaello 209  
 Rapeseed oil 7, 197  
 Raphael 209  
 Red dyes 372–4  
     *see also* Anthraquinones  
 Reference materials  
     lipids 104–15  
     proteins, paint binders 249  
     resins 80–8  
     solid phase microextraction 264–70  
 Reflectron 56–7, 57  
 Regalrez 346, 1094  
 Relbunium, chemical composition 23  
 Resins 12–14, 77–8, 327–30  
     animal 17–18  
     chemical composition 13  
     derivatisation 313–14  
     diterpenoid, *see* Diterpenoid resins  
     fossil 18–19  
     gas chromatography mass spectrometry 215–18  
         case studies  
             aromatic resin 228–9  
             bark tar 222–7  
             frankincense 218  
             mastic resin 227–8  
             pine pitch 218–22  
             terpenoid varnishes 229–32  
     graphite assisted laser desorption ionisation/MS 145–50  
     heating 19  
     phenolic 12, 17  
     pitch and tar 19  
     synthetic 26, 156–9, 342–6  
         *see also* Polymers  
     triterpenoid, *see* Triterpenoid resins  
 Reverse phase liquid chromatography (RPLC), *see* High performance liquid chromatography, reverse phase  
 Rhamnus bark 24  
 Ricinoleic acid 8  
 Rosin, *see* Colophony  
 Roty, Louis-Oscar 118  
 Rubber, graphite assisted laser desorption ionisation/MS 149–50  
*Rubia tinctorum* roots 370, 371  
 S/S ratio 199  
 Safflower dyes 25  
 Saffron 25, 376, 377–80  
 Saint Catherine, Znojimo 182, 183  
 Sample preparation  
     accelerator mass spectrometry 473–6  
     gas chromatography-mass spectrometry, proteins 243–4  
     lipids, gas chromatography mass spectrometry 192–3  
     secondary ion mass spectrometry 436–7  
     waxes, ESI/MS 103  
 Sandalwood, dyes, chemical composition 25  
 Sandarac 13, 15, 335  
 Sandaracopimaric acid 14  
 Santa Croce frock 477  
 Sapwood 443–4  
 Sawwort 24  
 Sebacic acid 107  
 Secondary ion mass spectrometry (SIMS) 434  
     applications  
         archaeological blood 450–2  
         archaeological soft tissues 449–50  
         complex mixtures 452–3  
         natural fibres 440–5  
         painting materials 445–9  
         polymers 438–40  
         wood 443–5  
     charge suppression 435  
     chemical imaging 435–6, 436–7, 437–8, 453, 454  
     data interpretation 437–8  
     instrumentation 434–6  
     process overview 433–4  
     sample preparation 436–7  
 Separation techniques 43  
 Sequential injection 468  
 Sesquiterpenes 13–14, 271  
     *see also* Terpenoid resins  
 Shell 462  
 Shellac 17–18, 147, 148, 314  
 Side-group elimination 348–9  
 Silicone paints 356, 357  
 Silk 6, 440, 443  
 Silver birch 25  
     *see also* Birch bark tar  
 Silylation 194, 196, 216–17, 310  
     proteins 246–7  
 Skin 411, 462  
 Smal discolouration 449  
 Soft ionisation 47–53  
     data interpretation 67–71

- Soft tissues
  - relative isotopic abundances 408–10, 410–12
  - secondary ion mass spectrometry 449–50
- Solid phase microextraction (SPME) 261–2
- case studies
  - archaeological samples
    - at 80°C 291–7
    - at room temperature 284–91
    - frankincense 275–81, **276–80**
    - incense 282
  - comparison with classical solvent extraction 273, 274
  - fibre coatings 271–3
  - optimization 270–4
  - process overview 262–4, 263
  - reference sample analysis 264–70
  - sampling temperature 270–1
  - sampling time 271–3
- Spermaceti wax 11, 99, **100**, 108–9
- Spilamberto Tower, wall painting 209
- Static-SIMS 434
- Stearic acid
  - ratio to oleic acid 199
  - ratio to palmitic acid 199, 356, 447
- Sterols 197
- Storax resin 17
- Strasbourg turpentine **13**
- Sugars, pyrolysis 314
- Sulfur, relative isotopic abundance **393**
- Sumac **25**
- Tandem accelerator 469–70
- Tandem mass spectrometry 60–3, 103
- Tapestries 440–2
- Tar, *see* Birch bark tar
- Tempera* 238
  - see also* Egg
- Terpenoid resins 13–14
  - direct mass spectrometry
    - case studies 88–94
    - reference samples
      - dehydroabietic acid 84–7
      - oleanolic acid 80–4
  - diterpenoid 14–16, 145–50, 333–9
  - gas chromatography-mass spectrometry 229–30
  - pyrolysis 330–3
    - di- and triterpenoids 333–9
    - trimethylsilylation 341–2
  - solid phase microextraction 271–3
    - archaeological samples 286–9, 291–7
  - triterpenoid
    - ageing 136–7
    - case studies 88–94
    - graphite assisted laser desorption ionisation-MS 133–8
- Tetramethylammonium hydroxide (TMAH) 305, 313, 340
- Textiles, *see* Fibres
- Thermal degradation, synthetic polymers 346–8
- Thermally-assisted hydrolysis and methylation 337–40
  - see also* Derivatisation
- THM gas chromatography
  - mass spectrometry 333, 337–40
- Tigaso oil 156, 157
- Time of flight mass analyser **5**, 56–7
  - see also* Secondary ion mass spectrometry
- Total lipid extracts (TLE) 192–3
- Tragacanth **21**
- Transmethylation 308–10
  - see also* Derivatisation
- Triacylglycerols 106, 108, 125, 124–5
- Japan wax 110–14
- Triglycerides 6
- Trimethylammonium hydroxide (TFTMTH) 340
- Trimethylchlorosilane 342
- Trimethylsilylation 217
  - lipids 194, **195**
  - proteins 246–7
  - resins 222–3, 313–14, 341–2
- N, O*-bis(trimethylsilyl) trifluoroacetamide 341
- Tripalmitin 110–14
- Triple quadrupole mass analyser 61
- Tristearin 108
- Triterpenoid resins 15, 16–17
  - ageing 136–7
  - direct mass spectrometry 88–94
  - fragmentation 80–8
  - graphite assisted laser desorption ionisation 133–8
  - oxidation 16–17
  - pyrolysis 333–9
- Triterpenes 133–8
- Trypsin 172, 174
- Tung oil **7**, 152
- Turin Shroud 476
- Turmeric **25**, 377
- Turpentine **13**, 333–5
- Tyrian Purple 380–1
- Unguentaria 203–5
- Unzipping 347
- Urate salts 453
- Ursane 332



- Valery, Paul 119, 120  
 Van der Weyden 446  
 Varnishes 327–30  
   direct temperature resolved mass  
     spectrometry 87–8, 93  
   gas chromatography mass  
     spectrometry 229–32  
   synthetic 342–5  
   transition temperature 26  
   *see also* Shellac; Terpenoid resins  
 Vat dyes 367  
 Vegetable oils 6–9, 99–100, 114–15, 192  
   distinguishing from animal fats 197  
   fatty acid profiles 197  
   graphite-assisted laser desorption/ionisation  
     mass spectrometry 152  
   in lamp residues 201–3  
   *see also* Lipids  
 Venice turpentine **13**, 333–5  
 Verdigris 447–9, 448  
*Vernice liquida* 328  
 Vinylite 343  
 Vinyl paints 351–4  
 Vinyl polymers **27**  
 ‘Virgin and Child’ 185  
 Vitruvius 3  
 Volatilisation, *see* Derivatisation  
 Wall paintings 244  
 Walnut galls **25**  
 Waxes **4**, **10**, 10–12, 97–8  
   gas chromatography mass  
     spectrometry 200  
   graphite assisted laser desorption ionisation  
     mass spectrometry 150–2  
   in sculptures 117–22  
   *see also* Beeswax; Lipids  
 Weld 22, **24**  
 Whey **179**  
 White varnish 329  
 Wien filter 464–5  
 Wiley Registry of Mass Spectral Data 67  
 Woad **23**  
 Wood  
   radiometric sample mass **462**  
   secondary ion mass spectrometry 443–5  
 Wool **6**, 440–2  
 Xylose 314  
 Yellow dyes 374–80  
   *see also* Flavonoid dyes  
 Young fustic, chemical composition **24**  
 Zonyl 438–40

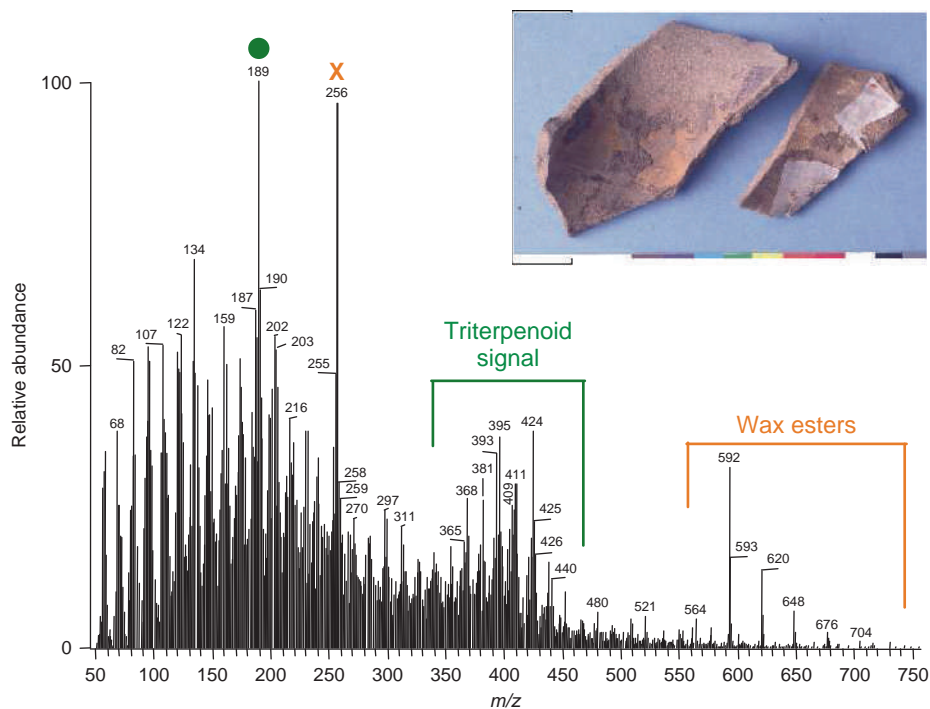


**Plate 1** Mass spectrum of an archaeological sample made of a mixture of beeswax and birch bark tar from a residue sampled on a ceramic sherd from the Iron Age site of Grand Aunay (Sarthe, France). The spectrum was obtained by DI EI-MS on a GCQ Finnigan device equipped with an ion trap analyser. Adapted from Regert and Rolando, 2002 (see Figure 4.11)

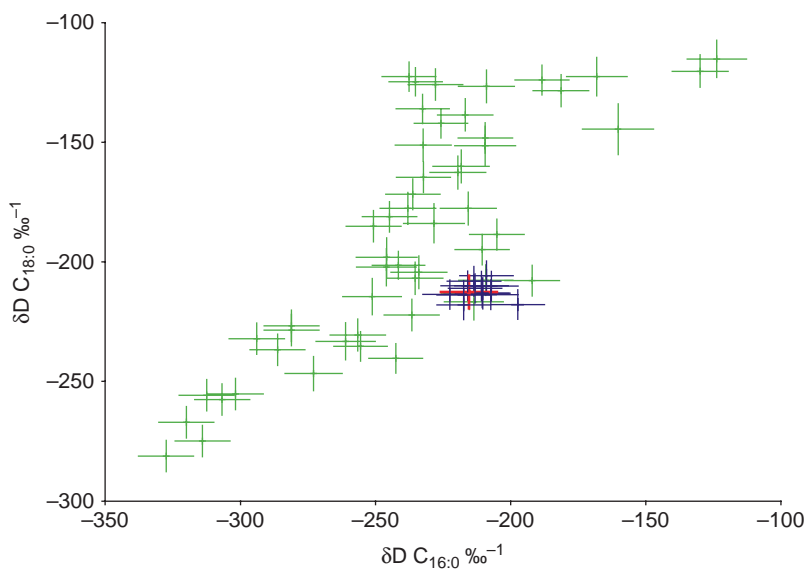


**Plate 2** Data from the simulated burial experiment superimposed on a plot of reference animal fatty acid  $\delta D$  values, showing how any change in  $\delta D$  value caused by burial is not significant compared with natural variations in  $\delta D$  values of animal fatty acids. Data from the burial experiment is blue, except for the raw lamb which is red. Reference animal fatty acid  $\delta D$  values are green and correspond to a wide range of terrestrial and marine species drawn from a wide geographical range (see Figure 14.21)

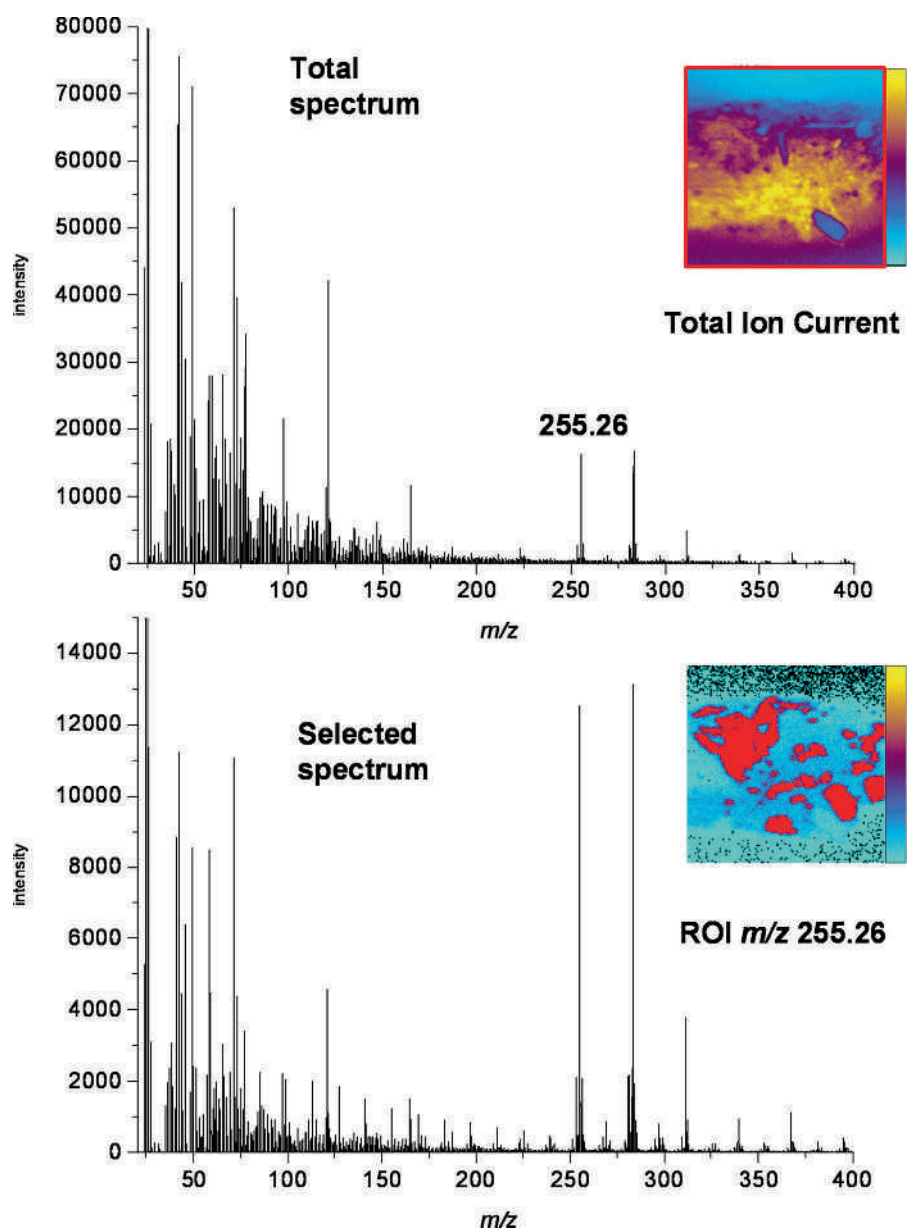


**Plate 3** Example of the use of a region of interest (ROI) on ToF-SIMS images to obtain a more specific spectrum. On account of the selected area on the image, signals from fatty acids are emphasized on the selected spectrum (see Figure 15.3)

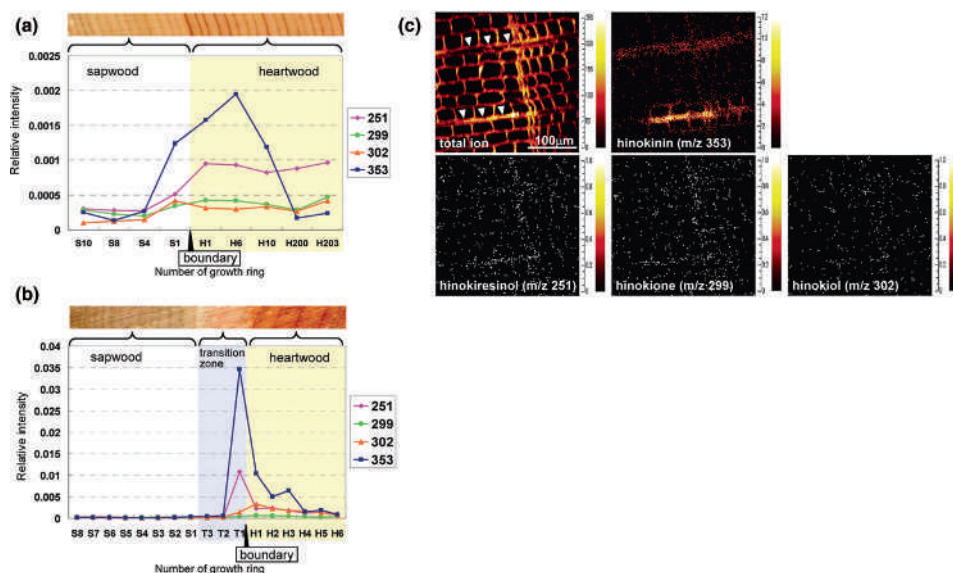


**Plate 4** Distribution of relative intensities of extractive ions at  $m/z$  251 for hinokiresinol,  $m/z$  299 for hinokione,  $m/z$  302 for hinokiol and  $m/z$  353 for hinokinin from sapwood to heartwood in Hinoki cypress. The values were obtained from the positive ToF-SIMS spectra of (a) naturally dried 233-year-old and (b) freeze-preserved 31-year-old Hinoki samples. The 'boundary' indicates the boundary between sapwood and heartwood. The growth rings determined were numbered by counting the number of years from the boundary. (c) Positive ion image ( $300 \times 300 \mu\text{m}^2$ ; scale bar,  $100 \mu\text{m}$ ) of the transverse section of the ancient Hinoki wood sample, including the ring boundary between the 44th and 45th rings; the total ion image and selected ion images for hinokinin, hinokiresinol, hinokione and hinokiol are shown. Yellow represents high intensity and black represents low yields. Adapted from *Analytical Chemistry*, **80**, 1552–1557, Saito et al., Copyright 2008 American Chemical Society (see Figure 15.8)

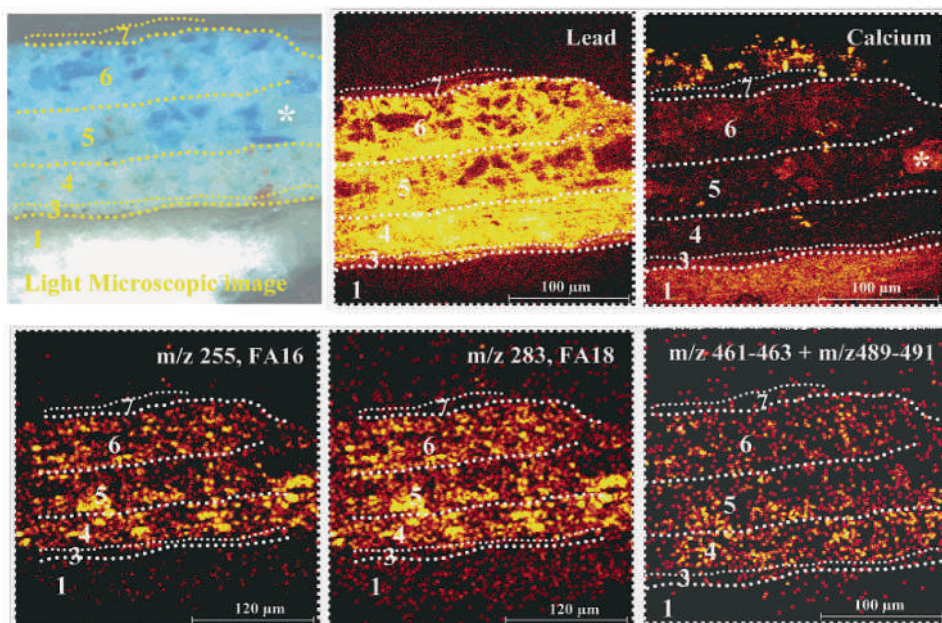


**Plate 5** Microscopic image and ToF-SIMS images of the cross-section from the painting 'The Descent from the Cross' (Museo del Prado, Madrid) by van der Weyden. Images of lead, calcium and lead soaps ( $m/z$  461–463 and 489–491) have been acquired in positive ion mode (image size  $250 \times 250 \mu\text{m}^2$ ). Images of palmitic ( $m/z$  255) and stearic ( $m/z$  283) acids have been acquired in negative ion mode (image size  $300 \times 300 \mu\text{m}^2$ ). Yellow represents high intensity and black represents low yields. The numbers on the images refer to the different layers. Adapted from *Analytical Chemistry*, 76, 1374–1385, Keune et al., Copyright 2004 American Chemical Society (see Figure 15.9)



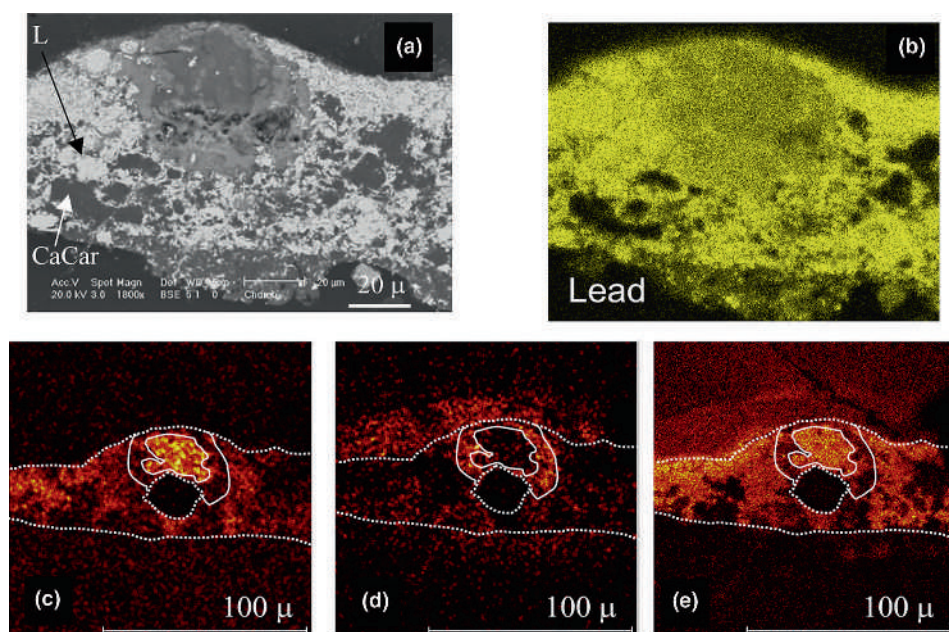


**Plate 6** Cross-section of a sample from a painting from the Hudson River School presenting a round protruding mass. (a) SEM image and EDX images of (b) lead, (c) lead soaps, (d) azelaic acid and (e) stearic acid. Reprinted from Boon et al., *Microscopy and Microanalysis*, **11**, Supplement 2, pp. 444–445, 2005, by permission of Cambridge University Press (see Figure 15.11)

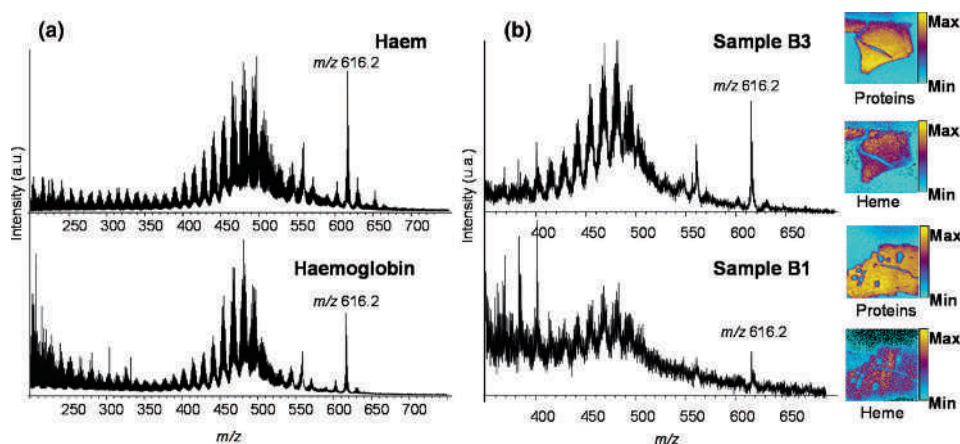


**Plate 7** Identification of blood. (a) ToF-SIMS spectra in positive ion mode of hemin and haemoglobin. (b) ToF-SIMS spectra in positive ion mode of two cross-sections of boliw patina (samples B1 and B3) and images of the localization of haem and proteins in the sample (see Figure 15.12)

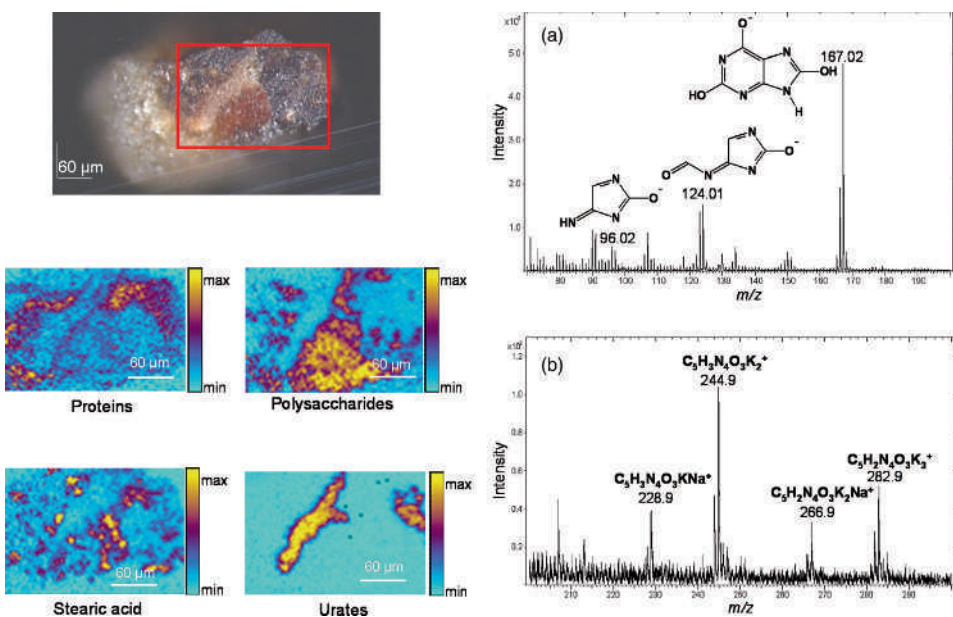


**Plate 8** Study of the sample from the Dogon statuette 73.1964.3.39. The area analysed by ToF-SIMS is outlined in red on the optical microphotograph. The spectra have been calculated from the area rich in urates in (a) negative and (b) positive ion mode (see Figure 15.13)



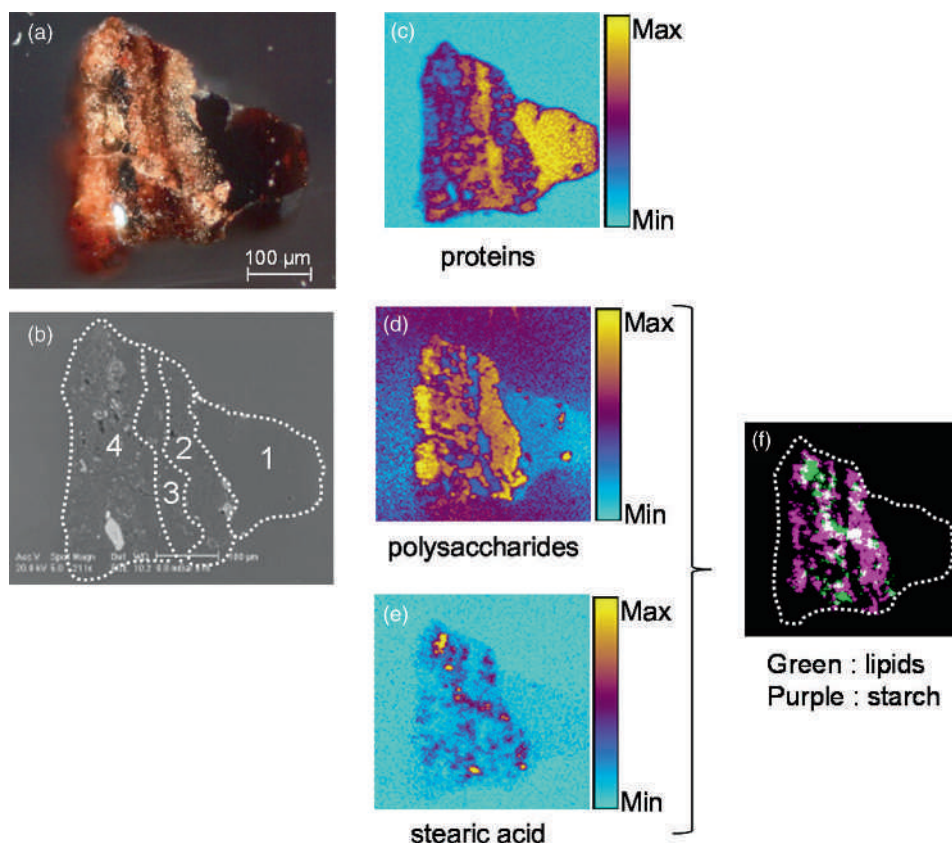


**Plate 9** Study of the sample from the Dogon statuette 71.1935.105.169. (a) Optical micro-photograph; (b) SEM micrograph showing the layer structure; ToF-SIMS images of (c) proteins, (d) polysaccharides and (e) stearic acid; (f) superposition of the distribution of polysaccharides and stearic acid (see Figure 15.14)